11-10-2020

A Spectroscopic and Photometric Survey of the W4 Hii Region and Its Young Stellar Population

Matt Wentzel-Long

A SPECTROSCOPIC AND PHOTOMETRIC SURVEY OF THE W4 HII REGION AND ITS YOUNG STELLAR POPULATION

by

MATT WENTZEL-LONG

A DISSERTATION

Presented to the Graduate Faculty of the

MISSOURI UNIVERSITY OF SCIENCE AND TECHNOLOGY

and

UNIVERSITY OF MISSOURI – ST. LOUIS

In Partial Fulfillment of the Requirements for the Degree

DOCTOR OF PHILOSOPHY

in

PHYSICS

2020

Approved by

Bruce A. Wilking, Advisor
Alexey Yamilov, Co-Advisor
J. Serena Kim
Erika Gibb
Shun Saito

PUBLICATION DISSERTATION OPTION

This dissertation consists of the following article which has been submitted for publication, or will be submitted for publication as follows:

Paper I: Pages 29-64 are intended for submission to the Astronomical Journal.

ABSTRACT

The W4 HII region is home to a large number of O and B-type stars as well as the young open cluster IC 1805. OB-type produce intense photoionizing radiation and stellar winds that can induce star formation in surrounding molecular clouds and sometimes carve out large regions of decreased particle density called superbubbles. During the star-formation process, young stellar objects (YSOs) are initially surrounded by circumstellar disks made of gas and dust which naturally dissipate after several million years. The dissipation of the disk is thought to occur for a variety of reasons, including photoevaporation by the encompassed protostar and the formation of planets. Photoionizing radiation can affect a YSO that is in close proximity to the OB stars by ablating the outer regions of a disk which cause it to dissipate faster and can disrupt the planet forming process.

The goals of this study are to contribute additional evidence for an earlier generation of star formation in the W4 HII region and to characterize the evolutionary status of disk-bearing YSOs. This was done by identifying members of IC 1805 that met several youth criteria. An average extinction of 2.7 ± 0.5 mag and median age of 2.2-2.8 Myr was found for the cluster members. A group of 15 YSOs are candidates for an earlier generation, with a mean age of 8.5 ± 2.8 Myr. Several YSOs located near bright-rimmed clouds support the theory that the OB stars are driving the expansion of the superbubble by their young ages. A total of 74 disk-bearing YSOs were identified with dereddened spectral energy distributions, and 51 were fit with a simple reprocessing disk model. Examination of the disk modeling parameters showed that most disks identified in this survey are in evolved stages. A small number of disk-bearing sources located within projected distances of $\lesssim 0.7$ pc of an O- or B-star showed evidence that their outer disks may be influenced by external photoionizing radiation.

ACKNOWLEDGMENTS

There are many people I would like to thank for helping to make this dissertation possible, including, first and foremost, my advisor Bruce Wilking. From the beginning of this research project to its conclusion, he has been a voice of reason and source of ideas. His patience, clarity of thought, and constant encouragement were instrumental in both building my own knowledge of astrophysics and aiding in my small contribution to the astronomical world. The sharing of his time, expertise, and funding made this research project possible, and best of all, an enjoyable experience.

I owe a great deal of thanks to J. Serena Kim, who shared the data that made this research possible, helped refine our work, and pushed the project in new directions. I would also like to thank the rest of my committee members for providing valuable feedback that greatly improved the quality and clarity of this research. In particular, the astrophysics course of Erika Gibb and her insights on this project helped me understand many of the abstract concepts that this research is built upon and gave the project a clear direction. Many thanks also go to several undergraduate research assistants–Justin Bryan, Tyler Hanke, and Matthew Sprague–for their assistance in analyzing the sizable spectroscopic sample. I would also like to thank Tim Sullivan for several useful discussions about the *emcee* sampler used in this project and for his advice throughout my graduate studies that calmed my anxieties about the process.

Many thanks also go to my wonderful spouse Mélanie, whose constant encouragement and aid in the dissertation editing process helped the final product come together. I'd also like to thank my parents, Larry and Linda, and my brother Joe, who convinced me that I could pursue a degree in physics and have always inspired me to literally reach for the stars! I would also like to acknowledge our cat Lara, whose insistence to get my attention always provided a good excuse to take a break.

TABLE OF CONTENTS

Page

PAPER

SECTION

LIST OF ILLUSTRATIONS

SECTION

LIST OF TABLES

SECTION

1. INTRODUCTION

The evolution of stars, from how they form in large clouds of gas and dust to how they end their lives as white dwarfs, neutron stars, or black holes, remains at best a partially understood process. In particular, the evolution of circumstellar disks around young stars, and the subsequent effects on planet formation, is still a field of intense study. In the 1970s, it first became suspected that young pre-main-sequence stars (i.e., before hydrogen fusion has ignited in the core) are surrounded by disks of gas and dust. These were identified by noting that the amount of flux at infrared wavelengths of visible stars was greater than that produced by the young stellar object (YSO) alone, as observed via their spectral energy distributions (SEDs). Since this discovery, thousands of disk-bearing objects have been found by infrared observations. In particular, their detections were greatly enhanced by the launch of the *Spitzer Space Telescope* in 2003, which provided near-infrared (NIR) to mid-infrared (MIR) photometry for this study.

As circumstellar disks age, it is theorized that planets form within the disks. This has been reinforced by a now growing number of detections of planetary-like clumps, using interferometry and polarimetric differential imaging, within circumstellar disks (e.g. Keppler *et al.* 2018, Pinte *et al.* 2018). Thus, planet formation is directly linked to how long a circumstellar disk survives around its host protostar. The survival of a disk can depend on several factors, the most relevant to this study being photoionizing radiation. Far-ultraviolet (FUV) to X-ray radiation from nearby O and early B type stars can have several consequences on disk-bearing YSOs. If disk-bearing YSOs are in close proximity to

OB-type stars, their outer disks can be ablated by the external radiation. At farther distances from OB stars, the effects may still be detected as external radiation can heat up the outer disk and cause it to expand (i.e., flare).

IC 1805 is a young open cluster located in the Perseus arm of the galaxy, at a distance of approximately 2350 pc (Massey *et al.*, 1995). It has been the subject of numerous studies over the years due to its youth and the presence of Cas OB6 (or OCL 352), the OB association located centrally in the nebula. However, many properties of the cluster itself are still debated, such as its age and its connection to young isolated areas of star formation near the edges of the region. In addition, the presence of the OB association makes this cluster of particular interest due to the effects that photoionizing flux and stellar winds from these O and B-type stars have on the surrounding nebula and on the disk-bearing YSOs in the cluster.

This study utilizes data from a multi-object spectrograph, as well as astrometric and photometric surveys such as Gaia and Pan-STARRS, to attempt to shed light on the star formation history of W4 and the evolutionary status of disk-bearing objects of IC 1805. This introduction will provide an overview of the star formation process (Section 1.1) which leads to the subsequent formation of circumstellar disks (Section 1.2), properties of an HII region (Section 1.3), and the effect of external radiation fields on disk-bearing stars (Section 1.4).

1.1. STAR FORMATION IN BRIEF

Interstellar space contains regions with higher densities of gas and dust called *molecular clouds*. In these cold clouds are the ingredients for potential star formation. Giant molecular clouds (GMCs) form throughout the spiral arms of the Milky Way. These are filamentary structures typically caused by turbulent motions (e.g., shock fronts) from supernovae or ionizing radiation from hot stars (Osterbrock, 1989), with temperatures around $\sim 15K$ and number densities $n \sim 10^8$ m^{-3} (Carroll and Ostlie, 2006). Within these

filaments exist small regions of even higher density called *cores*. External pressure from the cloud can trigger the gravitational collapse of matter along the lengths of these filaments, causing the formation of even smaller *dense cores*. Here the number density increases to around $n \sim 10^{10}$ m^{-3} and temperatures are typically ~ 10 K.

In order for a dense core to overcome thermal pressure and undergo gravitational collapse, its mass must meet the *Jeans criterion*. Based on the temperature T, mass density ρ_0, and average mass per particle $\bar{m}$, the minimum mass needed for a dense core to spontaneously collapse is

$$M_J \approx \left(\frac{5kT}{G\bar{m}}\right)^{3/2} \left(\frac{3}{4\pi\rho_0}\right)^{1/2}, \tag{1.1}$$

where k and G are the Boltzmann and gravitational constants, respectively. Using the given temperature and number density values for a dense core, this is roughly $M_J \sim 5.4 M_\odot$. However, this equation neglects influences from the external pressure of the surrounding cloud on the dense core. In this case, the minimum mass needed for gravitational collapse becomes

$$M_{BE} = 1.18 \left(\frac{kT}{\bar{m}}\right)^2 (P_0 G^3)^{-1/2}, \tag{1.2}$$

which is known as the *Bonnor-Ebert mass*, where P_0 is the external gas pressure. Again, using the values for a dense core, and assuming the pressure is ideal, $M_{BE} \sim 1 M_\odot$. Following the assumptions of the Jeans criterion, the *free-fall timescale* of the cloud can be approximated as

$$t_{ff} = \left(\frac{3\pi}{32 G\rho_0}\right)^{1/2}. \tag{1.3}$$

In words, this represents the timescale it would take a prestellar core to gravitationally collapse and become a protostar. For a dense core, $t_{ff} \sim 10^5$ yr.

During this gravitational collapse, matter accretes onto the dense core, the temperature rises, and it begins to radiate. This region of higher density will rotate around its center of mass as more matter accretes onto it. As the collapse proceeds, the conservation of angular momentum causes the surrounding mass of gas and dust to form a disk perpendicular

Table 1.1. YSO classes based on spectral indices.

Class	Spectral index	Physical Properties	Observational characteristics
0	-	$M_{env} > M_{star} > M_{disk}$	No optical or NIR emission
I	$\alpha_{IR} > 0.3$	$M_{star} > M_{env} \sim M_{disk}$	Optically obscured
FS	$-0.3 < \alpha_{IR} < 0.3$		Class I and II
II	$-1.6 < \alpha_{IR} < -0.3$	$M_{disk}/M_{star} \sim 1\%, M_{env} \sim 0$	Accretion; strong Hα and UV
III	$\alpha_{IR} < -1.6$	$M_{disk}/M_{star} \ll 1\%, M_{env} \sim 0$	Passive disk

Spectral index characteristics for YSOs. M_{env} refers to the mass of circumstellar material surrounding the protostar (envelope), M_{star} the mass of the YSO, and M_{disk} is the mass of the circumstellar disk. FS refers to a flat-spectrum source. Taken from Williams and Cieza (2011).

to the axis of rotation, which causes a small cavity to be carved out within the surrounding GMC. As matter continues to accrete onto the central protostar from the disk, jets/outflows of material occur along the poles of some protostars.

The next stages in the evolution of a protostar can be summarized using what is called the infrared *spectral index*. This method of detecting YSOs based on the infrared appearance of their SEDs was first proposed by Lada and Wilking (1984). They showed that YSOs in the Ophiuchus star-forming region could be separated into three groups based on whether the observed flux is (I) rising in the mid-IR, (II) declining but with an overall excess throughout the blackbody, or (III) has a negligible IR excess. Lada (1987) formalized this classification scheme by estimating the slope of the SED between 2-25μm:

$$\alpha_{IR} = \frac{d\log \nu F_\nu}{d\log \nu} = \frac{d\log \lambda F_\lambda}{d\log \lambda} \tag{1.4}$$

The classes have been modified and expanded since then, and their physical and observational properties are summarized in Table 1.1 following Williams and Cieza (2011).

A young star evolves through these classes sequentially in time. Class 0 objects are still in the free-fall phase, and the protostar and disk are still forming. Observationally, these objects are completely obscured by the surrounding envelope. Class I objects are nearing the end of the free-fall phase, where a disk has formed around the central protostar. These

objects can be seen in the infrared, since dust in the surrounding disk and envelope absorbs and re-radiates far-IR radiation. An intermediate class, called a flat-spectrum (FS) source, occurs as the accretion rate slows. This causes the infrared part of an FS source's SED to appear flat. Class II objects have disks that may still be accreting onto the protostar, but will soon cease accretion and develop an inner disk hole. Disks which are dissipating, and have inner disk holes are referred to as transition disks. Class III objects are pre-main-sequence stars with little to no disk material remaining. Those whose SEDs show small amounts of excess infrared flux are often referred to as debris disks.

The length of time from a Class II to main sequence object can be approximated by the *Kelvin-Helmholtz timescale*:

$$t_{KH} \approx \frac{GM_*^2}{R_* L_*}. \tag{1.5}$$

This represents the time it would take for the star to radiate its gravitational binding energy given its luminosity. For an A0V star, this would be approximately $t_{KH} \approx 2 \times 10^6$ yr, and for a K0V star this would be $t_{KH} \approx 6 \times 10^7$ yr. It is important to note that this method of classification does not provide completely unambiguous descriptions of YSOs. The orientation of a disk-bearing object has several consequences on the appearance of its SED. For example, a Class II object viewed at a high inclination can display characteristics similar to Class I object in its SED. This occurs because the light received from a nearly edge-on disk is highly extincted, which can be misinterpreted as a more embedded object. Moreover, Class II YSOs with high visual extinctions can be appear has Class I. So, the YSO classes based on SED slopes do not always accurately represent the evolutionary state of a YSO.

Before the Class II phase, there are no significant observational differences between high-mass and low-mass stars. Once the Class II phase begins, the central protostar begins radiating primarily at visible wavelengths. At this stage two types of stars are distinguished by mass, known as Classical T Tauri stars (CTTs) and Herbig AeBe stars (HAeBe). T Tauri stars are YSOs with masses ranging from 0.5-2 $M_\odot$ (which roughly spans the spectral types F-M, respectively). They are characterized by emission in $H\alpha$, $H\beta$, and Ca H & K as well as

occasional emission in the Ca II triplet lines. These spectral features are prominent in CTTs and faint in weak-line T Tauri stars (WTTs). WTTs, Class III objects, are also identified by X-ray emission likely caused by surface magnetic activity. Analogously, Herbig AeBe stars are YSOs with masses ranging from 2-10 $M_{\odot}$ (spanning A and B spectral types). HAeBe spectra have many characteristics in common with CTTs. X-ray emission is usually not seen in HAeBe objects, however, exceptions have been observed (see e.g., Testa *et al.* 2008). This could be a consequence of little to no surface magnetic activity in HAeBe stars.

The end of the Class III phase is brought on by the ignition of hydrogen fusion within the core of the pre-main-sequence star, thus becoming a main-sequence star. The main sequence is then where stars spend the majority of their lives in hydrostatic equilibrium. By the time a star reaches the main sequence its disk is likely dispersed, or only debris remains. For example, our solar system has two debris disks associated with the asteroid belt and Kuiper belt.

On a large scale, some theorize that star formation within a cloud begins with a global collapse of the cloud causing high star formation rates initially (Vázquez-Semadeni, 2015). Over time, this rate is slowed by ionization feedback and winds from the most massive stars formed, which disperses the clouds. Others theorize it is turbulent kinetic energy that stabilizes the overall cloud from collapse, while internally causing local compressions/shocks leading to individual star formation (McKee and Ostriker, 2007). It is likely a combination of the two mechanisms which stabilizes the overall cloud and causes the observed star formation rates.

Studies of star-forming regions find that only a small amount of the available mass of a GMC ends up forming stars. That is, the density throughout most of a GMC is too low to form dense cores. Recent models, such as Federrath (2015), suggest that several processes come into play as dense cores begin the process of gravitational collapse. To produce a more accurate star-formation rate, the gravitational collapse of dense cores are counteracted by a combination of the following processes: turbulence from the external

cloud, magnetic fields of the protostar and GMC, and jets/outflows from protostars. Shocks that are created by stellar winds and supernovae within expanding superbubbles are believed to be the primary mechanism for triggering star formation (Oey *et al.*, 2005).

1.2. CIRCUMSTELLAR DISK THEORY

This section will take a more detailed look at circumstellar disk properties during the Class I-III phases. Recall, once gravitational collapse of a dense core has occurred material from the surrounding cloud begins to accrete onto the growing central protostar. Initial rotation of the core is amplified as more mass accretes, resulting in a faster rotation rate of the core as well as the surrounding gas and dust. In addition, the conservation of angular momentum results in the formation of a disk by the infalling material. Disks typically form quickly, within $\sim 10^4$ years after initial core collapse (Hueso and Guillot, 2005).

The evolution of a disk during these stages is caused by a combination of several processes: the viscous accretion of material from the disk onto the central star, dust settling and coagulation, photoevaporative radiation, and the formation of planets. While the disk is forming, material from the inner disk accretes onto the central protostar via magnetic fields generated by the protostar, while the outer disk resupplies the inner disk material. Lynden-Bell and Pringle (1974) showed, via an energy balance equation, that mass is transported towards the inner disk while angular momentum is transported to the outer disk.

Photoevaporative radiation from the central protostar can be explained with the UV-switch model (Clarke *et al.*, 2001). Once the accretion rate onto the protostar drops below the photoevaporative rate, an inner disk hole forms because the outer disk cannot sufficiently resupply the material being lost. Since the inner disk edge is now exposed to extreme UV radiation from the central protostar, the disk will begin to dissipate rapidly from the inside out. Dust settling and planet formation will briefly be discussed in Section 1.4.

Most of the mass of a circumstellar disk is gas. Typically, about 1% of a disk's mass is composed of dust, which reflects the ratio of gas-to-dust of the interstellar medium (Williams and Cieza, 2011). Circumstellar disk masses are often determined by observations of dust emission in the millimeter wavelength regime. On scales larger than 10 AU, Williams and Cieza (2011) relate the total disk mass (i.e., gas and dust) to the observed flux for $\lambda > 1$mm,

$$M_{disk} = \frac{F_\nu d^2}{\kappa_\nu B_\nu(T)} \tag{1.6}$$

assuming the emission is optically thin, where κ_ν is the dust opacity, d is the distance to the source relative to Earth, and $B_\nu(T)$ is the Planck distribution. However, D'Alessio *et al.* (2001) noted that this method ignores dust growth, which in turn decreases dust mass opacity. Thus, disk masses estimated this way should be considered lower limits. Hartmann *et al.* (1998) found that disk masses could also be estimated from a combination of mass accretion rates and protostellar ages.

The distribution of gas and dust in disks has a profound effect on how disks can be observed. Different annuli and layers of the disk emit larger amounts of radiation at different wavelengths. In general, as one moves away from the central protostar the peak wavelength of dust emission grows longer. This dust emission includes both light scattered by the protostar and thermal continuum emission primarily from surface disk layers (in the infrared). Emission from dust grains and larger solids (up to ~1 cm in size) in the midplanes of disks are observed primarily at sub-millimeter and millimeter wavelengths (Andrews, 2020). Most knowledge about disk sizes and masses is due to observations at these wavelengths. Spectral line emission from molecular gas, such as CO, can be observed at millimeter wavelengths which allows for more precise estimates of the total mass of gas in a disk.

The innermost region of the disk, for radii $r < 1$ AU, is largely composed of gas. This is due to stellar winds and photoevaporative radiation from the central star clearing and subliming dust particles over time. Typically, the dust sublimation temperature is estimated to be 1500 K. However, sublimation temperature estimates have varied, from 1000-2000 K, for observed Herbig Ae/Be and T Tauri objects, based upon whether the model fitted to the object included both direct heating of the dust by the protostar and backwarming from the outer disk (Millan-Gabet *et al.*, 2007). The radius at which the temperature can sublime dust particles is referred to as the inner disk rim. Beyond the innermost region, a disk is composed of gas and dust where larger grains are found towards the midplane and smaller dust grains towards the disk surface.

Chiang and Goldreich (1997) (referred to as CG97, hereafter) developed a disk model for a passive (i.e., not accreting) disk in hydrostatic and radiative equilibrium. In this model, radiation from the disk is split into two layers: a superheated surface layer and an interior dust layer. Dust in the superheated surface layer absorbs and re-emits half of its radiation into space, and the other half into the disk. Radiation from this layer peaks in the near to far-IR. The radiation reprocessed by the interior can only be seen in far-IR to millimeter wavelengths in an SED. Since the interior disk layer is optically thick in the near IR, only radiation at long wavelengths can escape. Dullemond *et al.* (2001) found that a disk model which included a “puffed-up" inner disk rim could explain an SED feature often seen in disk-bearing stars called the NIR bump (around 2-3 μm). By including what is essentially a wall of dust at the sublimation radius in a disk model, they could reproduce a large increase in near IR flux evident in disk SEDs.

Observations and modeling of the SEDs of disk-bearing YSOs have shown two types of disk geometries: flat and flared. Kenyon and Hartmann (1987) (hereafter KH87) first proposed the flaring of protoplanetary disks based on evidence of far-infrared observations that could not be explained by a flat disk or accretion. The flaring is a result of vertical hydrostatic equilibrium considerations in the disk structure. The component of the star’s

gravitational force perpendicular to the disk midplane is balanced by the pressure gradient of the gas. So, the farther away from the central star one moves in the disk the weaker the gravitational force gets, which allows the pressure in the disk to expand material higher and higher above the midplane. KH87 found that a flared disk has a power law temperature distribution $T_d(r) \propto r^{-1/2}$ that can reproduce the SEDs seen in FS class YSOs. At the same time, Adams *et al.* (1987) affirmed that the SEDs of flat passive reprocessing or accretion disks could be fit with a temperature distribution $T_d(r) \propto r^{-3/4}$.

The SEDs of flared and flat passive disks can be approximated as blackbodies with radial dust temperature distributions. CG97 derived the dust temperature of a flared disk to be

$$T_d(r) = \left(\frac{\alpha}{2}\right)^{1/4} \left(\frac{R_*}{r}\right)^{1/2} T_*, \tag{1.7}$$

where α is the grazing angle at which stellar radiation strikes the disk, r is the distance from the center of the protostar, and R_* and T_* correspond to the stellar radius and effective temperature. The factor of $1/2$ accompanying the grazing angle approximates that half the absorbed stellar radiation is re-emitted into space by the dust grains, whereas the other half is re-emitted towards the interior of the disk. CG97 approximate the grazing angle as

$$\alpha \approx \frac{0.4R_*}{r} + r\frac{d}{dr}\left(\frac{H}{r}\right), \tag{1.8}$$

where H is the height above the disk midplane. The last term can be approximated as $0.03r^{2/7}$ where r is in units of AU (see the Disk Model Appendix for details).

For the flat disk, CG97 approximate the blackbody disk of Friedjung (1985) and Adams and Shu (1986). The original temperature distribution is given by

$$T_d(r) = \left(\frac{2}{3\pi}\right)^{1/4} \left(\frac{R_*}{r}\right)^{3/4} T_*. \tag{1.9}$$

CG97 approximate $\frac{2}{3\pi} \approx \frac{1}{5}$, which stems from an approximate form of the grazing angle, $\alpha \approx 0.4R_*/r$, when $r \gg R_*$. A detailed derivation of this model is given in the Disk Model Appendix. The SEDs for these models can then be computed as,

$$L_\lambda = 4\pi d^2 \lambda F_\lambda = 8\pi^2 \lambda \int_{r_i}^{r_o} r B_\lambda(T_d) dr$$

where d is the distance to the star and $B_\lambda(T) = \frac{2hc^2}{\lambda^5}\left(e^{hc/\lambda kT} - 1\right)^{-1}$. In terms of flux this equation is,

$$\lambda F_\lambda = \frac{2\pi\lambda}{d^2} \int_{r_i}^{r_o} r B_\lambda(T_d) dr. \tag{1.10}$$

Note, these models assume that the disk orientation is face-on.

The overall lifetime of a circumstellar disk depends on many factors, including the mass of the protostar and the environment in which the star forms (which will be discussed in Section 1.4). Haisch *et al.* (2001) studied disk fractions in intermediate age clusters, between 2.5-30 Myr, and found an overall disk lifetime of about 6 Myr. They found that the disk lifetime is even shorter for higher mass stars, around 2-3 Myr. Richert *et al.* (2018) compiled data from 69 young clusters with ages $\leq$ 5 Myr and found their estimated disk lifetimes heavily depended on the evolutionary model being used. The non-magnetic evolutionary models of Siess *et al.* (2000) and MIST (Dotter 2016 and Choi *et al.* 2016) resulted in mean disk lifetimes of 1.9-2.9 Myr, while the magnetic models of Feiden (2016) resulted in a mean lifetime of 5 Myr.

1.3. THE FORMATION OF HII REGIONS AND SUPERBUBBLES

The most massive protostars contract to the main sequence the fastest (O and B type stars). Due to their high rates of nuclear fusion, these stars produce intense stellar winds and photoionizing radiation that disperse the surrounding gas and molecular clouds. O and B stellar luminosities peak in the ultraviolet, producing plentiful radiation in wavelengths

shorter than Lyman limit (91nm) which ionizes the surrounding atomic hydrogen. The recombination of the ionized hydrogen nuclei with free electrons causes a cascade of radiation to be emitted in the visible spectrum, peaking around the Balmer Hα line. This process causes most HII regions to have reddish visual appearance.

An HII region can be defined as a region of space where the photoionization rate of atomic hydrogen gas is in equilibrium with the recombination rate of the ionized hydrogen nuclei. Assuming this equilibrium exists, one can approximate the size of an HII region caused by a central ionizing source. The result of this approximation is known as a *Strömgren sphere*, $R_{Strom} = \left(\frac{3Q_*}{4\pi\alpha(T)n_H^2}\right)^{1/3}$, where Q_* is the number of ionizing photons per second, $\alpha(T)$ is the recombination coefficient (a function of the temperature), and n_H the total number of hydrogen atoms. Strömgren spheres typically range from radii of about 23 pc for a B0 star to over 100 pc for an O5 star (Osterbrock, 1989).

Under the assumption given above, the Strömgren radius will now be derived. The recombination rate can be expressed as,

$$A_r = n_p n_e \langle \sigma v \rangle = n_p n_e \alpha(T) \tag{1.11}$$

where n_p and n_e are the number densities of free protons and electrons, and σ is a cross section averaged over velocities v (i.e $\langle \sigma v \rangle = \alpha(T)$). The recombination coefficient can be approximated as,

$$\alpha(T) = \int_0^\infty \sigma v f(v) dv \tag{1.12}$$

where $f(v)$ is given by the Maxwell-Boltzmann velocity distribution. It is important to note that the cross section σ must take into account *Coulomb focusing*. This correction considers how the electromagnetic interaction between a free electron and a proton (i.e., an ionized hydrogen nucleus) will affect the collisional cross section. If the gas is composed

primarily of neutral hydrogen then $n_p \sim n_e$. This tranforms the recombination rate into $A_r = n_e^2\alpha(T) = x^2 n_H^2\alpha(T)$, where $x = n_e/n_H$ and n_H accounts for both ionized and neutral hydrogen.

The recombination coefficient for hydrogen can take on several values depending on the electron transitions of interest. In the case where an ionized hydrogen nucleus combines with a free electron that indirectly reaches the ground state (emitting a series of spectral lines in the process), the recombination coefficient is typically, $\alpha_A(10^4K) = 4.2 \times 10^{-13}\text{cm}^3\text{s}^{-1}$ (Osterbrock, 1989). Recombinations that go directly to ground state result in the production of a photon with an energy greater than 13.6 eV. That is, the radiation emitted during the recombination is enough to ionize another neutral hydrogen atom. In an HII region, this type of transition does not impact the net recombination of the nebula. Excluding this type of transition results in a recombination coefficient more appropriate for an HII region, $\alpha_B(10^4K) = 2.6 \times 10^{-13}\text{cm}^3\text{s}^{-1}$.

Now suppose that inside the radius R_{Strom}, the gas is entirely ionized. At the center of this sphere is the source of the ionizing radiation which must be emitting photons with wavelengths shorter than the Lyman limit in order to ionize neutral hydrogen atoms. The rate at which these photons are emitted, Q_*, is,

$$Q_* = \int_{\nu=13.6\text{eV}/h}^{\infty} \frac{L_\nu}{h\nu} d\nu = \frac{8\pi^2 R_*^2}{c^2} \int_{\nu=13.6\text{eV}/h}^{\infty} \nu^2 (e^{h\nu/kT} - 1)^{-1} d\nu \tag{1.13}$$

where the star has been approximated as a blackbody, and L_ν is its luminosity and R_* its radius. If all of the ionizing photons are absorbed, then Q_* is balanced by the recombination rate integrated over the sphere. This means,

$$Q_* = A_r \frac{4}{3}\pi R_{Strom}^3 = x^2 n_H^2 \alpha(T) \frac{4}{3}\pi R_{Strom}^3 \tag{1.14}$$

which can be solved for R_{strom},

$$R_{Strom} = \left(\frac{3Q_*}{4\pi n_H^2 \alpha(T)} \right)^{1/3}, \tag{1.15}$$

where $x = 1$ implies a totally ionized region.

Simulations by Peters *et al.* (2010) have shown that once a protostar reaches a minimum mass of around $10M_\odot$, an HII region begins to form. Initially, the HII region around a protostar is relatively static due to the balance of gravitational and internal pressures of the cloud. Over time, the HII region will begin to fluctuate between static and expanding states. This alternation causes contractions of the HII region which leads to non-uniform expansions, and helps explain different morphologies seen in HII regions.

An OB association is a group of stars which contains roughly 10-100 O and B type main-sequence stars in a small volume of a GMC. OB type stars become Type II supernovae towards the end of their lives. Over tens of millions of years, repeated supernovae from an OB association will carve out a larger cavity within the HII region produced by the stellar winds. This type of cavity is often called a *superbubble*. A large, dense, and thin shell of interstellar material marks the boundary of a superbubble. *Bright rim clouds* are illuminated areas found at the boundaries of many superbubbles where stellar winds and shock fronts produced by supernovae collide with interstellar material (Mac Low and McCray, 1988). This collisional process can trigger star formation within these isolated regions if the pressure in the ionized boundary layers exceeds the internal pressure of clouds.

1.4. PHOTOEVAPORATION AND ITS EFFECTS ON PLANET FORMATION

Circumstellar disks provide the material necessary for planets, comets, and other extrasolar system objects to form. An understanding of the time evolution of circumstellar disks is essential for explaining the origin of planetary systems. Longer disk lifetimes allow for the formation of giant planets (Pollack *et al.*, 1996), which implies that studying the

evolution of disks in a variety of star-forming environments can provide information about the diversity of planets likely to form around YSOs. Observations of YSOs have shown that, in general, about 10 Myr after the formation of a protostar, the surrounding disks are entirely dispersed (Williams and Cieza, 2011). Thus, the formation of a planetary system must occur approximately within this time span.

The formation of planets is believed to be a consequence of dust settling and coagulation within a disk. Since dust grains are initially inherited from the interstellar medium, their initial sizes will be consistent with such grains (submicron sized). Over time, grains in the disk collide and form aggregates due to processes such as turbulence and Brownian motion. This causes their motions to decouple from the mostly Keplerian motions of gas which results in a strong drag force that settles the grains toward the disk midplane. The increased density of the midplane accelerates the coagulation process and leads to the formation of planetesimals. Planetesimals can then coalesce into rocky cores for planets (Dullemond and Dominik, 2005). If the core is massive enough and the environment cool, the continued accretion of gas will result in the formation of a gaseous giant planet (Lissauer, 1993). Alternatively, Boss (2019) has proposed that gravitational instabilities that occur in the inner gas disk can lead to the formation of giant planets on a much shorter timescale.

It is thought that all disks have an inner disk hole phase (Alexander *et al.*, 2006). The primary mechanisms for forming an inner disk hole are theorized to be photoevaporation from the central star and/or the formation of planets. Alexander et al. found that once accretion stops, the disks of T Tauri stars will completely disperse in about 10^5 yrs. Comparison with observations revealed that photoevaporization alone could not account for inner disk holes in several T Tauri sources with high accretion rates. For these, it is suspected that planet formation and/or grain growth are likely the cause (i.e. gas is still accreting onto the star while dust is coagulating into larger and larger bodies in the disk interior). Alonso-Albi *et al.* (2009) concluded a similar timescale for the dissiptation of

disks around Herbig Be stars. In this case, they theorize that intense UV radiation from the Be protostar disperses the outer disk which then leads to the quick dissipation of the inner disk.

An additional factor that can contribute to a shorter disk lifetime is the photoevaporation of the disk by far ultraviolet radiation (FUV) from a nearby OB star. Since stars often form in clusters, with the majority being low mass stars, the hottest OB stars among the cluster members can actively ablate, and in some cases destroy, the circumstellar disks of nearby stars (Anderson *et al.*, 2013). FUV radiation can strip material away from the outer disk regions, and in turn deplete the inner disk, hindering the planet formation process. Anderson et al. found that the dissipation of a disk with external FUV can depend on the viscosity of the disk. A dimensionless FUV flux parameter,

$$G_0 = \frac{1}{F_0}\frac{L_{FUV}}{4\pi d^2} \tag{1.16}$$

is often used, where F_0 is the typical interstellar FUV flux value of $1.6 \times 10^{-3} erg/s$, L_{FUV} the FUV luminosity in the star cluster, and d the true distance to a source. High values of $G_0 \sim 30,000$ correspond to stars in very close ($\sim$ 0.1pc) proximity to an OB star. At this distance, the FUV can directly threaten the planet formation process unless disk viscosity is very low. On the other hand, for low values of $G_0 \sim 300$, planet formation is likely not affected (e.g., separations $\gtrsim$ 1 pc).

Anderson *et al.* (2013), however, only considered photoevaporative effects on systems with $M_* = 1M_\odot$. Higher mass YSOs could resist photoevaporation due to their disks being in higher gravitational potentials. Also, initial conditions of the protostar were not taken into account. Xiao and Chang (2018) considered how properties of the pre-stellar core can later influence the severity of photoevaporative effects. If the pre-stellar core has a low angular velocity ($\omega \sim 0.3 \times 10^{-14} s^{-1}$), most of its material collapses either onto the protostar or onto the inner regions of the forming disk. This results in a deep gravitational potential

well which can suppress photoevaporation. The deep gravitational potential also causes the disk to be smaller in size and mass which means it will have a shorter lifetime. A core with a moderate angular velocity ($\omega \sim 1 \times 10^{-14} s^{-1}$) will have more material collapse onto the disk, resulting in a disk which is large in size and mass that leads to a longer disk lifetime. Although external photoevaporation is enhanced compared to the previous case, it cannot significantly deplete the disk during these early stages of evolution. A core with a high angular velocity ($\omega \sim 5 \times 10^{-14} s^{-1}$) will have a significant amount of its material collapse onto the outer disk regions, again resulting in an even smaller final mass for the protostar. In this case, the gravitational potential well of the disk is low enough that photoevaporation will ablate much of the disk.

Direct evidence for the external photoevaporation of disk-bearing YSOs is seen in the Orion Nebula Cluster (ONC). Studies such as Bally *et al.* (2000), have directly observed proplyds (protoplanetary disks) that are silhouetted against nebular emission from the ONC. Cometary-like tails of these proplyds point directly away from the nearby Trapezium OB stars, and show that these YSOs are being actively ablated by photoevaporative radiation. To directly detect ablation, photometry from far-IR to millimeter wavelengths is needed. Indirect methods involve examination of the fraction of disk-bearing sources in a cluster as compared to their separation from ionizing sources, or the amount of FUV flux incident upon the disks. These indirect methods can then be backed up by examination of the inner disk region. As previously described, a depletion of material in the outer disk leads to the dissipation of the inner disk. So, sources subject to ablation should either have, or be in the process of, developing an inner disk hole. In addition, they should exhibit an excess in flux in the outer regions of the disk.

As an example of an indirect method, Richert *et al.* (2015) tested several star forming regions for disk destruction by creating empirical cumulative distribution functions that test the frequency of disk-bearing and disk-less sources within 0.5 pc of O stars. A smaller frequency of disk-bearing stars near O-stars compared to nearby diskless stars would suggest

that disks are being actively destroyed. This analysis was based upon disk candidates in each region from the Massive Young Star-Forming Complex Study in Infrared and X-ray (MYStIX) catalog (Povich *et al.*, 2013).

2. LITERATURE REVIEW

W4 is an HII region in the W3/W4/W5 molecular cloud complex (see Figure 2.1[1]). It encompasses the young open cluster IC 1805 which contains a group of high mass O and B-type stars called OCL 352. The region is nicknamed the Heart Nebula due to its visual appearance. NGC 896, in the neighboring W3 region, was first discovered by William

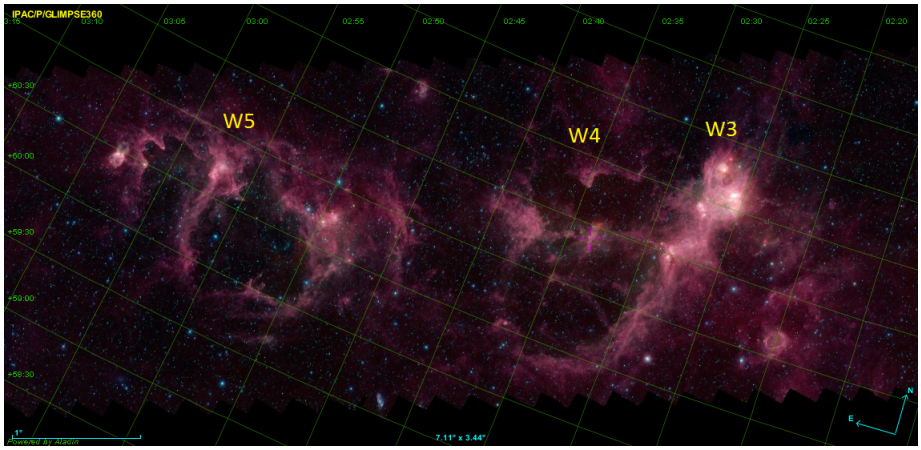

Figure 2.1. Infrared view of dust emission from the W3/W4/W5 molecular cloud complexes. From the GLIMPSE 360 survey, generated by *Aladin sky atlas*. IRAC bands 1,2, and 4 are shown in blue, green, and red (respectively).

Herschel in 1787, and was described as an “extremely faint, pretty large, irregular figure." IC 1805 was later observed in 1888 by Edward Barnard, and described as a “cluster, coarse, extremely large, nebula extends following" (Dreyer, 1895). The HII regions are named after Gart Westerhout who found W3/W4/W5 in a radio survey of the galaxy at 1390 MHz (Westerhout, 1958). The three HII regions correspond to the third, fourth, and fifth discrete sources in his catalog.

[1]This research has made use of *Aladin sky atlas* developed at CDS, Strasbourg Observatory, France

Table 2.1. Previous estimates of IC 1805 properties.

	Massey	Straižys	Panwar	Sung
Distance (kpc)	2.35	2.0	-	2.4±0.2
R_V	3.1	3.2	-	3.05±0.06
Age (Myr)	1-3	-	2.5 ±1.5	3.5
Mass function	-	-	-1.23±0.23	-1.3±0.2

Summary of results from IC 1805 studies over the past several years by Massey *et al.* (1995), Straižys *et al.* (2013), Panwar *et al.* (2017), and Sung *et al.* (2017).

IC 1805 has been the subject of numerous studies due to its young age and the presence of OCL 352. A large number of OB stars have profound effects on the surrounding star forming environment, and represent a unique opportunity to study hierarchical triggered star formation. Table 2.1 summarizes properties of IC 1805 from several studies since 1995. The following sections will expand on each property and construct a picture of our current understanding of the W4 HII region and the young IC 1805 cluster.

2.1. THE EVOLUTIONARY HISTORY AND SPATIAL PROPERTIES OF W4

The structure of the W4 HII region and superbubble have been gradually revealed over time as progressive observations have allowed for greater detail. Figure 2.2 shows the locations of the W3/W4/W5 HII regions, the larger W4 superbubble, the IC 1805 cluster, and the supernova remnant HB3. Normandeau *et al.* (1996) first noticed a $\sim$ 110 pc cavity above the W4 HII region through HI observations. This corresponds to the bright arc in the center of Figure 2.2 where the purple cross-hair lies. They suspected this cavity was formed by the stellar winds of OCL 352, whose location coincides with IC 1805. Dennison *et al.* (1997) observed an even larger cavity through a wide-field Hα image that extends about 230 pc above OCL 352. This corresponds to the northern top of the contours in Figure 2.2.

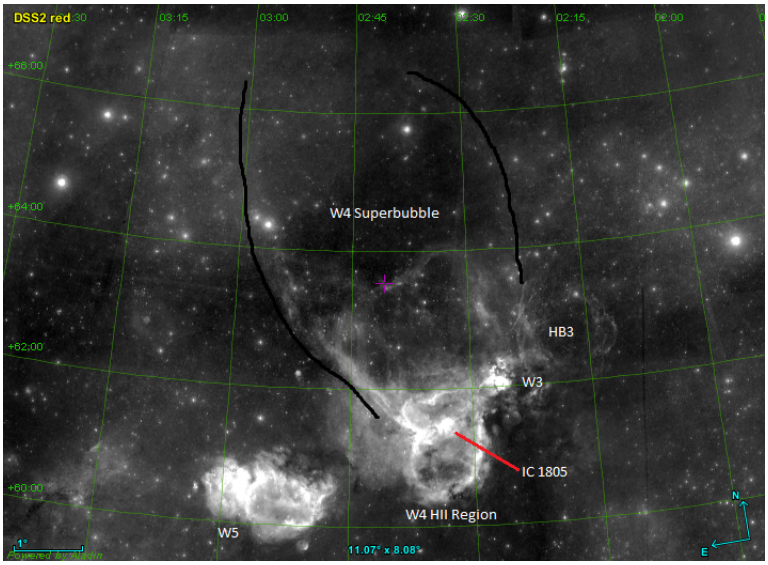

Figure 2.2. DSS2 F+R image (0.658 μm and 0.640 μm, respectively) which highlights Hα emission from ionized hydrogen of the W3/W4/W5 cloud complexes. The locations of the W4 HII region, IC 1805 cluster, W4 superbubble, W3 and W5 HII regions, and supernova remnant HB3 are labeled. Solid black curves roughly trace out the contours of the superbubble. This image was generated in Aladin.

However, based on the age of OCL 352 ($\lesssim$ 2.5 Myr), Dennison et al. suggested that this larger cavity was created by a previous generation of stars after estimating the dynamical age of the shell to be 6.4 – 9.6 Myr.

The idea of a generation of stars older than IC 1805/OCL 352 which produced the large $\sim$ 230 pc cavity continued to be explored. Dynamical simulations performed by Basu *et al.* (1999) found, to the contrary, that the 230 pc cavity could have been produced by OCL 352 in 2.5 Myr. Oey *et al.* (2005) later noted that Basu et al. estimated such a young age for the shell due the small galactic scale height they estimated for the ambient gas. Instead, Oey *et al.* (2005) suggested that the W3/W4 complexes are composed of three generations of stars whose formation was triggered by the expanding superbubble produced by the first generation of stars based on the Hα images of Reynolds *et al.* (2001). They suggested

that IC 1805 is located on the edge of the W4 superbubble along our line of sight, and represents the second generation of star formation (where isolated areas of star formation in W3 represent the third generation).

Carpenter *et al.* (2000) explored the connection between W3 and W4 by observing embedded clusters along the border of these two regions. They found that four of five then known embedded clusters in W3 are located along the border with W4, instead of being located in the interior regions of W3 where much of the molecular mass is concentrated. This result implied that star formation in these embedded clusters was triggered by the expansion of the W4 HII region. Radio observations by West *et al.* (2007) found two breaks in the ionized shell of the W4 superbubble, suggesting that it is in the process of fragmenting and forming a galactic chimney. One break is roughly 20 pc wide near the top of the superbubble (above a declination of 66° in Figure 2.2), and the other break is roughly 48 pc wide along the western edge of the shell, above HB3. They argued that OCL 352 is the dominant source of ionizing radiation for the superbubble, but that it is not solely responsible for the creation of the superbubble. Furthermore, they noted that Normandeau *et al.* (1996) and Dennison *et al.* (1997) did not account for the effects of magnetic fields when they derived their ages for the superbubble based on the expansion time of the bubble. Ferriere *et al.* (1991) found that interstellar magnetic fields would restrict the volume of a superbubble during its expansion by a factor of roughly 1/3 (i.e., relative to the volume of a superbubble not influenced by magnetic fields). So, this implies that the age of W4 superbubble may be older than previous estimates.

Most distance estimates for the IC 1805 cluster have been in the range 2.0-2.4 kpc. Massey *et al.* (1995) estimated a distance of 2.35 kpc to IC 1805 from the spectroscopic parallax of 38 high-mass cluster members. A shorter distance of 2.0 kpc was estimated by Straižys *et al.* (2013) from a color-magnitude diagram (CMD) in the Vilnius photometric system and a two-dimensional classification of OB stars in the central IC 1805 cluster. They noted that this corresponds well to a measurement of masers in the nearby W3 star-forming

by the Very Long Baseline Array (VLBA) (see Xu *et al.* 2006 and Hachisuka *et al.* 2006). However, Sung *et al.* (2017) (hereafter S17) considered VLBI astrometry of other SFRs, as well as the possible width of the Perseus spiral arm, and found no physical grounds for assuming that W3/W4 are at the same distance. S17 derived a distance of 2400 ± 200 pc using a modified zero-age main-sequence fitting technique that was verified using distances from the Gaia DR1 database. They selected members of 34 nearby open clusters and used their proper motion and parallactic measurements to test their ZAMS fitting. They found the parallactic distances to be consistent with the ZAMS-fitting distance within about ±0.2 milliarcseconds (where a distance d in parsecs is related the parallax angle p in arcseconds by $d = 1/p$).

Lim *et al.* (2020) used probable cluster members from S17 for their study on the kinematics of the stellar population in the W4 HII region. Using data from the Gaia DR2 data release (Gaia Collaboration *et al.* 2016; Gaia Collaboration *et al.* 2018), they estimated a distance of 2.1 ± 0.2 kpc to the IC 1805 cluster. Through the comparison of observed kinematics and the results of dynamical simulations of a model cluster, they found that cluster members near the core of IC 1805 were nearly in equilibrium while the population distributed over ~20 pc showed signs of radial expansion. Overall, this result demonstrated that the evolution of the IC 1805 cluster is likely responsible for much of the stellar population distributed across the W4 HII region.

Panwar *et al.* (2017) used AllWISE 12 μm data and Herschel 250 μm data to attempt to piece together the star formation history of IC 1805. AllWISE 12 μm data traces emission from polycyclic aromatic hydrocarbons (PAH) which surrounds HII regions as well as regions excited by B-type YSOs. Herschel 250 μm data traces dust emission throughout the region. PAH emission traced a filamentary distribution of emission elongated in the east-west direction, and coincides with several bright-rimmed clouds (BRCs). The distribution of 250 μm emission appears to be elongated in the north-south direction and bounded in the east-west direction. They suggested that IC 1805 began as a filamentary

cloud, with star formation first taking place along the high density east-west axis. Over time, the O stars of OCL 352 produced the HII region which expanded into the north-south low density regions.

Additional tracers of the expansion of the W4 HII region are isolated areas of star formation at its edges. Sugitani *et al.* (1991) found several BRCs in the W4 HII region, cataloged as BRCs 5 through 9. BRCs 5, 8, and 9 lie along the east-west photon-dominated region, corresponding to the elongated PAH region identified by Panwar *et al.* (2017), that intersects the center of IC 1805. BRCs 6 and 7 lie south and north of IC 1805, respectively. Morgan *et al.* (2009) investigated whether BRCs identified by Sugitani *et al.* (1991) are candidate regions for triggered star formation by analyzing the structure and kinematics of CO (J=2-1) molecular gas. They concluded that BRCs 5, 6, and 7 fit the candidate criteria. Consistent with this picture, Fukuda *et al.* (2013) found that the small cluster of YSOs around BRC 5 were nearly all < 1 Myr old. Later, Panwar *et al.* (2014) studied YSOs near both BRCs 5 and 7, where they found average ages of the isolated populations to be 2.2 Myr and 1.3 Myr, respectively.

2.2. THE REDDENING LAW TOWARDS IC 1805 AND PROPERTIES OF CLUSTER MEMBERSHIP

Studies of the reddening law towards IC 1805 have fallen into two groups in regards to the total-to-selective extinction ratio R_V: it is normal (3.1) or higher than normal. Guetter and Vrba (1989) and S17 found that R_V is normal and uniform across the cluster, and the dust size distribution of both the foreground medium and intracluster medium are approximately the same. This conclusion is backed up by many other studies (Sung and Lee 1995; Hillwig *et al.* 2006; Straižys *et al.* 2013). On the higher side, studies such as Ishida (1969), Kwon and Lee (1983), and Pandey *et al.* (2003) found R_V values of 3.82 ± 0.5, 3.44, and 3.56 ± 0.29, respectively.

Cluster members in the study by Wolff *et al.* (2011) were chosen based on the following criteria: (1) a reddening factor consistent with that chosen by Massey *et al.* (1995) for massive cluster members, (2) the presence of the interstellar feature λ4430, and (3) a source's position in a Hertzsprung-Russell (H-R) diagram. The reddening factor used by Massey *et al.* (1995) for stars with spectral types O4-B2.5V for cluster membership ranged from $0.68 < E(B-V) < 1.29$, where the reddening, $E(B-V) = (B-V)_{obs} - (B-V)_{int}$, is a measure of the difference in magnitude between observed $B-V$ wavelengths and theoretical intrinsic values. Wolff et al. expanded upon this reddening range based on stars containing the interstellar absorption feature λ4430, changing it to $0.5 < E(B-V) < 1.30$.

2.3. THE AGE AND INITIAL MASS FUNCTION OF IC 1805

The age of IC 1805 has differed in estimates over the years primarily due to the star formation history of the surrounding HII region. Guetter and Vrba (1989) found a scatter of early B stars in their reddening-corrected CMD which they interpreted as an older population of stars in IC 1805. More recent studies, such as those summarized in Table 2, have consistently estimated ages within 1-3.5 Myr. Massey *et al.* (1995) estimated an age of 1-3 Myr for IC 1805 members with masses greater than 25 $M_{\odot}$ using the evolutionary models of Schaller *et al.* (1992). S17 found that the massive main-sequence stars were well matched to an isochrone of 3.5 Myr using the stellar evolution models of Ekström *et al.* (2012), while the PMS stars had a median age of 2.4 Myr, using Siess *et al.* (2000) models, or 1.6 Myr using the models of Baraffe *et al.* (2015). S17 did find two evolved early-type stars in their sample that were left out of the previous main-sequence fitting. When included, a best-fit isochrone of 7.3 Myr was matched with the data, and fits within the age range of the superbubble. These two stars were suspected to belong to an older generation of stars. However, S17 were unable to find any other evolved counterpart stars in their field of view.

Panwar *et al.* (2017) found a mean age of 2.5 ± 1.5 Myr for the YSOs of their sample using the evolutionary models of Siess *et al.* (2000). They also investigated differences in age between their CTTs and WTTs sources. They found that the CTTs had a mean age of ∼ 2.3 Myr while the WTTs sources had a mean age of ∼ 2.6 Myr. This supports the idea that CTTs evolve into WTTs (an idea which has been debated; see e.g., Gras-Velázquez and Ray 2005). However, they do note that spectroscopic information is needed to reduce uncertainties in cluster membership for these sources.

Initial mass function (IMF) estimates of IC 1805 have primarily been computed using intermediate to high mass stars. The IMF slope is defined as $\Gamma = \frac{d\mathrm{Log}N}{d\mathrm{Log}M}$, where N is the number of stars with mass M (Salpeter, 1955). Three studies in 1995 derived three different estimates of the IMF: Sung & Lee derived a slope of $\Gamma = -1.0 \pm 0.2$ for $3 < M/M_{\odot} < 85$, Massey et al. derived a slope of $\Gamma = -1.3 \pm 0.2$ for $3 < M/M_{\odot} < 85$, and Ninkov *et al.* (1995) derived a slope of $\Gamma = -1.38 \pm 0.19$ for $2.5 < M/M_{\odot} < 30$. Given their uncertainties, all three estimates overlap with a typical Salpeter-type slope, that is $\Gamma \approx -1.35$. Recent studies such as S17 and Panwar *et al.* (2017) have attempted to examine the IMF of lower-mass members of IC 1805 using deep optical photometric data. S17 estimated an IMF slope of $\Gamma = -1.3 \pm 0.2$ using sources with > 1.8 $M_{\odot}$. Panwar et al. reported their survey was complete down to 0.3 $M_{\odot}$, and estimated a slope of $\Gamma = 1.23 \pm 0.14$ for sources between $0.3 < M/M_{\odot} < 2.5$.

2.4. OBSERVATIONS OF DISK-BEARING YSOS IN IC 1805

Most information regarding the disk-bearing YSOs of IC 1805 has been inferred from photometric surveys of the region that combined optical data with near and mid-infrared data. Panwar *et al.* (2017) found a total of 577 YSOs in the direction of IC 1805. Of these, 384 are probable cluster members. By spectral index, 101 sources are Class I/II objects while 283 sources are Class III objects. This number of YSOs is in agreement with that of Broos *et al.* (2013), as part of their MYStIX Probable Complex Members (MPCM)

catalog, which estimated 389 YSOs in the same field of view. This implies a disk fraction of 26% for Panwar et al., where 74% of the detected YSOs are in a more advanced stage of evolution.

S17 classified YSOs based on their infrared slopes according to the following criteria: Class I ($\alpha \geq 0.3$), Flat spectrum ($-0.3 \leq \alpha < 0.3$), Class II ($-1.8 \leq \alpha < -0.3$), Class III ($-2.55 \leq \alpha < -1.8$), and Class IV ($\alpha < -2.55$). Out of a total 11910 sources, from Class I to IV, they had 76, 85, 542, 1433, and 9681 sources. Excluding the Class IV sources, this means they found that about 33% of YSOs have young disks and 67% are in a more evolved state. S17 also identified pre-transition and transition disks by comparing the SED slope from the IRAC bands to the slope obtained between IRAC 4 and MIPS 1. Here they found 11 pre-transition disks and 37 transition disks.

Wolff *et al.* (2011) is the most recent survey of IC 1805 to combine spectroscopic observations with optical and infrared photometric data. In their survey, they found 548 cluster members of IC 1805, of which 63 had IR excesses. They split the IR excesses into 5 groups with the following properties:

- Optically thick disks (Herbig AeBe) stars that likely have accretion disks (7 sources).
- Optically thin disks (thin throughout infrared and at 24 μm, if detected) that they interpreted as either gas emission or dust emission from larger grains (5 sources).
- Thin/thick disks (thin in the near-infrared and thick at 24 μm) interpreted as possible extrasolar giant planet formation (2 sources).
- Empty/thin (no near-infrared excess and optically thin emission in mid-infrared bands) interpreted as second generation dust emission from planet formation (45 sources).
- Empty/thick (no near-infrared excess and optically thick emission at 24 μm) interpreted as photoevaporation or companion formation (4 sources).

So, approximately 11% of their IR excess sources have accretion disks (Class I/II YSOs) while the remaining 89% of sources have more evolved disks. Currie *et al.* (2009) suggested that optically thin disks represent a stage during which disks are transitioning from accretion to debris disks. They posit that the formation of planetesimals throughout all radii of the disk depletes it of small dust grains. It is also worth noting that Currie et al. found that optically thin disks outnumbered optically thick disks in their study of NGC 2362, which has been estimated to be 5 Myr old. In regards to the empty/thin sources, Wolff *et al.* (2011) noted that the nebular emission at 8 μm in IC 1805 often exceeds the theoretical 8 μm emission predicted in disk models with inner disk holes and optically thin outer disks, suggesting contamination from nebular PAH emission.

PAPER

I. A SPECTROSCOPIC AND PHOTOMETRIC SURVEY OF THE W4 HII REGION

Matt Wentzel-Long
Department of Physics & Astronomy
University of Missouri St. Louis
St. Louis, Missouri 63121
Email: mwhv2@umsl.edu

Bruce A. Wilking
Department of Physics & Astronomy
University of Missouri St. Louis
St. Louis, Missouri 63121

Jinyoung Serena Kim
Steward Observatory
University of Arizona
Tucson, Arizona 85721

Justin Bryan
Department of Physics & Astronomy
University of Missouri St. Louis
St. Louis, Missouri 63121

ABSTRACT

A growing amount of evidence suggests that the W4 HII region is composed of two generations of star formation. In order to investigate the ages and masses of different generations of young stars in W4, it is imperative that reliable estimates of extinction and effective temperature are determined for each source. We present optical spectroscopy for over 3000 stars in the direction of W4. Spectral types combined with published X-ray, proper motion, and near to mid-infrared photometric surveys are used to identify candidate cluster members for which extinction, age, and mass are estimated. The visual extinction towards W4 is found to have a mean value of $A_V = 2.2 \pm 0.3$ mag, while a subsample of 219 probable cluster members ranging in spectral type from B1 to M0 has a mean extinction of $A_V = 2.7 \pm 0.5$ mag. A median age of 2.2 Myr is found for probable cluster members, and a group of 15 sources with median age 8.5 ± 2.5 Myr are considered candidate young stars from an earlier generation of star formation.

Keywords: stellar evolution, IC 1805, young stellar object, HII region

1. INTRODUCTION

Star formation is often triggered along the edges of a superbubble where shock fronts collide with interstellar material, which can lead to gravitational collapse (e.g., Elmegreen 1998 and references therein). It has been proposed that the expansion of the W4 superbubble has triggered star formation in several of the surrounding regions including IC 1795, AFGL 333, and W3 (e.g., Carpenter *et al.* 2000; Oey *et al.* 2005; Kiminki *et al.* 2015). The locations and ages of several bright-rimmed clouds and compact star-forming regions in the high density layer adjacent to W3 show evidence for this picture. In general, progressively younger YSOs are seen as one moves west from the IC 1805 cluster. IC 1795 is estimated to be between 3-5 Myr old while several ultracompact star-forming regions are estimated to

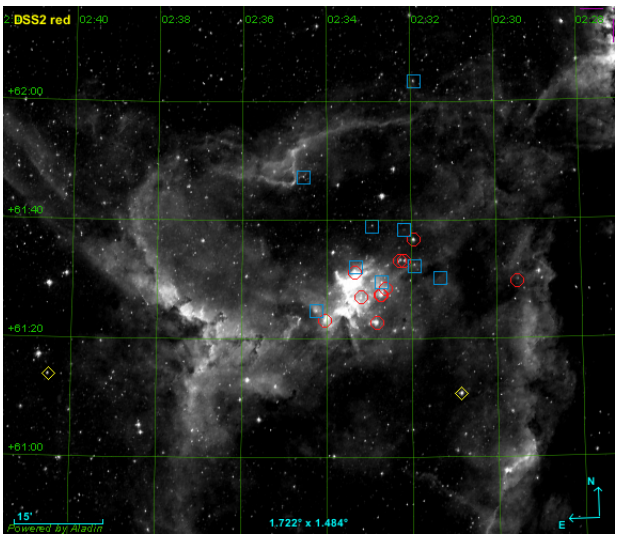

Figure 1. Locations of the 13 O4-B0.5 stars in IC 1805 (red circles) identified by Massey *et al.* (1995) two of which are in binary systems. Blue squares represent locations of nine additional O9.5-B0.5 stars from Roman-Lopes *et al.* (2019). The blue supergiant BD+60 493 (in the west) and X-ray binary LS I +61° 303 (in the east) are shown as yellow diamonds. Coordinates are overlaid on a DSS2 $F + R$ image (0.658 μm and 0.640 μm, respectively).

be between $10^4 - 10^5$ yr old (Oey *et al.*, 2005). However, the morphology of young clusters in IC 1795 and AFGL 333 have called this picture into question (Roccatagliata *et al.* 2011; Jose *et al.* 2016)

In this paper, IC 1805 will be used to refer to the young cluster which surrounds the group of OB-type stars called OCL 352. Figure 1 shows the locations of O-B0.5 stars identified by Massey *et al.* (1995) and Roman-Lopes *et al.* (2019) as well as the B0Iae star BD+60 493 and the X-ray binary LS I +61° 303. W4 is used to refer to the surrounding HII region outside the IC 1805 cluster. The W4 superbubble/chimney refers to the large cavity which extends above the W4 HII region. Distinguishing between these regions is detailed further in a brief recap of the region's observational history.

The evolutionary connection between the young open cluster IC 1805, located centrally in the W4 HII region, and the larger W4 superbubble/chimney is a debated topic. HI observations by Normandeau *et al.* (1996) revealed a cavity which stretched about 110

pc north of IC 1805, which was theorized to be a blow out produced by OCL 352. The time required for the O stars to produce this cavity was estimated to be 5.7 Myr. However, the youngest main-sequence O-star among OCL 352, BD+60 507 (O5V), places an age of less than 4.3 Myr on OCL 352. Dennison *et al.* (1997) observed a closed shell in Hα images located 230 pc north of OCL 352. They estimated that OCL 352 could create this clearing in 6.4-9.6 Myr. Due to the age discrepancy with OCL 352, Dennison et al. suggested that a previous generation of stars could have produced the region of lower ambient density. In contrast to this result, dynamical simulations by Basu *et al.* (1999) estimated that OCL 352 could have produced the observed 230 pc shell in 2.5 Myr.

Possible evidence of a supernova contribution to the W4 superbubble was suggested by Mirabel *et al.* (2004) from the presence of the X-ray binary LS I +61° 303 (a neutron star or black hole and B0Ve star). Its proper motion relative to IC 1805 suggests it could have escaped from the cluster due to an asymmetric explosion 1.7±0.7 Myr ago. Radial velocity measurements of 41.41 km/s by Aragona *et al.* (2009) combined with a Bailer-Jones *et al.* (2018) distance of 2445 pc suggests its original distance was roughly 2370 pc. Mirabel et al. note that if LS I +61° 303 were a member of IC 1805, then the progenitor mass must have been $\geq$60 $M_{\odot}$. However, mass estimates of the primary B0Ve star, the compact object, and mass loss during the supernova have been well below this threshold. So, a clear connection between LS I +61° 303 and IC 1805 is not yet established.

Evidence which suggests the existence of a previous episode of star formation in W4 was first highlighted by Oey *et al.* (2005). Oey et al. suggested that Hα images of Reynolds *et al.* (2001), which revealed a 1300 pc diameter shell of ionized hydrogen, was formed by an older generation of stars some 10-20 Myr ago. Additional evidence was provided by West *et al.* (2007), who found from radio observations that the superbubble may be in the process of fragmenting and forming a galactic chimney. Their observations showed an elongated superbubble, 164 pc wide and 246 pc above the galactic midplane at an assumed distance of 2.35 kpc.

This study utilizes optical spectroscopy to first assign spectral types to a large sample of stars in the direction of W4 and identify signatures of youth. Spectral types then allow for more accurate estimates of extinctions for each source using the *r* and *i* passbands from the PanSTARRS PS1 survey. The increased accuracy in extinction estimates allows for previous IC 1805 membership criteria to be updated and made more rigorous. Lastly, luminosities are estimated and used to create Hertzsprung-Russell (H-R) diagrams from which mass and age estimates are interpolated. The subsample of probable cluster members which results from this reduction procedure should represent a more accurate view of the stellar population in the HII region.

This paper is organized as follows: Section 2 outlines observations using the 90Prime wide-field imager and Hectospec spectrograph, and additional photometric data. Section 3 presents results of the data analysis including distance assumptions, the spectral classification of the sample, cluster membership criteria, extinction estimates, and H-R diagrams. Section 4 discusses the reliability of the extinction estimates, undersampling of intermediate-mass stars, and the age of the IC 1805 cluster as well as several stars which may belong to a previous generation of star formation in the complex. The possible triggering of star formation in clouds adjacent to the cluster is discussed.

2. OBSERVATIONS USING THE 90PRIME WIDE-FIELD IMAGER AND HECTOSPEC SPECTROGRAPH AT MMT

2.1. 90PRIME SURVEY AND SOURCE SELECTION

W4 was observed with the 90Prime wide-field imager (Williams *et al.*, 2004) at the Steward Observatory 2.3 m Bok Telescope in January 2006. The 90Prime imager consists of four 4k $\times$ 4k CCDs, each with a field of view of 30'$\times$30' and a pixel scale of 0.45"pix^{-1}.

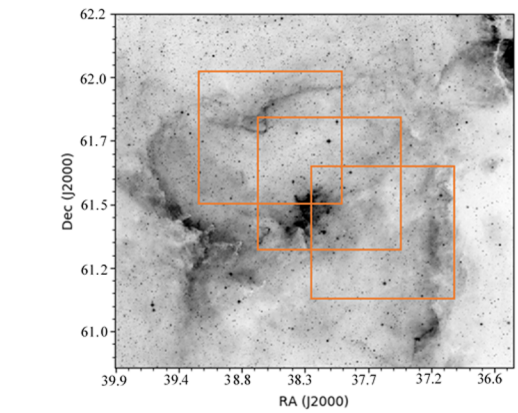

Figure 2. Overlay of 90Prime imaging areas on DSS2-R image.

These observations had a total coverage of 60'×60'. The observing and reduction procedure details are identical to those discussed in Kiminki *et al.* (2015), but will be briefly outlined below. Figure 2 shows the survey areas overlaid on a DSS2-R mosaic.

Data reduction of the measured photometry was performed using the Interactive Data Language (IDL) pipelines *Bokproc*, *Bokphot*, and *aperture_correct* written by William H. Sherry as described in Kiminki *et al.* (2015). This procedure removed the most saturated stars while less saturated stars and other problematic stars had to be identified manually. As shown in Figure 3, the spectroscopic sample was selected from a V vs $V - I$ color-magnitude diagram of 25,128 sources from the January 2006 observations as well as Hα emission sources from CFHT imaging data which are now published in Sung *et al.* (2017). The chosen sample is a subset, ~6000 stars, of stars above the 5-Myr isochrone which were designated as YSO candidates based on their positions relative to Siess *et al.* (2000) solar-metallicity pre-main-sequence (PMS) isochrones. For the purposes of target selection, the PMS isochrones were corrected for a distance of 2.0 kpc and a foreground extinction of A_V = 1.0 mag.

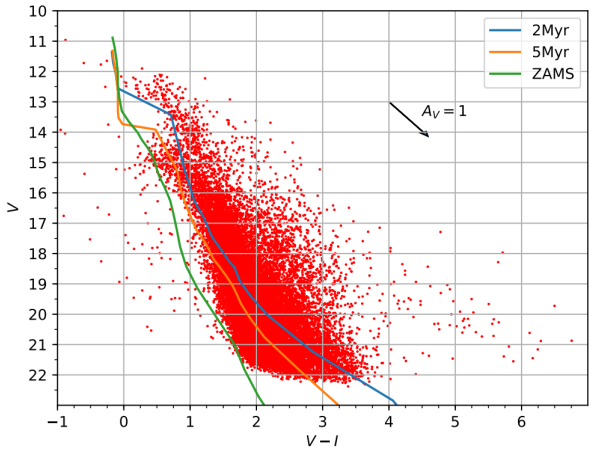

Figure 3. Color-magnitude diagram of over 25,000 sources in the direction of W4 with 90Prime photometry. The solid lines are isochrones for 2-Myr, 5-Myr, and the ZAMS for 2 kpc and $A_V = 1$ (Siess *et al.*, 2000). The sources targeted for spectroscopy were some 6,000 stars on or above the 5-Myr isochrone.

2.2. SPECTROSCOPY WITH HECTOSPEC

Candidate members of W4 were targeted for spectroscopic follow-up with the Hectospec multi-fiber spectrograph (Fabricant *et al.*, 2005) on the 6.5 m MMT Observatory on Mt. Hopkins, Arizona. As in Kiminki *et al.* (2015), a model of the foreground population, using the Besancon Galactic model (Robin *et al.*, 2003), was used to minimize the intrusion of foreground stars in the sample.

Seventeen Hectospec fiber configurations were observed in queue mode over 11 nights from 2011 to 2012. Exposure times were chosen to achieve a minimum signal-to-noise ratio of 25 at 6500Å. Details of each fiber configuration (date of observation, center of field of view, total on-source exposure time, magnitude range of sources observed, and number of targets observed) are given in Table 1. Over 3200 sources were observed one or more times with Hectospec's 270 lines mm^{-1} grating with a 1 degree field of view over a wavelength range of 3650-9200Å at a resolution of 5Å. These sources included the majority of objects lying redward of the 5 Myr Siess *et al.* (2000) PMS isochrone

Table 1. Log of Hectospec observations.

Date	RA(J2000) (hhmmss.s)	DEC(J2000) (° ’ ”)	Int. Time (sec)	Magnitude Range (mag)	Fibers Assigned
2011 Sept 23	02 31 49.3	+61 23 35.0	1800	12 < V < 16	245
2011 Oct 23	02 32 03.9	+61 25 51.8	2400	12 < V < 16	232
2012 Jan 24	02 32 47.8	+61 34 04.8	1260	12.5 < V < 16.5	244
2012 Feb 16	02 32 40.3	+61 34 54.1	5400	18.0 < V < 20.5	265
2012 Feb 20	02 34 22.8	+61 32 16.5	1260	12.5 < V < 16.5	246
2012 Mar 04	02 33 13.9	+61 37 36.1	1260	12.5 < V < 16.5	249
2012 Nov 04	02 34 17.9	+61 41 00.0	1260	12.5 < V < 16.5	228
2012 Nov 05	02 31 38.7	+61 31 26.0	1260	12.5 < V < 16.5	202
2012 Nov 05	02 34 14.8	+61 38 37.0	1260	12.5 < V < 16.5	191
2012 Nov 05	02 32 05.4	+62 03 44.2	1800	12.5 < V < 16.5	212
2012 Nov 05	02 32 26.1	+62 02 39.5	2400	12.5 < V < 16.5	169
2012 Nov 06	02 33 43.8	+61 43 24.0	3600	16.5 < V < 18.5	250
2012 Nov 06	02 32 16.1	+61 29 08.1	3600	16.5 < V < 18.5	257
2012 Nov 06	02 31 58.3	+61 54 53.6	3600	16.5 < V < 18.5	256
2012 Dec 03	02 32 39.0	+61 27 35.8	3600	14 < V < 20	258
2012 Dec 03	02 32 24.1	+61 27 29.0	3600	14 < V < 20	252
2012 Dec 04	02 32 24.7	+61 27 35.2	3600	14 < V < 20	247

with $13 < V < 16.5$ mag, as well as several hundred sources with $V > 16.5$ mag. The reduction of spectroscopic data (e.g., dark-current subtraction, aperture extraction, and cosmic ray removal) was performed in the IRAF[2]-based E-SPECROAD pipeline[3], following the procedures given in Kiminki *et al.* (2015).

2.3. PHOTOMETRY AND OTHER SURVEY DATA

Photometry for each star was assembled from several surveys. PanSTARRS PS1 data was retrieved for all $grizy$ bands at 0.481 μm, 0.617 μm, 0.752 μm, 0.866 μm, and 0.962 μm, respectively (Flewelling *et al.*, 2016). Survey parameters are described in Chambers et al. (2016). Photometry from the 2MASS Point Source Catalog was retrieved for bands

[2]IRAF is distributed by the National Optical Astronomy Observatory, which is operated by the Association of Universities for Research in Astronomy (AURA) under cooperative agreement with the National Science Foundation

[3]*http://astronomy.mnstate.edu/cabanela/research/ESPECROAD/*

JHK_s at 1.235 μm, 1.662 μm, and 2.159 μm, respectively (Cutri *et al.*, 2003). Spitzer data was retrieved from the Spitzer Enhanced Imaging Products catalog for the IRAC bands at 3.6 μm, 4.5 μm, 5.8 μm, and 8.0 μm, and the MIPS-1 band at 24.0μm. The IRAC and MIPS coverage did not include the entire survey area. Bands W1 and W2 (3.4 μm and 4.6 μm, respectively) were used from the AllWISE Release of the Wide-Field Infrared Survey Explorer (WISE) (Cutri and et al., 2013).

X-ray detections were collected for 161 sources from surveys using the XMM Newton and Chandra space telescopes. XMM Newton data is from Rauw and Nazé (2016), which covered an area of 26' x 27' centered on the IC 1805 cluster, but also includes unpublished data for fields to the north and east. Chandra data is from the Massive Star-Forming Regions (MSFRs) Omnibus X-ray Catalog (MOXC) from Townsley *et al.* (2014) which covered an area of 21' x 22' (centered on the cluster). Many sources in our survey are located outside these regions. Of the 161 sources, 126 were included as probable cluster members. Five of the remaining X-ray emitters had spectra too noisy to classify, while the other 30 sources were identified as foreground stars based on their low extinctions (on average, $A_V \approx 1.5$ mag) and reliable distance estimates that fell within 1000 pc.

Proper motion probabilities were assembled from Shi and Hu (1999), based on data from Vasilevskis *et al.* (1965). Gaia DR2 parallaxes and *G* band photometry were obtained for all sources (Gaia Collaboration *et al.* 2016; Gaia Collaboration *et al.* 2018). Inferred distances using Gaia DR2 data were obtained for the entire sample from Bailer-Jones *et al.* (2018).

3. RESULTS

3.1. THE DISTANCE TO W4

Most distance estimates for W4 have fallen within the range of about 2.0-2.4 kpc. Estimates made using spectroscopic parallax have generally sided on the higher side (e.g., Massey *et al.* 1995 or Sung *et al.* 2017), while VLBA measurements of a maser in W3, and Straižys *et al.* (2013), have sided near 2 kpc. Many studies have assumed the neighboring W3 complex is at the same distance as W4. However, Sung et al. found that there is no physical grounds for assuming this by comparing other VLBI astrometry to the width of the Perseus spiral arm.

The latest release of parallax measurements from the Gaia DR2 survey can be used to infer a distance, and uncertainty, to the cluster which will be used in this study. Errors reported by the survey claim that stars with a $G < 15$ mag will have parallax uncertainties of at most 0.04 mas. Using the estimated distances above, this would correspond to maximum distance errors of 2000^{+174}_{-148} pc and 2400^{+255}_{-210} pc. Most of the bright IC 1805 cluster members of Massey *et al.* (1995) have G magnitudes brighter than this limit and will be used to make the distance inference. Of these 38 cluster members, 34 stars were used since four stars had parallax errors higher than the limit quoted above.

Figure 4 shows two overlaid distributions for the distances to the 34 cluster members. The distribution labeled DR2 uses distances calculated by taking the inverse parallax for each star. The label Bailer-Jones refers to the inferred distances of Bailer-Jones *et al.* (2018). In Bailer-Jones et al., the distances to some 1.33 billion stars of the Gaia DR2 survey are estimated using Bayesian inference. A distance of 2300 ± 200 pc will be adopted for this study based on where the peaks of the two distributions coincide. The uncertainty of 200 pc is rounded up from the errors of the distributions and is consistent with the uncertainty adopted in Sung *et al.* (2017).

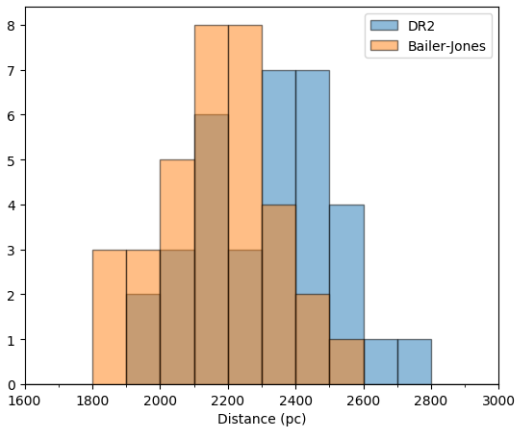

Figure 4. Histograms overlaying distance estimates taken directly from Gaia DR2 (inverse parallax), and inferred data from Bailer-Jones *et al.* (2018). Both estimates peak in the 2200-2400 pc range.

3.2. SPECTRAL CLASSIFICATION

A total of 4085 sources in the direction of W4 were assigned a spectral type and corresponding uncertainty. Three independent estimates of spectral type and uncertainty were made for all sources before being given a final spectral type and spectral range. Each reduced spectrum was first normalized in IRAF before being passed to the programs/methods below.

The spectral typing process was performed largely in *sptool*, a Python-based script created by Mark Pecaut (Pecaut *et al.*, 2012). The standards used for classification were those of Jacoby *et al.* (1984), which cover a spectral range of O to M-type stars, luminosity classes I, III, and V, and a wavelength range of 3510Å-7427Å at a resolution of 4.5Å. Standards from Gray and Corbally (2009) were used as well which covered a spectral range of O to K-stars over a wavelength range of 3800-5800Å at a resolution of 1.8Å. Two additional programs were used to help determine spectral types for the first 6 configurations. *SpTAssist* is an Interactive Data Language-based (IDL) tool developed by Danielle Kiminki (private

communication, 2013). This program used the previously mentioned Jacoby standards and Gray & Corbally standards, with an additional Danks and Dennefeld (1994) set of standards. The spectral typing program *SPTCLASS* was used on six datasets (Hernández *et al.*, 2004).

Many sources that could not be spectral typed using the programs above were classified manually via template matching using dwarf standards from Allen and Strom (1995), and dwarf and giant standards from STELIB by Le Borgne *et al.* (2003). About 70% of stars had small uncertainties in spectral type of ±1-2 subtypes. G and K-type stars had the largest uncertainties in spectral type (on average ±3 subtypes) due to limited spectral features to distinguish between G-type stars and early K-type stars.

A large number of sources had to be classified without the use of their hydrogen lines. These lines were often filled in with emission, some intrinsic to the source, and some due to nebular emission and/or a poor sky subtraction. This was indicated by the presence of nebular emission lines at 6582Å[N II], 6715Å[S II], and 6725Å[S II]. In these instances, B-stars were classified by the presence of He I absorption lines at 4026Å and 4471Å. In later B-stars and early A-stars, the strength of the Ca II K (3934Å) line and the relative strengths of Mg II (4481Å) to He I (4471Å) were used to distinguish spectral type. Occasionally, the wings of the Hβ absorption line could be fit to a digital standard for classification.

In F-stars, a key spectral feature used was the ratio between Mn (4030Å) and Fe I (4046Å), which strengthens as temperature becomes cooler. In early G-stars the strengths of Fe I lines at 4226Å, 4271Å, and 4383Å were used as well as the strength of the G-band (relative to digital standards). The G-band is a collection of absorption lines caused by electronic transitions in the diatomic CH molecule. Late G-stars and early K-stars were difficult to distinguish from one another due to small changes in spectral feature strengths over the observed spectral range (particularly without the aid of hydrogen lines). However, the strength of the blend at 6497Å, which is combination of Fe I, Ca I, and Ba II absorption lines, relative to digital standards provided a marker of spectral subtype as it increases with

decreasing temperature. In mid-K through M-type stars the increasing strength of TiO bands (at 6080-6390Å, 6651-6852Å, and 7053-7270Å) as well as Ca I (4227Å) feature were used.

In the cases where the hydrogen lines were not strongly affected, B-stars were classified using the presence of the hydrogen Balmer lines, as well as the strength/presence of the Ca II K and He I lines (wavelengths given above). The strength of the Ca II K relative to Balmer lines was primarily used for classifying A-stars . The classification of F and G-stars was largely based on the relative strengths of the G-band (4305Å) to Hγ, Ca II H and K (3969Å and 3934Å, respectively), and Fe I lines (primarily at 4046Å and 4384Å). Late G and K-stars use the relative strengths of Fe I (4325Å) and Hγ, as well as the relative strengths of Hα and the blend at 6497Å.

Giants were identified using several spectral features given by Torres-Dodgen and Weaver (1993) and Gray and Corbally (2009). For G and K stars the presence of strong absorption lines in the Ca II triplet, at {8498Å, 8542Å, 8662Å}, provided a reliable estimation of luminosity. In G stars the ratio between Ca I (4226Å) and Sr II (4216Å) as well as the strength of the CN band at 4215Å provided additional criteria. In late G and early K stars the ratio of Y II (4376Å) to Fe I (4384Å) was used. The ratio of Fe I lines at 5250Å and 5269Å also provided luminosity class information. A total of 165 stars were classified as giants or supergiants.

A full list of stars observed spectroscopically is presented in Table 2. Spectral types along with 90Prime and PanSTARRS r and i photometry are given for each source. The main-sequence luminosity classification given with the spectral types is meant to indicate that the spectral classifications were assigned using main-sequence standards. Giants are indicated in column 6. There were 844 sources observed more than once which have been combined into a single entry, resulting in a sample of 3241 unique sources. Additionally, an estimate of A_V is given for each source as well as a flag if the extinction was within the range $A_V = 1.6 - 4.2$ mag estimated for cluster members.

Table 2. IC 1805 spectral types and photometry.

Year	Date_No.[a] (MMDD_No.)	RA(J2000) (hhmmss.ss)	DEC(J2000) (° ' ")	SpTy Range	SpTy	A_V (r-i) (mag)	Assoc.?[b] (ext)	V(90P)[c] (mag)	rmag[d] (mag)	imag[d] (mag)	I(90P)[c] (mag)
2012	1106_3_66	2 28 26.92	62 10 32.80	F0-F4	F2V	2.8	1	...	17.59	17.06	...
2012	1105_4_183	2 28 27.08	61 59 14.30	F5-F6	F6V	1.8	1	14.93	14.94	14.54	13.78
2012	1105_2_177	2 28 27.17	61 48 38.20	F4-F7	F5V	2.5	1	14.55	15.77	15.27	14.48
2012	1105_4_202	2 28 27.19	62 08 15.90	G8-K1	G9V	1.5	0	15.86	15.64	15.18	14.32
2012	1105_4_203	2 28 27.22	62 12 40.80	F2-F4	F2V	2.1	1	14.69	14.70	14.30	13.45
2012	1105_4_188	2 28 27.53	61 56 32.89	F7-F9	F8V	2.4	1	15.45	15.10	14.58	13.97
2012	1105_4_197	2 28 27.69	62 06 02.00	G0-G3	G2V	1.1	0	14.03	14.12	13.79	12.95
2012	1106_3_51	2 28 28.23	62 08 55.20	K3-K5	K4V	2.0	1	...	17.17	16.47	...
2012	1106_3_50	2 28 28.44	61 57 34.90	F0-F3	F2V	4.3	1	...	16.74	15.92	...
2012	1106_3_45	2 28 29.47	61 59 03.90	G9-K5	K2V	1.9	1	...	17.50	16.92	...
2012	1106_3_32	2 28 29.54	61 49 49.20	G9-K2	K2V	2.0	1	...	16.73	16.13	...
2012	1106_3_53	2 28 30.03	62 08 15.20	F7-F9	F8V	2.8	1	...	17.56	16.94	...
2012	1105_2_180	2 28 30.14	61 46 36.90		K2V	1.4	0	15.68	15.49	15.01	14.25
2012	1106_3_40	2 28 30.47	61 52 09.61	F8-G0	F8V	3.0	1	...	17.38	16.75	...
2012	1106_3_38	2 28 30.71	61 51 41.10	A1-A3	A1V	5.5	0	...	16.94	16.09	...
2012	1105_2_175	2 28 31.04	61 49 04.50	F3-F6	F4V	2.6	1	15.39	15.30	14.79	14.21
2012	1105_4_283	2 28 31.13	62 15 46.71	B9-A0	B9V	2.6	1	14.79	14.80	14.57	13.86
2012	1106_3_57	2 28 31.28	62 06 33.41	G1-G6	G3V	2.4	1	...	17.55	16.97	...
2012	1106_3_56	2 28 31.74	62 03 49.40	K2-K3	K2V	1.7	0	...	17.37	16.83	...
2012	1106_2_44	2 28 31.97	61 31 03.10	F7-F9	F8V	3.5	1	18.23	17.70	16.96	16.29
2012	1105_4_176	2 28 32.10	61 48 51.70	G0-G3	G0V	2.4	1	13.61	13.67[e]	13.11[e]	12.81

[a] The month and day of the observation followed by the configuration number (if more than one) and the spectrum number in that configuration.
[b] A "1" denotes an extinction value between 1.8-4.6 mag, consistent with lying within the W4 region. A"0" denotes an extinction value outside of this range.
[c] Photometry from the 90Prime imager.
[d] Photometry from PanStarrs DR2 release except where noted.
[e] Photomerty from the IPHAS Second Data Release (Barentsen et al. 2014).
[f] i band photometry from the IPHAS Second Data Release (Barentsen et al).
[g] Spectrum indicates a likely giant or supergiant with a luminosity class of I-III. The two A type stars are possible supergiants.
(This table is available in its entirety in machine readable form. A portion is shown here for guidance regarding its form and content.)

3.3. THE EXTINCTION ACROSS W4

Extinction estimates were calculated for each source based on the assigned spectral type, and the PanSTARRS r and i passband photometry. The intrinsic colors of Pecaut and Mamajek (2013) for main sequence stars were used to calculate the reddening of each source. The colors were transformed from Cousins to SDSS using the transformations of Jordi *et al.* (2006). An extinction coefficient for the $(r - i)$ color was calculated from the extinction vector of Green *et al.* (2019) to yield an estimate for the visual extinction $A_V = 4.71E(r - i)$.

The entire spectroscopic sample of stars in the direction of W4 has an average extinction of 2.2 ± 0.3 mag. The average extinction of cluster members is $A_V = 2.7 \pm 0.5$ mag. The uncertainty for both the entire sample and cluster members are primarily due to uncertainties in spectral type. Uncertainty in the galactic visual extinction coefficient (which was assigned $R_V = 3.1 \pm 0.1$) and PanSTARRS photometric errors were the next

Table 3. Completeness limits.

Passbands	V	I_C	r	i	[3.6]	[4.5]
Limits (mag)	18	17	17	16	14	14

largest sources of uncertainty. The larger errors from PanSTARRS photometry typically resulted from very faint or very bright sources (r or $i < 15$ mag). Bright sources which were not assigned errors were given an error of ±0.02 mag. In general, over 90% of stars which had errors assigned by the PS1 survey fell well below 0.02 mag.

3.4. COMPLETENESS AND CLUSTER MEMBERSHIP

Completeness limits in the V, I_C, r, i, and IRAC 1-2 bands are estimated for the entire population using the method of Jose *et al.* (2016). This method determines completeness where data for 90% of the sources were obtained in a single photometric band. These particular bands were chosen because the 90Prime data were used to make the initial source selection, the PanSTARRS data were used to estimate extinctions, and the IRAC 1 and 2 bands were used in identifying young stars with circumstellar disks. The IRAC 3 and 4 bands, as well as MIPS1, were often saturated by bright nearby sources and nebular emission, and therefore do not represent the larger population. Figure 5 shows histograms for the V 90Prime and IRAC bands, where the vertical line denotes the 90th percentile. The completeness limits are summarized in Table 3. The 90th percentile limits of $V = 18$ and $I_C = 17$ correspond to 2 $M_\odot$ using the pre-main-sequence evolutionary models of Dotter (2016) and Choi *et al.* (2016).

To be considered a cluster member, each source with few exceptions, had to meet at least two of the following criteria: displaying an infrared excess (irx), X-ray detection, Hα emission (where EW(Hα) $\geq$ 5Å), proper motion probability greater than 50%, and/or a visual extinction within $A_V = 1.6 - 4.2$ mag. In total, 219 sources are considered probable

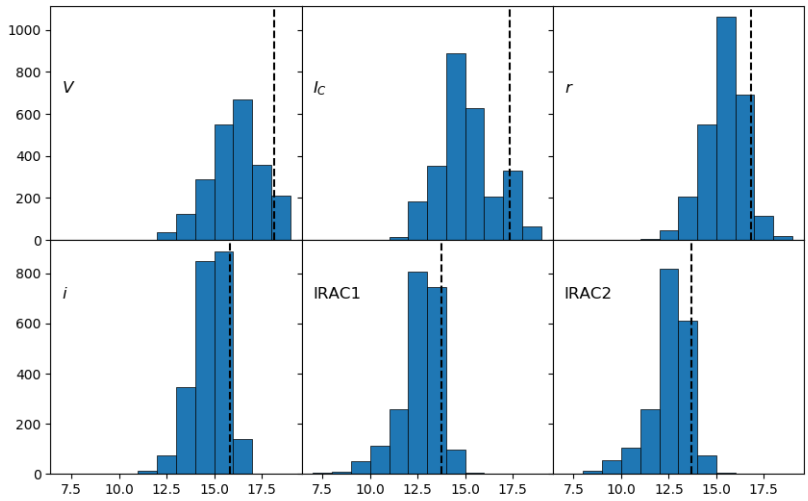

Figure 5. Completeness limits for each band used in the initial source selection (V & I), estimating extinction (r & i), and identifying sources exhibiting an excess in infrared flux (IRAC).

cluster members. Using PanSTARRS PS1 r and i photometry and the corresponding extinction laws from Green *et al.* (2019), the extinction range of 1.6-4.2 mag was determined for the cluster members identified by Massey et al. However, given uncertainties in extinction, at least one additional criterion was required to be considered a cluster member. Hα emission was considered weak if EW= 5 – 10Å and strong if EW> 10Å. Five stars which met only one criterion were included in the final list of cluster members. Three of these stars are irx sources and the other two are sources of strong Hα emission.

Stars exhibiting an excess in infrared flux indicating a dusty, reprocessing circumstellar disk were identified using dereddened spectral energy distributions (SEDs). Each source with an excess in the IRAC bands and/or MIPS1 bands was verified by visual inspection of the IRAC and MIPS1 mosaics available in the SEIP database. If no point source was visible in the mosaic, the source was not assigned the irx criterion. Additionally, the SEIP performed aperture photometry on each source using a 3.8 arcsec diameter aperture as well as a 5.8 arcsec diameter. Nebular contamination of the IRAC bands is evident by

comparison of the flux measured by these apertures, providing a second means of identifying true excess sources. Many SEDs showed signs of polycyclic aromatic hydrocarbon (PAH) emission which resulted in infrared excesses unrelated to the presence of a disk. Interstellar PAH emission is known to occur at 3.3, 6.2, 7.7, 8.6, 11.2, 12.7, and 16.4 μm, as well as weaker emission features in numerous other bands (Tielens, 2008). Towards W4, this emission typically appeared in IRAC bands 3 and 4. Visually, this resulted in a rising tail in the SED that is somewhat similar to the near infrared bump seen in many Herbig stars (e.g., Bans and Königl 2012). These stars are not identified as true irx sources.

The extinction criterion of $A_V = 1.6-4.2$ mag alone was not considered an indicator of cluster membership. Roughly 2257 stars in the 3241 spectral-typed sample met this criterion (Table 2). Stars possessing an irx, and/or Hα emission with an equivalent width greater than 5Å, were considered cluster members regardless of their extinction. This group of 75 stars spans an extinction range of $A_V = 0.8 - 5.1$ mag, above and below the criterion range, but consistent with this range given the uncertainties in spectral types. Additionally, no correlation was found between stars whose spectra showed strong giant luminosity indicators and their respective extinctions.

3.5. HERTZSPRUNG-RUSSELL DIAGRAMS

Table 4 lists all 219 probable cluster members along with their corresponding spectral types, effective temperatures, extinctions, luminosities, and association criteria. Additionally, sources which were also covered in the survey by Wolff *et al.* (2011) are identified with their corresponding number, an “S" if a spectrum was obtained for that source, and an “irx" if identified as a disk-bearing source. Our list does not include 33 O and early B type stars identified as members of OCL 352 by Massey *et al.* (1995). The last column in the table includes comments such as which sources displayed emission in the calcium triplet spectral lines.

Table 4. IC 1805 probable cluster members.

RA(J2000) (hhmmss.ss)	DEC(J2000) (° ' ")	Wolff et al.[a]	SpTy	log T_{eff}(K)	A_V (r-i) (mag)	log $L/L_\odot$	Mass $M_\odot$	Age Myr	Assoc. Criteria[b]	Comments[c]
2 28 27.53	61 56 32.89		F8V	3.789	2.1	1.272	2.3	3	irx,ext	
2 28 43.41	61 31 34.30		B8V	4.097	4.3	2.280	3.4	1.5	irx,ha	
2 28 43.45	61 29 41.60		G1V	3.769	4.0	1.634	3.2	1	irx,ext	
2 29 35.91	61 15 56.80		B6V	4.161	4.0	2.944	5.1	0.6	irx?,Ha,ext	Ca tr em[d]
2 29 40.18	61 10 20.40		A3V	3.932	3.4	1.069	1.8	18.9	irx,ext	
2 30 07.22	61 31 07.70	955	A2V	3.946	2.5	2.457	4.5	0.7	pm,ext	
2 30 26.40	61 27 43.40	941	B2.5V	4.267	4.0	3.782	9.1	0.1	pm,ext	
2 30 28.83	61 32 56.00	940	B3V	4.230	4.1	3.516	7.6	0.2	pm,ext	
2 30 29.51	61 19 45.00	939S	B3V	4.230	3.2	3.351	6.6	0.3	pm,ext	
2 30 31.32	61 30 13.20	938	F0V	3.857	1.7	1.732	2.8	2.2	pm,ext	
2 30 37.71	61 18 10.54		K2V	3.702	1.9	0.313	1.5	1.5	ha,ext	
2 30 39.44	61 31 57.20	931	F0V	3.857	2.1	1.991	3.5	1.1	pm,ext	
2 30 45.16	61 16 12.10		B4V	4.223	2.9	3.037	5.4	0.5	pm,ext	
2 30 50.77	61 30 22.40		G2V	3.761	4.0	1.037	2.3	3.4	irx,x,ext	
2 30 53.49	61 45 29.20	514S (B5)	B5V	4.196	3.4	2.854	4.8	0.6	pm,ext	
2 31 06.65	61 40 56.08		G2V	3.761	2.6	1.268	2.7	1.9	ha,ext	
2 31 13.95	61 30 45.99		G8V	3.740	3.1	0.479	1.6	8.5	x,ext	gen1?
2 31 15.10	61 19 21.20		F8V	3.789	3.0	0.880	1.7	6	irx,ext	gen1?
2 31 21.12	61 38 22.01		A7V	3.892	2.9	0.964	1.7	11.9	irx,ext	gen1?
2 31 25.07	61 45 59.35	489S (B5)	B4V	4.223	2.0	2.573	4.5	2.4	pm,ext	
2 31 37.48	61 28 13.94		G9V	3.728	3.5	0.557	1.8	2.4	x,ext	
2 31 47.00	61 32 03.43	297 (A2)	B9V	4.029	3.4	1.813	2.7	3	x,ext	
2 31 47.85	61 27 32.45	209S (B5)	A0V	3.987	2.6	1.601	2.3	4.3	x,ext	
2 31 48.48	61 34 55.96	208S	B3V	4.230	2.7	2.774	4.8	9.5	pm,ext	
2 31 49.79	61 32 41.42	206S (B5)	B4V	4.223	2.4	2.820	5.2	0.8	pm,ext	
2 31 50.22	61 35 59.90		F9V	3.781	2.8	1.214	2.2	3	x,ext	
2 31 50.73	61 33 32.34		F9V	3.781	2.5	1.033	2	3.4	x,ext	
2 31 55.15	61 31 22.95		K1V	3.713	2.9	0.693	2	1.7	x,ext	
2 31 56.92	61 32 35.86		K4V	3.665	2.3	0.060	1.2	2.7	x,ha,ext	
2 31 59.24	61 39 29.60		F3V	3.827	2.3	1.105	1.8	6.7	irx,ha,ext	gen1?
2 32 02.45	61 37 13.29	292/461	F0V	3.857	2.5	1.320	2	5.4	irx,ext	
2 32 06.33	61 32 51.90	190S (B8)	B9V	4.029	2.6	1.802	2.7	3	x?,ext	
2 32 06.99	61 32 42.90		K8V	3.599	4.6	1.168	0.6	0.1	irx,x,Ha	
2 32 07.04	61 45 34.00		G2V	3.761	2.9	1.134	2.4	2.4	irx,Ha,ext	Ca tr em

[a] Source number from the study of Wolff et al. (2011) with their reported spectral classification and identification of an infrared excess (irx).
[b] Association criteria include an infrared excess (irx, this study); X-ray emission (x, Townsley et al. 2014; Rauw & Naze 2016); Hα emission with EW>10Å (Ha) or 10Å > EW >5Å (ha), this study; proper motion member with probability >50% (Shi & Hu 1999); or extinction with A_V = 1.6-4.2 mag (this study).
[c] Sources noted with possible lithium absorption at 6707Å or calcium triplet emission at 8498, 8542, & 8662Å.
[d] This source exhibits a P Cygni Hα emission profile in its spectrum. It is suspected to be a post-main-sequence star.
(This table is available in its entirety in machine readable format.)

Hertzsprung-Russell (H-R) diagrams were created using the Mesa Isochrones and Stellar Tracks (MIST) pre-main-sequence evolutionary models (Dotter 2016; Choi *et al.* 2016; Paxton *et al.* 2018). Probable cluster members are plotted against solar metallicity isochrones and tracks for two groups: (1) 113 sources with an infrared excess (irx) and those displaying Hα emission which are not also irx sources in Figure 6 and (2) 107 sources with X-ray and/or proper motion measurements in Figure 7. A zoomed in view of the densely packed lower-mass stars in Figure 6 is shown in Figure 8.

Luminosities were calculated for each source using the estimated extinction and r band magnitude. The bolometric correction at the r band is estimated from the intrinsic colors of Pecaut and Mamajek (2013) as $BC_r = BC_V + (V - r)$, where $(V - r)$ is transformed from $(V - R_C)$ using the transformations of Jordi *et al.* (2006). The vertical error bars for

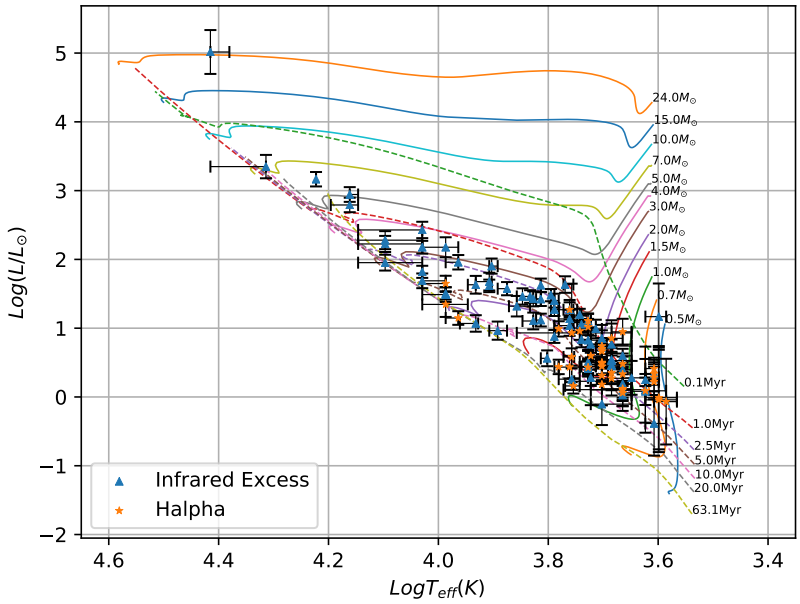

Figure 6. H-R diagram of 114 cluster members which met the minimum infrared excess (irx) criterion and those displaying Hα emission which are not irx sources. Among these two criteria, 34 sources are irx only, 41 are irx and Hα, and 39 are Hα only. Solid lines are mass tracks and dashed lines are isochrones.

luminosity represent the propagation of uncertainty due to the following: distance modulus, extinction, observational error in r magnitudes, and transformation of the $(V - r)$ color. Uncertainty in the distance modulus, using the adopted distance of 2300±200 pc, is the largest contribution to the luminosity uncertainty. Extinction errors were largely affected by uncertainty in spectral type. Horizontal error bars represent the uncertainty in spectral type.

In Figure 7 there is a clear separation between proper motion members and X-ray sources. Estimating proper motion is typically limited to more luminous stars, hence the grouping in the upper left corner. X-ray emission is seen mostly among low mass stars and can be an indicator of magnetic activity in classical T-Tauri stars and weak-line T-Tauri stars. X-ray emitters among A and B type stars, which do not have an apparent irx, are often attributed to a low mass YSO companion.

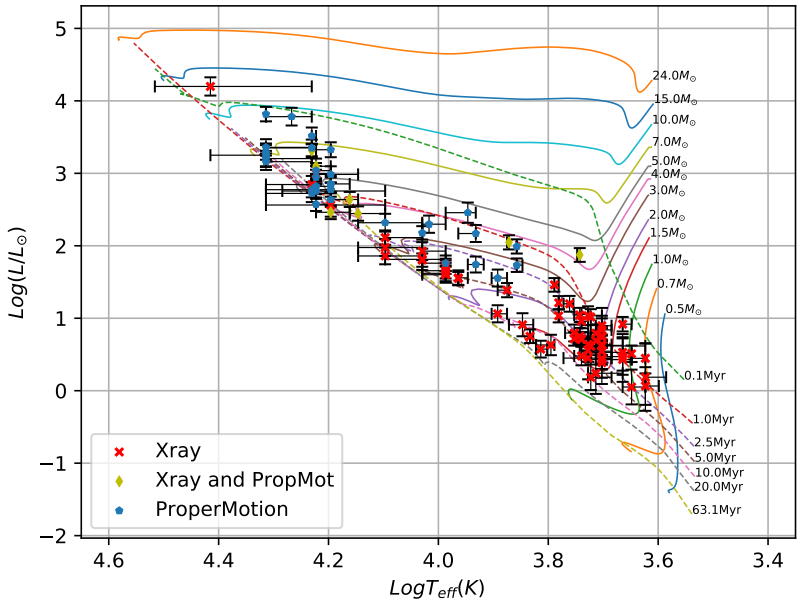

Figure 7. H-R diagram of the remaining 105 cluster members which met at minimum the proper motion and/or X-ray criteria. Among these two criteria, 33 sources are probable proper motion members, 8 are both proper motion and X-ray sources, and 64 are X-ray sources. Solid lines are mass tracks and dashed lines are isochrones.

Ages and masses were interpolated for each star using the full set of mass tracks and isochrones less than 25 Myr. Uncertainties in ages and masses are estimated by computing all four extremes defined by the error bars in the H-R diagrams, which are then reduced to the maximum and minimum in each category. Histograms of interpolated masses and ages are shown in the two panels of Figure 9. Both panels include an additional sample of 117 possible cluster members, which will be discussed in Section 4.1. Each distribution also includes 24 B-type cluster members from Massey *et al.* (1995) which were not observed in this survey. The error bars in panel (a) represent the $\pm\sqrt{N}$ count for each bin. Initial mass function (IMF) curves using the slopes of Sung and Lee (1995) ($\Gamma = -1.0$), Sung *et al.* (2017) ($\Gamma = -1.3$), and Panwar *et al.* (2017) ($\Gamma = -1.23$) are overlaid on the plot to visualize previous mass distributions. Each IMF is normalized using the 10 O-type stars in OCL 352.

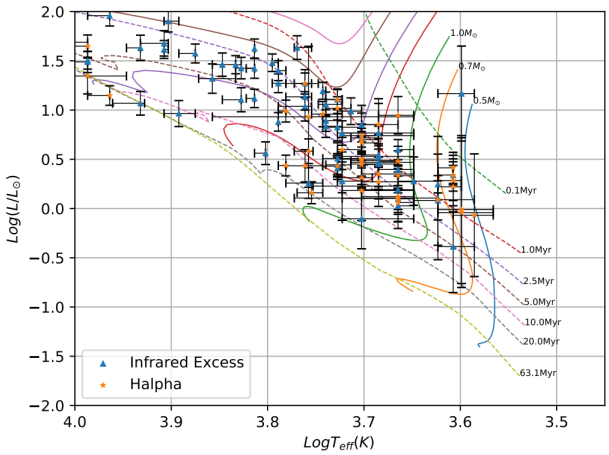

Figure 8. A zoomed in view of the left panel of Figure 5, showing the spread of lower mass irx and Hα sources.

4. DISCUSSION

4.1. COMPARISON WITH PREVIOUS STUDIES

A comparison of our 219 probable cluster members with previous studies of IC 1805 would suggest that our survey is undersampled for low mass YSOs. Panwar *et al.* (2017) identified 370 IC 1805 cluster members within a cluster radius of 9 arcmin centered around $\alpha_{J2000} = 2^h32^m42^s$, $\delta_{J2000} = +61°27'21"$. If this filter is applied to the stars in Table 4, a total of 120 probable cluster members results. Another study, Sung *et al.* (2017), identified 718 YSOs within an estimated cluster radius of 15 arcmin centered around $\alpha_{J2000} = 2^h32^m42^s$, $\delta_{J2000} = +61°28'2"$. Applying this spatial filter to our probable cluster members results in 154 stars.

Undersampling could be caused by a combination of the magnitude limit of our optical spectroscopic survey, X-ray variability, and missed irx coverage. Only seven of the 17 Hectospec configurations were specifically dedicated to observing sources with visual magnitudes fainter than 16.5 mag (see Table 1). Additionally, the skewed distributions of

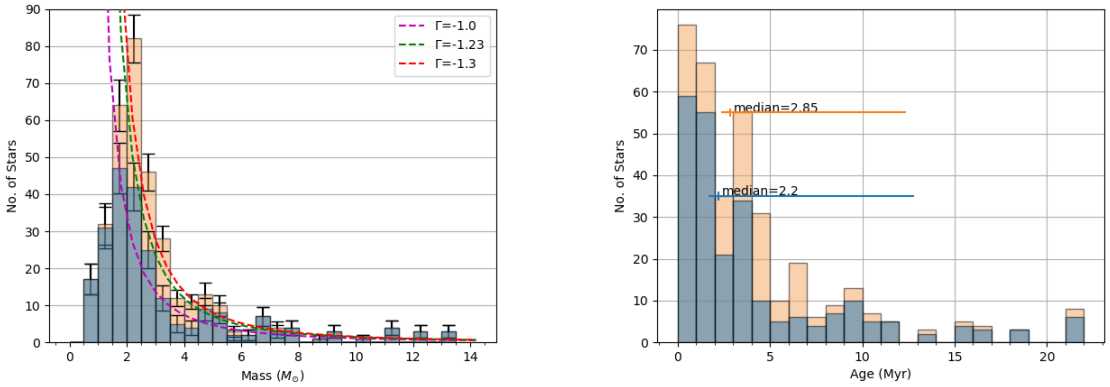

(a) (b)

Figure 9. Mass (a) and age (b) histograms for probable cluster members. The distributions also include 24 B-type stars from Massey *et al.* (1995) which were not observed in this survey. Probable cluster members are represented by the gray distribution, and the orange distribution represents the inclusion of an additional 117 possible cluster members. The slopes in panel (a) represent several estimated IMFs for IC 1805 (see Section 4.1). In (b), the same distributions are again represented by gray and orange, respectively. The vertical error bars represent the medians of the two distributions, and the horizontal error bars represent the 10th and 90th percentiles.

V and I_C in Figure 5 have clearly influenced the 90% completeness estimations. The V and I_C bands completeness limits are likely closer to 16.5 mag and 16 mag, respectively, than those given in Table 3.

As was noted in Section 2.3, the IRAC and MIPS data did not cover the entire survey. AllWISE data was compiled for all cluster members and was critical for sources that fell outside of the Spitzer coverage. However, AllWISE bands 3 and 4 often showed an irx in sources while Spitzer data did not. Due to the high rate of contamination from nebular emission, extended sources, and source confusion, these bands were not used precluding the identification of YSOs with evolved disks. Studies such as Dennihy *et al.* (2020) and Silverberg *et al.* (2018) have found high rates of false-positive irx identification in several surveys which relied on WISE photometry. AllWISE bands 1 and 2, which have larger aperture radii than IRAC 1 and 2, often agreed with Spitzer photometry, but several sources

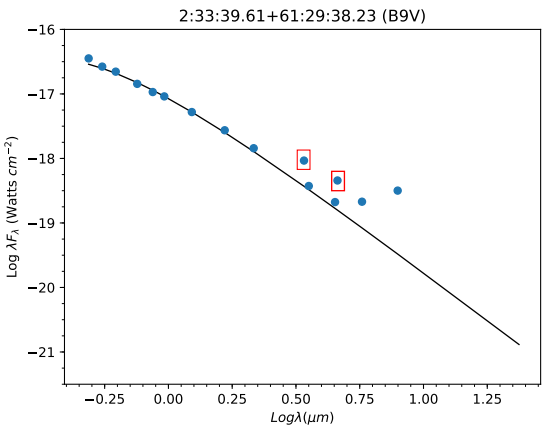

Figure 10. Example SED of a source with contaminated AllWISE data (red boxes) and PAH emission in IRAC 3 and 4 bands (as discussed in Section 3.4). The solid line is a blackbody with an effective temperature corresponding to a B9V star from Pecaut and Mamajek (2013), normalized to the *J* band. Photometric errors are smaller than the markers. In the dereddened SEDs, extinction ratios were formed from the extinction vector of Green *et al.* (2019) for the PanSTARRS and 2MASS bands. Extinction ratios for the remaining Spitzer and WISE bands were taken from Wang and Chen (2019).

did show signs of contamination in these bands too. Figure 10 shows an example of contaminated data in AllWISE bands 1 and 2 (in red boxes) where the IRAC 3 and 4 bands show an apparent excess due to PAH emission.

Our sample has a photometric completeness down to 2 $M_\odot$, where approximately 120 of 219 probable cluster members have masses greater than or equal to 2 $M_\odot$. Panwar *et al.* (2017) found that their survey was complete down to 0.2-0.3 $M_\odot$. However, based on the interpolated masses given in their Table 4, they only found roughly 50 stars between 2.0-7.0 $M_\odot$. Our study has found 113 stars in this mass range. In this regard, either our study is overestimating cluster members, or Panwar et al. was not able to identify all intermediate-mass cluster members. This discrepancy could be due to the fact that YSOs in this mass range have often dissipated their disks and are undersampled in X-ray surveys. By including proper motion surveys and making estimates for visual extinctions, we have more completely sampled this mass range.

Like this study, Wolff *et al.* (2011) surveyed IC 1805 using both optical spectroscopy and infrared photometry. In their study, they identified 62 irx sources, 57 of which were spectroscopically observed in this survey. Here, only 17 of these sources were classified as irx stars, and an additional 5 as non-irx cluster members. All 40 of the unconfirmed irx sources fall into categories which Wolff et al. called “empty/thin" and “empty/thick" excesses. In these sources, a slight irx appears only in the IRAC 4 band (sometimes in IRAC 3 also) of the SED for “empty/thin", and in the MIPS 1 band for “empty/thick". These sources are all located near areas of strong nebular emission at 8 μm and/or 24 μm which may have mimicked an irx.

Figure 9(a) shows the mass distribution of cluster members in Table 4. Our distribution fits between the IMF estimates of $\Gamma = -1.0$ and $\Gamma = -1.23$ (Sung and Lee 1995; Panwar *et al.* 2017, respectively). However, our cluster membership criteria could be excluding additional intermediate-mass young stars which have depleted their inner disks. Instead, if only extinctions and Gaia distance estimates are used to filter the entire 2257 extinction sources, excluding previously identified members, we find an additional 117 stars in the mass range 1.3-7.2 $M_{\odot}$. These stars have distance uncertainties less than the ±200 pc error assumed for W4. The inclusion of these stars would bring the number of cluster members up to 337. As seen in Figure 9, the addition of these stars would shift the mass distribution steeper than an IMF of $\Gamma = -1.3$, and the median age of the entire cluster up to 2.8 Myr.

4.2. THE AGES OF THE W4 HII REGION AND IC 1805

It has been suggested that an earlier generation of star formation is responsible for the creation of the 1300 pc shell identified by Reynolds *et al.* (2001), while recent star formation is responsible for carving the superbubble identified by Normandeau *et al.* (1996) and West *et al.* (2007). Figure 9(b) shows the distribution of ages for the entire probable cluster member list in Table 4. This distribution has a median age of 2.2 Myr, and the inclusion of 117 possible cluster members would bring the median age to 2.8 Myr. These

estimates are consistent with an age of 1.6-2.5 Myr found by Sung et al. and an age of 2.5±1.5 Myr derived by Panwar et al. While most cluster members are younger than about 5 Myr, a small rise in the number of stars can be seen around 10 Myr. This could be indicative of young stars from a previous generation of star formation which are still contracting to the main sequence.

Age estimates of an earlier generation of stars have been made in the range 6.4-20 Myr (see e.g., Dennison *et al.* 1997 or Oey *et al.* 2005). Several stars are located between the 5 Myr and 20 Myr isochrones in Figures 6 and 7, and a small gap with few sources can be seen between the 5 Myr and 10 Myr isochrones between log$T_{\rm eff}$=3.8-4.0. The two sections below examine the ages of stars located within: (1) an area of the H-R diagram which suggests they could be members of an older generation and (2) sources which are located near several bright-rimmed clouds (BRCs) and the cometary globule CG 7S.

4.2.1. Possible First Generation Stars. To isolate possible YSOs of an older generation, cluster members with interpolated ages greater than or equal to 6 Myr were examined. Those whose differences in age uncertainties were greater than ±10 Myr were excluded. This resulted in 15 sources, 14 of which are shown in Figure 11. They are indicated in the *Comments* column of Table 4. One higher mass star, EM* MWC 50 which can be seen near the top of Figure 6, is out of view. The median interpolated age of this group of stars is 8.5 ± 2.8 Myr.

Nine of these sources have an irx and/or Hα emission suggesting the presence of a circumstellar disk. However, one irx source, EM* MWC 50, is suspected to be a post-AGB star. Typically, the inner regions of a circumstellar disk have a median lifetime of about 2-3 Myr, however some disks have been observed to retain their inner disks upwards of 10 Myr (Williams and Cieza, 2011). Six of these objects are X-ray emitters with no other signatures of youth.

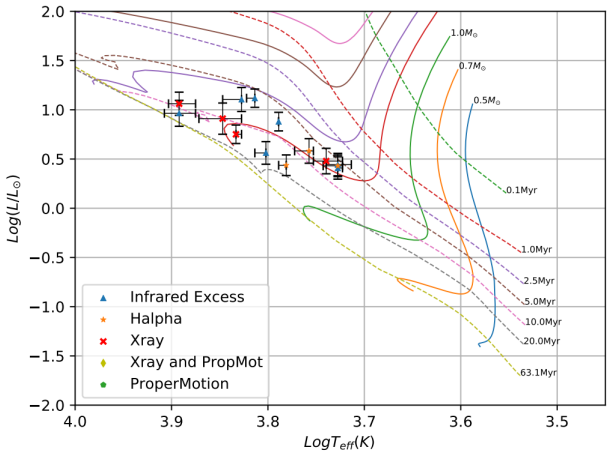

Figure 11. Fourteen of 15 possible cluster members whose interpolated ages suggest they could be members of a previous generation of star formation. EM* MWC 50, a higher mass star, is not included in this H-R diagram.

A closer look at the most massive stars in IC 1805 is shown in Figure 12, suggesting a mixture of first-generation stars and members of the younger OCL 352. Two sources identified as cluster members in Table 4 appear to be evolved stars: EM* MWC 50 (located on the $24.0M_{\odot}$ track of Figure 6) and the source 2:32:47.56+61:27:0.00 (located in between the $10M_{\odot}$ and $15M_{\odot}$ tracks in Figure 7) which is classified as a B1 star with X-ray emission. As shown in Figure 12, EM*MWC 50 (blue triangle) fits well along a 9 Myr isochrone and 2:32:47.56+61:27:0.00 (red X) has an interpolated age of 9.5 Myr. While not part of our survey, the blue supergiant BD+60 493 fits well along a 7.5 Myr isochrone, which is similar to the age found by Sung *et al.* (2017). These, as well as several B stars from Massey *et al.* (1995) which rise away from the main sequence between the 9 Myr and 11 Myr isochrones, could be evolved stars from an earlier generation of star formation in W4. Compared to cluster members, this group of stars is more spatially distributed in the east-west direction between IC 1805 and AFGL 333. The O-stars in Figure 12 sit primarily in between the 1 Myr and 5 Myr isochrones, with a grouping around the 3.5 Myr isochrone and a spread in ages very similar to that seen by most cluster members in the H-R diagrams of Section 3.5.

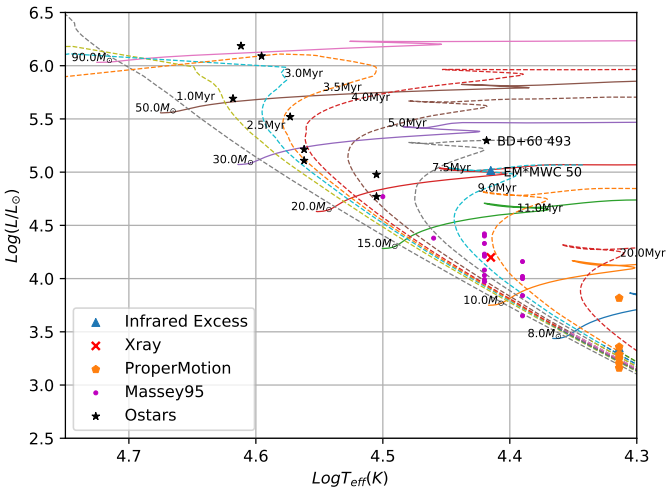

Figure 12. Zoomed in view of the high mass stars in W4 with main-sequence and post-main-sequence tracks and isochrones. Note the O-star which coincides with the 7.5 Myr isochrone is actually a B0.5Iae star (BD+60 493).

4.2.2. Sources in the Extended W4 HII Region. The YSOs not located within the IC 1805 cluster radii in Section 4.2, and not part of possible first generation stars, may represent a population dispersed by dynamical evolution (Lim *et al.*, 2020) or examples of isolated incidents of star formation which have occurred via the expansion of the W4 HII region and stellar winds from OCL 352. In the latter case, one would expect these stars to be slightly younger than the IC 1805 cluster. As indicated by the orange circles in Figure 13, the wider W4 HII region also features several BRCs (Sugitani *et al.*, 1991) and the cometary globule CG 7S (Lefloch and Lazareff, 1995) which host small populations of young stars (see also Panwar *et al.* 2019). Recent findings by Lim *et al.* (2020) support the idea that the observed stellar population, distributed over 20 pc in W4, is the result of the dynamical evolution of IC 1805. This section will investigate cluster members near each of these regions and Table 5 summarizes their spectral types, visual extinctions, association criteria, and age estimates.

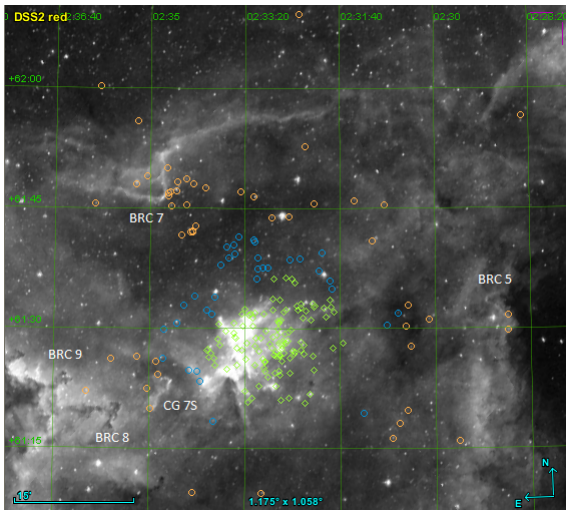

Figure 13. The spatial locations of the two IC 1805 groups (light green diamonds refer to the sources within Panwar et al.'s cluster radius and blue circles include additional sources within Sung et al.'s radius; Sung et al.'s cluster dimensions include the sources within the cluster dimensions of Panwar et al.) and sources outside of both IC 1805 cluster dimensions (orange circles). Several bright-rimmed clouds are denoted as well as cometary globule CG 7S. Coordinates are overlaid on a DSS2 $F + R$ image.

Two sources located along the western edge of the W4 HII region, near BRC 5, are both irx cluster members. They appear to be part of the small cluster identified by Hodapp (1994) and Fukuda *et al.* (2013), and were identified as Class II YSOs by Rivera-Ingraham *et al.* (2011).The more massive source near the edge of the BRC 5 bow shock is a B8 star and to the south is a cooler G1 source. Both of these objects have ages consistent with the proposal that ionizing radiation and winds from OCL 352 have triggered star formation along the edge of W4 (Fukada et al.). It should be noted that both sources also have visual extinctions higher than the cluster average, consistent with their location in gas and dust swept up by the HII region.

Our probable cluster member list includes two stars within the wake of BRC 7, and three sources which lie near the bow shock (see Figure 13). Although a small cluster is not evident in deep near-infrared imaging of BRC 7 (Carpenter *et al.*, 2000), Panwar *et al.*

Table 5. Probable cluster members near BRCs and CG 7S.

	RA (hh mm ss.ss)	Dec (° ′ ″)	SpTy	A_V (mag)	Assoc. Criteria	Age[a] (Myr)	AgeErUp (Myr)	AgeErLow (Myr)
BRC 5	2 28 43.41	+61 31 34.30	B8V	4.3	irx,ha	1.5	3.8	1.1
	2 28 43.45	+61 29 41.60	G1V	4.0	irx,ext	1	1.9	0.5
	2 35 03.53	+61 49 02.00	K8V	2.5	Ha,ext	0.9	–	–
	2 35 15.32	+61 48 03.29	K0V	2.6	irx,Ha,ext	1.2	3.4	0.7
BRC 7	2 34 41.26	+61 46 33.933	K3V	2.4	Ha,ext	1.4	–	–
	2 34 40.37	+61 46 52.706	G5V	2.3	x,ext	4.8	–	–
	2 34 41.74	+61 50 00.20	K2V	3.1	Ha,ext	1.4	–	–
	2 34 59.40	+61 19 59.00	A5V	3.6	irx,ha,ext	4	5	3
CG 7S	2 35 02.23	+61 22 30.43	G7V	2.0	irx,ext	2	2	1
	2 34 50.52	+61 24 16.71	A5V	2.8	irx,ext	4	5	4

[a]Stars without age uncertainties had spectral type errors too large to properly constrain the age.

(2019) did see an enhancement in density of YSOs identified through irx identification near BRC 7. With the exception of the G5 star, the ages of these cluster members are consistent with star formation triggered by OCL 352.

There are three probable cluster members located near CG 7S. Two stars are located in and near its clouds, and the other star is near the northern part of its tail. While the morphology of CG 7S is consistent with its formation through radiation driven implosion (Lefloch and Lazareff, 1995), our age estimates of these sources suggest they are more likely part of the dispersed IC 1805 cluster and that CG 7S has not yet started forming stars.

5. SUMMARY AND CONCLUSIONS

This study presents a sample of 3241 spectrally classified sources in the direction of W4. Spectral classifications were invaluable in the identification of cluster members, permitting estimates of their visual extinctions and establishing excess infrared emission relative to the underlying photospheres. A list of 219 probable cluster members were compiled based on extinction, proper motion, and/or the presence of X-ray emission, Hα emission, or an infrared excess. Ages and masses were interpolated for each source using the MIST evolutionary models. Estimations of the average visual extinction (2.7 ± 0.5

mag) and median age (2.2 Myr) of probable cluster members are in line with previous estimates. The mass distribution of cluster members largely follows the mass functions of previous IC 1805 studies. If a small sample of possible cluster members is included, whose memberships are based on extinctions and Gaia distances, the mass distribution more closely follows a Salpeter-type slope and the median age is 2.8 Myr.

The ages inferred from this spectroscopic sample of YSOs supports the proposal that an earlier generation of star formation has occurred within the W4 region. A group of 15 stars, one of which is an evolved B1 star, have a mean age of 8.5 ± 2.8 Myr, consistent with previous estimates for an earlier generation of stars that created the W4 superbubble. The evolved source, EM* MWC 50, is suspected to be a post-AGB star with an age around 9.0 Myr. Along with the blue supergiant BD+60 493, it may be another example of a star which predates the young IC 1805 cluster. Evidence of the influence of OCL 352 on the surrounding superbubble is supported by the ages of stars near/within BRCs 5 and 7.

ACKNOWLEDGMENTS

The observations in this study were obtained at the Bok Telescope which is operated by the Steward Observatory and the MMT Observatory, a joint venture of the University of Arizona and the Smithsonian Institution. This research has made use of “Aladin sky atlas" developed at CDS, Strasbourg Observatory, France (Bonnarel *et al.*, 2000) and the VizieR catalogue access tool, CDS, Strasbourg, France (Ochsenbein *et al.*, 2000). This work is based in part on archival data obtained with the Spitzer Space Telescope, which is operated by the Jet Propulsion Laboratory, California Institute of Technology under a contract with NASA. Spitzer photometries were obtained from the Source List of the Spitzer Enhanced Imaging Products (SEIP) database. This work has made use of data from the European Space Agency (ESA) mission *Gaia*[4], processed by the *Gaia* Data Processing

[4]*https://www.cosmos.esa.int/gaia*

and Analysis Consortium (DPAC)[5]. Funding for the DPAC has been provided by national institutions, in particular the institutions participating in the *Gaia* Multilateral Agreement. Part of this project (optical imaging and spectroscopy of the W4 region) is supported by the National Science Foundation through Astronomy and Astrophysics Research Grant AST-0907980. M. Wentzel-Long acknowledges support from the NASA Missouri Space Grant Consortium. We thank Hwankyung Sung for his input in the Hectospec target selection, Micaela Bagley for her work in reducing the 90Prime photometry, and Megan Kiminki for her work in reducing the Hectospec spectroscopy. J.S. Kim thanks to Dr. William H. Sherry for taking and processing optical images with the Bok/90Prime. M. Wentzel-Long thanks Tyler Hanke and Matthew Sprague for their assistance in inspecting spectral features and spectral classification. This research used the Python packages NumPy (van der Walt *et al.*, 2011), Matplotlib (Hunter, 2007), and Pandas (McKinney, 2010).

REFERENCES

Allen, L. E. and Strom, K. M., 'Moderate-Resolution Spectral Standards From λ5600 to λ9000 Angstrom,' Astronomical Journal, 1995, **109**, p. 1379.

Aragona, C., McSwain, M. V., Grundstrom, E. D., Marsh, A. N., Roettenbacher, R. M., Hessler, K. M., Boyajian, T. S., and Ray, P. S., 'The Orbits of the γ-Ray Binaries LS I +61 303 and LS 5039,' Astrophysical Journal, 2009, **698**(1), pp. 514–518.

Bailer-Jones, C. A. L., Rybizki, J., Fouesneau, M., Mantelet, G., and Andrae, R., 'Estimating Distance from Parallaxes. IV. Distances to 1.33 Billion Stars in Gaia Data Release 2,' Astronomical Journal, 2018, **156**(2), 58.

Bans, A. and Königl, A., 'A Disk-wind Model for the Near-infrared Excess Emission in Protostars,' Astrophysical Journal, 2012, **758**(2), 100.

Basu, S., Johnstone, D., and Martin, P. G., 'Dynamical Evolution and Ionization Structure of an Expanding Superbubble: Application to W4,' Astrophysical Journal, 1999, **516**(2), pp. 843–862.

[5]*https://www.cosmos.esa.int/web/gaia/dpac/consortium*

Bonnarel, F., Fernique, P., Bienaymé, O., Egret, D., Genova, F., Louys, M., Ochsenbein, F., Wenger, M., and Bartlett, J. G., 'The ALADIN interactive sky atlas. A reference tool for identification of astronomical sources,' Astronomy & Astrophysics Supplement, 2000, **143**, pp. 33–40.

Carpenter, J. M., Heyer, M. H., and Snell, R. L., 'Embedded Stellar Clusters in the W3/W4/W5 Molecular Cloud Complex,' Astrophysical Journal Supplement Series, 2000, **130**(2), pp. 381–402.

Choi, J., Dotter, A., Conroy, C., Cantiello, M., Paxton, B., and Johnson, B. D., 'Mesa Isochrones and Stellar Tracks (MIST). I. Solar-scaled Models,' Astrophysical Journal, 2016, **823**(2), 102.

Cutri, R. M. and et al., 'VizieR Online Data Catalog: AllWISE Data Release (Cutri+ 2013),' VizieR Online Data Catalog, 2013, II/328.

Cutri, R. M., Skrutskie, M. F., van Dyk, S., and et al., 'VizieR Online Data Catalog: 2MASS All-Sky Catalog of Point Sources (Cutri+ 2003),' VizieR Online Data Catalog, 2003, II/246.

Danks, A. C. and Dennefeld, M., 'An Atlas of Southern MK Standards from 5800 to 10,200A,' Publications of the Astronomical Society of the Pacific, 1994, **106**, p. 382.

Dennihy, E., Farihi, J., Fusillo, N. P. G., and Debes, J. H., 'A Word to the WISE: Confusion is Unavoidable for WISE-selected Infrared Excesses,' Astrophysical Journal, 2020, **891**(1), 97.

Dennison, B., Topasna, G. A., and Simonetti, J. H., 'Detection in Hα of a Supershell Associated with W4,' Astrophysical Journall, 1997, **474**(1), pp. L31–L34.

Dotter, A., 'MESA Isochrones and Stellar Tracks (MIST) 0: Methods for the Construction of Stellar Isochrones,' Astrophysical Journal Supplement Series, 2016, **222**(1), 8.

Elmegreen, B. G., 'Observations and Theory of Dynamical Triggers for Star Formation,' in C. E. Woodward, J. M. Shull, and J. Thronson, Harley A., editors, 'Origins,' volume 148 of *Astronomical Society of the Pacific Conference Series*, 1998 p. 150.

Fabricant, D., Fata, R., Roll, J., and et al., 'Hectospec, the MMT's 300 Optical Fiber-Fed Spectrograph,' Publications of the Astronomical Society of the Pacific, 2005, **117**(838), pp. 1411–1434.

Flewelling, H. A., Magnier, E. A., Chambers, K. C., and et al., 'The Pan-STARRS1 Database and Data Products,' arXiv e-prints, 2016, arXiv:1612.05243.

Fukuda, N., Miao, J., Sugitani, K., Kawahara, K., Watanabe, M., Nakano, M., and Pickles, A. J., 'Triggered Star Formation in a Bright-rimmed Cloud (BRC 5) of IC 1805,' Astrophysical Journal, 2013, **773**(2), 132.

Gaia Collaboration, Brown, A. G. A., Vallenari, A., Prusti, T., and et al., 'Gaia Data Release 2. Summary of the contents and survey properties,' Astronomy & Astrophysics, 2018, **616**, A1.

Gaia Collaboration, Prusti, T., de Bruijne, J. H. J., Brown, A. G. A., and et al., 'The Gaia mission,' Astronomy & Astrophysics, 2016, **595**, A1.

Gray, R. O. and Corbally, J., Christopher, *Stellar Spectral Classification*, Princeton University Press, 2009.

Green, G. M., Schlafly, E., Zucker, C., Speagle, J. S., and Finkbeiner, D., 'A 3D Dust Map Based on Gaia, Pan-STARRS 1, and 2MASS,' Astrophysical Journal, 2019, **887**(1), 93.

Hernández, J., Calvet, N., Briceño, C., Hartmann, L., and Berlind, P., 'Spectral Analysis and Classification of Herbig Ae/Be Stars,' Astronomical Journal, 2004, **127**(3), pp. 1682–1701.

Hodapp, K.-W., 'A K Imaging Survey of Molecular Outflow Sources,' Astrophysical Journal Supplement Series, 1994, **94**, p. 615.

Hunter, J. D., 'Matplotlib: A 2d graphics environment,' Computing in Science & Engineering, 2007, **9**(3), pp. 90–95.

Jacoby, G. H., Hunter, D. A., and Christian, C. A., 'A library of stellar spectra.' Astrophysical Journal Supplement Series, 1984, **56**, pp. 257–281.

Jordi, K., Grebel, E. K., and Ammon, K., 'Empirical color transformations between SDSS photometry and other photometric systems,' Astronomy & Astrophysics, 2006, **460**(1), pp. 339–347.

Jose, J., Kim, J. S., Herczeg, G. J., Samal, M. R., Bieging, J. H., Meyer, M. R., and Sherry, W. H., 'Star Formation in W3—AFGL 333: Young Stellar Content, Properties, and Roles of External Feedback,' Astrophysical Journal, 2016, **822**(1), 49.

Kiminki, M. M., Kim, J. S., Bagley, M. B., Sherry, W. H., and Rieke, G. H., 'The O- and B-Type Stellar Population in W3: Beyond the High-Density Layer,' Astrophysical Journal, 2015, **813**(1), 42.

Le Borgne, J. F., Bruzual, G., Pelló, R., Lançon, A., Rocca-Volmerange, B., Sanahuja, B., Schaerer, D., Soubiran, C., and Vílchez-Gómez, R., 'STELIB: A library of stellar spectra at R ∼2000,' Astronomy & Astrophysics, 2003, **402**, pp. 433–442.

Lefloch, B. and Lazareff, B., 'Cometary globules. II. Observational tests of radiation-driven implosion: the case of CG7S.' Astronomy & Astrophysics, 1995, **301**, p. 522.

Lim, B., Hong, J., Yun, H.-S., Hwang, N., Kim, J. S., Lee, J.-E., Park, B.-G., and Park, S., 'The Origin of a Distributed Stellar Population in the Star-forming Region W4,' Astrophysical Journal, 2020, **899**(2), 121.

Massey, P., Johnson, K. E., and Degioia-Eastwood, K., 'The Initial Mass Function and Massive Star Evolution in the OB Associations of the Northern Milky Way,' Astrophysical Journal, 1995, **454**, p. 151.

McKinney, W., 'Data structures for statistical computing in python,' in S. van der Walt and J. Millman, editors, 'Proceedings of the 9th Python in Science Conference,' 2010 pp. 56 – 61.

Mirabel, I. F., Rodrigues, I., and Liu, Q. Z., 'A microquasar shot out from its birth place,' Astronomy & Astrophysics, 2004, **422**, pp. L29–L32.

Normandeau, M., Taylor, A. R., and Dewdney, P. E., 'A galactic chimney in the Perseus arm of the Milky Way,' Nature, 1996, **380**(6576), pp. 687–689.

Ochsenbein, F., Bauer, P., and Marcout, J., 'The VizieR database of astronomical catalogues,' Astronomy & Astrophysics Supplement, 2000, **143**, pp. 23–32.

Oey, M. S., Watson, A. M., Kern, K., and Walth, G. L., 'Hierarchical Triggering of Star Formation by Superbubbles in W3/W4,' Astronomical Journal, 2005, **129**(1), pp. 393–401.

Panwar, N., Samal, M. R., Pandey, A. K., Jose, J., Chen, W. P., Ojha, D. K., Ogura, K., Singh, H. P., and Yadav, R. K., 'Low-mass young stellar population and star formation history of the cluster IC 1805 in the W4 H II region,' Monthly Notices of the Royal Astronomical Society, 2017, **468**(3), pp. 2684–2698.

Panwar, N., Samal, M. R., Pandey, A. K., Singh, H. P., and Sharma, S., 'Understanding Formation of Young, Distributed Low-mass Stars and Clusters in the W4 Cloud Complex,' Astronomical Journal, 2019, **157**(3), 112.

Paxton, B., Schwab, J., Bauer, E. B., Bildsten, L., Blinnikov, S., Duffell, P., Farmer, R., Goldberg, J. A., Marchant, P., Sorokina, E., Thoul, A., Townsend, R. H. D., and Timmes, F. X., 'Modules for Experiments in Stellar Astrophysics (MESA): Convective Boundaries, Element Diffusion, and Massive Star Explosions,' Astrophysical Journal Supplement Series, 2018, **234**(2), 34.

Pecaut, M. J. and Mamajek, E. E., 'Intrinsic Colors, Temperatures, and Bolometric Corrections of Pre-main-sequence Stars,' Astrophysical Journal Supplement Series, 2013, **208**(1), 9.

Pecaut, M. J., Mamajek, E. E., and Bubar, E. J., 'A Revised Age for Upper Scorpius and the Star Formation History among the F-type Members of the Scorpius-Centaurus OB Association,' Astrophysical Journal, 2012, **746**(2), 154.

Rauw, G. and Nazé, Y., 'X-ray and optical spectroscopy of the massive young open cluster IC 1805,' Astronomy & Astrophysics, 2016, **594**, A82.

Reynolds, R. J., Sterling, N. C., and Haffner, L. M., 'Detection of a Large Arc of Ionized Hydrogen Far above the Cassiopeia OB6 Association: A Superbubble Blowout into the Galactic Halo?' Astrophysical Journall, 2001, **558**(2), pp. L101–L104.

Rivera-Ingraham, A., Martin, P. G., Polychroni, D., and Moore, T. J. T., 'Star Formation and Young Stellar Content in the W3 Giant Molecular Cloud,' Astrophysical Journal, 2011, **743**(1), 39.

Robin, A. C., Reylé, C., Derrière, S., and Picaud, S., 'A synthetic view on structure and evolution of the Milky Way,' Astronomy & Astrophysics, 2003, **409**, pp. 523–540.

Roccatagliata, V., Bouwman, J., Henning, T., Gennaro, M., Feigelson, E., Kim, J. S., Sicilia-Aguilar, A., and Lawson, W. A., 'Disk Evolution in OB Associations: Deep Spitzer/IRAC Observations of IC 1795,' Astrophysical Journal, 2011, **733**(2), 113.

Roman-Lopes, A., Román-Zúñiga, C. G., Tapia, M., Hernández, J., Ramírez-Preciado, V., Stringfellow, G. S., Ybarra, J. E., Kim, J. S., Minniti, D., Covey, K. R., Kounkel, M., Suárez, G., Borissova, J., García-Hernández, D. A., Zamora, O., and Trujillo, J. D., 'Massive Stars in the SDSS-IV/APOGEE-2 Survey. II. OB-stars in the W345 Complexes,' Astrophysical Journal, 2019, **873**(1), 66.

Shi, H. M. and Hu, J. Y., 'Spectroscopic observations of young open clusters: IC 1805, NGC 654 and NGC 6823,' Astronomy & Astrophysicss, 1999, **136**, pp. 313–331.

Siess, L., Dufour, E., and Forestini, M., 'An internet server for pre-main sequence tracks of low- and intermediate-mass stars,' Astronomy & Astrophysics, 2000, **358**, pp. 593–599.

Silverberg, S. M., Kuchner, M. J., Wisniewski, J. P., and et al., 'Follow-up Imaging of Disk Candidates from the Disk Detective Citizen Science Project: New Discoveries and False Positives in WISE Circumstellar Disk Surveys,' Astrophysical Journal, 2018, **868**(1), 43.

Straižys, V., Boyle, R. P., Janusz, R., Laugalys, V., and Kazlauskas, A., 'The open cluster IC 1805 and its vicinity: investigation of stars in the Vilnius, IPHAS, 2MASS, and WISE systems,' Astronomy & Astrophysics, 2013, **554**, A3.

Sugitani, K., Fukui, Y., and Ogura, K., 'A Catalog of Bright-rimmed Clouds with IRAS Point Sources: Candidates for Star Formation by Radiation-driven Implosion. I. The Northern Hemisphere,' Astrophysical Journal Supplement Series, 1991, **77**, p. 59.

Sung, H., Bessell, M. S., Chun, M.-Y., Yi, J., Nazé, Y., Lim, B., Karimov, R., Rauw, G., Park, B.-G., and Hur, H., 'An Optical and Infrared Photometric Study of the Young Open Cluster IC 1805 in the Giant H II Region W4 ,' Astrophysical Journals, 2017, **230**(1), 3.

Sung, H. and Lee, S.-W., 'UBV(Ikc) CCD Photometry of Young Open Clusters. I. IC 1805,' Journal of Korean Astronomical Society, 1995, **28**(2), pp. 119–137.

Tielens, A. G. G. M., 'Interstellar polycyclic aromatic hydrocarbon molecules.' Annual Review of Astronomy and Astrophysics, 2008, **46**, pp. 289–337.

Torres-Dodgen, A. V. and Weaver, W. B., 'An Atlas of Low-Resolution Near-Infrared Spectra of Normal Stars,' Publications of the Astronomical Society of the Pacific, 1993, **105**, p. 693.

Townsley, L. K., Broos, P. S., Garmire, G. P., Bouwman, J., Povich, M. S., Feigelson, E. D., Getman, K. V., and Kuhn, M. A., 'The Massive Star-Forming Regions Omnibus X-Ray Catalog,' Astrophysical Journal Supplement Series, 2014, **213**(1), 1.

van der Walt, S., Colbert, S. C., and Varoquaux, G., 'The numpy array: A structure for efficient numerical computation,' Computing in Science & Engineering, 2011, **13**(2), pp. 22–30.

Vasilevskis, S., Sanders, W. L., and van Altena, W. F., 'Membership of the open cluster IC 1805.' Astronomical Journal, 1965, **70**, p. 806.

Wang, S. and Chen, X., 'The Optical to Mid-infrared Extinction Law Based on the APOGEE, Gaia DR2, Pan-STARRS1, SDSS, APASS, 2MASS, and WISE Surveys,' Astrophysical Journal, 2019, **877**(2), 116.

West, J. L., English, J., Normandeau, M., and Landecker, T. L., 'The Fragmenting Superbubble Associated with the H II Region W4,' Astrophysical Journal, 2007, **656**(2), pp. 914–927.

Williams, G. G., Olszewski, E., Lesser, M. P., and Burge, J. H., '90prime: a prime focus imager for the steward observatory 90-in. telescope,' in A. F. M. Moorwood and M. Iye, editors, '90prime: a prime focus imager for the Steward Observatory 90-in. telescope,' volume 5492 of *Society of Photo-Optical Instrumentation Engineers (SPIE) Conference Series*, 2004 pp. 787–798.

Williams, J. P. and Cieza, L. A., 'Protoplanetary Disks and Their Evolution,' Annual Review of Astronomy and Astrophysics, 2011, **49**(1), pp. 67–117.

Wolff, S. C., Strom, S. E., and Rebull, L. M., 'The Evolution of Circumstellar Disks Surrounding Intermediate-mass Stars: IC 1805,' Astrophysical Journal, 2011, **726**(1), 19.

SECTION

3. THE EVOLUTION OF DISK-BEARING YSOS IN IC 1805

In Paper I, we identified 75 irx sources using dereddened SEDs. During the analysis of probable cluster members, one source, named EM* MWC 50, was ruled to be a post-main-sequence star due to its position in the H-R diagram. This section will analyze the remaining 74 irx cluster members, present the results of disk modeling using a Markov chain Monte Carlo (MCMC) algorithm, and discuss the evolutionary implications. The contents of this section are intended to be adapted into a second journal article.

3.1. IDENTIFYING DISK-BEARING YSOS

Dereddened SEDs were produced using the spectral types identified in Paper One, extinctions computed from $A_V = 4.71 * E(r - i)$, and the extinction laws derived from Green *et al.* (2019) and Wang and Chen (2019). All sources whose SEDs showed an irx were automatically considered cluster members. Additional YSO membership criteria used were: Hα emission, X-ray emission, proper motion membership, and extinctions within $1.6 \leq A_V \leq 4.2$ mag. Among the 74 irx sources, 54% had Hα emission measured from their spectra, 39% had X-ray emission detected, 5% are proper motion members, and 94% are within the extinction bounds. However, with extinction uncertainties taken into account, all irx sources are within the cluster extinction bounds.

SEDs for B, A, and F-type stars were normalized to the PanSTARRS *r* band, while G, K, and M-type stars were normalized to the 2MASS *J* band. These normalization schemes are utilized to provide an accurate SED based on the average wavelength at which the flux of these different stars peaks. This also helps resolve differences in photometry which can

result from the observations occurring at different times. The PanSTARRS PS1 survey ran between 2010-2014, 2MASS between 1997-2001, and Spitzer IC 1805 observations were taken in 2005 and 2006 using the MIPS and IRAC instruments, respectively. AllWISE is a combination of data from the WISE cryogenic survey in 2010 and NEOWISE post-cryogenic survey that extended into 2011 (note, the NEOWISE survey observed minor solar system objects such as asteroids and comets). Disagreement between PanSTARRS and infrared data is particularly evident in several G and K type sources and is likely due to variability common in YSOs. Several sources were not fit with a disk model because the disagreement caused ambiguity in judging at which wavelength the irx initially begins, and sometimes could result in a source resembling a pre-transition disk or transition disk.

The 90Prime photometry presented in Paper I were not utilized in the disk fits presented here. Both V and I_C bands overlapped the PanSTARRS PS1 photometry and produced less accurate photometry. The Spitzer Enhanced Imaging Products (SEIP) database provides two aperture photometries for each IRAC band. We utilized flux densities from the smaller 3.8 arcsec diameter aperture for the IRAC bands, and the point-spread function (PSF) flux density for the MIPS 1 band. Additionally, each suspected irx source was verified by inspection of the super mosaics corresponding to each band the infrared excess appeared in. To be considered a disk candidate, each suspected irx band was required to have a corresponding point source in its super mosaic.

3.2. MODELING

3.2.1. Disk Modeling. The blackbody disk models of Chiang and Goldreich (1997), which correspond to flat and flared disk geometries, are adapted and implemented with an MCMC sampler to estimate the most probable fit to a disk+star SED. The temperature distribution of dust grains within the disk are modified from those in the Introduction as,

$$T_d(r) = \left(\frac{\alpha}{2}\right)^{1/4} T_* \left(\frac{R_*}{r}\right)^p , \tag{3.1}$$

for a flared disk, and

$$T_d(r) = \left(\frac{2}{3\pi}\right)^{1/4} T_* \left(\frac{R_*}{r}\right)^p \tag{3.2}$$

for a flat disk. Above, α is the grazing angle at which protostellar flux strikes the disk, T_* and R_* are the effective temperature and radius of the protostar, r is the distance from the center of the protostar, and p is the power law index.

The disk SED is then computed as

$$\lambda F_\lambda = 2\pi\lambda 10^{-f} \int_{r_i}^{r_o} r B_\lambda(T_d) dr, \tag{3.3}$$

where f is a scaling parameter that primarily accounts for the distance to and orientation of the source and B_λ is the Planck distribution. This integral is numerically approximated from an inner disk radius r_i to an outer disk radius r_o. The sampling process is performed on the sum of the disk SED and stellar blackbody SED which is normalized to either the r or J band.

SEDs were fit with four possible parameters: a scaling parameter, the temperature power law index, the inner disk radius, and the outer disk radius. The two parameters universal to all flared and flat disk fits are the scaling parameter f and the temperature power law index p. In the flared and flat temperature distributions above, the power law parameter p is sampled around the canonical “flared" $p = 0.5$ or “flat" $p = 0.75$ power law values (see e.g., Kenyon and Hartmann 1987; Adams *et al.* 1987). The outer disk radius is included only for sources which have MIPS 1 fluxes. This parameter was included in the sampling process as it was found to have some effect on the disk+star SED at 24 μm.

It is probable that all disk-bearing irx sources here have orientations, relative to Earth, that are approximately face-on. Chiang and Goldreich (1999) investigated how disk orientation would affect their radiative and hydrostatic equilibrium disk models. For inclinations less than 45°, the SED is insensitive to the inclination. However, at angles greater than 45° the flux in optical to mid-infrared wavelengths is greatly extinguished

by the outer disk along the line of sight. Given this restriction along with the adopted distance of 2.3 kpc to the cluster, it is unlikely that an optical spectrum was obtained for any disk-bearing source at a significant inclination. So, all sources are assumed to have face-on orientations.

For sources with an irx only in the IRAC 4 and MIPS 1 bands, a simple blackbody curve was fitted to the irx. This sampling only involved a scaling factor and the blackbody temperature, which was allowed to vary between 100 K and 2000 K. The upper bound represents a typical estimate for the dust sublimation temperature. Thus, this blackbody curve is representative of the inner dust rim in sources which have cleared out inner disk holes (Dullemond and Monnier, 2010). A theoretical dust rim radius is listed on the fitted SED of each of these sources.

3.2.2. *Emcee* Implementation. The disk modeling procedure utilizes the *emcee* ensemble sampler created by Foreman-Mackey *et al.* (2013). To be clear, *emcee* does not optimize the parameters. Instead, it creates sets of “walkers" in each parameter space which essentially test the total probability. In this case, the total log probability is the sum of the likelihood function and prior distribution. The samples it draws from the total log probability using the *stretch move* algorithm form the posterior distributions of the parameters. By using a large enough number of walkers in combination with a large number of iterations, the posterior distributions should cluster around the values which minimize the likelihood function relative to the prior information.

A recent review by Andrews (2020) notes that modeling the infrared SED of disk-bearing stars does not produce unique fits. There are often several sets of parameters that create fits to the SED that look acceptable, but may not correspond to the correct physical parameters. Some of this ambiguity can be avoided by combining the modeling with spatially resolved information of the disks. The purpose of using the *emcee* sampler in this study is to mitigate some of this ambiguity by allowing walkers to explore the parameter spaces and find the most likely set of parameters. In some cases, *emcee* was not able

to produce ideal posterior distributions, the shape of which should reflect the choice of likelihood function. This result is not a shortcoming of the MCMC process, but rather the choice of disk models being implemented to a variety of disks in different evolutionary stages and the limited data constraining the models.

3.2.3. Choosing Distributions. The first step in implementing Bayesian inference is choosing the proper distributions to represent the priors and likelihood function. For the sampling performed in this study, a uniform prior distribution was chosen for parameters based on typical values of disk parameters found in the literature. The scaling parameter f was allowed to sample between $36.5 < f < 42.0$, where f primarily accounts for the distance to the star. That is, the distance d can be expressed in terms of f as, $d \sim \sqrt{10^f}$. For example, an $f = 39.705$ is roughly 2300 pc. However, the inclination of the disk is also contained within this parameter. The temperature power law p is allowed to sample between $0.4 < p < 0.8$, for flared disks whose SEDs visually fall into the optically thick category. For optically thin disks, the power law of the flat disk model was allowed to vary between $0.5 < p < 1.5$. The bounds reflect the canonical power laws for flared and flat temperature distributions 0.5 and 0.75, respectively. The extension of the bounds above and below these canonical values allow for the *emcee* walkers to explore around these bounds, and also to aid in showing which disk-bearing sources deviate from these canonical values.

The other two parameters that could be included in the prior distribution, depending on the SED being fit, were the inner and outer disk radii. If an SED had clear indication of an inner disk hole, then the inner disk radius was allowed to sample between $R_* < R_{\rm in} < 2$ AU. These values are based on the wavelengths being observed which typically correspond to radii less than 10 AU from the protostar. If an SED had a MIPS1 flux, then the outer disk radius was included as a parameter which sampled between 2 AU $< R_{\rm out} <$ 200 AU. The reason the lower bound is so close to the inner disk is due to the presence of several disk-bearing sources in which the MIPS 1 point sits below the expected disk+star SED, requiring warmer dust.

A Gaussian distribution is used for the likelihood function. This means that the photometry and its associated errors are assumed to be normally distributed and independent. For x_i random variables, the total probability P is given by the product of the individual probability density functions $P = P(x_1)P(x_2)...P(x_i)$.

$$P = \prod_i \frac{1}{\sqrt{2\pi\sigma^2}} \exp\left(-\sum_i \frac{(x_i - \mu_i)^2}{2\sigma_i^2}\right), \tag{3.4}$$

where x_i represents the normally distributed random variable, μ_i is the expected value, and σ_i^2 is the variance associated with the random variable. To make the computations easier, the logarithm of the total probability, prior plus the likelihood, is taken. This transforms the Gaussian likelihood into,

$$\mathrm{Log}(P) = -\frac{1}{2}\sum_i \left(\frac{(x_i - \mu_i)^2}{\sigma_i^2} + \mathrm{Log}(2\pi\sigma_i^2)\right). \tag{3.5}$$

In terms of fluxes, this looks like,

$$\mathrm{Log}(P) = -\frac{1}{2}\sum_\lambda \left(\frac{((\lambda F_\lambda)_{obs} - (\lambda F_\lambda)_{model})^2}{\sigma_{obs,\lambda}^2} + \mathrm{Log}(2\pi\sigma_{obs,\lambda}^2)\right). \tag{3.6}$$

A total log probability that uses a uniform prior will return the sum of the prior and likelihood for each iteration. The uniform prior simply returns a 0 if the proposed parameter values are within the bounds, or it returns a negative infinity. In the latter case, the proposed move is rejected and the walker remains in the same location in parameter space.

3.3. HERTZSPRUNG-RUSSELL DIAGRAM AND RESULTS OF DISK MODELING

Table 3.1 presents the results of the flared and flat disk modeling as well as the SED slopes which were obtained using a simple linear regression. Parameter estimates are provided for the scaling factor f, inner disk radius R_{in} (when present), and temperature

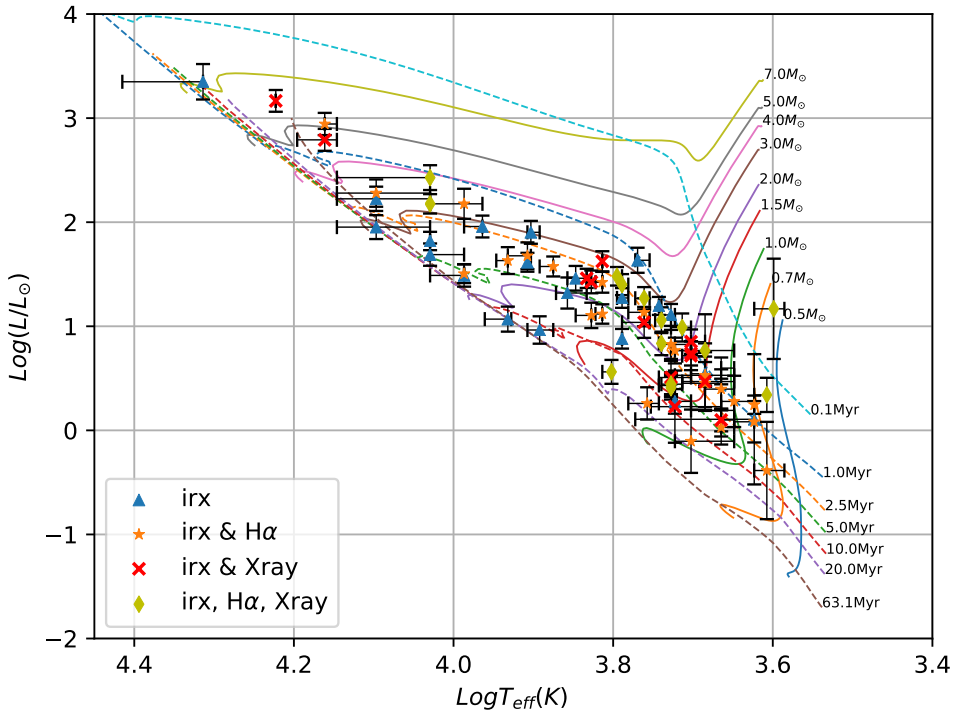

Figure 3.1. H-R diagram of all disk-bearing sources using the MIST evolutionary models. Solid lines are mass tracks and dashed lines are isochrones.

power law p. Standard deviations are not provided for power laws since they were primarily fit to a precision higher than has physical meaning. In the disk type category, “thick" refers to an optically thick disk, “thin" an optically thin disk, “pt" a pre-transition disk, “t" a transition disk, “trunc" refers to sources whose MIPS 1 flux could indicate a truncated disk, and “enh" refers to sources whose SEDs and proximities to O-stars suggest that their flared outer disks could be enhanced by external photoevaporative flux. Table 3.2 presents the results of sources either fit with the dust rim approximation or sources not modeled. Figure 3.1 shows an H-R diagram of all disk-bearing sources. It can be seen that some of this sample contains sources identified in Paper I as candidate members of an earlier generation of stars. Most disk-bearing sources sit between the 1 Myr and 5 Myr isochrones.

Table 3.1. Best fit parameters for flared and flat disk models.

RA(J2000) (hmmss.ss)	Dec(J2000) (deg ' ")	f	R_{in} (AU)	p	$\alpha_{\rm IRAC}$	α_{LW}	Disk Type	Model	Assoc. Criteria
2 28 43.41	+61 31 34.30	41.1798 ± 0.0079		0.66	-1.63		thin	flat	irx,Ha,x
2 28 43.45	+61 29 41.60	39.0836 ± 0.0006		0.37	0.10	-0.10	pt	flared	irx
2 29 35.91	+61 15 56.80	39.6768 ± 0.1813	0.023 ± 0.064	0.54	-0.70		thick	flared	irx,Ha
2 29 40.18	+61 10 20.40	39.4530 ± 0.0212	0.042 ± 0.000	0.62			thick	flared	irx
2 30 50.77	+61 30 22.40	39.0790 ± 0.0561		0.48	-0.79	-0.97	thin?/pt?	flared	irx,x
2 31 15.10	+61 19 21.20	39.7395 ± 0.0013		0.42	-0.47	0.27	pt	flared	irx
2 31 21.12	+61 38 22.01	40.2940 ± 0.0022		0.56	-1.76	0.15	pt	flared	irx
2 31 59.24	+61 39 29.60	39.1962 ± 0.0544	0.013 ± 0.003	0.53	-0.89	-0.38	thick	flared	irx,ha
2 32 02.45	+61 37 13.29	39.8057 ± 0.1866	0.036 ± 0.047	0.79	-1.51	-1.76	thin/trunc	flat	irx
2 32 06.99	+61 32 42.90	38.0784 ± 0.0140	0.018 ± 0.000	0.46	-1.08	0.11	pt-t/enh	flared	irx,Ha,x
2 32 07.04	+61 45 34.00	39.6227 ± 0.0087		0.60	-1.50		thin	flat	irx, Ha,x
2 32 07.91	+61 24 51.39	39.1186 ± 0.0086		0.67	-1.00	-1.20	thin	flat	irx,ha,x
2 32 15.94	+61 32 11.18	40.1522 ± 0.0652		0.60	-1.37	-1.91	thin/trunc	flat	irx,x
2 32 17.19	+61 20 39.11	37.5587 ± 0.0015	0.007 ± 0.000	0.54	-0.70		thick	flared	irx,Ha,x
2 32 21.40	+61 33 00.64	38.9116 ± 0.0276	0.018 ± 0.000	0.46	-1.32	-0.16	pt/enh	flared	irx,ha,x
2 32 23.51	+62 09 15.61	40.1564 ± 0.0402		0.46			thin	flat	irx,
2 32 33.94	+61 43 56.84	38.1817 ± 0.3055	0.085 ± 0.019	0.67	-1.48	0.69	t	flat	irx,Ha
2 32 34.10	+61 21 17.55	39.2324 ± 0.0028	0.005 ± 0.000	0.44	-1.11	0.39	pt	flared	irx,x
2 32 39.55	+61 26 57.87	37.4579 ± 0.4144	0.026 ± 0.007	0.82	0.43	-0.82	pt?-t?/trunc	flat	irx,x
2 32 42.53	+61 21 00.90	39.5092 ± 0.0041		0.65	-1.45	-1.10	thin	flat	irx,x
2 32 43.16	+61 30 58.91	38.8207 ± 0.0002		0.40	-0.06	-0.27	pt?	flared	irx,ha,x
2 32 43.28	+61 33 35.31	38.6394 ± 0.0140	0.018 ± 0.000	0.72	-0.74	-1.06	thick/trunc?	flat	irx,x
2 32 43.77	+61 28 09.79	39.6134 ± 0.0007		0.43	0.01		thick	flared	irx,Ha
2 32 44.98	+61 30 55.80	39.0260 ± 0.0035		0.60	-0.91		thin?	flat	irx,Ha
2 32 45.91	+61 29 11.17	39.4729 ± 0.0011		0.44	-1.10	0.77	pt/enh	flared	irx,Ha,x
2 32 47.08	+61 22 46.08	39.7763 ± 0.0012		0.58	-0.89		thick	flat	irx,
2 32 50.45	+61 28 57.40	38.7794 ± 0.0025		0.49	-0.91	0.03	pt	flared	irx,ha,x
2 32 50.83	+61 32 16.70	38.6062 ± 0.0016		0.76	-1.37	-1.19	thin	flat	irx,ha
2 32 58.95	+61 25 45.20	39.2984 ± 0.1846	0.035 ± 0.115	0.76	-1.47	-1.16	thin	flat	irx,ha,x,pm
2 33 00.78	+61 26 09.74	39.2139 ± 0.0011		0.48	-1.57	-0.29	pt	flared	irx,Ha,x
2 33 06.52	+61 38 52.91	38.8898 ± 0.0295	0.018 ± 0.000	0.70	-0.94	-1.12	thin	flat	irx
2 33 11.02	+61 46 24.80	38.9288 ± 0.0006		0.54	-1.25	0.22	thick?-pt	flared	irx,ha
2 33 11.42	+61 31 15.01	38.4538 ± 0.0026		0.85	-1.63		thin	flat	irx,x
2 33 19.84	+61 20 41.94	39.0818 ± 0.1628	0.007 ± 0.006	0.48	-0.48	-0.12	thick	flared	irx,Ha
2 33 20.14	+61 22 10.61	39.5923 ± 0.0024		0.68	-1.43		thin	flat	irx,Ha
2 33 22.56	+61 27 18.30	38.6158 ± 0.0007		0.64	-1.11	-0.84	thin	flat	irx,ha
2 33 23.16	+61 31 48.20	38.8168 ± 0.0037		0.64	-1.02		thin	flat	irx,x
2 33 30.72	+61 39 22.20	38.7939 ± 0.0006		0.51	-1.49	-0.07	pt	flared	irx,ha,x
2 33 36.64	+61 38 48.50	38.8764 ± 0.0012		0.64	-1.11	-0.83	thin	flat	irx,ha
2 34 10.27	+61 24 40.42	37.7372 ± 0.0322	0.034 ± 0.000	1.17	-0.94		thick-pt	flat	irx,Ha,x
2 34 13.98	+61 48 06.55	40.4818 ± 0.0005		0.42	0.76	0.11	thick	flared	irx,Ha
2 34 14.20	+61 09 30.80	38.6052 ± 0.0146	0.043 ± 0.000	0.89	-0.96	-1.43	thick	flat	irx
2 34 14.81	+61 42 11.70	41.7542 ± 0.1266	0.256 ± 0.009	0.55	-2.43	-0.87	pt-t	flared	irx
2 34 15.04	+61 42 01.54	39.9918 ± 0.0063	0.003 ± 0.000	0.40	-1.86	0.93	pt	flared	irx,Ha
2 34 18.89	+61 24 49.10	39.4039 ± 0.0022		0.60	-1.01		thin	flat	irx,Ha,x
2 34 45.42	+61 29 54.70	38.4851 ± 0.0013		0.50	-0.95	-0.54	thick	flared	irx,Ha
2 34 50.52	+61 24 16.71	40.1313 ± 0.0013	0.103 ± 0.000	0.50	-0.48		t?	flared	irx
2 34 59.40	+61 19 59.00	39.6950 ± 0.0009	0.016 ± 0.000	0.45	-0.02		thick	flared	irx,ha
2 35 15.32	+61 48 03.29	38.7997 ± 0.0131		0.61			thin?	flat	irx,Ha
2 35 40.67	+61 26 09.67	38.7502 ± 0.0049		0.55	-1.74	-0.19	pt	flared	irx,Ha
2 36 05.56	+61 22 05.10	37.8313 ± 0.2600	0.064 ± 0.004	0.72	0.35	-0.93	thick/trunc?	flared	irx,ha

A table of the 51 irx sources fit with the flat and flared disk models. Columns 3-5 give the best fit results (medians and standard deviations) for the scaling parameter, inner disk radius, and power laws. Columns 6 and 7 list the SED slopes of the IRAC points as well as the slope between the IRAC 4 and MIPS 1 band (α_{LW}), where the average error in IRAC slope is 0.2. Sources with blank inner disk radii were not fit with this parameter. Blank SED slopes refer to sources which lacked enough IRAC and /or MIPS data to estimate a slope. Disk Type refers to the class of disk the SED represents based on the IRAC slope and fit SED. The disk classes used are described in detail in Section 3.4. Association Criteria refers to the YSO criteria each source meets, in addition to irx. In this category, Ha and ha refer to Hα emission with equivalent widths >10 Åand $\leq$ 10 Å, respectively, x refers to X-ray emission, and PM refers to a proper motion member.

Table 3.2. Best fit parameters for dust rim sources & properties of sources not modeled.

RA(J2000) (hmmss.ss)	Dec(J2000) (deg ' ")	f_{rim}	T_{rim} (AU)	$\alpha_{\rm IRAC}$	α_{LW}	Disk Type	Assoc. Criteria
2 28 27.53	+61 56 32.89	17.7796 ± 0.2437	162.3 ± 17.2	-2.49	-0.93	t	irx
2 32 08.75	+61 33 01.91			-1.69	0.49	t/enh	irx,Ha
2 32 27.46	+61 25 08.27			-1.52		8 μm	irx?,x
2 32 28.05	+61 26 51.08			-1.73		8 μm	irx?,x
2 32 37.41	+61 32 19.32	18.1392 ± 0.0072	299.2 ± 1.2	-2.43	-0.93	t	irx,x,pm
2 32 38.60	+61 32 05.00			-2.37		8 μm	irx?,x
2 32 42.69	+61 28 12.31			-2.07		8 μm	irx?
2 32 43.53	+61 26 31.96	18.7498 ± 0.0179	390.1 ± 3.9	-2.54	-1.63	t	irx,x,pm
2 32 51.54	+61 43 46.75			-1.41	-0.15	pt-t	irx,Ha
2 32 58.84	+61 25 53.77			-1.79		8 μm	irx?,Ha
2 33 24.21	+61 47 01.74	16.1751 ± 0.1499	117.9 ± 7.5	-2.61	1.95	t	irx
2 33 26.48	+61 41 29.10			-1.00	-0.27	t	irx,ha
2 33 38.87	+61 40 15.00	18.0043 ± 0.0258	205.5 ± 3.2	-2.49	-0.20	t	irx
2 34 00.42	+61 32 15.30			-0.73	0.00	pt-t	irx,Ha
2 34 12.66	+61 34 02.26			-2.64	-2.49	t?	irx
2 34 16.92	+61 42 05.61			-2.11	-0.41	pt-t	irx
2 34 22.11	+61 45 26.00			-1.72	-0.68	t	irx,Ha
2 34 24.56	+61 32 53.80	18.9833 ± 0.0108	437.4 ± 2.4	-2.16	-2.03	t	irx,Ha
2 34 26.38	+61 41 43.50			-2.28		8 μm	irx?
2 34 35.87	+61 33 35.63			-1.02	-0.27	pt-t	irx,Ha,x
2 34 45.65	+61 26 14.30			-2.53		8 μm	irx?
2 35 02.23	+61 22 30.43			-2.20		8 μm	irx?
2 35 53.69	+62 00 11.80	19.7548 ± 0.0110	1390 ± 13.3	-2.16		thin?-t	irx

A table of the 23 irx sources either fit with the dust rim approximation or not fit with a disk model. Columns 3 and 4 give the best fit parameters (medians and standard deviations) for the scaling parameter f_{rim} and dust rim temperature T_{rim}. The remaining columns refer to the same criteria listed in Table 3.1. 8 μm irx sources were not assigned a disk type as their infrared excesses are quite uncertain. See Paper I for a brief discussion of these sources.

3.4. DISCUSSION

In the following sections, the disk types assigned to all modeled disk-bearing sources are first described in regards to their SED appearance and physical interpretations in the literature. Then the results of the disk modeling are discussed. The evolutionary status of disk-bearing sources is discussed relative to their disk modeling parameters and SED slopes. Lastly, several sources which displayed a deficit in their MIPS 1 flux are detailed and several issues encountered in the disk modeling process and how they effect best fit parameters are addressed.

3.4.1. Categories and Physical Interpretations of Disk Types. A total of 58 sources were fit using the *emcee* sampler. Seven of these sources were fit with the simple blackbody model approximation of the inner dust rim. Of the remaining 51 sources, 27 were fit with the flared disk model and 24 with the flat disk model. These sources were categorized into four types of disks based on the IRAC and 8-24 μm slopes of their SEDs ($\alpha_{\rm IRAC}$ and α_{LW}, respectively), as well as the best fit parameters from the modeling process: optically thick, optically thin, pre-transition, and transition disks. The IRAC slope ranges that correspond to optically thick, optically thin, and transition disks are provided in Section 3.4.3, while the 8-24 μm slope is required to identify pre-transition disks. Sources that were not fit with a disk model either possessed an irx at only the IRAC 4 band or a discrepancy between their PanSTARRS photometry and infrared photometry. For the former, a single photometric band displaying an irx is not enough information to sample several disk parameters. For the latter, the discrepancy in photometry, which is likely due to the variability in luminosity of these largely G and K-type YSOs, called into question where the initial excess in flux began in the SED (and, thus, the type of disk).

Following Wolff *et al.* (2011), SEDs categorized as possessing optically thick disks displayed an excess in the *H* band and all further bands. This corresponds roughly with “Flat Spectrum" and early Class II SEDs discussed in the Introduction which are relative to the slope determined by fitting a linear regression to the flux from 2-24 μm. Lada *et al.* (2006) noted in their study of IC 348, that flared optically thick sources often had the strongest Hα emission lines, which is a signature of matter accreting onto the protostar. Since accretion is a signature of young circumstellar disks, optically thick disks have also been referred to as “primordial" disks (see e.g., Mamajek 2009).

Sources identified as optically thin disks display an excess which also starts around the *H* band and continues into longer wavelengths. However, the excess emission steadily decreases at longer wavelengths unlike in optically thick disks. Hernández *et al.* (2010) referred to these as “evolved disks", Lada *et al.* (2006) called these “anemic" disks, and

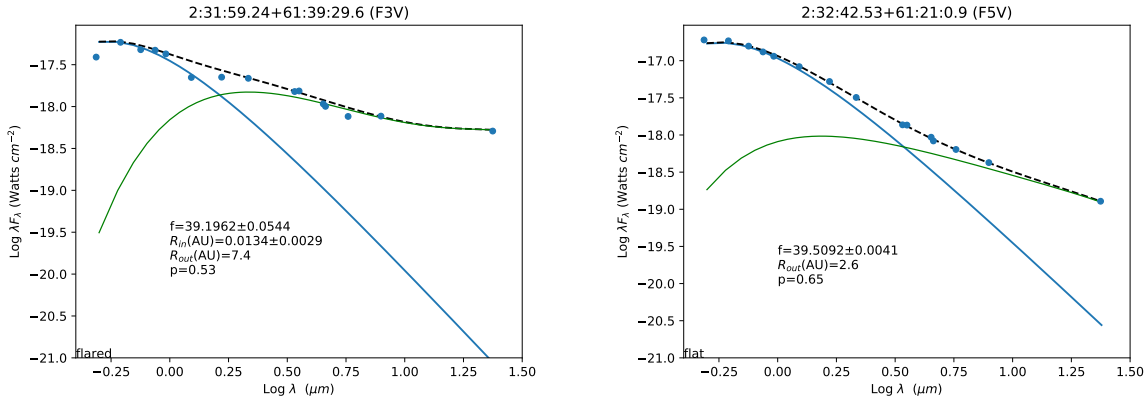

(a) (b)

Figure 3.2. SEDs of optically thick (a) and optically thin (b) disks fit with the flared disk model and flat disk model, respectively. The spectra of both (a) and (b) exhibit signs of weak Hα emission, while (b) is also an X-ray emission source. The solid blue line is the protostellar blackbody, the solid green line is the disk SED, and the dashed black line is the total disk+star SED.

Currie *et al.* (2009) called these “homologously depleted" disks. Here, the term optically thin is chosen as it more accurately describes the gradual decline in excess emission of an SED compared to the optically thick disks. Sicilia-Aguilar *et al.* (2011) and Espaillat *et al.* (2012) found that disk models which incorporate dust settling can accurately reproduce the SEDs of optically thin sources. Since dust settling is a function of the lifetime of a disk, these disks are typically regarded are being older than optically thick disks. Figure 3.2 shows example SEDs of (a) optically thick and (b) optically thin disks that have been fit with the flared and flat disk models, respectively.

The distinction between optically thin, pre-transition, and transition disks in this study is based, in part, on the distinctions of Espaillat *et al.* (2014). Here, the SED of an object identified as a pre-transition disk displays excess emission in the near to mid-infrared bands similar to an optically thin source while having optically thick excess emission in the MIPS 1 band (sometimes also at the IRAC 4 band). Wolff *et al.* (2011) referred to such sources as “thin/thick" disks. Sung *et al.* (2017) used the following criteria to

photometrically identify pre-transition disks: $-1.8 < \alpha_{\rm IRAC} < -0.3$ and $\alpha_{LW} > 0.3$. Based on disk modeling results, a pre-transition disk should, instead, have an 8-24 μm slope of $\alpha_{LW} \gtrsim -0.2$. Espaillat *et al.* (2012) fit the SEDs of such sources using a combination of an optically thick inner and outer disk that is separated by an optically thin gap. This suggests that pre-transition disks have begun the process of clearing out the inner disk caused by processes such as photoevaporative flux from the protostar and/or planet formation. In terms of age, Currie and Kenyon (2009) and Hernández *et al.* (2010) suggest that optically thin disks and pre-transitional disks represent two different evolutionary paths for circumstellar disks. That is as optically thick disks age, they can transform into optically thin or pre-transitional objects depending on which processes, such as dust settling or planet formation, are more prominent within the disks.

Sources labeled as transition disks possess SEDs that show no excess in the near-infrared, little to no excess in the mid-infrared, and an excess at the 24 μm MIPS 1 band. This lack of excess emission at near to mid-infrared wavelengths was attributed to be presence of an inner disk hole that has developed by several possible mechanisms such as photoevaporation, planet formation, or growth in dust grains (Espaillat *et al.*, 2014). Compared to the previous categories of disks, SEDs displaying transition disks are expected to be the oldest. The term debris disk is typically applied to objects which have dissipated their transition disks, and instead sustain a collection of small dust grains (Hughes *et al.*, 2018). This collection of dust grains can cause a small infrared excess to appear in the spectrum of a star with such a disk. Since the designation of debris disk requires knowledge of the entirety of a disk, all objects displaying small excesses at longer wavelengths were labeled as transition disks. Figure 3.3 shows example SEDs of a (a) pre-transition disk and (b) transition disk which were fit with a flared disk model and simple blackbody dust rim, respectively.

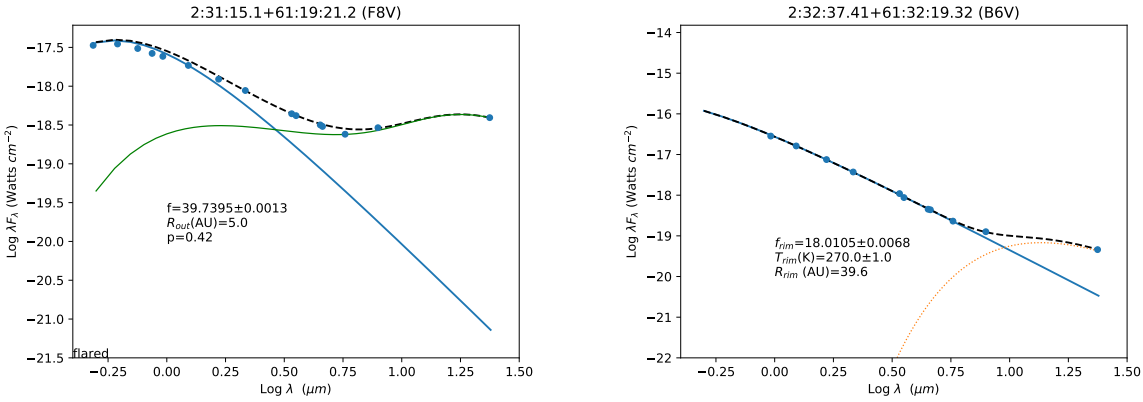

(a) (b)

Figure 3.3. SEDs of a (a) pre-transition disk and (b) transition disk fit with the flared disk model and blackbody dust rim model, respectively. Source (b) is an X-ray emission source and also a proper motion member of IC 1805. The lines of SED (a) are the same as described in Figure 3.2, while the orange dotted line in (b) represents the blackbody dust rim. The theoretical dust rim radius listed on (b) is computed from the best fit temperature T_{rim}.

3.4.2. Implications of Best Fit Disk Modeling Parameters. Table 3.1 lists the best fit parameters of three out of four possible parameters included in the models. The outer disk radii is excluded because it is viewed as a nuisance parameter. It was included in the sampling process as it is needed to fit sources with 24 μm emission. However, large changes in the outer disk radii result in small changes to the SED at 24 μm. So, the errors accompanying this parameter are often large. The flared and flat dust temperature approximations were found on occasion to underestimate the dust temperature in the inner disk, which sometimes leads to underestimates of the disk flux over the wavelength range being modeled. This is apparent when comparing between the flat and flared temperature distributions with the superheated surface and interior temperature distributions of Chiang and Goldreich (1997), two components of their radiative and hydrostatic equilibrium disk model (see Figure 3.4).

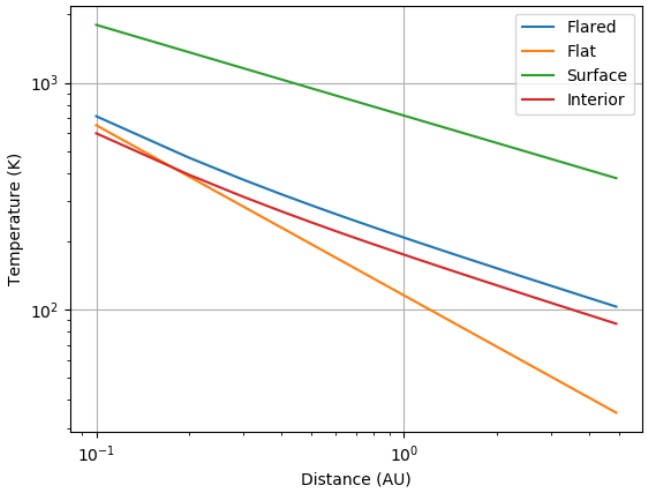

Figure 3.4. A comparison of the flared and flat temperature distributions to the surface and interior disk layers of Chiang and Goldreich (1997). These were computed for a stellar temperature of 6720 K.

This underestimation of dust temperature ultimately leads to small inner disk radii estimates and, occasionally, predictions of too much flux in the PanSTARRS and 2MASS bands. Overestimates in the PanSTARRS and 2MASS fluxes were the result of the steeper declines in dust temperatures of the flared and flat models in the inner disk. To fit the irx in sources, *emcee* would use the scaling parameter to effectively raise the dust temperature and then lower the inner disk radius to try and fit the initial excess in flux. In many sources, the model could not distinguish between the protostellar photosphere and the beginning of the disk which caused the walkers in the sampling process to crowd around the lower bound of the prior distribution while proposed positions in the Markov chain were rejected. If walkers in one parameter space get stuck, then, to an extent, so will the walkers in the other parameter spaces. So, many sources had their inner disk radii set to the photosphere which allowed the other walkers to explore unhindered.

The sharp drop in dust temperatures for the flared and flat distributions could also cause the model to overestimate the disk flux in the PanSTARRS and 2MASS bands. This occurred as the sampler fit more fluxes at longer wavelengths and overestimated the disk

fluxes at shorter wavelengths. It should also be noted that while the marginalization of the total log probability moves walkers in directions such that the difference between the observed and model flux values are brought closer to zero, it does not distinguish if the observed flux values lie above or below the protostellar blackbody. That is, the likelihood function marginalizes over the square of the difference. So, sources which have PanSTARRS photometry that falls below the protostellar blackbody are viewed by *emcee* as possessing an irx. To avoid this issue, these SEDs were sampled only in the 2MASS, AllWISE, and Spitzer bands.

Despite these shortcomings of the disk models, the best fit parameters still provide some useful diagnostics. Optically thick and pre-transition disks were well fit using the flared disk model, while optically thin disks were fit exclusively with the flat disk model. This separation is largely based on whether the best fit power laws aligned with values expected for such disks, that is, $p = 0.5$ for flared disks and $p = 0.75$ for flat disks. Optically thick disks fit with the flared disk model had an average power law of 0.5 ± 0.1, while optically thick disks fit with the flat disk model had an average power law of 0.8 ± 0.3. For the latter, this average is slightly higher than the canonical flat disk value, implying that this disk model is too simplistic to fit these sources.

Optically thin disks had an average power law of 0.7 ± 0.1. This suggests that the geometry of the inner disks of these sources does not quite fit the traditional flat geometry. Figure 3.5 shows an example of (a) an optically thick disk and (b) an optically thin disk with atypical power laws. Pre-transition disks had an average power law of 0.46, and, in general, were not well fit by the disk models. To fit these sources, the sampler often moved walkers towards power laws of 0.4, which corresponds with the power law of the superheated surface layer of Chiang and Goldreich (1997) (i.e., $T(r) \propto r^{-2/5}$). Then, by moving the inner disk radius close to the protostellar photosphere, the model produced the curve which could

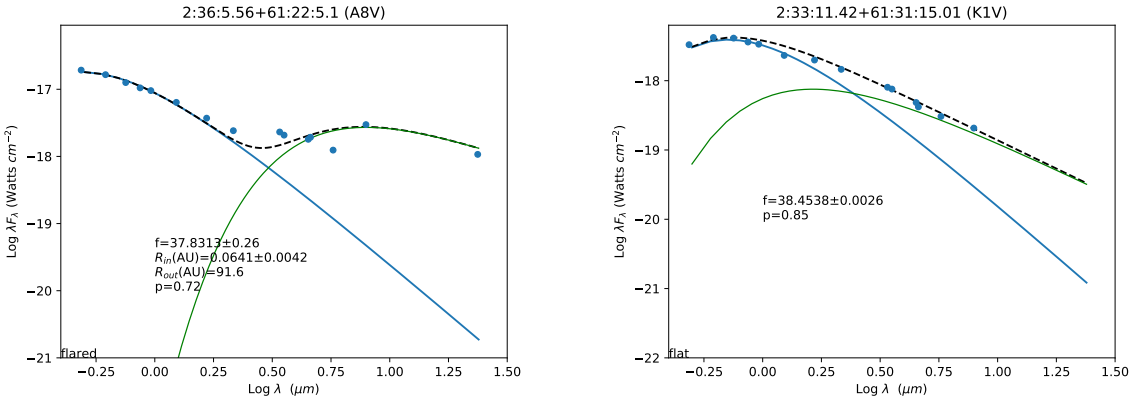

(a) (b)

Figure 3.5. SEDs of an (a) optically thick flared disk and (b) optically thin flat disk fit with atypical power laws.

replicate the mix of optically thin and optically thick dust emission. The resemblance of the power law to that of the superheated surface layer is indicative that a multi-layer disk model is needed to predict the flux in and around an optically thin gap in the disk.

While the values of the best fit inner disk radii represent at best lower limits, some significance can be placed on whether or not the disk models were able to fit the inner disk radius at all. That is, since the disk model had to scale the distribution of flux and push the inner disk radius towards the protostellar photosphere to fit the SEDs, those sources with best fit inner disk radii are highly suggestive of the presence of an inner disk hole. Ten out of 15 optically thick disks required the inner disk parameter to produce reasonable fits, three out of 18 optically thin disks required inner disk radii, and five out of 15 pre-transition disks were fit with the inner disk radii. This suggests that over half of the detected optically thick disks may be beginning their transitions towards a more evolved state. Figure 3.6 shows the fit SED of an optically thick disk suspected to be in a state of transition towards a pre-transition disk.

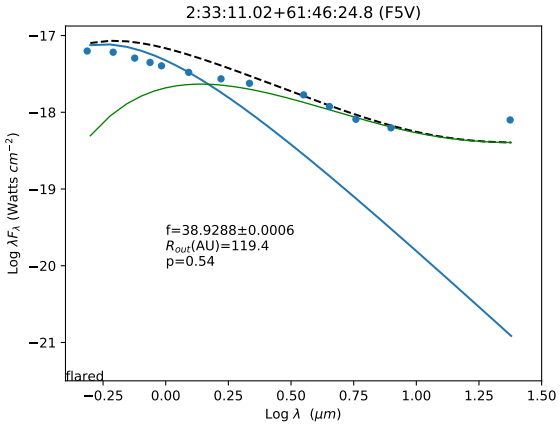

Figure 3.6. SED for a source whose IRAC slope would identify it as an optically thin source. However, its IRAC 4 to MIPS 1 slope identifies it as a pre-transition object (see Section 3.4.3). Given the best fit power law, it has been designated as a source evolving from an optically thick disk towards a pre-transition disk.

The average scaling parameter values of flared and flat disks are 39.26 and 39.10, respectively, which can be compared to the scaling parameter that corresponds to the cluster distance, 39.705. Since the orientation of disks in this study can be assumed to be approximately face-on, much of this difference likely stems from the scaling which *emcee* performed in order to make the flared and flat disks models have a higher dust temperature. Additionally, the disk models required theoretical protostellar radii to compute the SEDs. To be consistent with effective temperature estimates, theoretical radii were also taken from the main-sequence intrinsic parameters of Pecaut and Mamajek (2013). There are bound to be discrepancies with the actual YSOs which should be larger than their main-sequence counterparts, so it is likely that the scaling parameter accounted for these small differences as well.

Sources identified as transition disks were nearly all fit using a simple blackbody approximation of a dust rim, except for three sources that were either fit with the flared (two sources) or flat (one source) disk model. While the sources fit with the flared disk model provided inner disk estimates, these estimates were still found to be below a theoretical

dust sublimation radius. In contrast, the source fit with the flat disk model had an inner disk radius estimate that did not contradict the theoretical sublimation radius. The sources fit with the dust rim approximation mostly predicted cool dust rims with temperatures less than 500 K. Only one source fit with this model predicted a dust rim temperature within typical dust sublimation temperature estimates (1000-2000 K).

3.4.3. Evolution of Disk-Bearing Stars in IC 1805. In general, as a YSO ages its circumstellar disk will gradually dissipate. However, the age of the parent YSO does not provide stringent information regarding the evolutionary status of the disk. A classic method of analyzing the evolutionary status of a disk is by fitting a linear regression to the infrared SED. The disk-bearing members in this study have a median age of 2.4 Myr from H-R diagram interpolations, which is in line with IC 1805 age estimates. Optically thick disks have a mean age of 2.6 Myr, optically thin disks a mean age of 2.8 Myr, pre-transition disks a mean age of 1.7 Myr, and transition disks a mean age of 4.5 Myr. Two optically thick sources were excluded from this estimation since their large spectral type uncertainties produced large uncertainties in ages, and probable first generation irx members were excluded. These ages show the expected trends except for that of pre-transition disks. If these represent an alternative evolutionary path to optically thin disks, their ages should be similar. The discrepancy could be due to higher age uncertainties for cooler stars which dominate the pre-transition disk sources.

Figure 3.7 plots the IRAC spectral indices as a function of spectral type. The horizontal lines were estimated by a comparison of modeled SEDs and IRAC slopes. Sources with optically thick disks have slopes $\alpha \gtrsim -1.0$, and those with optically thin disks slopes of $-1.6 \lesssim \alpha \lesssim -1.0$. Transition disks had slopes in the range $-2.6 \lesssim \alpha \lesssim -1.6$, and corresponded well with diskless sources from Paper I whose slopes were approximately $\alpha \lesssim -2.6$. These IRAC slope estimates closely correspond with those found by Lada *et al.* (2006). They found that both thick and thin irx sources had slopes $\alpha > -1.8$, transition or “anemic disks" had slopes $-2.56 < \alpha < -1.8$, and diskless objects $\alpha < -2.56$.

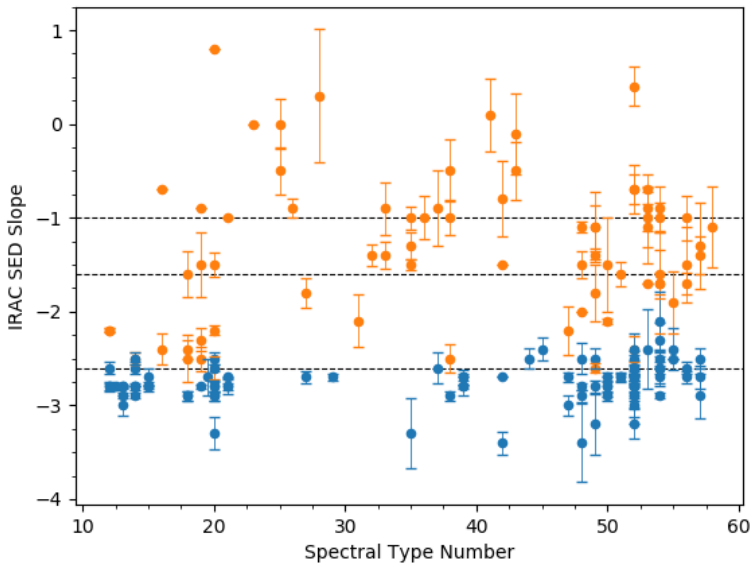

Figure 3.7. Spectral indices vs spectral number for irx sources (orange dots) and non-irx cluster members from Paper I (blue dotes). Spectral indices were determined from dereddened IRAC flux densities. Spectral type numbers correspond to B0, A0, F0, G0, and K0 as 10, 20, 30, 40, and 50, respectively (and subtypes within). The horizontal lines correspond to YSO classes that correspond to sources with the following SED irx emission profiles: thick $\alpha \gtrsim -1.0$, thin $-1.6 \lesssim \alpha \lesssim -1.0$, and transition $-2.6 \lesssim \alpha \lesssim -1.6$. Vertical error bars correspond to the standard errors of each ordinary least squares fit. Points with no uncertainties only had two IRAC fluxes.

The disk fraction, relative to the 219 cluster members of Paper I, is about 34%. When the sample is expanded to include 117 possible cluster members which had no irx, for a total of 336 cluster members, the disk fraction is about 22%. Mamajek (2009) plotted the fraction of optically thick primordial disks versus ages (often called a “Haisch-Lada" plot) for 22 star clusters and fit an exponential decay curve with timescale of $\tau_{\rm disk}$=2.5 Myr. In Paper I, a median age of 2.2 Myr was estimated using 219 probable members and 2.8 Myr with the additional 117 possible members. An age of 2.2 Myr would result in a theoretical disk fraction of about 41% and 2.8 Myr a disk fraction of 32%. The plot in Mamajek, however, represents the disk fraction for nearby star clusters where the disk samples were dominated by sources less than 2 $M_{\odot}$.

Previous studies have estimated similar disk fractions compared to their estimated cluster ages. Panwar *et al.* (2017) estimated a disk fraction of roughly 26% (Class I and II sources) along with a cluster age of 2.5 Myr. Sung *et al.* (2017) found a disk fraction of 18%, with an estimated age of 2.4 Myr for the PMS members using the evolutionary models Siess *et al.* (2000) and 1.6 Myr using the models of Baraffe *et al.* (2015). Surprisingly, the results presented here produce a similar disk fraction and cluster age, despite the fact that the results of Sung et al. correspond to a mass range of $0.3 < M/M_{\odot} < 1.0$ while the results here correspond roughly to the mass range $0.7 < M/M_{\odot} < 7.0$ (where this study is complete down to 2 $M_{\odot}$).

Richert *et al.* (2018) derived mean circumstellar disk lifetimes by analyzing YSO data from 69 young clusters using non-magnetic and magnetic PMS evolutionary models. They found that the disk fraction of a cluster detected in the IRAC bands should drop to 50% when the cluster is 1.3-2 Myr using the MIST and Siess *et al.* (2000) PMS models. In their analysis, they found that their derived disk lifetimes were not strongly affected by the initial disk fraction, stellar mass, star-forming environment, or criteria used to identify YSOs in the data. However, they do note that disk fraction could vary with stellar mass during the initial few Myr of life because their sample is not well represented for stars with >2 $M_{\odot}$. We estimated an age of 2.2-2.8 Myr for IC 1805 in Paper I along with disk fractions less than 50%. Since our sample is complete to 2 $M_{\odot}$, this suggests that disk fraction does not vary for the first few Myr of life in higher mass YSOs.

As noted in Paper I, Wolff *et al.* (2011) found 62 unique irx sources in their study of disk-bearing YSOs in IC 1805. A total of 57 of these sources were observed in Paper I and only 17 of these were confirmed as irx sources. Five of their sources were classified as non-irx cluster members, and six others as possible cluster members. Of the 40 sources that did not meet our probable cluster criteria, 38 were classified as empty/thin and two empty/thick. The requirement that fluxes displaying an irx have corresponding point sources in the Spitzer mosaics ruled out many sources that displayed an irx only at the IRAC 4 band

which can be dominated by PAH emission. Wolff et al. commented in their study that the 8 μm emission seen in many sources often exceeded that predicted by Kenyon and Bromley (2008). All of the sources Wolff *et al.* (2011) referred to as optically thick and optically thin were confirmed in this study.

Wolff *et al.* (2011) found no evidence of optically thick emission for sources with $M > 4M_{\odot}$. This study has found one source which falls into this category: 2 29 35.91+61 15 56.80, also called EM* GGA 173. It was spectral typed as B6 with an interpolated mass of $5.1M_{\odot}$ and age <1 Myr. The source is located towards the western edge of the W4 HII region (just outside of Wolff et al.'s coverage). There are four other disk-bearing sources in our sample located along the western edge of the W4 HII region. Three of these sources also have ages less than 3 Myr, while the other source's age (18 Myr) seems to disagree with its modeled SED (optically thick emission; $1.8M_{\odot}$).

The histograms of Figure 3.8 show the distributions of irx spectral numbers for the four identified disk types. Both the optically thick and transition disk types are largely composed of B and A-type YSOs along with small groups of late G and K-type YSOs, while the optically thin and pre-transition disks are largely composed of F, G, and K-type YSOs. This supports the hypothesis that circumstellar disks around hot YSOs evolve from optically thick disks to transition disks more rapidly than cooler YSOs. Not counting the apparent 8 μm irx sources (66 sources), about 23% of irx sources are optically thick, 27% are optically thin, 29% are pre-transitional, and 21% are transition disks. The small amount of low mass YSOs in the optically thick category is somewhat surprising for this young cluster. These low numbers may be due to the fact that our sample is not complete to lower mass objects. Additionally, low mass YSOs may retain their surrounding envelopes which obscure optical wavelength radiation for a longer time than higher mass YSOs. It is also possible that optically thin sources may be visible at higher inclinations than optically thick sources.

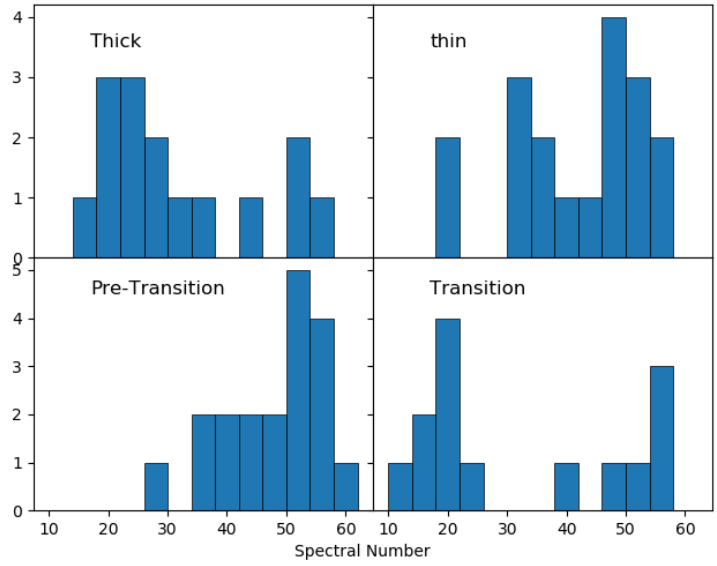

Figure 3.8. Histograms for the four types of disks by spectral number, described in Figure 3.7. These do not include the 8 μm irx sources which were not modeled.

3.4.4. Disk-Bearing Sources with a Deficit in MIPS 1 Flux. Five irx sources have curious SEDs where the MIPS1 displays a deficit in flux compared to the IRAC bands and disk fits. The *emcee* sampler attempted to fit these sources by truncating the outer disk radius but, due in part to the limitations of these models, was unsuccessful. Three of these sources were in the vicinity of an extended source, which makes their apparent deficits even more significant. Three of these sources have projected distances $\leq$0.7 pc away from an O star (assuming 2.3 kpc to the cluster). Disk truncation can be caused by the presence of a companion YSO, encounters with another star, and by external photoevaporative radiation.

Figure 3.9 shows two examples of sources within a projected distance $\leq$0.5 pc from two binary O star systems. In addition to these two sources, four other irx sources located within a projected distance of less than 0.5 pc of an O-star have SEDs which were identified as either pre-transition or transition disks. Each SED show a deficit in 2MASS and several IRAC bands accompanied by an optically thick MIPS 1 flux. These could be signs of disk flaring that has been enhanced by nearby photoevaporative flux from the O-stars. These few

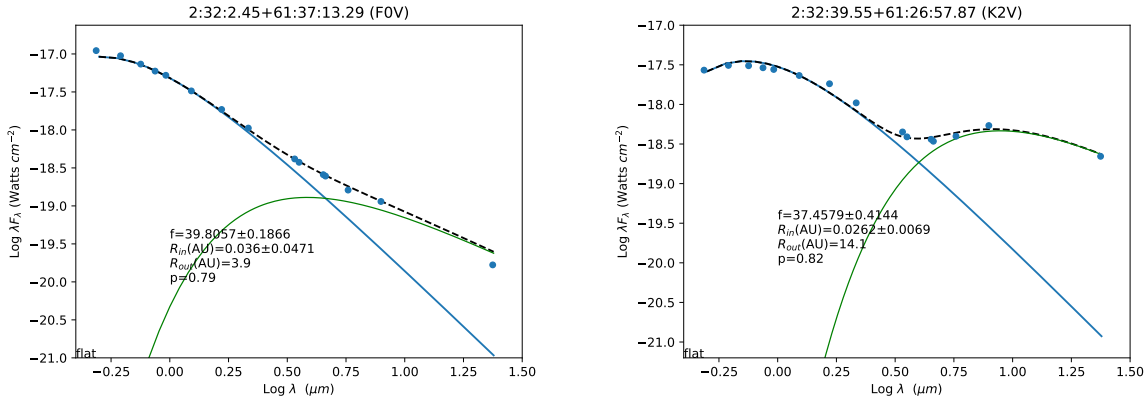

(a) (b)

Figure 3.9. SEDs of two disk-bearing sources that display small MIPS 1 fluxes relative to the IRAC bands and best fit disk models. Source (a) has a projected distance of 0.5 pc away from BD+60 497 (O6.5V+O8.5V), and source (b) has a projected distance of 0.4 pc away from HD 15558 (O4.5III+O7V).

diagnostics suggest that the O-stars of IC 1805 are not causing widespread disk ablation or destruction but it could be occurring to a few sources. This is in line with the findings of previous studies such as Richert *et al.* (2015) and Panwar *et al.* (2017).

4. ADDITIONAL ANALYSIS OF PROBABLE CLUSTER MEMBERS

In this section, additional details will be presented regarding how data was transformed and utilized for the results of Paper I, and how these affected the results presented there. Several Python packages should be briefly acknowledged that were extensively used throughout this study. NumPy (van der Walt *et al.*, 2011), Matplotlib (Hunter, 2007), SciPy (Virtanen *et al.*, 2020), and Pandas (McKinney, 2010).

4.1. SPECTRAL TYPES AMONG THE SAMPLE AND CLUSTER

Spectral types amongst the entire 3241 source sample ranged from B0 to M4, while the spectral types among the 219 cluster members ranged from B1 to M0. Errors in spectral subtypes were on average: ±1 subtypes for B star, ±2 subtypes for A stars, ±2 subtypes for F stars, ±4 subtypes for G stars, ±2 subtypes for K stars, and ±2 subtypes for M stars. Histograms of spectral types in both the full sample and cluster members are shown in Figure 4.1. The cluster members histogram in panel (b) has an additional distribution that includes 117 possible cluster members mentioned in Paper I, which met the extinction and distance criteria.

The shape of the distribution in Figure 4.1(a) shows several difficulties experienced during the spectral classification process in several spots. In particular, the dearth between 40-48 (i.e., G0-G8) highlights the difficulty in classifying G-types stars. The two peaks at 20-24 (A0-A4) show a location around which we lacked spectral standards. Jacoby *et al.* (1984) standard stars had gaps in late B-type stars and some confusion in mid to late A-type stars. Specifically, the catalog did not include an A4 star and the standards marked A6-A8 showed inconsistencies in the strength of the Ca II K absorption line. It is possible that some of the FITS files were mislabeled.

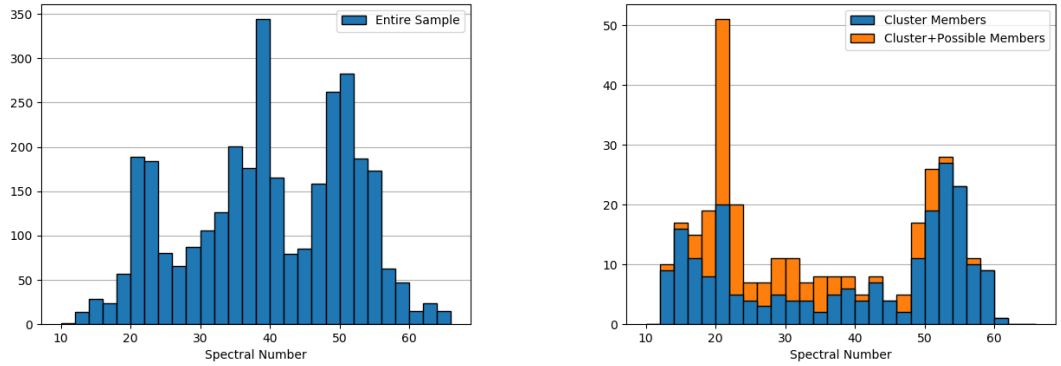

(a) (b)

Figure 4.1. Histograms of spectral types among (a) all 3241 spectrally classified sources and (b) the 219 cluster members. Plot (b) layers the distribution that includes 117 possible cluster members behind the 219 cluster member distribution. The spectral number system, 10-60, corresponds to B0 through M0 spectral types, and subtypes within.

Figure 4.1(b) shows that the cluster member distribution is top and bottom heavy. Since this survey is targeted towards YSOs, the criterion of proper motion will favor hotter YSOs that are more easily visible. Meanwhile, cooler YSOs more prominently feature X-ray emission which occurs as their circumstellar disks gradually dissipate. In Paper I, it was theorized that A-type YSOs are difficult to detect as they can dissipate their disks relatively quickly. If these particular YSOs emit no other indication of youth, such as Hα emission or X-rays, then they could be missed. The inclusion of the possible cluster members helps to fill in the gap, but results in a staggering number of A0-A1 type stars. Nearly 24% of the possible cluster members were A0-A1 stars. It may simply be the case that, with a visual magnitude completeness of $V \sim 16.5$ mag, diskless YSOs with no other indicators of youth will be limited to brighter YSOs. Or, not all of the possible cluster members are actual cluster members.

4.2. INTRINSIC COLORS AND EXTINCTIONS

The main-sequence intrinsic colors of Pecaut and Mamajek (2013) (hereafter PM13) were utilized in the assigning of effective temperatures based on spectral type, and the computing of reddenings based on spectral type. A web based[1] version of their Table 5 has been updated and expanded upon since the publishing of the 2013 paper. This study uses a version of the web-based table from March of 2019. It is important to note that PM13 has an additional table featuring the intrinsic colors of stars 5-30 Myr (Table 6 in the paper). However, this table does not have estimates for the colors used in this study to estimate reddening. Therefore, the main-sequence colors were used in place. On average, the colors differ between the two tables by less than half a magnitude.

The color $(r - i)$ was used to estimate reddening, and extinction, in this work. Several modifications were made to the PM13 intrinsic colors. The color $(R - I_C)$ was calculated taking the difference of $(V - I_C) - (V - R_C)$ given in the web-based table. This was transformed into SDSS ri passbands, which are approximately equivalent to PanSTARRS passbands, using the following transformation from Jordi *et al.* (2006) for metal-rich Population I stars: $(r - i) = (0.988 \pm 0.006)(R_C - I_C) - (0.221 \pm 0.004)$. Additionally, the color $(V - r)$ was needed for estimating luminosity. The transformation $(r - R_C) = (0.275 \pm 0.006)(V - R_C) + (0.086 \pm 0.004)$ from Jordi *et al.* (2006) for Population I stars with $(V - R_C) \leq 0.93$ was used to convert the given $(V - R_C)$ color. For the majority of our sample, the restriction of $(V - R_C)$ was not an issue because this would only effect stars cooler than a spectral type of M1. All but one M-star in the sample were determined to be foreground objects.

Visual extinction is calculated using the $(r - i)$ color. The extinction coefficient $R(r - i) = 0.658$ is calculated from Table 1 of Green *et al.* (2019) where the coefficients have been converted relative to $(B - V)$. It is combined with the typical expression for

[1]Hosted on Erik Mamajek's webpage at the Universty of Rochester.

Table 4.1. Average extinctions in IC 1805.

Filter	$\lambda_{mean}(\mu m)$	Extinction Law	A_λ (mag)
g	0.4866	1.156	3.1±0.6
r	0.6215	0.86	2.3±0.4
i	0.7545	0.648	1.7±0.3
z	0.8679	0.509	1.4±0.3
y	0.9633	0.415	1.1±0.2
J	1.235	0.261	0.7±0.1
H	1.662	0.154	0.42±0.08
K	2.159	0.099	0.27±0.05
W1	3.4	0.039	0.11±0.02
I1	3.55	0.037	0.1±0.02
I2	4.5	0.026	0.07±0.01
W2	4.6	0.026	0.07±0.01
I3	5.74	0.019	0.05±0.01
I4	7.92	0.025	0.07±0.01
M1	23.68	0.025	0.07±0.01

visual extinction,

$$\frac{A_V}{E(r-i)} = \frac{3.1E(B-V)}{0.658E(B-V)} = 4.71. \tag{4.1}$$

Coefficients were used from Table 1 of Green *et al.* (2019) to calculate extinction laws (relative to A_V) for the PanSTARRS $grizy$ and 2MASS JHK passbands. Extinction laws for Spitzer and WISE passbands were taken from Table 3 of Wang and Chen (2019). The usual visual extinction equation was combined with $A_\lambda = R_\lambda E(B-V)$ in the following manner to produce the extinction laws (when not provided),

$$\frac{A_\lambda}{A_V} = \frac{R_\lambda E(B-V)}{3.1E(B-V)} = \frac{R_\lambda}{3.1}. \tag{4.2}$$

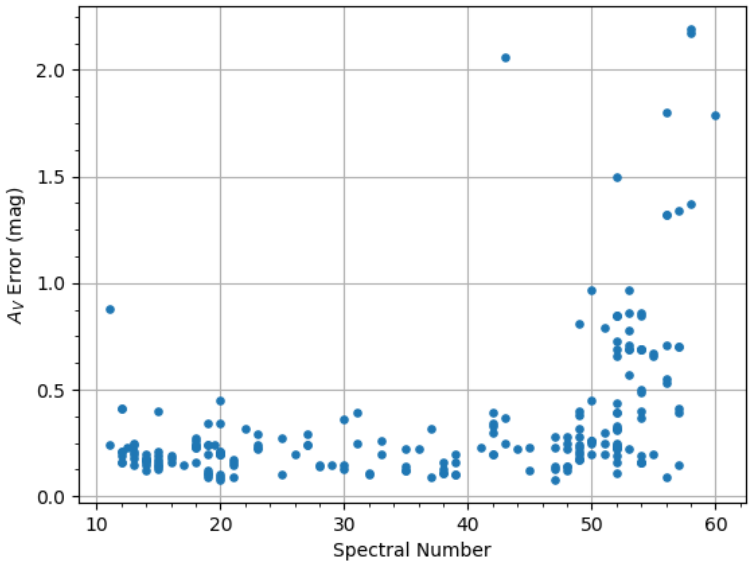

Figure 4.2. Extinction uncertainties as a function of spectral number for the 219 cluster members.

The 90Prime V and I passbands used the ratios $A_V/A_V = 1$ and $A_I/A_V = 0.482$ from Rieke and Lebofsky (1985). Average extinctions for IC 1805 in the PanSTARRS, 2MASS, AllWISE, and Spitzer bands are given in Table 4.1 for $A_V = 2.7$ mag in the V band (0.548 μm).

It is evident from Table 4.1 that the interstellar extinction has a minimal effect on the AllWISE and Spitzer bands. These extinctions are similar to those found by Wolff *et al.* (2011) (Table 5 of their paper), with many estimates being lower than their values. We found the average visual extinction of cluster members to be 2.7 ± 0.5 mag, which is exactly in line with the average visual extinction found by Wolff *et al.* (2011). Figure 4.2 shows the spread in extinction errors as a function of spectral number for all 219 cluster members. It is evident that the majority of the uncertainty in extinction is the result of large spectral type uncertainties in late G and K type sources.

A model of the foreground population was utilized in choosing spectroscopic targets to reduce the intrusion of these stars in the sample (Robin *et al.*, 2003). The model predicted that, given the range in visual magnitudes on which the targets are based, about 75% of the sample would be a foreground population. Consider the 2257 sources which met the extinction cluster member criterion. A sample of the foreground population can be extracted by using the distance estimates of Bailer-Jones *et al.* (2018). A total of 1417 sources have distance estimates which fall below 1900 pc accompanied by upper and lower distance uncertainties less than 200 pc. This foreground group of stars represents roughly 63% of the of the 2257 sources, slightly lower than the model prediction. Figure 4.3 shows the distribution of visual extinctions of the foreground population versus their distances. The histogram shows that the extinction due to gas and dust in the inter-arm region is roughly 1.5 mag. This implies that a remaining ∼1 mag of extinction lies in front of the IC 1805 cluster.

4.3. COVERAGE FROM DIFFERENT PHOTOMETRIC SURVEYS AND Hα EMISSION AMONG CLUSTER MEMBERS

Only the PanSTARRS PS1, 2MASS, and AllWISE surveys covered the entire spectroscopic survey area. Infrared data from Spitzer and the X-ray detections of Rauw and Nazé (2016) and Townsley *et al.* (2014) did not cover the entire area observed spectroscopically. Figure 4.4 shows approximately which spectroscopic targets (orange circles) were covered by Spitzer observations (red boxes) and X-ray observations (violet box). There are five X-ray sources, not boxed in, to the north and east of the pictured box that were obtained from unpublished data.

The first row of Table 4.2 lists how many sources of the entire observed sample have photometry in the Spitzer passbands. The second row lists the percentage of sources with photometry in the given band that had flux densities which the SEIP classified as *bandfill*. This means that a source was not detected at that band, but a flux density is provided if it was

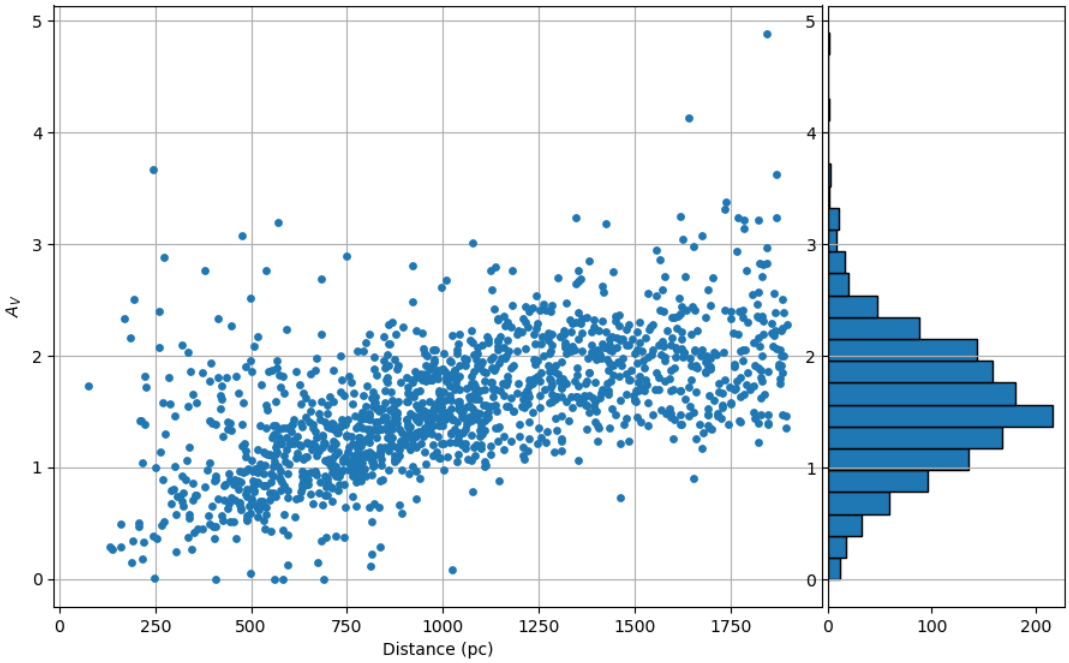

Figure 4.3. A plot of the extinction of foreground stars as a function of distance. The side histogram shows the spread in extinctions of the foreground population.

measured with S/N>3. Additionally, bandfill flux densities were provided if the source was extended in the IRAC band. In this case, the position chosen for the bandfill flux density was based on the MIPS-1 position. They note that the MIPS-1 position can be discrepant from the position coinciding with peak brightness. For the both the IRAC aperture photometry and MIPS point spread function photometry, normal flux densities were significant at a level greater than 10 sigma, while bandfill flux densities were significant at a level greater than 3 sigma.

Hα emission was detected in roughly 36% of our 219 probable cluster members, where these sources were classified as either strong or weak if the equivalent width of the spectral emission line was $>$ 10 Å or $\leq$ 10 Å in the spectra. Lada *et al.* (2006) regarded

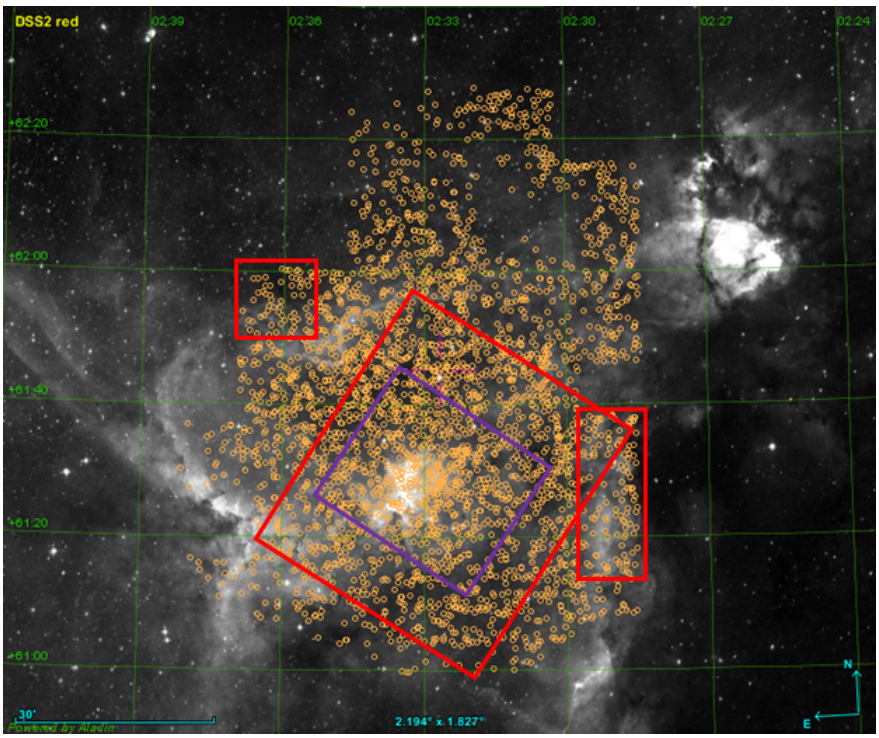

Figure 4.4. Areas covered by Spitzer infrared observations (red boxes) and X-ray surveys (violet box). The orange circles represent the entire spectroscopic sample. Additional X-ray sources in the east are not pictured.

strong emission sources as CTTs and weak emission sources as WTTs. This type of emission is typically regarded as a signature of accretion in YSOs, and can be variable in YSOs as the rate of material accreting onto the protostar will inevitably fluctuate.

Interestingly, only 51% of these sources were identified as disk-bearing sources from their SEDs. Among the non-irx sources with strong Hα emission, nearly 79% were classified as having spectral types of K0 or later. Mid-infrared photometry was often limited for these faint sources, and is likely the main cause of this apparent discrepancy. Since our sample of YSOs is located within the W4 HII region, their spectra were influenced by the varying Hα emission from the ionized hydrogen gas in the nebula. The sky subtraction procedure performed during the spectroscopic reduction process was mostly successful in

Table 4.2. Spitzer photometric coverage of the sample.

	IRAC 1	IRAC 2	IRAC 3	IRAC 4	MIPS 1
% of Total	54%	49%	52%	47%	6%
% Bandfill	1.8%	0.8%	6.4%	40.3%	71.4%

Percentages of sources with photometry in the given passband. % Bandfill represents how many of those sources with photometry were classified as bandfill by the SEIP.

removing noise produced by the nebula from individual spectra, but showed issues for sources in the faint spectroscopic samples. It is possible that the Hα emission measured for some faint sources has been inflated by nebular emission that was not fully subtracted.

In Sung *et al.* (2017), Hα emission was detected from the spread of sources in color-color diagrams. Figure 4.5 shows a color-color diagram comparison of our 219 cluster members whose spectra showed either strong or weak Hα emission to those without Hα emission using r, Hα, and i photometries from the IPHAS Data Release 2 survey (Barentsen *et al.*, 2014). While the separation of sources with and without is somewhat defined, this type of photometric Hα identification can miss sources. It should also be noted that the strength of a source's $(r - H\alpha)$ color was found not to correspond directly with our strong and weak Hα emission sources. This is likely due to the variability in Hα emission since the optical spectroscopy of our sample and the IPHAS survey did not occur simultaneously.

4.4. LUMINOSITY ESTIMATIONS AND H-R DIAGRAM CAUTIONS

Luminosity was estimated for each cluster member which had PanSTARRS r and i photometry. The luminosities were calculated using,

$$Log_{10}(L/L_{\odot}) = 0.4(M_{bol,\odot} - M_{bol}) = 1.89 - 0.4M_{bol} \tag{4.3}$$

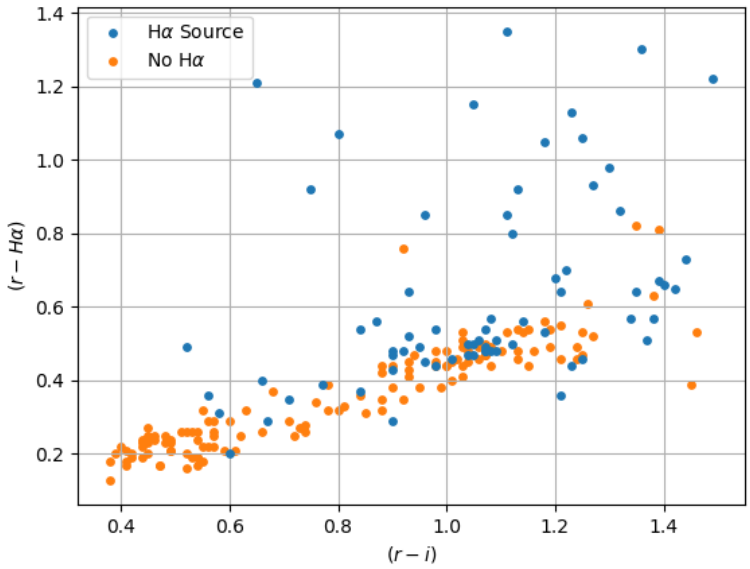

Figure 4.5. Color-color diagram of IPHAS colors $(r-H\alpha)$ versus $(r-i)$ for cluster members with either strong or weak Hα emission (blue dots) and without Hα emission (orange dots).

where $M_{bol,\odot}$ represents the solar bolometric magnitude of 4.74. The bolometric magnitude for each source was calculated by

$$M_{bol} = M_r + BC_r = [m_r - A_r - DM] + [BC_V + (V - r)] \tag{4.4}$$

where DM is distance modulus, BC_r and BC_V are the bolometric corrections at the r and V bands, $(V - r)$ is an intrinsic color, and m_r is the apparent (observed) r band magnitude. Here a distance of 2300 pc was assumed for each source resulting in a distance modulus of 11.81. Both BC_V and $(V - r)$ are taken from PM13, where $(V - r)$ is transformed from $(V - R)$ using the transformations of Jordi *et al.* (2006).

The age of a young cluster, derived from an H-R diagram, should be interpreted with caution. Baraffe *et al.* (2002) note that there are two primary reasons for complications which arise in theorizing how a YSO “contracts" to the main sequence. Since evolutionary models are based on observations, extinction from interstellar material as well as dust

which surrounds a YSO modify both the apparent magnitude and colors of the YSOs. Even if interstellar extinction is corrected for (and assumed static), the extinction due to the dust that surrounds a YSO changes over time and will affect the observed magnitudes. Second, the presence of an accretion disk and/or residual material from the formation of the protostellar nebula (i.e., protostar, disk, and envelope) will affect the spectra of YSOs. This results in uncertainties in effective temperature as well as derived luminosities where the uncertainty in absolute magnitude is also taken into account. Hosokawa *et al.* (2011) compared the protostellar evolutionary models that account for the effects of accretion to previous evolutionary models which neglect this process. For stars of $T_* \gtrsim 3500K$, they found that non-accreting models overestimate the protostellar ages while age estimates for protostars with $T_* \lesssim 3500$ K are not as different in non-accreting models.

4.5. INITIAL MASS FUNCTION ESTIMATES

Due to uncertainties in the distance to IC 1805 and interpolated masses from the MIST models, an estimate of the IMF slope for our sample of cluster members was not given in Paper I. This section will present a brief IMF analysis using our data to illustrate the possible slope values that are estimated from both the 219 probable cluster members and the 336 possible cluster members. The IMF slope refers to the following form of an equation originally derived in Salpeter (1955),

$$\Gamma = \frac{\mathrm{d\,Log}N}{\mathrm{d\,Log}M} \tag{4.5}$$

where N is the number of stars with mass M.

Based on the completeness estimated in Paper I, the following IMF estimates are for YSOs $\geq 2\,\mathrm{M}_\odot$. For the 219 cluster members, an IMF slope of $\Gamma = -1.1 \pm 0.2$ was found (see Figure 4.6). As inferred in Paper I, this sits in between IMF slope estimates of $\Gamma = -1.0$ and $\Gamma = -1.23$ by Sung and Lee (1995) and Panwar *et al.* (2017), respectively, and can be

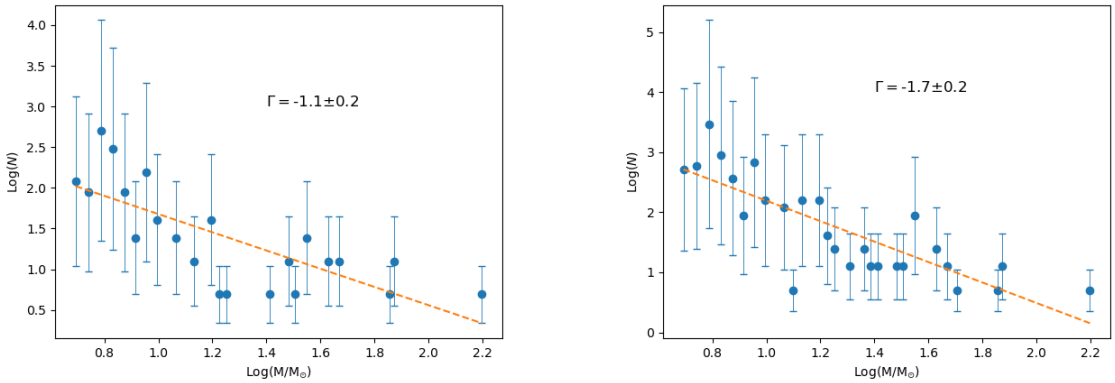

(a) (b)

Figure 4.6. IMF estimates for (a) probable cluster members and (b) probable members plus possible cluster members with masses ≥ 2 $M_{\odot}$. The vertical error bars represent the $\sqrt{N}$ errors, and the uncertain in the slope corresponds to the standard error of the linear regression.

called a Salpeter-type slope ($\Gamma \sim -1.35$) that is commonly found in star clusters and the field star population. With the additional 117 possible cluster members, an IMF slope of $\Gamma = -1.7 \pm 0.2$ was found. This is the steepest IMF slope yet measured for IC 1805, where the steepest previous estimate was $\Gamma = -1.38$ by Ninkov *et al.* (1995). This implies, again, that not all of the possible cluster members are actually located in the IC 1805 cluster.

5. SUMMARY AND FUTURE WORK

This section will summarize the findings of Paper I and the analysis of disk-bearing YSOs in the W4 HII region, and suggest next steps that the project can take to continue exploring the evolutionary history of this dynamic region.

5.1. SUMMARY

To investigate the young population of the W4 HII region, photometric and spectroscopic observations of probable YSOs were conducted between 2006 and 2012 at the Bok Telescope and MMT Observatory, respectively. In Paper I, this sample of 4085 stars were assigned spectral types which were then used to estimate visual extinctions and luminosities using photometry assembled from the PanSTARRS PS1 survey. Additional photometry was collected from 2MASS, WISE, and Spitzer surveys that allowed for the creation of SEDs from which sources exhibiting an excess in infrared flux, likely caused by the presence of a circumstellar disk, were found. Other indicators of youth such as Hα emission and X-ray emission were used to narrow the sample to only the most probable members of the young cluster.

A mean visual extinction of 2.7 ± 0.5 mag was found for 219 probable cluster members, which is in line with estimates found by previous studies (e.g., Straižys *et al.* 2013; Wolff *et al.* 2011). The MIST evolutionary models were used to create H-R diagrams that allowed for the ages and masses of all cluster members to be interpolated. A median age of 2.2 Myr was found for probable cluster members, and a median age of 2.8 Myr was found if a sample of possible cluster members is included. These age estimates are in line with those found in recent studies such as Panwar *et al.* (2017) and Sung *et al.* (2017). The mass distribution among cluster members was found to closely follow IMF estimates made

in the aforementioned studies, predicting a Salpeter-type slope of $\Gamma \sim -1.35$. A group of 15 YSOs was identified in H-R diagrams as candidate members of a previous generation of stars with a mean age of 8.5 ± 2.8 Myr. This age agrees with previous estimates made by Dennison *et al.* (1997) based upon the size of the W4 superbubble. Additionally, the source EM* MWC 50 was determined to be a post-main-sequence star with an age of 9.0 Myr.

Several cluster members are located near BRCs 5 and 7 along the western and northern edges of the W4 HII region, respectively. Two cluster members near BRC 5 have a mean age of 1.25 Myr while four cluster members near BRC 7 have a mean age of 1.2 Myr (a fifth cluster member near BRC 7 may be an older member of IC 1805). The age of the YSOs near BRC 5 agree with the age estimate of Fukuda *et al.* (2013), and those near BRC 7 are in line with the age estimate of Panwar *et al.* (2014). These ages support the idea that the photoevaporative flows of OCL 352 have triggered regions of star formation along the high density edges of the W4 HII region.

A total of 74 disk-bearing YSOs were identified from the SEDs of Paper I. The IRAC slopes estimated from their SEDs showed a variety of disks that broadly fit into three categories used in the literature: optically thick, optically thin, and transition. Another class of circumstellar disks was identified, pre-transition, using an additional estimated slope between the IRAC 4 and MIPS 1 bands as well as from the fit disk models. Fifty-One of these sources were then fit with either a flared or flat reprocessing disk model. Most disk-bearing sources fit with a flared disk showed a typical power law value of 0.5, and corresponded primarily with optically thick disks. Additionally, most of these optically thick sources had Hα emission present in their spectra, which is typically an indicator of accretion. All disk-bearing sources designated as optically thin were fit with a flat disk model. Interestingly, these sources had an average power law of 0.7, slightly lower than the typical flat power law of 0.75. This implies that the disk model had to shift the power law towards the regime of power laws typically occupied by optically thick sources.

Sources identified as pre-transition disks were primarily fit using the flared disk model. Due to the nature of pre-transition disk SEDs, optically thin at near-infrared wavelengths and optically thick at mid-infrared wavelengths, these sources were not well fit by the simple flared and flat disk models. In the literature, these types of sources are usually fit using a multi-layer disk model (see e.g., Espaillat *et al.* 2012). The prevalence of more massive YSOs among optically thick and transition disks, and less massive YSOs among optically thin and pre-transition disks, supports the theory that hot YSOs deplete their inner disks faster than cooler YSOs. Nearly 44% of disk-bearing sources were classified as possessing either a pre-transition or transition disk. The presence of planet formation around these types of objects has been confirmed in recent years by resolved interferometric data. For example, planets have been observed in the transition disk of PDS 70 (Mesa *et al.*, 2019) and in the transition disk of HD 97048 (Pinte *et al.*, 2019). Therefore, it is likely that this subgroup of the disk-bearing sources has already begun the process of planet formation.

5.2. FUTURE WORK

The investigation of the star formation history of the W4 HII region, and superbubble, can be continued with the inclusion of more precise distance measurements that will produce more accurate bolometric luminosities estimates for YSOs. These can be used to construct a three-dimensional view of the region that would provide more stringent observational limits for dynamical simulations of the evolution of the HII region. Gaia Data Release 3, scheduled for release in 2022 (a small early release is also scheduled for December of 2020), is estimated to improve parallax estimates by 20% compared to those in the second data release, allowing for more precise distance estimate to be made for more distant objects in the galaxy. A study similar to Thompson *et al.* (2004) that combines Hα, sub-millimeter, and CO observations of the BRCs and CG 7S in the W4 HII region could help trace the evolution of these compact star forming regions.

The work in this project on disk-bearing YSOs in IC 1805 could be continued and enhanced by the addition of far-infrared and longer millimeter wavelength data that would allow for a more sophisticated disk model to be fit to sources. Properties such as disk mass and size could be estimated, and provide a more complete view of the variety of disks in IC 1805. Resolved interferometric observations would provide even stricter bounds for the disk size and structure, and allow for more accurate SED modeling to be performed. Additionally, complete coverage of the W4 HII region in infrared, X-ray, and Hα wavelengths would allow for a more complete determination of YSOs throughout the region. An investigation of disk ablation by the large O-star population of IC 1805 would benefit from the inclusion of the faint low-mass population of YSOs in W4 which is not well covered by this study. With the retirement of the Spitzer Space Telescope, observations in the infrared regime must now look towards the launch of the James Webb Space Telescope. The James Webb Space Telescope is currently scheduled for launch in 2021, and will provide greater angular resolution than Spitzer over the wavlength range $0.6 - 28$ μm.

In regards to circumstellar disk theory, the disk analysis of this survey contributes additional evidence that cooler F, G, and K-type YSOs have longer phases than B and A-type YSOs in which their circumstellar disks evolve from optically thick disks to transition disks. Studies such as Currie and Kenyon (2009) and Hernández *et al.* (2010) have suggested that these disk types represent two possible evolutionary paths for circumstellar disks. Meanwhile, studies such as Xiao and Chang (2018), have detailed how the initial conditions of the prestellar core can affect the size and mass of the circumstellar disk that forms after the initial collapse phase. This suggests that the initial conditions of the prestellar core may influence if the resulting cirucmstellar disk is geometrically flared or flat, which were roughly correlated with pre-transition and optically thin disks, respectively. An investigation into the temporal evolution of circumstellar disks with varying physical geometries may establish a connection between the initial conditions of a prestellar core and the evolutionary path the resulting circumstellar disk is likely to follow.

APPENDIX A.

THE SPECTROSCOPIC SAMPLE

Table 1. IC 1805 Spectral Types and Photometry

Year	Date_No.[a] (MMDD_No.)	RA(J2000) (hhmmss.ss)	Dec(J2000) (° ′ ″)	SpTy Range	SpTy	A_V (r-i) (mag)	Assoc.?[b] (ext)	V(90P)[c] (mag)	r[d] (mag)	i[d] (mag)	I(90P)[c] (mag)
2012	1106_3_66	2 28 26.92	62 10 32.80	F0-F4	F2V	2.5	1	...	17.59	17.06	...
2012	1105_4_183	2 28 27.08	61 59 14.30	F5-F6	F6V	1.6	1	14.93	14.94	14.54	13.78
2012	1105_2_177	2 28 27.17	61 48 38.20	F4-F7	F5V	2.2	1	14.55	15.77	15.27	14.48
2012	1105_4_202	2 28 27.19	62 08 15.90	G8-K1	G9V	1.4	0	15.86	15.64	15.18	14.32
2012	1105_4_203	2 28 27.22	62 12 40.80	F2-F4	F2V	1.9	1	14.69	14.70	14.30	13.45
2012	1105_4_188	2 28 27.53	61 56 32.89	F7-F9	F8V	2.1	1	15.45	15.10	14.58	13.97
2012	1105_4_197	2 28 27.69	62 06 02.00	G0-G3	G2V	1.0	0	14.03	14.12	13.79	12.95
2012	1106_3_51	2 28 28.23	62 08 55.20	K3-K5	K4V	1.8	1	...	17.17	16.47	...
2012	1106_3_50	2 28 28.44	61 57 34.90	F0-F3	F2V	3.9	1	...	16.74	15.92	...
2012	1106_3_45	2 28 29.47	61 59 03.90	G9-K5	K2V	1.7	1	...	17.50	16.92	...
2012	1106_3_32	2 28 29.54	61 49 49.20	G9-K2	K2V	1.8	1	...	16.73	16.13	...
2012	1106_3_53	2 28 30.03	62 08 15.20	F7-F9	F8V	2.6	1	...	17.56	16.94	...
2012	1105_2_180	2 28 30.14	61 46 36.90		K2V	1.3	0	15.68	15.49	15.01	14.25
2012	1106_3_40	2 28 30.47	61 52 09.61	F8-G0	F8V	2.6	1	...	17.38	16.75	...
2012	1106_3_38	2 28 30.71	61 51 41.10	A1-A3	A1V	4.9	0	...	16.94	16.09	...
2012	1105_2_175	2 28 31.04	61 49 04.50	F3-F6	F4V	2.4	1	15.39	15.30	14.79	14.21
2012	1105_4_283	2 28 31.13	62 15 46.71	B9-A0	B9V	2.3	1	14.79	14.80	14.57	13.86
2012	1106_3_57	2 28 31.28	62 06 33.41	G1-G6	G3V	2.1	1	...	17.55	16.97	...
2012	1106_3_56	2 28 31.74	62 03 49.40	K2-K3	K2V	1.5	0	...	17.37	16.83	...
2012	1106_2_44	2 28 31.97	61 31 03.10	F7-F9	F8V	3.1	1	18.23	17.70	16.96	16.29
2012	1105_4_176	2 28 32.10	61 48 51.70	G0-G3	G0V	2.2	1	13.61	13.67[e]	13.11[f]	12.81
2012	1106_2_270	2 28 32.10	61 18 13.20	G0-G8	G7V	2.3	1	17.48	17.01	16.38	15.74
2012	1106_2_10	2 28 32.18	61 24 20.30	G8-K0	G8V	2.5	1	17.77	17.27	16.58	15.95
2012	1106_2_41	2 28 32.42	61 35 34.00	A1-A5	A3V	5.6	0	17.89	17.21	16.18	15.42
2012	1106_3_54	2 28 32.89	62 03 07.30	A2-A3	A3V	3.6	1	...	17.13	16.53	...
2012	1106_2_6	2 28 32.97	61 23 36.61	F7-F9	F8V	3.0	1	18.20	17.70	16.99	16.34
2012	1106_3_257	2 28 33.15	61 37 49.30	F9-G4	G3V	2.4	1	17.59	17.15	16.54	15.96
2012	1106_3_8	2 28 33.15	61 48 11.09	F5-F7	F6V	2.3	1	...	17.19	16.62	...
2012	1106_3_36	2 28 33.42	61 51 23.00	G0-K0	G5V	5.1	0	...	17.02	15.79	...
2012	1106_3_55	2 28 33.55	62 07 16.30	F7-F8	F7V	2.8	1	...	17.39	16.74	...
2012	1106_3_68	2 28 33.56	62 10 39.20	F9-K0	G5V	3.0	1	...	17.31	16.54	...
2011	0923_143	2 28 33.57	61 21 20.30		F1V	2.6	1	15.94	15.55	15.04	14.45
2012	1106_2_5	2 28 33.92	61 37 23.70	K4-K5	K4V	1.2	0	17.41	16.86	16.29	15.76
2011	0923_25	2 28 34.21	61 08 56.64	A0-A1	A1V	2.7	1	15.65	15.41	15.03	14.45
2012	1106_3_5	2 28 34.30	62 01 19.60	K4-K6	K5V	1.6	1	...	16.90	16.21	...
2012	1106_2_47	2 28 34.41	61 33 46.40	G1-G7	G6V	1.7	1	16.82	16.69	16.18	14.98
2011	0923_158	2 28 35.06	61 25 56.68	G1-G3	G2V	1.6	1	15.50	15.08	14.61	14.02
2011	0923_172	2 28 35.11	61 37 49.53	K2-K3	K2V	2.5	1	14.33	13.67	12.93	12.27
2012	1105_4_189	2 28 35.42	61 57 44.40	F2-F3	F2V[g]	2.6	1	15.51	15.38	14.83	14.03
2012	1106_3_52	2 28 35.71	62 02 32.70	G7-G9	G8V	1.9	1	...	16.96	16.40	...
2011	1023_257	2 28 35.74	61 32 07.94		F9V	2.0	1	15.79	15.39	14.87	14.29
2012	1105_4_284	2 28 35.93	62 00 46.90	G0-K0	G7V	1.2	0	15.96	15.75	15.34	15.19
2011	1105_5_266	2 28 35.96	61 58 00.80	G0-G7	G3V	2.2	1	15.72	15.50	14.91	14.09
2011	0923_135	2 28 36.11	61 15 48.43	F4-F5	F5V	2.2	1	15.83	15.48	14.98	14.39
2012	1106_2_265	2 28 36.24	61 20 25.20	G7-K0	G9V	5.1	0	18.41	17.48	16.22	15.38
2012	1105_2_168	2 28 36.33	61 37 36.89	F4-F5	F5V	2.4	1	16.02	15.61	15.06	14.52
2012	1106_2_34	2 28 36.53	61 25 26.89	G1-G6	G5V	2.2	1	17.17	16.69	16.08	15.48
2012	1105_4_194	2 28 37.11	62 03 16.20	G8-K2	K2V	1.8	1	15.18	14.89	14.29	13.45
2012	1106_3_259	2 28 37.13	61 37 39.60	G0-G5	G2V	1.9	1	16.54	16.10	15.56	15.04
2011	0923_157	2 28 37.29	61 27 13.50	G8-K1	K0V	1.2	0	14.80	14.37	13.94	13.35
2012	1106_3_7	2 28 37.44	62 00 52.50	G8-K3	K2V	1.8	1	...	17.33	16.73	...
2011	0923_27	2 28 38.05	61 08 34.76	G5-G6	G8V	1.0	0	14.72	14.42	14.06	13.51
2011	0923_159	2 28 38.14	61 26 30.02	F3-F6	F4V	2.3	1	15.07	14.72	14.22	13.66
2011	1023_295	2 28 38.41	61 27 10.05		A9V	2.8	1	15.91	15.50	14.98	14.36
2012	1106_2_266	2 28 38.82	61 17 29.50	K3-K5	K5V	1.6	0	18.20	17.61	16.93	16.34
2012	1106_3_44	2 28 39.35	61 55 56.60	F2-F5	F4V	4.0	1	...	16.61	15.76	...
2012	1105_2_272	2 28 39.54	61 28 49.89	F6-F7	F6V	3.1	1	16.12	15.60	14.88	14.26
2012	0124_217	2 28 40.16	61 37 17.39	K0-K2	K1V	1.2	0	16.40	15.90	15.45	14.91
2012	1105_4_177	2 28 40.23	61 52 48.70	G2-G7	G7V	1.3	0	15.28	15.08	14.66	13.91
2012	1106_3_3	2 28 40.58	62 01 49.00	G8-K2	G9V	1.9	1	...	17.47	16.90	...
2012	1105_2_125	2 28 40.68	61 13 30.70	F6-F7	F6V	2.1	1	16.20	15.83	15.33	14.71
2012	1106_2_2	2 28 40.88	61 21 51.00	M3-M4	M3V	0.5	0	16.64	16.17	14.96	14.25
2012	1105_4_208	2 28 40.89	62 09 49.31	F9-G0	F9V	1.3	0	14.98	14.96	14.59	13.76
2012	1106_3_64	2 28 40.95	62 08 58.21	G1-K2	G8V	3.4	1	...	17.20	16.32	...
2012	0923_163	2 28 41.26	61 33 35.68	F9-G2	G1V	1.4	0	15.29	14.94	14.54	13.92
2012	1105_4_184	2 28 41.43	61 55 38.90	A9-F0	A9V	2.2	1	14.35	14.36	13.97	13.23
2011	0923_273	2 28 41.49	61 36 42.20	G1-G3	G2V	1.2	0	14.80	14.45	14.07	13.56
2011	0923_167	2 28 41.66	61 32 27.90	K0-K2	K1V	0.6	0	14.45	14.27	13.96	13.06
2012	1105_2_147	2 28 41.75	61 27 20.00	K4-K5	K4V	0.7	0	15.17	14.65	14.19	13.60
2012	1106_3_67	2 28 42.84	62 12 48.40	A9-F3	F0V	2.3	1	...	16.71	16.28	...
2012	1105_4_201	2 28 43.04	62 12 25.70	G8-K1	G9V	2.6	1	15.64	15.13	14.41	13.51
2012	1105_4_207	2 28 43.13	62 11 09.80	A2-A5	A3V	2.3	1	15.80	15.71	15.39	14.62
2012	1106_3_59	2 28 43.13	62 05 20.80	F0-F3	F2V	2.9	1	...	16.84	16.22	...
2012	1105_2_179	2 28 43.24	61 46 59.81	F4-F7	F5V	2.5	1	15.60	15.41	14.85	14.28
2012	1106_2_50	2 28 43.32	61 33 03.60	K2-K4	K3V	2.4	1	17.78	17.22	16.44	15.69
2012	1106_3_60	2 28 43.40	62 04 52.70	G5-K0	G8V	3.3	1	...	17.10	16.24	...
2011	0923_169	2 28 43.41	61 31 34.30	B7-B9	B8V	4.3	0	15.95	15.49	14.84	14.18
2012	1106_3_63	2 28 43.43	62 13 42.90	K3-K5	K4V[g]	3.5	1	...	16.90	15.84	...
2012	1106_2_31	2 28 43.45	61 29 41.60	G0-G4	G1V	4.0	1	16.56	15.82	14.87	14.14
2011	0923_140	2 28 43.75	61 14 27.50		B8V	3.2	1	15.02	14.77	14.37	13.76
2012	1106_2_8	2 28 44.07	61 24 18.00	K1-K3	K2V	1.9	1	17.37	16.87	16.26	15.67
2012	1106_2_42	2 28 44.25	61 30 35.50	F9-G7	G5V	2.6	1	17.80	17.16	16.46	15.86
2012	1106_3_58	2 28 44.33	62 04 01.80	A2-A3	A3V	3.0	1	...	16.95	16.47	...
2012	1106_2_39	2 28 44.74	61 27 22.20	G0-G6	G5V	2.0	1	16.62	16.15	15.60	15.06
2012	1105_4_191	2 28 45.03	62 07 43.10	F6-F7	F6V	1.9	1	15.93	15.41	14.95	14.36
2012	1105_5_31	2 28 45.08	62 10 27.31	A3-A7	A5V	2.1	1	14.19	14.33	14.01	13.26
2012	1105_4_205	2 28 45.60	62 11 40.80	G2-G7	G6V	1.2	0	15.07	15.01	14.61	13.85

Table 1. IC 1805 Spectral Types and Photometry (Continued)

Year	Date_No.[a] (MMDD_No.)	RA(J2000) (hhmmss.ss)	Dec(J2000) (° ′ ″)	SpTy Range	SpTy	A_V (r-i) (mag)	Assoc.?[b] (ext)	V(90P)[c] (mag)	r[d] (mag)	i[d] (mag)	I(90P)[c] (mag)
2012	1105_2_133	2 28 45.88	61 23 31.89	B9-A0	B9.5V	3.4	1	16.05	15.71	15.22	14.65
2012	1106_2_262	2 28 45.91	61 16 13.20	K1-K3	K2V	1.5	0	17.39	16.90	16.37	15.75
2012	1105_4_273	2 28 46.59	61 47 48.00	F9-G7	G1V	2.8	1	15.63	15.28	14.58	13.73
2011	0923_29	2 28 46.62	61 08 50.50	F7-F8	F7V	1.1	0	13.90	13.60	13.29	12.72
2012	1106_2_267	2 28 46.64	61 20 18.60	G8-K4	K3V	2.0	1	18.26	17.64	16.97	16.40
2012	1105_2_121	2 28 46.92	61 15 48.70	G9-K2	K0V[g]	4.7	0	16.09	15.14	13.96	13.17
2012	1105_2_123	2 28 46.98	61 14 36.00	K3-K5	K4V	0.8	0	16.39	15.92	15.43	14.85
2012	1106_2_263	2 28 47.23	61 21 16.80	G8-K2	G9V	2.4	1	17.77	17.31	16.63	15.99
2012	1106_2_38	2 28 47.65	61 26 46.30	K4-K5	K4V	1.9	1	18.32	17.59	16.87	16.27
2012	1106_3_42	2 28 47.87	61 55 14.40	F4-F5	F4V	2.7	1	...	16.94	16.36	...
2012	1106_2_48	2 28 48.03	61 32 22.91	G5-G8	G6V	2.4	1	18.02	17.47	16.82	16.15
2012	1105_2_139	2 28 48.15	61 22 14.00	K4-K5	K5V	4.9	0	16.49	15.32	13.93	13.10
2012	1106_2_264	2 28 48.79	61 17 16.30	K2-K4	K3V	2.3	1	18.47	17.88	17.15	16.54
2011	0923_149*	2 28 48.81	61 19 50.30		A7V	2.9	1	14.57	14.16	13.64	13.03
2011	0923_279	2 28 49.39	61 34 27.20	F4-F5	F4V	1.8	1	14.93	14.61	14.22	13.63
2012	1105_2_186	2 28 49.39	61 51 11.60	F4-F7	F7V	1.7	1	15.00	14.80	14.37	13.61
2011	0923_166*	2 28 49.51	61 30 04.30	A9-F2	F0V	3.1	1	14.98	14.43	13.82	13.19
2011	1023_229	2 28 50.01	61 09 39.90	A7-F1	F0V	2.7	1	15.96	15.54	15.02	14.39
2012	1106_3_2	2 28 50.06	61 47 21.60	F0-F5	F6V	3.0	1	...	17.41	16.72	...
2012	1105_2_190	2 28 50.18	61 53 01.00	B2-B3	B3V	5.3	0	15.85	15.48	14.69	13.66
2011	0923_274	2 28 50.24	61 22 23.22	F7-G0	F8V	4.4	0	15.95	15.08	14.08	13.38
2012	1106_2_37	2 28 50.28	61 28 06.90	G6-K0	G8V	2.7	1	18.31	17.67	16.94	16.32
2012	1105_4_206	2 28 50.34	62 08 54.00	A3-A6	A5V	2.0	1	15.65	15.72	15.41	14.69
2012	1106_3_43	2 28 50.37	61 58 17.10	F9-G0	G0V	2.3	1	...	17.05	16.47	...
2012	1106_2_255	2 28 50.93	61 14 49.40	F7-F8	F7V	3.1	1	17.95	17.43	16.71	16.05
2012	1106_2_32	2 28 51.23	61 25 24.81	G2-K0	G7V	2.2	1	17.71	17.13	16.50	15.91
2012	1105_2_124	2 28 51.55	61 09 43.90	F4-F7	F6V	2.3	1	16.22	15.80	15.26	14.63
2011	0923_168	2 28 51.74	61 30 41.60	G7-K0	G8V	4.3	0	15.90	15.03	13.97	13.23
2012	1106_2_268	2 28 51.94	61 18 44.09	K2-K3	K2V	1.4	0	17.12	16.61	16.09	15.52
2011	1023_264	2 28 52.59	61 34 28.37	G2-G8	G5V	1.3	0	14.77	14.36	13.95	13.41
2012	1106_3_47	2 28 52.93	61 57 35.60	G1-G7	G5V	2.7	1	...	17.27	16.56	...
2012	0124_220	2 28 52.99	61 36 00.00	F8-G0	F8V	1.9	1	16.19	15.76	15.27	14.76
2012	1105_2_137	2 28 53.47	61 23 06.69	G6-G7	G7V	1.8	1	16.39	15.89	15.36	14.78
2012	1105_4_173	2 28 53.69	61 54 40.90	F6-F8	F8V	2.5	1	15.40	15.05	14.44	14.27
2011	0923_121	2 28 53.90	61 08 52.80		A2V	2.6	1	15.32	15.05	14.66	14.10
2012	1106_3_31	2 28 53.93	61 54 51.30	K2-K3	K2V	2.0	1	...	17.28	16.64	...
2012	1105_4_287	2 28 54.52	62 13 15.91	G8-K2	K0V[g]	3.6	1	15.72	15.18	14.24	13.49
2011	0923_161	2 28 54.73	61 33 42.70	G2-G4	G3V	1.6	1	15.98	15.57	15.10	14.51
2012	1105_5_293	2 28 54.74	61 50 31.71	F8-G0	F9V	1.6	1	15.16	14.67	14.24	13.70
2012	1106_2_253	2 28 54.98	61 16 11.60	G4-G8	G7V	1.5	0	16.89	16.49	16.01	15.28
2012	1106_3_46	2 28 55.03	61 56 15.10	B6-A0	B7V	5.7	0	...	16.69	15.78	...
2012	1105_5_44	2 28 55.09	62 10 46.81	K2-K4	K3V	0.9	0	15.31	15.00	14.56	14.44
2011	0923_139	2 28 55.50	61 15 43.60	F3-F4	F4V	1.9	1	15.22	14.87	14.45	13.89
2012	1105_4_286	2 28 55.62	62 01 22.70	F4-F6	F5V	1.9	1	15.50	15.38	14.96	14.19
2012	1106_3_16	2 28 55.87	62 15 30.41	A9-F2	F1V	2.2	1	...	17.59	17.14	...
2012	1106_2_43	2 28 56.01	61 33 45.21	F5-F7	F6V	2.3	1	17.16	16.70	16.15	15.53
2012	1106_3_69	2 28 56.33	62 10 54.00	K3-K5	K4V	1.1	0	...	17.10	16.55	...
2012	1106_3_70	2 28 57.46	62 09 46.51	G0-K0	G9V	2.0	1	...	17.54	16.94	...
2012	1106_2_258	2 28 57.50	61 12 33.20	G1-G8	G5V	2.1	1	17.54	17.08	16.49	15.79
2012	1105_5_263	2 28 57.77	62 01 35.60	F8-F9	F8V	1.4	0	14.53	14.55	14.19	13.37
2012	1106_3_10	2 28 57.82	61 49 47.00	A1-A3	A3V	3.5	1	...	16.75	16.17	...
2012	1105_4_282	2 28 58.00	62 00 16.49	F6-F7	F7V	1.3	0	14.65	14.73	14.38	13.66
2012	1105_2_134	2 28 58.03	61 20 22.00	G9-K1	K0V[g]	4.5	0	16.35	15.46	14.32	13.69
2012	1105_5_6	2 28 58.45	62 03 30.59	A6-A9	A8V	1.9	1	15.84	15.85	15.53	14.79
2012	1106_3_267	2 28 58.46	61 46 23.00	A6-A8	A7V	2.8	1	...	17.03	16.53	...
2011	0923_123	2 28 58.49	61 08 36.80	G3-G6	G6V	1.4	0	15.37	14.96	14.53	13.96
2012	1105_4_216	2 28 58.59	62 16 07.40	B9-A0	A0V	2.0	1	14.88	15.07	14.87	14.17
2012	1106_2_256	2 28 58.65	61 11 52.90	G8-K2	K0V	5.3	0	18.42	17.49	16.18	15.22
2012	1106_3_37	2 28 58.67	61 53 09.00	A1-A3	A2V	4.7	0	...	17.35	16.52	...
2012	1105_5_253	2 28 59.03	61 56 19.00	A9-F1	A9V	2.0	1	13.80	13.95	13.59	12.78
2012	1106_2_52	2 28 59.07	61 37 48.00	F4-F8	F6V	4.4	0	17.90	17.11	16.12	15.48
2012	0124_191	2 28 59.16	61 24 07.39	A5-A6	A2V	3.3	1	16.35	15.97	15.43	14.84
2012	1105_2_173	2 28 59.22	61 47 15.30	G7-K0	G9V	4.8	0	15.64	14.64	13.44	12.93
2012	1106_2_36	2 28 59.29	61 26 29.50	G2-K0	G7V[g]	4.6	0	17.98	17.04	15.92	15.16
2012	1106_2_260	2 28 59.41	61 13 27.21	A1-A6	A3V	4.0	1	17.48	17.01	16.33	15.56
2011	1023_232	2 28 59.55	61 16 30.40	G1-G6	G3V	1.4	0	15.82	15.40	14.98	14.45
2012	0124_193	2 28 59.70	61 23 11.80		B9V	3.6	1	16.35	16.00	15.49	14.87
2012	1105_2_182	2 28 59.73	61 47 47.80	G5-G7	G6V	1.4	0	15.35	15.24	14.79	14.02
2012	1105_2_188	2 29 00.59	61 50 27.50	G5-G7	G6V	1.5	0	15.96	15.66	15.20	14.42
2012	1105_5_295	2 29 00.78	61 50 08.70	G2-G7	G6V	1.0	0	15.29	14.83	14.48	13.94
2012	1106_2_54	2 29 01.34	61 38 17.80	G6-K0	G8V	4.3	0	16.73	15.76	14.69	14.00
2012	1106_3_61	2 29 01.71	62 13 30.00	F3-F6	F5V	2.3	1	...	16.79	16.28	...
2012	0124_213	2 29 01.94	61 38 09.70	G9-K1	K0V	2.2	1	16.39	15.77	15.11	14.63
2012	1106_3_34	2 29 02.05	61 50 51.00	G7-K0	G6V	2.7	1	...	16.87	16.14	...
2012	0124_289	2 29 02.21	61 30 49.60	A6-A8	A6V	3.0	1	16.05	15.59	15.08	14.50
2012	1105_4_195	2 29 03.09	62 06 05.30		A1V	2.2	1	15.48	15.42	15.16	14.42
2012	1106_3_33	2 29 03.33	61 54 22.50	G7-K0	G9V[g]	4.5	0	...	16.30	15.17	...
2012	1106_3_4	2 29 03.71	61 48 08.20	A0-A2	A1V	3.5	1	...	17.59	17.04	...
2012	1106_3_258	2 29 03.85	61 38 10.90	K3-K5	K4V	5.1	0	18.36	17.15	15.74	15.01
2012	1105_4_281	2 29 04.06	62 14 36.30	A6-A8	A7V	1.9	1	15.78	15.88	15.58	14.85
2012	1106_3_65	2 29 04.08	62 11 20.10	G0-G8	G3V	3.6	1	...	16.64	15.76	...
2012	1105_4_288	2 29 04.11	62 01 56.80	A1-A2	A1V	2.8	1	15.63	15.59	15.18	14.38
2012	1106_3_263	2 29 04.45	61 47 35.31	A5-A8	A7V	3.0	1	...	16.38	15.85	...
2012	1106_3_35	2 29 04.75	61 53 53.19	K4-K5	K4V	1.7	1	...	17.05	16.35	...
2012	1105_2_187	2 29 04.95	61 52 34.00	F2-F4	F3V	1.8	1	14.04	14.12	13.73	13.11
2012	1105_4_285	2 29 05.83	62 13 46.60	G6-K0	G9V	1.1	0	15.64	15.40	14.98	14.26
2012	1106_3_297	2 29 05.99	61 33 12.10	G8-K0	G9V	1.7	1	16.67	16.20	15.67	15.09

Table 1. IC 1805 Spectral Types and Photometry (Continued)

Year	Date_No.[a] (MMDD_No.)	RA(J2000) (hhmmss.ss)	Dec(J2000) (° ′ ″)	SpTy Range	SpTy	A_V (r-i) (mag)	Assoc.?[b] (ext)	V(90P)[c] (mag)	r[d] (mag)	i[d] (mag)	I(90P)[c] (mag)
2011	0923_275	2 29 06.12	61 34 41.17	A3-A6	A5V	2.2	1	15.71	15.48	15.13	14.57
2012	1105_4_192	2 29 06.20	62 02 56.19	G7-G9	G8V	0.9	0	14.13	14.13	13.77	13.20
2012	1106_3_295	2 29 06.37	61 34 34.60	A2-A7	A6V	4.5	0	18.26	17.67	16.83	16.09
2011	1023_269	2 29 06.66	61 35 35.69		F7V	2.2	1	15.53	15.15	14.62	14.09
2012	1105_2_185*	2 29 07.18	61 53 08.21	A0-A1	A1V	4.1	1	15.77	15.53	14.85	13.88
2012	1105_2_183	2 29 07.20	61 54 29.11	A3-A7	A5V	2.8	1	15.26	15.26	14.78	14.00
2012	1105_5_32	2 29 07.77	62 05 27.41	B9-A0	B9V	1.9	1	14.44	14.18	14.04	13.51
2012	1105_5_41	2 29 07.83	62 15 25.30	G7-K0	G9V[g]	2.4	1	15.43	15.10	14.43	13.59
2011	1023_253	2 29 07.86	61 32 22.20	F7-F8	F7V	1.5	0	14.90	14.62	14.23	13.74
2012	1106_3_9	2 29 08.01	61 59 23.80	K3-K5	K4V	1.7	1	...	18.19	17.51	...
2012	1105_5_36	2 29 09.52	62 06 06.70	A1-A0	A0V	2.3	1	15.66	15.58	15.31	14.75
2012	1105_4_187	2 29 09.63	61 59 01.00	G7-K2	G8V[g]	4.1	1	15.68	14.97	13.94	12.93
2012	1106_3_14	2 29 10.05	62 13 19.50	K3-K5	K3V	2.0	1	...	17.43	16.76	...
2011	0923_138	2 29 10.07	61 15 25.19		G3V	2.7	1	14.76	14.16	13.46	12.79
2012	1105_4_172	2 29 10.09	61 50 23.80	A0-A1	A1V	2.7	1	15.79	15.79	15.41	14.61
2011	0923_150	2 29 10.25	61 19 59.68		F8V	1.9	1	15.30	14.93	14.45	13.92
2012	1106_3_41	2 29 10.62	61 58 45.99		K3V	1.2	0	...	16.71	16.20	...
2012	1105_2_129	2 29 10.67	61 14 48.30		K4V	1.1	0	16.50	15.98	15.43	14.84
2011	1023_244	2 29 10.88	61 22 27.75	B9-A2	B9V	4.0	1	15.10	14.70	14.11	13.47
2012	0124_202	2 29 10.96	61 25 07.70	G9-K2	G8V	3.7	1	16.37	15.56	14.63	13.92
2012	1106_3_269	2 29 10.97	61 46 28.91	A2-A5	A3V	3.6	1	...	17.32	16.71	...
2012	1105_4_209*	2 29 11.23	62 09 13.70	B9-A1	A0V	2.1	1	13.98	14.20	13.97	13.15
2012	1105_2_189	2 29 11.24	61 51 08.61	G8-G9	G9V	1.0	0	13.09	13.45	13.07	12.39
2012	1105_2_184	2 29 11.31	61 48 22.79	F9-G3	G2V	1.9	1	15.83	15.66	15.13	14.33
2012	1105_4_193	2 29 11.35	62 06 52.70	F3-F5	F4V	1.8	1	15.30	15.10	14.71	14.57
2011	1023_294	2 29 11.44	61 15 19.82	A7-A9	A9V	1.9	1	15.48	15.28	14.93	14.41
2012	1105_4_279	2 29 11.89	61 47 26.81	G7-K2	K0V[g]	3.4	1	15.73	15.05	14.15	13.20
2012	1105_5_48	2 29 12.08	62 12 01.80	F5-F7	F6V	1.1	0	15.54	14.62	14.33	13.79
2012	1106_3_72	2 29 12.29	62 16 13.71	B7-A1	B9V	3.3	1	...	16.90	16.46	...
2012	1105_4_185	2 29 12.33	61 59 50.50	A7-A9	A8V	2.1	1	15.65	15.61	15.24	14.65
2012	1106_3_6	2 29 12.40	61 48 58.60	A2-A5	A3V	3.4	1	...	16.82	16.26	...
2011	0923_276	2 29 12.77	61 22 53.10		F7V	2.5	1	15.99	15.51	14.92	14.36
2012	1106_2_269	2 29 12.78	61 20 56.30	F9-K0	G5V	3.2	1	18.26	17.71	16.90	16.26
2012	1106_3_18	2 29 12.80	62 15 01.20	K4-K5	K5V	1.7	1	...	17.18	16.47	...
2012	1105_5_33	2 29 12.88	62 09 17.80	F1-F3	F2V	1.7	1	15.82	15.40	15.04	14.29
2012	1105_5_47	2 29 13.07	62 12 56.40	A1-A2	A2V	2.8	1	14.14	14.26	13.84	13.15
2012	1105_4_198	2 29 13.40	62 04 53.01	F3-F6	F4V	1.8	1	15.04	15.04	13.886	...
2012	1105_5_38	2 29 13.73	62 06 23.20	A9-F1	F0V	1.9	1	14.77	14.62	13.498	...
2012	1105_5_43	2 29 14.05	62 14 10.80	A9-F0	A9V	1.6	1	14.76	14.87	14.087	...
2012	0124_210	2 29 14.22	61 27 54.00	F6-F8	F7V	2.8	1	16.28	15.76	15.09	14.42
2012	1105_4_214	2 29 14.62	62 14 26.09	G6-K2	G9V	1.1	0	15.79	15.70	15.29	14.53
2012	1105_2_128	2 29 14.66	61 14 03.81	F7-F9	F8V	2.4	1	16.17	15.72	15.13	14.58
2012	1105_2_127	2 29 14.82	61 15 47.41	F6-F7	F6V	1.9	1	15.44	15.10	14.64	14.12
2012	0124_300	2 29 15.40	61 47 16.20	B6-B8	B8V	3.4	1	14.71	14.66	14.21	13.60
2012	1105_2_284	2 29 15.44	61 55 35.30	G8-K1	G9V[g]	3.8	1	14.45	13.91	12.94	12.15
2012	1106_2_297	2 29 15.61	61 08 43.80	A9-F5	F1V	3.4	1	18.29	17.74	17.05	16.43
2012	1105_4_196*	2 29 16.24	62 04 08.00	B9-A0	A0V	2.1	1	15.36	15.02	15.362	...
2011	0923_174	2 29 16.30	61 35 14.60	F4-F5	F5V	1.8	1	15.38	14.99	15.38	14.04
2012	1105_4_179	2 29 16.45	61 54 14.30	F4-F7	F6V	2.2	1	15.88	15.72	15.877	...
2011	1023_228	2 29 16.82	61 10 35.89		F6V	1.2	0	13.88	13.65	13.34	12.81
2012	1105_4_186	2 29 17.04	61 57 34.50	K2-K4	K3V	0.7	0	15.63	15.22	14.81	14.05
2012	1105_2_165	2 29 17.22	61 37 47.61		F8V	2.0	1	16.37	15.90	15.39	14.87
2012	1106_3_252	2 29 17.29	61 37 39.30	A0-A1	A1V	2.9	1	16.55	16.23	15.81	15.25
2012	1105_4_174	2 29 18.41	61 51 26.31	F7-F9	F8V	1.9	1	15.96	15.67	15.20	...
2012	1106_3_299	2 29 18.46	61 33 54.30	K1-K3	K2V	2.8	1	18.30	17.45	16.64	16.07
2012	1106_2_299	2 29 18.69	61 08 22.60	A9-F7	F3V	3.3	1	17.94	17.43	16.73	16.11
2012	1105_5_35	2 29 18.98	62 08 41.70	F7-F8	F8V	1.2	0	15.48	15.05	14.71	14.14
2012	1105_5_37	2 29 19.13	62 08 04.70	G7-K1	G9V	1.1	0	15.89	15.96	15.55	14.60
2012	0124_232	2 29 19.28	61 48 05.11	K0-K3	K2V	3.2	1	14.84	14.18	13.28	12.51
2012	1106_2_56	2 29 19.59	61 37 48.50	G2-K0	G6V[g]	4.0	1	17.15	16.28	15.29	14.62
2012	1106_3_293	2 29 20.20	61 37 28.00	K1-K3	K2V[g]	4.7	0	17.45	16.28	15.06	14.23
2011	0923_152	2 29 20.21	61 24 19.11	A0-A1	A0V	3.1	1	15.64	15.31	14.88	14.33
2011	1023_33	2 29 20.37	61 46 24.28	G5-G9	G8V	1.4	0	13.27	13.09	12.65	11.94
2012	1105_5_2	2 29 20.67	62 02 16.51	B9-A0	A0V	2.3	1	14.51	14.72	14.45	13.71
2012	1106_2_252	2 29 21.15	61 11 57.70	F8-G0	G0V	2.7	1	17.41	16.87	16.20	15.59
2012	1105_5_46	2 29 21.24	62 10 55.29		A1V	2.1	1	15.59	15.71	15.46	14.72
2011	0923_179	2 29 21.99	61 37 23.40	B7-B8	B8V	2.8	1	14.10	13.86	13.56	13.04
2012	1106_3_48	2 29 22.32	61 56 57.90	F9-G0	F9V	2.1	1	...	16.83	16.31	...
2011	0923_132	2 29 22.33	61 13 56.60	G1-G4	G4V	1.3	0	15.84	15.47	15.06	14.55
2012	1106_3_74	2 29 22.44	62 15 59.60	A9-F3	F2V	2.2	1	...	17.59	17.13	...
2012	1106_2_254	2 29 22.89	61 13 29.71	F0-F7	F4V	3.8	1	18.07	17.43	16.60	15.97
2012	1105_2_167	2 29 23.01	61 36 42.59	G6-K0	G7V	1.6	1	16.49	16.07	15.59	15.03
2012	1105_5_251	2 29 23.03	61 57 55.50	K4-K5	K4V[g]	3.3	1	15.22	14.33	13.31	12.49
2012	0124_197	2 29 23.65	61 23 20.61	F2-F5	F3V	2.5	1	16.16	15.71	15.16	14.60
2012	1106_2_7	2 29 23.99	61 35 17.30	A1-A2	A1V	3.9	1	17.43	16.93	16.30	15.69
2011	1023_296	2 29 24.17	61 17 02.44	G2-G8	G5V	1.2	0	15.11	14.75	14.35	13.88
2012	1105_5_8	2 29 24.36	62 03 53.30	F2-F5	F4V	1.8	1	15.87	15.79	15.39	14.64
2011	0923_178	2 29 24.39	61 36 08.00		F7V	1.5	0	15.41	15.08	14.70	14.19
2012	1106_2_295	2 29 24.62	61 10 40.50	G1-G7	G3V	2.8	1	17.69	17.12	16.39	15.73
2011	0923_277*	2 29 25.07	61 32 34.76	B7-B8	B8V	3.1	1	15.09	14.83	14.44	13.93
2012	0124_286	2 29 25.22	61 17 17.00	B7-B8	B8V	3.2	1	16.02	15.76	15.37	14.77
2011	1023_223	2 29 25.70	61 14 04.86	B9-A1	A0V	3.6	1	15.79	15.47	14.93	14.30
2012	1106_3_245	2 29 25.74	61 32 15.30	F0-F9	F5V	3.3	1	18.16	17.53	16.80	16.18
2012	1105_2_136	2 29 26.08	61 22 45.30	G5-G7	G6V	1.4	0	15.35	14.94	14.50	13.99
2012	1106_2_58	2 29 26.14	61 37 51.70	G2-G8	G5V	4.0	1	17.24	16.38	15.39	14.67
2012	0304_252*	2 29 26.17	61 49 56.70	F6-F7	F7V	2.0	1	15.27	15.21	14.73	13.85
2012	1105_5_10	2 29 26.47	62 05 01.30	A5-A8	A7V	2.1	1	15.86	15.82	15.48	14.75

Table 1. IC 1805 Spectral Types and Photometry (Continued)

Year	Date_No.[a] (MMDD_No.)	RA(J2000) (hhmmss.ss)	Dec(J2000) (° ′ ″)	SpTy Range	SpTy	A_V (r-i) (mag)	Assoc.?[b] (ext)	V(90P)[c] (mag)	r[d] (mag)	i[d] (mag)	I(90P)[c] (mag)
2012	1105_4_290	2 29 26.51	62 02 41.01	F4-F7	F7V	1.1	0	14.85	14.84	14.54	13.75
2011	1023_266	2 29 26.95	61 33 22.06	F8-F9	F8V	0.8	0	13.32	13.26	13.01	12.48
2011	1023_42	2 29 27.84	61 47 08.83		F8V	1.9	1	15.73	15.58	15.09	14.30
2011	1023_237	2 29 28.54	61 20 26.50		F6V	1.8	1	14.66	14.28	13.85	13.31
2011	0923_155	2 29 28.89	61 26 30.70		B7V	3.8	1	15.09	14.72	14.21	13.67
2012	1106_2_243	2 29 29.14	61 08 08.49	G1-G7	G5V	1.8	1	16.72	16.31	15.78	15.19
2012	0124_235	2 29 29.29	61 51 45.20	F8-F9	F9V	3.7	1	13.45	13.31	12.44	11.70
2012	1106_3_76	2 29 29.33	62 15 36.90	F7-F8	F8V	1.9	1	...	17.51	17.04	...
2012	0124_200	2 29 29.53	61 22 48.00	G9-K0	K0V	1.4	0	15.06	14.55	14.06	13.54
2012	1105_4_204	2 29 29.87	62 07 29.70	G7-K0	G9V	2.5	1	15.29	14.77	14.08	13.19
2012	1105_5_268	2 29 30.23	61 59 31.30	F8-G0	F9V	1.3	0	15.29	15.29	14.92	14.35
2012	1106_2_60	2 29 30.35	61 38 11.10		A1V	4.2	0	16.58	16.02	15.32	14.64
2011	0923_126	2 29 30.59	61 07 38.90	A1-A5	A3V	2.7	1	15.25	15.02	14.61	14.08
2012	1105_4_200	2 29 31.01	62 05 14.31	A1-A2	A1V	1.9	1	13.57	13.87	13.66	12.98
2012	1105_4_220	2 29 31.31	62 15 49.30	F1-F5	F2V	2.1	1	15.81	15.65	15.21	14.45
2011	1023_256	2 29 31.39	61 28 56.00	F8-F9	F8V	2.0	1	14.51	14.03	13.54	12.95
2012	1105_5_264*	2 29 31.57	61 58 48.40	A3-A8	A5V	2.5	1	15.50	15.44	15.04	14.26
2011	1023_263	2 29 32.11	61 36 07.50	B9-A1	A1V	2.8	1	15.13	14.80	14.39	13.83
2012	1106_3_243	2 29 32.33	61 34 39.70	G9-K2	K0V	4.3	0	17.99	16.90	15.80	15.07
2012	1105_2_156	2 29 33.07	61 32 03.99	F0-F2	F1V	3.1	1	16.47	15.96	15.33	14.73
2012	1105_2_126	2 29 33.13	61 15 44.30	G9-K1	G9V	3.5	1	16.23	15.43	14.52	13.80
2012	1105_5_270	2 29 33.72	61 59 58.20	F8-G0	F8V	1.7	1	15.46	15.38	14.95	14.18
2012	1105_5_4	2 29 34.11	62 02 39.40	G1-G7	G5V	1.4	0	14.88	15.08	14.65	13.57
2012	1105_2_192	2 29 34.23	61 56 39.80	G5-K0	G7V	2.0	1	15.59	15.31	14.74	13.93
2012	1106_3_78	2 29 35.40	62 15 53.70	F6-F8	F7V	2.0	1	...	17.56	17.07	...
2012	1105_5_39	2 29 35.53	62 06 39.39	G7-K2	G9V	1.0	0	15.38	15.35	14.97	14.35
2012	1105_5_45	2 29 35.84	62 13 20.40		A1V	1.9	1	15.98	15.70	15.50	14.97
2011	0923_136	2 29 35.91	61 15 56.80	B5-B7	B6V	4.0	1	14.30	13.90	13.36	12.81
2012	1105_4_165	2 29 35.98	61 47 53.30	A8-F3	F0V	2.0	1	14.20	14.30	13.92	13.15
2012	1105_2_288	2 29 36.50	61 54 05.31		G9V	3.3	1	13.05	12.64	11.77	11.76
2011	0923_133	2 29 36.58	61 18 43.70	A3-A4	A4V	2.5	1	14.79	14.47	14.07	13.52
2011	0923_128	2 29 36.78	61 09 18.00	B9-A3	A1V	2.8	1	14.67	14.38	13.98	13.34
2012	1105_2_163	2 29 37.04	61 37 13.21	G5-G7	G6V	4.0	1	16.21	15.36	14.36	13.60
2011	0923_147	2 29 37.66	61 21 27.40	B8-B9	B9V	3.2	1	15.45	15.14	14.71	14.18
2012	1106_2_245	2 29 37.77	61 07 54.20	M2-M4	M3V	0.3	0	17.47	16.83	15.65	14.90
2012	1105_5_257	2 29 38.07	61 56 56.90	G2-G6	G4V	0.9	0	15.21	15.14	14.81	13.99
2012	1105_5_5	2 29 38.32	62 15 35.40		K6V	1.1	0	15.87	15.51	14.84	14.02
2012	1105_2_166	2 29 38.51	61 35 01.70	G8-K0	G9V	3.7	1	16.23	15.41	14.45	13.74
2012	1106_3_247	2 29 38.59	61 32 52.60	F9-G4	G3V	4.9	0	17.82	16.82	15.65	14.85
2011	0923_280	2 29 38.95	61 23 52.30	B9-A0	A0V	3.2	1	15.88	15.55	15.08	14.50
2012	1105_2_115	2 29 39.00	61 13 35.50		A1V	3.2	1	16.38	16.05	15.56	14.97
2012	0304_228	2 29 39.68	61 28 42.20	G8-G9	G9V	1.0	0	15.16	14.76	14.38	13.90
2012	0124_288	2 29 39.99	61 19 01.80	A2-A8	A5V	2.9	1	16.22	15.85	15.36	14.80
2012	1106_2_241	2 29 40.18	61 10 20.40	A3-A5	A3V	3.4	1	17.33	16.94	16.37	15.74
2012	1105_2_118	2 29 40.32	61 10 51.81	A7-A8	A7V	3.2	1	16.08	15.69	15.12	14.50
2011	0923_127	2 29 40.38	61 11 23.00		F8V	1.3	0	14.07	13.82	13.47	13.01
2012	1105_2_158	2 29 40.53	61 32 25.80	G0-G5	G2V	1.3	0	15.52	15.16	14.77	14.27
2011	1023_50	2 29 41.58	61 49 30.06		F2V	4.0	1	14.31	13.97	13.12	12.28
2011	1023_298*	2 29 42.32	61 18 36.80		B8V	3.3	1	15.03	14.76	14.33	13.84
2012	1105_2_149	2 29 43.04	61 28 28.70	A7-A8	A7V	2.1	1	13.54	13.43	13.08	12.56
2012	1106_1_284	2 29 43.70	61 37 24.70	G7-G9	G8V	2.0	1	17.12	16.59	16.02	15.41
2012	0124_234	2 29 43.78	61 47 02.50	B3-B7	B5V	3.6	1	14.64	14.64	14.20	13.33
2012	1105_2_117	2 29 44.03	61 12 56.80	G7-G9	G8V	1.5	0	16.44	15.98	15.52	14.99
2012	1106_3_241	2 29 44.50	61 37 01.60	K2-K3	K2V	2.1	1	18.39	17.74	17.09	16.45
2012	1106_2_247	2 29 44.68	61 07 18.60	F8-G0	F9V	2.9	1	17.68	17.29	16.59	15.99
2011	0923_124	2 29 44.87	61 08 52.80	B7-B9	B8V	3.0	1	15.09	14.89	14.54	14.02
2012	1105_4_217	2 29 45.24	62 15 38.70	G6-K0	G7V[g]	2.7	1	15.53	15.21	14.49	13.65
2012	1204_248	2 29 45.84	61 36 50.83		F6V	2.3	1	16.26	15.83	15.29	14.70
2012	1106_3_20	2 29 45.91	62 11 24.00	K4-K5	K5V	1.2	0	...	16.79	16.20	...
2012	1203_1_163	2 29 45.93	61 34 42.10	F6-F7	F6V	3.1	1	17.17	16.56	15.84	15.21
2012	1203_2_296	2 29 45.97	61 44 59.46	G0-G7	G3V	2.1	1	...	16.34	15.76	...
2012	1105_5_7	2 29 46.00	62 14 43.91	G2-G7	G2V	1.3	0	15.64	15.62	15.23	14.47
2012	1203_2_194	2 29 46.49	61 23 23.92	K0-K3	K2V	2.4	1	18.52	17.87	17.15	16.53
2011	1023_226*	2 29 46.71	61 12 47.60	G8-K0	G9V	2.9	1	15.16	14.48	13.69	12.94
2012	1203_2_230	2 29 46.84	61 39 30.73		F8V	2.2	1	...	15.32	14.77	...
2012	1203_2_298	2 29 46.98	61 45 32.44	F9-G1	G0V	1.8	1	...	15.52	15.03	...
2011	0923_171	2 29 47.22	61 37 47.90	A5-A7	A6V	0.1	0	14.32	14.05	14.15	13.13
2012	1105_2_138	2 29 47.22	61 25 31.40	F6-F7	F7V	2.1	1	16.09	15.67	15.16	14.60
2012	1106_3_80	2 29 47.59	62 15 52.80	K2-K3	K2V	1.6	1	...	16.67	16.12	...
2011	0923_144	2 29 47.71	61 19 25.30	F2-F3	F2V	2.1	1	15.35	14.97	14.53	14.03
2012	1203_1_176	2 29 47.76	61 39 14.04	F9-G6	G2V	1.1	0	...	14.76	14.42	...
2012	1204_295	2 29 48.30	61 41 56.05		F8V	2.2	1	...	16.32	15.79	...
2011	0923_125	2 29 48.67	61 12 35.30	G7-K0	G9V	3.4	1	15.80	15.08	14.19	13.48
2011	0923_134	2 29 49.12	61 16 07.87	F4-F5	F5V	2.1	1	15.83	15.44	14.96	14.43
2012	1106_3_265	2 29 49.14	61 49 20.60	G1-G8	G5V	2.9	1	...	16.76	16.00	...
2012	1204_202	2 29 49.34	61 13 23.09	F8-G0	F8V	1.6	1	15.75	15.41	14.99	14.47
2012	1105_4_180	2 29 49.62	61 55 29.00	A4-A7	A6V	2.7	1	15.66	15.42	14.97	14.18
2012	1105_2_196	2 29 49.72	61 56 12.20	F9-G0	G0V	1.9	1	15.94	15.58	15.09	14.30
2012	1204_225	2 29 49.77	61 27 58.38		G9V	1.8	1	17.02	16.48	15.92	15.35
2011	1023_231	2 29 49.91	61 22 35.46	F2-F5	F3V	3.5	1	14.98	14.36	13.60	12.95
2012	1105_2_114	2 29 50.28	61 10 12.90	G3-G5	G4V	3.9	1	16.28	15.50	14.55	13.79
2012	1203_1_179	2 29 50.34	61 40 42.04	F2-F3	F3V	2.0	1	...	15.02	14.60	...
2011	0923_288	2 29 50.74	61 48 29.00		F4V	1.1	0	13.80	13.40	13.15	12.75
2011	1023_292	2 29 50.85	61 16 16.49	B0-B2	B1.5V	4.6	0	14.90	14.47	13.88	13.30
2011	0923_137	2 29 51.08	61 18 58.50	F5-F6	F6V	2.3	1	15.72	15.26	14.72	14.17
2012	1105_4_215	2 29 51.13	62 15 47.69	A7-F0	A8V	1.5	0	15.01	15.08	14.84	14.14
2012	1106_2_45	2 29 51.15	61 32 26.90	F8-F9	F8V	5.5	0	16.69	16.14	14.90	13.83

Table 1. IC 1805 Spectral Types and Photometry (Continued)

Year	Date_No.[a] (MMDD_No.)	RA(J2000) (hhmmss.ss)	Dec(J2000) (° ′ ″)	SpTy Range	SpTy	A_V (r-i) (mag)	Assoc.?[b] (ext)	V(90P)[c] (mag)	r[d] (mag)	i[d] (mag)	I(90P)[c] (mag)
2012	1105_5_269	2 29 51.22	62 00 30.41	K3-K5	K4V[g]	3.2	1	13.92	13.33	12.32	11.88
2012	1203_2_191	2 29 52.02	61 26 26.84	A0-A1	A1V	3.6	1	16.52	16.10	15.53	14.94
2012	1203_2_234	2 29 52.18	61 46 47.39	A7-A8	A8V	2.4	1	15.84	15.76	15.32	14.73
2012	1204_249	2 29 52.48	61 36 59.21		A5V	4.4	0	18.59	17.99	17.19	16.42
2012	1106_1_189	2 29 52.81	61 34 29.50	F8-F9	F8V	2.4	1	17.17	16.65	16.07	15.55
2011	0923_177	2 29 52.89	61 35 18.80	F7-F8	F8V	2.3	1	14.66	14.20	13.64	13.13
2012	0124_181	2 29 52.97	61 18 03.71	A3-A5	A4V	2.8	1	15.50	15.19	14.74	14.15
2011	1023_230	2 29 53.59	61 14 18.43	F9-G1	G0V	0.9	0	12.83	12.56	12.28	12.06
2012	1203_1_184	2 29 53.82	61 43 35.56	F9-G5	G0V	1.7	1	...	15.65	15.19	...
2012	1204_197	2 29 53.99	61 11 12.51	F3-F5	F4V	2.5	1	16.48	16.07	15.51	14.95
2012	1105_2_111	2 29 54.01	61 16 06.50	A7-F2	A9V	2.3	1	14.75	14.45	14.03	13.51
2012	1203_2_275*	2 29 54.11	61 08 03.21		A0V	3.4	1	15.81	15.48	14.99	14.37
2012	1204_224	2 29 54.31	61 26 00.73		A1V	4.3	0	17.52	16.97	16.26	15.60
2012	1105_2_181	2 29 54.55	61 48 21.90	F2-F5	F4V	2.2	1	14.98	14.93	14.44	13.58
2012	0124_188	2 29 54.56	61 12 51.20	F3-F6	F4V	2.8	1	16.26	15.77	15.17	14.58
2012	1105_5_1	2 29 54.57	62 15 22.91	G8-K2	K1V[g]	2.5	1	15.20	14.47	13.75	13.10
2012	1203_1_159	2 29 54.73	61 28 07.69	K4-K5	K4V	1.6	1	17.66	16.98	16.32	15.67
2011	1023_224	2 29 55.24	61 13 10.20	G9-K1	K0V	3.8	1	15.12	14.28	13.29	12.56
2012	1203_2_213	2 29 55.31	61 36 04.53	G5-G7	G6V	2.1	1	16.80	16.27	15.67	15.13
2012	1105_4_161	2 29 55.70	61 51 02.60	A9-F1	F0V	0.9	0	13.36	13.09	12.95	12.24
2012	1105_4_218	2 29 55.95	62 12 52.39	G8-K2	K0V[g]	2.2	1	15.79	15.05	14.41	13.72
2012	0124_287	2 29 56.15	61 32 05.79	F8-G0	G6V	5.2	0	16.42	15.32	14.08	13.26
2011	1023_235	2 29 56.28	61 21 37.61	G1-G6	G3V	1.4	0	15.84	15.44	15.01	14.71
2012	1204_288	2 29 56.31	61 05 20.14	G1-G8	G5V	1.8	1	...	15.52	15.02	...
2012	1106_3_242	2 29 56.35	61 30 17.19		F7V	2.4	1	16.95	16.47	15.89	15.34
2012	1105_2_27	2 29 56.43	61 22 51.60	G3-G6	G4V[g]	3.6	1	15.56	14.80	13.91	13.25
2012	1106_3_77	2 29 56.63	62 16 29.70	A1-A7	A4V	2.3	1	...	17.29	16.95	...
2012	1203_2_212	2 29 56.90	61 32 11.80	K4-K5	K4V	2.3	1	19.06	18.27	17.46	16.84
2012	0304_255	2 29 56.94	61 53 09.80	G6-G7	G6V	0.6	0	13.74	13.84	13.57	12.77
2012	1203_2_289	2 29 56.97	61 30 49.18	F6-F8	F7V	2.0	1	16.28	15.88	15.40	14.90
2012	1105_4_213	2 29 56.98	62 15 57.40	G9-K2	K2V	1.5	0	14.79	14.55	14.01	13.13
2011	0923_115	2 29 57.21	61 07 33.65	G5-K0	G9V	1.5	0	15.66	15.32	14.84	14.29
2012	0124_189	2 29 57.25	61 14 39.00	K2-K4	K3V	0.9	0	15.65	15.20	14.76	14.23
2012	0124_196	2 29 57.27	61 22 54.50	G0-G2	G1V	1.4	0	14.84	14.49	14.09	13.61
2012	1106_3_248	2 29 57.54	61 33 37.90	K7-K8	K7V	1.9	1	17.77	17.01	16.09	15.49
2012	1203_1_121	2 29 57.77	61 11 32.41		F8V	1.9	1	15.42	15.11	14.62	14.09
2012	1204_215	2 29 58.09	61 24 54.80	F9-G5	G3V	2.4	1	17.91	17.32	16.68	16.12
2012	1105_5_267	2 29 58.37	62 01 04.81	F8-F9	F8V	1.1	0	13.96	13.49	13.19	12.74
2012	1204_235	2 29 58.64	61 33 36.57		A0V	4.0	1	16.76	16.21	15.59	15.00
2012	1203_1_152	2 29 58.66	61 26 48.98	G3-G8	G7V	2.2	1	17.38	16.85	16.23	15.66
2011	0923_145	2 29 58.81	61 22 05.00	F8-F9	F8V	1.6	1	15.09	14.53	14.12	14.42
2012	1203_1_185	2 29 58.88	61 48 47.79	F9-G7	G5V	3.7	1	...	15.69	14.77	...
2012	1105_2_28	2 29 59.16	61 08 08.49	G8-G9	G8V	2.7	1	16.13	15.54	14.81	14.16
2012	1106_2_33	2 29 59.22	61 29 10.30	G9-K2	K0V	1.7	1	17.63	17.19	16.65	16.04
2012	1106_3_231	2 29 59.28	61 29 41.30		F8V	2.2	1	17.21	16.78	16.24	15.65
2012	1105_2_200	2 29 59.32	61 56 55.80	A1-A2	A1V	2.4	1	15.72	15.71	15.40	14.64
2012	1203_2_227	2 29 59.41	61 39 53.63		F8V	2.5	1	...	16.77	16.16	...
2012	1203_1_278	2 29 59.46	61 26 02.63	F4-F5	F4V	3.5	1	17.49	16.86	16.10	15.46
2012	1105_4_175	2 29 59.72	61 57 37.30	A2-A6	A4V	2.3	1	15.89	15.85	15.50	14.75
2012	1106_3_262	2 30 00.03	61 46 30.90	K0-K5	K2V[g]	5.3	0	...	16.76	15.43	...
2012	1203_1_277	2 30 00.11	61 35 34.59	F5-F7	F6V	2.3	1	15.99	15.56	15.02	14.48
2012	1106_1_173	2 30 00.36	61 30 04.00	A2-A3	A3V	3.3	1	17.06	16.65	16.12	15.51
2012	1203_1_170	2 30 00.63	61 32 41.57	G0-G3	G2V	2.1	1	16.42	15.87	15.30	14.75
2011	0923_176	2 30 00.87	61 31 50.60	F6-F9	F7V	3.0	1	15.81	15.15	14.46	13.79
2012	1203_1_140	2 30 00.98	61 17 24.99	F4-F6	F4V	2.6	1	15.26	14.82	14.26	13.67
2012	1203_1_175	2 30 01.02	61 40 58.29	B9-A0	A0V	3.9	1	...	16.74	16.13	...
2012	1105_4_164	2 30 01.16	61 47 18.70	B8-A0	B9V	3.3	1	14.77	14.53	14.07	13.89
2012	1105_2_197	2 30 01.19	61 58 28.40	G7-K0	G9V	2.5	1	14.86	13.93	13.21	12.67
2012	1105_5_54	2 30 01.42	62 15 18.31	F9-G7	G3V	1.2	0	15.90	15.86	15.48	15.01
2012	1203_1_148	2 30 01.50	61 21 55.27	K4-K5	K4V	1.0	0	17.02	16.48	15.94	15.37
2012	1106_1_184	2 30 01.83	61 32 19.99	F7-F8	F7V	2.4	1	16.96	16.46	15.89	15.33
2012	1106_3_246	2 30 02.12	61 33 05.11	G9-K2	K0V	2.0	1	17.55	16.97	16.37	15.83
2012	1203_1_166	2 30 02.33	61 31 33.85	B9-A0	B9.5V	3.1	1	15.16	14.85	14.43	13.91
2012	0304_287	2 30 02.39	61 18 48.30		K2V	0.8	0	14.87	14.44	14.06	13.56
2011	0923_120	2 30 02.40	61 07 40.60	G3-G6	G3V[g]	4.1	1	15.56	14.77	13.77	12.99
2011	1023_225	2 30 02.55	61 15 40.33		F2V	2.3	1	14.92	14.54	14.05	13.49
2011	1023_217	2 30 02.66	61 11 29.04	G0-G2	G1V	0.8	0	14.05	13.80	13.51	13.04
2012	1203_2_277	2 30 02.69	61 08 24.09	G0-G1	G0V	2.1	1	15.44	15.01	14.45	13.89
2011	0923_23	2 30 02.93	61 15 54.30	A0-A1	A0V	2.9	1	15.43	15.20	14.80	14.41
2012	1203_2_218	2 30 02.94	61 33 36.98	F4-F9	F8V	3.4	1	18.72	17.97	17.17	16.57
2012	1105_2_116*	2 30 03.03	61 13 50.31	B5-B6	B5V	3.0	1	13.88	13.69	13.36	12.79
2012	1203_2_183	2 30 03.35	61 20 57.80	F6-F7	F6V	2.2	1	16.63	16.23	15.70	15.16
2012	1203_1_126	2 30 03.58	61 06 29.52	B8-A0	B8V	3.6	1	...	15.02	14.55	...
2012	1106_3_270	2 30 03.61	61 48 52.90	F2-F5	F3V	2.8	1	...	16.80	16.20	...
2012	1203_2_189	2 30 03.64	61 19 05.28	F2-F3	F3V	2.9	1	16.72	16.26	15.65	15.11
2012	1105_5_256	2 30 03.93	61 56 18.30	G5-K0	G7V[g]	3.2	1	15.71	15.20	14.38	13.63
2012	1105_4_219	2 30 04.25	62 13 46.41	A7-F0	A9V	1.3	0	14.23	14.18	13.97	13.47
2012	1203_2_178	2 30 04.48	61 13 16.98	G1-G6	G5V	1.9	1	16.18	15.75	15.21	14.66
2012	1105_4_277	2 30 04.67	61 52 33.30	G5-K0	G8V	0.5	0	13.71	13.76	13.50	12.62
2012	0304_285	2 30 04.90	61 19 42.40	G8-G9	G9V	2.1	1	14.96	13.77	13.16	13.81
2012	1204_228	2 30 05.08	61 26 35.02	F8-F9	F8V	2.7	1	16.74	16.18	15.54	14.96
2011	0923_146	2 30 05.33	61 20 32.40		F8V	1.2	0	12.87	12.46	12.13	12.08
2012	1105_5_9	2 30 05.49	62 12 25.00	G8-K0	G8V	2.3	1	15.09	14.85	14.20	13.24
2012	1106_1_188	2 30 05.60	61 33 32.60	F9-G0	F9V	2.5	1	17.47	16.90	16.28	15.72
2012	1105_2_195	2 30 05.80	61 58 58.70	F5-F7	F6V	1.7	1	15.89	15.77	15.35	14.74
2012	1204_239	2 30 07.04	61 31 43.75		F8V	1.9	1	16.32	15.91	15.43	14.92
2012	1203_1_122	2 30 07.19	61 04 48.05	F0-F3	F2V	2.3	1	...	14.72	14.23	...

Table 1. IC 1805 Spectral Types and Photometry (Continued)

Year	Date_No.[a] (MMDD_No.)	RA(J2000) (hhmmss.ss)	Dec(J2000) (° ′ ″)	SpTy Range	SpTy	A_V (r-i) (mag)	Assoc.?[b] (ext)	V(90P)[c] (mag)	r[d] (mag)	i[d] (mag)	I(90P)[c] (mag)
2012	1203_1_143	2 30 07.21	61 24 10.84	K1-K2	K2V	2.2	1	17.56	16.90	16.22	15.63
2011	1023_251	2 30 07.22	61 31 07.70	A0-A3	A2V	2.5	1	12.98	12.67	12.32	12.37
2012	1204_246	2 30 07.41	61 35 13.62		F4V	2.4	1	16.33	15.89	15.36	14.82
2011	0923_162	2 30 07.44	61 27 18.70	K4-K7	K4V	1.4	0	15.10	14.49	13.87	13.31
2012	0124_231	2 30 07.73	61 50 05.50	B2-B4	B3V	4.3	0	13.09	12.70	12.12	12.37
2012	1105_2_119	2 30 07.92	61 15 57.40	G8-G9	G9V	1.4	0	15.99	15.60	15.13	14.83
2012	1203_2_186	2 30 08.11	61 18 27.81	F9-G7	G0V	2.3	1	16.83	16.34	15.75	15.20
2011	1023_233	2 30 08.15	61 22 42.30	F2-F3	F2V	2.3	1	15.59	15.22	14.73	14.20
2012	1204_284	2 30 08.15	61 04 31.83	A2-A7	A5V	3.3	1	...	15.84	15.26	...
2012	1203_1_190	2 30 08.16	61 44 35.61	F8-G0	F9V	1.7	1	...	15.57	15.13	...
2012	1106_3_233	2 30 08.28	61 30 46.29	K2-K4	K3V	1.7	1	17.85	17.24	16.63	16.04
2012	1106_3_235	2 30 08.51	61 30 01.50	K0-K4	K3V[g]	4.6	0	18.41	17.28	16.06	15.19
2012	1106_2_246	2 30 08.68	61 08 49.20	A3-A8	A6V	3.8	1	17.87	17.38	16.69	16.04
2012	1204_206	2 30 08.78	61 16 11.00	G1-G7	G6V	1.7	1	16.61	16.16	15.65	15.10
2012	1106_2_248	2 30 09.11	61 09 41.20	K3-K5	K4V	1.9	1	18.46	17.87	17.14	16.36
2011	1023_6	2 30 09.38	61 35 04.50	G7-G8	G7V	1.4	0	14.72	14.27	13.84	13.36
2012	0124_284	2 30 09.42	61 19 55.11	F7-F9	F8V	4.2	0	14.43	13.38	12.41	13.62
2011	0923_113	2 30 09.60	61 09 35.40	F7-F8	F8V	2.1	1	15.50	15.12	14.61	14.01
2012	0124_187	2 30 09.99	61 16 45.61	F3-F7	F6V	1.8	1	14.75	14.18	13.75	13.94
2012	1105_5_3	2 30 10.08	62 13 41.30	K0-K3	K2V	1.0	0	15.88	14.80	14.37	14.30
2012	0304_300	2 30 10.17	61 35 14.59	F4-F5	F5V	2.4	1	16.45	16.01	15.46	14.93
2012	1104_274	2 30 10.32	61 36 21.74	F7-F8	F8V	1.8	1	16.36	15.93	15.48	14.91
2012	0304_259	2 30 10.41	61 50 50.00		F8V	1.0	0	13.41	13.45	13.17	12.51
2012	1106_3_71	2 30 10.48	62 16 28.80	F2-F4	F2V	2.5	1	...	16.70	16.17	...
2011	1023_265	2 30 10.56	61 32 53.16	A9-F0	F0V	2.3	1	14.68	14.33	13.88	13.38
2012	1204_211	2 30 10.74	61 25 53.38	F7-F8	F8V	2.9	1	18.06	17.48	16.79	16.21
2012	1203_1_150	2 30 11.07	61 22 34.90	F8-G4	G0V	1.7	1	15.03	14.63	14.18	13.67
2012	0304_296	2 30 11.18	61 34 22.20	K0-K1	K0V	1.8	1	16.35	15.84	15.28	14.76
2012	1106_2_53	2 30 11.53	61 37 58.40	G0-K0	G5V[g]	4.9	0	17.74	16.78	15.60	14.84
2012	1203_2_206	2 30 11.55	61 27 31.77	K7-K8	K7V	2.8	1	18.74	17.94	16.83	16.12
2012	1203_2_221	2 30 11.55	61 40 35.42	F4-F5	F4V	3.0	1	...	17.03	16.38	...
2012	1106_1_175	2 30 11.59	61 30 08.71	A1-A2	A1V	3.5	1	17.10	16.68	16.14	15.54
2012	1203_1_271	2 30 11.66	61 36 25.76	G0-G6	G3V	2.0	1	15.52	15.01	14.47	13.97
2012	0124_218	2 30 11.67	61 34 57.10	F9-G1	F9V	1.3	0	14.65	14.31	13.95	13.50
2012	1106_2_57	2 30 11.86	61 37 02.70		K2V	1.8	1	16.96	16.38	15.78	15.28
2012	1106_3_249	2 30 11.88	61 36 51.51	F9-G4	G3V	4.5	0	18.30	17.32	16.24	15.49
2012	1106_3_244	2 30 12.14	61 33 51.80	A5-A7	A6V	4.1	1	18.47	17.85	17.09	16.46
2012	1106_3_237	2 30 12.34	61 29 42.70	F4-F6	F5V	3.5	1	16.70	16.11	15.34	14.68
2012	1106_1_181	2 30 12.66	61 37 26.50	F8-F9	F8V	2.4	1	17.16	16.67	16.08	15.57
2012	0124_219	2 30 12.95	61 35 44.39	F8-G0	F9V	1.8	1	16.09	15.69	15.23	14.76
2012	1204_252	2 30 12.98	61 40 40.89		K4V	2.1	1	...	18.31	17.55	...
2012	1203_2_176	2 30 13.14	61 13 42.79	A9-F3	F3V	2.7	1	16.76	16.37	15.78	15.16
2012	1203_2_179	2 30 13.35	61 15 18.59	K4-K5	K4V	0.8	0	15.21	14.65	14.16	13.61
2012	1204_299	2 30 13.47	61 38 29.82	F4-F6	F6V	3.5	1	...	17.54	16.74	...
2012	1204_296	2 30 13.86	61 29 42.83	F2-F3	F2V	3.1	1	15.97	15.48	14.83	14.22
2012	1203_2_238	2 30 14.06	61 45 37.05	G0-K0	G5V	2.2	1	...	16.91	16.30	...
2012	1105_2_143	2 30 14.93	61 30 14.20	G8-G9	G8V	1.5	0	16.39	15.95	15.48	14.85
2012	1203_1_135	2 30 15.14	61 20 00.33	F6-F7	F7V	2.2	1	15.18	14.76	14.23	13.71
2012	1203_2_271	2 30 15.48	61 12 43.99	A3-A6	A5V	2.4	1	15.78	15.53	15.14	14.61
2012	1203_2_216	2 30 15.52	61 32 47.06	A0-A2	A1V	3.8	1	17.09	16.74	16.14	15.19
2012	1106_3_84	2 30 15.57	62 17 11.30	G7-K2	K0V	1.3	0	...	17.50	17.05	...
2012	1204_181	2 30 15.60	61 04 28.99	G5-G7	G8V	1.6	1	...	16.04	15.54	...
2012	1105_4_227	2 30 16.01	62 17 34.00	F4-F6	F4V	1.6	1	15.61	15.58	15.23	14.49
2012	1106_1_182	2 30 16.13	61 31 32.20	G6-G9	G8V	4.5	0	16.59	15.62	14.51	13.78
2012	1105_5_265	2 30 16.20	62 01 40.50	A1-A2	A1V	1.7	1	14.53	14.61	14.45	13.76
2012	1204_293	2 30 16.22	61 39 52.67	A1-A2	A1V	3.9	1	...	17.03	16.41	...
2012	1203_2_300	2 30 16.31	61 42 32.06	G0-G2	G1V	1.3	0	...	15.31	14.92	...
2012	1105_4_232	2 30 16.39	62 25 05.00	G7-K0	G8V[g]	2.3	1	14.59	14.35	13.71	12.75
2012	1204_287	2 30 16.47	61 21 03.73	F3-F4	F3V	2.9	1	16.72	16.22	15.60	15.05
2012	1105_4_236	2 30 16.49	62 26 48.50	F9-G2	G0V	1.4	0	15.94	15.81	15.41	14.92
2012	0304_268	2 30 16.54	61 55 28.40	F5-F6	F5V	2.0	1	15.54	15.39	14.93	14.16
2012	1203_2_207	2 30 16.69	61 28 45.22	A1-A2	A1V	4.2	1	17.05	16.53	15.84	15.22
2012	1105_4_230*	2 30 17.00	62 16 16.30	B7-A0	B9V	2.2	1	13.84	14.08	13.86	13.08
2012	0124_299*	2 30 17.15	61 57 36.11	B6-B8	B7V	2.2	1	13.75	13.95	13.77	13.28
2011	1023_220	2 30 17.29	61 11 48.65	G9-K2	K2V	3.0	1	15.81	15.08	14.23	13.52
2012	1106_3_266	2 30 17.43	61 49 22.51	A0-A2	A1V	4.2	0	...	17.01	16.31	...
2012	1203_2_170	2 30 17.47	61 04 51.95	B7-A0	B9V	2.9	1	...	15.26	14.89	...
2011	1023_213	2 30 17.50	61 14 34.20		F8V	1.0	0	13.82	13.54	13.24	12.69
2012	1203_2_167	2 30 18.26	61 06 10.20		F7V	1.7	1	...	15.00	14.58	...
2012	1105_4_294	2 30 18.70	62 20 29.60		F8V	1.3	0	14.88	14.97	14.62	13.89
2012	1203_2_229	2 30 18.78	61 37 53.88	K4-K5	K4V	1.6	1	18.00	17.32	16.66	16.11
2012	1204_207*	2 30 18.87	61 18 56.59	F4-F5	F4V	2.8	1	16.01	15.51	14.90	14.55
2012	1203_1_125	2 30 18.94	61 11 21.63	F7-F8	F8V	2.5	1	16.87	16.38	15.78	15.20
2011	0923_165	2 30 19.03	61 27 48.34	B8-B9	B8V	4.3	0	15.89	15.43	14.80	14.18
2012	1203_1_144	2 30 19.04	61 21 34.89	G8-G9	G8V	1.8	1	16.13	15.62	15.08	14.76
2012	0304_203	2 30 19.39	61 17 51.19	F6-F7	F7V	2.0	1	16.44	16.04	15.56	15.04
2012	1106_1_215	2 30 19.39	61 58 32.49	K2-K3	K2V	1.3	0	...	16.76	16.27	...
2012	0304_265	2 30 19.48	61 58 43.40	G7-G9	G8V	1.2	0	15.09	14.99	14.57	13.83
2012	1105_4_167	2 30 19.73	61 52 05.71	F4-F5	F4V	2.3	1	15.71	15.52	15.01	14.23
2012	1203_1_113	2 30 19.84	61 04 52.22	B9-A0	B9.5V	2.6	1	...	15.25	14.94	...
2012	1106_1_176	2 30 20.10	61 26 25.40	F7-G0	F9V	3.6	1	18.10	17.37	16.52	15.89
2012	1106_2_18	2 30 20.14	61 45 35.90	G7-G9	G8V	1.7	1	16.94	16.52	16.00	15.41
2012	1105_2_142	2 30 20.14	61 27 47.60	G7-K0	G9V[g]	4.7	0	14.85	13.84	12.67	12.19
2012	1105_2_30	2 30 20.33	61 15 06.40	A1-A2	A1V	3.0	1	15.72	15.45	15.02	14.64
2012	1203_1_280	2 30 20.50	61 26 32.46	A1-A3	A2V	3.6	1	16.47	16.03	15.45	14.99
2012	1106_3_239	2 30 20.58	61 29 02.10	F8-F9	F8V	2.5	1	17.33	16.79	16.18	15.63
2012	1204_300	2 30 20.62	61 30 15.48	A1-A2	A1V	4.9	0	17.59	17.00	16.15	15.30

Table 1. IC 1805 Spectral Types and Photometry (Continued)

Year	Date_No.[a] (MMDD_No.)	RA(J2000) (hhmmss.ss)	Dec(J2000) (° ′ ″)	SpTy Range	SpTy	A_V (r-i) (mag)	Assoc.?[b] (ext)	V(90P)[c] (mag)	r[d] (mag)	i[d] (mag)	I(90P)[c] (mag)
2012	1105_3_222	2 30 20.71	61 30 05.40	G9-K1	K0V	3.2	1	12.98	12.66	11.80	11.73
2012	1105_4_300	2 30 20.97	62 23 03.21	A7-F0	A8V	1.8	1	15.62	15.64	15.34	14.61
2012	1105_5_67	2 30 20.98	62 24 39.50	A6-A8	A7V	1.9	1	15.96	15.99	15.68	14.96
2012	1106_3_82	2 30 21.05	62 15 06.80	F6-F8	F7V	2.3	1	...	17.39	16.84	...
2012	1106_1_205	2 30 21.09	61 48 55.09	G5-K1	G8V	3.1	1	17.32	16.75	15.95	15.21
2011	0923_286	2 30 21.55	61 41 05.90	F4-F5	F5V	1.1	0	13.98	13.78	13.52	13.01
2012	1106_2_74	2 30 21.60	61 47 35.20	G0-G8	G7V	2.2	1	16.74	16.24	15.64	15.04
2012	0304_283	2 30 21.61	61 22 15.59		K3V	4.7	0	16.35	15.20	13.94	14.19
2012	1105_4_229	2 30 21.72	62 16 28.21	G8-K2	G9V	1.6	1	14.93	14.81	14.29	13.41
2012	1105_4_238	2 30 22.07	62 26 53.60	B6-A0	B8V	2.6	1	15.63	15.68	15.41	14.71
2012	1105_5_59	2 30 22.16	62 16 06.61	A0-A1	A1V	2.6	1	15.82	15.95	15.59	14.82
2012	1105_2_198	2 30 22.27	61 50 10.60	F9-G2	G1V	1.7	1	15.50	15.50	15.03	13.94
2012	1106_3_87	2 30 22.28	62 21 12.00	F8-F9	F8V	1.5	0	...	16.87	16.49	...
2012	1203_2_223	2 30 22.30	61 39 09.33	F4-F5	F4V	2.2	1	15.65	15.30	14.82	14.26
2012	1105_4_223	2 30 22.36	62 17 47.10	F2-F5	F2V	1.8	1	15.78	15.84	15.46	14.72
2012	1106_3_253	2 30 22.43	61 47 24.50	F8-F9	F8V	2.4	1	17.30	16.85	16.26	15.65
2012	1106_2_78	2 30 23.25	61 48 51.70	G9-K2	K1V	4.2	1	17.54	16.66	15.57	14.82
2012	1106_1_195	2 30 23.27	61 44 03.50	K3-K5	K4V	1.2	0	16.82	16.28	15.71	15.10
2012	0124_245	2 30 23.30	61 53 59.80		K3V	4.6	0	15.14	14.25	13.02	12.16
2012	1105_2_191	2 30 23.32	61 57 00.59	A7-F0	A9V	2.3	1	15.48	15.49	15.06	14.30
2011	0923_290	2 30 23.40	61 42 03.20	F9-G0	G0V	1.0	0	14.58	14.32	14.02	13.51
2012	1203_1_183	2 30 23.54	61 46 19.03	B8-A0	B9V	3.5	1	15.75	15.45	14.95	14.34
2012	1106_2_14	2 30 23.70	61 43 53.51	M1-M2	M2V	0.4	0	18.49	17.85	16.82	16.10
2011	1023_44	2 30 23.92	61 40 14.29	G9-K0	G9V	2.2	1	14.90	14.35	13.71	13.09
2011	1023_48	2 30 23.94	61 41 40.76		A1V	2.8	1	15.50	15.28	14.87	14.31
2012	1105_4_296	2 30 24.03	62 20 35.21	F6-F7	F7V	1.0	0	14.08	14.26	13.98	13.26
2011	0923_284	2 30 24.19	61 39 59.51	A2.5-A4	A4V	1.3	0	13.85	13.72	13.59	12.96
2012	1204_223	2 30 24.25	61 28 17.86	A0-A1	A1V	4.0	1	16.30	15.81	15.16	14.54
2012	0304_207	2 30 24.27	61 16 30.60	F2-F4	F3V	1.6	1	13.01	12.97	12.62	12.17
2012	1106_3_238	2 30 24.34	61 28 26.70	A1-A2	A1V	3.5	1	16.89	16.49	15.95	15.39
2012	1106_1_204	2 30 24.46	61 46 12.19	F5-F7	F6V	2.5	1	16.85	16.43	15.85	15.26
2012	0304_256	2 30 24.48	61 47 59.11	G8-K0	G9V	3.6	1	16.32	15.57	14.65	13.93
2012	1204_213	2 30 24.51	61 25 55.49	A0-A1	A0V	3.2	1	15.83	15.52	15.05	14.53
2012	1204_243	2 30 24.62	61 36 15.39		F4V	2.5	1	16.69	16.22	15.66	15.12
2012	1106_2_244	2 30 24.69	61 10 17.01	F8-G0	F9V	2.4	1	16.90	16.44	15.85	15.22
2011	1023_293	2 30 24.79	61 26 48.20	F4-F6	F5V	2.0	1	14.33	13.95	13.49	12.98
2012	1105_5_61	2 30 24.90	62 26 38.31	G6-G8	G7V	1.4	0	15.78	15.63	15.18	14.68
2012	0124_175	2 30 25.11	61 11 54.89	G4-G8	G3V[g]	3.2	1	15.89	15.20	14.39	13.70
2012	1106_3_89	2 30 25.30	62 18 35.61	F8-G0	F9V	1.9	1	...	17.12	16.62	...
2012	1204_231	2 30 25.41	61 33 20.45		K2V	2.0	1	17.80	17.19	16.55	15.93
2011	0923_122	2 30 25.60	61 12 13.80	K1-K3	K2V	2.2	1	14.83	14.18	13.49	12.69
2012	1106_2_69	2 30 25.83	61 40 16.90	G4-K0	G7V	2.8	1	18.37	17.81	17.07	16.41
2012	1203_1_284	2 30 25.85	61 47 38.93		K6V	0.9	0	16.60	15.99	15.35	14.74
2012	1204_192	2 30 25.92	61 10 58.40		F5V	2.8	1	15.99	15.48	14.87	14.29
2012	1203_2_181	2 30 25.97	61 22 40.96	A0-A1	A0V	4.0	1	16.71	16.24	15.61	15.00
2012	1106_2_72	2 30 26.00	61 46 13.20	G9-K2	G9V	2.4	1	18.39	17.82	17.14	16.50
2012	1204_199	2 30 26.11	61 13 35.17	G6-G9	G8V	1.6	1	16.54	16.08	15.58	15.07
2012	1106_3_86	2 30 26.12	62 15 41.80	G6-K0	G7V	1.6	1	...	17.34	16.86	...
2012	1204_268	2 30 26.26	61 48 34.01		F7V	2.4	1	17.02	16.55	15.98	15.42
2012	1106_3_88	2 30 26.37	62 16 58.60	A9-F5	F1V	2.0	1	...	17.46	17.07	...
2012	1105_3_217	2 30 26.40	61 27 43.40	B2-B3	B2.5V	4.0	1	12.87	12.48	11.97	12.02
2012	1106_1_288	2 30 26.47	61 39 40.70	K0-K3	K1V	3.4	1	16.83	16.12	15.21	14.51
2012	1105_4_226	2 30 26.77	62 14 17.10	A2-A6	A4V	1.5	0	14.86	14.92	14.74	14.05
2012	1203_1_273	2 30 26.92	61 35 05.53	G8-K0	G9V	1.1	0	15.64	15.27	14.87	14.32
2012	1106_1_224	2 30 26.95	62 00 27.91	K2-K3	K3V	1.3	0	...	17.27	16.74	...
2012	1104_153	2 30 26.97	61 43 39.83	K2-K3	K3V	0.9	0	16.43	15.95	15.51	14.93
2012	1106_2_233	2 30 27.14	61 07 44.90		K6V	1.7	1	17.46	16.73	15.93	15.27
2012	1105_5_53	2 30 27.22	62 17 17.21	G1-K0V	G5V	2.7	1	15.42	15.38	14.66	13.79
2012	1106_2_20	2 30 27.26	61 45 17.10	A1-A2	A2V	3.7	1	17.58	17.15	16.54	15.88
2012	1105_5_51	2 30 27.37	62 17 58.01	G6-K1	G8V[g]	2.5	1	15.35	14.94	14.25	13.40
2012	0124_171	2 30 27.39	61 14 47.00		K2V	0.9	0	15.20	14.75	14.35	14.25
2012	1204_258	2 30 27.44	61 41 03.92	A3-A5	A3V	3.0	1	16.01	15.69	15.22	14.64
2012	1203_2_285	2 30 27.45	61 30 22.65	F7-F8	F8V	2.4	1	17.09	16.59	16.01	15.46
2012	1106_2_259	2 30 27.53	61 21 21.20	A0-A1	A1V	3.8	1	17.11	16.60	15.99	15.39
2012	1106_1_207	2 30 27.85	61 48 14.50	B9-A1	A0V	3.8	1	17.20	16.77	16.19	15.54
2012	1106_3_255	2 30 27.87	61 46 57.50	G6-K0	G8V	4.1	1	18.09	17.25	16.22	15.48
2012	1105_5_58*	2 30 27.94	62 14 09.70	A1-A2	A1V	2.1	1	14.70	14.87	14.61	13.88
2012	1204_195	2 30 28.04	61 15 06.24	A1-A2	A2V	3.3	1	16.66	16.30	15.77	15.18
2012	1105_5_70	2 30 28.26	62 21 44.00	F9-G3	G0V	1.5	0	14.52	14.40	13.99	13.25
2012	1106_2_68	2 30 28.38	61 39 02.79	F8-G0	F9V	2.9	1	18.29	17.80	17.09	16.45
2012	1104_155	2 30 28.56	61 43 10.06	F0-F3	F2V	1.8	1	14.85	14.56	14.19	13.62
2012	1106_3_260	2 30 28.59	61 46 27.20	F9-G7	G4V	3.8	1	16.73	16.02	15.08	14.40
2011	0923_186	2 30 28.83	61 32 56.00	B2-B3	B2V	4.2	0	13.32	12.96	12.43	12.02
2012	1106_2_67	2 30 29.35	61 40 25.51	G7-K0	G9V[g]	4.8	0	16.66	15.68	14.48	13.69
2012	1203_2_279	2 30 29.41	61 11 08.68	F9-G0	F9V	1.7	1	15.84	15.49	15.05	14.52
2012	1105_5_65	2 30 29.45	62 23 59.00	A9-F1	F0V	1.2	0	13.99	14.04	13.84	13.14
2012	0304_293	2 30 29.47	61 45 34.70		G9V	2.1	1	16.39	15.86	15.25	14.65
2012	1104_168	2 30 29.50	61 46 56.61	G0-G7	G4V	0.7	0	14.22	13.92	13.65	13.17
2012	0304_201	2 30 29.51	61 19 45.00	B2-B3	B3V	3.2	1	12.88	12.65	12.30	11.98
2012	1204_201	2 30 29.58	61 20 46.58	F4-F5	F4V	2.6	1	16.59	16.15	15.59	15.11
2012	1106_1_290	2 30 29.90	61 40 24.39	G8-K2	K0V	1.6	1	16.77	16.31	15.78	15.14
2012	1204_259	2 30 30.00	61 42 01.21		G6V	1.5	0	15.98	15.61	15.14	14.56
2012	0124_223	2 30 30.02	61 40 20.21	F0-F4	F2V	1.1	0	13.84	13.39	13.15	12.71
2012	1105_5_57	2 30 30.08	62 15 54.40	F4-F6	F4V	1.4	0	15.29	15.35	15.03	14.33
2012	1106_1_202	2 30 30.31	61 45 15.70	G7-K0	G9V	2.4	1	17.52	16.93	16.24	15.61
2012	1104_166	2 30 30.48	61 45 51.31	G8-K2	K0V	1.2	0	16.10	15.68	15.24	14.72
2012	1204_217	2 30 30.48	61 25 33.68	G9-K2	K1V	1.9	1	16.34	15.82	15.23	14.68

Table 1. IC 1805 Spectral Types and Photometry (Continued)

Year	Date_No.[a] (MMDD_No.)	RA(J2000) (hhmmss.ss)	Dec(J2000) (° ′ ″)	SpTy Range	SpTy	A_V (r-i) (mag)	Assoc.?[b] (ext)	V(90P)[c] (mag)	r[d] (mag)	i[d] (mag)	I(90P)[c] (mag)
2012	1203_1_189	2 30 30.56	61 43 05.72	F2-F3	F2V	2.0	1	16.07	15.75	15.33	14.77
2012	1105_5_56	2 30 30.60	62 13 08.20	A1-A2	A2V	1.8	1	14.87	14.89	14.67	13.94
2012	1203_2_236	2 30 30.71	61 42 42.96	G5-G7	G6V	1.6	1	16.28	15.88	15.39	14.83
2012	0124_233	2 30 30.93	61 46 57.90	K4-K5	K4V	1.0	0	16.49	15.92	15.39	14.86
2012	1203_1_174	2 30 31.00	61 35 38.19	F6-F7	F7V	2.0	1	16.37	15.94	15.44	14.91
2012	1106_2_65	2 30 31.30	61 40 57.50	F0-F3	F2V	3.2	1	17.68	17.22	16.56	15.94
2011	1023_270	2 30 31.32	61 30 13.20	F0-F1	F0V	1.7	1	13.88	13.63	13.32	12.84
2012	1106_1_226	2 30 31.51	62 00 38.10	A9-F3	F1V	2.3	1	...	17.77	17.31	...
2012	1106_1_211	2 30 31.55	61 59 00.61	F3-F6	F4V	2.4	1	...	17.60	17.06	...
2012	1203_1_136	2 30 31.63	61 18 25.99	F2-F3	F3V	2.2	1	15.65	15.28	14.80	14.65
2012	1105_4_240	2 30 31.97	62 25 46.30	A7-F0	F0V	1.8	1	15.86	15.60	15.27	14.77
2012	1106_3_256	2 30 32.20	61 46 09.10	F3-F7	F5V[g]	3.0	1	17.68	17.17	16.51	15.88
2012	1106_1_198	2 30 32.32	61 42 29.60		K6V	1.5	0	18.45	17.75	16.99	16.37
2011	1023_267	2 30 32.39	61 31 16.41	G9-K2	K0V	1.9	1	14.21	13.49	12.90	12.23
2012	1106_1_273	2 30 32.55	61 25 21.19	K4-K5	K5V	2.3	1	18.22	17.40	16.57	15.94
2012	1105_2_193	2 30 32.72	61 51 41.50	G8-G9	G9V[g]	2.8	1	13.03	12.67	11.91	11.86
2012	1105_4_190	2 30 32.73	62 01 15.30	G5-G8	G6V[g]	1.8	1	14.93	14.27	13.73	13.05
2012	1106_3_234	2 30 32.76	61 27 05.70	F9-G1	G0V	3.2	1	18.49	17.73	16.95	16.38
2012	1105_4_168*	2 30 32.88	61 52 36.00	B8-A0	A0V	2.8	1	15.31	15.36	14.97	14.21
2012	1105_2_105	2 30 32.93	61 11 25.20	K1-K2	K2V	1.1	0	16.21	15.81	15.37	14.80
2012	1106_2_257	2 30 32.96	61 22 25.19	G5-G8	G7V	2.0	1	16.64	16.19	15.61	15.05
2012	0304_2	2 30 33.03	61 59 01.80	G6-G8	G7V	1.1	0	15.53	15.07	14.68	14.15
2012	1105_2_204	2 30 33.21	61 57 03.70	G8-K0	G9V	1.0	0	15.73	15.59	15.21	14.48
2012	1105_4_235	2 30 33.24	62 27 11.00	F2-F5	F3V	1.3	0	14.03	14.15	13.86	13.13
2011	0923_175	2 30 33.25	61 31 36.71	A3-A5	A4V	2.3	1	14.84	14.54	14.19	13.66
2012	1105_2_101	2 30 33.42	61 14 14.20	K0-K3	K2V[g]	2.0	1	14.33	13.68	13.03	12.40
2012	1106_2_64	2 30 33.45	61 37 21.90	F9-G2	G0V	3.0	1	18.32	17.71	16.97	16.38
2012	1104_144	2 30 34.13	61 30 39.20		F6V	2.7	1	15.67	15.13	14.51	13.92
2012	1203_2_163	2 30 34.50	61 10 25.88	F9-G0	F9V	2.4	1	16.92	16.51	15.91	15.30
2011	1023_207	2 30 34.61	61 04 16.76	A3-A5	A5V	2.5	1	15.83	15.97	15.55	14.90
2012	1106_3_81	2 30 34.62	62 22 52.50	A1-A7	A4V	2.2	1	...	17.45	17.11	...
2011	0923_105	2 30 35.04	61 02 03.36		A5V	2.4	1	15.28	15.44	15.06	14.51
2012	1106_2_66	2 30 35.37	61 37 59.20	F2-F5	F4V	3.1	1	18.18	17.63	16.96	16.33
2012	1204_257	2 30 35.45	61 42 39.81		F8V	1.9	1	16.09	15.69	15.22	14.66
2012	1203_2_173	2 30 35.62	61 19 22.64		A0V	2.9	1	15.81	15.59	15.18	14.79
2011	0923_187	2 30 35.69	61 34 48.70	G2-G4	G3V	0.9	0	12.69	12.70	12.39	12.30
2012	1105_5_64	2 30 35.69	62 17 58.40	A8-F0	A9V	1.7	1	15.61	15.55	15.25	14.49
2012	1203_2_195	2 30 35.71	61 26 23.62	A3-A5	A4V	4.3	0	17.45	16.85	16.08	15.45
2011	1023_38	2 30 35.93	61 34 45.06	K8-M1	M0V	0.3	0	15.66	15.08	14.30	13.54
2012	1106_1_206	2 30 35.93	61 46 49.70	K6-K7	K7V	1.9	1	18.29	17.61	16.69	16.05
2012	1106_2_63	2 30 35.97	61 41 15.21	F6-F8	F7V	2.0	1	16.72	16.32	15.83	15.26
2012	1106_3_83	2 30 36.47	62 21 01.20	G1-G8	G7V	1.2	0	...	16.98	16.58	...
2012	1105_5_66	2 30 36.69	62 18 42.40	F6-F7	F7V	1.2	0	15.72	15.65	15.33	14.61
2012	1106_2_77	2 30 36.77	61 47 43.39	G1-G9	G8V	2.1	1	17.71	17.18	16.58	15.75
2012	1106_2_235	2 30 36.77	61 07 29.00	F7-F9	F8V	2.3	1	17.12	16.71	16.15	15.55
2012	0304_248	2 30 36.90	61 41 21.19	A2-A6	A5V	3.4	1	16.49	16.07	15.48	14.83
2012	1204_227	2 30 36.99	61 27 38.58	F6-F7	F7V	3.3	1	18.89	18.22	17.47	16.88
2012	1106_1_275	2 30 37.16	61 24 27.20	A7-A8	A7V	4.1	1	18.33	17.75	16.97	16.32
2012	1106_1_227	2 30 37.20	62 03 20.40	F6-F7	F7V	1.8	1	...	17.21	16.77	...
2011	1023_35	2 30 37.29	61 36 35.70		A7V	1.6	1	13.92	13.72	13.48	13.01
2012	1105_2_106	2 30 37.57	61 04 17.51	G7-G9	G7V	1.5	0	15.54	15.40	14.94	14.62
2012	1203_2_203	2 30 37.59	61 29 21.55	B9-A1	A0V	3.7	1	15.41	14.94	14.39	14.28
2012	1203_1_21	2 30 37.71	61 18 10.54	G9-K1	K2V	1.9	1	17.89	17.37	16.76	16.10
2012	1106_1_203	2 30 37.88	61 48 49.11	G7-K2	K0V	4.4	0	18.44	17.45	16.32	15.58
2012	1105_5_14	2 30 37.89	62 24 57.79	A3-A6	A5V	1.7	1	15.64	15.49	15.25	14.71
2012	1105_5_63	2 30 38.09	62 23 25.50		F8V	1.2	0	15.88	15.82	15.50	14.76
2012	1106_1_286	2 30 38.17	61 39 34.30		A3V	3.1	1	16.53	16.20	15.71	15.10
2012	1203_2_196	2 30 38.29	61 25 07.86	A5-A6	A6V	4.2	0	17.08	16.48	15.71	15.11
2012	1106_3_236	2 30 38.47	61 29 49.10	A2-A3	A2V	3.9	1	17.46	16.95	16.29	15.66
2011	1023_210	2 30 38.53	61 03 47.47	G5G9	G7V	1.9	1	15.71	15.47	14.91	14.38
2012	1105_5_16	2 30 38.83	62 25 48.19	A1-A2	A2V	2.0	1	15.71	15.78	15.53	14.81
2012	1105_5_69	2 30 38.84	62 20 56.80	G1-G8	G6V	1.0	0	15.04	15.00	14.65	13.85
2012	1105_5_60	2 30 38.93	62 13 45.71	A2-A5	A3V	1.2	0	13.65	13.48	13.38	12.87
2012	1204_233	2 30 38.98	61 32 15.63		F8V	3.8	1	17.65	16.93	16.06	15.43
2012	1106_2_16	2 30 39.03	61 42 42.40	K5-K6	K6V	1.7	1	17.65	16.93	16.11	15.48
2012	0304_266	2 30 39.03	61 52 53.70	F4-F5	F5V	2.2	1	15.98	15.28	14.78	14.19
2011	1023_31	2 30 39.33	61 36 56.80	G1-G3	G2V	5.1	0	16.51	15.90	14.70	13.72
2011	1023_214	2 30 39.39	61 13 21.76	G8-K0	K0V	2.7	1	15.24	14.52	13.75	13.81
2011	1023_4	2 30 39.44	61 31 57.20		F0V	2.1	1	13.26	13.32	12.93	12.33
2012	0216_266	2 30 39.51	61 43 07.29	K7-M1	M0V	1.8	1	19.83	19.08	17.98	17.29
2012	1106_1_279	2 30 39.53	61 23 38.29	K0-K4	K2V[g]	4.6	0	18.46	17.35	16.17	15.37
2012	1203_1_120	2 30 39.63	61 05 32.09	G6-G9	G8V	2.1	1	...	16.31	15.71	...
2012	1106_2_237	2 30 40.20	61 07 21.29	G6-K2	G9V	3.5	1	18.13	17.37	16.46	15.70
2012	1106_2_55	2 30 40.21	61 35 37.20	G0-G4	G3V	5.4	0	18.21	17.10	15.83	15.01
2012	1203_2_273	2 30 40.35	61 15 02.09	A2-A4	A3V	3.6	1	15.69	15.19	14.59	14.38
2012	1105_4_275	2 30 40.40	61 57 18.60	G5-K0	G8V	0.7	0	14.71	14.49	14.19	13.51
2012	1203_1_123*	2 30 40.42	61 15 08.84	B9-A0	A0V	2.4	1	15.33	15.03	14.74	14.65
2012	1204_298	2 30 41.09	61 29 36.20	F6-F7	F7V	2.2	1	16.67	16.23	15.71	15.20
2011	0923_114	2 30 41.23	61 11 24.78	F1-F4	F1V	1.4	0	12.16	11.72	11.45	11.68
2011	0923_198	2 30 41.27	61 42 27.73	G7-G8	G8V	3.4	1	15.37	14.66	13.78	13.08
2012	1105_2_24	2 30 41.61	61 18 20.20	B8-B9	B8V	2.9	1	14.59	13.82	13.48	13.91
2012	1105_3_299	2 30 41.62	61 50 31.40	G7-G8	G9V[g]	3.1	1	13.97	13.47	12.65	12.10
2012	1105_4_298	2 30 41.98	62 18 51.00	G5-K9	G8V	2.5	1	15.84	15.57	14.87	13.94
2012	1203_2_290	2 30 42.27	61 24 51.44	A7-A8	A8V	3.3	1	17.69	17.17	16.53	15.94
2011	1023_46	2 30 42.28	61 38 13.40	B7-B9	B8V	3.2	1	15.88	15.61	15.21	14.63
2012	1105_4_224	2 30 42.32	62 11 42.21	B9-A0	A0V	1.5	1	13.88	14.01	13.90	13.22
2012	1106_2_70	2 30 42.84	61 38 10.59	G7-G9	G8V	4.5	0	18.21	17.34	16.23	15.47

Table 1. IC 1805 Spectral Types and Photometry (Continued)

Year	Date_No.[a] (MMDD_No.)	RA(J2000) (hhmmss.ss)	Dec(J2000) (° ′ ″)	SpTy Range	SpTy	A_V (r-i) (mag)	Assoc.?[b] (ext)	V(90P)[c] (mag)	r[d] (mag)	i[d] (mag)	I(90P)[c] (mag)
2012	0220_219	2 30 42.91	61 19 14.80	B9-A0	A0V	3.3	1	16.42	16.08	15.61	15.10
2012	1106_1_194	2 30 42.95	61 41 24.30	F5-F7	F6V	2.8	1	17.50	16.99	16.34	15.72
2012	0124_249	2 30 43.02	61 49 27.60	K5-K7	M2V	3.3	1	15.89	14.36	12.73	12.45
2012	0124_184	2 30 43.33	61 17 22.40	F2-F4	F3V	2.5	1	14.10	13.70[e]	13.17[f]	13.09
2012	1106_1_191	2 30 43.33	61 44 51.60	A0-A1	A1V	4.3	0	17.78	17.29	16.57	15.89
2011	0923_197	2 30 43.55	61 43 42.20	A5-A8	A6V	1.9	1	14.33	14.10	13.81	13.31
2011	0923_196	2 30 43.66	61 40 03.50		F8V	1.9	1	15.61	15.21	14.74	14.17
2012	1106_2_75	2 30 43.82	61 47 24.80	G1-G7	G6V	2.1	1	17.16	16.83	16.24	15.18
2012	0304_244	2 30 44.07	61 40 08.30	K0-K1	K1V	1.0	0	16.02	15.56	15.16	14.61
2011	1023_47	2 30 44.10	61 39 57.59	G2-G4	G3V	0.3	0	14.10	13.79	13.59	12.92
2012	1104_167	2 30 44.49	61 47 42.60	F8-G2	F9V	3.4	1	15.73	15.09	14.28	13.63
2012	0216_229	2 30 44.57	61 28 41.90	K7-M1	K8V	2.9	1	20.16	19.27	18.07	17.24
2011	0923_109	2 30 44.67	61 03 06.50	K4-K6	K5V	1.5	0	15.80	15.52	14.86	14.38
2012	1203_1_130	2 30 44.95	61 14 00.89	F2-F3	F3V	1.7	1	15.07	14.78	14.42	13.91
2012	1105_2_103	2 30 45.16	61 16 12.10	B4-B5	B4V	2.9	1	13.16	13.09	12.80	12.36
2012	1106_1_192	2 30 45.31	61 41 01.40	A6-A9	A7V	3.5	1	17.78	17.31	16.65	15.99
2012	0304_236	2 30 45.33	61 36 42.70	G0-G2	G1V	1.6	1	16.34	15.97	15.52	15.01
2012	0124_291	2 30 45.57	61 57 42.90	F3-F5	F4V	2.0	1	14.52	14.44	14.00	13.15
2012	1104_162	2 30 45.72	61 44 43.30		B9V	4.3	0	16.10	15.66	14.99	14.32
2012	1105_4_221	2 30 45.75	62 16 01.80	F0-F3	F2V	1.8	1	15.63	15.26	14.88	14.34
2012	0304_208	2 30 45.82	61 17 36.80	K0-K2	K1V	2.8	1	13.69	13.21	12.41	12.11
2011	1023_206	2 30 46.29	61 03 26.85	G8-G9	G8V	2.6	1	15.46	14.83	14.13	14.89
2012	1104_146	2 30 46.50	61 31 58.15	G4-G7	G6V	3.3	1	15.20	14.25	13.40	12.59
2012	1105_4_242	2 30 46.61	62 27 26.60	G1-G6	G7V	1.2	0	15.70	15.59	15.18	14.46
2012	1106_3_254	2 30 46.75	61 47 08.20	F6-G0	F9V	3.1	1	18.35	17.80	17.05	16.45
2012	1105_5_68	2 30 47.13	62 17 51.10	G8-K0	G9V[g]	2.9	1	15.58	15.17	14.38	13.39
2012	1105_4_234	2 30 47.33	62 20 22.70	F2-F5	F3V	1.5	0	14.82	14.77	14.45	14.37
2012	1106_2_76	2 30 47.43	61 44 04.79	G6-K0	G8V	4.7	0	17.84	16.91	15.76	14.99
2011	0923_108	2 30 47.44	61 01 04.80	K4-K5	K4V	1.6	1	15.97	15.79	15.13	14.29
2011	1023_203	2 30 47.58	61 08 50.23		A7V	2.3	1	15.11	14.88	14.49	13.95
2012	0304_216	2 30 47.97	61 26 30.90		G7V	4.2	1	16.19	15.20	14.17	13.87
2012	1105_2_107	2 30 48.00	61 14 19.20	A1-A2	A2V	2.7	1	16.27	15.97	15.57	15.09
2012	0304_258	2 30 48.08	61 46 52.60	G9-K1	K0V	3.9	1	15.07	14.19	13.18	12.40
2012	1204_251	2 30 48.43	61 42 28.14		F6V	1.9	1	16.09	15.73	15.27	14.68
2012	1106_3_232	2 30 48.43	61 30 49.21	G0-G4	G2V	2.4	1	17.74	17.18	16.54	15.96
2012	1106_3_17	2 30 48.50	62 23 20.30	A3-A9	A8V	1.8	1	...	17.13	16.81	...
2012	1203_2_185	2 30 48.58	61 22 56.24	F4-F5	F4V	2.1	1	15.41	14.99	14.54	14.41
2012	1106_3_19	2 30 48.77	62 21 56.70	A8-F1	F0V	2.0	1	...	17.00	16.63	...
2012	1106_2_59	2 30 48.94	61 34 18.10	G2-K0	G6V	2.4	1	17.79	17.18	16.53	15.93
2012	1104_180	2 30 49.60	61 55 44.99	G4-K2	K0V[g]	3.1	1	13.56	12.68	11.84	11.89
2012	1105_4_233	2 30 49.61	62 23 51.51	B2-B4	B3V	2.3	1	14.95	15.07	14.90	14.21
2012	1106_3_300	2 30 49.70	61 29 21.40	A7-F0	A9V	3.1	1	17.24	16.79	16.21	15.62
2012	1106_2_73	2 30 49.73	61 47 29.80	F2-F5	F3V	2.9	1	17.34	16.85	16.22	15.61
2012	1203_2_217	2 30 49.80	61 32 28.01	G9-K0	G9V	1.7	1	16.65	16.17	15.63	15.11
2012	1105_2_209*	2 30 50.69	61 57 26.21	B9-A0	A0V	2.2	1	15.27	15.41	15.16	14.53
2012	1106_2_46	2 30 50.77	61 30 22.40	F8-G4	G2V	4.0	1	18.15	17.29	16.32	15.62
2012	1106_2_238	2 30 50.87	61 07 52.10	G0-G7	G0V	2.4	1	17.41	16.91	16.30	15.71
2012	1106_1_217	2 30 51.17	61 56 02.81	A0-A1	A1V	3.0	1	...	16.91	16.46	...
2012	1105_3_252	2 30 51.19	61 53 05.29	G0-G6	G2V	1.0	0	14.73	14.14	13.81	13.27
2011	1023_9	2 30 51.26	61 41 17.44		F7V	2.6	1	14.59	14.06	13.45	12.79
2012	1106_1_292	2 30 51.29	62 04 53.99	F9-G7	G3V	3.3	1	...	16.74	15.91	...
2011	1023_287	2 30 51.57	61 11 33.02		A9V	2.4	1	14.71	14.42	13.98	13.39
2012	1106_3_298	2 30 51.92	61 26 35.11	G7-K2	G9V	5.1	0	17.64	18.17	16.91	15.47
2011	1023_204	2 30 52.22	61 03 23.52	K1-K2	K1V	1.0	0	14.96	15.01	14.60	14.20
2011	0923_106	2 30 52.35	61 01 23.90	K0-K2	K1V	2.1	1	14.93	14.67	14.02	13.59
2011	0923_183	2 30 52.42	61 33 34.10	G0-G3	G0V	1.7	1	15.98	15.54	15.08	14.60
2012	1204_186	2 30 52.76	61 04 23.91	G7-K0	G9V[g]	3.0	1	...	15.97	15.16	...
2012	1203_1_131	2 30 52.94	61 22 58.89	F3-F6	F4V	3.0	1	16.44	15.95	15.31	14.75
2012	1106_1_174	2 30 52.98	61 28 51.20	G8-K0	G8V	1.4	0	16.62	16.19	15.73	15.17
2011	0923_193	2 30 53.10	61 45 10.15		K0V	3.5	1	15.50	14.69	13.77	13.06
2012	1106_2_240	2 30 53.24	61 09 48.50	K1-K3	K2V	1.4	0	16.71	16.13	15.62	15.13
2012	0304_191	2 30 53.26	61 14 06.50	F7-F8	F7V	1.7	1	16.25	15.90	15.47	15.03
2011	1023_1	2 30 53.49	61 45 29.20	B5-B6	B5V	3.4	1	13.87	13.81	13.41	12.90
2012	0124_293	2 30 53.68	61 55 49.50	F3-F5	F4V	2.7	1	15.74	15.45	14.87	14.04
2012	1105_4_162	2 30 53.81	61 53 58.00	A1-A2	A1V	2.5	1	15.72	15.68	15.33	14.60
2012	1106_3_15	2 30 53.83	62 22 39.11	A3-A8	A6V	2.1	1	...	17.15	16.83	...
2012	1203_2_153	2 30 53.99	61 04 55.35	K0-K3	K2V[g]	2.0	1	15.53	15.36	14.72	14.29
2012	1204_253	2 30 54.11	61 41 08.20		A0V	2.8	1	15.28	14.95	14.57	14.01
2012	1104_164	2 30 54.25	61 44 57.26		A1V	3.3	1	15.78	15.49	14.97	14.37
2012	1104_179	2 30 54.30	61 56 00.80	G0-G4	G0V	1.2	0	14.67	14.64	14.28	13.45
2011	0923_202	2 30 54.35	61 46 46.40	F9-G0	G0V	1.9	1	15.93	15.70	15.19	14.44
2012	1203_2_198	2 30 54.38	61 25 47.91	G8-K0	G9V	1.8	1	16.77	16.33	15.78	15.17
2012	1203_2_244	2 30 54.70	61 45 59.66	F4-F5	F4V	2.2	1	16.13	15.80	15.33	14.80
2011	1023_56	2 30 54.77	61 47 08.09	F5-F7	F6V	2.3	1	16.17	15.70	15.16	14.57
2012	0124_298	2 30 55.12	61 40 49.90	F6-F8	F8V	1.8	1	16.13	15.79	15.34	14.77
2012	1106_1_193	2 30 55.59	61 44 21.00	F3-F5	F4V	2.7	1	17.08	16.63	16.04	15.35
2012	1204_286	2 30 55.59	61 13 43.45	A5-A6	A5V	3.0	1	16.47	16.08	15.56	15.05
2012	1106_1_180	2 30 55.70	61 31 19.10	A1-F2	A5V	4.4	0	17.99	17.31	16.52	15.84
2012	0304_204	2 30 55.86	61 16 30.01	G0-K0	G5V	...	...	15.31	...	...	14.80
2011	1023_57	2 30 55.91	61 54 24.12	B7-A0	B9V	2.8	1	14.96	14.75	14.41	13.68
2012	1105_2_207	2 30 56.00	61 55 50.29	B9-A0	B9.5V	1.7	1	13.51	13.31	13.17	12.68
2012	1106_1_289	2 30 56.05	61 49 00.40	F7-F9	F8V	3.2	1	18.24	17.64	16.89	16.26
2012	1106_3_13	2 30 56.10	62 23 38.60	G9-K2	K2V	1.2	0	...	17.32	16.86	...
2012	1106_1_165	2 30 56.16	61 21 57.60	K1-K2	K2V	1.5	0	16.89	16.47	15.94	15.28
2012	1204_260	2 30 56.32	61 38 05.88	G6-G8	G7V	1.8	1	16.38	16.02	15.49	14.90
2012	1106_2_84	2 30 56.44	61 49 08.70	F2-F5	F3V	2.5	1	17.03	16.60	16.06	15.47
2012	1105_4_244	2 30 56.47	62 26 04.21	A3-A8	A6V	1.6	1	15.35	15.54	15.32	14.61

Table 1. IC 1805 Spectral Types and Photometry (Continued)

Year	Date_No.[a] (MMDD_No.)	RA(J2000) (hhmmss.ss)	Dec(J2000) (° ′ ″)	SpTy Range	SpTy	A_V (r-i) (mag)	Assoc.?[b] (ext)	V(90P)[c] (mag)	r[d] (mag)	i[d] (mag)	I(90P)[c] (mag)
2012	1106_2_85	2 30 56.59	61 56 17.50	G5-K2	G9V	3.1	1	...	17.10	16.26	...
2011	0923_24	2 30 56.69	61 10 45.00		F0V	3.3	1	15.37	17.41	16.76	15.97
2012	1105_3_297	2 30 56.75	61 50 00.00	A0-A1	A1V	2.7	1	...	14.52	14.15	...
2012	1203_2_214	2 30 56.92	61 30 34.35	B9-A0	A0V	4.0	1	16.66	16.24	15.62	14.99
2012	1106_1_186	2 30 57.76	61 35 39.11	G7-K3	K0V	1.8	1	18.13	17.60	17.03	16.46
2012	1106_1_287	2 30 58.05	61 49 21.50	F8-G0	F9V	2.0	1	17.44	16.86	16.35	15.79
2011	1023_7	2 30 58.28	61 40 23.30	F8-G0	F9V	1.1	0	14.72	14.41	14.09	13.57
2012	0124_179	2 30 58.44	61 15 36.80	F0-F3	F2V	2.9	1	16.28	15.82	15.22	14.80
2011	1023_283	2 30 58.86	61 15 26.20	F9-G0	F9V	1.1	0	14.62	14.33	14.01	13.53
2012	1105_5_18	2 30 59.18	62 21 46.60	A9-F0	A9V	1.7	1	15.58	15.60	15.32	14.59
2012	1106_2_236	2 30 59.28	61 08 51.60	F5-F7	F6V	3.6	1	17.42	16.78	15.97	15.23
2012	1106_2_82	2 30 59.28	61 47 44.80	A7-F0	A9V	3.8	1	18.32	17.74	17.01	16.37
2012	1105_4_178	2 30 59.42	61 59 31.20	B9-A1	A0V	2.3	1	15.51	15.44	15.16	14.43
2012	1203_1_111	2 30 59.54	61 11 46.28	F2-F3	F2V	2.3	1	15.46	15.06	14.59	14.32
2011	1023_43	2 30 59.73	61 37 53.60	F6-F7	F7V	2.1	1	14.98	14.51	14.00	13.47
2012	1203_2_219	2 31 00.07	61 31 33.59	G9-K2	K2V	3.4	1	17.75	16.94	16.01	15.29
2011	1023_247	2 31 00.50	61 25 27.18	A8-A9	A9V	2.5	1	15.93	15.58	15.13	14.65
2012	1105_5_254	2 31 00.69	61 58 39.20	F9-G0	F9V	0.9	0	14.26	14.38	14.10	13.32
2012	1105_2_104	2 31 00.85	61 11 23.90	A1-A2	A1V	3.5	1	16.18	15.80	15.24	14.76
2012	1204_221	2 31 01.66	61 28 56.29	A9-F0	A9V	3.5	1	16.77	16.31	15.64	15.08
2012	0304_34	2 31 01.76	62 01 11.80	G8-G9	G8V	2.2	1	14.09	13.84	13.21	12.64
2012	0124_248	2 31 01.78	61 46 25.90	G1-G7	G3V	4.1	1	15.01	14.18	13.19	12.43
2012	1106_2_61	2 31 02.15	61 39 01.20	F2-F5	F5V	3.2	1	18.22	17.71	16.99	16.29
2011	0923_28	2 31 02.33	61 14 08.89	F7-F8	F8V	2.0	1	13.20	12.87	12.37	12.13
2011	1023_40	2 31 02.40	61 33 29.30	F6-F8	F7V	0.5	0	13.50	13.23	13.06	12.41
2012	0304_10*	2 31 03.00	61 59 26.09	B9-A0	A0V	1.7	1	14.46	14.51	14.36	13.68
2012	1203_1_178	2 31 03.02	61 34 23.63	G0-G7	G3V	3.3	1	18.40	17.65	16.82	16.15
2012	1105_4_246	2 31 03.11	62 24 55.20	A1-A2	A2V	1.7	1	15.05	15.28	15.09	14.37
2012	1204_247	2 31 03.34	61 32 25.53		F9V	3.1	1	17.86	17.29	16.55	15.87
2012	1104_159	2 31 03.55	61 41 23.78		F8V	4.6	0	16.44	15.52	14.47	13.71
2012	0220_230	2 31 03.75	61 25 43.50	F0-F3	F1V	2.1	1	14.36	13.97	13.56	12.94
2012	0124_254	2 31 03.81	61 55 40.50	K0-K2	K1V	2.5	1	15.83	15.45	14.72	13.77
2012	1105_2_93	2 31 03.87	61 05 59.29	A3-A4	A4V	2.1	1	14.77	14.62	14.31	14.39
2012	1106_2_250	2 31 03.87	61 19 09.20	F5-F7	F6V	2.9	1	18.09	17.59	16.93	16.32
2012	1106_1_208	2 31 04.45	61 46 40.80	G7-K1	K0V	4.2	0	17.04	16.07	14.99	14.21
2012	0124_256	2 31 04.77	61 56 48.80	F2-F6	F4V	1.7	1	13.83	13.84	13.46	12.79
2012	1203_2_164	2 31 05.06	61 11 37.71	K4-K5	K4V	1.2	0	16.90	16.29	15.70	15.18
2012	1203_1_171	2 31 05.31	61 36 48.97	K7-K8	K7V	2.5	1	18.61	17.83	16.77	16.11
2012	1106_3_294	2 31 05.81	61 29 13.80	F9-G0	G0V	2.0	1	17.26	16.82	16.30	15.67
2012	1204_254	2 31 05.83	61 35 25.15		K4V	1.0	0	16.22	15.60	15.05	14.56
2012	1106_2_71	2 31 05.87	61 44 26.90	G7-K0	G8V	3.9	1	18.42	17.55	16.56	15.72
2012	1104_170	2 31 06.03	61 46 33.10	A9-F3	F1V	2.4	1	16.43	16.05	15.56	15.04
2012	1203_1_118	2 31 06.05	61 10 28.47	A3-A5	A4V	3.1	1	16.62	16.25	15.74	15.18
2012	1203_2_248	2 31 06.06	61 44 55.14	F8-F9	F8V	2.5	1	16.65	16.10	15.49	14.80
2012	1106_2_234	2 31 06.16	61 09 57.60	F0-F2	F0V	3.4	1	17.42	16.93	16.26	15.61
2012	1106_2_88	2 31 06.18	61 49 06.40	G7-K0	G9V	3.4	1	18.06	17.30	16.40	15.74
2012	1104_149	2 31 06.22	61 34 37.09	G6-G8	G7V	1.4	0	16.13	15.73	15.27	14.83
2012	0304_36	2 31 06.42	62 01 27.51	G9-K1	K0V	0.9	0	15.87	15.68	15.30	14.74
2012	1204_171	2 31 06.62	61 05 09.91	F6-F7	F7V	2.5	1	...	16.32	15.72	...
2012	1204_266	2 31 06.65	61 40 56.08	F9-G6	G2V	2.6	1	16.00	15.50	14.83	14.20
2012	1105_2_108	2 31 06.84	61 18 15.41	F2-F3	F2V	1.7	1	14.91	14.36	14.01	14.16
2012	1106_3_92	2 31 06.88	62 23 48.90	A3-A6	A6V	2.2	1	...	17.12	16.77	...
2012	1104_143	2 31 07.03	61 36 08.89	G6-G9	G8V	2.4	1	14.67	13.89	13.23	12.50
2012	0220_289	2 31 07.03	61 13 58.90	B8-A0	B9V	3.2	1	16.22	15.92	15.49	15.05
2012	1105_5_55	2 31 07.11	62 12 19.39	F2-F4	F2V	1.8	1	15.36	15.20	14.83	14.09
2011	0923_102	2 31 07.23	61 03 13.98	A3-A6	A5V	2.4	1	15.25	15.25	14.87	14.68
2011	0923_93	2 31 07.31	61 01 46.00	F3-F4	F3V	2.1	1	15.93	15.85	15.41	14.87
2012	1204_267	2 31 07.35	61 43 42.03	F6-F7	F7V	2.1	1	16.19	15.79	15.27	14.72
2012	1105_5_74	2 31 07.42	62 23 27.01	F4-F6	F4V	1.4	0	15.78	15.49	15.18	14.63
2012	1203_2_184	2 31 07.50	61 22 15.32	F6-F7	F7V	1.8	1	15.51	15.16	14.72	14.52
2012	1106_1_178	2 31 07.58	61 31 45.89	F8-F9	F9V	2.8	1	17.38	16.84	16.16	15.54
2012	0124_257	2 31 07.63	62 01 19.20	G6-K0	G4V	2.8	1	15.79	15.33	14.60	13.76
2012	1203_2_284*	2 31 07.69	61 24 57.82	A7-A9	A8V	2.5	1	15.78	15.47	15.01	14.56
2011	1023_285	2 31 07.74	61 15 04.72		F7V	1.0	0	13.38	12.99	12.72	12.45
2012	0124_240	2 31 07.84	61 42 31.09	G9-K0	K0V	3.3	1	16.06	15.35	14.45	13.76
2012	1203_1_124	2 31 07.90	61 14 59.11		F8V	1.6	1	15.12	14.77	14.36	14.17
2011	1023_3	2 31 08.13	61 40 02.30	G4-G6	G5V	1.4	0	14.71	14.30	13.87	13.31
2012	1106_1_167	2 31 08.18	61 22 57.60	F6-F7	F7V	2.3	1	16.96	16.50	15.95	15.41
2011	0923_95	2 31 08.36	61 00 05.80	G6-G8	G7V	2.2	1	14.52	14.10	13.50	13.90
2012	1105_5_72	2 31 08.47	62 22 03.70	G1-G7	G4V	0.9	0	14.81	14.52	14.20	13.66
2012	1105_2_203	2 31 08.57	61 55 21.00	A9-F2	F0V	2.3	1	15.52	15.44	14.99	14.23
2012	1203_2_160	2 31 08.91	61 05 31.20	F6-F7	F7V	3.0	1	...	17.05	16.35	...
2011	1023_195	2 31 09.12	61 01 24.80	G1-G5	G3V	1.5	0	15.53	15.42	14.97	14.65
2012	1203_1_290	2 31 09.31	61 43 44.32	F8-F9	F8V	2.0	1	15.97	15.54	15.04	14.42
2012	1105_4_248	2 31 09.36	62 24 23.30	F1-F3	F2V	1.2	0	14.35	14.54	14.29	13.48
2011	1023_191	2 31 09.45	61 04 33.97	B9-A0	A0V	2.6	1	14.79	14.75	14.41	14.41
2012	1104_139	2 31 09.66	61 29 12.23	G0-G1	G0V	1.5	0	14.69	13.87	13.44	13.93
2012	1105_3_209*	2 31 09.93	61 19 27.30	B9-A0	B9.5V	2.6	1	14.91	14.67	14.35	13.84
2012	1106_2_79	2 31 09.98	61 40 42.80	G8-K1	K0V	2.5	1	17.32	16.66	15.95	15.33
2012	0216_259	2 31 10.07	61 39 41.51	M1-M2	M2V	0.9	0	19.30	18.62	17.49	16.68
2012	1106_2_300	2 31 10.15	61 08 47.10	G8-K0	G9V	2.1	1	17.97	17.44	16.81	16.21
2012	1105_4_157	2 31 10.33	61 54 10.20	G8-K0	G9V	3.3	1	14.70	14.17	13.31	12.55
2012	1106_2_86	2 31 10.63	61 46 39.61	F5-F7	F6V	2.7	1	17.70	17.19	16.57	15.98
2011	1023_58	2 31 10.67	61 43 57.50		F5V	1.2	0	14.29	14.05	13.76	13.23
2012	1203_1_133*	2 31 10.80	61 23 35.08		A0V	2.6	1	14.97	14.72	14.38	13.88
2012	1203_1_276	2 31 11.06	61 26 37.65	A7-F0	F0V	2.1	1	15.68	15.38	14.98	14.49
2012	0304_38	2 31 11.38	62 01 30.80	G2-G4	G3V	0.9	0	15.27	15.08	14.77	14.05

Table 1. IC 1805 Spectral Types and Photometry (Continued)

Year	Date_No.[a] (MMDD_No.)	RA(J2000) (hhmmss.ss)	Dec(J2000) (° ′ ″)	SpTy Range	SpTy	A_V (r-i) (mag)	Assoc.?[b] (ext)	V(90P)[c] (mag)	r[d] (mag)	i[d] (mag)	I(90P)[c] (mag)
2012	1105_4_152	2 31 11.39	61 51 51.80	F9-G7	G0V	1.7	1	15.94	15.73	15.27	14.54
2012	1203_1_199	2 31 11.62	61 47 37.85	G8-K1	G9V	2.6	1	17.28	16.63	15.91	15.30
2012	1105_2_208	2 31 11.78	61 43 38.50	B4-B5	B5V	2.3	1	13.82	13.66	13.49	12.96
2012	1106_1_168	2 31 11.80	61 21 29.91	G7-G9	G8V	1.9	1	17.48	17.02	16.46	15.85
2012	0220_247	2 31 11.89	61 38 46.60	K2-K3	K2V	3.9	1	16.33	15.42	14.37	13.61
2012	1105_4_249	2 31 12.06	62 26 24.70	A1-A3	A2V	1.9	1	15.51	15.36	15.13	14.62
2012	0220_264*	2 31 12.06	61 51 31.20	G5-G7	G6V	2.5	1	15.00	14.69	14.02	13.19
2011	0923_209	2 31 12.11	61 49 28.91	F8-F9	F9V	1.4	0	15.37	15.06	14.67	13.96
2012	1106_3_223	2 31 12.36	61 26 05.40	F8-G0	F9V	4.0	1	17.63	16.91	15.98	15.18
2012	1204_289*	2 31 12.44	61 23 43.22	A1-A2	A1V	2.7	1	15.53	15.21	14.83	14.67
2012	1106_2_298	2 31 12.64	61 08 16.01	F2-F4	F3V	3.1	1	17.24	16.76	16.11	15.47
2011	0923_199	2 31 13.00	61 33 31.05	A7-A8	A7V	2.2	1	15.08	14.64	14.28	14.10
2012	1203_2_241	2 31 13.36	61 49 56.93	F4-F7	F7V	2.5	1	...	16.75	16.15	...
2012	1203_1_196	2 31 13.47	61 45 03.13	A3-A5	A3V	3.3	1	16.00	15.59	15.06	14.45
2011	1023_59	2 31 13.51	61 45 26.09	G8-K0	G9V	3.0	1	15.70	15.00	14.19	13.57
2012	1105_5_78	2 31 13.62	62 26 58.20	G2-G5	G3V	2.5	1	15.51	15.17	14.51	13.87
2012	1203_1_165	2 31 13.95	61 30 45.99	G5-K0	G8V	3.1	1	18.78	17.96	17.15	16.52
2012	1104_21	2 31 13.96	61 25 52.25		A9V	2.9	1	16.19	15.77	15.23	14.72
2012	0304_294	2 31 14.03	61 35 06.70		F3V	0.7	0	13.77	13.50	13.36	12.77
2012	1203_2_166	2 31 14.03	61 14 57.73	A0-A1	A1V	3.0	1	15.86	15.60	15.16	14.77
2012	1204_229	2 31 14.13	61 27 16.37	F6-G0	F8V	3.1	1	18.33	17.70	16.96	16.34
2012	1106_3_94	2 31 14.18	62 22 16.01	G2-G8	G6V	1.3	0	...	16.83	16.42	...
2012	1105_4_231	2 31 14.25	62 17 10.60	G8-K0	G9V[g]	2.7	1	15.21	14.82	14.08	13.22
2012	1106_1_201	2 31 14.30	61 47 57.00	K4-K5	K5V	1.6	1	18.40	17.68	17.00	16.40
2012	1104_272*	2 31 14.64	61 36 35.71		A0V	3.1	1	16.06	15.78	15.35	14.76
2012	1106_3_96	2 31 14.97	62 24 12.60	F4-F7	F6V	1.7	1	...	17.27	16.84	...
2012	1105_2_201	2 31 14.98	61 55 19.79	A0-A1	A1V	2.5	1	14.96	14.46	14.12	13.56
2012	1104_154	2 31 14.99	61 40 08.58	G2-G4	G3V	3.1	1	16.00	15.31	14.52	13.88
2012	0124_258	2 31 15.06	61 55 40.81	B7-B9	B9V	2.3	1	15.84	15.72	15.47	14.77
2012	1106_2_242	2 31 15.10	61 19 21.20		F8V	3.0	1	17.40	16.84	16.13	15.51
2012	1203_2_155	2 31 15.28	61 09 31.58	A1-A2	A2V	3.1	1	16.38	16.06	15.57	15.05
2012	1204_261	2 31 15.56	61 45 46.02	K4-K5	K4V	1.2	0	17.29	16.63	16.05	15.48
2012	1105_5_76	2 31 15.70	62 21 59.71	F6-F9	F8V	1.2	0	15.41	15.45	15.11	14.38
2012	0304_198	2 31 15.79	61 11 42.21	A1-A3	A2V	2.7	1	16.09	15.85	15.46	14.98
2012	1203_2_225	2 31 16.07	61 33 59.13	A2-A3	A3V	3.8	1	17.29	16.80	16.15	15.55
2012	1203_1_27	2 31 16.12	61 19 43.02	B9-A0	B9V	3.0	1	15.35	14.99	14.60	14.65
2012	0220_218	2 31 16.21	61 20 09.40	F9-G1	G0V	1.5	0	15.43	15.03	14.62	14.64
2012	1204_184	2 31 16.32	61 10 22.60	F2-F4	F3V	2.6	1	16.95	16.54	15.98	15.40
2011	0923_153*	2 31 16.39	61 24 10.90	A4-A5	A5V	2.4	1	15.95	15.68	15.29	14.85
2012	1203_2_243	2 31 16.41	61 48 16.66	F7-F8	F8V	1.8	1	15.10	14.71	14.26	13.78
2012	1104_280	2 31 16.92	61 39 09.14		F5V	1.8	1	16.22	15.87	15.46	14.96
2012	1105_4_247	2 31 17.09	62 26 46.60	G7-G9	G8V	1.1	0	...	14.91	14.52	...
2012	1104_163	2 31 17.44	61 47 50.14		B9V	2.7	1	14.53	14.25	13.93	13.40
2012	1104_123	2 31 17.58	61 21 33.95	G5-G7	G6V	1.2	0	16.02	15.69	15.29	14.78
2012	1106_2_87	2 31 17.70	61 47 28.60	F0-F3	F2V	3.2	1	17.89	17.35	16.68	16.07
2012	1204_218	2 31 17.78	61 25 40.06		F4V	2.0	1	16.06	15.69	15.24	14.76
2012	1106_1_164	2 31 17.80	61 19 46.30	F6-F7	F7V	2.4	1	17.24	16.78	16.21	15.63
2011	0923_26	2 31 17.84	61 16 41.50	F4-F5	F5V	1.8	1	15.40	15.06	14.65	14.47
2012	1105_2_202	2 31 17.85	61 40 08.90	A2-A5	A3V	2.2	1	16.28	16.06	15.75	15.28
2012	1106_2_296	2 31 17.85	61 09 03.80	F6-F8	F7V	2.8	1	17.94	17.41	16.75	16.10
2012	0124_178	2 31 17.91	61 17 25.90	A9-F0	A9V	2.8	1	16.35	15.94	15.41	14.95
2012	1203_2_165	2 31 17.94	61 16 51.44	B9-A0	A0V	2.8	1	15.67	15.46	15.09	14.81
2012	0124_253	2 31 17.96	62 00 30.50	F3-F5	F5V	1.0	0	14.22	14.10	13.85	13.33
2011	1023_208	2 31 18.04	61 14 40.60		F0V	1.8	1	14.51	14.26	13.93	13.43
2012	1106_3_225	2 31 18.09	61 28 03.90	G1-G6	G3V	2.8	1	18.24	17.58	16.87	16.19
2012	1106_3_221	2 31 18.28	61 34 38.20	K4-K5	K5V	1.5	0	18.33	17.61	16.93	16.37
2012	0220_235	2 31 18.32	61 34 44.30	A8-F0	A9V	2.5	1	16.34	16.00	15.55	15.06
2012	1106_2_232	2 31 18.45	61 13 04.90	A5-A8	A7V	3.3	1	17.63	17.16	16.55	15.94
2012	0124_297	2 31 18.51	61 48 57.80	B9-A1	A0V	2.5	1	14.58	14.34	14.04	13.46
2012	1105_2_289	2 31 19.06	61 54 22.20	F3-F5	F4V	2.5	1	15.97	15.77	15.24	14.44
2011	0923_191	2 31 19.18	61 35 44.60		F2V	1.7	1	14.40	14.11	13.75	13.29
2012	1204_256	2 31 19.24	61 34 28.18	A1-A5	A3V	3.6	1	17.00	16.55	15.96	15.38
2012	1104_121	2 31 19.30	61 22 30.47	G7-K0	G9V	3.4	1	15.28	14.44	13.55	13.73
2012	1203_1_117	2 31 19.35	61 13 54.65	F6-F7	F7V	2.4	1	16.93	16.50	15.93	15.35
2012	1106_1_177	2 31 19.50	61 34 36.90	A3-A6	A5V	2.9	1	17.39	17.03	16.55	16.02
2012	1106_3_11	2 31 19.71	62 16 17.30	G5-K0	G7V	2.5	1	...	16.03	15.36	...
2012	1104_188	2 31 20.02	61 59 27.10	K0-K2	K1V	0.8	0	15.14	15.07	14.71	13.90
2012	1106_2_294	2 31 20.10	61 08 31.80	A3-A5	A3V	3.3	1	17.95	17.56	17.03	16.04
2012	1105_5_80*	2 31 20.47	62 26 02.81	B8-A0	B9V	1.6	1	13.71	13.65	13.56	13.12
2012	0304_267	2 31 20.54	61 50 44.81	F3-F5	F4V	0.8	0	13.44	12.74	12.55	13.26
2012	0124_161	2 31 20.69	61 08 26.10	K3-K6	K5V	5.1	0	15.35	14.40	12.98	14.33
2012	1106_1_185	2 31 21.12	61 38 22.01	A5-A8	A7V	2.9	1	16.93	16.58	16.07	15.34
2012	0304_260	2 31 21.13	61 45 13.29	A9-F1	F0V	2.3	1	16.38	16.06	15.63	15.09
2012	1203_1_195	2 31 21.45	61 48 06.73	G7-K0	G9V	1.3	0	15.91	15.51	15.07	14.59
2012	1106_3_227	2 31 21.53	61 25 47.70	G7-K0	G8V	2.9	1	17.76	17.12	16.36	15.71
2012	1203_2_156	2 31 21.63	61 05 01.05		A1V	2.8	1	15.43	15.53	15.14	14.52
2012	1106_2_83	2 31 21.82	61 47 49.51	G5-K1	K0V[g]	3.6	1	16.91	16.04	15.10	14.38
2012	1203_2_161	2 31 21.94	61 17 56.72		F8V	1.7	1	15.76	15.40	14.96	14.86
2011	0923_104	2 31 22.01	61 11 28.49		F9V	1.4	0	13.74	13.45	13.06	12.48
2012	1106_1_285	2 31 22.10	61 49 06.90	A9-F3	F2V	2.5	1	16.67	16.23	15.69	15.15
2012	1105_2_110	2 31 22.19	61 26 21.00		F9V	1.6	1	16.29	15.95	15.53	15.07
2012	1105_4_274	2 31 22.26	61 51 19.50	G0-G8	G2V	1.5	0	15.82	15.45	15.01	14.28
2011	1023_54	2 31 22.66	61 37 49.27	K7-M1	M0V	1.1	0	15.86	15.15	14.22	13.63
2012	1203_1_24	2 31 22.79	61 05 37.58	F7-F8	F7V	1.8	1	15.07	14.91	14.46	14.11
2012	1104_165	2 31 22.80	61 47 06.79		G6V	4.1	1	15.84	14.95	13.94	13.22
2012	1104_136	2 31 23.24	61 27 55.66	A9-F0	F0V	2.2	1	16.11	15.82	15.40	14.85
2012	1105_5_20	2 31 23.46	62 17 08.40	G7-K0	G8V	2.2	1	15.26	15.08	14.45	13.61

Table 1. IC 1805 Spectral Types and Photometry (Continued)

Year	Date_No.[a] (MMDD_No.)	RA(J2000) (hhmmss.ss)	Dec(J2000) (° ′ ″)	SpTy Range	SpTy	A_V (r-i) (mag)	Assoc.?[b] (ext)	V(90P)[c] (mag)	r[d] (mag)	i[d] (mag)	I(90P)[c] (mag)
2011	1023_45	2 31 23.53	61 34 05.20	G9-K2	K2V	1.5	0	15.08	14.47	13.93	13.97
2012	1105_2_205	2 31 23.86	61 41 34.41	A2-A4	A3V	2.3	1	16.29	16.08	15.74	15.07
2012	0220_257*	2 31 24.21	61 47 13.70	F5-F7	F6V	2.3	1	16.19	15.74	15.19	14.57
2011	1023_62	2 31 24.22	61 48 48.80	G3-G9	G5V	2.8	1	14.00	13.42	12.70	12.21
2012	0124_230	2 31 24.40	61 36 57.40	F4-F6	F5V	1.9	1	15.63	15.28	14.85	14.35
2011	0923_207	2 31 24.45	61 43 37.34	G5-G7	G6V	0.5	0	14.01	13.77	13.51	13.03
2012	1204_185	2 31 24.48	61 16 42.50	F4-F5	F4V	2.3	1	16.19	15.82	15.32	14.87
2012	1105_4_245	2 31 24.60	62 25 35.60	F7-F8	F8V	1.3	0	15.28	15.33	14.99	14.26
2012	1106_3_98	2 31 24.66	62 22 35.00	K6-K7	K7V	1.2	0	...	16.85	16.07	...
2012	1203_2_294	2 31 25.05	61 33 38.63	G5-G7	G6V	1.5	0	15.86	15.47	15.00	14.58
2011	0923_205	2 31 25.07	61 45 59.35		B4V	2.0	1	13.75	13.53	13.42	12.82
2012	0220_217	2 31 25.42	61 22 27.71	B9-A0	A0V	2.6	1	15.99	15.80	15.47	14.99
2012	0304_32	2 31 25.53	61 56 32.19	F6-F7	F6V	0.9	0	13.89	13.71	13.47	12.85
2012	0124_262*	2 31 25.68	62 01 47.41	G9-K1	K0V	2.6	1	13.21	12.96	12.21	11.59
2012	1203_2_249	2 31 25.76	61 40 43.99	K4-K5	K4V	1.6	0	17.29	16.58	15.92	15.36
2011	1023_199	2 31 26.06	61 04 53.43	K1-K2	K1V	1.1	0	15.18	15.19	14.76	14.14
2012	1105_4_243	2 31 26.29	62 26 41.81	F7-F8	F7V	1.4	0	15.22	15.29	14.93	14.21
2012	0220_229*	2 31 26.31	61 26 50.50	B9-A0	A0V	2.6	1	15.77	15.57	15.23	14.76
2012	1105_2_283	2 31 26.37	61 50 00.90	G5-G7	G6V	0.0	0	13.62	13.38	13.31	12.60
2012	1106_1_151	2 31 26.46	61 19 10.10	K6-K7	K7V	1.9	1	17.69	17.01	16.09	15.42
2012	0220_268	2 31 26.68	61 52 08.40	B7-B8	B8V	2.5	1	14.81	14.26	14.00	13.46
2012	1104_277	2 31 26.74	61 49 04.40		F7V	1.1	0	14.61	14.31	14.01	13.54
2012	1203_2_295*	2 31 27.35	61 49 31.69	A1-A2	A2V	2.3	1	14.84	14.88	14.56	14.04
2011	1023_36	2 31 27.37	61 28 11.20		F3V	1.4	0	14.42	14.19	13.89	13.45
2011	0923_204	2 31 27.54	61 33 22.30	G8-K1	K0V	2.9	1	15.81	15.04	14.24	13.57
2012	1105_3_283	2 31 27.56	61 26 39.20	G4-G6	G6V	1.1	0	15.27	14.97	14.59	14.09
2012	1105_3_207	2 31 27.65	61 22 04.40	A3-A6	A4V	2.8	1	15.86	15.54	15.08	14.72
2011	0923_97	2 31 27.95	61 08 32.60	G8-K0	G9V	5.0	0	14.65	13.62[e]	12.39[f]	12.22
2012	0304_251*	2 31 28.21	61 47 04.41	G7-G9	G8V	2.7	1	15.21	14.52	13.78	13.18
2012	1204_205	2 31 28.34	61 24 21.81		G0V	1.4	0	15.68	15.34	14.95	14.54
2011	1023_197	2 31 28.35	61 08 49.24		F7V	1.8	1	15.37	14.98	14.53	14.18
2012	1106_3_100	2 31 28.55	62 24 24.30	A1-A2	A2V	2.7	1	...	17.19	16.79	...
2012	1105_2_99	2 31 29.09	61 17 41.90	G8-G9	G8V	1.4	0	16.35	15.95	15.48	15.03
2011	1023_236	2 31 29.17	61 23 53.00	G9-K0	K0V	2.6	1	13.89	13.41	12.68	12.20
2012	1105_5_75	2 31 29.27	62 26 35.11	F6-F8	F7V	1.4	0	15.23	15.40	15.04	14.11
2011	0923_203	2 31 29.41	61 45 16.30	F9-G0	G0V	1.8	1	15.67	15.27	14.78	14.27
2012	1106_3_229	2 31 29.41	61 28 53.79	K7-K8	K7V	1.9	1	18.07	17.57	16.65	15.76
2012	1104_140	2 31 29.44	61 30 00.11	G6-G7	G7V	1.3	0	16.03	15.69	15.27	14.74
2012	1105_3_264	2 31 29.46	61 58 02.41	A0-A1	A0V	2.4	1	13.22	13.43	13.14	12.59
2012	1105_2_98	2 31 30.55	61 14 10.60	B9-A0	B9.5V	2.8	1	16.35	15.79	15.43	15.03
2012	0304_210*	2 31 30.79	61 24 29.00	G7-G8	G8V	2.2	1	16.18	15.63	15.00	14.51
2012	0124_215	2 31 30.94	61 35 14.31	A3-A7	A4V	0.6	0	12.79	12.22	12.22	12.16
2012	1106_2_81	2 31 30.98	61 45 00.49	K4-K5	K4V	1.3	0	17.28	16.62	16.02	15.47
2012	1104_142	2 31 31.06	61 32 28.93	G5-G9	G7V	2.9	1	15.31	14.52	13.77	13.87
2012	1204_297	2 31 31.63	61 32 39.49	A7-A8	A7V	3.5	1	17.58	17.05	16.40	15.80
2012	1106_3_230	2 31 31.73	61 26 32.50	F2-F3	F3V	2.6	1	17.17	16.74	16.19	15.62
2011	0923_103	2 31 32.21	61 19 01.57	F7-F8	F7V	2.0	1	13.37	13.49	13.00	12.39
2012	1105_4_241	2 31 32.25	62 24 57.90	B9-A0	A0V	1.8	1	14.92	15.06	14.90	14.18
2012	1104_148	2 31 32.39	61 33 59.08	F7-F8	F7V	0.9	0	13.92	13.70	13.44	12.93
2012	1106_2_19	2 31 32.70	61 46 46.40	G8-K1	G9V[g]	4.3	0	18.07	17.10	16.03	15.30
2011	1023_64	2 31 32.78	61 44 24.80	A1-A2.5	A2V	2.5	1	15.93	15.66	15.30	14.77
2011	1023_194	2 31 32.87	61 00 13.32	F2.5-F4	F3V	2.1	1	15.12	14.97	14.51	14.44
2012	1204_175	2 31 33.00	61 11 20.86	G3-G6	G4V	2.0	1	16.32	15.82	15.25	14.78
2012	1203_2_222	2 31 33.08	61 30 19.14	F4-F6	F5V	2.9	1	17.20	16.68	16.03	15.44
2012	1203_2_152	2 31 33.11	61 05 45.23	A0-A1	A1V	3.1	1	15.67	15.70	15.24	14.57
2012	1106_3_99	2 31 33.19	62 24 30.09	G9-K2	K2V	1.1	0	...	17.22	16.77	...
2012	1106_2_223	2 31 33.40	61 09 49.10	K3-K5	K4V	1.9	1	18.43	17.81	17.07	16.44
2012	1105_2_11	2 31 34.09	61 27 24.10	M0-M2	M2V	0.4	0	16.03	16.89	15.87	14.65
2011	0923_99	2 31 34.63	61 11 37.19	F8-G0	F9V	1.5	0	14.86	14.52	14.12	13.64
2012	1105_4_299	2 31 34.78	62 26 23.01	A2-A6	A3V	2.2	1	15.67	15.72	15.41	14.69
2012	1105_4_276	2 31 34.86	61 55 28.60	F3-F5	F4V	0.7	0	13.60	13.42	13.26	12.59
2012	1105_4_153	2 31 35.07	61 59 47.30	K2-K4	K3V	0.8	0	14.31	13.77	13.36	13.42
2012	0220_214	2 31 35.15	61 20 30.10	B9-A1	A0V	3.0	1	16.10	15.83	15.42	14.92
2012	1106_2_225	2 31 35.28	61 07 39.00	A5-AA7	A6V	4.0	1	18.09	17.51	16.78	16.13
2012	1105_5_297	2 31 35.48	61 59 43.60	G5-K0	G8V	0.3	0	14.31	13.23	13.02	12.79
2011	0923_96	2 31 35.51	61 02 44.50	F7-F8	F8V	2.0	1	15.09	15.08	14.58	14.04
2011	0923_116	2 31 35.60	61 22 05.60	F4-F5	F5V	2.1	1	15.77	15.33	14.85	14.74
2012	1105_5_73	2 31 36.01	62 25 40.81	A0-A1	A1V	1.7	1	15.17	15.10	14.92	14.43
2012	1203_2_202	2 31 36.35	61 27 29.98	A2-A3	A2V	3.2	1	16.18	16.18	15.67	14.62
2012	1204_242	2 31 36.46	61 30 18.64	K4-K5	K4V	1.3	0	16.60	15.97	15.38	14.89
2012	1204_36	2 31 36.69	61 46 48.20	A3-A6	A5V	2.9	1	16.05	15.69	15.20	14.67
2012	1203_1_116	2 31 36.94	61 15 39.63	G8-K0	G8V	2.9	1	16.91	16.27	15.50	14.96
2012	1204_173*	2 31 37.07	61 14 28.21	F6-F7	F7V	2.3	1	16.15	15.67	15.12	14.75
2011	0923_201	2 31 37.16	61 35 26.71	F3-F4	F4V	1.8	1	15.21	14.78	14.38	14.29
2012	1203_1_155	2 31 37.48	61 28 13.94	G7-K2	G9V	3.5	1	18.92	18.17	17.25	16.60
2012	1204_180	2 31 37.55	61 06 50.15	A1-A2	A2V	3.5	1	...	16.12	15.54	...
2012	1105_3_262*	2 31 37.63	61 55 55.20	G6-G8	G7V	2.1	1	15.34	14.81	14.21	13.40
2011	0923_180	2 31 37.64	61 24 33.43		A3V	1.9	1	13.08	13.12	12.89	12.44
2012	1105_5_77	2 31 37.86	62 21 36.50	G8-K1	G8V	2.0	1	14.33	14.17	13.59	12.64
2012	1203_2_252	2 31 37.99	61 48 55.15	F4-F5	F4V	2.7	1	17.18	16.67	16.09	15.54
2012	1203_2_157	2 31 38.15	61 14 24.24	G5-G7	G6V	1.4	0	15.95	15.54	15.09	14.77
2012	1204_190	2 31 38.50	61 15 59.51	F6-F7	F7V	3.2	1	17.23	16.62	15.88	15.25
2012	1106_3_97	2 31 38.74	62 22 41.70	K3-K4	K4V	1.0	0	...	17.23	16.70	...
2012	1105_5_238	2 31 39.03	61 55 55.71	K2-K3	K2V	0.6	0	15.29	14.62	14.27	13.58
2012	1106_3_228	2 31 39.40	61 28 51.29	G9-K1	K0V	2.1	1	17.68	17.10	16.47	15.92
2012	1106_2_221	2 31 39.82	61 15 15.90	K4-K5	K4V	1.2	0	17.64	17.06	16.48	15.91
2012	0124_266	2 31 39.99	62 01 36.10	F6-F8	F7V	1.2	0	15.08	15.14	14.83	14.07

Table 1. IC 1805 Spectral Types and Photometry (Continued)

Year	Date_No.[a] (MMDD_No.)	RA(J2000) (hhmmss.ss)	Dec(J2000) (° ′ ″)	SpTy Range	SpTy	A_V (r-i) (mag)	Assoc.?[b] (ext)	V(90P)[c] (mag)	r[d] (mag)	i[d] (mag)	I(90P)[c] (mag)
2012	1104_127	2 31 40.04	61 22 33.53	G7-G8	G7V	2.7	1	15.46	14.72	13.99	14.07
2012	1203_2_174	2 31 40.18	61 22 40.86	G7-G9	G8V	1.1	0	15.34	14.89	14.50	14.38
2012	1105_4_145	2 31 40.24	61 55 04.21	F6-F7	F7V	1.5	0	15.36	15.28	14.90	14.18
2011	1023_66	2 31 40.56	61 45 14.20	A9-F0	F0V	1.5	1	13.67	13.41	13.14	12.57
2012	1105_2_13	2 31 40.61	61 16 41.01	A1-A2	A1V	2.9	1	16.38	16.11	15.70	15.19
2012	1106_2_227	2 31 40.71	61 09 18.39	G3-G5	G4V	3.1	1	18.10	17.47	16.67	15.94
2012	1203_2_154	2 31 40.78	61 09 38.32	F6-F7	F7V	2.2	1	16.39	16.00	15.46	14.89
2012	1203_1_206	2 31 40.91	61 47 53.25		F8V	2.2	1	16.86	16.37	15.83	15.28
2012	1203_1_139*	2 31 41.20	61 24 52.73	B9-A0	B9V	2.8	1	15.32	15.03	14.70	14.51
2012	1203_1_198	2 31 41.26	61 40 12.38	A5-A6	A6V	2.0	1	15.38	15.17	14.88	14.36
2012	1203_2_276	2 31 41.45	61 04 08.07	K4-K5	K4V	1.4	0	...	16.14	15.52	...
2012	1105_2_70	2 31 41.78	61 31 03.60	G5-G7	G6V	1.4	0	16.26	15.86	15.41	14.96
2012	1203_1_107*	2 31 41.78	61 04 35.52	B9-A1	A0V	2.6	1	15.91	14.90	14.57	15.85
2012	1106_3_226	2 31 41.84	61 26 57.00	F9-G6	G3V	2.2	1	17.37	16.86	16.26	15.68
2012	0304_288	2 31 41.90	61 10 35.81		F7V	2.8	1	17.45	16.96	16.31	15.68
2012	1106_2_11	2 31 41.94	61 55 08.51	A1-A2	A2V	2.8	1	...	17.41	17.00	...
2011	1023_60	2 31 41.96	61 33 50.00		A0V	2.4	1	14.83	14.44	14.14	14.12
2012	1204_174	2 31 42.24	61 04 30.79	K4-K5	K4V	0.7	0	15.88	15.52	15.04	14.76
2012	0124_264	2 31 42.32	61 59 46.60	G6-G9	G4V	0.9	0	15.27	15.25	14.92	14.22
2012	1105_2_214	2 31 42.34	61 50 14.20	K2-K4	K3V	1.3	0	13.82	13.46[e]	12.93[f]	12.62
2012	1105_4_297	2 31 42.51	62 24 33.90	F9-G2	G0V	1.1	0	15.75	15.79	15.46	14.71
2012	1106_2_17	2 31 42.59	61 44 25.60	G8-K2	G9V	2.0	1	17.53	16.99	16.41	15.85
2012	0220_231	2 31 42.74	61 35 08.50	K5-K7	K6V	4.2	1	16.42	15.21	13.87	13.77
2012	0304_263	2 31 42.85	61 49 12.10	A7-A8	A7V	2.1	1	14.95	14.66	14.32	13.82
2012	1204_238	2 31 42.90	61 28 06.94	G0-G7	G5V	2.0	1	16.96	16.47	15.90	15.33
2012	1105_5_300	2 31 43.04	61 55 33.50	A7-A9	A8V	1.6	1	13.30	13.30	13.03	12.52
2012	1204_219	2 31 43.80	61 27 27.59	F4-F5	F5V	3.3	1	17.35	16.80	16.07	15.43
2011	1023_196	2 31 44.03	61 09 06.05	B5-B7	B6V	3.3	1	14.96	14.68	14.27	13.73
2012	0124_163	2 31 44.32	61 13 52.50	F3-F5	F4V	1.9	1	16.20	15.85	15.43	15.02
2012	1106_2_94	2 31 44.32	61 56 05.00	M1-M2	M2V	0.3	0	...	16.79	15.78	...
2012	1105_2_218	2 31 44.51	61 41 58.60		A3V	1.8	1	14.31	14.11	13.88	13.33
2011	1023_53	2 31 44.67	61 36 51.85	B5-B7	B6V	4.3	0	...	17.94	17.33	...
2012	1104_278	2 31 44.93	61 39 13.90		G5V	3.9	1	15.65	14.76	13.81	13.08
2012	0216_193	2 31 45.06	61 22 00.90	K7-M1	M0V	2.1	1	20.01	19.11	17.96	17.19
2012	1203_1_286	2 31 45.45	61 34 54.30		F8V	1.8	1	15.98	15.61	15.15	14.66
2012	1203_2_286*	2 31 45.46	61 26 57.49	B9-A0	A0V	2.7	1	16.26	15.29	14.92	14.96
2012	0304_44	2 31 45.62	62 03 09.01	F7-F8	F7V	0.9	0	13.53	13.57	13.30	12.57
2012	0304_224	2 31 45.70	61 33 22.79	K0-K2	K1V	4.7	0	15.39	14.17	12.98	13.88
2012	1106_3_93	2 31 45.90	62 00 09.11	F6-F8	F7V	2.0	1	...	17.54	17.05	...
2012	1106_3_224	2 31 46.21	61 39 59.40	G9-K2	K2V	1.4	0	16.89	16.74	16.23	15.05
2012	1105_4_295	2 31 46.35	62 22 56.60		F8V	1.0	0	14.31	14.39	14.09	13.26
2012	1204_237	2 31 46.61	61 28 47.13		F7V	2.1	1	16.07	15.68	15.17	14.74
2012	1203_2_232	2 31 47.00	61 32 03.43	B8-A0	B9V	3.4	1	15.90	15.51	15.03	14.71
2012	1105_2_216	2 31 47.31	62 00 51.00	F8-F9	F8V	1.3	0	15.87	15.79	15.44	14.72
2012	1105_2_298	2 31 47.37	61 33 24.50	G5-K2	G8V[g]	2.9	1	15.64	14.91	14.14	14.26
2011	1023_299	2 31 47.38	61 25 42.41		F6V	2.0	1	15.99	15.61	15.12	14.74
2012	1203_1_204	2 31 47.52	61 44 36.52	F7-F8	F7V	2.4	1	17.30	16.81	16.23	15.66
2012	1203_1_156	2 31 47.85	61 27 32.45	B9-A0	A0V	2.6	1	15.38	15.12	14.78	14.54
2012	1105_5_82	2 31 48.16	62 20 26.90	A2-A5	A3V	1.9	1	14.23	14.36	14.12	13.55
2011	0923_217	2 31 48.34	61 25 27.40	K3-K4	K3V	0.7	0	15.33	14.83	14.43	14.53
2012	1104_150	2 31 48.48	61 34 55.96	B2-B3	B3V	2.7	1	13.93	13.68	13.43	12.86
2012	1105_2_15	2 31 48.53	61 04 46.19	B9-A0	A0V	2.6	1	15.80	15.75	15.41	14.85
2011	0923_285	2 31 48.55	61 43 01.40		G8V	2.9	1	15.61	14.93	14.16	13.53
2012	0220_215	2 31 48.58	61 24 06.60	F8-G1	G0V	1.7	1	16.12	15.76	15.30	14.80
2011	1023_69	2 31 48.59	61 49 35.00		F8V	1.4	0	15.18	14.50	14.13	13.63
2012	0304_46	2 31 48.71	62 04 38.90	F4-F6	F5V	1.6	1	15.71	15.68	15.31	14.57
2012	1106_2_230	2 31 48.76	61 09 24.30	G3-G6	G5V	1.9	1	17.22	16.76	16.21	15.62
2011	0923_13	2 31 48.77	61 20 05.74		F5V	1.4	0	12.96	12.63	12.30	12.14
2012	1105_4_293	2 31 48.79	62 26 08.90	F9-G2	G0V	1.0	0	14.55	14.60	14.28	13.54
2012	1203_2_280	2 31 49.03	61 10 45.94		F8V	1.4	0	15.28	14.94	14.57	13.81
2012	0220_191	2 31 49.12	61 09 10.20	K1-K2	K2V	3.4	1	16.17	15.32	14.38	13.68
2011	0923_212	2 31 49.79	61 32 41.42	B4-B7	B4V	2.4	1	13.44	13.24	13.05	12.69
2012	1203_2_293*	2 31 49.92	61 41 13.02	A1-A2	A1V	2.4	1	14.97	14.74	14.43	13.95
2011	1023_5	2 31 50.09	61 28 42.70	F6-F7	F7V	0.8	0	13.83	13.56	13.32	12.83
2012	1203_2_247	2 31 50.22	61 35 59.90		F9V	2.8	1	16.39	15.82	15.15	14.62
2012	0216_3	2 31 50.58	61 57 32.61	A0-F0	A5V	3.8	1	...	18.41	17.73	...
2012	1204_270	2 31 50.73	61 33 32.34		F9V	2.5	1	16.58	16.02	15.41	14.88
2012	1204_193	2 31 50.81	61 24 03.26	F6-F7	F7V	2.1	1	15.37	14.88	14.38	14.24
2012	1106_2_229	2 31 50.84	61 14 57.80	K6-K7	K6V	1.8	1	18.27	17.51	16.67	16.07
2012	0304_247	2 31 50.91	61 39 45.50	A1-A2	A2V	1.9	1	14.58	14.42	14.18	13.70
2012	1106_3_104	2 31 51.06	62 03 23.80	K2-K5	K4V[g]	3.8	1	...	15.22	14.09	...
2012	0124_195	2 31 51.35	61 31 24.31	F3-F5	F5V	1.1	0	12.77	12.59	12.34	12.15
2012	1203_1_209	2 31 51.49	61 46 48.66	G0-G3	G1V	2.1	1	15.95	15.47	14.92	14.39
2012	0124_207	2 31 51.49	61 32 28.91	G9-K1	G9V	3.0	1	16.46	15.70	14.88	14.56
2012	1203_1_110	2 31 51.59	61 05 43.34	F8-F9	F9V	2.7	1	...	15.42	14.76	...
2012	1105_2_215*	2 31 51.69	61 41 01.20	B9-A0	B9V	2.6	1	14.81	14.60	14.31	13.84
2012	1204_187	2 31 51.87	61 21 28.85	F2-F3	F2V	2.1	1	16.12	15.78	15.34	14.91
2012	1104_29	2 31 51.90	61 26 21.73	F9-G0	F9V	1.2	0	15.32	14.99	14.65	14.33
2012	0220_299	2 31 52.21	61 39 33.20	F4-F6	F5V	2.1	1	16.42	16.02	15.54	15.00
2012	1106_1_212	2 31 52.32	61 48 41.00	G5-G8	G7V	2.9	1	18.05	17.32	16.57	15.94
2012	1106_3_213	2 31 52.38	61 44 14.00	A6-A8	A7V	2.0	1	16.78	16.69	16.37	15.30
2011	1023_65	2 31 52.58	61 51 03.80		F8V	1.1	0	15.02	14.73	14.43	13.76
2012	1105_5_84	2 31 52.69	62 24 45.70	G9-K1	K0V	1.5	0	14.68	14.20	13.71	13.10
2012	1105_3_237	2 31 52.81	61 41 09.51	A7-A8	A8V	1.8	1	13.47	13.44	13.12	12.60
2012	1106_2_228	2 31 52.87	61 09 29.81	F1-F3	F2V	3.0	1	16.71	16.22	15.59	14.99
2011	0923_15	2 31 53.05	61 00 46.53		F4V	2.2	1	15.09	15.12	14.63	14.38
2011	1023_288	2 31 53.57	61 12 17.40	F8-G0	F9V	0.4	0	13.72	13.33	13.17	12.65

Table 1. IC 1805 Spectral Types and Photometry (Continued)

Year	Date_No.[a] (MMDD_No.)	RA(J2000) (hhmmss.ss)	Dec(J2000) (° ′ ″)	SpTy Range	SpTy	A_V (r-i) (mag)	Assoc.?[b] (ext)	V(90P)[c] (mag)	r[d] (mag)	i[d] (mag)	I(90P)[c] (mag)
2012	1203_2_143	2 31 53.61	61 04 14.66		F8V	2.1	1	15.63	15.52	15.01	14.41
2011	1023_284	2 31 53.73	60 59 28.88		K2V	4.8	0	...	14.43	13.20	...
2012	1203_2_297	2 31 53.78	61 38 46.31	F4-F5	F4V	2.5	1	16.52	16.06	15.51	14.90
2011	0923_214*	2 31 53.84	61 31 50.43	A0-A1	A1V	2.7	1	15.94	15.68	15.30	14.82
2012	1106_2_96	2 31 53.93	61 48 06.00	F2-F3	F3V	3.1	1	16.87	16.32	15.66	15.08
2012	1106_3_102	2 31 54.00	62 14 23.59	K3-K5	K4V	1.2	0	...	17.37	16.79	...
2012	1203_1_275	2 31 54.06	61 30 13.18	G5-G7	G6V	1.2	0	15.89	15.53	15.14	14.72
2012	1105_2_224	2 31 54.22	61 39 34.81	K0-K3	K2V	3.6	1	16.42	15.49	14.51	13.76
2012	1203_1_202	2 31 54.40	61 41 29.71	G8-G9	G9V	1.2	0	16.05	15.67	15.25	14.75
2011	0923_83	2 31 54.60	61 15 32.94	B7-A0	A0V	2.6	1	14.77	14.12	13.79	14.10
2012	1106_3_217	2 31 54.66	61 47 43.60	G0-G4	G3V	4.9	0	18.40	17.32	16.15	15.36
2012	1104_175	2 31 54.86	61 52 36.50	G8-K0	G9V	0.9	0	15.77	15.40	15.04	14.98
2012	1203_1_177	2 31 55.15	61 31 22.95	K0-K2	K1V	2.9	1	18.05	17.29	16.48	15.88
2012	1203_2_205	2 31 55.23	61 27 53.30	B3-B5	B4V	4.0	1	16.67	16.27	15.75	15.21
2012	1203_2_278	2 31 55.30	61 11 45.57	F8-F9	F8V	2.0	1	16.02	15.58	15.08	14.84
2012	1105_4_252	2 31 55.32	62 20 37.20	G8-G9	G9V[g]	2.3	1	14.86	14.62	13.96	13.01
2012	1105_4_72	2 31 55.57	62 04 55.00	G9-K2	K0V[g]	3.1	1	15.22	14.33	13.49	12.89
2012	1203_2_260	2 31 55.67	61 49 38.57		F9V	1.8	1	...	15.78	15.32	...
2012	1105_2_219	2 31 55.72	61 49 59.41	G0-G7	G3V	0.4	0	15.31	14.06	13.85	13.78
2012	1106_3_110	2 31 55.72	62 02 28.60	A9-F3	F2V	2.1	1	...	17.03	16.58	...
2012	1106_3_211	2 31 55.89	61 31 04.39	G0-G7	G4V	2.9	1	18.39	17.74	17.00	16.37
2012	1204_178	2 31 55.95	61 12 06.84	B9-A0	B9.5V	3.1	1	16.06	15.74	15.32	14.96
2012	1105_5_86	2 31 56.10	62 24 38.90	G5-K0	G8V	1.0	0	15.49	15.51	15.14	14.40
2011	0923_60	2 31 56.21	61 22 24.99	B6-B8	B7V	2.7	1	14.66	14.25	13.97	14.12
2011	1023_198	2 31 56.27	61 21 14.37	G1-G2	G1V	1.6	0	...	15.89	15.45	...
2012	1104_156	2 31 56.34	61 40 50.88	F1-F3	F2V	1.8	1	14.43	14.13	13.76	13.22
2012	1106_2_226	2 31 56.38	61 08 41.80	F6-F8	F7V	3.2	1	18.43	17.86	17.10	16.46
2012	0124_269	2 31 56.51	62 01 25.90	G0-G4	K2V	3.7	1	15.51	14.82	13.81	13.02
2012	0216_31	2 31 56.52	61 43 36.90	K6-M1	K8V	2.2	1	19.70	18.80	17.75	17.13
2012	1106_1_155	2 31 56.64	61 23 01.39	A7-A8	A7V	2.7	1	17.15	16.78	16.32	15.79
2012	0304_233	2 31 56.74	61 38 30.21	A3-A7	A5V	2.4	1	16.45	16.18	15.81	15.31
2012	1204_198	2 31 56.78	61 23 41.10	F4-F5	F4V	2.1	1	16.38	16.00	15.54	15.04
2012	1203_2_231	2 31 56.92	61 32 35.86	K4-K5	K4V	2.3	1	19.44	18.57	17.75	17.05
2012	1105_5_88	2 31 56.99	62 27 42.00	F6-F7	F6V	1.2	0	15.82	15.80	15.48	14.79
2012	1105_4_149	2 31 57.06	62 00 39.50	G8-K0	G9V	1.7	1	13.40	13.46	12.92	12.33
2012	1105_2_220*	2 31 57.89	61 58 21.40	B9-A0	B9V	3.3	1	15.67	15.58	15.14	14.36
2011	0923_89	2 31 57.99	61 19 44.90		A5V	2.1	1	15.75	15.50	15.17	14.74
2012	0304_232	2 31 58.00	61 36 52.40	F9-G1	G0V	...	...	16.50	...	...	15.09
2012	1104_276	2 31 58.06	61 39 04.75		F8V	3.2	1	15.60	14.94	14.19	13.56
2012	1105_4_135	2 31 58.15	61 56 14.51	G1-G7	G6V	0.7	0	14.19	14.29	14.00	13.32
2011	0923_20	2 31 58.18	61 21 29.75	A8-F0	A9V	1.3	0	12.67	11.25	11.05	12.03
2012	1106_3_106	2 31 58.19	62 09 07.50		F8V	2.2	1	...	17.68	17.15	...
2012	1106_2_13	2 31 58.45	61 41 53.30	M1-M2	M2V	0.5	0	17.80	17.07	16.04	15.37
2012	1106_3_107	2 31 58.49	62 02 10.00		K3V	1.1	0	...	17.36	16.88	...
2012	1105_3_241	2 31 58.53	61 45 56.70		A2V	2.7	1	15.59	15.27	14.86	14.37
2012	1106_2_98	2 31 58.54	61 44 59.30	F4-F8	F7V	2.6	1	17.87	17.38	16.76	15.94
2012	1203_2_145	2 31 58.61	61 06 12.27	F2-F4	F3V	3.2	1	...	17.23	16.53	...
2012	1106_1_231	2 31 58.78	62 08 03.50	F9-G2	G0V	1.8	1	...	17.49	17.00	...
2012	0304_48	2 31 58.83	62 04 02.19	G0-G2	G1V	1.3	0	14.20	14.08	13.71	12.97
2012	1204_32	2 31 58.88	61 38 12.23	G8-G9	G9V	1.1	0	16.11	15.73	15.33	14.82
2011	1023_12*	2 31 59.17	61 38 06.45	A0.5-A2	A1V	2.4	1	15.89	15.67	15.35	14.87
2012	0124_244	2 31 59.24	61 39 29.60	F1-F3	F3V	2.3	1	16.50	15.68	15.20	14.69
2012	1106_3_215	2 31 59.57	61 38 05.10	F9-G7	G4V	3.4	1	17.69	17.07	16.22	15.55
2012	0220_291	2 31 59.68	61 41 35.20	A6-A8	A7V	2.3	1	16.10	15.82	15.44	14.91
2012	0124_225	2 32 00.16	61 36 06.30	A1-A6	A2V	2.3	1	16.44	16.19	15.82	15.33
2012	1105_2_19	2 32 00.39	61 04 17.40		A1V	3.1	1	15.75	16.09	15.64	14.99
2011	1023_286	2 32 00.46	61 14 53.24	F6-F7	F6V	1.7	1	14.83	14.48	14.06	13.58
2012	1203_1_203	2 32 00.56	61 48 46.02	G7-K0	G9V	1.0	0	15.97	15.58	15.20	14.68
2012	0220_265	2 32 00.56	61 50 49.30	G9-K0	K0V	2.1	1	13.99	13.54	12.92	12.24
2012	1203_2_274	2 32 00.58	61 12 58.24	F4-F5	F4V	3.0	1	15.89	15.43	14.77	14.24
2012	1204_31	2 32 00.62	61 49 19.61		K7V	1.4	0	18.15	17.44	16.63	16.03
2012	0216_44	2 32 01.12	61 44 20.39	M2-M3	M3V	0.6	0	19.80	19.10	17.87	17.19
2011	1023_181	2 32 01.13	61 09 17.70	A3-A4	A3V	2.2	1	13.15	13.12	12.81	12.36
2012	1105_4_159	2 32 01.25	62 02 10.60	F0-F5	F3V	1.5	0	15.83	15.76	15.44	14.74
2012	0220_243*	2 32 01.32	61 38 15.10	B7-B9	B8V	2.4	1	14.49	14.34	14.11	13.65
2012	1105_4_256	2 32 01.54	62 25 06.71	F6-F7	F7V	1.2	0	15.25	15.25	14.94	14.23
2011	1023_14*	2 32 01.54	61 32 06.70	A9-F0	F0V	2.2	1	15.32	14.94	14.53	14.47
2011	0923_223	2 32 01.90	61 26 48.90	F8-F9	F9V	0.7	0	12.77	12.68	12.44	12.16
2012	1204_177	2 32 01.95	61 20 38.35	G7-G9	G8V	1.4	0	16.40	16.03	15.58	15.04
2011	0923_213	2 32 01.99	61 29 38.48	G4-G9	G5V	1.5	0	12.30	11.52	11.07	11.71
2012	1204_4	2 32 02.17	61 35 46.43	F4-F5	F4V	2.7	1	16.74	16.24	15.65	15.11
2012	1203_1_207	2 32 02.23	61 44 05.52	G5-G8	G6V	1.4	0	...	15.71	15.28	14.67
2012	1203_2_272	2 32 02.38	61 11 39.24	F4-F5	F4V	2.3	1	16.10	15.68	15.18	14.87
2012	1104_125	2 32 02.38	61 25 29.46	B9-A0	B9V	3.0	1	15.23	14.94	14.55	14.51
2011	0923_218	2 32 02.45	61 37 13.29	A9-F2	F0V	2.5	1	15.73	15.33	14.86	14.52
2012	1106_2_224	2 32 02.46	61 15 21.70	F5-F8	F7V	3.2	1	18.27	17.66	16.92	16.27
2012	1106_3_220	2 32 02.85	61 44 34.40	F6-F8	F7V	2.7	1	17.64	17.11	16.47	15.82
2012	1106_3_112	2 32 02.94	61 57 36.79	G7-K0	G9V	1.9	1	...	17.62	17.05	...
2012	0124_177	2 32 03.04	61 26 48.91	F6-F9	F8V	...	...	16.38	...	...	14.78
2012	1203_2_254	2 32 03.10	61 36 34.52	G9-K0	G9V	1.1	0	15.38	14.91	14.51	14.34
2012	1203_2_158	2 32 03.25	61 20 37.03	F4-F5	F4V	2.1	1	15.71	15.35	14.88	14.55
2012	1105_4_260	2 32 03.26	62 11 19.81	A9-F2	F0V	1.4	0	14.37	14.53	14.29	13.50
2012	1203_1_109	2 32 03.33	61 13 14.00	A6-A8	A7V	2.2	1	15.85	15.56	15.18	14.83
2012	1203_1_191	2 32 03.42	61 37 51.79	G8-K0	G9V	2.4	1	17.44	16.74	16.06	15.46
2012	1203_2_245*	2 32 03.59	61 33 11.31	A8-A9	A9V	2.3	1	15.64	15.35	14.94	14.61
2012	1106_3_108	2 32 03.65	62 12 59.00	F0-F5	F3V	2.3	1	...	17.12	16.62	...
2012	1105_4_255	2 32 03.76	62 07 37.31	A7-F0	A9V	2.2	1	15.51	15.29	14.89	14.32

Table 1. IC 1805 Spectral Types and Photometry (Continued)

Year	Date_No.[a] (MMDD_No.)	RA(J2000) (hhmmss.ss)	Dec(J2000) (° ′ ″)	SpTy Range	SpTy	A_V (r-i) (mag)	Assoc.?[b] (ext)	V(90P)[c] (mag)	r[d] (mag)	i[d] (mag)	I(90P)[c] (mag)
2012	1104_115	2 32 03.81	61 17 19.32	G2-G8	G5V	3.1	1	16.34	15.55	14.75	14.42
2012	1105_3_240	2 32 03.89	61 40 43.61	G5-G7	G6V[g]	3.0	1	16.12	15.47	14.69	14.05
2012	1203_1_26	2 32 03.98	61 17 33.70	K4-K6	K5V	2.1	1	18.90	18.07	17.28	16.65
2012	1204_277	2 32 04.05	61 04 07.07	G8-K2	G9V	3.4	1	...	18.62	17.72	...
2012	1105_4_258	2 32 04.07	62 19 59.60	F4-F6	F4V	1.0	0	14.12	13.85	13.62	13.15
2012	1106_3_28	2 32 04.36	62 00 01.50	G2-G7	G5V	1.5	0	...	16.72	16.26	...
2012	1105_2_230	2 32 04.60	61 41 31.21	G9-K1	K0V	2.9	1	16.49	15.77	14.97	14.31
2012	1203_2_257	2 32 04.82	61 48 51.80	F6-F7	F6V	2.0	1	16.51	16.07	15.59	15.07
2012	1105_5_89	2 32 04.99	62 24 45.10	G8-K2	G8V	1.9	1	14.83	14.54	13.97	13.14
2011	1023_183	2 32 05.13	61 11 55.21	B9-A0	A0V	2.7	1	15.74	15.52	15.18	14.87
2012	1204_263	2 32 05.15	61 33 53.02	F4-F5	F5V	2.5	1	17.29	16.78	16.21	15.65
2012	0124_265	2 32 05.26	62 02 37.30	F4-F6	F4V	1.5	0	13.03	13.08	12.75	12.30
2012	1204_179	2 32 05.26	61 20 24.89	G7-G8	G7V[g]	2.9	1	16.71	16.06	15.30	14.64
2012	1105_4_253	2 32 05.71	62 06 33.70	K4-K5	K4V[g]	2.2	1	13.05	12.46	11.68	11.85
2012	1204_33	2 32 05.86	61 43 56.76		F8V	1.9	1	15.76	15.59	15.11	14.55
2012	1106_2_222	2 32 06.28	61 04 37.01	A1-A3	A2V	3.2	1	...	16.83	16.33	...
2011	1023_16	2 32 06.33	61 32 51.90		B9V	2.6	1	15.05	14.84	14.53	14.11
2012	1204_241	2 32 06.36	61 28 43.25		F8V	1.9	1	15.53	15.11	14.65	14.50
2012	1106_3_285	2 32 06.43	61 48 19.80	G5-G8	G7V	1.7	1	17.37	16.73	16.21	15.66
2012	1203_1_23	2 32 06.44	61 24 57.86	K5-K6	K6V	2.0	1	18.89	18.23	17.35	16.68
2012	1105_2_5*	2 32 06.51	61 29 54.40	B2-B3	B2V	3.8	1	13.94	13.71	13.27	12.73
2012	1203_1_288	2 32 06.99	61 32 42.90	K6-M0	K8V	4.6	0	18.53	18.14	16.58	16.02
2012	1106_2_99	2 32 07.04	61 45 34.00	F9-G4	G2V	2.9	1	16.76	16.10	15.36	14.68
2012	1105_4_134	2 32 07.09	61 53 34.60	G0-G6	G2V	1.3	0	14.72	14.73	14.34	13.52
2012	1106_3_103	2 32 07.17	62 05 19.19	A5-A8	A7V	3.1	1	...	16.89	16.33	...
2012	1105_3_295	2 32 07.19	61 45 44.30	G8-K0	G9V	3.2	1	16.06	15.24	14.40	13.76
2012	1203_1_106	2 32 07.29	61 09 18.24	A0-A1	A0V	3.2	1	16.17	15.84	15.38	14.92
2012	1203_2_259	2 32 07.33	61 42 36.77	G6-G7	G6V	1.6	1	15.90	15.50	15.02	14.44
2012	1106_2_219	2 32 07.51	61 24 10.59	K4-K5	K4V	1.2	0	16.94	16.33	15.75	15.10
2012	0124_283	2 32 07.60	61 33 08.40	K0-K2	K1V	2.6	1	14.71	14.04	13.29	12.72
2012	1105_2_217	2 32 07.90	61 56 42.60	G8-K1	K0V	3.5	1	15.30	14.65	13.72	12.74
2012	1203_2_151	2 32 07.91	61 24 51.39	F4-F5	F5V	3.2	1	16.08	15.69	14.98	14.52
2012	1203_1_114	2 32 08.02	61 22 03.59	K4-K5	K4V	0.9	0	16.02	15.26	14.76	14.61
2012	1105_4_23	2 32 08.11	61 58 37.70	F9-G5	G1V	0.9	0	14.52	14.57	14.27	13.49
2012	1204_275	2 32 08.17	61 10 21.72	A9-F0	F0V	2.8	1	16.69	16.30	15.75	15.16
2012	1105_4_124	2 32 08.20	62 00 32.09	B7-A0	B8V	3.4	1	14.76	14.69	14.24	13.57
2012	0304_219	2 32 08.25	61 33 20.10	F8-G0	F9V	2.0	1	...	17.23	16.71	...
2012	1204_279	2 32 08.36	61 05 13.47	B4-B7	B4V	4.1	1	...	16.38	15.83	...
2011	1023_185	2 32 08.38	61 08 59.80	F3-F8	F7V	1.7	1	14.82	14.47	14.05	13.53
2012	1105_5_87	2 32 08.51	62 24 16.50	K3-K5	K4V[g]	1.5	0	13.96	13.54	12.90	11.95
2012	1106_1_223	2 32 08.71	61 54 20.70	G1-G7	G6V	1.8	1	16.99	16.59	16.06	15.45
2012	1106_2_100	2 32 08.75	61 33 01.91	K5-K6	K6V	1.9	1	18.16	18.34	17.49	16.35
2012	1106_3_116	2 32 08.80	61 56 22.50	G6-K1	G9V	1.7	1	18.32	17.89	17.35	16.75
2011	0923_221	2 32 09.06	61 26 30.20	A8-A9	A9V	2.0	1	13.19	13.11	12.76	12.38
2012	1204_208	2 32 09.22	61 26 55.31	G9-K0	G9V	2.4	1	16.33	15.70	15.02	14.58
2012	1203_2_256	2 32 09.23	61 35 33.59	B9-A0	A0V	2.7	1	15.53	15.24	14.87	14.52
2012	1105_4_257	2 32 09.32	62 16 23.80	F4-F7	F6V	1.1	0	14.44	14.54	14.26	13.58
2012	1106_1_229	2 32 09.33	61 52 58.70	G9-K2	K1V	3.4	1	16.94	16.21	15.29	14.59
2012	1106_3_216	2 32 09.35	61 45 23.40	K0-K3	K2V	2.0	1	17.82	17.24	16.60	15.99
2012	1203_2_149	2 32 09.40	61 06 16.83	A9-F0	A9V	2.9	1	...	16.06	15.50	...
2012	1105_4_79	2 32 09.44	62 04 32.50	A9-F0	F0V	1.7	1	15.43	15.48	15.17	14.63
2012	0124_153	2 32 09.73	61 04 43.20	B8-B9	B9V	3.4	1	15.57	15.39	14.93	14.50
2012	1104_117	2 32 10.07	61 17 20.40	B8-A0	B9V	3.2	1	16.48	16.13	15.71	15.12
2012	1106_2_218	2 32 10.15	61 25 39.50	G0-G4	G2V	3.8	1	18.28	17.52	16.58	15.89
2012	1106_2_97	2 32 10.84	61 46 19.71	G4-G6	G5V	3.1	1	17.88	17.16	16.37	15.71
2012	1203_1_187	2 32 11.12	61 31 02.88	B9-A0	A0V	2.4	1	15.11	14.86	14.57	14.25
2012	1104_284	2 32 11.15	61 59 13.60	F9-G3	G1V	0.8	0	14.25	13.99	13.70	13.14
2012	1104_189	2 32 11.17	61 55 32.90	K0-K2	K1V	0.9	0	15.76	15.39	15.01	14.50
2012	0220_293*	2 32 11.26	61 39 48.90	F3-F4	F4V	2.4	1	15.36	14.95	14.42	14.02
2011	0923_88	2 32 11.28	61 12 13.85		F6V	1.4	0	14.17	13.93	13.58	13.06
2012	1105_2_294	2 32 11.29	61 39 37.40	K1-K3	K2V[g]	3.8	1	14.96	14.05	13.02	12.41
2012	0216_9	2 32 11.37	61 44 26.70	M1-M3	M2V	0.8	0	18.93	18.37	17.27	16.43
2012	1106_3_22	2 32 11.42	62 05 49.81	A9-F3	F1V	2.1	1	...	16.89	16.47	...
2011	1023_173	2 32 11.45	61 21 45.20	B0-B2	B1V	5.1	0	12.19	11.18	10.52	11.53
2012	0304_47	2 32 11.64	62 04 01.60		F8V	1.1	0	15.41	14.94	14.62	14.10
2012	0304_42	2 32 11.65	61 55 05.50		F7V	2.2	1	16.29	15.93	15.41	14.85
2012	1105_5_85	2 32 11.69	62 22 10.71	G3-G7	G5V	1.0	0	14.73	14.64	14.29	13.54
2012	1106_2_93	2 32 11.71	61 39 00.01	G3-G7	G6V	2.0	1	17.96	17.51	16.94	16.36
2012	1106_2_105	2 32 11.78	61 32 00.00	G5-G9	G7V	3.5	1	17.38	16.58	15.69	14.99
2012	1104_174	2 32 11.79	61 48 12.96		F3V	2.4	1	15.70	15.31	14.81	14.23
2012	1106_3_219	2 32 11.82	61 32 22.00	G1-G4	G2V	3.4	1	17.78	17.06	16.22	15.45
2012	1106_2_217	2 32 11.88	61 11 58.60	F5-F7	F6V	2.4	1	17.24	17.00	16.44	15.53
2012	1106_2_108	2 32 11.98	61 33 44.79	K4-K5	K4V	1.1	0	16.77	16.12	15.55	15.06
2012	0124_192	2 32 12.03	61 31 48.20	F3-F5	F3V	2.2	1	16.29	15.92	15.46	14.90
2012	0124_294	2 32 12.16	61 36 17.39		A2V	2.2	1	15.65	15.43	15.13	14.73
2012	1106_1_234	2 32 12.17	61 58 58.50	K6-K7	K7V	1.0	0	18.27	17.49	16.75	16.13
2012	1106_2_95	2 32 12.25	61 58 33.40	K2-K5	K4V[g]	4.5	0	17.88	16.84	15.57	14.77
2012	1106_1_213	2 32 12.28	61 50 45.40	G8-K2	K0V[g]	3.6	1	17.31	16.60	15.64	14.96
2012	1106_2_103	2 32 12.46	61 30 51.80	G4-G8	G6V	3.4	1	17.11	16.29	15.43	14.74
2012	1104_152	2 32 12.65	61 39 59.54	K4-M0	K7V	0.3	0	15.87	15.26	14.69	14.15
2012	1106_2_216	2 32 12.66	61 26 35.20	F7-F8	F8V	2.1	1	16.70	16.26	15.74	15.22
2012	0220_6	2 32 12.69	61 54 26.70	A0-A1	A0V	2.2	1	14.03	13.91	13.66	13.09
2012	0220_193	2 32 13.12	61 12 23.80	F6-F8	F7V	2.0	1	16.46	16.08	15.60	15.12
2012	0220_295	2 32 13.39	61 39 18.11		F8V	1.3	0	15.20	14.91	14.57	14.18
2012	1203_1_289	2 32 13.49	61 47 53.23	A9-F0	F0V	2.5	1	16.00	15.62	15.14	14.65
2012	1106_3_114	2 32 13.52	61 59 29.99	A9-F7	F6V	2.6	1	18.04	17.52	16.92	16.35
2011	0923_224	2 32 13.57	61 33 24.10	F7-F8.5	F8V	1.6	1	15.92	15.57	15.16	14.75

Table 1. IC 1805 Spectral Types and Photometry (Continued)

Year	Date_No.[a] (MMDD_No.)	RA(J2000) (hhmmss.ss)	Dec(J2000) (° ′ ″)	SpTy Range	SpTy	A_V (r-i) (mag)	Assoc.?[b] (ext)	V(90P)[c] (mag)	r[d] (mag)	i[d] (mag)	I(90P)[c] (mag)
2012	1203_1_151	2 32 13.71	61 28 03.02	G9-K3	K0V	2.8	1	19.23	18.48	17.70	17.04
2012	1105_2_87	2 32 13.81	61 10 16.31	B8-B9	B8V	3.1	1	15.46	15.17	14.80	14.51
2012	0220_10	2 32 13.88	61 55 32.50	G0-G3	G2V	1.9	1	16.09	15.65	15.11	14.53
2012	1203_2_262	2 32 13.93	61 45 51.47	F7-F8	F7V	2.6	1	17.56	17.06	16.44	15.83
2012	0304_212	2 32 13.95	61 31 45.89	A5-A6	A5V	2.1	1	15.98	15.75	15.43	14.90
2011	0923_51	2 32 13.98	61 19 41.11		F5V	0.7	0	13.63	13.34	13.17	12.58
2012	0220_4	2 32 14.02	61 51 49.41	G8-K0	G9V	1.0	0	16.08	15.71	15.32	14.79
2012	1106_1_294	2 32 14.07	61 54 15.89	G6-K0	G8V	3.4	1	17.67	16.94	16.07	15.35
2012	1105_4_3	2 32 14.09	62 05 28.70	F3-F5	F4V	1.9	1	15.27	15.21	14.79	14.23
2011	0923_87	2 32 14.09	61 03 38.70		A0V	2.9	1	15.82	15.96	15.57	14.99
2012	1105_2_213	2 32 14.17	61 55 24.50	F5-F7	F6V	2.1	1	16.31	15.94	15.44	14.86
2012	0124_263	2 32 14.47	61 59 42.00	A2-A4	A3V	1.4	0	14.08	13.97	13.85	13.29
2011	1023_189	2 32 14.69	61 09 14.70	A0-A3	A1V	2.2	1	13.33	13.26	12.99	12.62
2012	1106_3_208	2 32 14.73	61 49 04.41	G5-G8	G7V	3.7	1	17.98	17.23	16.30	15.64
2012	0124_164	2 32 14.75	61 17 04.30	G9-K1	K0V	2.7	1	16.17	15.46	14.71	14.60
2011	0923_54	2 32 14.76	61 21 35.23	B7-B8	B8V	3.3	1	14.81	14.47	14.05	13.49
2012	1106_2_127	2 32 14.85	61 30 04.20	F3-F6	F5V	3.1	1	17.71	17.11	16.43	15.79
2012	1105_4_25	2 32 14.88	61 54 19.70	K3-K5	K4V^g	3.1	1	14.85	13.91	12.94	12.34
2012	1105_5_83	2 32 14.92	62 17 15.81	F6-F7	F7V	1.1	0	15.30	15.22	14.92	14.21
2012	1105_4_259	2 32 14.92	62 24 31.70	A6-A8	A7V	1.6	1	15.70	15.55	15.31	14.79
2012	0216_195	2 32 15.00	61 28 25.60	M2-M3	M2V	2.2	1	...	19.26	17.86	...
2012	1105_4_4	2 32 15.04	62 07 21.80	G8-K1	K0V	1.6	1	14.38	13.91	13.38	12.58
2011	0923_72	2 32 15.07	61 16 47.98	G2-G3	G2V	1.8	1	13.35	13.40	12.89	12.29
2012	0304_185	2 32 15.08	61 12 44.50	F4-F5	F5V	2.1	1	16.21	15.85	15.38	14.96
2012	1106_2_102	2 32 15.15	61 40 07.81	F3-F5	F4V	2.7	1	17.13	16.65	16.07	15.50
2011	1023_82	2 32 15.38	61 29 41.80		F0V	2.0	1	15.98	15.67	15.30	14.88
2012	1104_173	2 32 15.43	61 51 23.44		A1V	1.9	1	14.62	14.49	14.29	13.79
2012	1105_2_233*	2 32 15.43	61 36 40.20	F4-F5	F5V	2.3	1	15.05	15.44	14.92	14.52
2012	0304_50*	2 32 15.48	62 00 00.49	B7-B8	B8V	1.9	1	13.92	13.83	13.71	13.22
2012	1105_2_73	2 32 15.65	61 19 14.10	B7-B9	B8V	2.7	1	15.40	15.20	14.90	14.63
2012	1203_1_93	2 32 15.85	61 09 12.97	G9-K1	G9V	2.3	1	16.26	15.95	15.29	14.66
2011	1023_187	2 32 15.91	61 00 46.43	B2-B5	B3V	3.5	1	15.52	15.64	15.22	14.66
2012	1204_273	2 32 15.92	61 19 09.86	G8-K0	G9V	2.9	1	16.64	15.99	15.20	14.64
2012	1203_1_194	2 32 15.94	61 32 11.18	F2-F5	F3V	2.5	1	15.51	15.05	14.52	14.36
2012	1203_2_264	2 32 16.14	61 41 01.73		F4V	2.3	1	16.36	15.94	15.42	14.91
2012	1106_2_207	2 32 16.16	61 28 27.00	G8-K2	K0V^g	2.9	1	18.21	17.47	16.67	15.61
2012	1105_3_269	2 32 16.29	61 55 15.19	A7-A8	A8V	2.2	1	15.06	14.82	14.43	13.84
2012	1203_1_197	2 32 16.29	61 33 11.78		F8V	5.2	0	...	16.11	14.93	...
2012	1106_3_109	2 32 16.32	62 17 09.30	A9-F3	F2V	1.5	0	...	16.53	16.22	...
2012	1204_48	2 32 16.34	61 49 14.99	G8-K0	G9V	1.8	1	17.07	16.61	16.06	15.50
2012	1106_3_30	2 32 16.36	62 03 17.21	G0-G5	G3V	1.5	0	...	17.24	16.79	...
2012	0124_268	2 32 16.46	61 47 39.70	G8-K0	G8V	1.1	0	16.10	15.75	15.36	14.90
2012	1106_1_239	2 32 16.46	62 00 08.50	G7-K1	K0V	2.8	1	17.79	17.56	16.78	15.85
2012	1106_2_214	2 32 16.59	61 25 49.80	G9-K2	K2V	1.9	1	17.11	16.52	15.90	15.32
2012	1204_42	2 32 16.81	61 37 54.79		G8V	2.3	1	16.52	15.93	15.29	14.70
2012	1106_3_138	2 32 16.85	61 56 26.49	F9-G3	G2V	1.9	1	17.34	16.92	16.39	15.79
2011	1023_18	2 32 16.87	61 44 09.67	F1-F5	F2V	3.0	1	14.52	18.24	17.61	16.99
2012	1106_1_225	2 32 16.92	61 52 42.61	G7-G9	G8V	3.7	1	18.14	17.41	16.48	15.78
2012	1105_3_253	2 32 17.09	61 51 29.60	A3-A5	A3V	2.2	1	16.14	15.94	15.65	15.12
2012	1203_1_103	2 32 17.19	61 20 39.11	K0-K5	K3V	3.2	1	18.28	17.49	16.55	15.74
2012	0304_33	2 32 17.51	61 51 34.70	F6-F7	F6V	2.1	1	16.05	15.65	15.15	14.58
2012	1106_3_186	2 32 17.53	61 52 24.00	G4-G7	G5V	2.0	1	16.90	16.43	15.87	15.30
2011	1023_76	2 32 17.59	61 35 14.33		A7V	2.3	1	13.92	15.99	15.60	14.88
2012	1203_1_146	2 32 18.01	61 26 51.41	G0-K3	G9V	3.5	1	19.10	18.41	17.49	16.82
2012	1104_183	2 32 18.16	61 56 40.50		K6V^g	4.1	1	15.23	14.25	12.94	12.27
2012	1105_5_81	2 32 18.26	62 23 46.40	G7-K0	G8V	2.6	1	15.81	15.54	14.84	13.97
2011	1023_13	2 32 18.38	61 27 52.74		B2V	2.3	1	12.33	11.19	11.06	12.08
2012	1105_3_198	2 32 18.60	61 18 46.40		F7V	2.2	1	16.20	15.76	15.23	14.71
2012	1105_5_17	2 32 18.68	62 08 13.70	B3-B4	B3V	3.0	1	14.17	14.04	13.73	12.93
2012	1203_2_258	2 32 18.71	61 31 18.06	K4-K5	K4V	2.1	1	18.49	17.71	16.94	16.11
2012	1204_40	2 32 18.78	61 33 01.00		F4V	1.6	1	14.87	14.93	14.57	13.55
2012	0220_208	2 32 18.90	61 16 29.20		F3V	2.3	1	16.29	15.89	15.39	14.97
2012	1106_2_220	2 32 18.94	61 10 55.20	K1-K3	K2V	1.9	1	18.16	17.56	16.93	16.32
2012	1105_4_45	2 32 18.95	62 06 17.60	K3-K5	K4V^g	3.3	1	15.29	14.19	13.17	12.65
2012	1104_138	2 32 19.03	61 32 50.46	F8-F9	F8V	1.2	0	13.74	13.32	12.99	12.53
2012	1106_2_191	2 32 19.08	61 28 40.90	F0-F3	F2V	2.4	1	17.55	17.24	16.73	15.91
2012	1105_3_263	2 32 19.16	61 56 43.30	F5-F6	F5V	2.3	1	16.21	16.01	15.48	14.72
2012	1106_3_287	2 32 19.17	61 45 42.30	G0-G3	G2V	3.5	1	18.05	17.34	16.47	15.77
2012	1106_2_26	2 32 19.50	61 32 35.20	F9-G7	G6V	1.9	1	17.32	16.84	16.29	15.67
2012	0304_8	2 32 19.55	61 46 49.30	F6-F7	F6V	1.3	0	14.61	14.35	14.01	13.54
2012	0216_189	2 32 19.58	61 09 23.70	M2-M4	M3V	1.7	1	20.38	19.77	18.30	17.35
2011	0923_82	2 32 19.67	61 09 30.24		A7V	2.1	1	15.00	14.62	14.27	14.36
2012	1204_49	2 32 19.80	61 40 41.31		A1V	2.3	1	15.33	15.13	14.84	14.37
2012	1204_38	2 32 20.00	61 31 10.26		F9V	1.6	1	15.38	14.98	14.57	14.48
2012	0304_195	2 32 20.06	61 27 55.40	G8-G9	G9V	2.0	1	15.19	15.24	14.64	14.08
2012	1106_1_238	2 32 20.22	61 58 54.80		A1V	3.3	1	16.81	16.45	15.95	15.32
2012	0220_199	2 32 20.30	61 09 37.90	K2-K3	K3V	4.5	0	16.19	15.07	13.86	13.79
2012	1104_286	2 32 20.38	61 59 27.10	F6-F9	F8V	2.3	1	15.87	15.43	14.86	14.26
2012	1105_5_92	2 32 20.45	62 06 25.30	G8-K2	K0V	1.3	0	13.27	13.02	12.55	12.08
2012	1203_2_266	2 32 20.58	61 45 28.03	F2-F3	F3V	2.0	1	15.08	14.78	14.35	13.79
2012	0304_257	2 32 20.61	61 41 46.90	B9-A0	A0V	2.7	1	16.03	15.78	15.43	14.96
2012	1203_2_146	2 32 20.65	61 05 40.21	G7-G8	G8V	1.4	0	...	15.46	15.00	...
2012	0304_238	2 32 20.69	61 37 25.61	F6-F7	F7V	1.6	1	16.32	15.98	15.58	15.08
2012	1106_1_300	2 32 20.90	61 55 41.30	K3-K5	K4V^g	2.6	1	16.85	16.09	15.21	14.57
2012	0304_43	2 32 20.93	62 01 49.20	G8-K0	G9V	0.4	0	14.28	13.98	13.73	12.88
2012	1203_1_274	2 32 20.94	61 27 19.24	G4-K0	G7V	2.5	1	...	16.28	15.60	...
2012	1203_2_133	2 32 20.95	61 23 34.00	F6-F7	F6V	2.4	1	16.11	15.67	15.10	14.63

Table 1. IC 1805 Spectral Types and Photometry (Continued)

Year	Date_No.[a] (MMDD_No.)	RA(J2000) (hhmmss.ss)	Dec(J2000) (° ′ ″)	SpTy Range	SpTy	A_V (r-i) (mag)	Assoc.?[b] (ext)	V(90P)[c] (mag)	r[d] (mag)	i[d] (mag)	I(90P)[c] (mag)
2012	1106_3_156	2 32 21.02	61 55 26.40	G0-G7	G3V	2.2	1	16.59	16.11	15.51	14.96
2012	1203_1_287	2 32 21.13	61 43 13.58	F0-F3	F2V	2.3	1	15.22	14.81	14.33	13.79
2012	0220_285	2 32 21.25	61 21 55.20	G7-G9	G8V	3.8	1	16.40	15.55	14.59	14.54
2012	1204_161	2 32 21.32	61 21 00.85	F6-F7	F7V	2.2	1	16.14	15.73	15.21	14.72
2012	1203_2_268	2 32 21.40	61 33 00.64	K6-K7	K7V	2.5	1	...	18.34	17.28	...
2012	1105_3_208	2 32 21.41	61 26 14.30	G9-K2	K1V[g]	2.8	1	15.95	15.26	14.46	14.35
2011	0923_237	2 32 21.49	61 28 19.64	B9-A0	A0V	1.5	1	13.82	13.78	13.67	13.17
2012	1106_1_170	2 32 21.56	61 32 37.00	G5-G8	G7V	2.6	1	16.69	16.08	15.39	14.82
2012	1105_2_46	2 32 21.92	61 30 07.40	G6-G8	G8V	1.3	0	16.18	15.75	15.32	14.86
2012	1105_2_89	2 32 21.95	61 09 23.30	A1-A2	A2V	2.8	1	16.25	15.94	15.53	15.05
2012	0216_54	2 32 22.22	61 45 20.50	K6-K8	K7V	3.0	1	19.67	18.96	17.79	17.05
2012	1204_163	2 32 22.26	61 10 46.90	A1-A2	A2V	2.8	1	16.10	15.79	15.36	14.90
2012	0304_231	2 32 22.29	61 38 43.90	A6-A8	A7V	1.8	1	14.59	14.18	13.90	13.78
2012	1105_4_263	2 32 22.30	62 10 16.90	F4-F6	F4V	1.3	0	14.08	13.99	13.69	13.01
2012	1105_4_262	2 32 22.33	62 17 23.70	K0-K2	K1V	2.1	1	15.87	15.20	14.56	13.90
2012	1105_4_6	2 32 22.41	62 08 10.40	K4-K5	K4V	1.0	0	15.93	15.61	15.08	14.27
2012	1106_2_287	2 32 22.41	61 23 26.40	F6-F7	F7V	2.6	1	17.86	17.34	16.72	16.12
2012	1106_3_118	2 32 22.44	61 59 34.10	F8-F9	F8V	2.1	1	17.10	16.65	16.13	15.57
2012	1105_4_269	2 32 22.58	62 11 57.00	G6-G9	G7V[g]	2.7	1	15.12	14.71	13.99	13.10
2012	1106_2_104	2 32 22.64	61 44 39.70	K3-K4	K3V	1.1	0	17.12	16.59	16.11	15.56
2011	1023_190	2 32 22.78	61 03 53.43	F9-G2	G0V	1.9	1	15.06	15.04	14.54	14.26
2012	1106_2_110	2 32 22.78	61 39 09.80	F9-G8	G6V	3.2	1	17.45	16.70	15.87	15.20
2012	1105_4_96	2 32 22.94	62 02 35.00	A1-A2	A1V	1.6	1	13.25	13.32	13.18	12.60
2012	0304_37	2 32 23.22	61 49 38.70	A7-A9	A8V	2.5	1	16.25	15.92	15.47	14.88
2012	1106_1_156	2 32 23.28	61 23 23.11	F9-G0	F9V	3.2	1	18.11	17.49	16.72	16.05
2012	0124_157	2 32 23.31	61 05 39.79	A3-A5	A4V	3.0	1	15.40	15.33	14.84	14.33
2012	1106_3_105	2 32 23.35	62 16 17.91	F4-F6	F6V	1.9	1	...	17.15	16.70	...
2011	1023_184	2 32 23.50	61 11 07.10	G1-G3	G2V	1.5	0	15.16	14.68	14.24	14.51
2012	1106_3_24	2 32 23.51	62 09 15.61	G7-K0	G9V	2.2	1	...	17.34	16.70	...
2012	1104_176	2 32 23.52	61 47 54.38		G9V	0.6	0	14.66	14.34	14.03	13.56
2011	0923_71	2 32 23.71	61 10 13.97		F0V	2.2	1	14.34	14.03	13.61	13.09
2012	0220_206	2 32 23.76	61 16 25.60	A1-A2	A1V	2.7	1	16.24	15.95	15.56	15.10
2012	0124_238	2 32 23.90	61 35 53.31		G4V	...	...	16.13	...	...	14.44
2012	0304_299	2 32 23.96	61 39 49.40	F4-F6	F5V	2.2	1	14.36	13.95	13.46	12.88
2012	1106_1_235	2 32 23.98	62 00 20.70	G7-K1	G9V[g]	3.1	1	17.78	17.03	16.20	15.48
2012	1105_5_13	2 32 24.17	62 12 06.40	F0-F3	F2V	1.4	0	14.77	14.78	14.49	13.80
2012	1105_2_222*	2 32 24.29	61 58 09.00	F6-F7	F6V	1.8	1	15.24	14.87	14.44	13.87
2012	0216_5	2 32 24.49	61 43 03.20	A8-F0	A9V	5.3	0	18.67	17.75	16.70	15.90
2012	1204_47	2 32 24.53	61 32 20.24		K2V	2.7	1	18.57	17.88	17.10	16.43
2012	1105_2_245	2 32 24.58	61 35 53.20	F2-F3	F2V	2.1	1	13.25	13.05	12.62	12.19
2012	1203_2_270	2 32 24.88	61 32 51.52	K2-K3	K2V	2.8	1	18.03	17.28	16.47	15.81
2012	1104_182	2 32 25.06	61 50 52.87		M0V	0.4	0	16.20	15.57	14.79	14.21
2012	1106_2_286	2 32 25.29	61 28 15.60	K2-K3	K2V	2.9	1	18.07	17.28	16.46	15.77
2012	0124_4	2 32 25.34	62 01 44.00	A1-A6	A3V	1.9	1	15.62	15.68	15.45	14.96
2012	1106_3_125	2 32 25.37	61 58 10.40	G5-K0	G6V	1.3	0	16.70	16.31	15.88	15.29
2011	0923_265	2 32 25.37	61 23 52.38	F2-F3	F2V	2.1	1	15.20	14.83	14.39	14.15
2012	1105_2_266	2 32 25.41	61 33 09.71	A7-A9	A7V	1.4	0	13.34	13.08	12.87	12.59
2012	1204_167	2 32 25.53	61 04 28.03	G5-G7	G7V	2.5	1	...	16.98	16.31	...
2012	0216_58	2 32 25.54	61 47 45.50	G9-K1	K0V	4.2	0	18.61	17.66	16.58	15.84
2012	1106_2_144	2 32 26.04	61 30 22.10	F6-G0	F8V	2.5	1	17.93	17.39	16.78	16.17
2012	1203_1_283	2 32 26.17	61 45 11.77	K2-K4	K2V	2.3	1	18.58	17.95	17.25	16.61
2012	0220_202	2 32 26.33	61 15 35.01	A0-A2	A1V	2.7	1	16.49	16.24	15.87	15.30
2012	1104_186	2 32 26.44	61 52 20.68		F9V	3.7	1	16.06	15.38	14.51	13.83
2012	1203_1_97	2 32 26.56	61 08 08.88	G0-G4	G3V	1.6	1	16.17	15.76	15.30	14.85
2012	0124_155	2 32 26.74	61 15 54.70	F6-F9	F8V	3.9	1	21.06	20.46	19.55	18.87
2012	0304_45	2 32 26.75	62 01 19.80		F3V	1.5	0	15.10	14.94	14.61	14.11
2011	1023_72	2 32 26.79	61 47 46.72	K1-K3	K2V	2.5	1	14.96	14.21	13.48	12.84
2012	1203_2_131	2 32 26.81	61 06 28.83	A0-A1	A0V	3.3	1	...	15.92	15.44	...
2012	1106_2_134	2 32 26.83	61 31 03.41	K2-K3	K2V	3.3	1	18.14	17.31	16.39	15.66
2012	1104_118	2 32 26.86	61 18 29.23	F6-F7	F7V	1.9	1	16.50	16.12	15.65	15.10
2011	0923_228	2 32 27.46	61 37 35.26	F1-F2	F2V	1.9	1	15.67	15.36	14.96	14.43
2012	1203_2_138	2 32 27.46	61 25 08.27	G5-K4	K0V	3.3	1	19.46	18.76	17.88	17.10
2012	0304_196	2 32 27.48	61 27 01.10	B4-B6	B5V	2.3	1	14.03	13.89	13.71	13.18
2012	1105_4_27	2 32 27.53	61 41 52.70	G8-K2	K0V[g]	3.1	1	16.25	15.48	14.64	13.99
2012	1106_1_277	2 32 27.61	61 35 43.80	K2-K3	K2V	2.6	1	18.25	17.65	16.89	16.18
2012	1203_1_212	2 32 27.99	61 46 20.94		F8V	2.1	1	16.29	15.85	15.32	14.79
2012	1203_1_138	2 32 28.05	61 26 51.08	K4-K5	K4V	2.8	1	19.70	18.86	17.95	17.20
2012	1106_3_26	2 32 28.29	62 10 08.40	F6-F7	F7V	2.5	1	...	17.47	16.87	...
2012	1105_5_15	2 32 28.40	62 21 58.40	A1-A2	A2V	2.0	1	15.89	15.70	15.44	14.90
2012	1105_5_100	2 32 28.49	62 08 29.70	K2-K5	K4V[g]	2.8	1	15.39	14.76	13.84	12.92
2012	1104_161	2 32 28.53	61 45 15.52		F3V	2.1	1	16.44	16.08	15.64	15.13
2012	1204_157	2 32 28.54	61 25 18.11	A9-F0	A9V	2.3	1	15.43	15.08	14.65	14.39
2012	0124_247	2 32 28.56	61 36 32.50	G1-G7	G3V	0.8	0	14.37	14.06	13.76	13.24
2012	0216_55	2 32 28.81	61 53 00.20	K8-M1	M0V	1.6	0	19.80	19.10	18.06	17.38
2011	1023_275	2 32 28.90	61 19 05.20	F8-G0	F9V	1.1	0	14.09	13.74	13.42	12.84
2012	1106_1_296	2 32 28.92	61 52 52.80	K6-K7	K7V	1.5	0	17.49	16.87	16.02	15.40
2012	1105_2_35	2 32 29.00	61 30 44.80		F7V	1.8	1	16.27	15.89	15.45	14.94
2012	1106_3_127	2 32 29.51	61 59 29.90	G9-K2	K0V[g]	3.2	1	17.74	16.98	16.12	15.47
2011	0923_73	2 32 29.86	61 09 36.60	F9-A1	A0V	4.7	0	14.17	13.89	13.11	12.39
2011	0923_248	2 32 29.92	61 27 07.68	B3-B5	B4V	2.7	1	13.35	13.05	12.80	12.51
2012	1105_2_59	2 32 30.13	61 27 13.90	K4-K5	K4V	0.9	0	15.69	15.12	14.60	14.37
2012	1204_43	2 32 30.14	61 43 12.87	G8-G9	G8V	2.7	1	16.35	15.71	14.98	14.33
2012	1204_169	2 32 30.15	61 17 11.19	F4-F5	F5V	2.1	1	16.47	16.09	15.61	14.93
2012	1106_3_195	2 32 30.24	61 49 12.40	K4-K5	K4V	0.8	0	16.99	16.45	15.96	15.44
2012	1106_2_202	2 32 30.24	61 24 55.80	F4-F6	F5V	3.1	1	18.27	17.74	17.05	16.41
2012	1106_3_139	2 32 30.32	61 57 12.10	A5-F9	F2V	4.2	0	18.27	17.58	16.70	16.03
2012	1203_1_100	2 32 30.34	61 08 19.70	F0-F2	F0V	3.2	1	17.37	16.92	16.30	15.65

Table 1. IC 1805 Spectral Types and Photometry (Continued)

Year	Date_No.[a] (MMDD_No.)	RA(J2000) (hhmmss.ss)	Dec(J2000) (° ′ ″)	SpTy Range	SpTy	A_V (r-i) (mag)	Assoc.?[b] (ext)	V(90P)[c] (mag)	r[d] (mag)	i[d] (mag)	I(90P)[c] (mag)
2012	1106_3_210	2 32 30.49	61 44 26.70	G6-G9	G8V	3.0	1	18.07	17.43	16.64	15.97
2012	1203_1_285	2 32 30.53	61 36 08.28	K3-K4	K4V	2.1	1	18.21	17.32	16.55	15.94
2012	1106_3_199	2 32 30.56	61 50 57.00	K3-K4V	K3V	2.0	1	18.50	17.92	17.24	16.44
2012	1104_192	2 32 30.58	61 59 38.21	F8-G0	F9V	1.4	0	16.00	15.65	15.26	14.73
2012	1204_45	2 32 30.95	61 34 55.96	F2-F3	F2V	2.0	1	15.22	14.86	14.44	14.21
2011	1023_127	2 32 31.09	61 26 32.10	F4-F6	F5V	1.2	0	13.50	13.34	13.05	12.57
2012	1106_2_106	2 32 31.43	61 51 22.10	F9-G1	G0V	2.5	1	18.20	17.64	17.01	16.42
2011	0923_222	2 32 31.43	61 43 57.30		B0V	4.6	0	12.20	18.18	17.72	17.11
2012	1106_1_228	2 32 31.48	61 49 24.10	F8-F9	F8V	2.2	1	16.82	16.33	15.78	15.23
2012	1105_2_74	2 32 31.48	61 18 30.80	G8-G9	G9V[g]	3.1	1	16.24	15.50	14.66	14.31
2012	1203_2_37	2 32 31.52	61 29 50.14	K2-K5	K3V	2.3	1	18.60	17.91	17.17	16.50
2012	1106_1_276	2 32 31.62	61 19 29.40	F7-F8	F8V	2.7	1	18.04	17.52	16.86	16.27
2012	0124_160	2 32 31.68	61 14 53.81	G4-G8	G7V	3.5	1	16.07	15.27	14.38	14.47
2012	0220_267	2 32 31.72	61 45 57.90	F3-F4	F3V	2.1	1	16.21	15.86	15.42	14.87
2012	1106_2_283	2 32 31.79	61 17 16.00	K0-K3	K2V	3.6	1	18.23	17.40	16.41	15.64
2012	1105_2_242	2 32 32.70	61 38 34.20	B6-B8	B7V	2.6	1	14.04	13.87	13.61	13.13
2012	1106_3_204	2 32 32.71	61 47 01.50	K7-K8	K7V	1.8	1	18.02	17.30	16.40	15.79
2012	0124_261	2 32 32.79	61 51 05.20	F0-F2	F2V	2.2	1	15.39	15.03	14.58	14.02
2012	0216_56	2 32 32.79	61 40 32.40	M2-M3	M2V	2.7	1	20.36	19.52	18.01	17.23
2012	0124_6	2 32 32.84	61 57 26.30	F8-F9	F8V	1.7	1	15.68	15.27	14.83	14.33
2012	1106_3_206	2 32 32.93	61 45 38.00	F9-G6	G3V	1.9	1	17.70	17.29	16.76	15.41
2012	1203_1_112	2 32 32.98	61 26 19.23	K0-K5	K4V	3.3	1	19.45	18.47	17.45	16.75
2012	1203_1_98	2 32 33.07	61 10 42.44	G5-G7	G6V	1.1	0	15.40	15.05	14.66	14.46
2011	1023_78	2 32 33.08	61 41 26.00	A7-A8	A7V	1.7	1	14.24	14.05	13.78	13.29
2011	0923_269	2 32 33.12	61 24 27.50	A1-A2	A1V	2.9	1	15.66	15.38	14.96	14.51
2012	1104_279	2 32 33.17	61 45 29.59		G4V	0.0	0	14.12	13.88	13.77	12.99
2011	1023_171	2 32 33.21	61 07 16.55	K1-K2	K2V	3.5	1	15.79	14.86	13.90	13.16
2012	1105_4_270	2 32 33.23	62 17 44.80	A1-A3	A2V	1.5	0	13.86	14.19	14.05	13.38
2011	0923_86	2 32 33.23	61 00 55.37	F4-F7	F7V	1.6	1	...	14.62	14.21	...
2012	0220_238	2 32 33.33	61 32 41.10	G5-G7	G6V	1.5	0	16.33	15.89	15.43	14.94
2012	1105_2_226	2 32 33.42	61 56 14.00		K4V	0.6	0	16.18	15.64	15.18	14.65
2012	1105_5_98	2 32 33.44	62 13 31.79	G8-K1	G9V[g]	2.5	1	15.63	15.27	14.56	13.71
2012	1104_290	2 32 33.54	61 57 50.00	F9-G2	G0V	1.8	1	16.09	15.64	15.16	14.57
2012	1106_3_128	2 32 33.76	62 01 04.70	F8-G0	F9V	2.1	1	...	17.47	16.94	...
2012	0220_253	2 32 33.77	61 42 28.80	G8-K0	G9V	2.6	1	15.22	14.55	13.83	13.19
2012	0304_194	2 32 33.89	61 27 30.70	G0-K0	G5V	2.1	1	...	20.37	19.79	...
2011	0923_235	2 32 33.93	61 29 30.24	B7-B9	B8V	2.3	1	14.99	14.74	14.54	14.30
2012	1203_2_269	2 32 33.94	61 43 56.84		K6V	1.9	1	18.68	17.97	17.11	16.37
2011	1023_164	2 32 34.03	61 21 24.30		F7V	1.1	0	14.17	13.90	13.60	13.08
2012	1203_1_95	2 32 34.10	61 21 17.55	K1-K5	K3V	2.5	1	18.29	17.59	16.81	16.11
2012	1204_164	2 32 34.11	61 13 10.25	G7-G9	G9V	3.1	1	16.83	16.09	15.27	14.80
2012	1203_1_161	2 32 34.13	61 27 48.60	F9-F8	F9V	1.2	0	15.34	15.02	14.68	14.46
2012	1203_1_214	2 32 34.21	61 33 53.50	K7-M0	K7V	1.4	0	16.51	16.00	15.18	14.47
2012	1204_155	2 32 34.41	61 18 54.04	G6-G8	G8V	2.6	1	16.71	16.11	15.40	14.79
2012	1105_3_4	2 32 34.57	61 56 41.90	K2-K4	K4V	0.0	0	14.29	13.84	13.51	13.00
2012	1105_4_36	2 32 34.68	62 10 18.30	F9-G1	G0V	1.2	0	15.65	15.58	15.22	14.50
2012	1105_3_293	2 32 34.70	61 45 04.90	B3-B5	B4V	3.3	1	16.45	16.18	15.80	15.29
2012	1204_153	2 32 34.87	61 16 39.85	F2-F3	F2V	2.4	1	16.44	16.04	15.54	15.06
2012	1203_2_267	2 32 35.04	61 40 51.76	A1-A2	A2V	2.5	1	15.49	15.24	14.89	14.37
2012	0124_273	2 32 35.14	61 28 54.91	G9-K0	K1V	3.5	1	16.21	15.32	14.38	14.31
2012	1106_1_242	2 32 35.14	61 59 18.60	G0-G8	G5V	4.1	1	17.54	16.75	15.76	15.06
2012	1106_3_202	2 32 35.16	61 47 32.39	K4-K5	K4V	1.5	0	17.62	16.98	16.34	15.68
2012	1105_3_232	2 32 35.26	61 38 55.50	A7-A8	A8V	2.1	1	16.08	15.81	15.45	14.92
2012	0304_253	2 32 35.30	61 41 03.51		F7V	1.9	1	16.44	16.05	15.57	15.00
2012	1203_2_56	2 32 35.33	61 28 28.88	F0-K5	G3V	4.6	0	...	18.09	16.99	...
2012	1203_1_96	2 32 35.36	61 15 22.47	G0-G7	G4V	1.3	0	15.49	15.09	14.67	14.79
2011	1023_74*	2 32 35.50	61 50 41.09	G3-G7	G5V	2.6	1	15.49	14.90	14.22	13.60
2012	1105_5_99	2 32 35.52	62 10 25.80	G5-K0	G7V	2.1	1	14.75	14.32	13.72	12.92
2012	0124_270	2 32 35.69	61 41 53.30	B9-A1	A0V	2.4	1	15.93	15.75	15.46	15.00
2012	1204_168	2 32 35.96	61 04 52.95		A1V	3.0	1	15.87	15.69	15.25	14.83
2012	1204_166	2 32 35.96	61 08 34.72	A0-A1	A0V[g]	3.5	1	16.19	15.84	15.32	14.82
2012	1106_2_107	2 32 36.03	61 45 53.81	G1-G7	G4V	3.5	1	17.70	16.92	16.05	15.39
2012	1203_2_135	2 32 36.03	61 06 55.53		F9V	3.1	1	...	16.32	15.58	...
2012	1106_2_30	2 32 36.16	61 35 28.11	G2-G6	G4V	2.9	1	18.44	17.78	17.02	16.34
2012	1204_9	2 32 36.20	61 41 19.79	G6-G7	G7V	1.4	0	16.25	15.85	15.39	14.87
2012	0124_158	2 32 36.27	61 04 33.40	G5-G9	G8V	3.0	1	14.67	14.36	13.55	14.41
2012	1106_3_205	2 32 36.95	61 42 05.80	K1-K3	K2V	2.6	1	18.43	17.72	16.95	16.31
2012	1203_1_173	2 32 37.01	61 28 11.87	G9-K2	G9V	3.1	1	17.28	16.64	15.80	15.20
2012	1106_3_197	2 32 37.21	61 49 02.89	K5-K6	K6V	1.0	0	17.92	17.19	16.52	15.95
2012	1203_1_216	2 32 37.31	61 42 44.73	G6-K0	G8V[g]	2.3	1	16.45	15.86	15.20	14.57
2011	1023_138	2 32 37.32	61 25 11.60	G6-G7	G6V	0.4	0	14.72	14.19	13.95	13.96
2012	1106_3_173	2 32 37.32	61 51 56.51	F4-F7	F6V	2.6	1	17.59	17.11	16.51	15.90
2011	0923_232	2 32 37.41	61 32 19.32	B5-B7	B6V	2.2	1	12.93	12.78	12.60	12.29
2012	1203_2_4	2 32 37.41	61 36 19.65		A1V	2.3	1	15.14	14.89	14.59	14.28
2012	1204_41	2 32 37.47	61 47 15.78	K4-K5	K5V	1.5	0	18.07	17.35	16.69	16.17
2012	1106_2_277	2 32 37.72	61 28 32.30	K3-K4	K4V	0.4	0	17.20	16.60	16.20	15.60
2012	1106_3_177	2 32 38.13	61 53 08.21	G8-K0	G9V	2.0	1	17.48	16.99	16.40	15.75
2012	1203_2_5	2 32 38.23	61 29 18.58	K0-K5	K2V	2.6	1	18.97	18.33	17.56	16.72
2012	0124_172	2 32 38.33	61 30 16.10	G7-K0	K0V	2.7	1	15.95	15.28	14.54	14.23
2012	1105_2_236	2 32 38.35	61 42 28.00	F4-F6	F5V	2.0	1	16.22	15.83	15.37	14.83
2012	1105_2_228	2 32 38.59	61 57 10.61	F8-F9	F9V	0.6	0	14.04	13.75	13.55	13.04
2012	1106_1_153	2 32 38.60	61 32 05.00	K2-K3	K2V	2.8	1	17.99	17.16	16.33	15.73
2011	0923_69	2 32 38.76	61 16 12.04	F8-F9	F8V	2.6	1	...	19.87	19.24	...
2012	1106_3_203	2 32 38.80	61 40 11.10	K4-K5	K4V[g]	3.7	1	17.86	17.08	15.97	15.18
2012	1105_3_10	2 32 38.96	61 58 04.70	F6-F8	F8V	1.8	1	16.15	15.75	15.30	14.76
2012	1106_1_232	2 32 38.98	61 53 30.30	G8-K1	G9V	2.1	1	17.86	17.36	16.74	16.11
2012	0304_223*	2 32 39.10	61 37 16.30	B8-B9	B9V	2.2	1	14.68	14.53	14.30	13.87

Table 1. IC 1805 Spectral Types and Photometry (Continued)

Year	Date_No.[a] (MMDD_No.)	RA(J2000) (hhmmss.ss)	Dec(J2000) (° ′ ″)	SpTy Range	SpTy	A_V (r-i) (mag)	Assoc.?[b] (ext)	V(90P)[c] (mag)	r[d] (mag)	i[d] (mag)	I(90P)[c] (mag)
2012	1104_181	2 32 39.26	61 54 58.40	K4-K5	K4V	0.7	0	16.35	15.82	15.36	14.82
2012	1203_1_94	2 32 39.36	61 06 52.73	G8-K0	G9V	1.2	0	13.38	15.08	14.65	14.57
2012	1203_1_30	2 32 39.55	61 26 57.87	K2-K3	K2V	3.1	1	17.71	17.06	16.19	15.41
2012	1203_1_11	2 32 39.69	61 13 44.69	F8-F9	F8V	2.2	1	15.60	15.13	14.58	14.52
2012	1106_2_278	2 32 39.78	61 30 01.61	G9-K2	K2V	3.2	1	17.57	16.74	15.83	15.16
2012	1105_3_214	2 32 39.97	61 32 44.91	G9-K2	K0V[g]	3.5	1	16.30	15.44	14.52	14.21
2012	1106_3_117	2 32 40.11	62 03 37.90	F4-F6	F6V	1.8	1	...	16.71	16.27	...
2012	1106_3_160	2 32 40.14	61 54 38.00	G5-G7	G6V	2.4	1	17.48	16.84	16.18	15.63
2012	1203_2_65	2 32 40.21	61 28 14.72	K2-K5	K4V	2.0	1	19.09	18.14	17.39	16.67
2012	1106_3_126	2 32 40.21	62 02 50.40	F8-F9	F8V	1.7	1	...	16.71	16.28	...
2012	1106_2_290	2 32 40.26	61 25 20.70	F4-F8	F7V	3.1	1	18.06	17.51	16.80	16.15
2012	0220_228	2 32 40.29	61 28 42.20	F6-F7	F7V	1.5	0	16.30	15.94	15.55	15.06
2012	1204_19	2 32 40.32	61 28 24.27	K6-M0	K6V	2.4	1	19.70	18.73	17.78	17.08
2011	1023_167	2 32 40.60	61 19 25.80	G0-G2	G1V	0.6	0	12.42	12.20	11.98	11.90
2011	0923_44	2 32 40.66	61 21 35.63		F4V	2.3	1	15.20	14.80	14.30	13.90
2012	1106_2_180	2 32 40.80	61 27 29.60	K0-K4	K2V	2.9	1	17.41	17.49	16.65	15.87
2011	1023_26	2 32 40.89	61 27 48.40	F8-F9	F9V	3.0	1	14.04	16.54	15.83	14.93
2012	0124_259	2 32 41.01	61 37 32.60	A9-F0	F1V	2.0	1	16.00	15.90	15.50	14.69
2012	1105_2_254	2 32 41.01	61 35 26.50	F4-F6	F5V	2.2	1	15.87	15.47	14.97	14.53
2012	1106_1_230	2 32 41.18	61 49 07.80	F8-F9	F9V	2.0	1	16.78	16.40	15.89	15.31
2012	0124_8	2 32 41.18	61 45 18.31	A0-A2	A1V	2.4	1	16.19	15.96	15.64	15.16
2012	1204_7	2 32 41.28	61 45 03.08	K4-K5	K4V	2.3	1	19.11	18.33	17.52	16.80
2011	1023_96*	2 32 41.29	61 30 58.10		B5V	2.3	1	13.48	13.26	13.09	12.73
2012	1104_187	2 32 41.32	61 53 33.11		K2V	1.3	0	15.90	15.49	14.99	14.36
2012	0304_241	2 32 41.37	61 38 35.90	F4-F5	F4V	1.4	0	12.69	12.84	12.53	12.18
2012	1106_3_25	2 32 41.37	61 59 56.80	G7-K2	K1V	1.8	1	18.44	17.91	17.33	16.81
2012	1203_1_81	2 32 41.46	61 25 53.80	F8-F9	F8V	2.8	1	15.86	15.27	14.59	14.21
2011	0923_297	2 32 41.49	61 27 45.24		B8V	3.6	1	13.30	12.99[e]	12.50[f]	12.54
2011	0923_78	2 32 41.49	61 07 33.50		F7V	1.3	0	14.16	13.92	13.57	13.08
2011	1023_179	2 32 41.86	61 09 56.40	F3-F6	F4V	0.7	0	13.78	13.42	13.24	12.57
2012	1105_3_248	2 32 42.03	61 42 04.80	F9-G0	G0V	1.8	1	16.25	15.86	15.38	14.85
2012	1106_1_160	2 32 42.12	61 31 05.40	K0-K2	K2V	2.3	1	17.24	16.67	15.96	15.32
2011	0923_46	2 32 42.53	61 21 00.90		F5V	3.2	1	15.78	15.20	14.49	14.30
2012	1203_2_134	2 32 42.66	61 17 52.12	F2-F3	F2V	1.9	1	15.36	15.01	14.61	14.40
2012	1105_2_41	2 32 42.69	61 28 12.31	F0-F2	F1V	2.0	1	15.00	14.58	14.18	13.90
2012	1106_1_152	2 32 42.74	61 26 40.69	K6-K8	K6V	3.2	1	18.15	19.49	18.37	17.58
2012	0220_283	2 32 42.80	61 24 13.79	G6-G7	G7V	2.5	1	14.83	13.94	13.27	14.09
2012	1204_154	2 32 43.09	61 20 33.13		F8V	2.3	1	16.32	15.86	15.30	14.78
2012	1203_1_213	2 32 43.16	61 30 58.91	G0-G4	G2V	2.0	1	16.17	15.01	14.46	14.36
2012	1105_4_268	2 32 43.18	62 22 53.80	A9-F1	F0V	0.3	0	13.05	13.27	13.25	12.43
2012	1104_126	2 32 43.23	61 28 04.51	B2-B8	B5V	2.5	1	13.97	13.77	13.56	12.99
2012	1106_1_162	2 32 43.28	61 33 35.31	K1-K3	K2V	2.6	1	17.65	17.04	16.26	15.58
2011	1023_177	2 32 43.35	61 07 31.44	F7-F9	F8V	1.8	1	15.97	15.65	15.20	14.64
2012	1106_3_23	2 32 43.45	61 59 34.90	A1-A2	A1V	3.1	1	16.86	16.57	16.10	15.54
2012	1105_2_68	2 32 43.47	61 24 17.69	G5-G7	G6V	1.5	0	16.49	16.10	15.64	15.11
2012	1105_3_238	2 32 43.48	61 39 57.79	F4-F5	F4V	2.1	1	16.19	15.85	15.39	14.76
2011	0923_291	2 32 43.53	61 26 31.96		B4V	2.9	1	12.91	12.80	12.50	12.22
2011	1023_176	2 32 43.65	61 13 44.19	B9-A0	B9V	3.3	1	14.68	14.19	13.74	13.91
2012	1203_1_48	2 32 43.72	61 27 28.00	F8-K2	G6V	0.4	0	16.68	15.72	15.49	14.93
2012	0304_286	2 32 43.77	61 28 09.79	A2-A3	A3V	1.5	0	14.09	13.88	13.72	13.07
2012	1106_3_175	2 32 43.92	61 52 06.50	A5-A8	A6V	3.7	1	17.25	16.85	16.19	15.56
2012	0124_156	2 32 44.09	61 25 23.60	F6-F8	F7V	1.3	0	14.88	14.57	14.22	13.91
2012	1106_2_24	2 32 44.09	61 43 11.80	F4-F5	F4V	2.6	1	17.13	16.73	16.17	15.58
2012	1203_1_220	2 32 44.09	61 46 08.56	G6-G8	G7V	3.0	1	16.14	15.43	14.64	13.99
2012	1203_2_33	2 32 44.12	61 30 39.80	K1-K3	K2V	2.8	1	17.47	16.75	15.93	15.34
2012	1104_111	2 32 44.19	61 25 14.38	F8-F9	F8V	1.2	0	13.90	13.65	13.32	12.81
2011	1023_95	2 32 44.35	61 30 28.70		F6V	1.9	1	15.66	15.26	14.81	14.45
2012	1105_3_225	2 32 44.43	61 37 13.80		F8V	1.8	1	16.21	15.85	15.40	14.89
2012	1104_196	2 32 44.51	61 58 49.00	A0-A2	A1V	2.1	1	12.89	13.04	12.79	12.29
2011	0923_229	2 32 44.67	61 40 43.76	F1.5-F3	F2V	2.0	1	14.95	14.63	14.21	13.81
2011	1023_140	2 32 44.69	61 24 38.90		A0V	1.6	1	14.03	13.88	13.76	13.15
2012	1105_5_94	2 32 44.70	62 22 22.60	F4-F6	F4V	1.3	0	15.96	15.94	15.64	14.91
2011	1023_162	2 32 44.84	61 20 34.00		A0V	2.2	1	14.44	13.90	13.65	13.89
2012	1106_3_283	2 32 44.98	61 30 55.80	K4-K5	K4V	2.6	1	18.10	17.46	16.58	15.89
2012	1204_162	2 32 45.00	61 04 51.03	K0-K2	K2V	1.9	1	...	17.01	16.40	...
2012	0124_10	2 32 45.12	61 47 45.50	F4-F6	F5V	1.5	0	14.52	14.29	13.94	13.42
2012	1104_26	2 32 45.14	61 14 53.27	F8-F9	F9V	1.5	0	16.35	15.99	15.59	15.16
2012	1106_3_184	2 32 45.16	61 50 55.30	F6-F8	F7V	2.6	1	17.64	17.21	16.60	15.97
2012	1106_2_109	2 32 45.22	61 52 40.60	F3-F5	F4V	3.4	1	17.98	17.47	16.74	16.10
2012	1106_1_236	2 32 45.25	61 53 55.30	F4-F6	F5V	3.0	1	18.03	17.61	16.94	16.29
2012	0220_294	2 32 45.31	61 31 00.10	G7-G9	G8V	1.9	1	14.14	13.23	12.67	12.51
2011	1023_86	2 32 45.52	61 38 36.93	G9-K2	K0V	3.2	1	14.78	13.93	13.07	13.85
2012	1106_1_280	2 32 45.55	61 26 31.30	K2-K3	K2V	2.8	1	18.06	17.21	16.40	15.65
2012	1105_3_282	2 32 45.56	61 15 11.70		F8V	1.4	0	15.53	15.15	14.77	14.86
2012	1203_2_265	2 32 45.56	61 49 01.44	G7-K0	G8V	3.8	1	18.24	17.39	16.43	15.70
2012	1203_1_298	2 32 45.76	61 29 59.42	G9-K6	K2V	4.1	1	19.12	18.50	17.42	16.67
2012	1106_1_219	2 32 45.81	61 48 01.10	A7-A8	A7V	3.1	1	17.06	16.64	16.09	15.49
2012	1105_4_266	2 32 45.89	62 25 16.59	F9-G0	G0V	1.3	0	15.78	15.69	15.31	14.57
2012	1204_20	2 32 45.91	61 29 11.17	G9-K0	G9V	3.7	1	19.70	18.64	17.70	16.91
2012	0216_182	2 32 45.94	61 09 31.30	K6-K8	K7V	1.7	1	18.73	17.96	17.07	16.41
2012	1204_5	2 32 45.99	61 44 57.93	F6-F8	F7V	1.7	1	16.18	15.81	15.39	14.82
2012	1105_4_127	2 32 46.05	61 43 44.19	A0-A1	A0V	2.5	1	16.01	15.81	15.49	14.93
2012	1104_119	2 32 46.46	61 22 58.62	G7-K0	G9V	4.1	1	16.50	15.62	14.58	14.08
2012	1106_2_208*	2 32 46.60	61 20 10.90	G8-K0	G9V	2.6	1	16.72	16.07	15.35	14.83
2012	1105_5_208*	2 32 46.77	61 44 14.00	G0-G5	G2V	2.3	1	16.44	15.85	15.24	14.62
2011	0923_38	2 32 47.08	61 22 46.08		A3V	3.2	1	14.36	14.39	13.87	13.51
2012	0124_154	2 32 47.24	61 27 56.80	F8-G4	F8V	...	...	15.15	...	...	14.61

Table 1. IC 1805 Spectral Types and Photometry (Continued)

Year	Date_No.[a] (MMDD_No.)	RA(J2000) (hhmmss.ss)	Dec(J2000) (° ′ ″)	SpTy Range	SpTy	A_V (r-i) (mag)	Assoc.?[b] (ext)	V(90P)[c] (mag)	r[d] (mag)	i[d] (mag)	I(90P)[c] (mag)
2012	1204_113	2 32 47.35	61 26 37.11	K1-K3	K2V	3.8	1	19.48	18.68	17.67	16.96
2012	1204_57	2 32 47.36	61 36 17.35	B9-A0	A0V	2.3	1	15.03	14.87	14.60	14.13
2011	1023_124	2 32 47.56	61 27 00.00	B0-B3	B1V	4.4	0	12.72	12.62	12.11	11.99
2012	1105_5_95	2 32 47.59	62 13 31.40	A1-A2	A1V	2.6	1	15.87	15.49	15.13	14.56
2012	1106_2_22	2 32 47.76	61 45 41.60	F2-F4	F3V	2.8	1	17.36	16.88	16.29	15.65
2012	1105_2_71	2 32 47.76	61 07 32.20	B9-A0	B9.5V	3.0	1	15.77	15.57	15.17	14.54
2012	1203_2_139*	2 32 47.78	61 04 44.57	A1-A2	A1V	3.0	1	15.56	15.34	14.91	14.62
2012	1203_1_219	2 32 47.79	61 45 10.42	G6-G8	G7V	1.4	0	15.87	15.43	14.99	14.45
2012	1106_1_244	2 32 48.01	61 56 25.30	F9-G7	G4V	3.9	1	16.53	15.78	14.81	14.02
2012	1105_4_34	2 32 48.03	62 13 34.20	F3-F5	F4V	1.5	0	15.63	14.69	14.36	14.35
2012	1105_4_123	2 32 48.05	61 37 02.40	F4-F6	F5V	1.8	1	15.37	15.04	14.63	14.24
2012	1105_5_127	2 32 48.08	62 03 39.00	G9-K2	K0V[g]	3.1	1	15.36	14.83	13.98	12.96
2012	1106_2_196	2 32 48.13	61 23 33.20	G6-G8	G7V	3.0	1	18.19	17.51	16.72	15.87
2012	1106_1_147	2 32 48.19	61 15 24.60	G7-K0	G8V	3.4	1	16.81	15.99	15.11	14.65
2012	1204_151	2 32 48.43	61 04 30.04	K6-K7	K7V	2.2	1	...	18.10	17.11	...
2012	1203_1_82	2 32 48.51	61 24 27.28	K4-K5	K5V	3.6	1	19.51	18.64	17.53	16.83
2012	0304_3*	2 32 48.59	62 04 24.30	A8-F0	A9V	1.9	1	13.83	14.01	13.67	12.99
2012	1105_2_72	2 32 48.66	61 16 14.50	G8-G9	G9V	1.5	0	16.37	15.90	15.42	14.99
2011	0923_75	2 32 48.68	61 04 02.96	B7-B8	B8V	2.9	1	14.38	14.40	14.06	13.92
2012	1204_143*	2 32 48.70	61 21 16.91	A0-A1	A0V	2.9	1	15.70	15.43	15.04	14.55
2012	1105_3_183	2 32 48.79	61 13 58.81	B9-A0	B9V	3.3	1	16.28	15.95	15.50	15.04
2012	0124_32	2 32 48.92	62 03 25.60	F1-F3	F2V	1.4	0	14.79	14.67	14.38	13.73
2012	1104_191	2 32 48.97	62 05 37.50	F6-F8	F7V	1.3	0	14.79	14.75	14.41	13.54
2012	0220_263	2 32 49.12	61 45 10.30		F7V	2.1	1	16.22	16.00	15.50	14.78
2012	0220_220	2 32 49.35	61 26 41.70	B2-B4	B3V	2.7	1	13.72	13.45	13.21	12.78
2012	1105_4_53	2 32 49.38	62 05 42.60	G0-G7	G7V	1.7	1	14.62	14.05	13.54	12.93
2012	1203_2_36	2 32 49.39	61 36 14.90	G8-K0	G9V	2.2	1	17.43	16.84	16.20	15.52
2012	1203_2_124	2 32 49.81	61 21 29.00	G0-G3	G1V	1.9	1	16.04	15.62	15.11	14.74
2011	0923_10	2 32 49.84	61 23 43.80		G9V	2.4	1	14.85	13.81	13.12	14.18
2012	1106_3_167	2 32 49.98	61 54 10.59	G1-K0	G6V[g]	3.5	1	17.30	16.54	15.66	14.97
2012	1106_2_285	2 32 50.31	61 08 18.60	F2-F6	F4V	3.3	1	17.28	16.75	16.03	15.36
2012	1203_1_228	2 32 50.36	61 33 41.88	G6-K0	G7V	2.2	1	17.10	16.52	15.90	15.36
2012	1105_4_2	2 32 50.45	62 17 37.30		F8V	1.4	0	15.18	15.17	14.80	13.98
2011	1023_24	2 32 50.45	61 28 57.40	F7-F8	F7V	2.1	1	15.15	14.57	14.06	14.16
2012	0124_276*	2 32 50.45	61 25 42.10	B5-B7	B6V	3.0	1	14.48	14.23	13.90	13.36
2012	1105_2_293	2 32 50.51	61 36 46.00	F8-F9	F8V	2.8	1	14.45	13.74[e]	13.07[f]	13.37
2012	1106_1_233	2 32 50.51	61 54 47.80	F6-F7	F7V	2.8	1	17.83	17.45	16.80	16.10
2011	0923_53*	2 32 50.54	61 16 28.10	G4-G6	G5V	3.7	1	15.07	14.03	13.10	13.92
2012	1105_4_37	2 32 50.58	62 09 46.90	G5-K0	K0V[g]	1.1	0	13.75	13.61	13.19	12.52
2012	0304_226	2 32 50.81	61 36 46.10	F8-F9	F9V	...	0	16.07	...	...	14.33
2012	1106_2_136	2 32 50.83	61 32 16.70	G7-K2	G9V	2.4	1	17.88	17.28	16.60	15.75
2012	1203_2_27	2 32 50.87	61 20 19.14	A0-A1	A1V	2.6	1	15.45	15.22	14.86	14.44
2012	1105_2_223	2 32 50.96	61 51 43.80	A3-A5	A3V	2.4	1	15.51	15.31	14.96	14.43
2012	1106_3_286	2 32 51.02	61 48 57.50	K1-K3	K2V	2.4	1	18.07	17.35	16.63	15.97
2012	1106_3_201	2 32 51.19	61 35 08.19	G8-K0	G9V	1.7	1	17.23	16.75	16.21	15.67
2012	1105_5_139	2 32 51.19	62 02 55.30	A0-A1	A0V	1.8	1	14.47	14.63	14.46	13.73
2012	1106_3_158	2 32 51.26	61 55 17.20	G9-K2	K2V	2.8	1	17.89	17.13	16.32	15.67
2012	1203_2_111	2 32 51.32	61 22 45.38	B4-B7	B5V	9.1	0	...	15.08	13.45	13.61
2012	1203_1_215	2 32 51.54	61 43 46.75	K4-M0	K7V	0.8	0	19.78	18.65	17.96	17.20
2012	1104_198	2 32 51.66	61 58 45.99	F7-F8	F8V	1.8	1	15.44	15.12	14.67	14.24
2012	1104_28	2 32 51.69	61 17 51.97	A7-F0	A8V	2.6	1	16.35	15.96	15.48	15.00
2012	1106_1_143	2 32 51.71	61 21 43.20	A2-A4	A3V	3.6	1	17.62	17.17	16.56	15.99
2012	1104_184	2 32 51.73	61 49 12.61		B9V	2.4	1	14.06	13.92	13.67	13.18
2012	0220_290	2 32 51.79	61 10 22.50	G7-G8	G7V	3.3	1	16.38	15.61	14.76	14.64
2012	1106_2_198	2 32 51.86	61 22 09.31	F5-F7	F6V	3.0	1	17.46	16.87	16.18	15.56
2012	1104_30	2 32 51.96	61 20 27.31	F8-G0	F9V	1.2	0	14.89	14.40	14.05	14.00
2012	0216_177	2 32 52.01	61 27 36.00	K7-M1	M0V	2.0	1	20.17	19.16	18.03	17.24
2012	1204_56	2 32 52.27	61 42 47.82	F4-F5	F4V	1.8	1	15.38	15.11	14.71	14.26
2012	1105_4_38	2 32 52.30	62 11 33.50	A9-F0	A9V	1.2	0	13.79	14.00	13.81	13.13
2012	1106_2_118	2 32 52.44	61 39 14.00	F2-F4	F4V	2.8	1	17.47	17.00	16.40	15.81
2012	0220_225*	2 32 52.46	61 29 43.10	F0-F3	F1V	1.9	1	16.08	15.78	15.41	14.93
2012	0124_34*	2 32 52.46	62 03 28.00	F2-F4	F3V	1.9	1	15.34	15.12	14.72	14.02
2012	0304_5	2 32 52.48	61 58 47.60	K2-K4	K3V	1.0	0	16.16	15.67	15.21	14.66
2012	1105_4_78	2 32 52.94	62 04 33.60	A3-A7	A6V	2.0	1	15.96	16.00	15.69	15.01
2012	1106_2_201	2 32 52.94	61 12 42.51	F0-F2	F1V	3.1	1	17.77	17.33	16.70	16.03
2012	0304_183	2 32 53.04	61 29 16.91	A0-A1	A1V	2.4	1	15.57	15.37	15.05	14.62
2012	1105_2_32	2 32 53.13	61 31 19.01	F8-F9	F8V	0.6	0	14.63	14.29	14.08	13.84
2012	1204_69	2 32 53.30	61 33 37.64		M2V	1.1	0	19.40	18.58	17.41	16.69
2012	1106_2_168	2 32 53.66	61 28 23.50	F2-F3	F2V	2.8	1	17.49	17.04	16.44	15.87
2012	1106_3_124	2 32 53.68	62 06 09.00	F8-F9	F8V	1.8	1	...	17.45	16.99	...
2011	0923_246	2 32 53.74	61 30 10.86	G1-G5	G3V	0.2	0	14.54	14.08	13.90	13.28
2012	0220_246	2 32 53.76	61 34 53.20	A1-A2	A2V	2.6	1	16.24	15.97	15.59	15.10
2012	0124_145	2 32 53.84	61 29 54.51	G1-G5	G3V	4.1	1	...	17.27	16.28	...
2012	1203_2_136	2 32 53.87	61 09 33.50	F8-F9	F9V	2.1	1	16.12	15.69	15.17	14.79
2012	1203_1_265	2 32 53.96	61 28 04.26	G9-K2	K0V	2.6	1	17.87	17.23	16.49	15.89
2012	1106_2_27	2 32 54.05	61 34 12.00		M4V	...	...	18.14	17.51	16.15	15.43
2012	1105_4_126	2 32 54.09	61 43 18.71		A1V	2.5	1	16.05	15.83	15.51	14.99
2012	1203_1_226	2 32 54.23	61 37 50.11	F2-F3	F2V	1.7	1	15.41	15.20	14.84	14.26
2012	0220_31	2 32 54.37	61 59 42.20	A3-A5	A4V	1.9	1	15.18	14.95	14.69	14.22
2012	1105_2_246	2 32 54.41	61 40 33.80	A7-A8	A8V	2.3	1	15.17	14.91	14.50	14.04
2012	0124_36	2 32 54.52	62 00 54.00	G5-G9	G8V[g]	2.2	1	14.64	14.39	13.77	12.98
2012	1105_5_97	2 32 54.53	62 18 07.40	A2-A6	A4V	2.3	1	15.55	15.62	15.26	14.51
2012	1106_1_249	2 32 54.92	61 58 33.50	A1-A2	A1V	4.2	0	16.88	16.40	15.70	15.00
2012	1203_1_17	2 32 55.00	61 13 51.76	F5-F7	F6V	2.1	1	15.86	15.44	14.94	14.64
2012	0220_209	2 32 55.00	61 21 14.80	K6-K7	K7V	4.3	0	...	13.88	12.45	...
2012	1106_1_246	2 32 55.20	61 55 39.01	K3-K4	K4V	1.2	0	17.86	17.26	16.68	16.07
2012	1105_5_96	2 32 55.32	62 27 13.69	A7-F0	A8V	1.7	1	15.72	15.75	15.47	14.77

Table 1. IC 1805 Spectral Types and Photometry (Continued)

Year	Date_No.[a] (MMDD_No.)	RA(J2000) (hhmmss.ss)	Dec(J2000) (° ′ ″)	SpTy Range	SpTy	A_V (r-i) (mag)	Assoc.?[b] (ext)	V(90P)[c] (mag)	r[d] (mag)	i[d] (mag)	I(90P)[c] (mag)
2012	1106_1_214	2 32 55.46	61 45 38.80	G0-G2	G1V	3.0	1	17.65	17.10	16.35	15.43
2012	0304_184	2 32 55.58	61 20 26.99	K2-K3	K3V	2.4	1	16.14	14.86	14.10	13.77
2012	1203_2_2	2 32 55.83	61 49 03.18	G0-G1	G0V	1.5	0	16.05	15.69	15.26	14.75
2011	1023_133	2 32 55.84	61 23 52.40		B4V	3.3	1	13.87	13.69	13.31	12.91
2012	1106_3_289	2 32 55.91	61 32 26.41	K3-K5	K4V	0.7	0	16.77	16.26	15.78	15.26
2012	1106_3_207	2 32 55.94	61 37 34.00	G9-K2	K1V	2.6	1	17.58	16.84	16.08	15.47
2012	1106_2_210	2 32 56.34	61 15 56.80	G7-K0	G8V	3.7	1	17.93	17.10	16.16	15.47
2012	1105_5_126	2 32 56.42	62 05 48.80		A0V	1.5	0	14.03	14.10	14.00	13.39
2012	1105_2_57*	2 32 56.58	61 24 19.30	B5-B7	B6V	3.5	1	14.97	14.68	14.25	13.96
2012	1106_2_275	2 32 56.81	61 27 03.00	G7-K0	G9V	3.6	1	17.71	16.92	15.98	15.25
2012	1105_4_267	2 32 56.83	62 23 25.91	G7-G9	G8V	0.9	0	14.33	13.98	13.62	13.08
2011	1023_71	2 32 56.84	61 45 36.60		F8V	1.4	0	14.91	14.58	14.21	13.76
2012	1105_4_77	2 32 57.12	62 02 51.50	G1-G8	G7V	1.2	0	14.21	14.16	13.76	13.24
2012	0304_188	2 32 57.20	61 27 22.50	A9-F0	A9V	2.4	1	16.36	16.06	15.62	15.07
2012	0304_182	2 32 57.26	61 19 18.00	F4-F5	F5V	1.9	1	16.31	15.93	15.51	15.03
2012	1106_3_277	2 32 57.29	61 53 04.10	G2-G7	G5V	2.5	1	16.69	16.16	15.49	14.89
2012	1105_2_253	2 32 57.41	61 34 43.60	G9-K2	K0V	2.8	1	15.50	14.76	13.99	13.76
2012	0124_148	2 32 57.60	61 29 42.70		B2V	2.4	1	12.79	12.59	12.44	12.31
2011	1023_168*	2 32 57.76	61 17 18.91	G8-K0	G9V	3.0	1	14.80	14.05	13.24	12.63
2012	1105_5_204	2 32 57.80	61 41 38.80	F1-F3	F2V	3.0	1	14.57	14.10	13.47	12.84
2012	1106_3_149	2 32 57.86	61 57 56.90	K3-K4	K3V	1.2	0	17.27	16.77	16.26	15.70
2012	0304_41	2 32 57.87	61 46 45.89		F7V	1.5	0	15.33	14.99	14.61	14.13
2012	1105_4_128	2 32 57.91	61 40 52.40	G8-K1	G9V	0.7	0	14.92	14.56	14.23	13.92
2012	0304_54	2 32 58.12	62 02 55.70	F7-F8	F7V	1.2	0	15.11	15.19	14.87	13.80
2012	1106_1_150	2 32 58.58	61 16 29.31	F9-G6	G3V	1.9	1	17.27	16.77	16.24	15.70
2012	1203_2_109	2 32 58.64	61 24 39.71	K2-K5	K2V	2.9	1	18.81	18.00	17.16	16.53
2011	0923_77	2 32 58.68	61 01 16.90	K6-K8	K7V	1.0	0	15.83	15.27	14.53	14.50
2012	1203_1_64	2 32 58.84	61 25 53.77	G8-K1	G9V	2.2	1	15.97	17.33	16.68	15.22
2011	1023_29	2 32 58.95	61 25 45.20	B7-B9	B9V	2.9	1	13.67	13.46	13.11	12.62
2012	1106_3_152	2 32 59.34	61 57 08.60	K3-K5	K4V[g]	3.8	1	16.91	15.93	14.80	14.02
2012	1106_1_245	2 32 59.40	62 00 10.30	M1-M2	M2V	0.7	0	17.98	17.34	16.26	15.61
2012	0304_1	2 32 59.42	61 58 41.20	G8-G9	G8V	3.1	1	16.26	15.52	14.71	14.05
2012	0124_278	2 32 59.52	61 04 26.80	A2-A3	A2V	3.1	1	15.74	15.48	15.00	14.68
2012	0216_180	2 32 59.67	61 19 42.60	K7-M1	M0V	2.2	1	20.06	19.23	18.05	17.32
2012	0124_38	2 32 59.78	61 59 58.81	G0-G5	G0V	1.3	0	16.21	15.84	15.47	14.97
2012	1106_1_248	2 32 59.80	61 55 38.59	G7-K2	K0V	3.4	1	18.09	17.29	16.39	15.65
2012	1203_1_238	2 32 59.89	61 31 46.95	K4-K6	K5V	2.1	1	19.26	18.46	17.67	17.11
2012	1203_1_70	2 32 59.92	61 25 03.22	K5-K6	K6V	3.2	1	19.35	18.59	17.46	16.65
2012	1106_1_247	2 32 59.97	61 58 15.80	G7-K0	G8V	3.6	1	17.26	16.44	15.51	14.80
2012	0220_258	2 33 00.06	61 38 36.70	A6-A8	A7V	2.2	1	16.00	15.75	15.39	14.84
2012	0304_9	2 33 00.30	61 47 08.40		F8V	1.7	1	14.79	14.41	13.98	13.58
2012	1106_1_295	2 33 00.42	62 12 22.20	F3-F6	F5V	1.7	1	...	16.95	16.56	...
2012	0216_61	2 33 00.45	61 45 42.81	K6-K7	K6V	2.2	1	19.86	19.07	18.15	17.39
2012	1106_3_27	2 33 00.49	62 02 39.60	G0-G6	G3V	1.6	1	...	17.12	16.66	...
2012	1106_3_153	2 33 00.61	61 54 27.60	F7-F9	F8V	2.8	1	18.06	17.55	16.88	16.24
2012	1105_2_225	2 33 00.78	61 57 06.80	G9-K1	K0V[g]	3.2	1	16.01	15.25	14.39	13.72
2012	1203_2_96	2 33 00.78	61 26 09.74	K2-K5	K4V	1.8	1	...	17.81	17.10	...
2012	1106_2_113	2 33 00.81	61 37 37.90	G9-K0	G8V	2.5	1	17.39	16.88	16.19	15.56
2012	1105_4_52	2 33 00.93	62 08 28.69	A1-A5	A3V	1.5	0	15.30	15.54	15.39	14.75
2012	1105_2_248	2 33 01.10	61 40 33.90	G7-G9	G8V	0.6	0	14.72	14.43	14.15	13.82
2012	1106_3_154	2 33 01.29	61 56 37.10	G3-K1	G7V	3.2	1	17.40	16.79	15.96	15.29
2011	0923_64	2 33 01.49	61 13 51.50	G9-K2	K1V	3.2	1	15.77	14.94	14.06	13.79
2012	1106_3_284	2 33 01.57	61 48 22.70	F8-G0	F9V	2.3	1	17.63	17.14	16.57	15.93
2011	0923_238	2 33 01.62	61 35 24.42		F8V	1.6	1	14.56	14.06	13.65	13.59
2012	1203_1_222	2 33 01.62	61 45 33.59	G0-G6	G3V	3.6	1	17.91	17.13	16.23	15.47
2012	0124_37	2 33 01.90	61 47 50.70	K1-K2	K2V	0.7	0	15.53	15.11	14.75	14.30
2012	1105_3_254	2 33 01.96	61 43 39.70	A2-A6	A5V	2.0	1	16.35	16.17	15.87	15.36
2012	0304_213	2 33 01.98	61 36 57.70		F7V	1.4	0	15.39	15.05	14.68	14.45
2012	1105_3_31	2 33 02.01	62 06 02.49	A1-A2	A1V	1.9	1	15.52	15.63	15.42	14.77
2012	1106_2_185	2 33 02.29	61 25 04.80	A0-A7	A2V	4.3	0	18.18	17.68	16.94	16.25
2012	1104_147*	2 33 02.38	61 38 40.67		F3V	1.8	1	16.24	15.92	15.53	15.03
2012	1104_25	2 33 02.38	61 34 02.50	A2-A6	A4V	2.0	1	15.15	14.94	14.64	14.44
2011	1023_73	2 33 02.42	61 49 11.00		F4V	2.1	1	14.04	13.71	13.25	12.73
2011	0923_14	2 33 02.50	61 09 23.34		B5V	3.1	1	13.79	13.58	13.25	12.75
2012	1203_1_224	2 33 02.62	61 44 08.15	G1-G7	G6V	1.3	0	...	15.40	14.99	...
2012	1106_3_133	2 33 02.65	61 59 23.70	A1-A2	A2V	3.4	1	18.12	17.73	17.18	16.62
2011	0923_32	2 33 02.79	61 23 13.84		B9V	3.2	1	15.55	15.19	14.76	14.41
2012	1105_2_75	2 33 02.82	61 06 06.39	B9-A0	B9.5V	2.9	1	15.80	15.64	15.26	14.85
2012	0216_77	2 33 02.84	61 41 23.30	K6-M1	K8V	1.4	0	18.88	18.17	17.30	16.66
2011	1023_28*	2 33 02.97	61 28 42.52	B7-B9	B8V	2.4	1	14.76	14.54	14.32	14.18
2012	1105_5_137	2 33 03.01	62 02 57.80	A1-A3	A3V	1.8	1	14.99	14.65	14.45	14.01
2012	1106_2_276	2 33 03.14	61 30 56.10	G7-K1	G9V	1.7	1	17.84	17.38	16.84	16.23
2012	0304_186	2 33 03.20	61 28 46.90	B5-B6	B5V	1.9	1	13.34	13.12	13.02	12.67
2012	0220_34	2 33 03.23	61 48 08.70	F0-F1	F0V	1.9	1	15.39	15.10	14.74	14.28
2012	0220_237	2 33 03.52	61 33 23.00	A1-A3	A2V	2.8	1	16.32	16.09	15.67	15.16
2012	1203_1_85	2 33 03.67	61 13 33.24	B9-A0	B9V	3.3	1	15.09	14.67	14.22	14.19
2012	1105_4_56	2 33 03.97	62 07 34.30	F6-F7	F6V	1.3	0	14.61	14.18	13.84	13.47
2012	1105_5_24	2 33 04.02	62 11 04.70	A7-A9	A8V	0.9	0	14.06	14.04	13.93	13.39
2012	1106_3_275	2 33 04.18	61 52 26.00	G4-K0	G6V	3.4	1	17.31	16.56	15.71	15.04
2012	1105_3_242	2 33 04.24	61 40 34.10	A3-A5	A4V	2.8	1	16.47	16.17	15.71	15.16
2012	1105_3_243	2 33 04.26	61 41 55.40	B9-A0	A0V	2.0	1	14.53	14.42	14.22	13.77
2012	1106_2_193	2 33 04.28	61 19 01.70	G6-K3	G9V	3.8	1	18.31	17.40	16.42	15.70
2012	0220_38	2 33 04.29	61 49 39.09	G0-G2	G1V	1.3	0	16.04	15.69	15.30	14.77
2012	0304_177	2 33 04.31	61 10 42.00	F4-F5	F4V	1.5	0	14.28	14.04	13.70	13.24
2012	1105_3_195	2 33 04.33	61 28 26.51	F1-F5	F3V	3.5	1	16.00	16.88	16.14	14.92
2011	0923_63	2 33 04.35	61 10 02.20	K2-K4	K3V	5.0	0	14.25	13.13[e]	11.82[f]	12.03
2012	1204_59	2 33 04.36	61 43 35.25	G7-G8	G8V	3.2	1	16.89	16.15	15.32	14.66

Table 1. IC 1805 Spectral Types and Photometry (Continued)

Year	Date_No.[a] (MMDD_No.)	RA(J2000) (hhmmss.ss)	Dec(J2000) (° ′ ″)	SpTy Range	SpTy	A_V (r-i) (mag)	Assoc.?[b] (ext)	V(90P)[c] (mag)	r[d] (mag)	i[d] (mag)	I(90P)[c] (mag)
2012	0220_36	2 33 04.48	61 48 44.00	G6-G8	G7V	1.6	1	16.49	15.99	15.50	14.99
2011	1023_23	2 33 04.50	61 25 10.60		G6V	0.4	0	13.74	13.52	13.30	12.80
2012	1106_3_111	2 33 04.51	62 08 50.30	F8-G0	F9V	1.5	0	...	17.16	16.74	...
2012	1204_152	2 33 04.53	61 13 54.81	K2-K3	K2V	1.5	0	16.27	15.72	15.21	14.87
2012	1203_1_300	2 33 04.67	61 33 42.43	K7-M1	M0V	1.3	0	19.08	18.29	17.31	16.59
2012	1105_5_116	2 33 04.69	62 07 54.90	B6-B9	B8V	3.2	1	15.25	15.02	14.62	13.88
2012	1105_4_35	2 33 04.78	62 11 33.20	F4-F5	F4V	1.5	0	15.56	15.55	15.22	14.53
2012	1105_4_265	2 33 04.94	62 24 40.00		K2V	0.9	0	13.92	13.78	13.38	12.69
2011	0923_253	2 33 05.28	61 27 07.24	B3-B4	B4V	3.0	1	13.03	13.07	12.75	12.36
2012	1105_2_37	2 33 05.37	61 30 37.30	F5-F7	F6V	2.1	1	16.47	16.05	15.56	15.01
2012	1203_2_26	2 33 05.38	61 22 50.60	K1-K3	K2V	2.5	1	17.19	17.13	16.38	15.41
2012	1203_1_78*	2 33 05.58	61 22 09.18	B9-A0	A0V	2.5	1	14.97	14.71	14.40	14.07
2012	1104_199	2 33 05.60	61 56 20.60		K6V	0.6	0	15.58	15.03	14.45	13.86
2012	1105_5_136	2 33 05.78	62 04 35.30	K3-K4	K4V[g]	4.5	0	15.21	14.27	13.00	12.14
2012	1104_197	2 33 05.87	61 57 54.89	F2-F5	F3V	1.6	1	16.17	15.96	15.61	15.05
2012	1106_3_288	2 33 06.02	61 46 24.60	G7-K0	G7V	3.5	1	17.68	16.88	15.99	15.29
2012	1106_2_128	2 33 06.11	61 37 30.60	G7-G8	G8V	2.1	1	17.10	16.51	15.91	15.35
2012	1105_2_296	2 33 06.16	61 51 57.70	G8-G9	G8V[g]	3.6	1	16.43	15.61	14.69	13.98
2012	1106_3_136	2 33 06.22	62 01 35.00	A9-F1	F0V	2.8	1	...	17.43	16.89	...
2012	1105_5_128	2 33 06.28	62 06 09.59	G8-K0	K0V	0.8	0	15.42	15.38	15.02	14.24
2012	1106_1_197	2 33 06.38	61 42 53.80	G7-K0	G9V	3.4	1	18.30	17.48	16.58	15.87
2011	0923_225	2 33 06.39	61 44 26.80	A6-A8	A7V	2.2	1	15.67	15.77	15.40	14.85
2012	1106_1_163	2 33 06.52	61 38 52.91	K2-K3	K3V	2.4	1	17.82	17.30	16.55	15.80
2012	1204_58	2 33 06.57	61 46 33.76		A1V	2.5	1	15.76	15.30	14.97	14.49
2012	1106_2_205	2 33 06.61	61 09 51.00	A1-A2	A1V	3.8	1	17.59	17.14	16.53	15.92
2012	1106_3_179	2 33 06.73	61 51 56.30	G1-G8	G6V	3.3	1	17.89	17.18	16.34	15.60
2012	0220_183	2 33 06.83	61 06 36.19	F2-F3	F3V	2.7	1	15.40	15.32	14.75	14.32
2012	0124_133	2 33 06.93	61 28 20.70	F6-F8	F7V	...	...	14.40	...	...	13.42
2012	0124_40	2 33 07.09	61 57 14.90	B7-B9	B9V	2.5	1	14.24	14.04	13.77	13.32
2012	1203_1_294	2 33 07.13	61 36 09.62	G9-K2	K2V	2.8	1	17.64	17.07	16.27	15.61
2012	1204_134	2 33 07.16	61 22 56.75	F2-F3	F3V	2.2	1	15.60	15.26	14.79	14.48
2012	1105_2_53	2 33 07.38	61 22 06.30	G8-G9	G8V	1.2	0	15.72	15.35	14.95	14.55
2012	1106_3_144	2 33 07.41	61 58 52.60	F6-F8	F7V	2.6	1	17.92	17.42	16.80	16.26
2012	1203_2_38	2 33 07.43	61 40 44.25		F9V	2.1	1	16.53	16.14	15.61	14.95
2012	1203_1_19	2 33 07.48	61 04 54.89	F5-F7	F6V	1.5	0	15.51	14.92	14.55	15.03
2012	1203_2_23	2 33 07.75	61 08 58.15	K1-K3	K2V	1.3	0	16.25	15.78	15.29	14.86
2012	1204_64	2 33 07.88	61 39 54.26	F0-F2	F1V	2.1	1	15.97	15.64	15.21	14.67
2012	1105_4_115	2 33 08.01	61 47 17.91	K1-K4	K2V[g]	1.6	1	14.61	13.89	13.33	12.58
2012	1105_3_190	2 33 08.24	61 14 19.80	F8-F9	F9V	1.6	1	16.24	15.89	15.46	15.05
2012	1105_5_93	2 33 08.28	62 19 39.90	F6-F8	F8V	0.0	0	13.55	13.55	13.48	12.67
2012	1106_3_120	2 33 08.41	62 12 20.70	G4-G8	G8V	1.1	0	...	16.61	16.21	...
2011	1023_274	2 33 08.59	61 20 52.30		F7V	1.5	0	13.91	13.54	13.15	12.66
2012	0304_179	2 33 08.79	61 14 07.99		F8V	2.1	1	16.48	16.03	15.50	15.04
2012	1106_2_179	2 33 08.88	61 25 22.31	G8-G9	G8V	2.9	1	17.28	16.58	15.81	15.22
2011	0923_293	2 33 08.89	61 28 45.60	B9-A0	A0V	2.2	1	14.85	14.63	14.38	14.04
2011	0923_35	2 33 08.95	61 21 52.22	A5-A7	A6V	2.5	1	14.80	14.50	14.09	13.59
2012	1106_2_204	2 33 08.97	61 14 50.80	F8-G0	F9V	3.0	1	18.25	17.67	16.95	16.28
2011	0923_258	2 33 09.03	61 27 46.05	B2-B3	B2V	2.9	1	12.92	12.88	12.61	12.30
2012	1203_2_132	2 33 09.14	61 06 25.63	F4-F5	F4V	2.0	1	15.29	15.30	14.86	14.46
2012	1105_2_247	2 33 09.15	61 40 51.90	B5-B7	B6V	1.9	1	13.12	12.91	12.80	12.51
2011	1023_106	2 33 09.19	61 31 58.10	B3-B4	B4V	2.4	1	14.91	13.20	13.02	14.33
2012	1105_5_110	2 33 09.34	62 12 54.89	F9-G6	G0V	0.8	0	14.33	13.37	13.10	13.38
2012	1105_2_78	2 33 09.39	61 09 14.80	G5-G7	G6V	3.5	1	16.08	15.32	14.44	14.16
2012	1106_1_218	2 33 09.41	61 45 27.40	G6-G9	G8V	1.7	1	17.51	17.12	16.59	15.95
2012	0220_232	2 33 09.51	61 31 57.99	B4-B5	B4V	2.4	1	13.33	13.20	13.02	12.62
2012	0304_173	2 33 09.54	61 31 48.90	G7-G8	G7V	1.5	0	16.38	16.01	15.54	14.98
2011	1023_85	2 33 09.71	61 40 49.10		F8V	0.7	0	13.30	13.24	13.01	12.58
2012	0304_7	2 33 09.76	61 44 47.39	F6-F7	F7V	1.5	0	15.14	14.84	14.47	13.99
2012	1105_5_91	2 33 10.27	62 18 09.80	A9-F1	A9V	0.6	0	13.08	13.29	13.24	12.48
2012	1105_5_149*	2 33 10.31	62 02 49.51	A3-A6	A5V	1.9	1	14.76	14.79	14.50	13.73
2012	1106_3_193	2 33 10.32	61 41 06.29	K0-K3	K2V	2.9	1	18.44	17.65	16.83	16.14
2012	1105_4_54*	2 33 10.37	62 08 34.70	A6-A8	A7V	1.6	1	15.06	15.15	14.91	14.45
2012	1106_2_132	2 33 10.44	61 35 19.89	G0-G3	G2V	2.4	1	17.23	16.70	16.07	15.49
2012	0304_58	2 33 11.02	61 46 24.80	F4-F5	F5V	2.4	1	15.18	15.73	15.19	14.17
2012	1203_2_16	2 33 11.02	61 29 12.14	F8-F9	F9V	3.4	1	19.14	18.30	17.50	16.85
2012	1106_2_280	2 33 11.13	61 30 19.30	K3-K5	K4V	2.6	1	17.29	16.57	15.70	15.02
2012	1106_2_114	2 33 11.18	61 44 56.40	F6-F8	F7V	2.2	1	17.13	16.69	16.15	15.59
2012	1105_5_104	2 33 11.31	62 16 16.51	G2-K0	G6V	2.6	1	15.45	15.10	14.40	13.45
2012	1203_1_243	2 33 11.42	61 31 15.01	G9-K2	K1V	2.8	1	17.59	16.47	15.68	15.35
2012	0220_194	2 33 11.63	61 16 58.60		K2V	3.3	1	12.92	12.19	11.28	11.32
2011	1023_105	2 33 11.94	61 30 57.70		F0V	0.4	0	13.61	12.92	12.89	12.73
2011	0923_33	2 33 12.06	61 21 17.81		A0V	2.5	1	14.99	14.77	14.45	14.09
2011	0923_55	2 33 12.14	61 14 42.67	G8-K2	K0V	0.9	0	14.91	14.42	14.04	14.21
2011	1023_180	2 33 12.19	61 00 18.07		F8V	1.3	0	15.01	14.77	14.41	14.72
2012	0216_176	2 33 12.25	61 13 54.40	M2-M4	M3V	1.6	0	20.22	19.49	18.05	17.20
2012	1104_178	2 33 12.37	61 45 16.78		A1V	3.0	1	16.43	16.13	15.70	15.13
2011	1023_115	2 33 12.61	61 28 00.90	B7-B9	B8V	2.4	1	14.58	14.42	14.20	13.76
2012	0304_271	2 33 12.64	61 32 41.40		G7V	1.5	0	16.21	15.80	15.34	14.91
2012	1105_5_122	2 33 12.86	62 08 30.10	A6-F0	A8V	1.3	0	13.63	13.75	13.55	12.82
2011	0923_58	2 33 12.90	61 16 11.30	G5-G9	G7V	3.6	1	15.93	15.08	14.16	13.43
2012	1105_2_260	2 33 12.95	61 36 35.40	F2-F5	F4V	1.8	1	16.11	15.78	15.38	14.93
2012	0220_187	2 33 13.03	61 04 24.50	F4-F5	F5V	2.0	1	15.60	15.52	15.07	14.57
2011	0923_50*	2 33 13.13	61 19 25.90	G7-G8	G9V	2.9	1	14.97	13.93	13.14	13.50
2012	1105_3_44	2 33 13.14	62 05 04.71	F0-F2	F2V	1.5	0	15.00	15.10	14.79	14.00
2012	1105_2_299	2 33 13.19	61 39 38.40		F2V	1.8	1	16.35	16.05	15.67	15.15
2011	1023_83	2 33 13.24	61 40 42.30	A5-F3	F0V	2.9	1	...	18.55	17.99	...
2012	1105_5_112	2 33 13.28	62 10 59.00	F3-F5	F4V	1.7	1	15.59	15.39	15.01	14.31

Table 1. IC 1805 Spectral Types and Photometry (Continued)

Year	Date_No.[a] (MMDD_No.)	RA(J2000) (hhmmss.ss)	Dec(J2000) (° ′ ″)	SpTy Range	SpTy	A_V (r-i) (mag)	Assoc.?[b] (ext)	V(90P)[c] (mag)	r[d] (mag)	i[d] (mag)	I(90P)[c] (mag)
2012	1105_3_8	2 33 13.28	61 49 14.50	F0-F3	F2V	2.1	1	16.47	16.07	15.63	15.06
2012	1203_2_55	2 33 13.43	61 31 52.23	K6-K7	K7V	2.4	1	18.89	18.07	17.04	16.18
2012	1105_4_67	2 33 13.53	62 06 15.31	F3-F5	F2V	1.6	1	15.78	14.71	14.38	14.37
2012	1105_2_79	2 33 13.54	61 05 59.90		K4V	0.4	0	14.85	14.84	14.44	14.13
2012	1105_4_10	2 33 13.68	62 19 20.50	G8-K0	G9V	1.1	0	14.97	14.55	14.16	13.42
2012	0304_180	2 33 13.70	61 24 03.00	G0-K0	G5V	...	...	15.05	...	...	14.06
2012	1105_4_122	2 33 13.73	61 40 50.01	G8-K0	G9V[g]	1.0	0	13.52	13.43	13.05	12.48
2011	0923_231	2 33 13.75	61 34 10.16	B6-B9	B8V	2.2	1	14.30	14.20	14.00	13.53
2012	1105_3_46	2 33 13.79	62 06 10.80	F8-F9	F8V	1.1	0	15.06	14.59	14.29	13.83
2012	1105_3_294	2 33 14.16	61 37 47.70	F2-F3	F2V	1.3	0	14.55	14.22	13.94	13.67
2012	1106_2_119	2 33 14.49	61 43 15.20	K3-K4	K4V[g]	2.4	1	16.84	16.00	15.16	14.45
2012	1106_2_148	2 33 14.58	61 31 49.20	K2-K3	K2V	1.5	0	17.05	16.57	16.03	15.41
2011	0923_6	2 33 14.65	61 24 02.86		A9V	1.5	0	12.58	12.24	11.99	11.92
2012	1105_3_257	2 33 14.70	61 44 24.01		K5V	0.9	0	15.76	15.33	14.80	14.16
2012	1203_1_88	2 33 14.81	61 13 29.16	F9-G0	F9V	1.5	0	15.37	14.98	14.57	14.40
2012	1105_3_256	2 33 14.86	61 43 08.60	G7-G9	G8V	0.9	0	15.99	15.68	15.33	14.79
2012	1203_1_254	2 33 14.93	61 30 11.01	K0-K6	K2V	4.2	0	19.39	18.49	17.37	16.67
2011	1023_15	2 33 15.04	61 38 41.92		K2V	3.2	1	15.85	14.99	14.10	13.57
2012	1105_3_236	2 33 15.17	61 39 05.80	B9-A0	A0V	2.3	1	15.54	15.42	15.18	14.70
2012	1203_2_125	2 33 15.17	61 13 39.70	F2-F4	F3V	2.2	1	16.15	15.73	15.24	15.02
2012	1106_1_241	2 33 15.40	61 55 27.50	K1-K3	K2V[g]	3.3	1	18.11	17.40	16.49	15.72
2012	0216_178	2 33 15.41	61 08 10.20	M2-M3	M2V	2.6	1	20.38	19.53	18.04	17.10
2012	1204_84	2 33 15.56	61 31 44.44		K7V	2.7	1	19.28	18.46	17.37	16.60
2012	1204_18	2 33 15.60	61 34 56.49		F9V	2.0	1	16.23	15.78	15.28	14.79
2012	1106_2_138	2 33 15.62	61 33 57.61	G4-G9	G7V[g]	3.3	1	16.85	16.07	15.21	14.62
2012	1204_274	2 33 15.69	61 12 56.60	A1-A2	A1V	3.5	1	16.45	16.03	15.47	14.97
2012	1104_114	2 33 16.00	61 27 36.22	F0-F2	F1V	1.9	1	15.23	14.88	14.50	14.35
2012	1203_1_20	2 33 16.18	61 20 48.40	K0-K3	K2V	3.0	1	17.73	17.01	16.17	15.53
2012	0304_60	2 33 16.28	61 50 15.80	A1-A2	A2V	2.8	1	16.46	16.23	15.80	15.08
2012	0304_178	2 33 16.31	61 22 54.01	F5-F6	F5V	2.1	1	16.29	15.93	15.46	14.96
2012	1106_1_299	2 33 16.53	61 57 29.01	F9-G9	G7V	3.3	1	17.98	17.21	16.35	15.68
2012	0124_35	2 33 16.86	62 00 08.50	G1-G7	G4V	1.2	0	15.65	15.28	14.90	14.40
2012	0220_2*	2 33 16.88	61 41 30.50	A0-A2	A1V	2.1	1	15.58	15.42	15.18	14.73
2012	1104_202	2 33 16.95	61 59 00.00	F3-F5	F4V	1.7	1	16.22	15.90	15.52	15.07
2012	1105_3_191	2 33 16.99	61 31 09.50	G8-K2	K0V[g]	2.8	1	15.77	14.96	14.18	13.80
2012	1203_1_10	2 33 17.47	61 28 08.39	G8-K1	G9V	2.7	1	16.96	16.32	15.57	15.05
2012	0220_8	2 33 17.50	61 44 16.49	B9-A0	B9V	2.3	1	15.17	15.03	14.80	14.37
2012	0220_270	2 33 17.70	61 39 31.70		A9V	2.0	1	16.29	16.00	15.64	15.15
2012	1105_4_113	2 33 17.83	61 42 57.81	F9-G3	G0V	1.6	1	16.36	16.00	15.55	14.98
2012	0304_167	2 33 18.01	61 35 19.89	F7-F8	F8V	1.6	1	16.46	16.13	15.73	15.22
2012	1105_2_42	2 33 18.07	61 28 49.80	G1-G3	G2V	1.6	1	15.71	15.28	14.82	14.53
2012	1106_1_254	2 33 18.22	62 11 47.79	F6-F7	F7V	1.5	0	...	16.92	16.54	...
2012	1106_3_274	2 33 18.23	61 57 54.10	G9-K1	K0V	3.4	1	18.09	17.26	16.36	15.66
2012	1204_62	2 33 18.31	61 43 26.30	G8-G9	G8V	1.4	0	15.98	15.56	15.10	14.54
2012	1105_4_55	2 33 18.40	62 07 51.51		K2V[g]	3.3	1	15.24	14.65	13.74	12.77
2012	1203_2_123	2 33 18.47	61 11 18.47	F4-F5	F4V	2.4	1	15.93	15.92	15.41	14.75
2012	1104_190	2 33 18.62	61 47 28.18		G9V	3.5	1	13.66	13.01	12.10	11.83
2012	1105_3_288	2 33 18.66	61 26 13.39	B2-B5	B3V	2.5	1	13.73	13.64	13.43	12.91
2012	0220_255	2 33 18.89	61 37 45.00	F3-F5	F4V	1.4	0	14.85	14.46	14.13	14.08
2012	1105_4_116	2 33 18.90	61 48 26.10	K3-K4	K3V	0.8	0	16.06	15.51	15.09	14.61
2012	1106_1_293	2 33 18.98	61 59 22.80	M1-M2	M2V	0.5	0	16.87	16.20	15.15	14.51
2012	1106_3_164	2 33 19.14	61 54 10.50	K6-K8	K7V	1.4	0	18.49	17.79	16.97	16.23
2011	1023_178	2 33 19.42	60 59 45.88	K2-K3	K3V	0.7	0	14.79	14.97	14.57	14.37
2011	0923_239	2 33 19.42	61 37 39.24	F6-F7	F7V	1.3	0	15.22	14.93	14.59	14.15
2012	1106_3_163	2 33 19.73	61 52 51.00	K7-K8	K7V	1.7	1	18.02	17.28	16.40	15.73
2012	1105_5_276	2 33 19.79	62 02 30.31	G5-K0	G7V[g]	2.7	1	15.64	14.72	14.01	13.38
2012	1203_2_112	2 33 19.84	61 20 41.94	F9-G7	G3V	3.0	1	18.37	18.37	17.62	16.55
2012	1106_1_144	2 33 19.86	61 20 38.70	F9-K0	G6V	2.3	1	18.37	17.85	17.22	16.55
2012	1203_1_65	2 33 20.14	61 22 10.61	F2-F3	F2V	2.6	1	15.52	15.10	14.55	14.44
2012	1104_193	2 33 20.49	61 56 26.45		F5V	2.1	1	16.49	16.13	15.64	15.02
2012	1105_2_10	2 33 20.52	61 32 23.30	B2-B3	B2V	2.0	1	12.91	12.46	12.39	12.43
2012	1105_2_300	2 33 20.73	61 53 01.39	G9-K0	G9V	1.3	0	16.32	16.03	15.59	15.08
2012	1105_3_296	2 33 20.85	61 38 23.60	F8-G0	F9V	1.9	1	16.31	15.89	15.40	14.87
2012	1106_1_297	2 33 21.22	61 56 28.20	F2-F5	F3V	2.3	1	18.04	17.64	17.15	16.42
2012	1203_1_260	2 33 21.63	61 30 14.78	G0-G4	G2V	2.6	1	16.36	15.74	15.05	14.43
2012	1105_4_40	2 33 21.72	62 16 32.60	F3-F5	F3V	1.4	0	13.81	13.98	13.68	12.90
2012	0220_234*	2 33 21.86	61 32 27.90		K2V	2.8	1	15.19	14.90	14.09	13.61
2011	0923_74	2 33 22.06	60 59 49.16	B7-A0	A0V	3.3	1	15.42	15.10	14.62	14.48
2012	1104_205	2 33 22.12	62 08 26.40	A2-A4	A3V	1.5	0	14.14	14.14	13.98	13.35
2012	1106_3_190	2 33 22.33	61 47 08.10	G9-K0	G9V	2.4	1	17.32	16.65	15.97	15.34
2012	1106_2_161	2 33 22.56	61 27 18.30	G6-K0	G8V	3.3	1	17.25	16.66	15.81	14.76
2012	1204_156	2 33 22.62	61 04 03.72	A1-A5	A3V	4.0	1	...	16.14	15.46	...
2012	1106_3_157	2 33 22.64	61 54 56.60	G0-G7	G6V	1.9	1	16.86	16.38	15.83	15.19
2012	1106_2_188	2 33 22.68	61 23 58.21	A3-A4	A3V	4.1	1	16.85	16.35	15.65	14.99
2012	1106_3_129	2 33 22.78	62 08 46.09	G0-G7	G2V	1.6	1	...	16.90	16.44	...
2012	0124_31	2 33 22.85	61 56 17.80	F6-F8	F7V	1.7	1	16.10	15.78	15.36	14.83
2012	0304_59	2 33 22.85	62 00 58.20	A2-A5	A4V	2.1	1	15.92	15.76	15.45	14.76
2012	1105_5_124	2 33 22.86	62 08 52.91	A6-A8	A7V	1.5	0	15.12	15.06	14.84	14.16
2012	1204_55	2 33 22.90	61 47 10.08	G7-G8	G8V[g]	2.8	1	16.26	15.57	14.82	14.17
2012	0124_44	2 33 22.90	61 52 35.70	A1-A5	A3V	2.8	1	15.82	15.61	15.17	14.63
2012	1203_2_128	2 33 22.94	61 13 14.30	F8-F9	F9V	1.4	0	...	14.67	14.28	...
2011	0923_236	2 33 23.15	61 39 22.31	F4-F5	F5V	1.5	0	15.25	14.96	14.61	14.16
2012	0216_135	2 33 23.16	61 31 48.20	G0-K6	K6V	2.0	1	19.28	18.40	17.52	16.68
2012	0124_33	2 33 23.18	62 00 07.90	F6-F8	F7V	1.0	0	13.00	13.07	12.80	12.29
2012	0124_105	2 33 23.24	61 32 41.50	G5-G7	G6V	0.8	0	14.81	14.49	14.16	13.88
2012	1105_3_48	2 33 23.25	62 04 14.50	A0-A1	A1V	1.8	1	14.12	14.07	13.88	13.22
2012	1105_4_111	2 33 23.54	61 39 34.70	K1-K3	K2V[g]	3.3	1	16.17	15.29	14.38	13.87

Table 1. IC 1805 Spectral Types and Photometry (Continued)

Year	Date_No.[a] (MMDD_No.)	RA(J2000) (hhmmss.ss)	Dec(J2000) (° ′ ″)	SpTy Range	SpTy	A_V (r-i) (mag)	Assoc.?[b] (ext)	V(90P)[c] (mag)	r[d] (mag)	i[d] (mag)	I(90P)[c] (mag)
2012	1105_5_26	2 33 24.00	62 13 54.91		F8V	1.4	0	15.78	15.74	15.37	14.93
2012	1106_1_252	2 33 24.03	61 58 06.80	K3-K4	K4V	1.5	0	18.34	17.67	17.04	16.46
2012	1203_2_77	2 33 24.06	61 27 42.77	F7-F8	F8V	1.7	1	16.18	15.80	15.36	14.81
2012	1106_3_180	2 33 24.12	61 51 20.90	F3-F5	F4V	2.5	1	17.02	16.58	16.03	15.45
2012	1203_1_229	2 33 24.21	61 47 01.74	B9-A0	A0V	2.2	1	15.23	15.05	14.80	14.34
2011	0923_31	2 33 24.78	61 20 26.35		F7V	0.2	0	...	10.55	10.45	...
2012	1105_2_20	2 33 24.83	61 10 04.80	F9-G0	F9V	1.8	1	15.90	15.28	14.83	15.11
2012	1106_3_122	2 33 24.90	62 12 21.50	A2-F0	A8V	3.2	1	...	17.60	17.00	...
2012	0304_53	2 33 24.93	61 49 16.90	B8-A0	B9V	2.5	1	15.90	15.70	15.43	14.92
2012	1204_280	2 33 24.98	61 09 02.37	F6-F8	F7V	2.1	1	...	15.80	15.30	...
2012	1105_3_266	2 33 25.31	61 44 54.70	G7-G9	G8V	3.4	1	16.21	15.46	14.58	13.98
2012	1104_105	2 33 25.40	61 20 52.55	G7-K0	G8V	2.3	1	13.06	12.55	11.90	11.95
2012	1105_5_197	2 33 25.57	61 39 36.60	G8-K0	G9V[g]	2.2	1	13.12	12.69	12.05	11.92
2012	1203_2_100	2 33 26.35	61 24 30.97	K2-K4	K2V	1.1	0	15.93	15.47	15.02	14.59
2012	0124_104	2 33 26.46	61 33 04.30	F8-G0	F9V	1.8	1	16.13	15.74	15.26	14.68
2012	1106_2_122	2 33 26.48	61 41 29.10	K1-K4	K3V	2.1	1	18.35	17.34	16.63	16.08
2012	1203_1_223	2 33 26.63	61 43 11.30	F6-F7	F7V	1.7	1	16.02	15.65	15.23	14.80
2012	1203_1_87	2 33 26.88	61 05 14.02	F4-F5	F4V	1.8	1	15.63	15.38	14.98	14.72
2012	1105_4_44	2 33 27.14	62 14 02.50	G0-G7	G5V	0.7	0	12.99	12.88	12.59	12.06
2012	1105_5_106	2 33 27.18	62 20 41.00	A2-A6	A4V	1.9	1	15.67	14.92	14.64	14.59
2012	1203_2_45	2 33 27.20	61 37 26.51	F2-F3	F2V	2.3	1	16.13	15.87	15.39	14.81
2012	0304_57	2 33 27.28	62 02 53.41		F8V	1.9	1	13.81	13.49[e]	13.02[f]	12.82
2011	1023_174	2 33 27.34	60 59 54.96	A7-A9	A9V	2.1	1	15.16	14.90	14.53	14.34
2012	1203_1_84	2 33 27.60	61 10 15.72	F1-F3	F2V	2.2	1	...	15.50	15.04	...
2012	1203_2_121	2 33 27.67	61 07 36.81	A7-F0	A8V	2.3	1	15.51	15.30	14.88	14.73
2012	1105_5_103	2 33 28.01	62 16 31.50	K0-K1	K0V	2.8	1	15.35	14.10	13.32	13.44
2012	1105_3_194	2 33 28.08	61 29 48.00	G1-G9	G5V	1.6	1	16.28	15.75	15.28	14.74
2012	1203_2_130	2 33 28.09	61 11 04.41	G9-K1	K0V	1.3	0	...	14.96	14.49	...
2012	1106_2_163	2 33 28.22	61 27 30.70	G9-K4	K1V	2.2	1	18.45	17.86	17.19	16.55
2012	0304_280*	2 33 28.29	61 35 03.90		B9V	2.1	1	14.68	14.59	14.40	13.91
2012	1203_1_237	2 33 28.34	61 36 24.12		F8V	1.4	0	15.56	15.24	14.87	14.39
2012	1106_1_258	2 33 28.41	62 10 23.90	A3-A6	A4V	3.2	1	...	16.79	16.25	...
2012	1203_1_52	2 33 28.57	61 25 27.20	G9-K3	K2V	2.6	1	18.25	17.54	16.77	16.09
2012	1105_5_153	2 33 28.58	62 00 52.41	G6-K5	K1V[g]	1.7	1	15.64	15.31	14.76	13.91
2012	1104_204	2 33 28.65	61 56 51.50	B9-A1	A1V	2.5	1	16.47	16.23	15.89	15.39
2012	1204_142	2 33 28.66	61 18 13.09	F2-F3	F2V	2.2	1	...	15.47	15.01	...
2012	1204_100	2 33 28.79	61 29 36.23	G3-G6	G5V	1.0	0	15.23	14.89	14.54	14.16
2011	1023_84	2 33 29.11	61 52 37.50	K1-K4	K2V	0.6	0	14.42	14.06	13.72	13.26
2012	1204_93	2 33 29.38	61 28 44.58	A7-A9	A8V	2.0	1	15.13	14.79	14.43	14.17
2012	0220_35	2 33 29.38	61 46 51.10		F4V	2.2	1	15.77	15.33	14.85	14.33
2012	1204_141	2 33 29.49	61 11 04.56	F0-F3	F2V	3.1	1	...	16.25	15.60	...
2012	0220_244	2 33 29.62	61 33 34.21	F4-F5	F4V	1.8	1	16.22	15.92	15.52	15.03
2012	1106_3_29	2 33 29.75	62 06 50.39	F2-F5	F4V	2.2	1	...	17.58	17.09	...
2011	0923_16	2 33 29.88	61 03 15.30	B7-B9	B8V	3.8	1	14.86	14.90	14.38	14.01
2012	0220_242	2 33 29.93	61 33 12.30		A0V	2.4	1	15.83	15.63	15.34	14.82
2012	1203_1_80	2 33 30.07	61 14 18.91	B9-A0	B9.5V	3.3	1	...	14.57	14.10	...
2011	1023_117	2 33 30.09	61 28 54.00	B8-B9	B8V	1.9	1	13.94	13.83	13.70	13.12
2012	1105_3_32	2 33 30.34	61 48 13.61		A1V	2.7	1	16.40	16.09	15.71	15.24
2012	1106_1_145	2 33 30.72	61 39 22.20	G7-K0	G8V	2.4	1	17.17	16.47	15.80	15.24
2012	0220_195	2 33 30.76	61 23 55.20	G6-G9	G7V	1.4	0	16.04	15.62	15.18	14.68
2012	0304_174	2 33 30.78	61 10 25.91	F8-G0	F9V	4.1	1	...	20.36	19.40	...
2012	1106_1_133	2 33 30.88	61 20 02.21	K6-K7	K6V	1.6	1	16.82	16.17	15.37	14.72
2012	1106_3_135	2 33 30.88	62 01 51.10	F6-F8	F8V	1.6	1	...	16.91	16.48	...
2012	0304_55	2 33 30.93	62 05 35.80	G8-G9	G9V	0.8	0	15.46	15.38	15.03	14.35
2012	0124_136	2 33 30.98	61 24 24.40		G0V	2.1	1	16.48	16.04	15.49	14.97
2012	1203_2_20	2 33 31.19	61 29 24.61	K2-K4	K3V	2.9	1	17.69	16.99	16.12	15.36
2012	1105_2_38	2 33 31.27	61 30 39.19	A0-A1	A1V	2.6	1	16.30	16.09	15.74	15.23
2012	1105_3_38	2 33 31.32	61 51 04.01		A3V	2.4	1	16.22	15.98	15.64	15.15
2012	0220_198	2 33 31.53	61 22 20.80		B9V	2.2	1	14.26	14.14	13.92	13.43
2012	0216_15	2 33 31.60	61 40 25.70	K6-K8	K7V	2.5	1	19.23	18.45	17.40	16.55
2012	1203_1_89	2 33 31.79	61 04 31.38	F9-G0	F9V	1.6	1	14.72	14.73	14.30	14.02
2012	0124_149	2 33 31.82	61 10 35.50	F0-F5	F5V	...	...	14.81	...	...	14.38
2012	1105_5_109	2 33 32.10	62 18 21.50	F9-G7	G2V	0.8	0	14.70	14.33	14.03	13.51
2012	0304_64	2 33 32.13	61 50 53.00	B8-B9	B8V	2.6	1	14.39	14.18	13.90	13.38
2012	1106_2_143	2 33 32.14	61 32 02.80	F2-F3	F2V	2.7	1	17.42	16.99	16.43	15.76
2012	1106_1_256	2 33 32.24	61 47 02.70	K4-K5	K4V	1.2	0	17.23	16.52	15.94	15.40
2012	1105_4_63	2 33 32.25	62 05 50.90	G8-K1	G8V[g]	2.1	1	...	14.15	13.56	...
2012	1106_3_113	2 33 32.46	62 15 06.30		K6V	0.8	0	...	16.57	15.95	...
2012	1106_1_260	2 33 32.58	61 56 25.90	F9-G9	G6V	1.6	1	17.02	16.56	16.08	15.58
2012	1204_114	2 33 32.63	61 25 15.00	G0-G5	G3V	3.9	1	19.40	18.41	17.44	16.74
2012	1105_2_63	2 33 32.70	61 14 13.29	F8-F9	F9V	1.3	0	15.18	14.46	14.10	15.09
2012	1203_2_3	2 33 32.72	61 35 37.39	G5-G7	G6V	1.0	0	15.49	15.17	14.82	14.35
2012	1105_5_111	2 33 32.83	62 11 02.39	F2-F3	F2V	1.1	0	14.03	14.10	13.86	13.09
2012	0124_144	2 33 33.00	61 16 29.20		F7V	2.2	1	15.89	15.88	15.35	14.76
2012	0220_256	2 33 33.02	61 35 45.20	K3-K5	K4V	1.3	0	16.34	15.81	15.21	14.60
2012	1203_1_86	2 33 33.14	61 07 16.20	B9-A0	B9.5V	3.6	1	14.95	15.02	14.48	14.13
2012	1105_5_199	2 33 33.19	61 38 42.30	K4-K5	K4V	0.3	0	12.87	12.58	12.19	11.98
2012	1106_2_192	2 33 33.33	61 16 48.50	A7-A9	A8V	3.2	1	...	17.08	16.47	...
2012	0220_251	2 33 33.37	61 37 30.80	F4-F6	F5V	1.9	1	16.27	15.94	15.51	14.99
2012	1106_2_116	2 33 33.45	61 50 11.00	G7-G9	G9V	3.3	1	16.53	15.75	14.88	14.20
2012	1106_2_195	2 33 33.54	61 13 11.70	K0-K2	K1V	3.1	1	...	17.07	16.22	...
2012	0220_44	2 33 33.66	61 49 23.49	F0-F3	F1V	2.3	1	16.02	15.65	15.19	14.71
2012	0216_72	2 33 33.67	61 54 48.70	M2-M3	M2V	1.8	1	18.67	18.00	16.67	15.92
2012	0304_70	2 33 34.12	61 48 24.20	K0-K2	K1V	2.9	1	16.14	15.34	14.53	13.92
2011	0923_259	2 33 34.22	61 28 30.83	F7-F8	F8V	1.2	0	15.21	14.94	14.61	14.31
2012	1106_2_288	2 33 34.24	61 18 17.80	G9-K2	K0V	3.1	1	18.32	17.64	16.80	16.04
2012	1105_5_130	2 33 34.30	62 07 57.91	A5-A7	A6V	1.4	0	14.62	14.58	14.40	13.76

Table 1. IC 1805 Spectral Types and Photometry (Continued)

Year	Date_No.[a] (MMDD_No.)	RA(J2000) (hhmmss.ss)	Dec(J2000) (° ′ ″)	SpTy Range	SpTy	A_V (r-i) (mag)	Assoc.?[b] (ext)	V(90P)[c] (mag)	r[d] (mag)	i[d] (mag)	I(90P)[c] (mag)
2012	1106_2_125	2 33 34.62	61 40 06.10	F9-G5	G2V	2.3	1	17.65	17.09	16.48	15.88
2012	1106_2_271	2 33 34.90	61 24 45.10	K4-K5	K5V	0.8	0	16.69	16.10	15.58	15.04
2011	0923_244	2 33 34.90	61 35 32.56	A0-A1	A0V	1.9	1	14.28	14.21	14.03	13.52
2012	1106_3_134	2 33 34.98	62 04 47.40	F8-G0	F9V	1.5	0	...	16.79	16.39	...
2011	0923_37	2 33 35.03	61 21 36.47		F6V	2.0	1	15.68	15.33	14.86	14.40
2012	1105_5_140	2 33 35.10	62 05 02.30		A1V	1.9	1	15.82	15.76	15.55	15.58
2012	0220_43	2 33 35.17	61 59 58.81		A2V	2.1	1	16.07	15.83	15.56	15.05
2012	0304_30	2 33 35.19	61 37 53.20		F8V	1.6	1	16.04	15.74	15.33	14.85
2011	1023_93	2 33 35.61	61 35 38.40		B8V	2.1	1	13.87	13.81	13.65	13.14
2012	0304_62	2 33 35.64	61 59 55.40	G6-G7	G7V	0.9	0	14.34	13.96	13.62	13.11
2012	1105_2_267	2 33 35.71	61 33 60.00	F6-F7	F7V	1.1	0	14.57	14.29	13.98	13.87
2012	1106_1_259	2 33 35.81	61 52 23.30	G8-K2	K1V	3.5	1	18.13	17.34	16.40	15.70
2012	1104_110	2 33 35.86	61 19 11.14		F8V	1.0	0	14.04	13.79	13.50	12.93
2012	0304_168	2 33 35.92	61 29 58.00	G3-G6	G4V	1.4	0	16.37	16.07	15.63	15.10
2012	1106_1_19	2 33 35.94	61 44 57.71	G7-K2	G9V	3.7	1	18.45	17.59	16.62	15.90
2012	1105_2_240	2 33 36.00	61 50 43.41	F4-F6	F5V	2.2	1	16.36	15.93	15.43	14.91
2011	1023_19	2 33 36.32	61 43 18.00	B6-B8	B8V	3.1	1	15.14	14.86	14.49	14.11
2012	1105_2_234	2 33 36.54	61 54 17.50	F4-F7	F5V	2.1	1	16.42	16.00	15.52	14.99
2012	1204_66	2 33 36.57	61 45 52.03	A9-F0	A9V	2.3	1	16.00	15.63	15.21	14.69
2012	1105_4_8	2 33 36.62	62 25 22.10	A3-A8	A6V	0.1	0	13.18	13.35	13.44	12.46
2012	1106_1_131	2 33 36.64	61 38 48.50	G8-K2	G9V	2.5	1	17.75	16.63	15.92	15.68
2012	1104_22	2 33 36.66	61 25 19.24	F2-F3	F3V	1.5	0	14.68	14.42	14.09	13.60
2012	1106_3_148	2 33 36.75	62 00 18.90	F2-F5	F3V	2.1	1	17.10	16.70	16.26	15.73
2012	1105_3_35	2 33 36.82	61 51 53.50	K4-K5	K4V	0.4	0	15.39	14.87	14.46	13.95
2012	1105_3_33	2 33 36.97	61 53 46.60	K4-K5	K4V	0.9	0	16.24	15.64	15.14	14.65
2012	1105_5_108	2 33 37.00	62 21 46.21	G5-K3	K1V[g]	2.8	1	15.48	14.66	13.87	13.16
2011	1023_161	2 33 37.11	61 06 19.03		K2V	0.9	0	15.97	15.27	14.87	14.69
2012	0304_74	2 33 37.30	61 43 28.80	G9-K0	G9V	1.0	0	16.12	15.69	15.30	14.88
2011	1023_126	2 33 37.52	61 27 28.56	K1-K4	K2V	4.7	0	...	17.39	16.18	...
2012	1105_3_34	2 33 37.55	61 47 22.40	B9-A0	A0V	2.5	1	15.98	15.75	15.42	14.95
2012	1105_2_12	2 33 37.65	61 12 14.70	F9-G0	F9V	1.4	0	15.93	15.68	15.30	14.91
2011	1023_94	2 33 37.75	61 39 51.00	G9-K2	K1V	3.3	1	13.75	13.25	12.35	12.17
2012	1105_2_256	2 33 37.96	61 38 38.60	G8-K2	K2V[g]	2.9	1	15.18	14.28	13.45	13.27
2012	0124_5	2 33 38.01	61 45 59.51	A5-A9	A9V	2.4	1	...	17.34	16.92	...
2012	0304_277	2 33 38.07	61 19 53.20	M0-M2	M0V	0.5	0	15.82	15.20	14.39	14.08
2012	1106_1_253	2 33 38.09	61 47 36.40	K3-K5	K4V	1.5	0	17.69	16.98	16.34	15.76
2012	0216_168	2 33 38.37	61 21 00.90	M2-M4	M3V	1.9	1	20.30	19.55	18.04	17.19
2012	0220_281	2 33 38.38	61 29 21.30		B3V	4.9	0	16.06	15.53	14.83	14.35
2012	1104_201	2 33 38.61	62 04 15.30	F8-G0	F9V	1.1	0	14.92	14.97	14.66	13.98
2012	1204_88	2 33 38.62	61 33 10.94	G0-G1	G1V	1.3	0	15.78	15.47	15.09	14.61
2012	1105_2_259	2 33 38.62	61 37 34.70	B9-A0	B9V	1.8	1	14.26	14.19	14.05	13.59
2012	1106_1_135	2 33 38.66	61 24 56.00	G1-G7	G4V	1.6	0	17.99	17.41	16.95	16.39
2012	0304_90	2 33 38.87	61 40 15.00	B7-B9	B8V	2.2	1	14.57	14.45	14.27	13.83
2012	1106_3_187	2 33 39.10	61 44 53.50	G7-G9	G8V	2.5	1	17.91	17.30	16.60	16.00
2012	1203_1_225	2 33 39.56	61 48 47.91	G9-G2	K2V	1.2	0	16.57	16.09	15.62	15.11
2012	1105_5_290	2 33 39.59	61 43 59.10	F9-K0	G5V	3.5	1	...	17.55	16.68	...
2012	1203_1_270	2 33 39.61	61 29 38.23	B9-A0	B9V	4.2	0	16.38	15.87	15.23	14.64
2012	1106_3_192	2 33 39.76	61 41 08.60	K0-K2	K1V[g]	2.5	1	17.89	17.19	16.47	15.84
2012	1105_4_31	2 33 39.78	62 16 34.80	G5-G8	G7V	0.5	0	...	11.46	11.21	...
2012	1106_1_255	2 33 39.79	61 55 30.09	G7-K0	G9V[g]	2.9	1	16.94	16.21	15.42	14.76
2012	1105_2_291	2 33 40.03	61 39 38.10	B9-A0	B9.5V	2.2	1	15.14	14.95	14.71	14.43
2012	1105_5_118	2 33 40.07	62 12 20.30	B6-B8	B8V	1.4	0	13.30	13.82	13.81	12.90
2012	1105_3_43	2 33 40.15	62 08 00.20	F2-F3	F2V	1.5	0	15.02	14.85	14.53	13.85
2012	1105_4_117	2 33 40.20	61 40 30.09	A7-F0	A9V	2.1	1	15.97	15.68	15.30	14.86
2011	1023_104	2 33 40.28	61 35 33.10	A0-A2	A2V	2.2	1	15.56	15.39	15.09	14.55
2012	0220_297	2 33 40.39	61 34 29.00		A2V	1.3	0	12.91	12.79	12.68	12.39
2012	1105_3_188	2 33 40.48	61 25 19.51		F8V	1.4	0	15.69	15.45	15.08	14.57
2012	1105_2_241	2 33 40.54	61 42 18.50	A1-A2	A1V	2.2	1	15.58	15.40	15.13	14.73
2012	1104_206	2 33 40.55	61 53 48.20	G3-G8	G6V	1.5	0	16.05	15.58	15.11	14.61
2012	1203_2_14	2 33 40.79	61 30 44.99	B9-A0	A0V	2.6	1	15.42	15.18	14.85	14.41
2011	1023_11	2 33 40.86	61 40 51.40		A1V	2.6	1	15.23	14.94	14.58	14.25
2012	1204_278	2 33 40.86	61 04 26.62	A1-A2	A2V	3.5	1	...	16.49	15.92	...
2012	0124_46*	2 33 41.00	61 59 24.01	B5-B8	B7V	2.9	1	14.72	14.45	14.13	13.65
2012	1105_3_184	2 33 41.11	61 21 19.30	G5-G8	G6V	3.4	1	15.77	15.00	14.13	14.18
2012	0220_197	2 33 41.19	61 24 54.20	K0-K2	K1V	0.6	0	15.03	14.64	14.31	14.19
2012	0124_129	2 33 41.27	61 28 13.50		F7V	1.1	0	14.50	14.22	13.92	13.44
2012	1203_1_45	2 33 41.45	61 25 01.63	K4-K5	K4V	1.0	0	16.16	15.75	15.22	14.60
2012	0216_124	2 33 41.50	61 34 58.50	K7-M1	M0V	2.0	1	20.34	19.40	18.28	17.39
2012	1105_4_41	2 33 41.53	62 13 23.00	B4-B9	B7V	1.3	0	12.98	13.41	13.42	12.60
2012	1105_4_48	2 33 42.23	62 14 45.20	G8-K2	K2V[g]	2.1	1	14.62	14.35	13.70	12.90
2012	1106_1_269	2 33 42.25	61 46 18.50	K4-K5	K4V	1.2	0	17.30	16.72	16.13	15.55
2012	1105_5_196	2 33 42.41	61 39 10.90	G8-K1	G9V[g]	2.6	1	15.92	15.26	14.53	14.24
2012	0304_21	2 33 42.57	61 35 29.60	G2-G4	G3V	...	...	15.65	...	...	14.43
2012	1106_1_270	2 33 42.72	61 48 17.70	K4-K5	K4V	1.1	0	17.20	16.53	15.97	15.44
2012	1106_1_257	2 33 42.84	62 07 18.40	F5-F7	F6V	1.7	1	...	16.92	16.51	...
2012	0220_50	2 33 42.88	61 51 37.01		F4V	2.1	1	15.64	15.27	14.81	14.31
2012	1105_3_173*	2 33 42.94	61 18 31.50	B9-A0	B9.5V	3.5	1	15.18	14.34	13.83	14.48
2012	1106_2_137	2 33 43.15	61 35 03.70	K0-K3	K2V[g]	2.9	1	17.43	16.63	15.80	15.11
2012	1105_4_109	2 33 43.16	61 51 28.81	A1-A2	A1V	2.5	1	15.91	15.74	15.41	14.77
2012	1105_4_24	2 33 43.48	61 47 41.60	F5-F7	F6V	2.2	1	16.06	15.61	15.09	14.55
2012	1106_2_206	2 33 43.58	61 05 30.30	F6-F8	F7V	3.7	1	...	17.31	16.46	...
2012	1104_207*	2 33 43.61	61 57 10.50	A5-A9	A7V	2.1	1	15.50	15.20	14.84	14.38
2012	1105_2_64	2 33 43.79	61 17 00.70	B8-A0	B9V	3.4	1	15.97	15.98	15.51	14.98
2012	1105_5_22	2 33 43.93	62 19 10.50		K6V	...	0	13.07	...	...	12.00
2012	1203_1_56	2 33 44.31	61 23 10.31	F4-F5	F4V	2.2	1	16.10	15.70	15.21	14.71
2011	0923_300	2 33 44.38	61 45 51.84	K0-K3	K3V	1.5	0	...	9.77	9.19	...
2012	0124_29	2 33 44.53	61 25 38.50	F6-F8	F7V	1.4	0	14.76	14.47	14.10	13.60

Table 1. IC 1805 Spectral Types and Photometry (Continued)

Year	Date_No.[a] (MMDD_No.)	RA(J2000) (hhmmss.ss)	Dec(J2000) (° ′ ″)	SpTy Range	SpTy	A_V (r-i) (mag)	Assoc.?[b] (ext)	V(90P)[c] (mag)	r[d] (mag)	i[d] (mag)	I(90P)[c] (mag)
2012	1104_109	2 33 44.55	61 26 56.51		F1V	1.8	1	14.86	14.46	14.10	13.90
2012	1105_3_49	2 33 44.56	61 54 54.50	F4-F6	F4V	2.0	1	16.16	15.77	15.33	14.80
2012	1106_2_112	2 33 44.79	61 55 09.40	G9-K2	K0V	2.2	1	18.31	17.57	16.91	16.40
2012	1105_2_268	2 33 44.82	61 35 07.70	G8-G9	G8V	0.7	0	14.75	14.44	14.13	13.65
2012	1105_5_274*	2 33 45.04	62 02 47.71	A1-A3	A2V	1.9	1	14.35	14.26	14.04	13.38
2012	1105_5_123	2 33 45.12	62 07 21.80	A9-F3	F2V	1.4	0	15.07	14.61	14.32	13.87
2012	1204_110	2 33 45.12	61 28 25.56	F6-F7	F7V	1.7	1	15.94	15.58	15.16	14.64
2012	0220_37	2 33 45.19	61 41 28.20		F0V	2.1	1	15.70	15.37	14.97	14.55
2012	1105_3_45	2 33 45.32	62 07 35.91	G5-G8	G7V	1.0	0	15.78	15.69	15.34	14.65
2012	1105_4_69	2 33 45.34	62 07 26.59	F6-F7	F6V	1.0	0	14.91	14.45	14.18	13.74
2012	1106_1_25	2 33 45.43	61 37 59.59	G8-K0	K0V	2.3	1	16.52	15.93	15.27	14.84
2012	1106_1_262	2 33 45.45	61 52 11.30	F7-F8	F8V	2.2	1	16.87	16.42	15.88	15.35
2012	0220_46	2 33 45.64	61 46 13.40		B8V	2.8	1	15.10	14.85	14.54	14.07
2012	1203_1_32	2 33 45.68	61 27 53.04	K6-M0	K6V	2.6	1	19.80	18.67	17.68	17.00
2012	1203_2_108	2 33 45.95	61 21 30.25		F7V	2.0	1	16.20	15.81	15.32	14.77
2012	1105_3_42	2 33 45.95	61 51 41.70	B9-A0	A0V	3.0	1	16.16	15.82	15.40	14.89
2012	1104_210	2 33 46.21	61 54 36.70	F3-F5	F5V	1.9	1	16.08	15.68	15.25	14.78
2012	1106_2_140	2 33 46.33	61 35 51.10	G8-K1	K0V	2.2	1	17.07	16.50	15.86	15.21
2012	1106_1_139	2 33 46.41	61 13 40.50	F4-F7	F5V	2.6	1	...	16.91	16.32	...
2012	1106_3_115	2 33 46.64	62 19 06.90	G7-K1	G8V	3.4	1	...	16.97	16.09	...
2012	1104_285	2 33 46.83	62 09 10.31	F4-F7	F6V	1.3	0	14.88	14.47	14.14	13.61
2012	1105_4_106	2 33 46.87	61 52 45.20	G9-K2	K2V[g]	2.4	1	15.12	14.43	13.71	13.11
2011	1023_116	2 33 46.89	61 30 33.90	B6-B9	B8V	2.1	1	13.58	13.49	13.32	12.88
2012	0220_287	2 33 47.07	61 29 04.60	F8-G0	F9V	1.5	0	16.50	16.11	15.72	15.21
2012	1106_2_183	2 33 47.17	61 19 22.70	G8-K1	K0V	2.2	1	17.50	16.93	16.28	15.65
2012	1204_127*	2 33 47.18	61 22 53.24	A9-F0	A9V	3.2	1	16.12	15.64	15.05	14.51
2012	1105_5_173*	2 33 47.19	61 52 22.69	B9-A0	B9.5V	1.8	1	13.55	13.36	13.23	12.81
2012	1105_4_103	2 33 47.32	61 49 47.50	A9-F3	F1V	1.9	1	15.17	14.86	14.47	13.98
2012	1203_1_71	2 33 47.40	61 06 51.30	G5-G7	G6V	1.3	0	14.97	15.02	14.61	14.56
2012	1105_3_186	2 33 47.53	61 26 17.29	F1-F2	F2V	0.9	0	13.49	13.37	13.19	12.71
2012	1105_4_65	2 33 47.61	62 06 35.70	G5-K0	G8V	1.9	1	14.54	14.24	13.69	12.81
2012	0220_205	2 33 47.76	61 28 23.40		F8V	1.1	0	13.44	13.31	13.01	12.55
2012	1105_3_255	2 33 48.07	61 42 03.81		M3V[g]	2.8	1	13.61	12.83	11.13	11.62
2012	1203_1_292	2 33 48.36	61 49 27.38	G5-G7	G6V	1.9	1	16.46	15.97	15.42	14.86
2012	1106_1_137	2 33 48.36	61 28 37.80	G9-K2	K0V	2.7	1	17.83	17.34	16.58	15.88
2012	0124_45	2 33 48.37	61 53 36.00	F6-F8	F7V	0.9	0	14.26	14.01	13.76	13.36
2012	0304_275	2 33 48.44	61 08 55.60	F9-G2	G0V	1.6	1	15.19	14.41	13.98	15.06
2012	0304_161	2 33 48.45	61 18 14.01	F5-F7	F6V	2.4	1	15.96	15.86	15.31	14.87
2012	1106_3_143	2 33 48.45	61 59 32.91	G1-K0	G9V	3.3	1	17.98	17.17	16.30	15.63
2012	1105_3_187	2 33 48.60	61 31 25.30	B9-A1	A0V	2.9	1	16.43	16.18	15.79	15.26
2012	1105_3_258	2 33 48.66	61 41 01.40	G6-G9	G8V	...	...	15.57	15.72	...	14.06
2012	1105_5_284	2 33 48.68	61 44 48.90	F0-F3	F2V	0.8	0	13.69	13.40	13.24	12.59
2012	1106_1_125	2 33 48.85	61 41 10.19	A9-F1	F0V	3.1	1	...	17.61	17.00	...
2012	0304_66	2 33 48.88	62 02 02.59	F0-F1	F0V	2.1	1	14.95	14.94	14.54	13.72
2012	0220_45	2 33 48.88	61 53 07.60	F3-F4	F4V	2.2	1	15.59	15.21	14.73	14.21
2012	1203_1_75	2 33 49.06	61 08 46.40	F8-G1	F9V	2.7	1	...	16.02	15.37	...
2012	0220_9	2 33 49.07	62 00 00.10	G7-G9	G8V	1.5	0	16.41	15.92	15.44	14.89
2012	1105_4_9	2 33 49.09	62 13 19.60	G8-K0	G8V	0.7	0	14.14	14.19	13.89	13.21
2012	1204_73	2 33 49.10	61 35 51.34	A7-A8	A7V	2.0	1	15.42	15.22	14.89	14.35
2012	1204_70	2 33 49.23	61 46 44.38	F6-F7	F7V	2.0	1	16.08	15.64	15.15	14.66
2012	1105_4_112	2 33 49.38	61 44 07.01	A3-A5	A3V	2.5	1	16.13	15.88	15.51	15.06
2012	1203_1_76	2 33 49.38	61 13 47.50	F2-F5	F4V	1.5	0	...	14.88	14.56	...
2012	1105_3_47	2 33 49.43	61 53 49.90	A2-A5	A3V	2.5	1	16.10	15.82	15.46	14.99
2012	1106_1_97	2 33 49.64	61 43 53.09		K6V	1.7	1	18.49	17.74	16.94	16.33
2011	0923_245	2 33 49.66	61 33 51.40	F6-F9	F8V	1.3	0	14.55	14.16	13.81	13.53
2012	1204_63	2 33 49.75	61 42 53.66	G3-G5	G4V	1.4	0	15.41	15.01	14.57	14.24
2012	1104_104	2 33 49.75	61 23 13.49	F7-F9	F8V	3.1	1	...	16.68	15.96	...
2012	1105_5_278	2 33 49.95	62 01 55.40	A6-A8	A7V	2.3	1	15.19	15.24	14.91	14.23
2012	1105_5_107	2 33 50.20	62 22 12.30	G7-K1	G9V	0.9	0	15.29	15.22	14.86	13.70
2012	1106_2_111	2 33 50.21	61 46 26.39	F9-G9	G6V	3.5	1	17.30	16.47	15.60	14.93
2012	1106_2_197	2 33 50.49	61 10 47.21	A5-A8	A6V	3.5	1	...	16.96	16.35	...
2012	0304_96	2 33 50.55	61 40 20.60	F7-F8	F8V	1.4	0	13.13	13.40	13.03	12.48
2012	1104_289	2 33 51.20	61 57 07.20	B9-A0	A0V	1.9	1	14.07	13.93	13.74	13.32
2012	1105_3_285	2 33 51.23	61 37 05.50	B9-A0	B9.5V	2.2	1	14.88	14.71	14.49	14.11
2012	1105_4_118	2 33 51.33	61 40 09.30	A0-A1	A1V	2.2	1	16.49	16.33	16.07	15.57
2012	1105_5_113	2 33 51.45	62 13 21.49	G4-K0	G8V[g]	2.4	1	13.04	13.24	12.58	11.83
2012	1204_115	2 33 51.66	61 24 15.88	F9-G7	G2V	4.0	1	19.57	18.83	17.85	17.06
2012	1203_2_17	2 33 51.76	61 25 25.91	K4-K5	K4V	2.2	1	17.51	16.82	16.03	15.42
2012	1203_1_252	2 33 51.76	61 33 55.11	G4-G6	G5V	2.4	1	16.82	16.25	15.60	14.98
2012	0124_48	2 33 51.87	62 01 57.40	F4-F7	F6V	1.4	0	14.94	14.67	14.31	13.54
2012	1203_1_73	2 33 52.12	61 06 55.42	B9-A0	A0V	3.3	1	...	16.06	15.58	...
2012	1106_3_131	2 33 52.21	62 02 07.61	G7-K0	K0V	1.3	0	...	17.35	16.88	...
2012	0220_39	2 33 52.29	61 38 40.30	F5-F6	F6V	1.6	1	16.26	15.95	15.56	15.05
2012	1204_145	2 33 52.38	61 07 55.42	A1-A2	A1V	3.5	1	...	16.07	15.52	...
2012	1106_1_140	2 33 52.40	61 13 38.40	G0-K2	G6V	1.9	1	...	16.62	16.07	...
2011	1023_146	2 33 52.56	61 20 49.20	A8-F0	A9V	1.1	0	13.53	13.41	13.24	12.70
2012	1105_5_166	2 33 52.66	61 59 19.30		K7V[g]	2.8	1	13.08	12.40	11.27	11.71
2012	0304_69	2 33 52.68	61 57 10.10	A1-A3	A2V	2.1	1	15.14	14.94	14.66	14.19
2012	1203_1_35	2 33 52.71	61 26 17.80	K2-K5	K4V	2.3	1	17.66	17.34	16.53	15.68
2012	0220_207	2 33 52.92	61 27 53.20		F6V	1.1	0	14.04	13.78	13.49	13.00
2012	0220_188	2 33 53.27	61 18 26.50	B2-B3	B2V	3.1	1	13.57	13.48	13.19	12.42
2012	1106_1_264	2 33 53.42	61 56 16.10	A9-F2	F2V	2.6	1	17.32	16.83	16.28	15.72
2011	1023_129	2 33 53.93	61 27 19.27	F3-F7	F5V	2.1	1	...	17.18	16.70	...
2012	1106_3_191	2 33 54.29	61 31 46.60	K1-K4	K2V	2.8	1	18.34	17.72	16.92	16.16
2012	1106_3_140	2 33 54.35	62 04 42.29	F9-G5	G2V	1.4	0	...	16.99	16.56	...
2012	1105_4_58	2 33 54.44	62 10 25.30	G0-G6	G2V	0.8	0	14.90	14.95	14.66	13.86
2012	1106_1_36	2 33 54.44	61 47 33.40	G5 -G9	G7V[g]	3.9	1	16.87	15.94	14.96	14.27

Table 1. IC 1805 Spectral Types and Photometry (Continued)

Year	Date_No.[a] (MMDD_No.)	RA(J2000) (hhmmss.ss)	Dec(J2000) (° ′ ″)	SpTy Range	SpTy	A_V (r-i) (mag)	Assoc.?[b] (ext)	V(90P)[c] (mag)	r[d] (mag)	i[d] (mag)	I(90P)[c] (mag)
2012	1203_2_30	2 33 54.53	61 16 43.64	F9-G0	G0V	1.7	1	...	15.92	15.46	...
2012	0304_164	2 33 54.58	61 25 10.80	G0-K0	G5V	...	...	16.39	...	...	14.86
2012	1203_1_296	2 33 54.67	61 48 01.18	B9-A0	A0V	2.5	1	15.14	14.91	14.61	14.12
2012	0220_7	2 33 54.76	61 56 53.49		B9V	2.1	1	14.55	14.41	14.21	13.79
2012	1105_5_192*	2 33 54.79	61 38 55.30	A7-A9	A8V	1.7	1	14.79	14.50	14.20	14.09
2011	1023_27	2 33 55.22	61 25 10.60	F9-G0	F8V	0.8	0	13.33	13.25	13.00	12.55
2012	1104_91	2 33 55.28	61 24 35.35	G7-G9	G8V	4.4	0	16.15	15.13	14.04	13.79
2012	1204_65	2 33 55.52	61 44 59.97		K6V	1.1	0	16.19	15.52	14.83	14.23
2012	1203_2_87	2 33 55.53	61 26 54.96	K0-K5	K4V	2.0	1	18.85	18.13	17.39	16.60
2012	1106_1_44	2 33 55.71	61 45 15.30	F4-F7	F6V	2.6	1	18.02	17.50	16.89	16.24
2012	1203_2_42	2 33 55.92	61 47 19.07	G8-K0	G9V	0.7	0	15.08	14.71	14.39	14.00
2012	1104_134*	2 33 56.19	61 38 57.95	B9-A0	A0V	1.7	1	14.63	14.48	14.33	14.16
2012	1105_3_9	2 33 56.26	62 06 09.80	G5-G8	G7V	0.9	0	15.82	15.57	15.23	14.57
2012	1105_5_156	2 33 56.47	62 01 09.20	F4-F6	F4V	1.2	0	15.05	14.51	14.24	13.81
2012	0304_61	2 33 56.53	61 51 54.71	G8-G9	G9V	2.6	1	15.35	14.70	13.98	13.35
2012	1106_3_147	2 33 57.03	62 00 23.80	F3-F7	F6V	2.3	1	17.63	17.18	16.64	16.02
2011	0923_270	2 33 57.20	61 26 27.81	B7-B9	B8V	2.5	1	14.90	14.64	14.39	14.22
2012	1106_2_142	2 33 57.44	61 35 43.30	K4-K5	K5V	1.5	0	18.11	17.42	16.75	16.14
2012	1105_3_215	2 33 57.45	61 38 20.40	G8-K0	G9V[g]	1.8	1	14.39	13.71	13.15	12.99
2012	1106_2_178	2 33 57.49	61 23 24.20	F1-F3	F2V	2.5	1	17.17	16.69	16.17	15.60
2012	1106_1_136	2 33 57.49	61 19 50.40	B9-A0	B9.5V	3.3	1	16.95	16.62	16.15	15.58
2012	0124_139	2 33 57.64	61 16 03.30	G4-G9	G9V	1.3	0	14.19	14.10	13.65	13.01
2012	1105_5_25	2 33 57.95	62 07 27.80	F8-F9	F8V	1.5	0	15.16	14.93	14.54	13.85
2012	1106_1_267	2 33 57.97	61 52 33.80	F9-G7	G6V	1.8	1	17.26	16.79	16.26	15.71
2012	1105_5_138	2 33 58.01	62 06 30.10	F8-G0	F8V	1.4	0	14.97	14.74	14.37	13.64
2012	0124_9	2 33 58.30	61 53 37.40	G6-K0	G7V	3.2	1	16.34	15.55	14.73	14.07
2012	1105_5_183	2 33 58.53	61 45 25.60	G8-K0	G9V[g]	2.9	1	15.69	14.93	14.15	13.65
2012	1204_108	2 33 58.56	61 28 51.68	F0-F2	F1V	2.3	1	16.08	15.71	15.25	14.76
2012	1105_2_243	2 33 58.71	61 44 19.10	F2-F3	F2V	2.0	1	15.82	15.47	15.05	14.53
2012	0304_68	2 33 58.79	62 03 43.90	B8-B9	B9V	2.2	1	15.04	15.19	14.97	14.32
2012	1105_3_205	2 33 58.85	61 36 15.90	G8-K2	K0V	1.5	0	14.66	13.99	13.49	12.73
2012	1105_3_290	2 33 59.01	61 35 22.20	F9-G0	G0V	1.5	0	16.19	15.88	15.46	14.98
2012	0216_147	2 33 59.01	61 27 25.00	K6-K8	K7V	2.3	1	19.46	18.46	17.45	16.67
2012	0124_95	2 33 59.37	61 33 12.10	F8-F9	F8V	1.6	1	16.46	16.14	15.73	15.19
2012	1106_2_153	2 33 59.51	61 28 47.39	F2-F3	F2V	2.6	1	17.16	16.71	16.16	15.61
2012	1203_1_36	2 33 59.68	61 27 19.02	K2-K5	K4V	2.5	1	18.32	17.64	16.79	16.14
2012	1106_1_27	2 33 59.76	61 33 08.90	G8-K2	K0V[g]	3.1	1	17.21	16.49	15.64	14.95
2011	1023_97	2 34 00.08	61 39 49.17	G4-G9	G5V	2.8	1	14.81	14.19	13.45	13.52
2012	1105_3_36	2 34 00.16	61 42 52.60	K4-K5	K4V	1.2	0	16.45	15.86	15.29	14.81
2012	1106_1_268	2 34 00.39	62 00 04.70	K2-K4	K4V	0.7	0	16.96	16.45	15.98	15.44
2011	1023_153	2 34 00.41	61 10 30.35		F9V	2.1	1	15.17	15.04	14.52	14.08
2012	1204_92	2 34 00.42	61 32 15.30	G6-K6	K0V	2.2	1	19.34	18.62	17.96	17.01
2012	1105_3_7	2 34 00.43	62 07 18.70	F6-F7	F7V	0.0	0	13.45	13.69	13.63	12.68
2012	0220_48	2 34 00.83	61 42 45.29	A1-A2	A1V	2.2	1	15.86	15.70	15.43	15.00
2012	1105_3_280	2 34 00.91	61 39 47.91	K0-K2	K1V	1.0	0	16.39	16.00	15.59	15.04
2012	1106_1_56	2 34 01.17	61 45 08.41	K4-K5	K4V	1.4	0	17.16	16.50	15.89	15.30
2011	0923_256	2 34 01.40	61 31 07.33		A1V	1.7	1	13.32	13.42	13.27	12.80
2012	1203_1_236	2 34 01.43	61 44 31.90	F2-F3	F2V	1.9	1	15.10	14.77	14.38	13.96
2012	1105_3_41	2 34 01.45	61 47 36.90	B9-A0	B9.5V	2.4	1	13.52	13.33	13.06	12.59
2011	1023_163	2 34 01.65	61 01 58.54	G4-K0	G6V	1.3	0	15.47	15.12	14.70	14.63
2012	1106_1_42	2 34 01.71	61 47 32.00	K3-K5	K4V	1.4	0	17.65	17.25	16.64	15.82
2012	0124_135*	2 34 01.71	61 12 09.20	B9-A1	A1V	2.7	1	14.94	14.41	14.04	13.87
2012	1203_2_126	2 34 01.81	61 06 08.92	F0-F3	F4V	3.0	1	...	16.54	15.89	...
2012	1106_1_21	2 34 02.24	61 23 44.30	A6-A9	A7V	3.1	1	17.01	16.57	16.01	15.37
2012	1106_1_34	2 34 02.63	61 50 16.60	G2-K1	G8V	3.2	1	17.60	16.83	16.00	15.36
2012	1106_2_284	2 34 02.69	61 15 43.20	A2-A4	A3V	3.8	1	...	17.19	16.54	...
2012	0304_157	2 34 02.87	61 26 22.00	G7-G9	G8V	2.3	1	14.52	13.67	13.02	13.48
2012	0220_41	2 34 02.93	61 48 33.51	G7-G9	G8V	3.0	1	16.24	15.51	14.71	14.21
2012	1106_1_4	2 34 03.18	61 52 38.20	G9-K2	K2V	3.3	1	18.02	17.18	16.26	15.54
2012	1105_4_68	2 34 03.24	62 08 12.30		K5V[g]	3.3	1	15.87	15.08	14.02	12.90
2012	1203_1_72	2 34 03.24	61 11 41.26	K7-K8	K7V	2.0	1	...	16.86	15.91	...
2012	1106_2_129	2 34 03.29	61 45 33.21	M1-M2	M2V	0.5	0	17.63	16.91	15.87	15.23
2012	0216_71	2 34 03.39	61 53 21.80	K7-M1	M0V	1.5	0	19.59	18.77	17.74	17.00
2012	1104_212	2 34 03.43	62 00 12.50	F2-F5	F4V	1.6	1	15.62	15.26	14.90	14.38
2012	1105_5_120	2 34 03.48	62 15 05.60	F8-G0	F9V	1.4	0	15.96	15.93	15.56	14.83
2012	1105_4_26	2 34 03.58	61 43 58.30	A7-F0	A9V	2.1	1	14.92	14.59	14.23	14.05
2012	0220_173	2 34 04.13	61 16 37.50	G7-G8	G7V	1.2	0	14.94	14.92	14.52	13.59
2012	1105_4_43	2 34 04.26	62 16 43.20		F8V	0.4	0	13.40	13.58	13.42	12.91
2012	1105_4_12	2 34 04.30	62 06 01.60	F3-F5	F4V	1.4	0	15.56	15.53	15.21	14.55
2012	1204_139	2 34 04.36	61 14 56.77		F8V	2.3	1	15.79	15.65	15.08	14.52
2012	1104_93	2 34 04.59	61 24 34.06	G9-K1	K0V	1.2	0	16.48	16.13	15.69	15.20
2012	0216_140	2 34 04.75	61 30 34.70	M3-M4	M3V	2.3	1	19.70	19.11	17.51	16.70
2012	0216_27	2 34 04.83	61 32 34.61	K6-M1	K8V	2.2	1	20.37	19.48	18.43	17.66
2012	0220_185	2 34 05.13	61 26 40.90	G9-K0	K0V	1.1	0	15.11	14.36	13.95	14.16
2012	0124_101	2 34 05.46	61 29 51.71	G4-G8	G6V	0.6	0	14.76	14.41	14.13	13.90
2012	1106_1_33	2 34 05.46	61 48 45.00	G8-K2	K1V	1.7	1	17.53	16.99	16.44	15.88
2012	1105_3_5	2 34 05.66	61 58 43.60	F6-F7	F7V	1.5	0	16.03	15.70	15.32	14.85
2012	1106_3_194	2 34 05.91	61 37 01.50	G5-G8	G7V	2.3	1	17.26	16.70	16.06	15.48
2012	1106_3_166	2 34 06.07	61 53 36.50		K6V	1.4	0	18.42	17.76	17.01	16.33
2012	0220_5*	2 34 06.32	61 48 11.90	A8-A9	A9V	2.2	1	15.55	15.25	14.85	14.33
2012	1105_3_179	2 34 06.38	61 31 08.01		A2V	2.2	1	16.32	16.13	15.83	15.36
2011	1023_139	2 34 06.38	61 22 08.96	G1-G5	G3V	3.7	1	15.45	14.66	13.74	13.94
2012	1106_3_272	2 34 06.43	61 59 57.01	F6-F8	F7V	3.7	1	17.44	16.88	16.04	15.30
2011	1023_103	2 34 06.62	61 34 18.90	A6-A8	A7V	2.1	1	15.68	15.45	15.11	14.70
2012	0216_78	2 34 06.70	62 00 10.60	K6-M1	K7V	1.7	1	18.51	17.83	16.96	16.29
2012	1105_2_269	2 34 06.86	61 34 58.00	G8-G9	G8V	1.2	0	16.23	15.85	15.44	14.97
2012	1106_2_147	2 34 07.03	61 33 58.50	G0-G3	G1V	1.9	1	17.22	16.78	16.27	15.67

Table 1. IC 1805 Spectral Types and Photometry (Continued)

Year	Date_No.[a] (MMDD_No.)	RA(J2000) (hhmmss.ss)	Dec(J2000) (° ′ ″)	SpTy Range	SpTy	A_V (r-i) (mag)	Assoc.?[b] (ext)	V(90P)[c] (mag)	r[d] (mag)	i[d] (mag)	I(90P)[c] (mag)
2012	0216_154	2 34 07.28	61 23 22.50	K6-M1	K8V	2.2	1	20.06	19.00	17.96	17.21
2012	1105_3_189	2 34 07.31	61 36 29.51	A1-A2	A2V	1.9	1	15.40	15.25	15.03	14.67
2012	0220_288	2 34 07.39	61 28 19.30	M2-M4	M3V	1.7	1	16.48	15.93	14.46	14.14
2012	1204_80	2 34 07.52	61 38 57.20		F8V	1.8	1	15.71	15.29	14.83	14.49
2012	0304_135	2 34 07.56	61 32 52.10	G9-K0	K0V	2.6	1	15.92	15.24	14.51	14.01
2012	1104_100	2 34 07.67	61 29 33.70	A9-F3	F1V	1.8	1	16.05	15.80	15.44	14.95
2012	0304_67	2 34 07.70	62 02 05.40	G0-G2	G1V	1.1	0	14.57	14.32	13.99	13.31
2012	0304_274	2 34 07.78	61 29 38.10	K2-K4	K3V	1.4	0	16.00	15.44	14.88	14.54
2012	1106_3_171	2 34 07.79	61 45 40.00	G7-K0	G8V	3.2	1	18.42	17.70	16.87	16.13
2012	1105_4_46	2 34 07.85	62 18 41.50	F5-F6	F6V	1.4	0	15.53	15.54	15.19	14.47
2012	0304_170	2 34 08.14	61 16 36.20	A6-A8	A7V	2.1	1	15.01	14.86	14.52	14.59
2012	1105_3_176	2 34 08.20	61 27 59.80	A7-A8	A7V	2.7	1	16.18	15.83	15.36	14.84
2012	1106_3_121	2 34 08.27	62 12 12.99	F2-F6	F4V	2.7	1	...	16.74	16.15	...
2012	1204_149	2 34 08.29	61 06 41.58	K3-K5	K4V	1.4	0	...	16.46	15.85	...
2012	1203_2_44	2 34 08.48	61 49 15.02	G1-G8	G7V	1.5	0	16.24	15.84	15.37	14.96
2012	1104_116	2 34 08.94	61 40 36.62		G0V	1.7	1	16.37	15.98	15.52	15.00
2012	1106_2_175	2 34 08.95	61 20 50.70	F6-F8	F7V	2.6	1	17.16	16.71	16.09	15.45
2012	1203_1_232	2 34 09.34	61 47 41.39	G9-K3	K2V	0.8	0	15.26	14.88	14.50	14.29
2012	1105_5_148	2 34 09.77	62 04 25.31	B2-B4	B3V	2.9	1	15.68	14.61	14.33	14.35
2012	0220_3	2 34 09.80	61 46 47.10	G7-G8	G8V	3.2	1	15.26	14.47	13.63	13.55
2012	1105_4_50	2 34 09.87	62 17 41.50	F6-F7	F7V	1.2	0	14.01	14.14	13.82	13.10
2012	0304_13	2 34 10.27	61 42 46.30	G2-G3	G2V	1.6	1	16.35	15.99	15.54	15.01
2011	0923_263	2 34 10.27	61 24 40.42		B9V	2.6	1	14.24	13.85	13.56	13.03
2012	1105_3_3	2 34 10.39	61 50 36.80	G2-G6	G5V	1.8	1	16.11	15.62	15.09	14.78
2012	1106_1_26	2 34 10.50	61 39 06.60	G8-K0	K1V	1.4	0	16.55	16.10	15.60	15.11
2012	0220_33	2 34 10.59	61 35 53.71	B8-B9	B9V	2.3	1	15.49	15.36	15.14	14.67
2011	1023_144	2 34 10.79	61 20 26.07	K0-K2	K2V	3.2	1	15.57	14.77	13.87	13.66
2012	1106_1_118	2 34 11.18	61 37 13.00		K6V	1.1	0	18.40	17.71	17.03	16.48
2012	1203_1_77*	2 34 11.18	61 04 06.77	B4-B7	B7V	3.3	1	14.56	14.64	14.24	14.42
2012	0124_43	2 34 11.44	62 01 56.50	G7-K0	G8V	1.3	0	14.14	13.63	13.20	12.46
2011	1023_17	2 34 11.48	61 49 26.40		B9V	2.1	1	14.63	14.34	14.15	14.07
2012	1106_2_189	2 34 11.65	61 18 36.71	K1-K3	K2V	3.8	1	18.36	17.44	16.42	15.67
2012	0220_184	2 34 11.69	61 25 22.40	A6-A8	A7V	2.7	1	16.46	16.13	15.66	15.13
2012	1104_98	2 34 11.73	61 38 13.52	B9-A0	A0V	2.0	1	14.31	13.88	13.68	13.95
2012	1106_1_106	2 34 11.77	61 41 46.50	K1-K3	K2V[g]	3.0	1	17.07	16.31	15.46	14.79
2012	0304_63	2 34 11.78	62 00 43.90	G8-G9	G8V	3.1	1	15.72	15.28	14.47	13.63
2012	1105_2_250	2 34 11.78	61 47 32.00	G9-K2	G9V[g]	3.1	1	16.49	15.71	14.88	14.21
2012	1203_2_114	2 34 11.90	61 13 04.66	F2-F3	F3V	3.2	1	...	16.56	15.87	...
2012	0124_41	2 34 12.03	61 59 24.80	F4-F6	F5V	1.1	0	14.11	13.84	13.57	13.14
2012	1104_287	2 34 12.03	61 42 49.36		B9V	2.2	1	13.59	13.50	13.29	12.80
2011	0923_56	2 34 12.10	61 11 20.93	G0-G2	G1V	0.6	0	13.32	13.31	13.08	11.96
2012	0304_18	2 34 12.41	61 53 57.40	B7-B8	B8V	2.2	1	14.16	13.99	13.81	13.23
2012	0124_61	2 34 12.48	61 40 51.81	A5-A8	A5V	2.0	1	16.22	16.02	15.73	15.21
2012	1204_81	2 34 12.66	61 34 02.26	G8-K0	G9V	2.7	1	16.81	16.10	15.35	14.75
2012	0220_52	2 34 12.86	61 49 57.80	K5-K6	K6V	0.7	0	16.25	15.58	14.98	14.73
2012	0304_73	2 34 12.92	61 47 46.70	G8-K0	G9V	2.1	1	14.56	13.77	13.16	13.39
2012	0304_111	2 34 12.92	61 37 04.20	G7-G8	G8V	3.1	1	16.16	15.45	14.64	14.30
2012	1105_5_125	2 34 12.93	62 10 11.20	G4-K0	G7V	2.0	1	15.38	15.16	14.58	13.69
2012	1106_1_266	2 34 12.94	62 09 45.70	G1-G9	G6V	1.4	0	...	17.67	17.22	...
2011	0923_249	2 34 13.16	61 37 43.92		A3V	2.2	1	15.76	15.55	15.25	14.86
2012	1106_3_188	2 34 13.20	61 43 25.70	K1-K5	K2V	3.3	1	17.92	17.11	16.20	15.46
2012	1106_1_94	2 34 13.24	61 42 42.00	G8-K1	K0V[g]	3.6	1	16.54	15.66	14.71	14.22
2012	0304_14*	2 34 13.29	61 55 55.29	A5-A7	A6V	2.6	1	16.34	15.97	15.54	15.04
2012	1105_5_131	2 34 13.56	62 05 01.40	A6-A8	A7V	1.2	0	13.29	13.60	13.44	12.80
2012	1104_216	2 34 13.93	62 09 22.60	G6-K1	G8V	1.2	0	15.86	15.28	14.88	14.38
2012	1104_214	2 34 13.98	61 48 06.55		A0V	2.4	1	15.36	15.16	14.87	14.51
2012	1105_3_52	2 34 14.19	61 49 35.89	F3-F4	F2V	1.0	0	13.69	13.48	13.29	12.68
2012	0304_165	2 34 14.20	61 09 30.80	A0-A1	A1V	3.0	1	14.44	14.41	13.98	13.99
2012	1106_3_183	2 34 14.38	61 41 04.60	K2-K3	K3V	1.2	0	17.28	16.77	16.25	15.63
2012	0124_124*	2 34 14.48	61 24 27.10	B7-B9	B8V	2.3	1	14.42	14.28	14.08	13.56
2012	1105_2_251	2 34 14.52	61 37 25.70	F2-F4	F3V	2.3	1	16.36	15.96	15.48	15.00
2011	0923_233	2 34 14.81	61 42 11.70	B7-B9	B8V	1.7	1	13.47	13.38	13.29	12.71
2012	1105_4_33	2 34 14.82	62 22 27.20	F7-F8	F7V	1.3	0	15.37	15.40	15.07	14.36
2012	1105_2_51	2 34 15.02	61 14 28.80	M1-M2	M1V	0.3	0	15.71	15.32	14.39	13.32
2012	1203_1_231	2 34 15.04	61 42 01.54	K4-K6	K5V	2.5	1	19.11	18.25	17.37	16.70
2011	1023_134	2 34 15.06	61 23 56.20	G2-G7	G5V	1.5	0	14.98	14.58	14.13	14.04
2012	1106_2_139	2 34 15.06	61 37 43.90	K1-K5	K3V	2.8	1	17.59	16.78	15.93	15.27
2012	1204_12	2 34 15.17	61 46 47.41	G0-G7	G5V[g]	2.9	1	17.66	17.02	16.27	15.55
2012	1106_2_199	2 34 15.18	61 06 52.80	F4-F8	F7V	3.2	1	...	16.88	16.13	...
2012	1204_30	2 34 15.27	61 24 42.83	F6-F7	F5V	4.5	0	...	15.17	14.20	...
2012	1104_218	2 34 15.41	61 55 28.60	A5-A8	A7V	1.4	0	14.28	14.13	13.93	13.47
2012	1105_4_110	2 34 15.71	61 48 28.10	G8-K0	K0V	2.8	1	16.08	15.33	14.56	13.97
2012	0304_24	2 34 15.72	61 38 53.00	G0-G1	G0V	1.4	0	15.84	15.60	15.21	14.61
2012	0304_79	2 34 15.72	61 50 46.80	F5-F7	F6V	1.7	1	16.28	15.89	15.47	15.08
2012	1105_4_100	2 34 15.80	61 53 50.20	G0-G6	G1V	1.7	1	16.23	15.79	15.32	14.81
2012	1106_1_108	2 34 15.92	61 40 53.60	G5-G9	G7V	3.1	1	17.01	16.28	15.48	14.87
2012	0124_140	2 34 16.09	61 12 04.40	G5-G6	G5V	1.2	0	13.98	14.02	13.64	12.66
2012	1104_96	2 34 16.15	61 30 03.74	F6-F8	F7V	1.7	1	16.30	15.95	15.52	14.99
2012	1105_5_30	2 34 16.15	62 21 26.20	A6-A8	A7V	2.7	1	14.58	13.88	13.39	13.74
2012	1106_2_158	2 34 16.22	61 29 48.90	K1-K3	K2V	3.2	1	17.86	17.07	16.18	15.46
2012	0304_65	2 34 16.27	62 04 03.20	F4-F6	F5V	1.7	1	15.27	15.34	14.94	14.02
2012	1203_1_63	2 34 16.84	61 13 08.86	F2-F3	F2V	2.2	1	15.23	15.18	14.73	14.30
2012	1106_3_189	2 34 16.92	61 42 05.61	G9-K2	K0V	2.0	1	18.25	17.58	16.96	16.22
2012	1104_220	2 34 17.02	61 47 04.85		B9V	2.4	1	15.22	15.03	14.77	14.44
2012	1203_2_89	2 34 17.08	61 26 54.84	K4-K5	K5V	1.1	0	17.15	16.53	15.95	15.41
2012	0216_136	2 34 17.21	61 30 52.41	K6-M1	K8V	1.7	1	20.20	19.53	18.59	17.77
2012	1105_4_57	2 34 17.38	62 11 17.01	A1-A5	A2V	2.6	1	15.72	15.59	15.21	14.45

Table 1. IC 1805 Spectral Types and Photometry (Continued)

Year	Date_No.[a] (MMDD_No.)	RA(J2000) (hhmmss.ss)	Dec(J2000) (° ′ ″)	SpTy Range	SpTy	A_V (r-i) (mag)	Assoc.?[b] (ext)	V(90P)[c] (mag)	r[d] (mag)	i[d] (mag)	I(90P)[c] (mag)
2012	1104_213	2 34 17.42	61 44 05.60		F3V	0.7	0	13.78	13.48	13.32	12.68
2012	1204_144	2 34 17.48	61 08 31.54	A9-F0	F0V	3.1	1	15.94	15.75	15.13	14.49
2011	1023_102	2 34 17.51	61 39 53.20	F9-G1	G0V	1.7	1	13.16	12.77[e]	12.30[f]	12.44
2012	1105_3_54	2 34 17.69	61 45 26.70	F4-F5	F5V	2.6	1	15.91	15.41	14.84	14.27
2012	0220_175	2 34 17.88	61 27 21.50	F5-F7	F6V	1.5	0	16.50	16.18	15.80	15.30
2012	1204_135	2 34 17.96	61 11 24.64	K4-K5	K4V	0.8	0	14.91	14.70	14.21	13.26
2012	1203_2_120	2 34 18.20	61 09 38.87	G8-K0	G9V	1.3	0	15.81	15.64	15.19	14.24
2012	1106_2_124	2 34 18.20	61 50 03.00	G0-G6	G3V	1.7	1	17.15	16.74	16.25	15.75
2012	0304_82	2 34 18.22	61 47 37.81		B9V	2.3	1	14.83	14.62	14.39	14.21
2012	1106_1_105	2 34 18.36	61 39 16.90	K5-K6	K6V[g]	3.8	1	17.11	15.97	14.71	14.27
2012	0220_54	2 34 18.43	61 43 55.80	A9-F2	F0V	2.3	1	16.09	16.25	15.81	15.10
2012	1204_111	2 34 18.45	61 21 52.99	K2-K3	K2V	0.9	0	15.94	15.57	15.16	14.70
2012	1204_140	2 34 18.53	61 13 51.42	G5-G7	G6V	1.1	0	14.90	14.67	14.29	13.66
2012	1106_1_263	2 34 18.68	62 00 26.00	G8-K0	G9V	3.7	1	17.84	16.92	15.96	15.37
2012	1105_4_95	2 34 18.71	61 52 13.10	G0-G7	G1V	1.5	0	16.44	16.05	15.62	15.18
2012	1104_224	2 34 18.77	61 42 23.11		G9V	2.8	1	13.17	12.90	12.13	12.15
2012	0304_156	2 34 18.89	61 24 49.10	F8-F9	F8V	2.8	1	15.69	15.38	14.71	14.29
2012	1105_5_23	2 34 19.62	62 08 25.50	A2-A5	A3V	1.7	1	14.80	15.06	14.86	14.00
2012	1105_4_7	2 34 19.64	62 15 22.70	F3-F5	F4V	1.3	0	14.84	14.95	14.67	13.98
2012	1105_3_275	2 34 19.65	61 21 10.60	B9-A1	A0V	0.8	0	13.95	13.75	13.79	12.91
2012	1106_2_165	2 34 19.68	61 26 22.80	K3-K5	K4V	1.8	1	18.30	17.53	16.83	16.29
2012	1105_2_270	2 34 19.92	61 35 35.00	K1-K3	K2V	0.9	0	15.76	15.40	15.00	14.65
2012	1106_1_6	2 34 20.06	61 56 05.31	A7-F0	A8V	3.3	1	17.53	17.00	16.38	15.80
2012	1105_3_60	2 34 20.31	61 44 16.21	F2-F3	F2V	1.6	1	14.51	14.13	13.81	13.49
2012	1106_3_174	2 34 20.58	61 49 15.90	F9-G7	G4V	2.2	1	18.17	17.66	17.06	15.84
2011	0923_266	2 34 21.13	61 27 35.68	G2-G3	G7V	1.3	0	15.94	15.51	15.08	14.65
2012	1105_4_66	2 34 21.20	62 09 04.89	A6-A8	A7V	1.4	0	14.19	14.43	14.23	13.48
2012	1106_1_16	2 34 21.40	61 43 50.59	F0-F3	F2V	2.6	1	16.95	16.51	15.95	15.33
2012	1204_126	2 34 21.49	61 20 46.30	F2-F3	F2V	2.4	1	15.69	15.33	14.83	14.42
2012	1204_132	2 34 21.58	61 16 16.40	A7-F3	F0V	3.7	1	...	17.85	17.12	...
2012	0220_176	2 34 21.76	61 21 09.59	F8-F9	F8V	1.7	1	16.35	16.02	15.60	15.08
2012	0220_56	2 34 21.79	61 48 37.60	B1-B2	B2V	1.9	1	12.73	12.24	12.20	12.31
2012	1106_1_66	2 34 22.11	61 45 26.00	K3-K5	K4V	1.9	1	18.14	17.36	16.63	15.91
2012	1104_77	2 34 22.35	61 39 42.26	G5-G7	G6V	2.7	1	15.23	14.51	13.79	13.76
2012	1104_85	2 34 22.41	61 38 10.86		F5V	1.3	0	15.00	14.71	14.41	14.10
2012	1106_1_2	2 34 22.57	61 59 49.40	A7-F0	F0V	3.2	1	18.15	17.58	16.95	16.37
2012	1204_119	2 34 22.64	61 23 39.02		A0V	2.4	1	14.23	14.10	13.81	13.27
2012	1105_2_49	2 34 22.81	61 25 16.59	K1-K2	K2V	0.5	0	14.80	14.28	13.96	14.34
2012	0304_76	2 34 23.15	61 53 09.30		F8V	1.5	0	15.47	15.03	14.64	14.43
2012	1105_3_58	2 34 23.50	61 51 09.59	B6-A0	B9V	3.0	1	15.75	15.45	15.06	14.74
2012	1106_2_156	2 34 23.63	61 30 20.60	K2-K4	K3V	1.6	1	17.28	16.71	16.10	15.54
2011	1023_160	2 34 23.96	61 09 56.52	K0-K4	K2V	2.6	1	15.02	14.53	13.76	12.42
2012	1203_2_49	2 34 24.07	61 48 48.65	F3-F5	F4V	1.9	1	15.07	14.71	14.29	14.21
2011	1023_156	2 34 24.18	61 12 01.10		F4V	1.2	0	14.04	13.84	13.56	12.79
2012	1106_1_14	2 34 24.26	61 44 30.41	G7-K0	G8V	1.8	1	17.46	16.97	16.43	15.81
2012	1204_98	2 34 24.45	61 31 45.41		F4V	1.5	0	15.24	14.96	14.62	14.25
2011	1023_114	2 34 24.56	61 32 53.80	B9-A1	A0V	2.7	1	13.88	13.73	13.38	12.90
2012	0304_16	2 34 24.64	61 58 05.70	G5-G8	G7V	1.1	0	15.91	15.55	15.17	14.62
2012	1106_1_265	2 34 24.64	62 03 54.00	F4-F7	F6V	1.9	1	...	17.05	16.60	...
2012	0124_64	2 34 24.69	61 46 23.50	A1-A3	A1V	2.0	1	14.44	14.05	13.82	13.89
2012	1203_1_18	2 34 24.92	61 09 22.17	K4-K5	K5V	1.3	0	...	15.70	15.08	...
2012	1105_2_258	2 34 25.07	61 41 06.10	A7-A8	A7V	1.4	0	13.59	13.44	13.24	12.68
2012	1203_2_116	2 34 25.36	61 10 41.67	G7-G8	G7V	1.8	1	15.94	15.78	15.26	14.40
2012	1105_5_114	2 34 25.89	62 20 51.49	G8-K2	K0V	0.8	0	14.99	13.80	13.45	12.39
2012	0304_20	2 34 25.89	61 56 52.81	A4-A6	A5V	2.2	1	16.19	15.94	15.61	15.08
2012	0124_94	2 34 25.96	61 34 15.41	G5-G9	G7V[g]	2.7	1	15.67	15.06	14.33	14.11
2012	0124_70	2 34 26.01	61 45 21.70	A0-A2	A0V	2.2	1	15.29	15.13	14.88	14.55
2012	1104_265	2 34 26.10	61 40 35.80		G4V	1.1	0	15.15	14.77	14.41	14.24
2012	1104_83	2 34 26.31	61 34 22.08	A7-F0	A9V	2.5	1	16.47	16.15	15.68	15.15
2012	1105_3_64	2 34 26.38	61 41 43.50	B9-A0	B9V	2.1	1	14.84	14.64	14.45	14.21
2012	1104_219	2 34 26.67	62 01 42.81	A5-A6	A2V	2.6	1	15.10	14.85	14.46	13.74
2012	1105_2_2	2 34 26.75	61 33 41.00	F7-F9	F7V	1.6	1	15.96	15.71	15.31	14.87
2011	1023_108	2 34 26.76	61 38 31.00	G2-G4	G3V	1.8	1	15.34	14.88	14.38	14.10
2012	1106_3_162	2 34 26.79	61 54 19.70	A7-F7	F0V	3.5	1	18.31	17.71	17.02	16.42
2011	1023_155	2 34 27.00	61 07 49.70		F0V	1.6	1	13.54	13.73	13.45	12.52
2012	1105_5_174	2 34 27.03	61 51 32.20	F6-F7	F7V	1.9	1	15.87	15.47	15.02	14.76
2012	1104_229	2 34 27.10	61 45 03.41	G8-K2	K2V	2.4	1	14.98	14.22	13.50	13.60
2012	1104_231	2 34 27.24	61 42 45.40		F4V	2.2	1	15.19	14.75	14.26	14.13
2012	1106_3_279	2 34 27.72	61 50 49.70	G0-G8	G3V	3.8	1	17.73	16.92	15.99	15.33
2012	0220_58	2 34 27.82	61 51 00.10	B8-B9	B9V	1.7	1	13.55	13.42	13.32	12.78
2012	0304_72	2 34 27.83	61 56 14.00	G7-G8	G7V	1.4	0	15.51	15.06	14.62	14.15
2012	1106_1_39	2 34 27.85	61 53 53.30	K1-K3	K2V	2.7	1	17.24	16.51	15.73	15.11
2012	1204_138	2 34 28.00	61 13 34.43	F3-F5	F4V	2.2	1	15.68	15.60	15.12	14.19
2012	1105_5_187	2 34 28.01	61 41 30.50	F6-F8	F7V	1.8	1	16.35	15.99	15.55	15.06
2012	1203_1_54	2 34 28.12	61 20 35.59	G8-G9	G8V	1.0	0	15.10	14.76	14.40	14.19
2012	0216_134	2 34 28.23	61 30 44.60	M0-M2	M2V	0.8	0	19.21	18.51	17.39	16.68
2012	1105_5_115	2 34 28.41	62 17 54.30	G8-K2	K0V[g]	1.2	0	14.34	13.93	13.49	12.61
2012	1105_4_94	2 34 28.61	61 54 20.50	G2-G7	G6V	1.3	0	16.20	15.85	15.43	14.91
2012	1105_5_144	2 34 28.66	62 05 02.40	G9-K2	K0V[g]	1.4	0	15.45	14.47	14.00	13.15
2012	1104_266	2 34 28.69	61 41 43.26		K3V	1.1	0	16.27	15.79	15.32	14.83
2012	1106_1_10	2 34 28.95	61 57 30.20	F1-F3	F3V	2.5	1	16.83	16.38	15.84	15.29
2012	1203_1_66	2 34 29.04	61 15 38.16	K1-K3	K2V	0.6	0	14.85	14.85	14.50	13.56
2012	1203_1_46	2 34 29.04	61 25 16.75	A9-F0	A9V	1.7	1	15.09	14.80	14.50	14.24
2012	1106_2_174	2 34 29.22	61 21 57.00	F0-F3	F2V	3.5	1	18.10	17.50	16.76	16.10
2012	1105_3_56	2 34 29.27	62 03 08.50	K0-K3	K2V[g]	2.1	1	15.96	15.02	14.36	13.79
2012	0304_17	2 34 29.32	61 45 03.90	A0-A1	A0V	1.8	1	14.75	14.68	14.52	13.79
2012	1203_1_14	2 34 29.35	61 10 10.76	G7-K3	K2V	2.0	1	15.54	15.21	14.58	13.56

Table 1. IC 1805 Spectral Types and Photometry (Continued)

Year	Date_No.[a] (MMDD_No.)	RA(J2000) (hhmmss.ss)	Dec(J2000) (° ′ ″)	SpTy Range	SpTy	A_V (r-i) (mag)	Assoc.?[b] (ext)	V(90P)[c] (mag)	r[d] (mag)	i[d] (mag)	I(90P)[c] (mag)
2012	0304_137	2 34 29.40	61 31 34.70	G8-G9	G8V	2.4	1	15.04	14.42	13.75	13.43
2012	0304_94	2 34 29.41	61 43 50.40	F3-F5	F4V	1.7	1	15.53	15.21	14.84	14.51
2012	0124_51	2 34 29.50	61 47 40.50	B7-B8	B9V	2.1	1	14.52	14.10	13.91	14.13
2012	1106_2_135	2 34 29.56	61 37 56.11	K7-K8	K7V	1.9	1	17.52	16.77	15.86	15.23
2012	1105_5_150	2 34 29.61	62 04 10.50	G0-G7	G3V	0.7	0	14.37	14.47	14.19	13.44
2012	1105_3_55	2 34 29.81	61 46 40.90	G8-K0	G9V	1.3	0	16.11	15.69	15.23	14.79
2012	1106_1_130	2 34 30.03	61 26 24.60		A5V	3.0	1	16.54	16.14	15.64	15.07
2012	1106_3_178	2 34 30.06	61 48 04.10	G7-K0	G9V	1.6	1	17.48	16.95	16.43	15.87
2012	0220_276	2 34 30.24	61 31 06.30	G8-K0	G9V	2.8	1	16.31	15.62	14.86	14.30
2012	1105_4_14	2 34 30.37	62 05 57.10	A1-A2	A2V	1.5	0	14.77	14.89	14.74	14.01
2012	0124_3	2 34 30.43	61 56 18.60	F4-F6	F6V	1.6	1	15.89	15.54	15.15	14.71
2011	0923_3	2 34 30.65	61 12 06.70	G4-G9	G5V	1.5	0	15.58	15.88	15.43	14.42
2012	1106_3_185	2 34 30.68	61 39 49.20	F9-G7	G5V	3.6	1	17.95	17.16	16.27	15.63
2012	1106_1_17	2 34 30.71	61 42 18.01	F8-F9	F8V	2.1	1	16.55	16.19	15.66	15.05
2012	1106_1_121	2 34 30.80	61 19 41.80	G0-G7	G3V	3.4	1	18.48	17.82	16.97	16.32
2012	0124_110	2 34 30.90	61 30 39.50	F6-F9	G0V	2.1	1	16.09	16.38	15.85	14.92
2012	1203_1_34	2 34 31.00	61 27 41.87	K4-K5	K4V	0.5	0	16.04	15.58	15.16	14.71
2012	1105_5_177	2 34 31.16	61 48 16.00	G8-K0	G9V	2.3	1	16.39	15.74	15.08	14.67
2012	1105_5_27	2 34 31.17	62 10 17.40	B9-A0	B9V	2.2	1	...	14.25	14.04	...
2012	1203_1_259	2 34 31.36	61 34 09.17	G5-G7	G6V	1.2	0	15.63	15.25	14.86	14.52
2011	0923_257	2 34 31.49	61 30 35.07	B2-B3	B3V	1.4	0	12.26	11.19	11.22	12.08
2012	0304_121	2 34 31.55	61 34 36.20	A9-F4	F2V	2.2	1	16.23	15.90	15.43	14.98
2012	0220_273	2 34 31.57	61 18 50.80	F4-F5	F4V	2.2	1	16.13	15.78	15.29	14.75
2012	1203_1_9	2 34 31.59	61 22 04.48	G5-G7	G6V	1.0	0	15.43	15.13	14.78	14.48
2012	1106_1_127	2 34 31.64	61 25 02.30	F6-F8	F7V	2.3	1	17.22	16.80	16.23	15.63
2012	1203_2_107	2 34 31.71	61 16 27.08	A7-A8	A7V	2.6	1	15.08	15.08	14.63	13.64
2012	0304_75	2 34 31.73	61 51 33.00	A1-A3	A2V	2.1	1	14.49	14.25	13.96	13.50
2012	1105_3_17	2 34 31.77	61 40 06.29	G5-G7	G6V[g]	3.2	1	15.26	14.50	13.68	13.74
2011	1023_25	2 34 31.89	61 24 39.20	A9-F0	F0V	2.1	1	15.74	15.44	15.05	14.55
2012	0304_127	2 34 31.90	61 35 26.60		F7V	1.1	0	14.60	14.29	14.00	14.03
2012	1105_4_81	2 34 32.04	61 56 56.20	A7-F0	A9V	1.7	1	15.65	15.42	15.13	14.62
2012	0216_88	2 34 32.18	61 54 11.90	M0-M1	M1V	0.5	0	20.18	19.32	18.34	17.68
2012	1105_4_108	2 34 32.23	61 47 08.00	B4-B5	B5V	1.8	1	13.17	12.63	12.57	12.50
2012	1105_3_167	2 34 32.25	61 24 31.70	A1-A2	A2V	2.5	1	16.20	16.00	15.65	15.14
2012	1106_2_173	2 34 32.95	61 18 40.40	F2-F3	F2V	2.8	1	16.71	16.29	15.71	15.15
2012	1106_3_276	2 34 33.14	61 59 45.50	G6-K1	G8V	4.0	1	18.32	17.45	16.45	15.71
2012	0216_93	2 34 33.19	61 43 37.91	M0-M2	M1V	2.3	1	19.50	19.33	17.98	17.18
2012	1105_5_143	2 34 33.22	62 03 13.30	G8-K1	G7V	2.3	1	15.66	15.10	14.46	13.67
2012	1104_87	2 34 33.42	61 34 34.00	F3-F4	F4V	2.1	1	16.20	15.84	15.38	14.93
2012	1106_1_128	2 34 33.44	61 26 43.19	A9-F0	F0V	2.6	1	16.94	16.51	16.00	15.43
2012	1105_4_47	2 34 33.81	62 19 56.70	F7-F8	F8V	1.2	0	15.15	15.06	14.73	14.04
2012	1203_2_94	2 34 33.91	61 22 46.75	A1-A2	A1V	2.8	1	15.34	15.09	14.70	14.50
2012	1105_2_66	2 34 34.06	61 10 24.81	G7-G8	G7V[g]	2.4	1	14.64	14.28	13.63	12.62
2012	1105_4_16	2 34 34.22	62 05 36.80	G8-K2	K2V[g]	2.0	1	14.84	14.00	13.35	12.91
2012	1105_3_165	2 34 34.43	61 20 37.40	G9-K0	G9V[g]	2.4	1	14.67	14.00	13.33	12.73
2012	1104_228	2 34 34.63	61 50 21.80	F3-F4	F3V	1.5	0	14.68	14.41	14.10	13.62
2012	1105_4_42	2 34 34.88	62 24 07.50	F6-F7	F7V	0.9	0	14.17	14.17	13.91	13.23
2011	1023_113	2 34 35.29	61 29 56.40	A0-A1	A1V	1.9	1	15.04	14.91	14.69	14.38
2012	1104_92	2 34 35.40	61 15 18.32	F7-F8	F8V	0.1	0	13.60	13.49	13.38	12.53
2012	1203_1_295	2 34 35.46	61 37 30.65		F8V	1.8	1	15.43	15.04	14.59	14.39
2012	1203_1_62	2 34 35.48	61 16 33.36	A0-A1	A1V	2.9	1	...	15.57	15.15	...
2012	1106_3_123	2 34 35.59	62 16 20.70	G8-K0	G9V	1.4	0	...	16.93	16.46	...
2012	1106_1_57	2 34 35.68	61 47 23.61	G8-K2	K1V	2.3	1	17.45	17.05	16.37	15.66
2012	1105_5_184*	2 34 35.73	61 44 41.30	B9-A0	A0V	2.1	1	14.88	14.69	14.47	14.34
2012	1105_3_59*	2 34 35.81	61 56 12.50	B4-A0	B9V	2.2	1	13.87	13.73	13.51	13.06
2012	1203_2_12	2 34 35.87	61 33 35.63	F5-F6	F6V	3.1	1	18.45	17.75	17.04	16.15
2012	1104_14	2 34 36.07	61 38 23.96	G2-G8	G5V	1.4	0	14.52	13.81	13.39	12.78
2011	1023_154	2 34 36.13	61 11 19.31	K0-K2	K1V	2.4	1	14.55	13.96	13.25	12.45
2012	1105_4_11	2 34 36.19	61 54 20.00	G7-G9	G8V	2.3	1	13.82	13.30	12.66	12.17
2012	1105_4_74	2 34 36.22	62 04 14.00	A9-F1	F0V	1.6	1	15.06	15.25	14.97	14.10
2012	0124_1	2 34 36.36	61 56 48.91	F3-F5	F5V	1.3	0	15.10	14.66	14.35	14.00
2012	1203_1_235	2 34 36.68	61 46 58.36	A7-A8	A8V	2.5	1	15.02	14.71	14.26	13.82
2012	0220_161	2 34 36.71	61 23 28.90	B5-B6	B5V	1.7	1	13.91	13.80	13.75	13.10
2012	1106_1_95	2 34 36.92	61 39 53.61	G7-K1	K0V[g]	2.9	1	17.19	16.44	15.64	15.04
2012	0124_69	2 34 36.96	61 45 50.70	G9-K3	K1V	1.2	0	16.45	16.01	15.56	15.06
2012	1203_1_74	2 34 37.07	61 04 37.82	A0-A1	A1V	4.1	1	...	16.24	15.57	...
2012	1104_232	2 34 37.22	61 45 16.70	B4-B7	B5V	2.5	1	12.80	12.73	12.51	12.35
2012	0124_103	2 34 37.39	61 28 51.80		F7V	1.6	1	16.24	15.89	15.47	14.98
2012	0124_80	2 34 37.51	61 39 38.20	G2-G5	F9V	1.0	0	16.36	14.34	14.04	15.14
2012	1203_2_115	2 34 37.66	61 04 36.61	A1-A2	A2V	4.1	1	...	16.57	15.88	...
2012	0124_113*	2 34 37.82	61 23 25.30	A1-A5	A3V	2.7	1	15.85	15.58	15.18	14.67
2012	1203_1_47	2 34 38.11	61 23 12.19	K4-K5	K4V	0.9	0	16.39	15.79	15.28	14.74
2012	1104_17	2 34 38.11	61 25 11.06	G8-K0	G9V	4.5	0	16.01	14.93	13.80	13.91
2012	1104_296	2 34 38.31	61 47 00.20	B6-B8	B4V	2.4	1	13.51	13.39	13.20	12.77
2012	0220_59	2 34 38.55	61 58 44.00	G9-K1	K0V	3.3	1	15.43	14.52	13.63	12.91
2012	1203_2_74	2 34 38.75	61 30 29.02	F2-F3	F2V	1.6	1	15.33	15.16	14.82	14.47
2012	1106_2_184	2 34 38.98	61 17 43.81	G4-G6	G5V	2.0	1	...	17.09	16.53	...
2012	1203_2_104	2 34 39.06	61 18 31.02	A1-A2	A2V	2.2	1	14.61	14.76	14.46	13.59
2012	0304_159	2 34 39.23	61 19 29.30	K0-K2	K1V	1.1	0	15.87	15.51	15.09	14.59
2012	1204_133	2 34 39.30	61 07 07.26	F9-G0	F9V	1.8	1	...	14.76	14.31	...
2011	0923_261	2 34 39.48	61 24 36.00		A9V	2.0	1	15.46	15.19	14.84	14.50
2012	1105_4_88	2 34 39.53	61 58 54.49	A9-F0	F0V	1.6	1	14.71	14.44	14.16	13.66
2012	0124_60	2 34 39.64	61 53 21.20		K2V	0.6	0	15.42	15.00	14.66	14.52
2012	0216_280	2 34 39.91	61 19 55.70	K6-K8	K7V	1.9	1	19.15	18.38	17.46	16.80
2011	1023_99	2 34 39.96	61 45 23.13	A6-A7	A7V	2.3	1	14.80	14.41	14.01	13.90
2012	0216_108	2 34 39.98	61 42 14.40	K6-K8	K7V	1.3	0	18.54	17.82	17.02	16.33
2012	0124_66	2 34 40.07	61 47 47.90	B7-B9	B8V	2.2	1	14.42	14.03	13.83	13.77

Table 1. IC 1805 Spectral Types and Photometry (Continued)

Year	Date_No.[a] (MMDD_No.)	RA(J2000) (hhmmss.ss)	Dec(J2000) (° ′ ″)	SpTy Range	SpTy	A_V (r-i) (mag)	Assoc.?[b] (ext)	V(90P)[c] (mag)	r[d] (mag)	i[d] (mag)	I(90P)[c] (mag)
2012	1105_3_156	2 34 40.12	61 30 60.00	G6-G8	G7V	2.2	1	15.99	15.68	15.06	14.16
2012	1105_5_171	2 34 40.22	61 44 51.10		K7V[g]	2.1	1	14.56	13.42	12.44	13.14
2012	1105_5_273	2 34 40.26	61 51 50.70	F2-F5	F3V	2.2	1	16.46	16.09	15.63	15.02
2012	1106_2_121	2 34 40.37	61 46 52.71	G1-G7	G5V	2.3	1	16.99	16.44	15.82	15.25
2012	1106_2_152	2 34 40.62	61 31 37.90	G8-K1	G9V	3.1	1	17.33	16.59	15.77	15.09
2012	1106_1_111	2 34 40.69	61 28 30.10	K4-K5	K4V	0.8	0	16.99	16.46	15.97	15.42
2012	0216_11	2 34 41.06	61 47 42.10	K6-M0	K8V	2.0	1	20.01	19.22	18.22	17.40
2012	1203_1_258*	2 34 41.14	61 35 45.41	A1-A3	A2V	2.3	1	15.41	15.20	14.87	14.60
2012	1203_1_233	2 34 41.26	61 46 33.93	K2-K5	K3V	2.4	1	18.50	17.86	17.08	16.30
2012	1106_1_126	2 34 41.60	61 25 11.01	G1-G7	G7V	1.4	0	...	16.47	16.02	...
2012	1105_4_87	2 34 41.67	61 57 42.30	F8-G0	F8V	1.3	0	14.75	14.43	14.09	13.59
2012	1105_5_175	2 34 41.69	61 46 34.70	G6-K0	G7V	1.7	1	16.46	16.03	15.52	14.93
2012	1106_1_41	2 34 41.74	61 50 00.20	K0-K5	K2V	3.1	1	17.94	17.36	16.49	15.69
2012	0304_71*	2 34 41.81	61 51 46.40	A1-A3	A2V	2.1	1	15.91	15.70	15.43	15.03
2012	0220_57	2 34 42.10	61 52 34.50	F5-F6	F6V	1.7	1	15.84	15.60	15.18	14.76
2012	1106_2_150	2 34 42.19	61 35 42.71	K7-K8	K8V	1.3	0	17.79	17.08	16.23	15.61
2012	1106_1_74	2 34 42.27	61 43 53.51	K4-K5	K4V	2.3	1	17.75	16.93	16.12	15.52
2012	1105_3_170	2 34 42.45	61 19 44.60	B9-A1	A1V	2.6	1	16.07	15.87	15.51	15.01
2012	1105_2_39	2 34 42.50	61 29 33.00	G8-G9	G9V[g]	2.4	1	16.15	15.51	14.82	14.33
2012	1104_60*	2 34 42.51	61 38 46.50		A1V	2.2	1	15.05	14.80	14.54	14.44
2012	1105_3_63	2 34 42.57	61 46 12.70	G7-K0	G8V[g]	2.8	1	15.51	14.79	14.05	13.94
2012	1204_91	2 34 42.58	61 29 22.95	F8-F9	F8V	1.4	0	15.45	15.13	14.76	14.38
2012	0304_155	2 34 42.62	61 16 12.70	A1-A3	A2V	3.0	1	15.87	15.40	14.93	14.45
2012	1106_3_169	2 34 42.70	61 52 50.30	A1-A2	A1V	4.4	0	17.52	16.92	16.18	15.56
2012	0304_19	2 34 42.78	61 46 51.31	B9-A0	A0V	2.4	1	15.15	14.90	14.60	14.34
2012	1106_1_30	2 34 43.12	61 33 23.80	F7-F9	F8V	2.8	1	17.84	17.34	16.68	16.02
2012	1106_1_38	2 34 43.54	61 57 49.70	K0-K4	K4V[g]	3.0	1	16.87	15.95	15.00	14.28
2012	1105_2_9	2 34 43.58	61 21 21.20	A4-A5	A5V	2.4	1	15.62	15.46	15.07	14.46
2012	0216_97	2 34 43.72	61 45 08.10	K6-K8	K7V	2.5	1	20.07	19.25	18.21	17.51
2012	1104_31	2 34 43.87	61 40 08.87	A1-A3	A2V	2.4	1	15.52	15.28	14.94	14.55
2012	1105_2_58	2 34 44.08	61 16 25.50	K0-K2	K1V	0.9	0	14.38	14.27	13.87	13.01
2012	0220_162	2 34 45.06	61 25 10.70	M2-M4	M3V[g]	2.5	1	13.69	12.70	11.07	11.48
2012	1203_2_117	2 34 45.06	61 04 04.35	G6-K3	K2V	1.3	0	...	16.33	15.84	...
2012	0304_104*	2 34 45.22	61 41 55.70	F3-F4	F3V	1.8	1	15.95	15.68	15.29	14.82
2012	1105_3_124	2 34 45.31	61 37 16.10	F4-F6	F5V	1.9	1	15.85	15.49	15.05	14.71
2012	1106_1_117	2 34 45.42	61 29 54.70	K4-K5	K4V	2.0	1	18.39	18.32	17.58	16.38
2012	1106_2_279	2 34 45.43	61 24 15.50	G8-K2	K0V	2.6	1	17.78	17.27	16.53	15.74
2012	1106_2_145	2 34 45.46	61 35 00.39	G4-G7	G5V	3.4	1	16.96	16.23	15.37	14.81
2012	1105_3_162	2 34 45.65	61 26 14.30		B9V	2.2	1	14.50	14.40	14.19	13.77
2012	1203_1_59	2 34 45.67	61 17 03.78	A7-F0	A9V	3.1	1	...	16.53	15.95	...
2012	1105_5_151	2 34 45.89	61 57 22.70	F3-F5	F4V	1.7	1	15.82	15.48	15.10	14.69
2012	0304_78	2 34 45.92	61 57 07.50	G8-K0	G9V	2.5	1	...	12.96	12.25	...
2012	0304_120	2 34 46.00	61 37 10.40	A4-A6	A5V	1.9	1	16.32	16.13	15.85	15.38
2012	1105_3_168	2 34 46.23	61 20 13.40	K3-K5	K2V[g]	3.5	1	15.14	14.36	13.39	14.55
2012	1105_3_148	2 34 46.34	61 33 25.50	F2-F4	F2V	2.1	1	16.30	15.99	15.55	15.00
2012	0220_163	2 34 46.69	61 17 53.20	G2-G4	G3V	1.3	0	15.95	14.89	14.48	14.60
2012	0220_62	2 34 46.78	61 49 32.69		K0V	0.5	0	14.12	13.80	13.50	13.07
2012	1203_2_1	2 34 46.84	61 43 23.66	F9-G1	F9V	1.4	0	15.68	15.27	14.88	14.58
2012	0124_54	2 34 46.90	61 57 35.20	G4-G8	G6V	1.1	0	15.30	14.92	14.54	14.39
2012	1104_38	2 34 46.90	61 40 39.36	G2-G8	G6V	1.3	0	16.18	15.82	15.40	14.92
2012	0220_138	2 34 47.03	61 29 15.51	G7-G9	G8V	2.4	1	15.45	14.85	14.18	13.70
2012	1105_3_164	2 34 47.31	61 24 21.20	G1-G4	G2V	1.5	0	16.30	15.96	15.51	14.99
2012	0220_55	2 34 47.59	61 55 16.80	F1-F3	F2V	1.2	0	14.85	14.47	14.23	14.25
2012	1104_260	2 34 47.63	61 43 10.00	F3-F5	F4V	2.9	1	13.64	13.95	13.32	12.76
2012	1105_3_70	2 34 47.76	61 49 58.10	K3-K5	K4V	0.8	0	16.09	15.58	15.11	14.78
2012	0220_121	2 34 47.77	61 31 13.71	F4-F6	F5V	2.0	1	16.49	16.15	15.70	15.18
2012	1204_117	2 34 47.91	61 22 08.87	F6-F7	F7V	2.2	1	16.17	15.77	15.24	14.66
2012	1106_3_278	2 34 47.98	61 59 42.81	K6-K7	K6V	1.5	0	18.30	17.53	16.77	16.17
2012	1106_1_115	2 34 48.11	61 28 23.71	A3-A4	A3V	2.6	1	16.69	16.43	16.04	15.53
2012	1105_3_53	2 34 48.12	61 55 37.40	B3-B7	B4V	2.9	1	14.99	14.69	14.40	14.35
2012	0124_123	2 34 48.20	61 15 58.90	B9-A1	A0V	2.5	1	15.81	15.48	15.18	14.76
2012	1203_1_38	2 34 48.22	61 26 57.44	F4-F6	F5V	1.7	1	15.94	15.62	15.22	14.76
2012	1203_1_251	2 34 48.79	61 33 05.85	F7-F8	F7V	1.8	1	15.36	14.96	14.50	14.27
2012	1106_1_124	2 34 48.79	61 24 07.39	A7-F2	F0V	3.4	1	18.23	17.71	17.03	16.38
2012	0304_77	2 34 48.95	61 55 49.10	F8-F9	F9V	1.0	0	...	13.68	13.39	...
2012	1106_2_177	2 34 49.05	61 18 29.50	F3-F5	F4V	2.9	1	17.48	16.98	16.35	15.76
2012	0220_111	2 34 49.16	61 31 38.40	G5-G8	G7V	1.2	0	16.39	16.05	15.64	15.18
2012	1105_3_27	2 34 49.31	61 35 47.40	A5-A6	A6V	1.1	0	12.46	11.65	11.54	12.27
2012	0124_58	2 34 49.33	61 55 49.00	B7-B8	B8V	2.7	1	13.92	13.68	13.39	12.94
2012	1203_2_64	2 34 49.34	61 37 51.85	F9-G0	F9V	1.3	0	15.16	14.84	14.47	14.38
2012	1203_2_80	2 34 49.65	61 29 25.19	G9-K0	K0V	1.7	1	16.25	15.75	15.20	14.64
2012	1204_76	2 34 50.05	61 45 11.12	G8-K2	K1V[g]	2.8	1	16.63	15.91	15.12	14.60
2012	0220_167	2 34 50.21	61 18 51.19	A0-A2	A1V	2.5	1	16.40	16.16	15.82	15.30
2012	1105_5_157	2 34 50.22	61 58 28.70	G1-G7	G6V	1.0	0	16.16	15.81	15.45	14.99
2012	1105_4_83	2 34 50.22	61 56 48.50	F2-F5	F2V	1.5	0	15.60	15.31	15.00	14.64
2012	1203_2_97	2 34 50.23	61 19 14.57	K8-M1	M0V	1.6	0	18.01	17.30	16.25	15.57
2012	1104_223	2 34 50.31	61 52 22.30	F8-G0	F9V	1.5	0	15.90	15.53	15.14	14.82
2012	1203_2_60	2 34 50.47	61 41 56.42	F4-F5	F4V	1.9	1	15.77	15.42	15.01	14.63
2012	0304_141	2 34 50.52	61 24 16.71	A5-A6	A5V	2.5	1	15.05	14.71	14.30	14.25
2012	0124_65	2 34 50.80	61 46 13.00	G2-G6	G5V	1.5	0	16.00	15.56	15.11	14.65
2012	0304_88	2 34 50.86	61 50 56.91	F3-F4	F3V	1.8	1	15.48	15.11	14.72	14.60
2012	0216_30	2 34 51.21	61 38 38.90	K0-K2	K1V	3.1	1	18.75	17.98	17.13	16.41
2012	1203_2_99	2 34 51.27	61 19 38.89	G1-G3	G2V	1.6	1	15.44	15.05	14.57	14.35
2012	1106_2_274	2 34 51.52	61 33 57.61	G7-K4	K0V[g]	3.7	1	17.90	17.01	16.04	15.29
2012	0304_129	2 34 51.55	61 35 10.60	G0-G1	G1V	1.6	1	16.24	15.84	15.40	14.93
2012	1105_4_93	2 34 51.62	61 48 49.81	F6-F7	F7V	0.8	0	13.95	13.68	13.44	12.99
2012	1105_2_34	2 34 51.80	61 30 42.30	G1-G3	G2V	1.3	0	15.74	15.40	15.00	14.53

Table 1. IC 1805 Spectral Types and Photometry (Continued)

Year	Date_No.[a] (MMDD_No.)	RA(J2000) (hhmmss.ss)	Dec(J2000) (° ′ ″)	SpTy Range	SpTy	A_V (r-i) (mag)	Assoc.?[b] (ext)	V(90P)[c] (mag)	r[d] (mag)	i[d] (mag)	I(90P)[c] (mag)
2012	1106_1_37	2 34 51.81	61 57 33.20	A9-F3	F1V	2.6	1	16.85	16.34	15.80	15.24
2012	0220_165	2 34 52.21	61 15 52.30	G7-G8	G8V	0.5	0	14.20	14.09	13.82	13.12
2012	1104_16	2 34 52.28	61 34 56.60	F0-F2	F2V	1.4	0	15.34	15.12	14.82	14.46
2012	0124_109	2 34 52.67	61 29 15.09	G8-K2	K0V	0.7	0	14.23	13.95	13.63	13.16
2012	0124_125	2 34 52.68	61 16 04.39	K2-K3	K3V	1.0	0	15.95	15.36	14.89	14.42
2012	1105_4_84	2 34 52.79	61 59 47.00	A1-A2	A2V	2.5	1	16.29	15.94	15.59	15.08
2011	1023_152	2 34 52.88	61 10 20.01		B9V	2.9	1	15.13	15.20	14.85	13.98
2012	1106_1_64	2 34 53.14	61 47 21.50	M0-M1	M1V	0.8	0	18.43	17.69	16.66	16.02
2011	1023_121	2 34 53.41	61 25 50.40	A1-A6	A3V	1.6	1	13.75	13.66	13.48	13.09
2012	0220_53	2 34 53.66	61 57 23.80	F5-F6	F6V	1.5	0	16.24	15.89	15.51	15.07
2012	1104_245	2 34 53.97	61 45 34.00	G4-K0	K0V[g]	2.1	1	14.93	14.27	13.65	13.52
2012	1203_2_24	2 34 54.03	61 11 22.11		F8V	1.4	0	15.18	14.71	14.32	13.98
2012	0304_124	2 34 54.30	61 35 41.19	G8-K0	G9V	2.9	1	15.55	14.79	14.00	13.98
2011	1023_141*	2 34 54.55	61 13 12.49	F3-F4	F3V	2.7	1	15.82	15.52	14.94	14.17
2012	1106_1_9	2 34 54.67	61 50 55.60	G7-K0	G8V	1.9	1	17.47	16.91	16.36	15.81
2011	0923_40	2 34 54.92	61 20 08.30	K2-K3	K2V	2.4	1	17.25	16.70	15.99	14.77
2012	1104_299	2 34 55.08	61 44 37.51	F6-F8	F8V	1.7	1	16.07	15.69	15.25	14.79
2012	1106_2_151	2 34 55.30	61 28 17.59	G8-K2	G8V	3.7	1	18.08	17.50	16.56	15.69
2012	1105_5_161	2 34 55.54	61 52 51.60	F7-F8	F7V	1.7	1	15.98	15.62	15.19	14.87
2012	1204_128	2 34 56.01	61 18 14.98	G5-G7	G6V	1.7	1	16.60	16.15	15.64	15.09
2012	0124_30	2 34 56.05	61 25 31.10	B7-B9	B8V	2.6	1	14.64	14.21	13.94	14.23
2012	1106_3_273	2 34 56.10	61 48 32.39	K3-K5	K4V[g]	5.9	0	17.28	15.83	14.25	13.60
2012	1204_96	2 34 56.39	61 33 22.04	G7-G8	G8V	2.1	1	17.29	16.74	16.13	15.48
2012	1104_84	2 34 56.66	61 26 32.68	G7-K0	G9V	3.0	1	16.30	15.55	14.76	14.58
2012	1104_270	2 34 56.85	61 42 07.69	G3-K1	G7V	2.1	1	15.17	14.55	13.96	13.72
2012	0124_96	2 34 56.96	61 33 32.60	A1-A4	A1V	2.3	1	15.90	15.73	15.44	14.98
2012	0124_24	2 34 57.18	61 26 36.20	G2-G7	G7V	1.2	0	15.87	15.53	15.13	14.83
2012	1104_50	2 34 57.31	61 39 13.75		F5V	2.3	1	16.39	15.96	15.43	14.95
2012	1105_3_51	2 34 57.35	61 59 51.29	G4-G7	G5V	0.5	0	14.10	13.78	13.54	13.09
2012	1203_1_263	2 34 57.52	61 30 37.05	F8-F9	F9V	2.1	1	16.97	16.53	16.00	15.43
2012	1104_86	2 34 57.66	61 25 10.96	G8-K0	G9V	0.5	0	13.92	13.63	13.34	12.96
2012	1203_2_110	2 34 57.67	61 15 24.49		F8V	1.7	1	15.54	15.58	15.14	14.06
2012	1203_2_54	2 34 57.77	61 43 44.76	G3-G7	G6V	0.9	0	15.15	14.80	14.45	14.40
2012	1106_1_71	2 34 57.84	61 42 34.90	F9-G7	G0V	2.0	1	17.20	16.73	16.22	15.65
2012	1105_4_86	2 34 58.03	61 58 41.30	F9-G0	G0V	1.3	0	14.82	14.44	14.06	13.61
2012	1203_1_41	2 34 58.27	61 21 16.16	F8-F9	F9V	3.4	1	16.92	16.25	15.45	14.78
2012	1203_1_42	2 34 58.35	61 24 45.96	G6-K1	G9V	2.3	1	16.80	16.17	15.50	14.91
2012	1104_237	2 34 58.60	61 48 17.00	F8-F9	F9V	1.6	1	15.93	15.53	15.11	14.76
2012	1203_1_8	2 34 58.78	61 29 20.41	F0-F2	F1V	2.7	1	16.47	16.00	15.46	14.90
2012	1105_3_140	2 34 58.86	61 34 44.00	K3-K4	K3V	1.2	0	16.27	15.81	15.30	14.80
2012	1105_5_158	2 34 58.92	61 59 07.20	G9-K1	G9V	0.8	0	15.62	15.22	14.87	14.44
2012	1106_1_99	2 34 59.05	61 39 16.20	G6-G8	G7V	2.0	1	17.14	16.60	16.02	15.49
2012	0216_148	2 34 59.19	61 24 04.40	M2-M3	M2V	1.6	0	19.07	18.40	17.13	16.43
2012	1104_81	2 34 59.23	61 13 23.92	A1-A2	A1V	2.4	1	14.90	15.06	14.76	13.90
2011	1023_135	2 34 59.40	61 19 59.00	A3-A6	A5V	3.2	1	15.38	15.18	14.62	14.34
2012	0124_17	2 34 59.59	61 35 32.50	G6-G7	G7V	1.2	0	16.43	16.07	15.67	15.15
2012	1106_1_120	2 34 59.96	61 27 44.10	K4-K5	K4V	1.1	0	17.54	16.99	16.43	15.85
2012	0124_67	2 34 59.97	61 47 39.40	F8-F9	F8V	1.8	1	16.18	15.74	15.29	14.88
2012	1204_112	2 35 00.10	61 23 30.82	G0-G9	G7V	3.5	1	17.54	16.67	15.78	15.22
2012	1105_3_155	2 35 00.46	61 23 43.10	B9-A0	A0V	2.9	1	16.42	16.15	15.75	15.23
2012	1204_71	2 35 00.60	61 41 54.06	K0-K3	K2V	1.6	1	17.18	16.63	16.08	15.57
2012	1106_2_170	2 35 00.80	61 25 49.50	F8-F9	F9V	2.0	1	16.97	16.58	16.07	15.55
2012	0216_19	2 35 00.81	61 53 03.10	M3-M4	M3V	1.9	1	20.08	19.35	17.85	17.10
2012	0304_158	2 35 01.01	61 16 01.61	F5-F7	F6V	1.5	0	15.45	15.75	15.38	14.44
2011	0923_43	2 35 01.17	61 14 00.92		F5V	1.2	0	13.94	14.05	13.76	13.06
2012	0124_53	2 35 02.17	61 53 24.51	F4-F6	F6V	1.5	0	15.66	15.31	14.93	14.59
2012	1204_118	2 35 02.23	61 22 30.43	G7-G8	G7V	1.8	1	15.53	15.05	14.52	14.58
2012	1204_75	2 35 02.68	61 43 39.48	G9-K2	K0V	0.9	0	15.50	15.11	14.72	14.46
2012	1105_3_166	2 35 02.94	61 15 37.51	G8-K0	G9V	2.6	1	15.03	14.53	13.81	12.93
2012	1104_298	2 35 03.30	61 52 50.30	F0-F3	F2V	1.7	1	15.67	15.36	15.02	14.73
2012	1204_24	2 35 03.48	61 25 37.00	G9-K1	K0V	2.3	1	16.37	15.75	15.07	14.58
2012	0216_96	2 35 03.53	61 49 02.00	K6-M1	K8V	2.5	1	20.25	19.33	18.22	17.19
2011	0923_299*	2 35 03.55	61 38 37.90	G6-G9	G8V	2.6	1	15.43	14.73	14.02	13.84
2012	0124_59	2 35 03.60	61 56 19.60	F6-F8	F7V	1.6	1	16.30	15.95	15.54	15.08
2012	1106_2_157	2 35 03.60	61 29 50.50	G8-K2	K0V	3.7	1	18.49	17.64	16.67	15.94
2012	0216_113	2 35 03.89	61 36 14.61	K7-M1	M0V	1.6	1	18.53	17.75	16.70	16.01
2012	1105_3_69	2 35 04.24	61 54 24.51	G8-K0	G9V	1.1	0	16.36	15.99	15.59	15.08
2012	1104_295	2 35 04.38	61 44 58.50	B7-B9	B8V	2.8	1	16.09	15.87	15.56	15.11
2012	0220_66	2 35 04.55	61 56 39.50	G0-G2	G1V	0.9	0	14.98	14.57	14.27	14.11
2012	0124_126	2 35 04.75	61 18 12.21	A0-A1	A1V	2.3	1	15.45	15.56	15.27	14.36
2012	1105_2_6	2 35 04.79	61 32 46.90	G2-G4	G3V[g]	3.0	1	15.96	15.57	14.81	13.79
2011	0923_5*	2 35 04.82	61 10 32.06	B9-A1	A0V	2.9	1	14.68	14.52	14.12	13.41
2012	1104_53	2 35 04.99	61 36 42.23	F5-F7	F6V	1.8	1	16.27	15.92	15.49	15.09
2012	1106_1_104	2 35 05.10	61 37 10.80	G8-K2	G9V	3.6	1	17.91	17.10	16.17	15.42
2012	1104_48	2 35 05.25	61 39 24.20	F0-F3	F2V	2.1	1	15.91	15.53	15.08	14.66
2012	0304_152	2 35 05.62	61 18 19.59	G1-G3	G2V	1.3	0	16.38	16.05	15.65	15.03
2012	0220_69	2 35 05.63	61 50 27.30	A6-A7	A6V	1.6	1	13.78	13.58	13.36	12.90
2012	1105_5_162	2 35 05.78	61 56 19.30	F8-G0	F9V	1.6	1	16.43	16.03	15.61	15.10
2012	1106_2_164	2 35 05.78	61 27 42.79		F8V	2.0	1	16.73	16.32	15.83	15.31
2012	0124_18	2 35 06.09	61 43 39.40	F8-G2	G0V	1.6	1	16.18	15.76	15.31	14.92
2012	1105_2_56	2 35 06.11	61 15 14.30	G3-G5	G4V	0.7	0	13.84	13.77	13.49	12.77
2012	1106_1_75	2 35 06.39	61 43 32.30	F9-G6	G0V	4.4	0	18.38	17.46	16.43	15.69
2011	0923_7	2 35 06.51	61 10 55.40	G5-G9	G7V	2.0	1	14.15	13.95	13.36	12.31
2012	1104_63	2 35 06.76	61 34 36.66	G3-G4	G4V	2.8	1	15.86	15.22	14.48	14.10
2012	0220_115	2 35 07.01	61 31 53.81		F3V	2.0	1	16.42	16.03	15.61	15.20
2012	0304_85	2 35 07.09	61 51 07.30	K2-K4	K3V	0.4	0	14.97	14.48	14.14	13.66
2012	1104_78	2 35 07.29	61 30 22.82		F7V	1.6	1	15.79	15.47	15.05	14.63

Table 1. IC 1805 Spectral Types and Photometry (Continued)

Year	Date_No.[a] (MMDD_No.)	RA(J2000) (hhmmss.ss)	Dec(J2000) (° ′ ″)	SpTy Range	SpTy	A_V (r-i) (mag)	Assoc.?[b] (ext)	V(90P)[c] (mag)	r[d] (mag)	i[d] (mag)	I(90P)[c] (mag)
2012	0220_64	2 35 07.70	61 59 51.90	F4-F5	F4V	1.7	1	15.33	14.96	14.58	14.08
2012	0124_102	2 35 07.79	61 31 14.50	F8-F9	F9V	1.5	0	16.45	16.10	15.69	15.17
2012	0304_86	2 35 07.88	61 53 46.60	F1-F2	F2V	1.4	0	12.83	12.87	12.58	12.23
2012	1203_1_69	2 35 08.04	61 08 53.30	G1-G7	G7V	1.1	0	15.14	15.18	14.79	13.90
2012	1106_1_82	2 35 08.13	61 42 07.80	F8-G0	F8V	2.6	1	17.67	17.12	16.49	15.94
2012	1105_3_20	2 35 08.19	61 49 17.70	A1-A3	A2V	2.2	1	14.44	14.06	13.77	13.86
2012	1105_4_19	2 35 08.19	61 54 43.90	M1-M2	M1V[g]	2.4	1	14.60	13.14	11.76	12.95
2012	1105_3_82	2 35 08.24	61 46 08.99	F4-F6	F5V	1.6	1	14.73	14.26	13.89	13.92
2012	1203_1_264	2 35 08.24	61 33 37.83	G0-G3	G0V	1.7	1	15.98	15.62	15.15	14.74
2012	1106_1_28	2 35 08.75	61 30 16.80	K4-K5	K5V	1.5	0	18.20	17.55	16.89	16.30
2012	1105_4_91	2 35 08.81	61 45 51.50	K3-K5	K4V	0.7	0	16.08	15.57	15.11	14.76
2012	1203_2_76	2 35 09.02	61 30 48.16	K3-K5	K4V	0.8	0	16.88	16.38	15.88	15.31
2012	1104_70	2 35 09.36	61 35 08.84		A1V	2.4	1	16.26	16.08	15.77	15.27
2012	1203_2_28	2 35 09.52	61 07 54.60	B4-B7	B6V	4.5	0	...	16.21	15.55	...
2012	1204_105	2 35 09.71	61 27 03.26	G6-G8	G7V	1.8	1	15.83	15.47	14.95	14.14
2012	1203_1_31	2 35 09.72	61 24 51.45	G6-G8	G6V	1.6	1	15.82	15.56	15.08	14.26
2012	0220_29	2 35 09.85	61 29 34.31		F5V	1.7	1	14.95	14.66	14.28	13.79
2012	1203_2_81	2 35 10.34	61 24 21.32	G5-G7	G6V	1.8	1	...	16.24	15.72	...
2012	1106_1_54	2 35 10.71	61 51 10.01	K6-K7	K6V	1.6	0	17.93	17.18	16.40	15.81
2012	1203_1_250	2 35 11.08	61 45 42.19	A9-F2	A9V	1.9	1	15.07	14.75	14.42	14.22
2011	0923_243	2 35 11.24	61 40 44.14	F5-F6	F6V	2.2	1	14.93	14.50	13.98	13.41
2012	1104_58	2 35 11.28	61 37 11.50	G2-K2	G8V	1.0	0	14.88	14.55	14.18	13.68
2012	0304_149	2 35 11.42	61 24 27.80	G5-G7	G6V	1.9	1	15.86	15.66	15.11	14.25
2012	1203_2_63	2 35 11.97	61 35 25.11	K4-K5	K4V	1.2	0	17.11	16.51	15.93	15.38
2012	1105_3_153	2 35 12.19	61 18 34.10	K5-K6	K5V	1.4	0	15.83	15.46	14.82	13.85
2012	1203_1_244	2 35 12.34	61 48 32.49	K1-K3	K2V[g]	1.9	1	15.61	14.95	14.34	14.07
2012	1204_121	2 35 12.40	61 13 48.14	F2-F3	F2V	2.5	1	...	16.17	15.64	...
2012	1106_3_151	2 35 12.95	61 54 43.40	G7-K2	K0V	3.3	1	17.53	16.72	15.83	15.03
2012	1203_1_61	2 35 12.95	61 04 51.17	A1-A2	A1V	3.7	1	...	15.89	15.30	...
2012	1203_1_40	2 35 12.96	61 26 28.53	B9-A0	A0V	3.0	1	15.33	15.29	14.88	13.91
2012	1106_1_96	2 35 12.99	61 38 44.60	G0-G6	G3V	3.4	1	17.73	17.02	16.16	15.51
2012	1105_3_160	2 35 13.31	61 21 36.80	F6-F7	F7V	1.3	0	14.92	14.97	14.62	13.73
2012	0304_100	2 35 13.31	61 45 26.70	A1-A2	A1V	2.2	1	15.78	15.61	15.33	14.94
2012	1106_1_45	2 35 13.42	61 54 10.10	F8-F9	F8V	3.5	1	18.45	17.78	16.97	16.34
2012	1105_3_144	2 35 13.51	61 31 07.31	G8-K0	G9V	3.0	1	16.03	15.30	14.49	14.31
2012	1203_1_256	2 35 13.69	61 38 11.24	F8-F9	F8V	1.8	1	16.20	15.82	15.37	14.97
2012	1104_292	2 35 13.70	61 59 42.14		F3V	1.6	1	16.14	15.83	15.49	15.03
2012	1104_300	2 35 13.78	61 54 48.50	A0-A2	A1V	1.6	1	14.09	14.02	13.88	13.37
2012	1106_1_48	2 35 13.81	61 55 53.91	B9-A2	A0V	4.5	0	17.93	17.34	16.61	15.94
2012	1203_1_241	2 35 13.92	61 42 48.15	A9-F0	A9V	2.0	1	15.40	15.12	14.77	14.57
2012	1105_3_276	2 35 14.60	61 27 23.20	K0-K2	K1V[g]	2.7	1	13.62	12.96	12.19	11.83
2012	0304_136	2 35 14.77	61 29 50.10		F3V	1.4	0	14.79	14.58	14.29	13.80
2012	1106_3_155	2 35 15.06	61 55 34.80	F0-F6	F3V	3.4	1	18.35	17.77	17.04	16.42
2012	1203_2_103	2 35 15.18	61 10 51.57	G4-G6	G5V	1.0	0	15.17	15.02	14.67	14.04
2012	1104_71	2 35 15.19	61 23 42.43		A6V	2.0	1	14.62	14.56	14.25	13.48
2012	1204_136	2 35 15.30	61 08 14.41	A1-A2	A1V	4.5	0	...	17.28	16.52	...
2012	1203_1_267	2 35 15.31	61 31 57.53	G9-K2	K0V	3.2	1	17.67	16.87	16.01	15.30
2012	1203_1_246	2 35 15.32	61 48 03.29	G9-K2	K0V	2.6	1	17.63	16.80	16.07	15.39
2012	0124_68	2 35 15.56	61 51 17.00	K0-K2	K2V	0.9	0	15.71	15.28	14.87	14.62
2011	1023_101	2 35 15.92	61 38 30.58	K6-M0	K6V	0.2	0	14.48	13.85	13.37	12.68
2012	0124_120	2 35 16.38	61 21 30.00	F3-F5	F4V	1.7	1	15.25	15.22	14.85	14.07
2012	1104_294	2 35 16.56	61 58 35.00		F8V	1.1	0	14.64	14.15	13.85	13.96
2012	0304_143	2 35 16.57	61 21 44.41	F4-F5	F4V	1.3	0	14.50	14.54	14.25	13.37
2012	1105_3_149	2 35 16.63	61 28 18.29	G7-G9	G8V	1.6	1	15.93	15.75	15.25	14.32
2012	1104_89	2 35 17.16	61 17 26.12	F5-F7	F6V	1.7	1	15.74	15.71	15.30	14.39
2012	1204_122	2 35 17.40	61 18 31.78		F9V	1.7	1	...	15.61	15.18	...
2012	1105_3_151	2 35 17.52	61 14 56.59	F2-F3	F2V	1.7	1	14.60	14.48	14.13	13.38
2012	0220_168	2 35 17.69	61 08 03.00	G7-G8	G7V	2.4	1	14.33	14.01	13.36	12.92
2012	1204_23	2 35 17.69	61 11 00.73	A7-A9	A8V	2.4	1	15.21	15.16	14.73	13.85
2012	1105_4_71	2 35 17.98	62 00 01.20	G4-G7	G5V	1.6	1	15.56	15.10	14.63	14.06
2012	1203_1_293	2 35 18.02	61 40 34.80	G2-G8	G5V	1.4	0	15.58	15.17	14.73	14.58
2012	1106_1_76	2 35 18.06	61 43 50.31		K6V	1.2	0	17.73	17.05	16.35	15.73
2012	1105_3_86	2 35 19.16	61 46 42.60	G6-G8	G6V	1.4	0	16.24	15.84	15.41	15.00
2012	0304_87	2 35 19.34	61 52 59.31	K2-K3	K3V	0.7	0	13.59	13.37	12.96	12.48
2012	1104_47	2 35 19.67	61 38 04.10	A0-A6	A1V	2.0	1	14.88	14.67	14.44	14.40
2012	0124_16	2 35 19.75	61 46 38.40	G9-K1	K0V	3.1	1	16.19	15.50	14.64	14.44
2012	1203_1_58	2 35 20.21	61 15 45.68		F8V	2.4	1	15.25	14.93	14.34	13.60
2011	1023_30	2 35 20.43	61 35 46.78	K0-K2	K1V	2.7	1	14.93	14.06	13.30	13.25
2012	0220_68	2 35 20.51	61 59 54.80	F4-F5	F4V	1.7	1	16.04	15.67	15.29	14.75
2012	0220_157	2 35 20.52	61 17 48.11	F8-F9	F9V	1.6	1	15.24	15.15	14.73	14.19
2012	1203_1_57	2 35 20.68	61 13 49.52	G6-G8	G7V	1.3	0	15.31	15.08	14.65	13.89
2012	0304_114	2 35 20.97	61 38 18.20	A6-F0	F0V	1.9	1	16.40	16.13	15.77	15.34
2012	0304_27	2 35 21.00	61 32 15.90	A1-A3	A2V	2.4	1	16.44	16.22	15.87	15.37
2011	0923_45	2 35 21.23	61 11 52.45	F8-G0	F9V	1.1	0	14.85	14.45	14.14	13.76
2012	0304_113	2 35 21.50	61 36 29.30	G7-G8	G8V	2.2	1	16.00	15.43	14.81	14.63
2012	1203_1_257	2 35 21.59	61 36 34.33	F4-F6	F5V	1.5	0	15.75	15.43	15.08	14.85
2012	0304_92	2 35 21.96	61 48 25.20	F4-F5	F5V	1.7	1	15.79	15.49	15.11	14.71
2012	1106_1_92	2 35 22.45	61 39 04.19	A3-A6	A5V	2.7	1	...	18.03	17.58	...
2012	1203_2_106	2 35 22.72	61 14 54.22	A0-A1	A1V	2.4	1	...	15.14	14.84	...
2012	0216_28	2 35 22.77	61 40 06.40	K6-M1	K8V	2.6	1	20.14	19.24	18.10	17.30
2012	1106_1_109	2 35 22.96	61 32 55.80	K4-K5	K4V	1.3	0	18.14	17.49	16.90	16.30
2012	0124_74	2 35 23.07	61 44 26.40	G4-G6	G7V[g]	2.6	1	15.14	14.52	13.83	13.23
2011	0923_9	2 35 23.08	61 10 14.59	F4-F6	F5V	1.9	1	15.54	15.48	15.05	14.20
2012	0220_70	2 35 23.09	61 59 04.30	B9-A0	A0V	2.4	1	16.48	16.25	15.96	15.43
2012	1105_3_78	2 35 23.21	61 49 50.90		K6V	1.6	1	15.90	15.20	14.41	14.12
2012	1203_1_269	2 35 23.28	61 32 39.47	F6-F7	F7V	1.5	0	15.93	15.61	15.21	14.83
2012	0216_125	2 35 23.35	61 32 26.20	M2-M3	M3V	1.4	0	20.48	19.75	18.35	17.55

Table 1. IC 1805 Spectral Types and Photometry (Continued)

Year	Date_No.[a] (MMDD_No.)	RA(J2000) (hhmmss.ss)	Dec(J2000) (° ′ ″)	SpTy Range	SpTy	A_V (r-i) (mag)	Assoc.?[b] (ext)	V(90P)[c] (mag)	r[d] (mag)	i[d] (mag)	I(90P)[c] (mag)
2012	0304_102	2 35 24.08	61 44 43.91	A7-A9	A8V	2.3	1	16.36	16.11	15.70	15.20
2012	1105_3_67*	2 35 24.11	61 59 14.20	A1-A2	A2V	2.1	1	15.25	15.04	14.76	14.25
2012	1106_2_190	2 35 24.32	61 11 28.50	K4-K5	K5V	1.4	0	...	16.87	16.22	...
2012	0124_111	2 35 24.43	61 18 07.80	F3-F5	F4V	1.7	1	...	15.13	14.76	...
2012	1104_56	2 35 24.57	61 36 40.91	G1-G8	G5V[g]	2.8	1	15.99	15.57	14.84	13.96
2012	1023_107	2 35 24.71	61 41 12.28	F4-F5.5	F5V	1.9	1	14.89	14.39	13.96	14.15
2012	0220_166	2 35 24.83	61 07 25.10	F3-F4	F4V	1.4	0	14.14	14.27	13.96	13.21
2012	1203_1_7	2 35 24.95	61 19 02.70	K3-K5	K4V	1.3	0	...	16.40	15.79	...
2012	0220_108	2 35 25.07	61 33 54.90	F4-F5	F4V	2.4	1	16.39	16.00	15.49	15.06
2012	1106_2_133	2 35 25.41	61 41 09.30		K6V	1.7	1	18.33	17.60	16.80	16.15
2012	1106_3_165	2 35 25.45	61 50 55.00	A3-A6	A5V	4.1	1	17.93	17.31	16.57	15.94
2012	0304_26	2 35 25.79	61 39 47.21		F9V	1.6	1	16.44	16.06	15.62	15.21
2012	1105_5_154	2 35 25.88	61 59 52.69	F6-F8	F7V	1.5	0	16.30	15.94	15.55	15.01
2012	1204_89	2 35 26.17	61 41 02.90	G5-K0	G7V[g]	3.6	1	17.84	17.01	16.10	15.41
2012	1104_236	2 35 26.18	61 55 16.72		F7V	1.8	1	15.79	15.45	15.01	14.64
2012	1104_8	2 35 26.42	61 41 35.30	F2-F6	F4V	2.4	1	16.35	16.00	15.48	14.94
2012	0304_145	2 35 26.65	61 21 21.10	G7-G9	G8V	2.9	1	15.08	14.57	13.81	12.72
2012	1106_1_15	2 35 26.94	61 39 28.30	K4-K5	K4V	1.8	1	18.20	17.53	16.84	16.19
2012	1106_2_167	2 35 27.37	61 24 51.60	F0-F3	F2V	2.7	1	...	17.13	16.56	...
2012	1106_3_168	2 35 27.40	61 52 29.20		K6V	1.4	0	18.10	17.38	16.64	16.06
2011	0923_4*	2 35 27.63	61 24 22.70	B9-A0	B9V	2.6	1	14.81	14.95	14.65	13.74
2012	1106_3_176	2 35 27.88	61 45 44.40	G5-K0	G8V[g]	2.9	1	16.72	16.08	15.32	14.82
2012	1104_242*	2 35 27.91	61 50 46.30	B3-B7	B4V	4.1	1	15.50	15.04	14.48	14.28
2011	0923_260	2 35 27.95	61 34 14.80		B8V	3.4	1	15.39	17.76	17.33	16.63
2012	1203_2_82	2 35 28.00	61 27 59.07	K0-K2	K1V[g]	3.1	1	...	17.03	16.16	...
2012	0304_140	2 35 28.02	61 28 21.80	F3-F5	F4V	1.4	0	15.26	14.34	14.02	13.99
2012	1203_1_2	2 35 28.14	61 30 56.11	G9-K2	K1V[g]	3.4	1	18.02	17.22	16.29	15.55
2012	1105_4_17	2 35 28.33	61 53 17.41	G0-G5	G1V	0.8	0	13.12	13.09	12.81	12.41
2012	1105_2_257	2 35 28.46	61 42 15.10	F2-F5	F4V	2.4	1	16.26	15.84	15.31	14.94
2012	1106_1_116	2 35 28.73	61 23 57.90	F0-F5	F4V	2.4	1	...	17.64	17.11	...
2012	0304_84	2 35 28.83	61 57 53.09	F4-F6	F5V	1.5	0	15.95	15.65	15.30	14.90
2011	0923_42*	2 35 28.86	61 16 16.53	A0-A1	A0V	2.5	1	14.94	15.06	14.75	13.83
2012	1106_1_68	2 35 28.87	61 48 05.11	F8-K0	G1V	3.6	1	18.44	17.72	16.86	16.21
2012	1104_10	2 35 29.04	61 41 14.79	G8-K3	K0V	3.0	1	16.10	15.36	14.54	14.27
2012	1203_1_68	2 35 29.67	61 08 28.68	B8-A0	B9V	3.2	1	15.41	15.25	14.82	14.17
2012	1105_3_93	2 35 29.81	61 42 00.10	A3-A5	A3V	2.5	1	15.50	15.24	14.88	14.70
2012	1106_2_162	2 35 29.84	61 27 45.20	F6-G0	F8V	2.4	1	...	17.50	16.92	...
2012	0124_63	2 35 29.90	61 48 52.50	F6-F8	F8V	4.3	0	16.41	15.42	14.43	14.17
2012	0304_126	2 35 30.33	61 34 31.50	A5-A6	A5V	2.6	1	16.49	16.21	15.77	15.27
2012	1105_3_157	2 35 30.37	61 15 54.20		A1V	2.6	1	15.72	15.78	15.43	14.52
2012	1106_2_182	2 35 30.37	61 13 43.91	G9-K2	K0V	3.3	1	...	16.87	15.99	...
2012	1204_130	2 35 30.66	61 15 29.86	K3-K4	K4V	0.7	0	...	16.04	15.57	...
2012	1104_74	2 35 30.67	61 27 29.59	A3-A5	A4V	1.6	1	13.43	13.60	13.39	12.60
2012	1105_2_265	2 35 30.70	61 36 01.09	F2-F4	F2V	1.7	1	16.00	15.73	15.37	15.06
2012	1105_3_29	2 35 31.01	61 34 20.60	F9-G4	G1V	1.6	1	15.75	15.40	14.95	14.69
2012	1104_267	2 35 31.04	61 42 56.60	G0-G9	G7V[g]	2.5	1	15.32	14.65	13.97	14.19
2012	1104_66	2 35 31.07	61 33 34.80	G1-G8	G5V	0.0	0	13.77	13.55	13.41	12.88
2012	1204_125	2 35 31.22	61 14 17.21		F8V	1.4	0	15.44	15.31	14.93	14.19
2012	0220_67	2 35 31.42	61 58 34.60	B8-B9	B9V	2.3	1	15.42	15.18	14.94	14.64
2012	0124_83	2 35 31.63	61 37 01.60	A6-A8	A7V	1.9	1	15.53	15.31	15.01	14.71
2012	0220_16	2 35 31.66	61 51 12.60		F8V	1.0	0	14.82	14.55	14.27	13.84
2012	1105_3_143	2 35 31.80	61 25 41.60	G8-K0	G9V[g]	2.5	1	15.30	14.93	14.23	13.19
2012	0304_109	2 35 32.04	61 42 34.99	F4-F5	F4V	1.9	1	15.64	15.34	14.92	14.75
2012	0304_278	2 35 32.06	61 15 25.30	A9-F0	F0V	1.9	1	15.56	15.59	15.23	14.32
2012	1106_1_7	2 35 32.57	61 54 27.60	A5-F0	A8V	5.7	0	17.83	17.50	16.35	15.56
2012	0220_151	2 35 32.85	61 10 03.30	F6-F7	F6V	2.0	1	15.97	15.77	15.30	14.59
2012	1203_2_86	2 35 33.50	61 26 59.82	K4-K5	K4V	0.6	0	15.39	15.03	14.58	13.78
2012	1106_3_161	2 35 33.53	61 49 29.00	K4-K5	K4V	1.3	0	17.09	16.39	15.80	15.30
2011	0923_254	2 35 33.69	61 36 28.50	F5-F6	F6V	1.0	0	14.22	13.85	13.59	13.72
2012	1203_1_268	2 35 33.89	61 33 50.67	K2-K4	K2V	2.5	1	18.31	17.60	16.84	16.12
2012	1106_1_62	2 35 34.02	61 49 46.40	F9-G7	G0V	2.8	1	18.25	17.62	16.92	16.29
2012	1106_1_73	2 35 34.16	61 42 36.51	K2-K4	K3V	1.9	1	18.26	17.59	16.92	16.36
2012	1204_124	2 35 34.52	61 17 07.46	G6-G8	G7V	1.2	0	14.73	14.72	14.32	13.79
2012	0220_112*	2 35 35.54	61 32 33.70	F9-G0	F9V	3.2	1	15.55	14.90	14.14	14.10
2012	1106_2_160	2 35 35.94	61 30 09.11	K4-K5	K4V	1.4	0	18.00	17.38	16.75	16.16
2012	0124_73	2 35 36.04	61 41 23.71	G3-G7	G5V	2.8	1	15.82	15.13	14.40	14.19
2012	0304_115	2 35 36.13	61 36 44.41		G8V	2.5	1	15.82	15.17	14.47	14.20
2012	0124_118*	2 35 36.25	61 20 33.11	G9-K1	K5V	1.9	1	15.48	14.98	14.22	13.24
2012	1204_94	2 35 36.66	61 35 04.91	F6-F7	F7V	1.5	0	16.04	15.70	15.31	14.96
2012	0220_63	2 35 36.78	61 56 27.80	B2-B4	B3V	4.1	1	15.53	15.08	14.54	14.44
2012	1204_97	2 35 37.07	61 32 00.52	A7-F0	A8V	3.9	1	18.52	17.94	17.17	16.48
2012	0220_123	2 35 37.19	61 29 32.40		F4V	1.4	0	14.35	14.12	13.80	13.30
2012	1204_25	2 35 37.50	61 09 29.64	A0-A2	A1V	2.9	1	14.66	14.65	14.24	13.33
2012	0220_65	2 35 37.93	61 58 18.29	G6-G8	G7V	1.3	0	16.08	15.69	15.27	14.85
2011	0923_47	2 35 37.97	61 12 15.06		A1V	1.8	1	13.45	13.75	13.57	12.90
2012	0216_112	2 35 37.99	61 39 26.10	M2-M3	M2V	1.8	1	20.06	19.18	17.85	17.05
2012	0220_153	2 35 38.91	61 09 05.00		F8V	2.0	1	15.71	15.42	14.91	14.22
2012	1106_1_87	2 35 39.63	61 41 03.70	F4-F7	F6V	2.5	1	17.65	17.17	16.59	15.98
2012	1105_3_14	2 35 39.90	61 58 43.10	F4-F5	F4V	1.4	0	14.21	13.91	13.60	13.16
2012	1105_3_104	2 35 39.97	61 41 33.80	A1-A3	A2V	2.2	1	16.32	16.11	15.80	15.41
2011	1023_143	2 35 40.08	61 11 26.00	B8-B9	B9V	2.8	1	14.45	14.70	14.36	13.21
2012	1105_3_61	2 35 40.17	61 59 49.40	G5-K0	G7V[g]	3.2	1	16.30	15.55	14.73	14.14
2012	1104_238	2 35 40.26	61 57 37.60	K4-K5	K4V[g]	3.1	1	16.31	15.35	14.36	13.66
2012	0304_276	2 35 40.41	61 15 08.20	G8-K0	G9V	2.7	1	15.43	15.02	14.28	13.22
2012	1106_1_107	2 35 40.50	61 30 22.80	F6-F7	F8V	2.9	1	17.39	16.89	16.20	15.56
2012	1203_2_88	2 35 40.67	61 26 09.67	K0-K5	K3V	2.8	1	...	17.69	16.85	...
2012	0220_155*	2 35 40.73	61 10 07.70	B7-B8	B8V	3.1	1	15.03	14.92	14.54	13.86

Table 1. IC 1805 Spectral Types and Photometry (Continued)

Year	Date_No.[a] (MMDD_No.)	RA(J2000) (hhmmss.ss)	Dec(J2000) (° ′ ″)	SpTy Range	SpTy	A_V (r-i) (mag)	Assoc.?[b] (ext)	V(90P)[c] (mag)	r[d] (mag)	i[d] (mag)	I(90P)[c] (mag)
2012	1105_3_125	2 35 40.87	61 34 57.10	G9-K2	K2V[g]	2.4	1	15.47	14.74	14.01	14.16
2012	1203_1_50	2 35 41.50	61 21 32.24	G8-K2	G9V	2.1	1	...	16.82	16.21	...
2012	1203_2_68	2 35 41.65	61 40 01.71	G7-G9	G8V[g]	3.1	1	16.74	16.01	15.20	14.81
2012	1105_3_87	2 35 41.71	61 47 01.70	F4-F5	F4V	1.9	1	16.00	15.63	15.21	14.90
2012	0304_22	2 35 42.17	61 41 07.10	G8-K0	G9V	3.1	1	14.96	14.17	13.34	13.63
2012	1203_2_59	2 35 42.20	61 45 15.50	G1-K0	G8V	2.9	1	16.92	16.25	15.48	14.92
2012	1104_54	2 35 42.74	61 36 25.61	G1-G9	G9V[g]	...	0	12.91	13.41	...	11.83
2012	1105_5_168	2 35 42.95	61 52 43.90	G8-K0	G9V	1.2	0	14.63	14.27	13.84	13.32
2012	1203_2_73	2 35 43.23	61 28 44.00	G8-K2	G9V	2.9	1	...	16.59	15.79	...
2012	1104_67	2 35 43.26	61 30 45.31	F8-F9	F9V	1.4	0	14.94	14.42	14.04	13.89
2012	0124_78	2 35 43.30	61 44 04.30	G1-G7	G5V	2.2	1	14.68	14.13	13.54	12.98
2012	1105_4_73	2 35 43.49	62 00 07.70	A3-A8	A5V	2.1	1	14.82	14.50	14.17	13.67
2011	1023_148	2 35 43.71	61 14 53.29	G2-G7	G5V	3.3	1	15.69	15.24	14.41	13.31
2012	1105_3_113	2 35 43.72	61 36 28.81	F8-F9	F8V	1.6	1	16.26	15.92	15.49	14.99
2012	0124_76	2 35 44.04	61 44 49.21	F4-F6	F5V	2.0	1	15.44	15.08	14.63	14.42
2012	1105_3_137	2 35 44.10	61 29 56.31	F2-F4	F3V	1.6	1	15.17	14.90	14.56	14.08
2012	1104_261	2 35 44.62	61 42 29.20	K3-K5	K4V	0.9	0	16.42	15.86	15.36	14.99
2012	1104_234	2 35 44.87	62 00 05.33		A1V	2.8	1	15.66	15.16	14.76	14.37
2012	0216_118	2 35 44.98	61 38 22.10	K7-M1	K8V	2.0	1	19.01	18.32	17.32	16.65
2012	1105_3_16	2 35 45.14	61 58 50.50	K4-K5	K4V	0.5	0	15.83	15.28	14.84	14.54
2012	1104_35	2 35 45.26	61 39 56.60	F6-F8	F8V	1.3	0	14.13	13.83	13.48	12.96
2012	0124_26	2 35 45.59	61 23 08.80	A9-F2	F1V	2.2	1	15.90	15.83	15.38	14.52
2012	1105_3_109	2 35 45.86	61 40 26.10	F9-G3	G0V	1.4	0	15.65	15.30	14.90	14.66
2012	0124_117	2 35 46.04	61 18 36.71	F7-F9	G0V	1.8	1	15.96	15.81	15.33	14.51
2012	0220_17	2 35 46.14	61 39 14.21	G7-G9	G8V	2.6	1	15.65	15.03	14.34	14.36
2012	1106_1_93	2 35 46.26	61 33 47.01	K2-K4	K3V	2.4	1	18.25	17.68	16.92	16.05
2012	0304_150	2 35 46.48	61 21 20.70	F3-F5	F4V	1.6	1	15.84	15.79	15.42	14.84
2012	0220_82	2 35 46.86	61 44 15.00	G8-K0	G9V	3.4	1	15.21	14.32	13.41	13.85
2012	1105_3_103	2 35 47.09	61 39 03.00	B9-A0	A0V	1.9	1	12.81	12.92	12.75	12.52
2012	1106_1_59	2 35 47.12	61 52 21.29	K2-K4	K3V[g]	4.4	0	18.05	16.99	15.79	15.08
2012	0220_20	2 35 47.29	61 51 30.19	F2-F3	F2V	1.4	0	14.49	14.25	13.96	13.53
2012	0220_14	2 35 47.42	61 56 24.20		F8V	1.6	1	13.26	13.42	13.01	12.45
2012	0220_18	2 35 47.86	61 53 43.40	F7-F8	F8V	1.1	0	13.43	13.02	12.72	12.56
2012	1105_3_96	2 35 48.24	61 44 08.80	F8-F9	F8V	0.9	0	14.24	13.99	13.73	13.28
2012	0220_139	2 35 48.72	61 24 30.30	B8-B9	B9V	2.6	1	15.68	15.62	15.33	14.52
2012	1104_75	2 35 49.88	61 17 40.16	F7-F8	F8V	1.4	0	15.45	15.30	14.92	13.93
2012	1106_2_176	2 35 50.00	61 17 20.80	G9-K2	K1V	3.7	1	...	16.30	15.33	...
2012	1105_3_95	2 35 50.09	61 43 11.70	B9-A0	B9.5V	2.3	1	14.38	14.05	13.80	13.90
2012	0220_61	2 35 50.09	61 57 49.40	G1-G2	G1V	3.5	1	15.30	14.49	13.65	13.63
2012	0220_84	2 35 50.14	61 44 07.20	F5-F7	F6V	1.7	1	16.45	16.12	15.71	15.28
2012	1104_243	2 35 50.42	61 50 58.10	G1-G8	G8V	0.8	0	15.44	15.07	14.74	14.54
2012	0220_75	2 35 50.67	61 46 31.90	G7-G8	G7V	1.3	0	16.05	15.65	15.24	14.86
2012	0220_28*	2 35 50.68	61 33 10.81	K0-K1	K0V	2.6	1	16.12	15.45	14.71	14.45
2012	1106_1_77	2 35 50.82	61 43 43.80	G5-K1	G8V	3.2	1	16.92	16.18	15.35	14.87
2012	0304_106	2 35 51.12	61 44 27.10	K3-K4	K3V	0.5	0	15.10	14.49	14.14	13.95
2012	1104_239	2 35 51.20	61 59 02.98		K3V	0.7	0	14.72	15.15	14.75	14.34
2012	1105_3_18	2 35 51.58	61 59 07.31	F2-F3	F2V	1.3	0	13.45	13.20	12.93	12.49
2012	1105_3_94	2 35 51.60	61 44 47.39	B8-A0	B9V	2.2	1	15.56	15.40	15.19	14.90
2012	0124_77	2 35 51.74	61 43 39.50	F0-F4	F4V	1.9	1	16.25	15.92	15.51	15.14
2012	1105_4_13	2 35 51.76	61 50 31.60	F8-G0	F9V	1.3	0	15.33	14.95	14.59	14.37
2012	1106_1_58	2 35 52.10	61 53 09.89	G7-K0	G9V	2.6	1	17.01	16.38	15.65	15.15
2012	1106_1_98	2 35 52.24	61 35 56.60	G9-K3	K0V[g]	3.1	1	17.00	16.25	15.42	14.97
2012	0124_89	2 35 52.45	61 39 19.09	G4-K0	G8V	2.2	1	13.51	13.14	12.50	12.34
2012	1106_2_141	2 35 52.48	61 35 54.60	K2-K4	K3V	1.2	0	17.18	16.72	16.20	15.62
2012	0124_115	2 35 52.54	61 17 19.40	F7-F9	F8V[g]	1.9	1	15.58	15.47	14.99	14.16
2012	0124_14	2 35 52.96	61 49 51.00	G4-G8	G6V	0.7	0	15.15	14.78	14.47	14.39
2012	1104_18	2 35 53.34	61 24 32.69		F7V	1.5	0	15.05	15.06	14.67	14.09
2012	1105_5_280	2 35 53.69	62 00 11.80	B0-B2	B1V	4.8	0	14.91	14.24	13.64	13.14
2011	0923_36	2 35 53.85	61 20 53.20	A7-F0	A7V	1.8	1	15.23	15.27	15.00	14.44
2012	1104_42	2 35 54.31	61 38 45.39	A0-A3	A1V	2.0	1	14.64	14.49	14.26	13.78
2012	1104_79*	2 35 54.82	61 19 23.23	A9-F1	F0V	1.8	1	15.84	15.73	15.40	14.62
2012	1106_1_13	2 35 54.90	61 37 41.10	G7-K0	G9V	3.0	1	16.85	16.16	15.35	14.89
2012	1106_1_20	2 35 55.51	61 45 19.50	F4-F7	F6V	2.3	1	17.97	17.51	16.98	16.45
2012	0304_139	2 35 55.75	61 25 30.70	A2-A4	A3V	2.3	1	15.38	15.06	14.75	14.17
2012	1104_9	2 35 56.72	61 36 25.70	A2-A6	A5V	2.2	1	16.24	16.01	15.68	15.23
2012	0216_114	2 35 57.47	61 39 22.71	K6-K7	K6V	2.0	1	18.82	18.09	17.22	16.60
2012	1105_3_13	2 35 57.84	61 45 30.10	A1-A3	A3V	2.6	1	13.52	13.49	13.09	12.67
2012	1106_1_47	2 35 58.04	62 00 11.91	F2-F5	F4V	3.0	1	17.55	17.28	16.62	15.77
2012	0220_74	2 35 58.57	61 52 32.60		F4V	1.4	0	14.37	14.10	13.79	13.35
2012	0124_84	2 35 58.73	61 40 44.01	G1-G9	G5V[g]	2.0	1	14.19	13.61	13.05	12.50
2012	0216_26	2 35 59.30	61 41 36.79	M2-M4	M3V	1.6	0	19.21	18.64	17.20	16.39
2012	0304_110	2 35 59.47	61 43 49.89	K0-K2	K1V	1.0	0	15.94	15.53	15.12	14.83
2012	0220_272	2 35 59.47	61 17 50.10	A9-F0	F0V	2.6	1	15.84	15.69	15.18	14.19
2011	1023_137	2 35 59.95	61 18 17.50	F3-F5	F4V	2.0	1	14.90	14.88	14.43	13.86
2012	0304_112	2 36 00.48	61 39 11.01	F6-F7	F6V	1.4	0	14.73	14.30	13.94	13.96
2012	1105_3_154	2 36 00.76	61 13 02.50	G8-G9	G9V	1.1	0	15.07	15.07	14.66	13.78
2012	0220_100	2 36 01.37	61 38 11.10	B9-A0	B9V	2.8	1	16.39	16.16	15.82	15.38
2012	0220_95	2 36 01.38	61 37 13.91	A5-A6	A6V	2.0	1	13.33	13.35	13.05	12.63
2012	1104_76	2 36 02.11	61 20 24.83	A3-A5	A4V	2.3	1	15.54	15.41	15.06	14.23
2012	0304_15	2 36 02.34	61 53 21.00		A1V[g]	2.5	1	15.38	15.06	14.73	14.59
2012	1105_3_99	2 36 02.41	61 44 10.80	A2-A4	A3V	2.4	1	16.23	16.02	15.66	15.20
2011	1023_120	2 36 02.67	61 34 35.10		A0V	2.3	1	15.93	15.47	15.20	15.04
2012	0304_146	2 36 02.83	61 20 47.10	F9-G2	G0V	1.1	0	14.11	14.20	13.86	12.96
2012	0220_73	2 36 02.87	61 47 38.09	A2-A3	A2V	2.1	1	16.32	16.09	15.82	15.37
2012	1105_4_75	2 36 02.88	62 00 22.80	G6-G8	G7V	1.5	0	16.35	15.87	15.41	14.86
2012	0220_158	2 36 03.08	61 09 32.20		K2V	0.7	0	15.21	15.06	14.69	13.86
2012	1106_2_149	2 36 03.16	61 38 56.70	K1-K4	K4V[g]	3.7	1	16.86	15.82	14.71	14.34

Table 1. IC 1805 Spectral Types and Photometry (Continued)

Year	Date_No.[a] (MMDD_No.)	RA(J2000) (hhmmss.ss)	Dec(J2000) (° ′ ″)	SpTy Range	SpTy	A_V (r-i) (mag)	Assoc.?[b] (ext)	V(90P)[c] (mag)	r[d] (mag)	i[d] (mag)	I(90P)[c] (mag)
2012	0220_116	2 36 03.72	61 31 59.70		F2V	1.7	1	16.10	15.85	15.49	15.09
2012	1104_233	2 36 04.11	61 58 21.22		G2V	1.8	1	16.29	15.82	15.31	14.90
2012	0220_156	2 36 04.23	61 10 14.91	F9-G1	G0V	1.2	0	14.59	14.67	14.31	13.38
2012	1104_264	2 36 04.40	61 45 58.20	G8-K2	K1V	1.7	1	16.04	15.44	14.88	14.59
2012	0304_142	2 36 04.45	61 22 34.20		B4V	2.9	1	15.57	15.52	15.23	14.44
2012	0220_78*	2 36 04.58	61 52 02.40	G7-G8	G8V	1.8	1	15.31	14.80	14.27	14.20
2012	0220_160	2 36 04.78	61 07 39.90	B1-B3	B2V	3.9	1	15.47	15.43	14.96	14.06
2012	1104_244	2 36 04.80	61 55 27.50	F8-F9	F8V	1.5	0	16.08	15.70	15.31	14.94
2012	0124_71	2 36 05.24	61 42 19.20	F8-F9	F8V	1.0	0	14.69	14.35	14.06	14.07
2012	0220_278	2 36 05.32	61 14 11.89	F8-G0	F9V	1.8	1	15.48	15.50	15.04	14.12
2011	1023_132	2 36 05.56	61 22 05.10	A7-A8	A8V	2.1	1	14.49	14.38	14.01	13.06
2012	1105_3_274	2 36 05.59	61 18 02.50	F4-F6	F4V	1.5	0	14.15	14.23	13.90	13.13
2012	1104_20*	2 36 05.66	61 21 33.80	B6-B8	B7V	2.3	1	13.86	14.06	13.86	13.11
2012	1106_1_12	2 36 05.68	61 47 35.20	G7-K1	G9V	2.2	1	17.39	16.76	16.11	15.51
2012	0124_72	2 36 05.72	61 47 42.90	B7-B9	B9V	2.3	1	14.92	14.61	14.36	14.43
2012	0124_98*	2 36 05.82	61 32 50.40	G4-K0	G8V	2.5	1	14.98	14.31	13.62	13.69
2012	0220_72	2 36 05.91	61 54 36.91	K6-M0	K8V	0.8	0	14.83	14.17	13.41	12.85
2012	0304_95	2 36 06.40	61 47 37.30	A1-A3	A2V	1.1	0	13.67	13.45	13.38	13.05
2012	0124_13	2 36 06.48	61 35 01.90	G6-K0	G7V	1.1	0	16.26	15.92	15.54	15.18
2012	0220_128	2 36 06.61	61 28 56.40	G7-G8	G8V	3.6	1	13.24	13.36	12.43	11.52
2012	0124_28	2 36 06.83	61 21 26.50	G1-G3	G2V	1.2	0	15.28	15.22	14.85	14.06
2012	1105_3_118	2 36 07.09	61 36 35.30	F2-F3	F3V	1.9	1	16.21	15.87	15.46	15.08
2012	1105_3_146	2 36 07.46	61 24 13.20	G8-K0	G9V[g]	2.0	1	13.60	13.40	12.79	12.10
2012	0304_122	2 36 07.83	61 34 51.61	G6-G8	G7V	0.9	0	14.67	14.40	14.06	13.54
2012	0220_76	2 36 07.83	61 53 45.50	K1-K3	K2V	3.8	1	15.80	14.80	13.78	13.75
2012	0124_75	2 36 08.24	61 43 34.01	K2-K4	K3V	0.9	0	16.19	15.75	15.30	14.94
2011	1023_123	2 36 08.41	61 25 57.05		K2V	2.0	1	14.29	13.89	13.24	12.12
2012	1104_34	2 36 08.94	61 41 06.29	A5-A8	A6V	2.0	1	15.18	14.92	14.62	14.42
2012	0220_80	2 36 09.51	61 50 44.90	F8-F9	F8V	2.5	1	15.04	14.48	13.88	13.31
2012	0220_101	2 36 09.54	61 33 52.40		A7V	1.5	1	14.27	14.09	13.86	13.42
2012	0304_103	2 36 09.89	61 42 25.70	G8-K0	G9V	4.0	1	15.34	14.48	13.47	13.54
2011	1023_128	2 36 09.94	61 29 22.90		A9V	1.9	1	15.18	14.93	14.61	14.05
2012	1106_1_81	2 36 10.00	61 38 56.81	F5-F7	F6V	1.9	1	17.92	17.56	17.11	16.59
2012	0124_93	2 36 10.09	61 30 02.71	K2-K3	K3V	0.9	0	16.33	15.85	15.40	14.94
2012	0304_147	2 36 10.16	61 16 42.70		F8V	0.1	0	13.96	13.89	13.79	12.80
2012	0220_23	2 36 10.20	61 25 51.41	A3-A5	A4V	2.7	1	15.52	15.45	15.01	14.13
2012	1104_68	2 36 10.57	61 28 55.61	B9-A5	A0V	1.9	1	14.88	14.66	14.48	13.95
2012	0220_71	2 36 11.10	61 48 03.50		A2V	2.1	1	15.76	15.55	15.28	14.96
2012	0304_148	2 36 11.34	61 19 12.00	K7-M2	M0V	0.3	0	14.63	14.37	13.61	12.92
2012	1104_6	2 36 11.44	61 42 35.30	F3-F5	F4V	1.5	0	14.69	14.32	13.98	13.76
2012	0220_117	2 36 11.56	61 31 26.50	G2-G4	G3V	1.0	0	15.41	15.11	14.77	14.57
2012	0124_87	2 36 11.59	61 38 41.40	A1-A6	A2V	2.2	1	15.75	15.60	15.31	14.98
2012	1106_1_88	2 36 11.63	61 40 49.80		K6V	0.9	0	17.40	16.79	16.16	15.60
2012	0304_107	2 36 11.74	61 43 14.30	B9-A1	A0V	2.5	1	15.56	15.36	15.04	14.66
2012	0124_116	2 36 11.84	61 18 29.10	F5-F7	F6V	1.9	1	15.90	15.68	15.23	14.42
2012	0220_83	2 36 11.87	61 43 05.70		F7V	1.0	0	13.88	13.67	13.40	12.95
2012	1106_1_102	2 36 12.59	61 31 08.40	F8-G0	F9V	2.4	1	17.65	17.16	16.56	15.96
2012	1104_46	2 36 13.41	61 38 04.70	A6-F0	A8V	1.8	1	16.35	16.12	15.81	15.39
2012	0220_15	2 36 13.42	61 41 14.00	G7-G8	G8V	0.9	0	15.42	15.09	14.73	14.54
2012	1104_247	2 36 13.83	61 54 37.73		G0V	3.0	1	16.48	15.76	15.01	14.69
2012	1105_3_15	2 36 14.50	61 47 28.91	A3-A8	A5V	1.8	1	16.19	15.99	15.73	15.33
2012	0220_87	2 36 14.60	61 45 02.50	A9-F0	A9V	1.9	1	16.08	15.83	15.50	15.15
2012	1104_297	2 36 15.47	61 51 49.90	G2-K2	G8V	1.7	1	14.78	14.28	13.77	13.24
2012	0124_20	2 36 15.78	61 48 48.60	B9-A1	A0V	1.9	1	13.57	13.44	13.24	12.83
2012	0220_134	2 36 15.85	61 24 19.40	K4-K6	K5V	0.8	0	14.74	14.51	13.99	13.12
2012	1104_249	2 36 17.15	61 55 37.19	A9-F2	A9V	1.5	0	15.28	15.02	14.78	14.57
2012	1105_3_79	2 36 17.61	61 57 47.00	A7-A8	A7V	1.8	1	15.11	14.78	14.49	14.45
2012	0220_152	2 36 18.14	61 10 00.31		K3V	0.9	0	15.43	15.23	14.79	14.15
2012	1106_1_89	2 36 18.14	61 40 10.90	F9-K1	G8V	3.1	1	17.10	16.40	15.58	15.09
2012	0216_104	2 36 18.23	61 49 07.60	M2-M4	M3V	1.7	1	19.70	18.93	17.47	16.70
2012	1105_3_141	2 36 18.65	61 16 55.40	G0-G2	G1V	1.8	1	15.85	15.71	15.21	14.27
2012	0220_97	2 36 18.66	61 38 28.30	G6-G8	G7V	2.0	1	16.29	15.81	15.23	14.85
2012	1104_248	2 36 18.77	61 56 19.90	F8-G0	F9V	0.7	0	14.48	14.14	13.91	13.43
2012	1106_1_60	2 36 18.96	61 54 47.91	F8-G0	F9V	2.1	1	17.60	17.12	16.59	16.07
2012	1104_256	2 36 19.47	61 50 24.89	F6-F7	F7V	1.4	0	16.25	15.94	15.58	15.18
2012	1105_3_127	2 36 19.47	61 33 18.70	F8-F9	F9V	1.4	0	15.73	15.44	15.06	14.76
2012	1105_3_84	2 36 20.52	61 53 55.41	F7-F8	F8V	1.0	0	14.91	14.54	14.25	14.22
2012	0124_112	2 36 20.58	61 19 08.70	G2-G8	G6V[g]	1.0	0	14.77	14.74	14.39	13.49
2012	0220_88	2 36 20.90	61 46 56.70	A8-F0	A9V	1.8	1	16.06	15.82	15.52	15.13
2012	0124_97*	2 36 21.44	61 31 05.09	A1-A6	A3V	2.4	1	15.72	15.47	15.12	14.72
2012	0124_11	2 36 21.59	61 34 08.40	F8-F9	F8V	1.5	0	15.80	15.52	15.14	14.82
2012	1105_3_115	2 36 22.03	61 35 57.30	G9-K0	G9V[g]	2.0	1	14.35	13.79	13.20	12.72
2012	0220_127	2 36 22.54	61 27 52.90	F3-F5	F4V	2.5	1	15.92	15.75	15.20	14.34
2012	0220_110	2 36 23.09	61 35 36.50	G6-G7	G6V	1.3	0	15.98	16.14	15.71	15.18
2012	0304_116	2 36 23.34	61 38 14.00	M1-M3	M1V[g]	1.9	1	15.63	14.63	13.37	13.42
2012	1105_3_77	2 36 23.70	61 57 52.00	F8-F9	F8V	1.2	0	15.08	14.65	14.32	14.18
2012	1105_3_131	2 36 23.96	61 23 48.20	B9-A0	A0V	2.1	1	15.04	15.04	14.81	14.02
2012	0220_154	2 36 24.06	61 07 52.00	B8-B9	B9V	3.3	1	15.96	15.99	15.54	14.69
2012	1105_3_26	2 36 24.08	61 38 44.30	A5-A8	A7V	1.9	1	16.13	16.02	15.71	15.27
2012	1105_5_159	2 36 24.15	61 56 33.80	F5-F7	F6V	1.5	0	15.73	15.40	15.04	14.74
2012	0220_13	2 36 24.88	61 41 46.20	F7-F8	F7V	1.8	1	16.49	16.11	15.66	15.23
2012	1106_1_5	2 36 25.10	61 59 07.31	F8-G0	F9V	1.7	1	18.15	17.69	17.23	16.76
2012	1105_3_88	2 36 25.22	61 53 20.61	G8-K0	G9V	2.3	1	13.48	13.15	12.50	12.13
2012	0220_25	2 36 25.71	61 25 18.60	F3-F4	F4V	1.6	1	15.31	14.90	14.53	13.97
2012	0220_104	2 36 25.74	61 37 07.51	G2-G4	G3V	3.2	1	16.13	15.41	14.61	14.60
2012	0304_133	2 36 26.14	61 21 29.30	G9-K0	K0V	1.7	1	14.41	14.03	13.48	12.59
2012	0124_106	2 36 26.34	61 27 28.40	G5-G7	G7V	1.4	0	14.63	14.24	13.80	12.84

Table 1. IC 1805 Spectral Types and Photometry (Continued)

Year	Date_No.[a] (MMDD_No.)	RA(J2000) (hhmmss.ss)	Dec(J2000) (° ′ ″)	SpTy Range	SpTy	A_V (r-i) (mag)	Assoc.?[b] (ext)	V(90P)[c] (mag)	r[d] (mag)	i[d] (mag)	I(90P)[c] (mag)
2012	1105_3_73	2 36 27.83	61 56 49.20	F6-F7	F7V	1.4	0	16.29	15.95	15.59	15.16
2012	0304_28	2 36 28.28	61 40 14.60	G1-G3	G2V	3.2	1	15.94	15.27	14.46	13.83
2012	0304_138	2 36 28.63	61 24 32.31		F4V	1.0	0	13.48	13.59	13.37	12.45
2012	0220_94	2 36 28.95	61 41 21.50		F8V	1.6	1	16.33	15.96	15.54	15.16
2012	0220_274	2 36 29.01	61 12 24.90		F4V	1.9	1	15.24	14.77	14.35	13.93
2012	0304_105	2 36 29.02	61 43 22.61	F2-F4	F3V	1.7	1	15.46	15.21	14.85	14.57
2012	0220_77	2 36 29.58	61 53 07.40	F7-F8	F7V	1.4	0	15.51	15.13	14.77	14.59
2012	0220_280	2 36 29.64	61 08 20.00		F8V	1.4	0	13.48	13.57	13.20	12.27
2012	1104_72	2 36 29.67	61 16 50.48	F8-F9	F9V	1.3	0	14.72	14.79	14.42	13.67
2012	0124_99	2 36 29.69	61 31 45.19	F8-F9	F8V	1.3	0	15.42	15.13	14.78	14.72
2012	1104_61	2 36 30.04	61 22 13.40	F8-F9	F8V	1.6	1	15.83	15.28	14.87	14.00
2012	1104_57	2 36 30.23	61 30 39.50	G1-G8	G8V	0.9	0	15.09	14.74	14.40	14.52
2012	0304_93	2 36 30.55	61 48 23.49	A9-F0	F0V	3.4	1	14.00	14.10	13.43	13.10
2012	0304_134	2 36 30.65	61 25 43.50	G7-G8	G7V	2.8	1	15.46	15.07	14.32	13.36
2012	1104_257	2 36 30.98	61 48 53.90	B8-A0	B9V	2.1	1	14.61	14.33	14.14	14.20
2012	1104_5	2 36 31.07	61 33 44.60	G1-K0	G9V[g]	3.4	1	16.30	15.51	14.61	14.41
2012	1105_3_145	2 36 31.30	61 17 04.10	B4-B5	B5V	3.3	1	14.18	14.22	13.83	12.88
2012	0124_81	2 36 31.69	61 37 35.60	A1-A6	A2V	2.1	1	16.08	15.92	15.65	15.25
2012	0304_125	2 36 31.91	61 30 56.80	B7-B8	B8V	2.7	1	14.02	13.83	13.54	13.05
2012	0220_85	2 36 31.92	61 46 05.79	F0-F1	F0V	1.7	1	16.14	15.91	15.60	15.21
2012	1106_1_85	2 36 32.29	61 39 04.30	G8-K3	K0V	2.9	1	17.50	16.77	15.96	15.37
2012	1106_1_63	2 36 33.23	61 48 37.30	F8-G7	G0V	3.3	1	18.40	17.70	16.89	16.23
2012	1105_3_71	2 36 33.28	61 56 39.50	F6-F7	F6V	1.9	1	15.93	15.48	15.02	14.71
2012	0220_96	2 36 33.31	61 41 09.91	G8-K0	G9V	2.7	1	16.11	15.40	14.65	14.53
2012	1106_1_100	2 36 33.44	61 32 50.70	A9-F0	A9V	2.4	1	16.58	16.31	15.88	15.36
2012	1104_258*	2 36 33.62	61 50 35.10	B8-A0	B9V	1.8	1	14.94	14.50	14.37	14.39
2012	1105_3_112	2 36 33.64	61 37 24.70	F4-F5	F4V	2.0	1	15.98	15.68	15.25	14.94
2012	1105_3_83	2 36 33.98	61 50 36.59	G8-K1	G9V[g]	4.0	1	16.22	15.40	14.37	14.23
2012	0304_128	2 36 34.28	61 32 36.90		A0V	1.8	1	12.89	12.98	12.81	12.55
2012	1104_33	2 36 34.37	61 39 03.21	G7-G8	G8V	0.8	0	15.12	14.81	14.49	14.59
2012	1104_246	2 36 34.39	61 58 56.35		F8V	1.0	0	15.22	14.88	14.58	14.36
2012	0220_147	2 36 34.66	61 14 41.30	G0-G2	G1V	1.7	1	15.74	15.62	15.15	14.24
2012	0220_149	2 36 35.28	61 15 47.30		F9V	1.3	0	14.71	14.77	14.41	13.54
2012	1106_1_86	2 36 35.45	61 40 41.70	K4-K5	K4V[g]	3.4	1	18.27	17.31	16.27	15.54
2012	0124_100	2 36 36.34	61 32 12.40	K0-K2	K1V	1.5	0	16.21	15.77	15.25	14.86
2012	1105_3_98	2 36 36.81	61 46 23.80	G8-K0	G9V[g]	2.3	1	15.40	14.74	14.08	14.24
2012	0220_89	2 36 37.11	61 47 47.40	G6-G7	G7V	1.4	0	16.10	15.66	15.22	14.96
2012	0220_143	2 36 37.47	61 12 29.90	A1-A2	A1V	2.4	1	15.81	15.78	15.46	14.60
2012	0304_108	2 36 38.65	61 45 54.09	G1-G3	G2V	2.4	1	14.43	13.69	13.06	13.54
2012	1104_253	2 36 38.83	61 48 20.90	F8-G4	G1V	1.6	1	16.40	15.96	15.51	15.13
2012	1104_32	2 36 38.87	61 41 38.00	F6-F8	F8V	0.7	0	13.90	13.67	13.44	13.01
2012	1104_241	2 36 39.57	61 55 32.27		F8V	1.4	0	13.00	13.19	12.82	12.37
2012	1105_3_75	2 36 39.94	61 58 54.70	G6-G8	G7V	1.2	0	16.13	15.76	15.36	14.90
2012	1104_37	2 36 40.79	61 39 48.00	F9-G1	G0V	1.7	1	16.14	15.75	15.30	14.97
2012	1104_254	2 36 41.28	61 52 24.91	A1-A6	A3V	2.0	1	15.57	15.34	15.08	14.79
2012	1105_3_117	2 36 41.87	61 35 56.40	G0-G7	G1V	2.4	1	16.18	15.68	15.07	14.68
2012	1105_3_24	2 36 42.71	61 39 36.21	F2-F4	F4V	1.1	0	13.79	13.62	13.37	12.99
2012	1105_3_81	2 36 44.20	61 51 00.41	F8-G2	G0V	1.4	0	15.34	14.95	14.55	14.34
2012	0124_82*	2 36 44.21	61 43 23.20	A2-A6	A4V	1.7	1	15.01	14.50	14.27	14.25
2012	1105_3_128	2 36 44.59	61 32 52.10	G0-G5	G2V	2.6	1	15.34	14.72	14.05	14.15
2012	1105_3_85	2 36 44.84	61 52 27.40	G0-G8	G6V	1.3	0	16.34	15.92	15.51	15.18
2012	0220_93	2 36 44.96	61 39 06.41		F5V	1.7	1	15.54	15.22	14.82	14.60
2012	0220_113*	2 36 47.20	61 29 59.79	G8-G9	G9V	1.9	1	14.49	13.91	13.35	12.74
2012	0304_117	2 36 48.48	61 36 21.10	F8-F9	F8V	1.5	0	16.38	16.05	15.67	15.25
2012	1105_3_100*	2 36 48.92	61 46 38.09	F2-F3	F2V	1.8	1	15.53	15.22	14.85	14.63
2012	0220_107	2 36 49.38	61 35 46.00	F2-F3	F2V	1.6	1	13.18	13.36	13.03	12.58
2012	0220_145	2 36 49.54	61 11 25.40		B9V	2.6	1	14.37	14.53	14.22	13.27
2012	1105_3_147	2 36 49.56	61 15 16.60	F8-G0	F8V	2.0	1	15.94	15.81	15.30	14.52
2012	0220_114	2 36 50.09	61 32 14.10	F1-F2	F2V	1.5	0	16.36	16.09	15.77	15.32
2012	0220_30	2 36 50.15	61 33 09.01		F5V	1.5	0	16.50	16.22	15.88	15.39
2012	1106_1_78	2 36 50.21	61 44 08.20	A6-A8	A7V	2.0	1	17.23	16.96	16.64	16.10
2012	0220_118	2 36 50.30	61 31 36.80		F8V	2.1	1	...	17.72	17.20	...
2012	1104_293	2 36 52.57	61 53 56.60	F2-F3	F2V	1.7	1	16.16	15.83	15.48	15.10
2012	0220_92	2 36 52.91	61 43 38.70	B2-B3	B2V	2.8	1	15.13	16.10	15.86	14.63
2012	0220_19	2 36 53.81	61 45 49.10	F6-F7	F6V	1.8	1	16.35	15.96	15.52	15.06
2012	0220_98	2 36 54.15	61 42 01.99	G7-G8	G8V	2.4	1	15.46	14.90	14.22	14.17
2012	0220_81	2 36 54.52	61 46 38.70	G7-G8	G8V	2.3	1	15.11	14.52	13.89	13.33
2012	0220_26	2 36 54.69	61 34 08.70	G6-G8	G7V	1.9	1	16.06	15.55	15.01	14.63
2012	1105_3_97	2 36 55.11	61 46 09.50	A1-A2	A2V	2.1	1	15.90	15.72	15.44	15.08
2012	0220_103	2 36 56.42	61 35 04.60		F2V	1.9	1	16.31	15.97	15.57	15.16
2012	1104_7	2 36 56.54	61 32 57.00	F7-G0	F9V[g]	2.3	1	14.43	13.74	13.17	13.15
2012	0220_126	2 36 56.73	61 28 14.70		B9V	2.8	1	15.23	15.30	14.97	14.02
2012	0220_148	2 36 58.90	61 13 51.50		B9V	2.9	1	15.71	15.77	15.40	14.51
2012	1105_3_126	2 37 01.90	61 32 33.20	F2-F4	F3V	1.4	0	15.45	15.48	15.17	14.68
2012	0220_109	2 37 05.75	61 36 40.70	F7-F8	F7V	1.4	0	15.60	15.42	15.05	14.33
2012	1105_3_114	2 37 06.11	61 36 49.41	G8-K2	K0V[g]	3.3	1	15.21	14.70	13.82	12.89
2012	0220_144	2 37 10.94	61 14 22.61	B5-B7	B6V	4.1	1	15.65	15.51	14.93	13.98
2012	0220_133	2 37 12.32	61 15 58.80		A4V	1.2	0	13.23	13.44	13.32	12.21
2012	0220_146	2 37 12.40	61 12 44.50	F5-F6	F5V	2.0	1	15.70	15.62	15.17	14.30
2012	1104_43	2 37 12.95	61 34 04.60	A3-A6	A5V	2.0	1	15.14	14.82	14.51	14.03
2012	1105_3_121	2 37 14.33	61 29 08.20	G0-G6	G5V	1.3	0	15.53	15.43	15.01	14.16
2012	1105_3_116	2 37 15.18	61 36 18.51	G0-G7	G3V	1.3	0	15.69	15.62	15.22	14.50
2012	1105_3_122	2 37 15.66	61 33 00.51	A8-F3	F0V	1.5	0	15.61	15.56	15.30	14.58
2012	0220_150	2 37 16.54	61 11 01.90	G6-G7	G7V	0.9	0	15.51	14.50	14.17	14.18
2012	0220_135	2 37 20.42	61 16 06.61	G6-G7	G7V	0.8	0	14.17	13.71	13.38	12.87
2012	1105_3_129	2 37 22.53	61 30 56.70	A9-F1	F1V	1.7	1	15.78	15.82	15.49	15.02
2012	1104_3*	2 37 24.99	61 30 32.60	A9-F3	F1V	2.0	1	14.88	14.73	14.33	13.55

Table 1. IC 1805 Spectral Types and Photometry (Continued)

Year	Date_No.[a] (MMDD_No.)	RA(J2000) (hhmmss.ss)	Dec(J2000) (° ′ ″)	SpTy Range	SpTy	A_V (r-i) (mag)	Assoc.?[b] (ext)	V(90P)[c] (mag)	r[d] (mag)	i[d] (mag)	I(90P)[c] (mag)
2012	1105_3_123	2 37 25.62	61 28 48.30	B3-B5	B5V	2.8	1	14.08	14.14	13.86	12.90
2012	0220_131	2 37 30.43	61 13 36.20		B7V	4.4	0	15.86	15.65	15.02	14.56
2012	1105_3_120	2 37 30.57	61 35 19.70	G0-G7	G5V	0.9	0	14.72	14.79	14.47	13.54
2012	0220_124	2 37 34.08	61 27 39.20		K2V	1.6	1	15.91	15.65	15.09	14.14
2012	1104_45	2 37 34.51	61 32 49.30	F9-K1	G9V[g]	2.6	1	15.50	15.14	14.42	13.55
2012	0220_24	2 37 35.70	61 34 56.10		A1V	1.8	1	14.99	15.07	14.88	14.12
2012	0220_137	2 37 41.49	61 14 56.59	A5-A6	A5V	2.0	1	14.78	14.94	14.64	13.72
2012	0220_140	2 37 43.62	61 15 59.70	A7-A8	A7V	2.9	1	15.56	15.45	14.93	14.21
2012	0220_136	2 37 54.84	61 16 41.71		K3V	0.7	0	14.61	14.42	14.01	13.22
2012	0220_122*	2 37 58.06	61 27 22.00	A7-A8	A8V	2.2	1	14.76	14.78	14.40	13.43
2012	0220_105	2 38 00.29	61 36 54.29	G6-G8	G7V	2.3	1	14.49	14.09	13.45	12.80
2012	0220_120	2 38 08.29	61 30 09.30	G8-G9	G9V	3.1	1	15.54	15.13	14.29	14.61

[a] The month and day of the observation followed by the configuration number (if more than one) and the spectrum number in that configuration. A "*" after a name indicates the source is a *possible* cluster member.

[b] A "1" denotes an extinction value between 1.6-4.2 mag computed assuming main sequence colors, consistent with lying within the W4 region. A"0" denotes an extinction value outside of this range.

[c] Photometry from the 90Prime imager.

[d] Photometry from PanStarrs DR2 release except where noted.

[e] r band photometry from the IPHAS Second Data Release (Barentsen et al. 2014).

[f] i band photometry from the IPHAS Second Data Release (Barentsen et al. 2014).

[g] Spectrum indicates a likely giant or supergiant with a luminosity class of I-III. The two A type stars are possible supergiants.

APPENDIX B.

DISK MODEL DERIVATIONS

In this appendix, the equations used for modeling the dust temperature in both flat and flared disks will be derived. These two equations have a long history of being used in circumstellar disk theory. However, a clear derivation of these expressions is difficult to find. The following section attempts to provide a step-by-step derivation which states all assumptions being made to derive the classic results.

1. THE FLAT DISK APPROXIMATION

Consider an extremely thin circumstellar disk which surrounds a protostar of effective temperature T_* and radius R_*. The brightness, I_*, from the protostar that strikes a small surface area of the disk, a distance r from the center of the protostar, can be estimated by setting a spherical coordinate system at the surface area under consideration. Let the z-axis of the coordinate system point towards the center of the protostar. The flux that passes through this surface, F_d, is given by

$$F_d = I_* \int \sin\theta\cos\phi \mathrm{d}\Omega, \tag{1}$$

where $\mathrm{d}\Omega$ is the differential solid angle (i.e., $\mathrm{d}\Omega = \sin\theta \mathrm{d}\theta \mathrm{d}\phi$). Since the surface of the disk is exposed to radiation from half the protostar, the integration bounds for θ and ϕ become

$$F_d = I_* \int_{-\pi/2}^{\pi/2} \cos\phi \mathrm{d}\phi \int_0^{\arcsin(R_*/r)} \sin^2\theta \mathrm{d}\theta. \tag{2}$$

The solution is

$$F_d = I_* \left[\arcsin\left(\frac{R_*}{r}\right) - \left(\frac{R_*}{r}\right)\sqrt{1 - \frac{R_*^2}{r^2}} \right]. \tag{3}$$

Equation 3 can be expressed in terms of the disk temperature by equating $F_d = \sigma T_d^4$ and relating the protostellar brightness to its flux by $I_* = \frac{\sigma T_*^4}{\pi}$, where σ is the Stefan-Boltzmann constant. Making the substitutions results in

$$T_d^4 = \frac{T_*^4}{\pi}\left[\arcsin\left(\frac{R_*}{r}\right) - \left(\frac{R_*}{r}\right)\sqrt{1 - \frac{R_*^2}{r^2}}\right]. \tag{4}$$

To simplify this equation, consider distances which are far away from the stellar surface $R_*/r \ll 1$. A Taylor series expansion of the bracketed term reduces the equation to

$$T_d^4 = \frac{T_*^4}{\pi}\frac{2}{3}\frac{R_*^3}{r^3} \tag{5}$$

where higher order terms have been ignored. This is equivalent to the flat disk approximation cited in Chiang and Goldreich (1997) (CG97)

$$T_d = \left(\frac{2}{3\pi}\right)^{1/4}\left(\frac{R_*}{r}\right)^{3/4} T_*, \tag{6}$$

where they have borrowed this form of the equation from, for example, Ruden and Pollack (1991).

The bracketed term in Equation 3 is actually related to the grazing angle. That is, the angle at which protostellar radiation strikes the surface of the disk. To make this clear, parameterize the flux striking the disk as $F_d = \alpha\Omega I_*$, where Ω is the solid angle of the protostellar flux on a surface area of the disk. So, the grazing angle is

$$\alpha = \frac{1}{\Omega}\left[\arcsin\left(\frac{R_*}{r}\right) - \left(\frac{R_*}{r}\right)\sqrt{1 - \frac{R_*^2}{r^2}}\right], \tag{7}$$

which can likewise be approximated as $\alpha = \frac{1}{\Omega}\frac{2}{3}\frac{R_*^3}{r^3}$. Then, the solid angle is simply

$$\Omega = \int_{\pi/2}^{\pi/2} \mathrm{d}\phi \int_0^{\arcsin(R_*/r)} \sin\theta \mathrm{d}\theta = \pi\left(1 - \sqrt{1 - \frac{R_*^2}{r^2}}\right) \approx \frac{\pi}{2}\frac{R_*^2}{r^2}. \tag{8}$$

Substituting this back into the equation for the grazing angle results in

$$\alpha = \frac{4}{3\pi}\frac{R_*}{r} \approx \frac{0.4R_*}{r}, \tag{9}$$

an approximate form of the grazing angle that has been widely used for flat disks.

2. THE FLARED DISK APPROXIMATION

The dust temperature for a flared disk used in CG97 is more readily derived. Consider the flux, F_{inc}, incident on a flared disk from a protostar of luminosity L_* at some distance r from the center of the protostar. It strikes the surface of the disk at some grazing angle α. So, the incident flux can be approximated as

$$F_{inc} = \alpha\frac{L_*}{4\pi r^2} = \alpha\frac{\sigma R_* T_*^4}{r}. \tag{10}$$

Then, assume that half of the incident flux that is absorbed by dust grains gets re-emitted into space, and the other re-emitted into the disk interior. This means that flux of the disk is $F_d = \sigma T_d^4 = \frac{1}{2}F_{inc}$. Equating and solving for the dust temperature results in

$$T_d = \left(\frac{\alpha}{2}\right)^{1/4}\left(\frac{R_*}{r}\right)^{1/2} T_*, \tag{11}$$

equation (1) of CG97.

Unlike the flat disk, the grazing angle for a flared disk will have a significant impact on the dust temperature as the distance from the protostar increases. CG97 approximate the grazing angle as

$$\alpha \approx \frac{0.4R_*}{r} + \arctan\left(\frac{dH}{dr}\right) - \arctan\left(\frac{H}{r}\right), \tag{12}$$

where H is the height above the disk midplane. This equation for the grazing angle represents a parameterization that accounts for radii close to the star where the disk is approximately flat, and distances beyond this where the degree of flaring depends on the disk height above the midplane. The first term is from Equation 9 and the second term represents the deviation from a flat disk due to the addition of an angle that represents differential changes in height and distance relative to a position on the disk surface. In the limit where $r >> H$, these small angles can be approximated as

$$\alpha \approx \frac{0.4R_*}{r} + \frac{dH}{dr} - \frac{H}{r} = \frac{0.4R_*}{r} + r\frac{d}{dr}\left(\frac{H}{r}\right), \tag{13}$$

the form of the grazing angle given in CG97.

The ratio of the height above of the midplane to the distance from the protostar is estimated by CG97 by assuming the gas in the disk is isothermal and uniformly mixed with the dust. Assuming a ratio of $H/h = 4$, where h is the scale height, they arrive at

$$\frac{H}{r} \approx 4\left(\frac{T_*}{T_c}\right)^{4/7}\left(\frac{r}{R_*}\right)^{2/7}, \tag{14}$$

where the temperature $T_c = \frac{GM_*\mu m_p}{kR_*}$ is a measure of the gravitational potential at the photosphere of the protostar. CG97 does note that the factor H/h will actually decrease from 5 in the inner disk to 4 in the outer disk. In this equation, G is the gravitational constant, k is the Boltzmann constant, μ is the mean molecular weight of the gas, and m_p is the mass of an ionized hydrogen atom. CG97 assume a $H/h = 4$ and further simplify the

grazing angle to something of the form

$$\alpha \approx \frac{0.4R_*}{r} + \beta r^{2/7}, \tag{15}$$

where $\beta = 4\left(\frac{T_*}{T_c}\right)^{4/7}\left(\frac{1}{R_*}\right)^{2/7}$. Using the intrinsic stellar parameters of Pecaut and Mamajek (2013), β can be approximated as 0.03 (technically, this has units of $AU^{-2/7}$).

APPENDIX C.

BAYESIAN INFERENCE AND THE DISK MODELING CODE

1. BAYESIAN INFERENCE USING *EMCEE*

This section will briefly detail the theory behind Bayesian inference and the Markov-chain Monte Carlo (MCMC) sampling method which the Python package *emcee* utilizes to produce posterior distributions. First it will start with Bayesian Inference and the Monte Carlo method, Markov chains, the Metropolis-Hastings algorithm, and a modification to the Metropolis-Hastings algorithm called the “stretch-move" which is used by default in *emcee*. Much of the information presented in this section is based on Foreman-Mackey *et al.* (2013) and a review by Sharma (2017).

1.1. BAYES’ THEOREM AND MCMC

The Bayesian to statistical inference is based upon Bayes’s theorem: Given a set of model parameters $\theta = \{\theta_1, \theta_2, ..., \theta_N\}$ and observed data x, then

$$p(\theta|x) = \frac{p(x|\theta)p(\theta)}{p(x)}. \tag{1}$$

In words, $p(\theta|x)$ (posterior) is the degree of belief about the model after having seen the data, which is equivalent to the product of the likelihood of the data given the parameters, $p(x|\theta)$, and our assumptions about the parameters $p(\theta)$ (prior) normalized by the evidence $p(x)$ (marginal likelihood).

The end goal of Bayesian inference is to compute the posterior probability density function (pdf) for each parameter in the set θ. However, the marginal likelihood is notoriously difficult to calculate. To avoid this, MCMC methods draw samples from the posterior pdf without ever having to calculate the marginal likelihood. In theory, by drawing enough

samples from the posteriors one can then statistically infer from those distributions the most likely parameter values. In actuality, it is impossible to explore the entire parameter space, and, therefore, produce a complete posterior.

An algorithm that utilizes Monte Carlo methods is one that uses repeated random sampling from probability distributions to generate numerical results. The general idea is to generate random inputs from a predefined domain, or state space, of possible inputs. Then, use the chosen inputs to perform computations using a deterministic model, in this case a model representing a physical system. Lastly, collect the computation results which will be in the form of a probability distribution.

A Markov chain is a sequence of random variables $X_1, ..., X_n$ such that the past and future states of the variables are independent given the present state. It has three basic elements:

1. The state space, X, which is the domain over which the chain takes values from
2. A transition operator, $K(x, y)$, that gives the probability of moving from state x to y
3. An initial conditional distribution π_0 which gives the probabilities of being in any of the possible states in the first iteration

The transition probability can be mathematically represented as,

$$P(X_{n+1} = x|X_1 = x_1, X_2 = x_2, ...X_n = x_n) = P(X_{n+1} = x|X_n = x_n). \quad (2)$$

This means that the conditional probability distribution X_{n+1} only depends upon the present state X_n. The transition operator is given by the transition probability described in Equation 2 (i.e., $K(x, y) = P(X_{n+1} = y|X_n = x)$).

For what follows, the transition operator is assumed to be independent of time. Given this assumption, a state space of a Markov chain has a stationary distribution χ if the chain can move from any state x to any state y a finite number of times. Mathematically,

$$\chi(y) = \int \chi(x)K(x,y)dx. \tag{3}$$

That is, if the transition operator is applied to all states x in a state space, the final distribution will approach the stationary distribution. A law of large numbers says that the expectation value of a function $f(x)$ over the stationary distribution π approaches the average of that function taken over the output of a Markov chain,

$$E_\pi\left[f(x)\right] = \int f(x)\pi(x)dx \tag{4}$$

This guarantees that parameter estimates can be computed from the Markov chain.

One requirement of *emcee* is that the Markov chain satisfies the condition of detailed balance. Detailed balanced simply means that if a state space X has a stationary distribution, then the chain looks identical whether n is progressed forwards or backwards in the parameter space. That is, $P(X_n, X_{n+1}) = P(X_{n+1}, X_n)$. While this condition is not required for Markov chains in general, by requiring detailed balance it is guaranteed that the created Markov chains will have stationary distributions. To satisfy detailed balance, symmetric pdfs should be used for the likelihood function.

1.2. METROPOLIS-HASTINGS ALGORITHM

The Metropolis-Hastings Algorithm (MH algorithm) is an iterative procedure that implements the MCMC technique of sampling from a probability distribution. The MH algorithm constructs a transition operator $K(x, y)$ in the following two steps:

- Given an initial state x sample a proposed position y from what is called the transition distribution $Q(y|x)$
- Accept the proposal with probability given by the acceptance ratio α:

$$\alpha(x, y) = min\left(1, \frac{P(y|d)Q(x|y)}{P(x|d)Q(y|x)}\right)$$

Then, the transition operator is given by $K(x, y) = Q(y|x)\alpha(x, y)$. So, to sample from a distribution $P(x|d)$ on a state space E, where $x \in E$, the MH algorithm constructs the transition operator to obtain a new sample y from the distribution $Q(y|x)$. If a uniform random variable U is less than $\frac{P(y|d)Q(x|y)}{P(x|d)Q(y|x)}$, then $x_{n+1} = y$. If not, then $x_{n+1} = x$. Essentially, if the acceptance ratio for each state $x \in E$ is minimized by the next state y then x is updated to y. If not, then the "position" remains x and the process is repeated.

It is important to note exactly what the acceptance ratio does. Specifically, it is the ratio of the posterior of the proposed state over the posterior of the current state. If this is re-written using Bayes theorem it would look like,

$$\frac{\frac{P(y|d)Q(x|y)}{P(d)}}{\frac{P(x|d)Q(y|x)}{P(d)}} = \frac{P(y|d)Q(x|y)}{P(x|d)Q(y|x)}. \tag{5}$$

The marginal likelihood, which does not change since it is based on the evidence d, actually cancels out of the ratio. Thus, the MH algorithm is able to draw samples from the posterior without ever needing to know the marginal likelihood.

This process is implemented by using a "walker". For each parameter to be optimized a walker is created based on an initial guess of what value the parameter should be. This walker is what undergoes the MCMC process of being moved in a random direction around the posterior distribution (walking closer and closer towards the optimum value based on if it minimizes the difference between the model and measured data). The MH algorithm varies walkers for each parameter simultaneously.

1.3. THE STRETCH MOVE

Goodman and Weare (2010) improved upon the MH method by utilizing what has been called the "stretch move". This method evolves an ensemble of walkers simultaneously for each parameter. For each parameter an ensemble of K walker $S = \{X_k\}$ is created where the proposal distribution for a single walker k is based on the current positions of the walkers in the complementary ensemble $S_{[k]} = \{X_j, \forall j \neq k\}$.

For a walker's "position" X_k to be updated (that is, their vector in the θ-dimensional parameter space) a new walker X_j is randomnly drawn from the complementary ensemble $S_{[k]}$ and the new position is proposed

$$X_k(t) \rightarrow Y = X_j + Z[X_k(t) - X_j] \tag{6}$$

where Z is a random variable drawn from a distribution $g(Z = z)$. If g satisfies the condition $g(z^{-1}) = zg(z)$, then the proposed position Y is symmetric. This implies the chain satisfies detailed balance (i.e., walkers can move in one direction as easily as the opposite) and the proposed position is accepted based on the new acceptance probability

$$\alpha = min\left(1, Z^{\theta-1}\frac{P(Y)}{P(X_k(t))}\right) \tag{7}$$

The procedure gets repeated for each walker in the ensemble in series.

The stretch move then splits the ensemble into two subsets of the original: $S^0 = \{X_k, \forall k = 1, ..., K/2\}$ and $S^1 = \{X_k, \forall k = K/2, ..., K\}$. Now it updates the positions of all the walkers in S^0 simultaneously based on the positions of the walkers in S^1. This allows the optimization of large numbers of walkers to be run in parallel.

2. DISK MODELING CODE

The following disk modeling code samples over all four possible parameters. Several variants of this code were used for sources that required different normalizations and fewer parameters.

```
# This program will produce model disk-bearing SEDs using a flared
# blackbody disk model. Input photometry should be dereddened and
# in units of Watts cm^-2 mu^-1.

import math
import numpy as np
import matplotlib.pyplot as plt
import matplotlib.backends.backend_pdf
import emcee
import corner
from scipy.integrate import quad

#Define constants to be used in disk model
h = 6.626e-34
c = 2.998e8
hc=h*c
bnum=2*np.pi*h*c**2
k = 1.381e-23
G = 6.674e-11
RsunAU = 0.0046525    # Solar radius in AU
au2=(1.496e11)**2     #Conversion between meters and AU

# Set burn-in and regular sampling iterations
burn=500
steps=800

```

```
# Wavelength scale for PanSTARRS, 2MASS, AllWISE, and Spitzer (in order of increasing wavelength)
lam = [0.486,0.617,0.752,0.866,0.962, 1.235, 1.662, 2.159, 3.4,3.55, 4.5,4.6, 5.74, 7.92, 23.68]
lam2=np.array(lam)*10**(-6.0)

#Define Planck distribution, prior, and total log probability
def bbmodel(Teff,lamb):
    bbmodel = (bnum/lamb**5)*(np.exp(hc/(lamb*k*Teff))-1)**(-1.0)*10**(-10.0)
    return bbmodel

def prior(theta):
    f,hole,p,out = theta
    if (37.0 < f < 42.0 and RstarAU < hole < 2.0 and 0.4 < p < 1.5 and 0.3 < out < 2.8):
        return(0.0)
    return(-np.inf)

def lnprob(theta):
    lp = prior(theta)
    if not np.isfinite(lp):
        return -np.inf
    return lp + lnlike(theta)

# Open a text document that will record best fit parameter values
pfile=open("/CGdisk/Flared/paramsFlareAll4r.txt",'w')

# Open text file containing all information of sources to be fitted (dereddened photometries, extinction, temeprature, and stellar radius
file=open("/CGdisk/Flared/IRXemceeABF_NoRin3p.txt")
for line in file:
    row = line.replace("\n","").split("\t")
```

```
55      name=row[0]
56      av=float(row[1])
57      obs=[float(row[2]),float(row[4]),float(row[6]),float(row[8]),float(
        row[10]),float(row[12]),float(row[14]),float(row[16]),float(row[18])
        ,float(row[20]),float(row[22]),float(row[24]),float(row[26]),float(
        row[28]),float(row[30])]
58      err=[float(row[3]),float(row[5]),float(row[7]),float(row[9]),float(
        row[11]),float(row[13]),float(row[15]),float(row[17]),float(row[19])
        ,float(row[21]),float(row[23]),float(row[25]),float(row[27]),float(
        row[29]),float(row[31])]
59      sptyp=row[32]
60      T=float(row[33])
61      Rstar=float(row[34])
62      n2=row[35]
63
64      # Estimate protostellar radius in AU and the thin disk grazing angle
         coefficient
65      RstarAU=Rstar*RsunAU
66      A=0.4*RstarAU
67
68      # Open PDFs that will record fit SEDs and Corner plots for each
        source
69      pdf = matplotlib.backends.backend_pdf.PdfPages("/CGdisk/Flared/
        IndiFlare/MCMCdiskAll4rFlare_"+n2+".pdf")
70      pdf2 = matplotlib.backends.backend_pdf.PdfPages("/CGdisk/Flared/
        IndiFlare/MCMCcornerAll4rFlare_"+n2+".pdf")
71
72      # Trim photometry and wavelength lists to weed out zeroes
73      obs2=[]
74      err2=[]
75      lamB=[]
76      for i in range(len(obs)):
77          if obs[i] != 0 and err[i] != 0:
```

```
78              obs2.append(obs[i])
79              err2.append(err[i])
80              lamB.append(lam[i])
81
82      lamB2=(np.array(lamB))*10**(-6.0)
83      fluxm=np.array(obs2)
84      err2=np.array(err2)
85      fluxm2=np.log10(fluxm)
86      err3=fluxm2-np.log10(fluxm-err2)
87      errax=err3
88
89      # These ranges can be adjusted to skip PanSTARRS photometry if
    necessary
90      fluxm2=fluxm2[1:]
91      err3=err3[1:]
92      lb=lamB[1:]
93      lb2=lamB2[1:]
94
95      obs3=np.log10(np.array(obs2))
96      llam=np.log10(np.array(lamB))
97
98      # Estimate normalization factor for stellar blackbody curve
99      scale2=obs[1]/(lam[1]*np.pi*bbmodel(T,lam2[1]))
100
101     # Define the likelihood function
102     def lnlike(theta):
103         f,hole,p,out = theta
104         totes = []
105         sflux = []
106         bb = np.pi*scale2*bbmodel(T,lb2)
107         blfl=lb*bb
108         sflux=blfl
109         for i in range(len(fluxm2)):
```

```
110             l1 = lb2[i]
111             integ=lambda r: r*bbmodel((0.5*(A/r+0.03*r**(2/7)))**(1/4)*T
    *(RstarAU/(r))**(p),l1)
112             q = quad(integ,hole,10**(out),epsabs=0)
113             flux = np.pi*lb[i]*au2*q[0]
114             totes.append(flux)
115         totes = np.array(totes)*10**(-f)
116         total = totes + sflux
117         total = np.log10(total)
118         return -0.5*(np.sum((fluxm2-total)**2/err3**2 + np.log(2*np.pi*
    err3**2)))
119
120     # Set up the sampler and create distributions of walkers
121     ndim, nwalkers = 4, 50
122     pos1 = np.random.normal(40.0,1.0,nwalkers)
123     pos2 = np.random.normal(0.2,0.01,nwalkers)
124     pos3 = np.random.normal(0.625,0.1,nwalkers)
125     pos4 = np.random.normal(1.8,0.1,nwalkers)
126     pos=np.stack((pos1,pos2,pos3,pos4),axis=-1)
127
128     # Run MCMC
129     sampler = emcee.EnsembleSampler(nwalkers, ndim, lnprob)
130
131     print("Burn-in")
132     posB, prob, state = sampler.run_mcmc(pos,burn,thin_by=1)
133     sampler.reset()
134     print("Sizzling")
135
136     print("Running MCMC...RadTrans")
137     sampler.run_mcmc(posB, steps,thin_by=1)
138     print("Done.")
139
140     # Estimate median and standard deviations for each parameter chain
```

```
141     samples=sampler.get_chain(discard=0,flat=True)
142     f_e,h_e,p_e,o_e = np.median(samples,axis=0)
143     f_std,h_std,p_std,o_std = np.std(samples,axis=0)
144
145     # Write best fit parameters to text file
146     pfile.write(n2+'\t'+str(round(f_e,6))+'\t'+str(round(h_e,6))+'\t'+
    str(round(o_e,6))+'\t'+str(round(p_e,6))+'\t'+str(round(f_std,7))+'\
    t'+str(round(h_std,7))+'\t'+str(round(o_std,7))+'\t'+str(round(p_std
    ,7))+'\n')
147
148     # Reset the sampler before the next source
149     sampler.reset()
150
151     # Make the corner plot and save to PDF. Note: show_titles=TRUE
    displays the 0.16,0.5, and 0.84 quantiles
152     name2 = name + " " +"(" + sptyp+ ")"
153     fig = corner.corner(samples, labels=["f",r'$R_{in}$',"p",r'$R_{out}$
    '],quantiles=[0.16,0.5,0.84],
154                         show_titles=True,title_fmt='.4f',title_kwargs
    ={"fontsize" : 16},label_kwargs={"fontsize" : 14})
155     fig.gca().annotate(name2,
156                        xy=(1.0, 1.0), xycoords="figure fraction",
157                        xytext=(-20, -10), textcoords="offset points",ha="
    right", va="top",fontsize=18)
158     pdf2.savefig()
159     plt.close(fig)
160
161     # Plot SEDs of the results using medians
162     fig=plt.figure()
163     ax1 = fig.add_subplot(111)
164
165     # Use a finer spread of wavelengths to produce smoother curves in
    the SEDs
```

```
166     lmb1=np.arange(0.5,24.0,0.1)
167     lmb2=lmb1*10**(-6)
168     lmb3=np.log10(lmb1)
169
170     # Convert the outer disk radius and standard deviation to AU
171     routs=samples[:,3]
172     routs=10**(routs)
173     ro_e=np.median(routs)
174     ro_std=np.std(routs)
175
176     # Reproduce the star, disk, and star+disk SEDs using median
    parameter values from the sampler
177     totes = []
178     sflux = []
179     star=[]
180     bb = np.pi*scale2*bbmodel(T,lmb2)
181     blfl=lmb1*bb
182     sflux=blfl
183     star=np.log10(sflux)
184     for i in range(len(lmb1)):
185         l1 = lmb2[i]
186         integ=lambda r: r*bbmodel((0.5*(A/r+0.03*r**(2/7)))**(1/4)*T*(
    RstarAU/(r))**(p_e),l1)
187         q = quad(integ,h_e,10**(o_e),epsabs=0)
188         flux = np.pi*lmb1[i]*au2*q[0]
189         totes.append(flux)
190     totes = np.array(totes)*10**(-f_e)
191     total = totes + sflux
192     total = np.log10(total)
193     disk=np.log10(totes)
194
195     name2 = name + " " +"(" + sptyp+ ")"
196
```

```
197     # Assemble the actual SED, save to PDF, and repeat
198     ax1.scatter(llam,obs3,s=20.0,zorder=3)
199     ax1.plot(lmb3,star,zorder=2)
200     ax1.plot(lmb3,total,'--',color='k',zorder=2)
201     ax1.plot(lmb3,disk,color='g',linewidth=1,zorder=2)
202     plt.title(name2)
203     plt.xlim(-0.4,1.5)
204     plt.ylim(bottom=-22)
205     plt.xlabel(r'Log $\lambda$  $(\mu m)$')
206     plt.ylabel(r'Log $\lambda F_{\lambda}$ (Watts $cm^{-2})$')
207     plt.text(0,-20,"f="+str(round(f_e,4))+r'$\pm$'+str(round(f_std,4))+'
    \n'+r'$R_{in}$(AU)='+str(round(h_e,4))+r'$\pm$'+str(round(h_std,4))+
    '\n'+r'$R_{out}$(AU)='+str(round(ro_e,1))+r'$\pm$'+str(round(ro_std
    ,1))+'\n'+'p='+str(round(p_e,2)),fontsize='medium')
208     plt.text(0,0,"flared",transform=ax1.transAxes)
209     pdf.savefig()
210     plt.close(fig)
211
212     pdf.close()
213     pdf2.close()
214
215 file.close()
216 pfile.close()
```

APPENDIX D.

DISK FIT SEDS AND CORNER PLOTS

This appendix contains the SEDs of all disk-bearing sources which have their corresponding modeled disk+star SEDs overlaid on the plots. The black dashed line represents the disk+star SED which used the median parameter values obtained from the posterior distributions, and the solid blue and green line correspond to the stellar blackbody and disk SED, respectively. Photometry from PanSTARRS ($grizy$), 2MASS (JHK), AllWISE (bands 1 and 2), and Spitzer (IRAC bands and MIPS 1 band) are plotted as solid blue points. Their photometric errors are smaller than the points themselves. Sources fit with a blackbody dust rim approximation show the blackbody rim as an orange dotted line.

The plots below each SED are corresponding *corner* plots. These plots shows histograms of each parameter space on the diagonal and covariance plots between each set of parameters. Each source was fit with at least two of the following four parameters: a scaling factor f, the inner disk radius R_{in}, the outer disk radius R_{out}, and the temperature power law index p. Every disk-bearing source sampled the scaling factor and temperature power law index, except for the dust rim sources. Histograms represent the distribution of walkers in each parameter space after the total number of iterations had been performed by the code. The median of each distribution is listed above the corresponding histogram, and the errors represent the 16th and 84th percentiles. Dotted lines on the individual histograms correspond to these three percentiles.

In the figure descriptions, disks types have the following correspondences: “thick" is an optically thick disk, “thin" is an optically thin disk, “pt" is a pre-transition disk, “t" is a transition disk, and “8 μm" is a source with an infrared excess only in its IRAC 4 band. Additionally, “trunc" refers to disks which may be truncated and “enh" refers to sources whose outer disks may be enhanced by external photoionizing radiation.

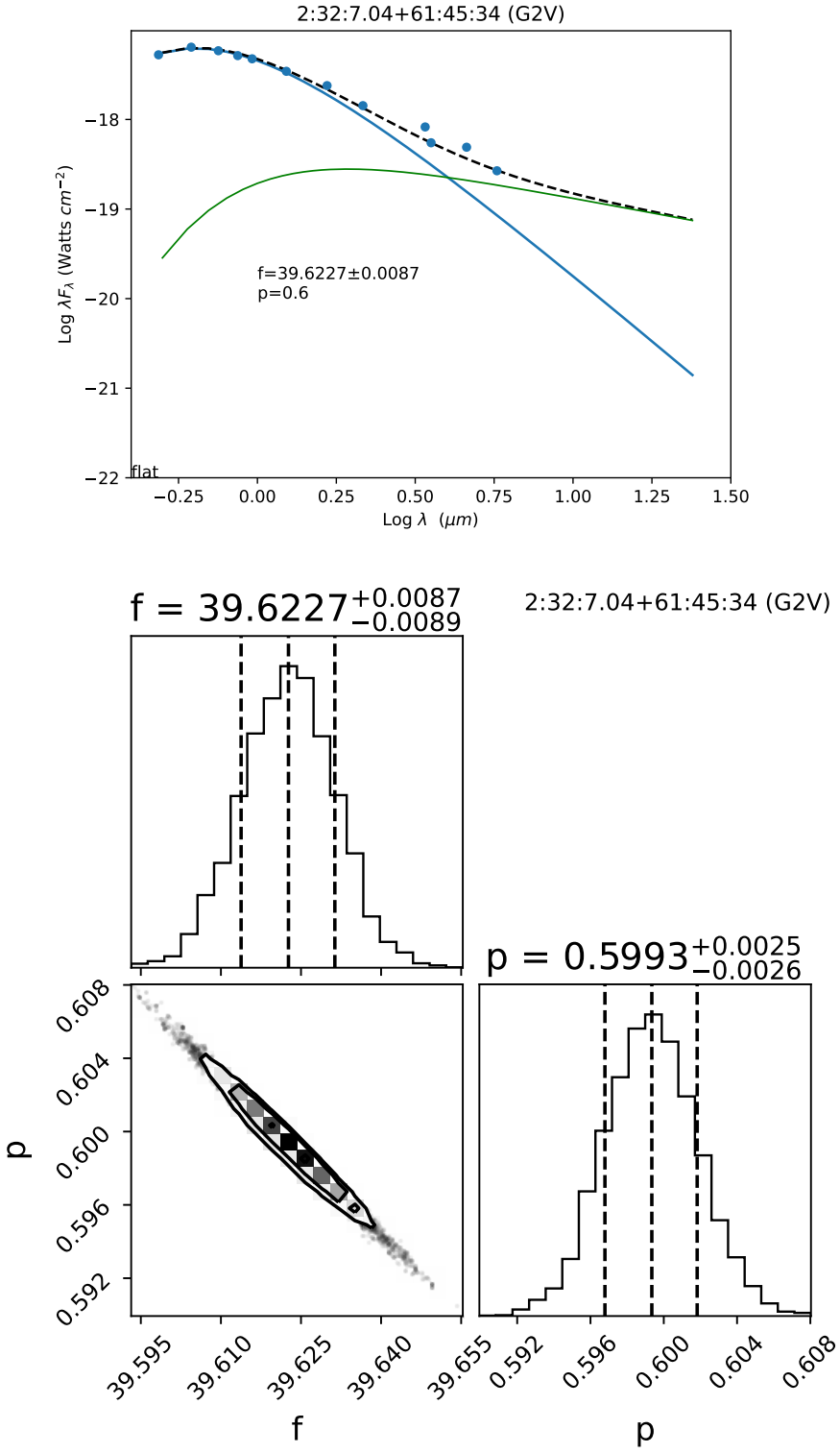

Figure 1. SED and corner plot of source 2:32:7.04+61:45:34 which is classified as a thin disk.

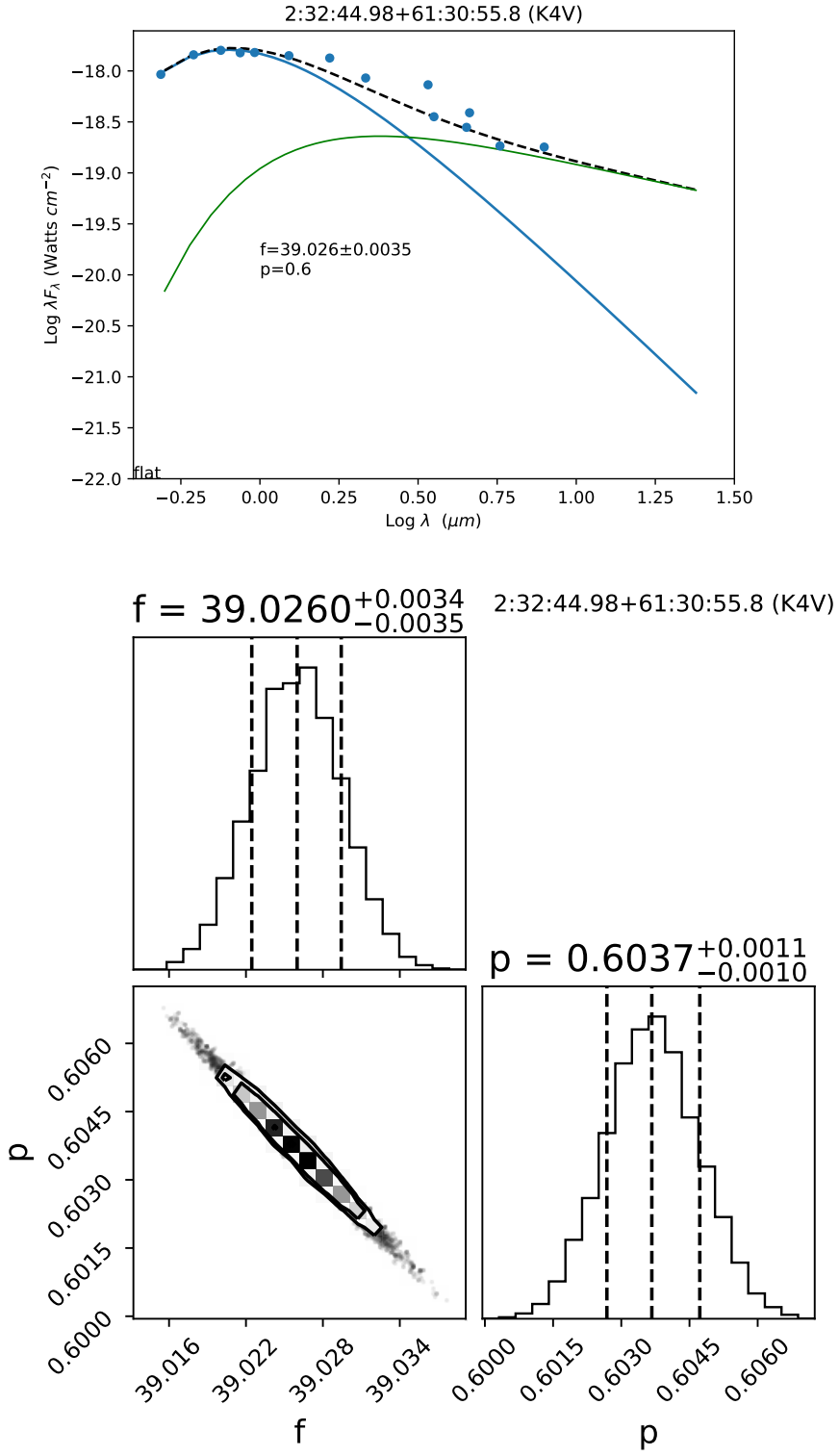

Figure 2. SED and corner plot of source 2:32:44.98+61:30:55.8 which is classified as a thin? disk.

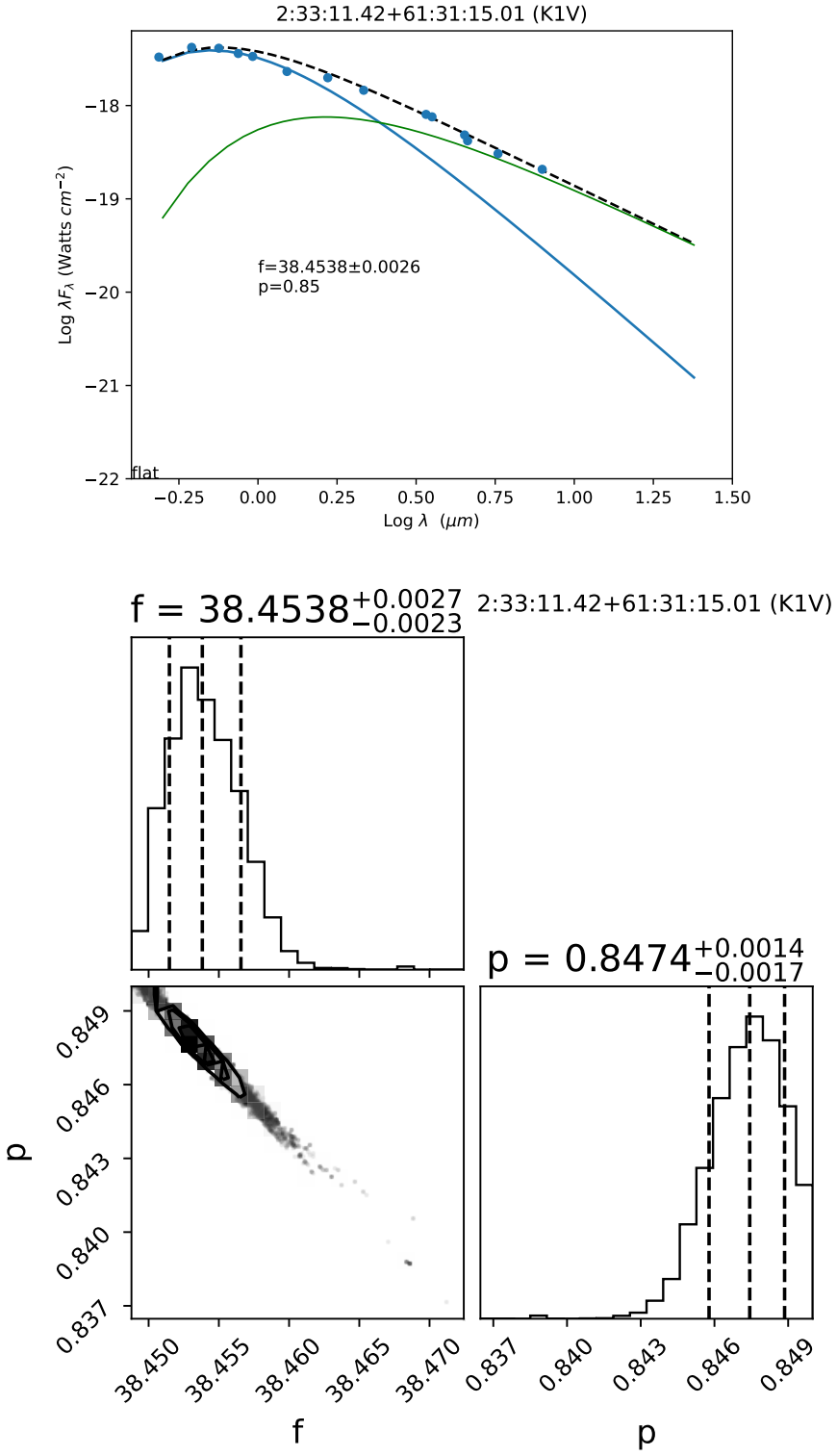

Figure 3. SED and corner plot of source 2:33:11.42+61:31:15.01 which is classified as a thin disk.

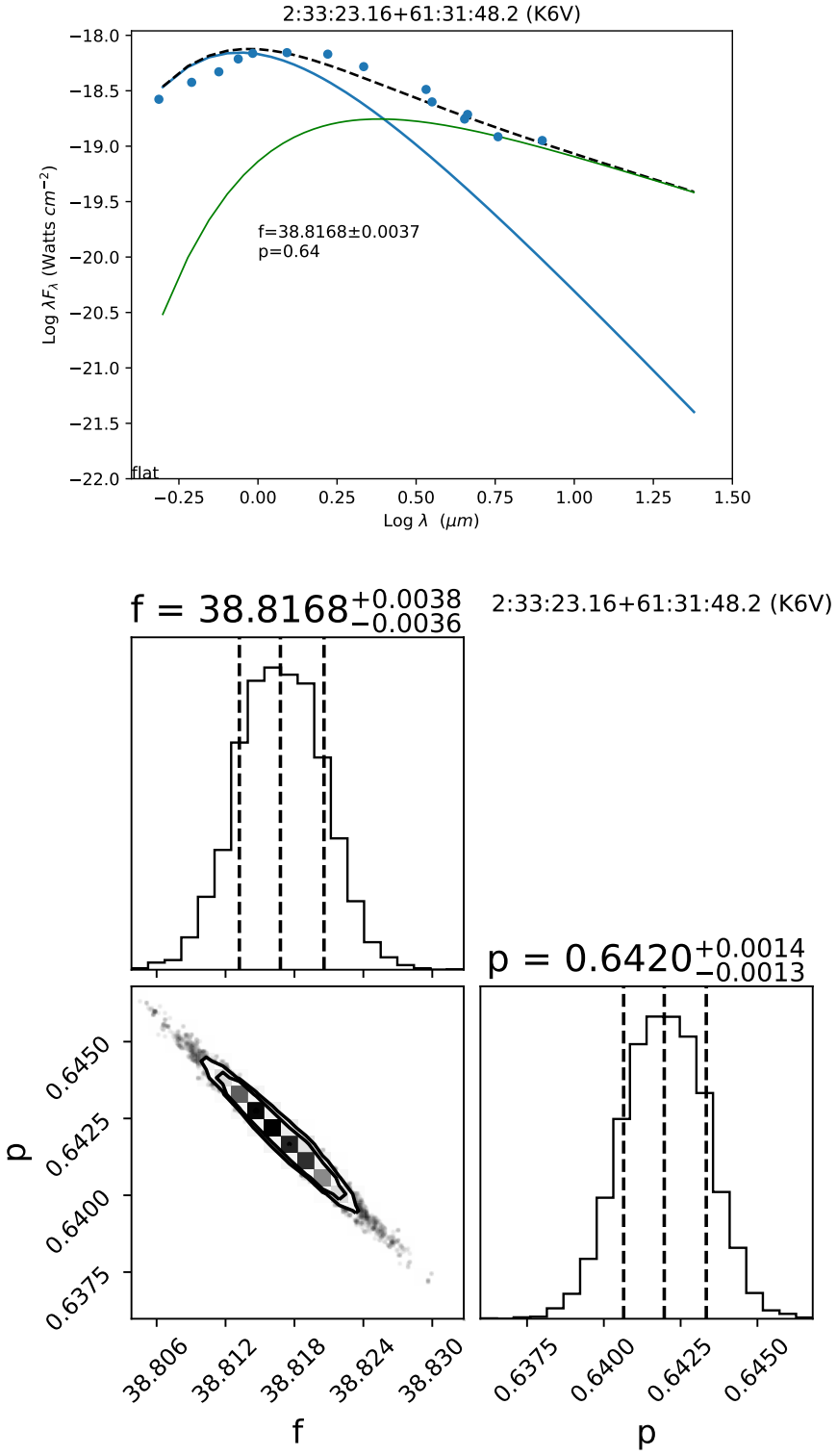

Figure 4. SED and corner plot of source 2:33:23.16+61:31:48.2 which is classified as a thin disk.

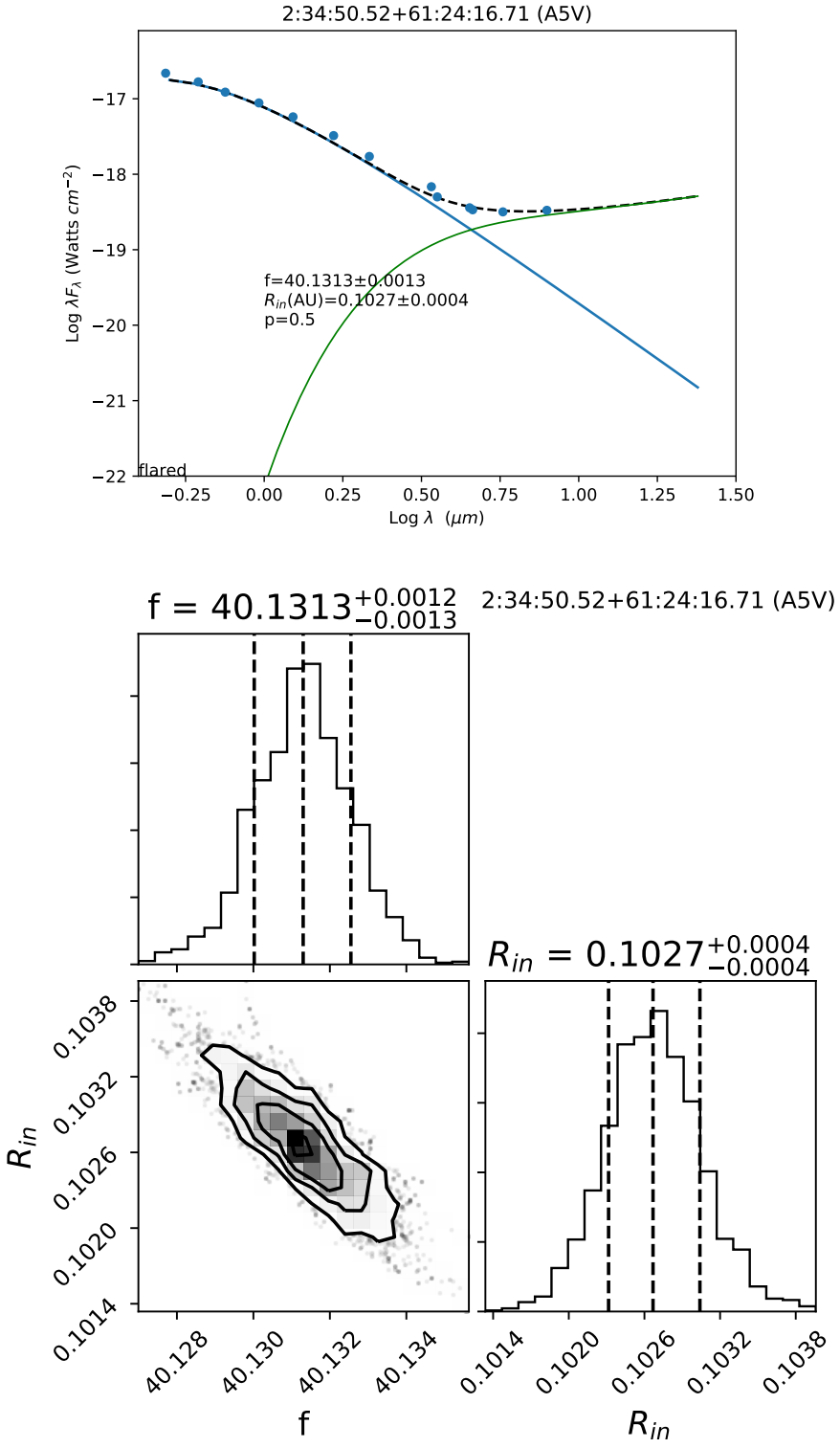

Figure 5. SED and corner plot of source 2:34:50.52+61:24:16.71 which is classified as a t? disk.

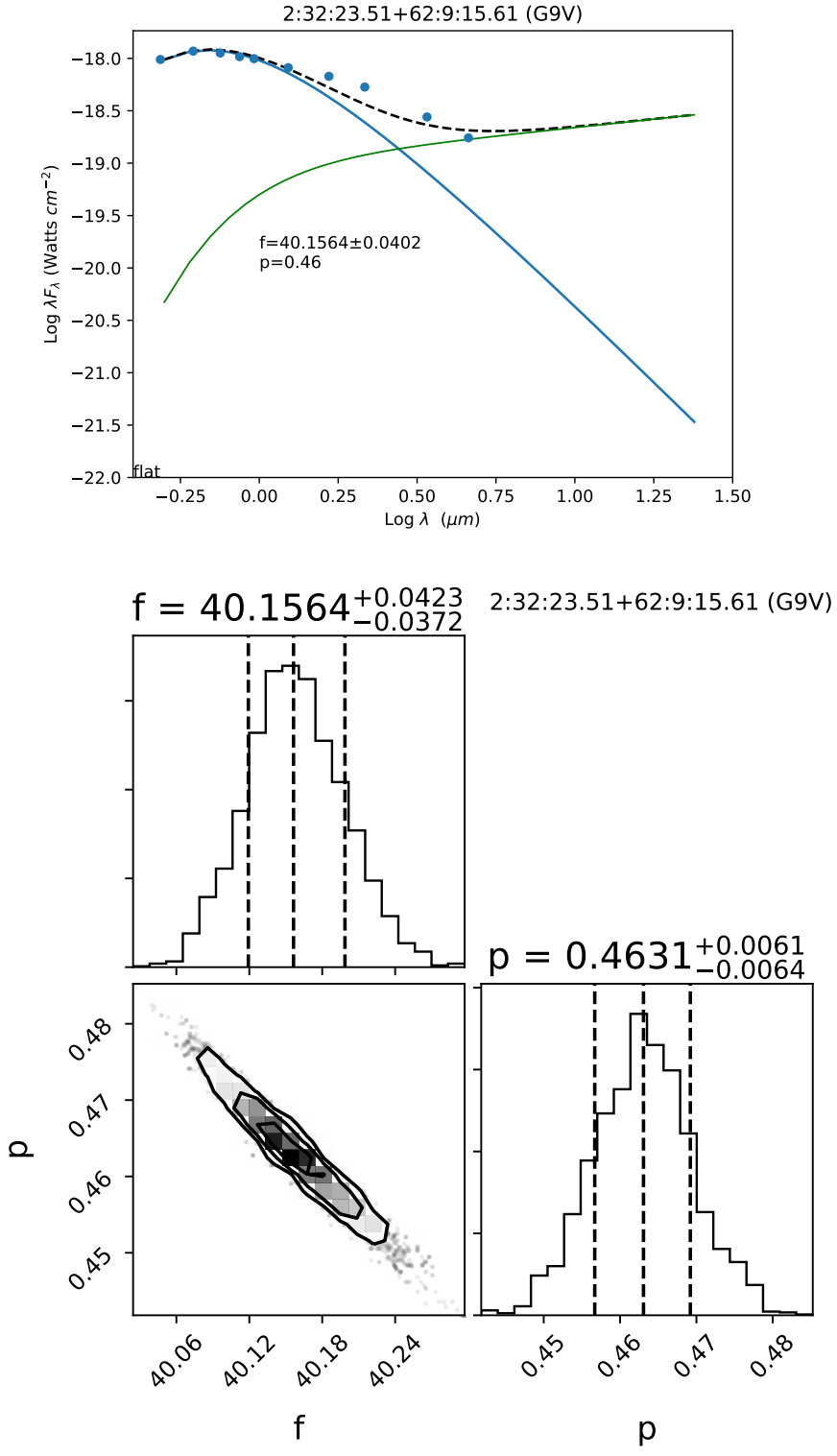

Figure 6. SED and corner plot of source 2:32:23.51+62:9:15.61 which is classified as a thin disk.

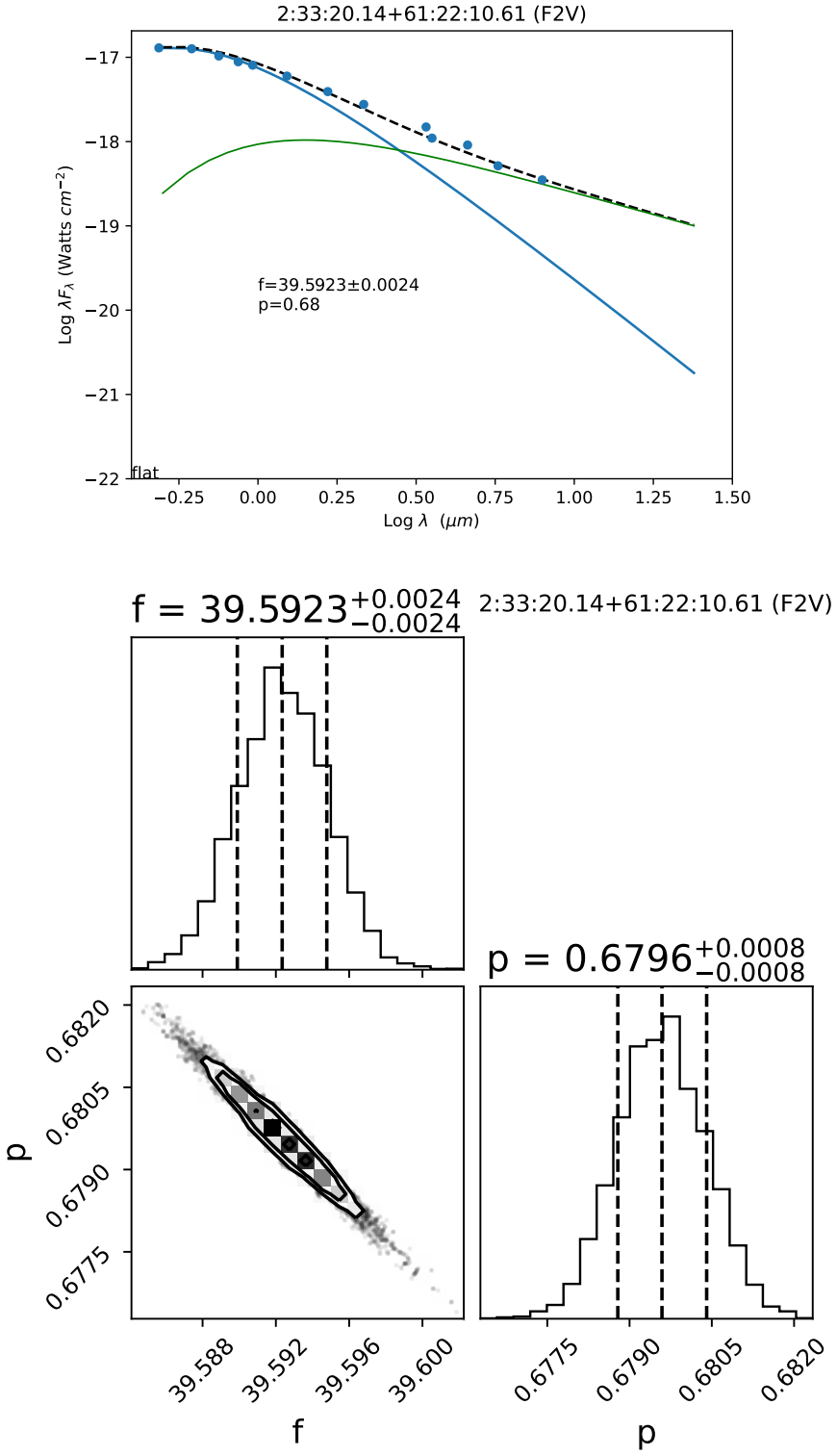

Figure 7. SED and corner plot of source 2:33:20.14+61:22:10.61 which is classified as a thin disk.

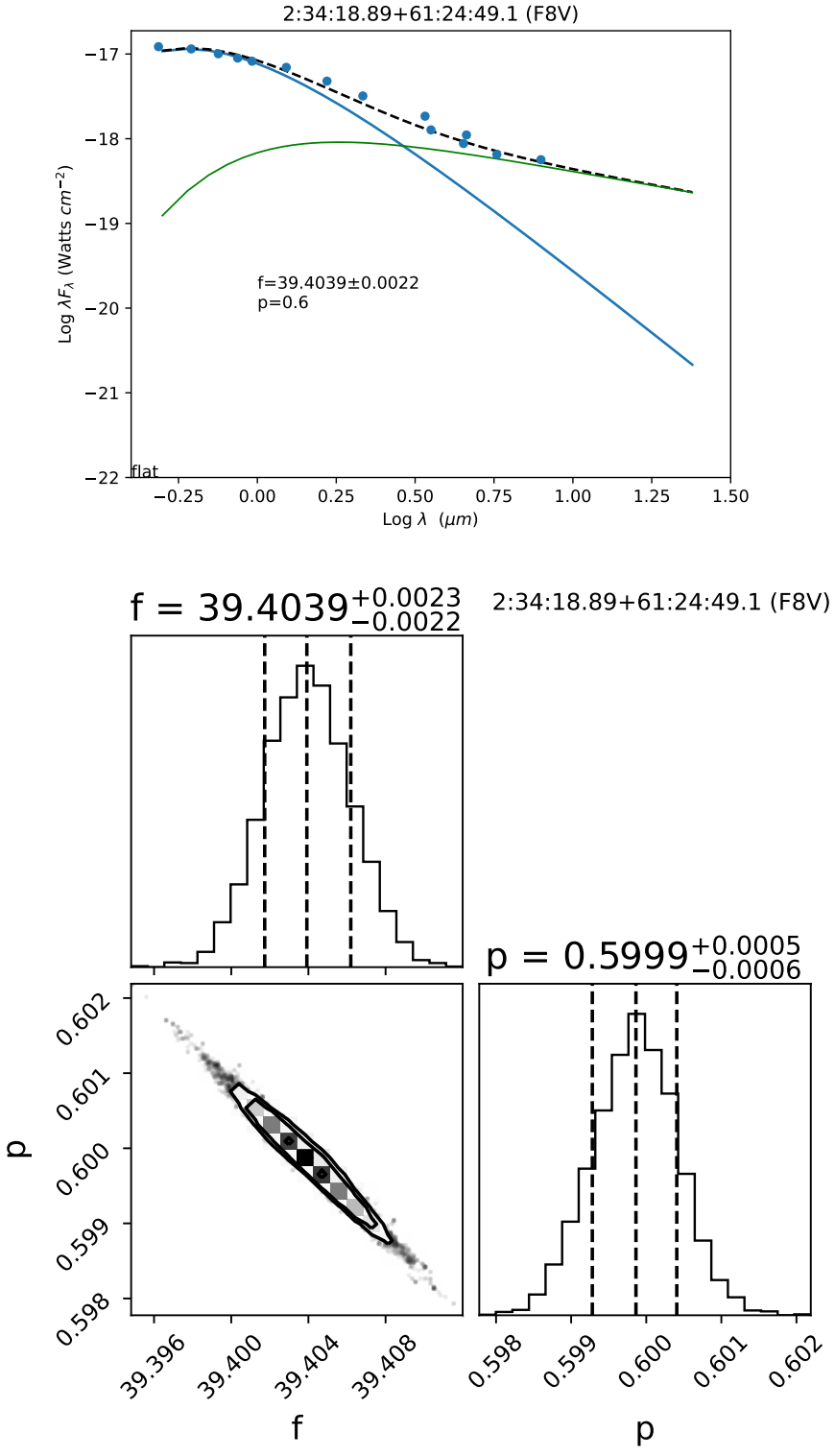

Figure 8. SED and corner plot of source 2:34:18.89+61:24:49.1 which is classified as a thin disk.

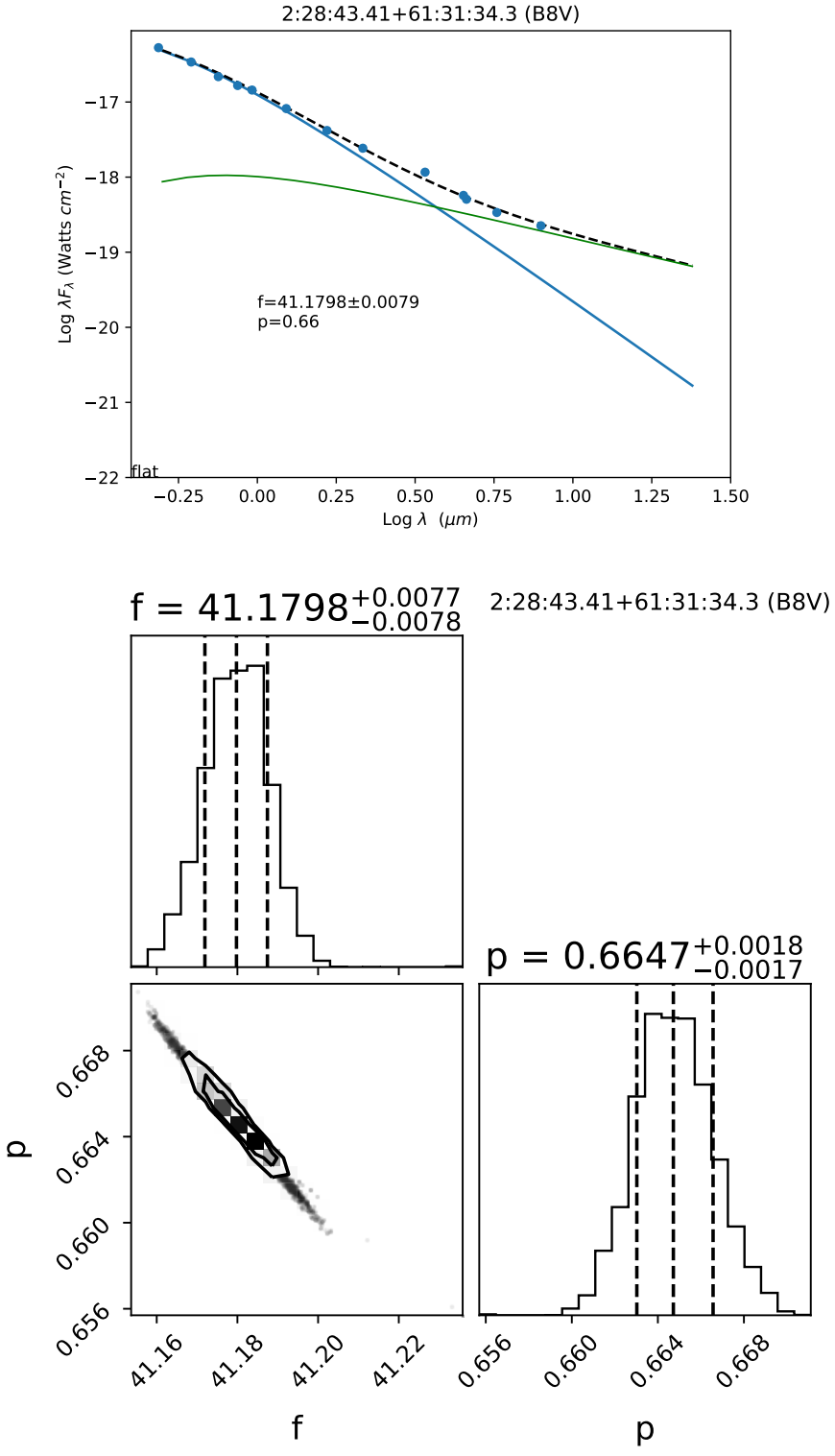

Figure 9. SED and corner plot of source 2:28:43.41+61:31:34.3 which is classified as a thin disk.

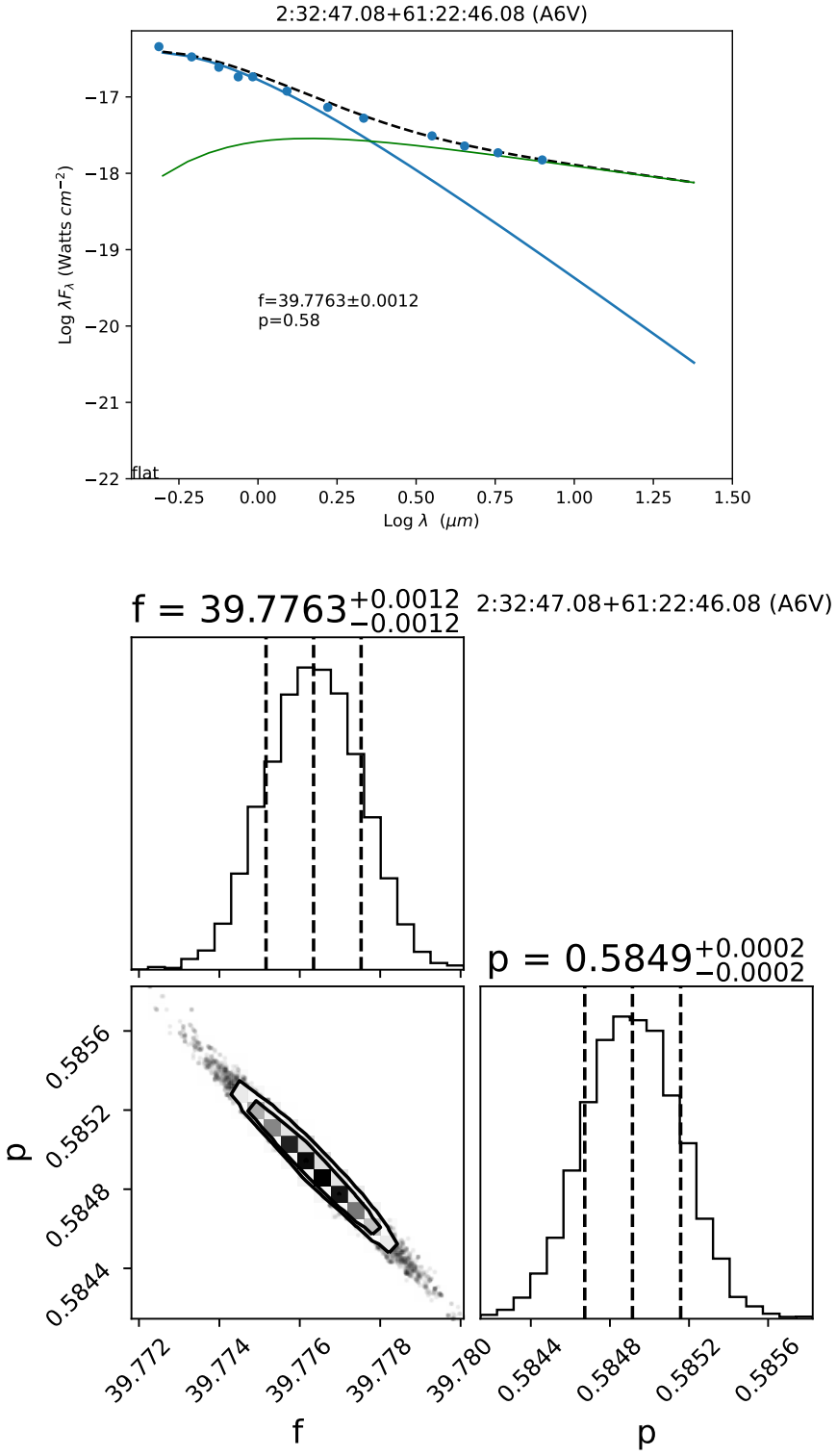

Figure 10. SED and corner plot of source 2:32:47.08+61:22:46.08 which is classified as a thick disk.

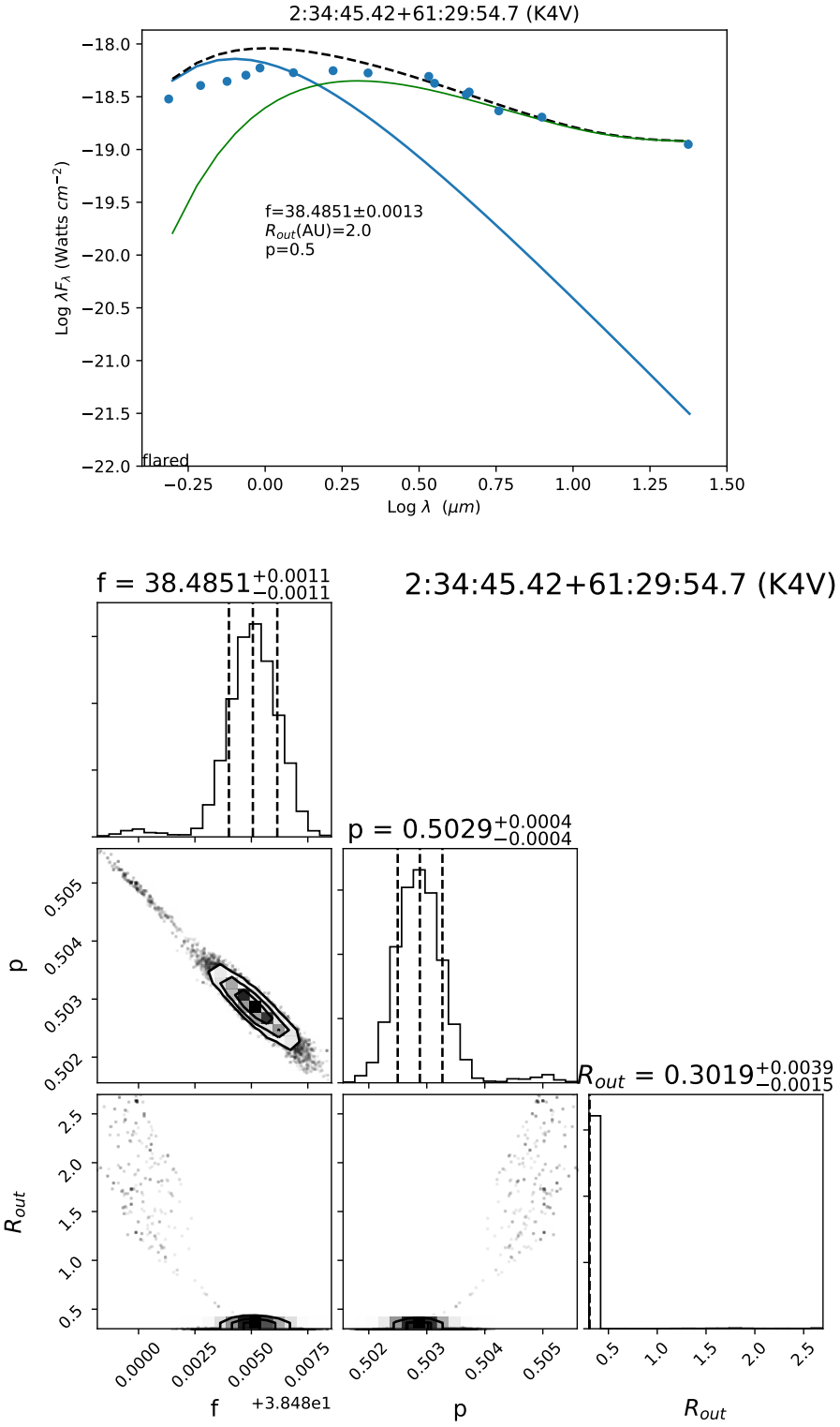

Figure 11. SED and corner plot of source 2:34:45.42+61:29:54.7 which is classified as a thick disk.

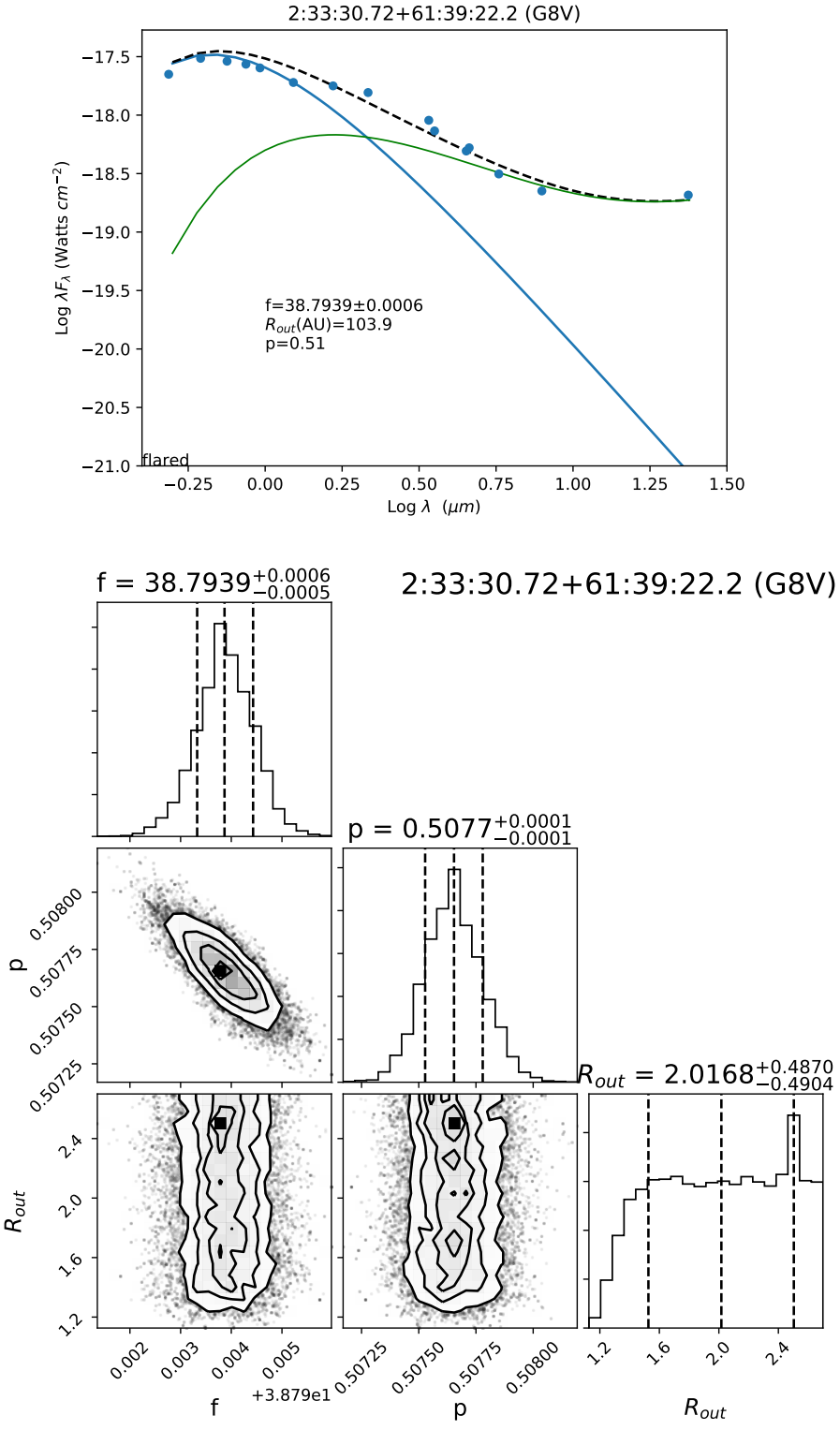

Figure 12. SED and corner plot of source 2:33:30.72+61:39:22.2 which is classified as a pt disk.

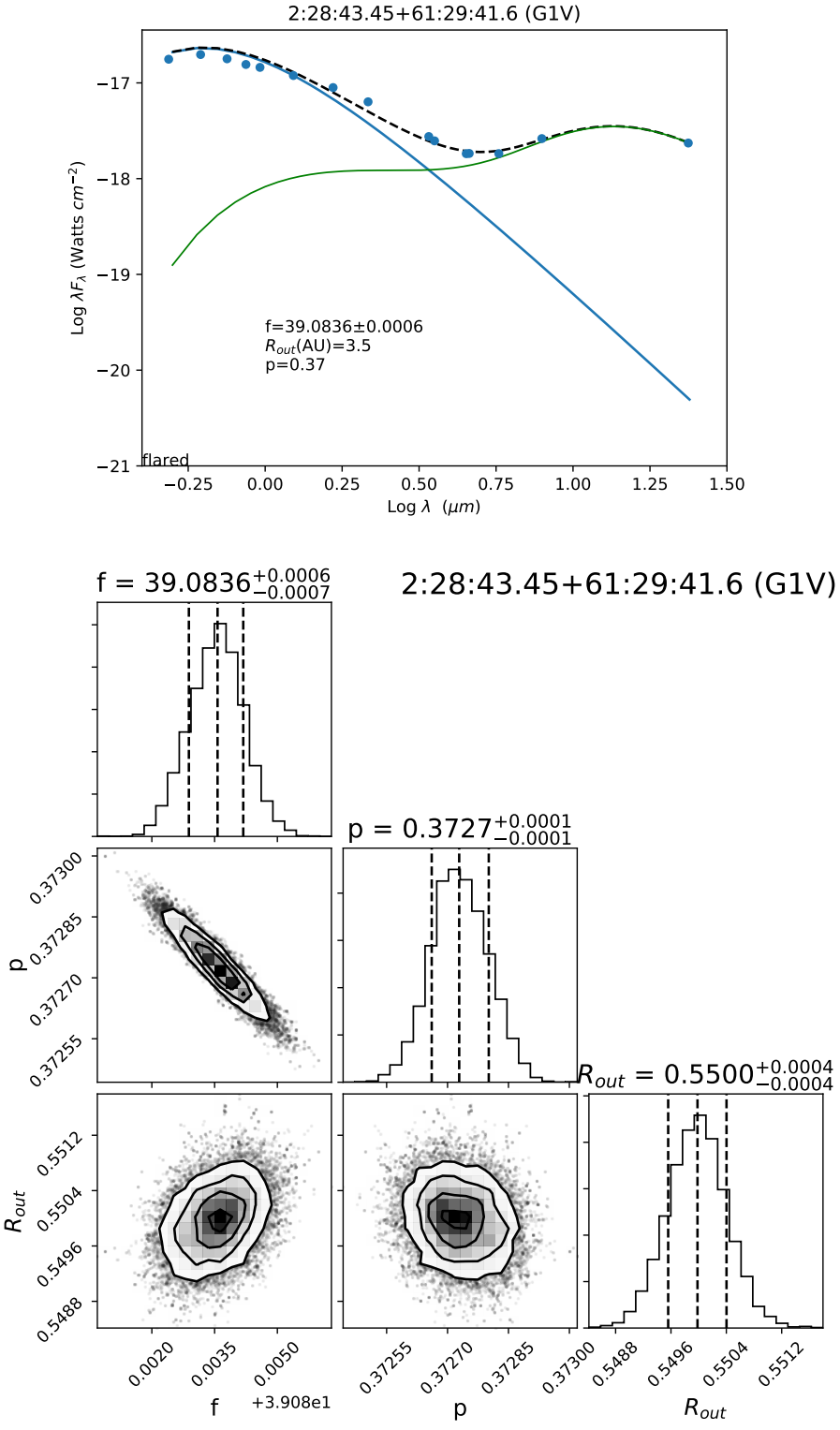

Figure 13. SED and corner plot of source 2:28:43.45+61:29:41.6 which is classified as a pt disk.

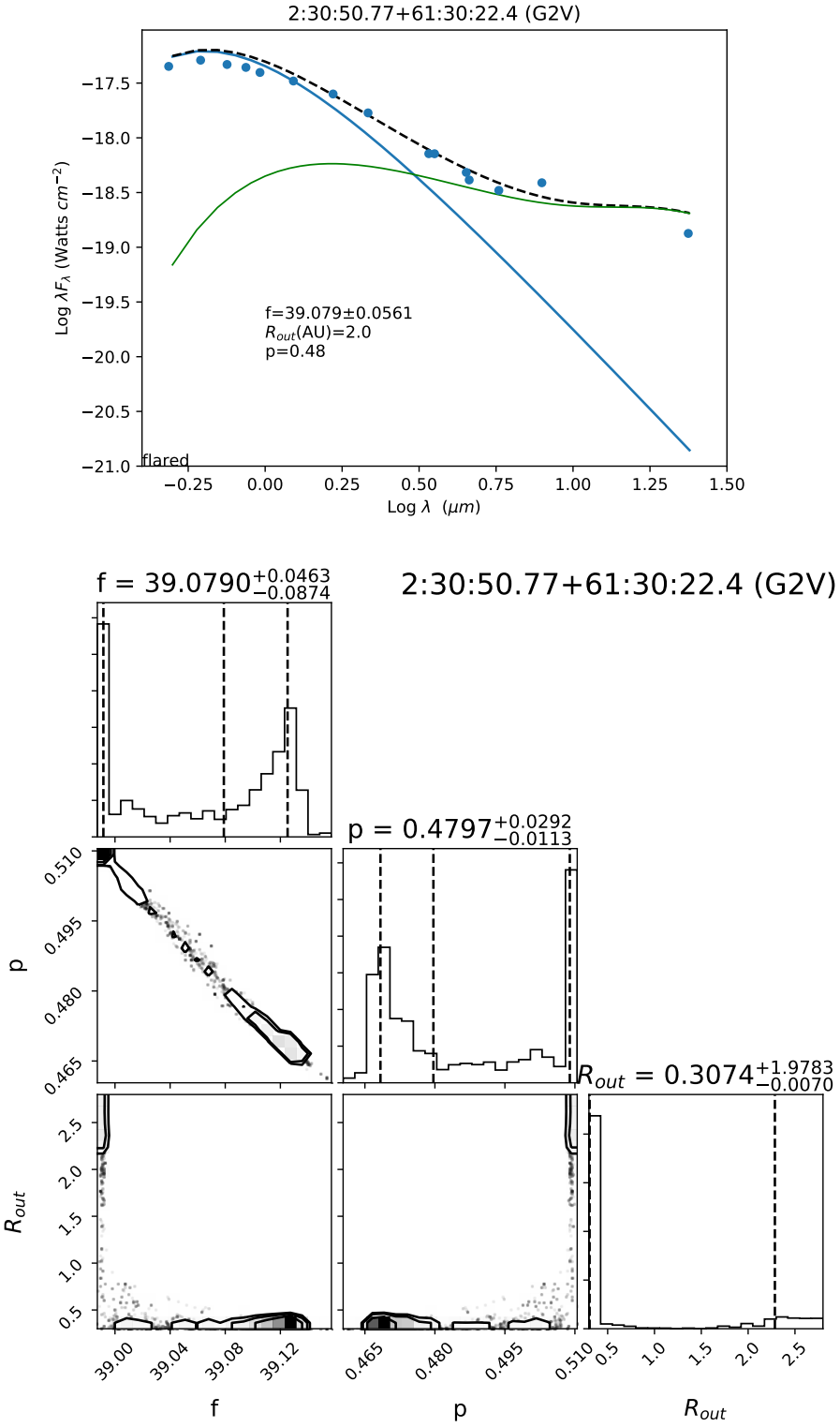

Figure 14. SED and corner plot of source 2:30:50.77+61:30:22.4 which is classified as a pt? disk.

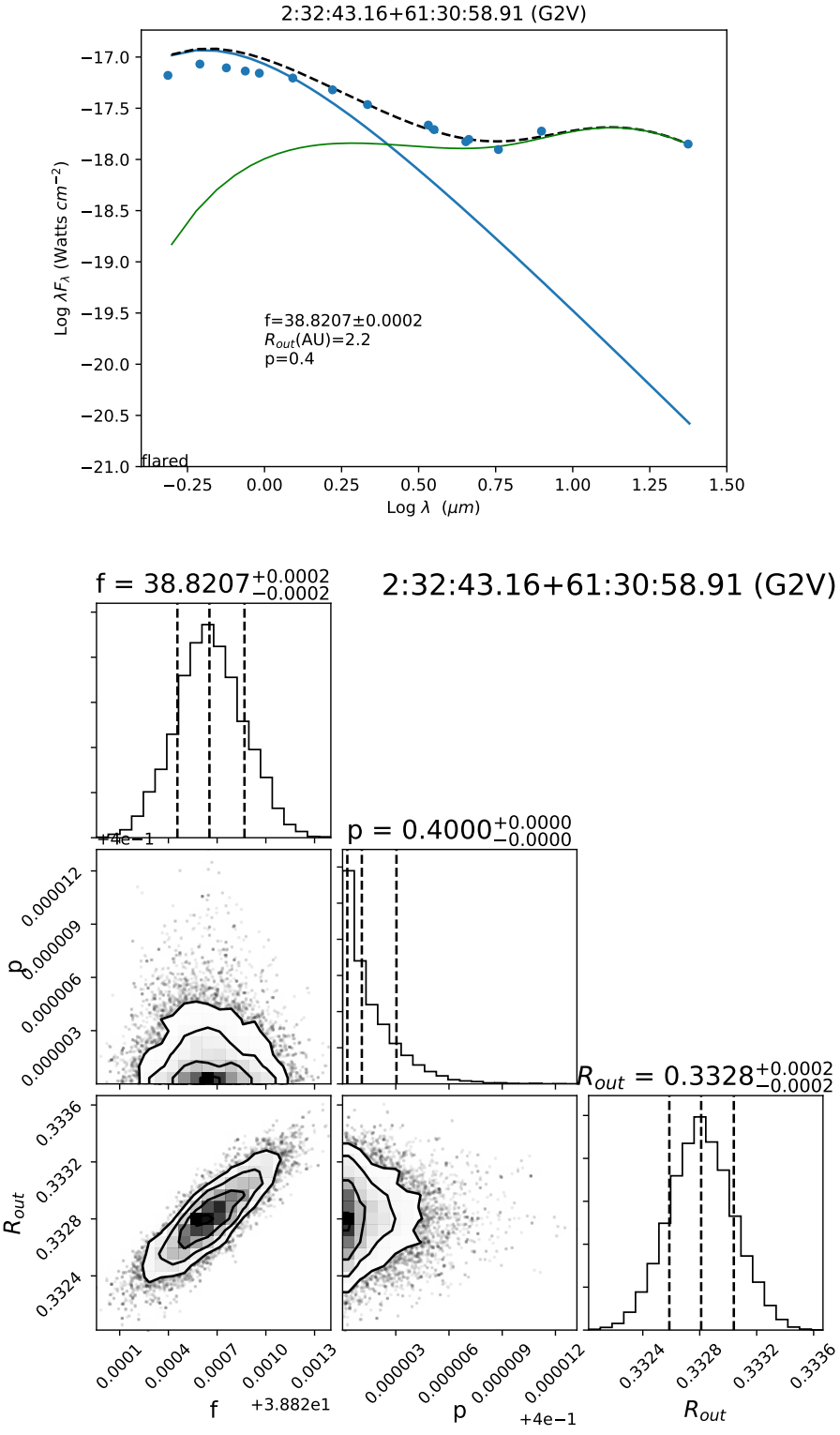

Figure 15. SED and corner plot of source 2:32:43.16+61:30:58.91 which is classified as a pt? disk.

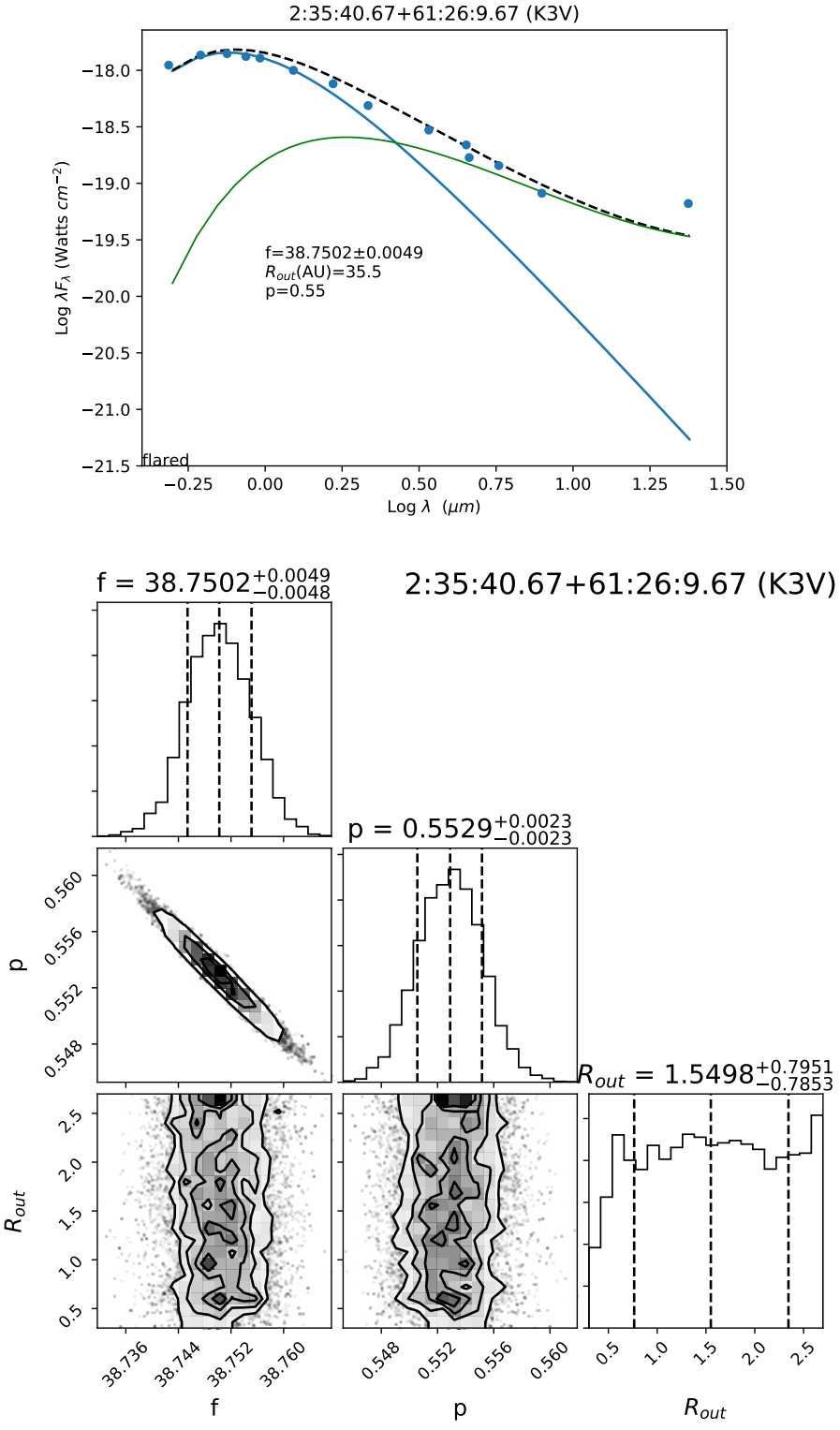

Figure 16. SED and corner plot of source 2:35:40.67+61:26:9.67 which is classified as a pt disk.

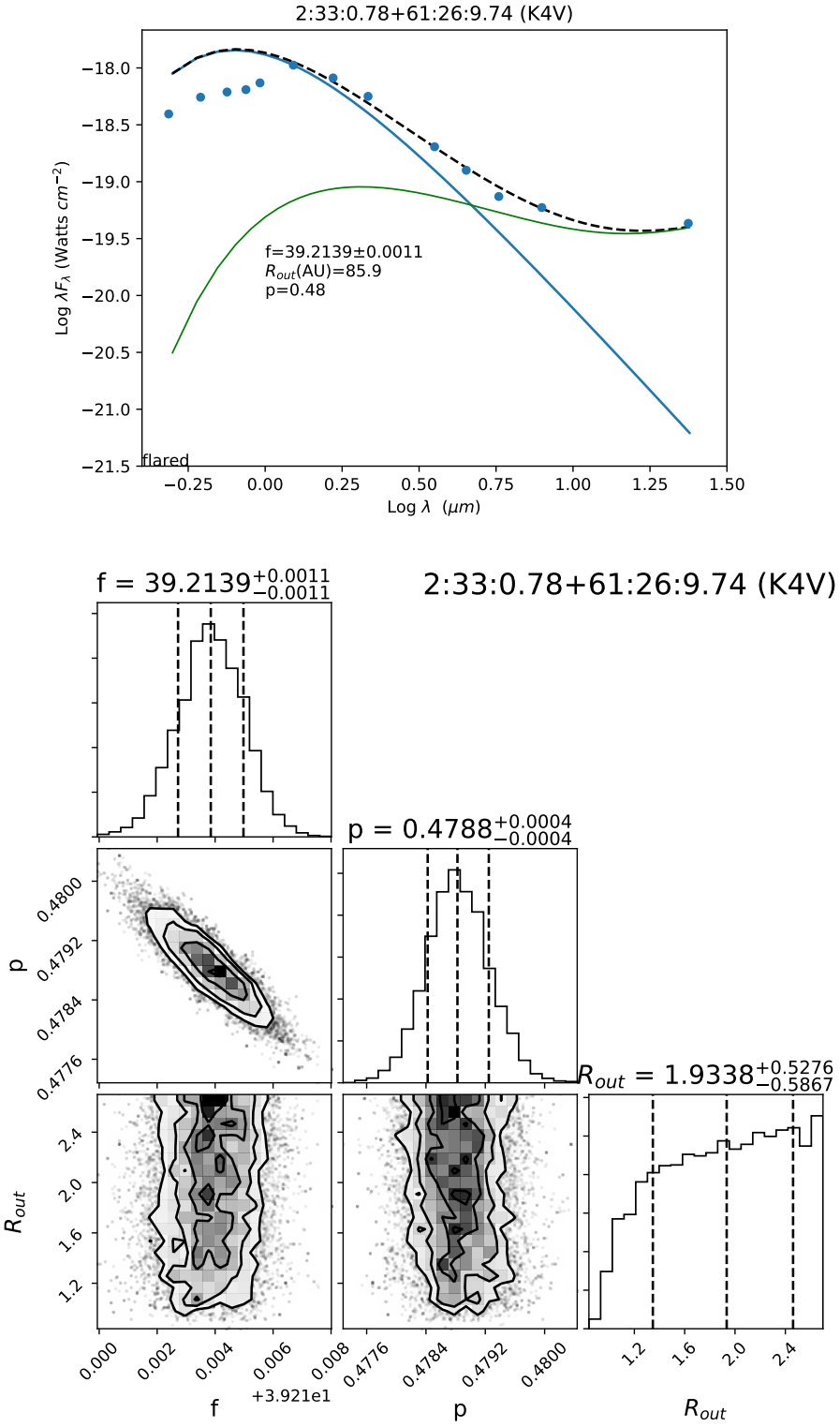

Figure 17. SED and corner plot of source 2:33:0.78+61:26:9.74 which is classified as a pt disk.

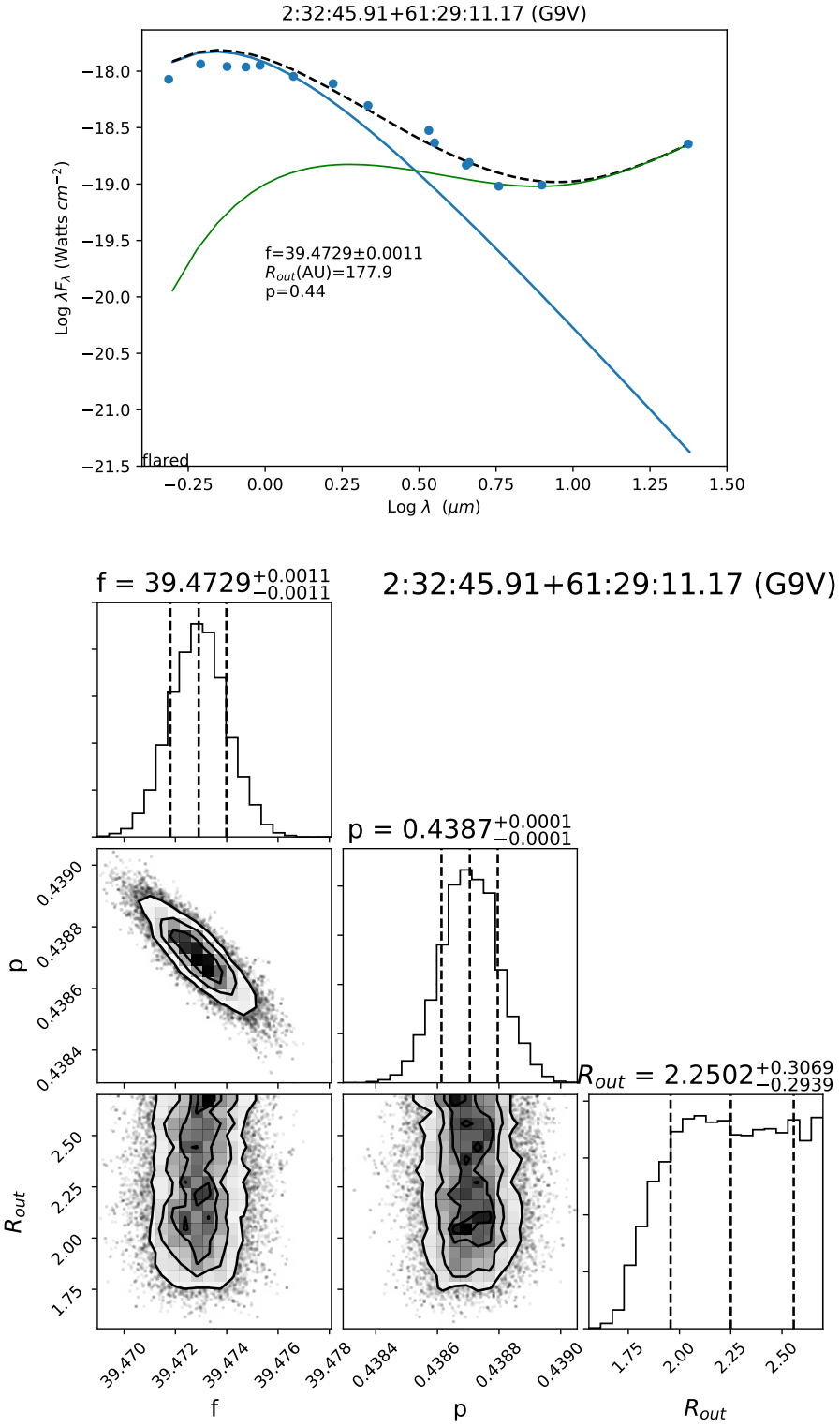

Figure 18. SED and corner plot of source 2:32:45.91+61:29:11.17 which is classified as a pt/enh disk.

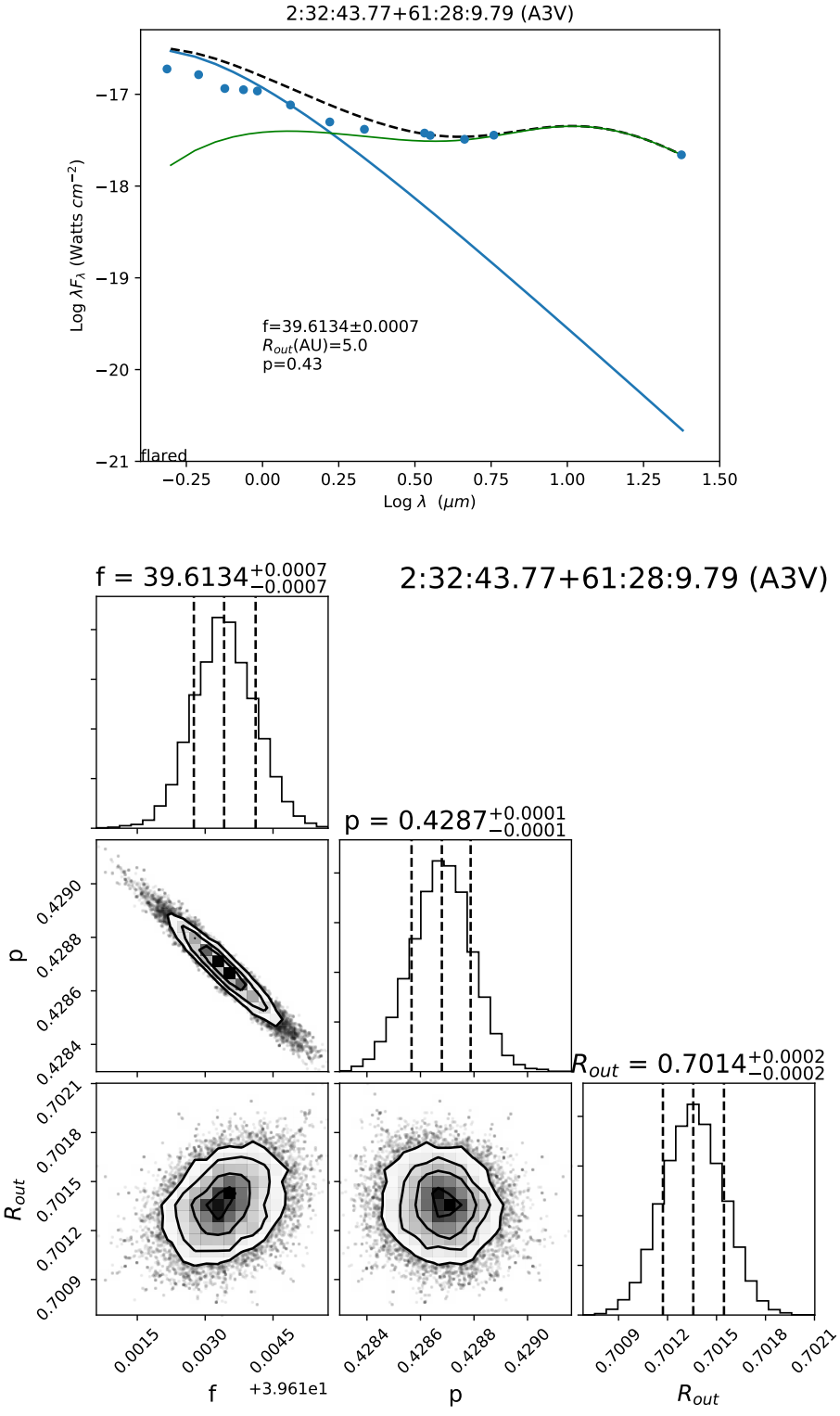

Figure 19. SED and corner plot of source 2:32:43.77+61:28:9.79 which is classified as a thick disk.

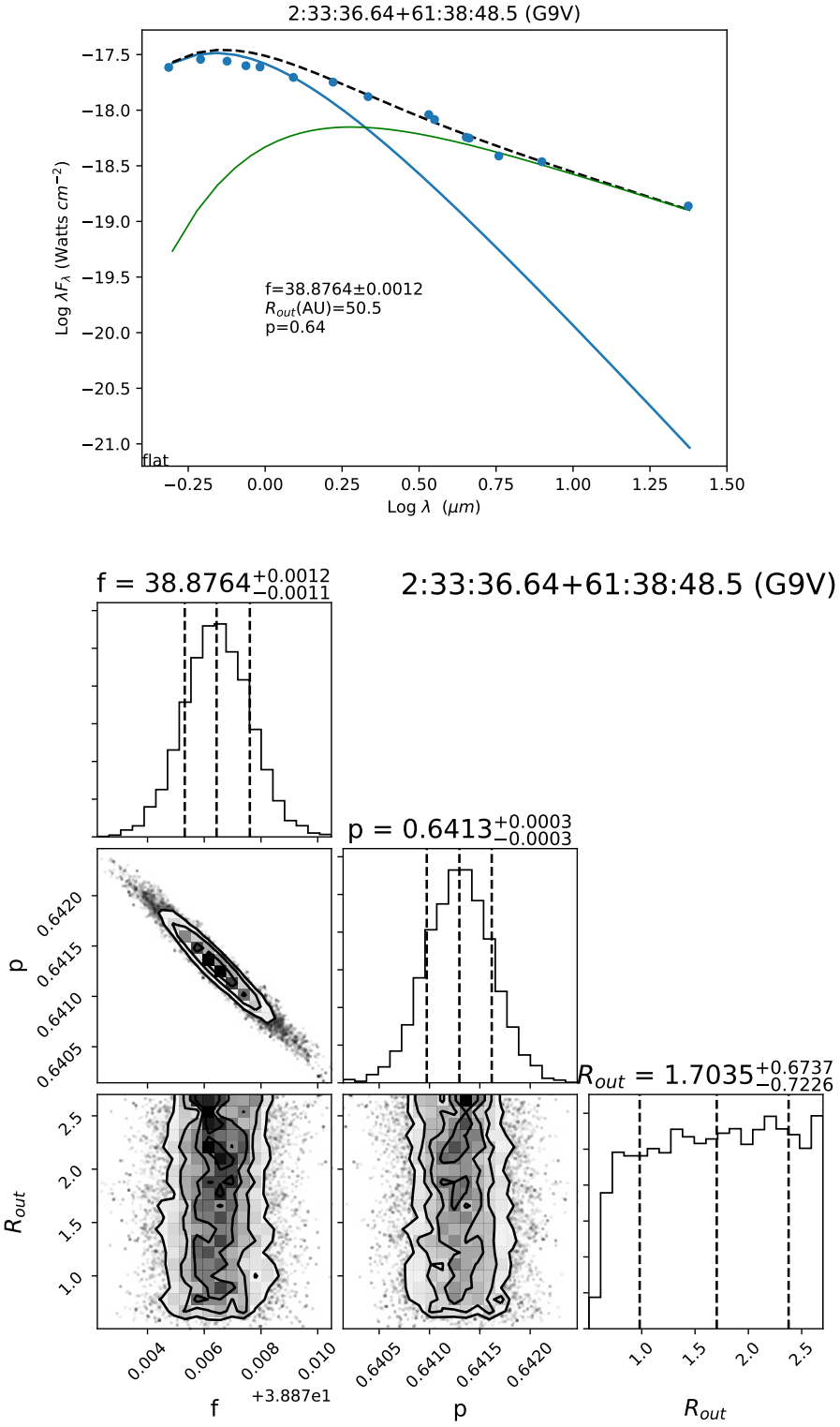

Figure 20. SED and corner plot of source 2:33:36.64+61:38:48.5 which is classified as a thin disk.

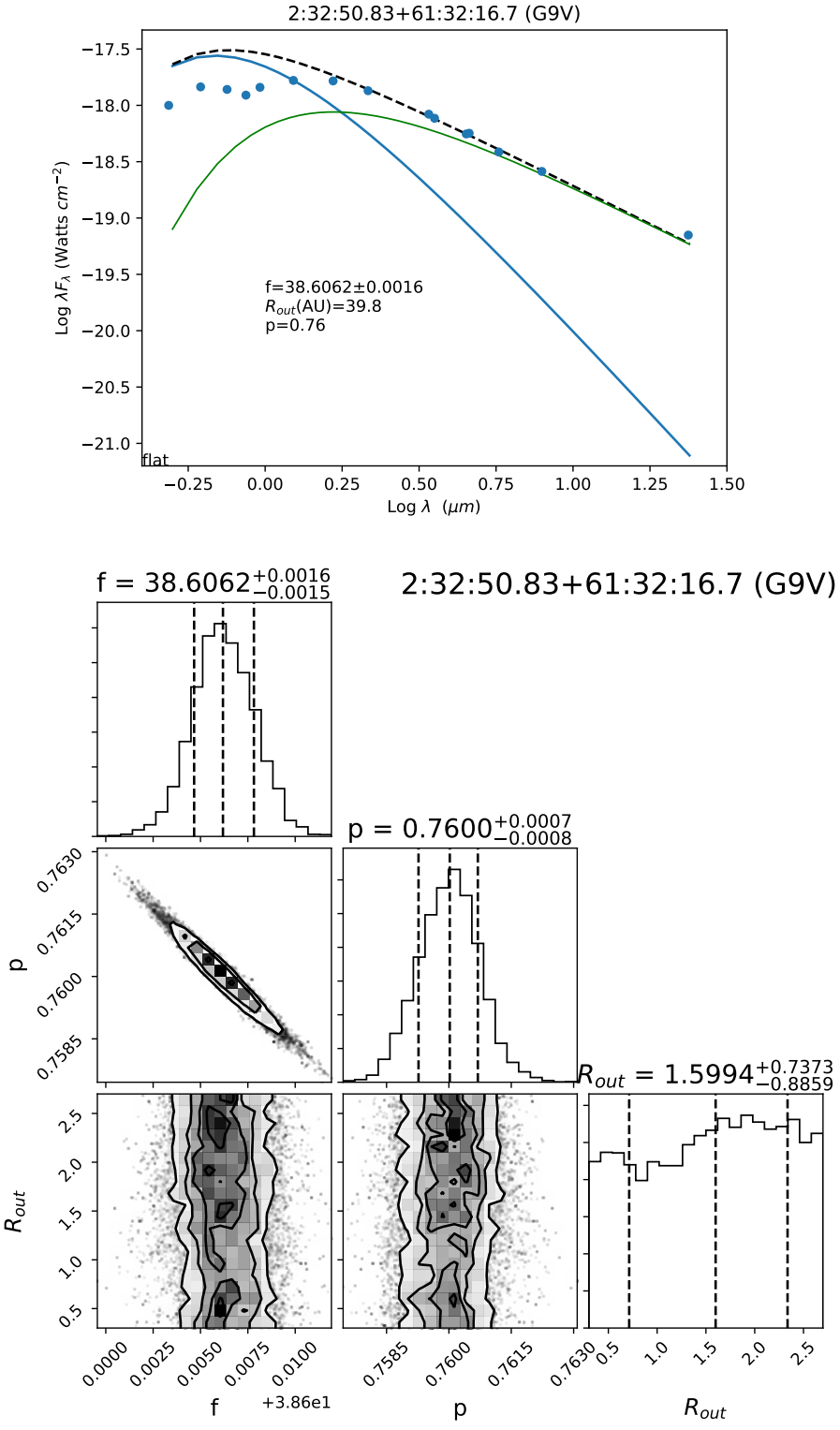

Figure 21. SED and corner plot of source 2:32:50.83+61:32:16.7 which is classified as a thin disk.

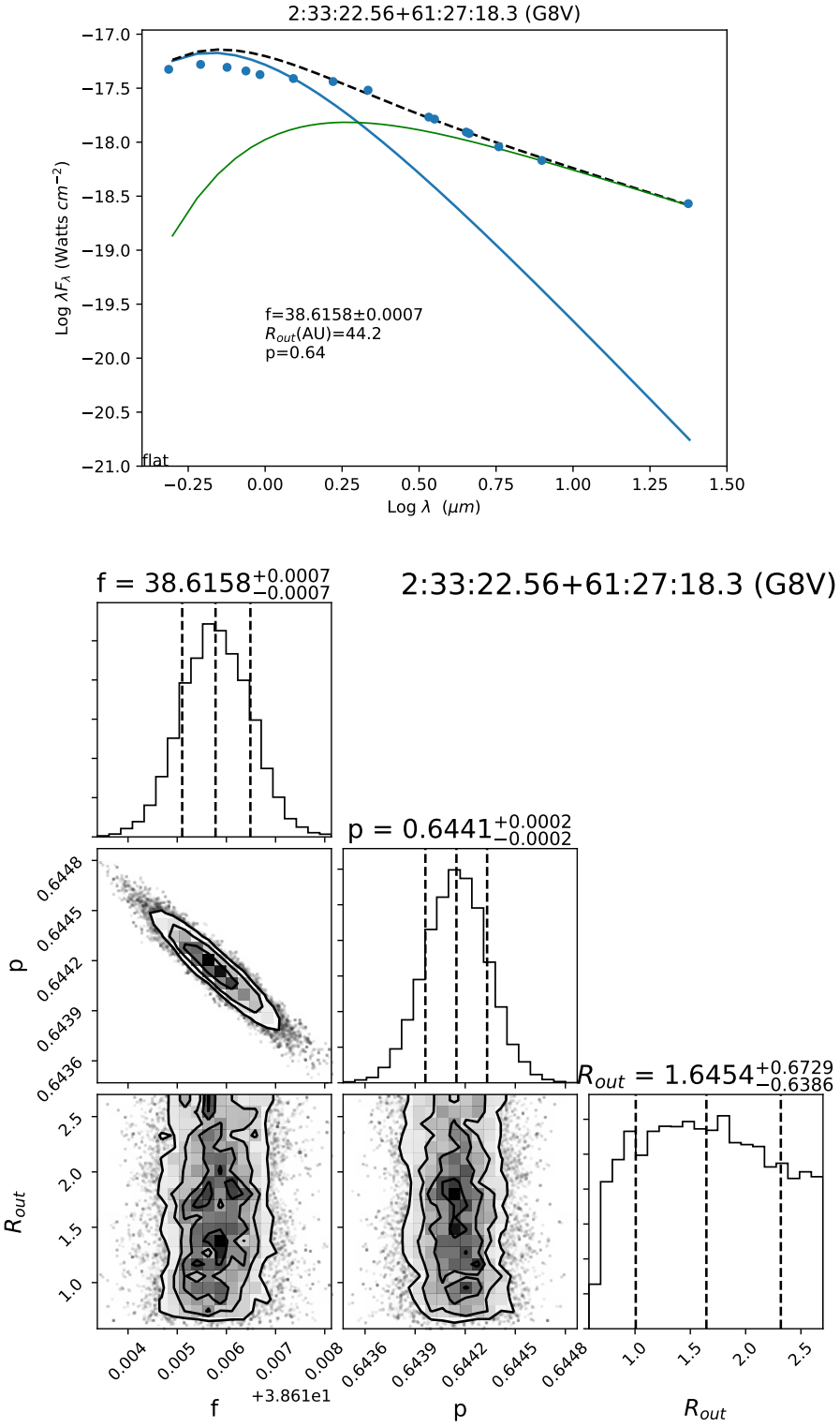

Figure 22. SED and corner plot of source 2:33:22.56+61:27:18.3 which is classified as a thin disk.

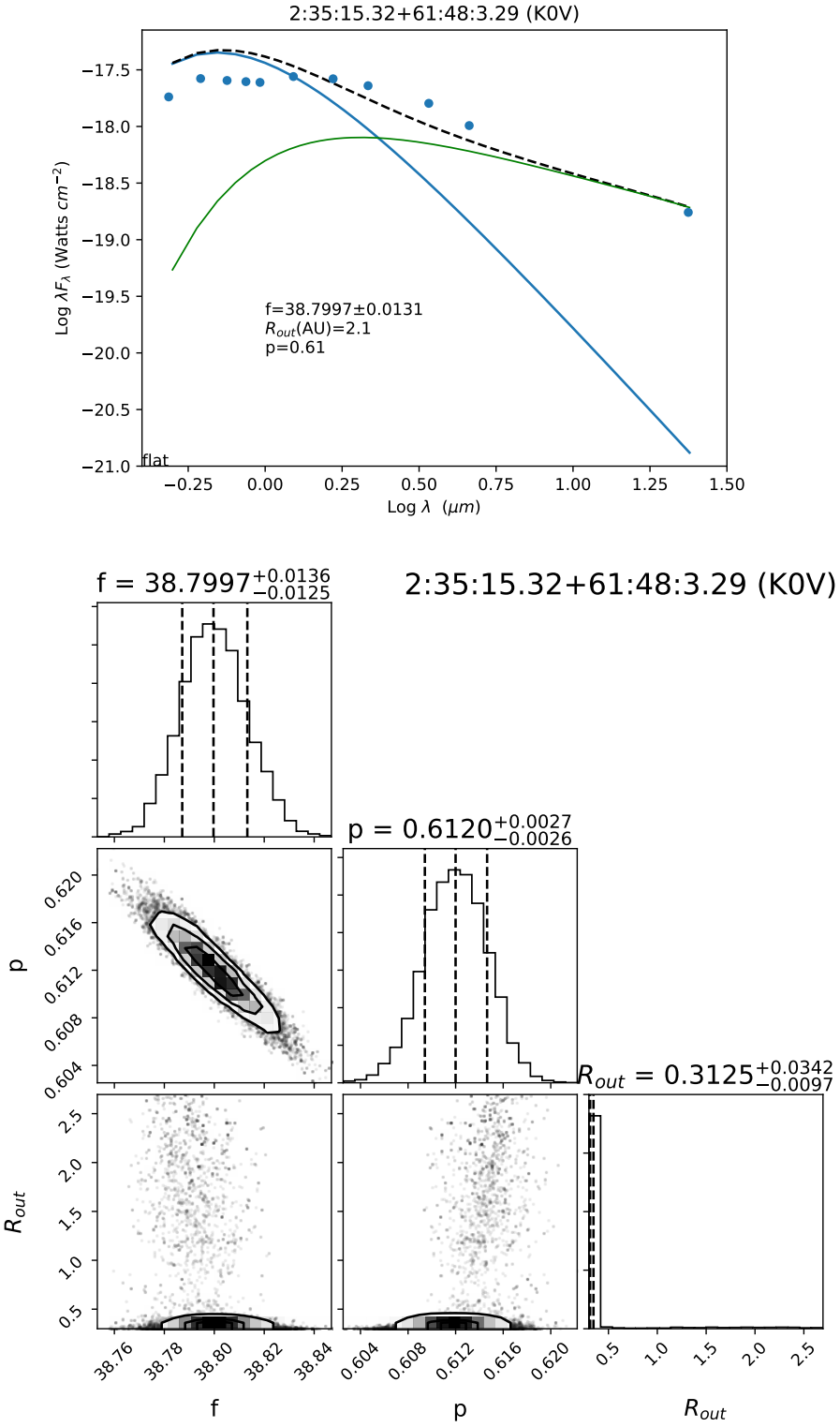

Figure 23. SED and corner plot of source 2:35:15.32+61:48:3.29 which is classified as a thin? disk.

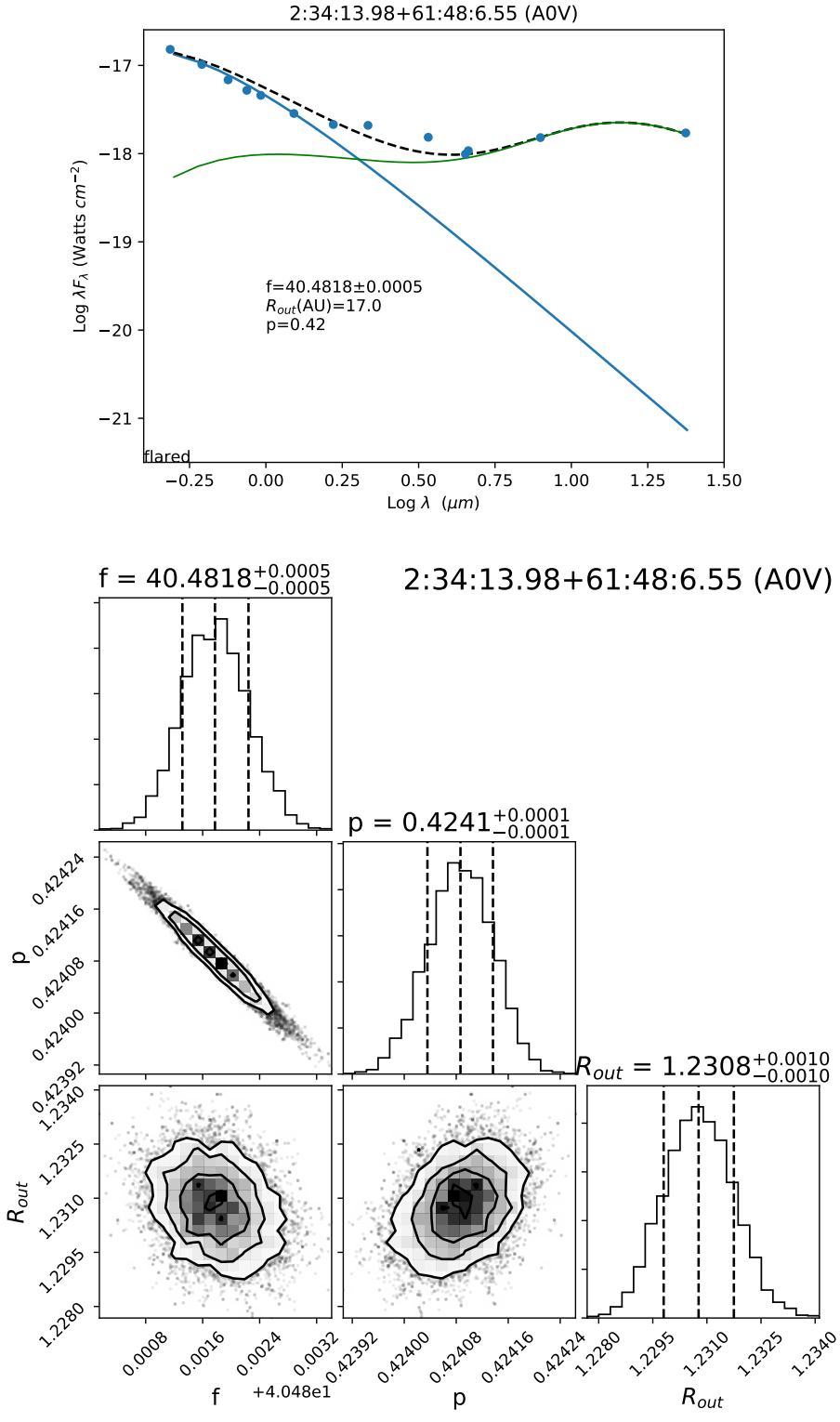

Figure 24. SED and corner plot of source 2:34:13.98+61:48:6.55 which is classified as a thick disk.

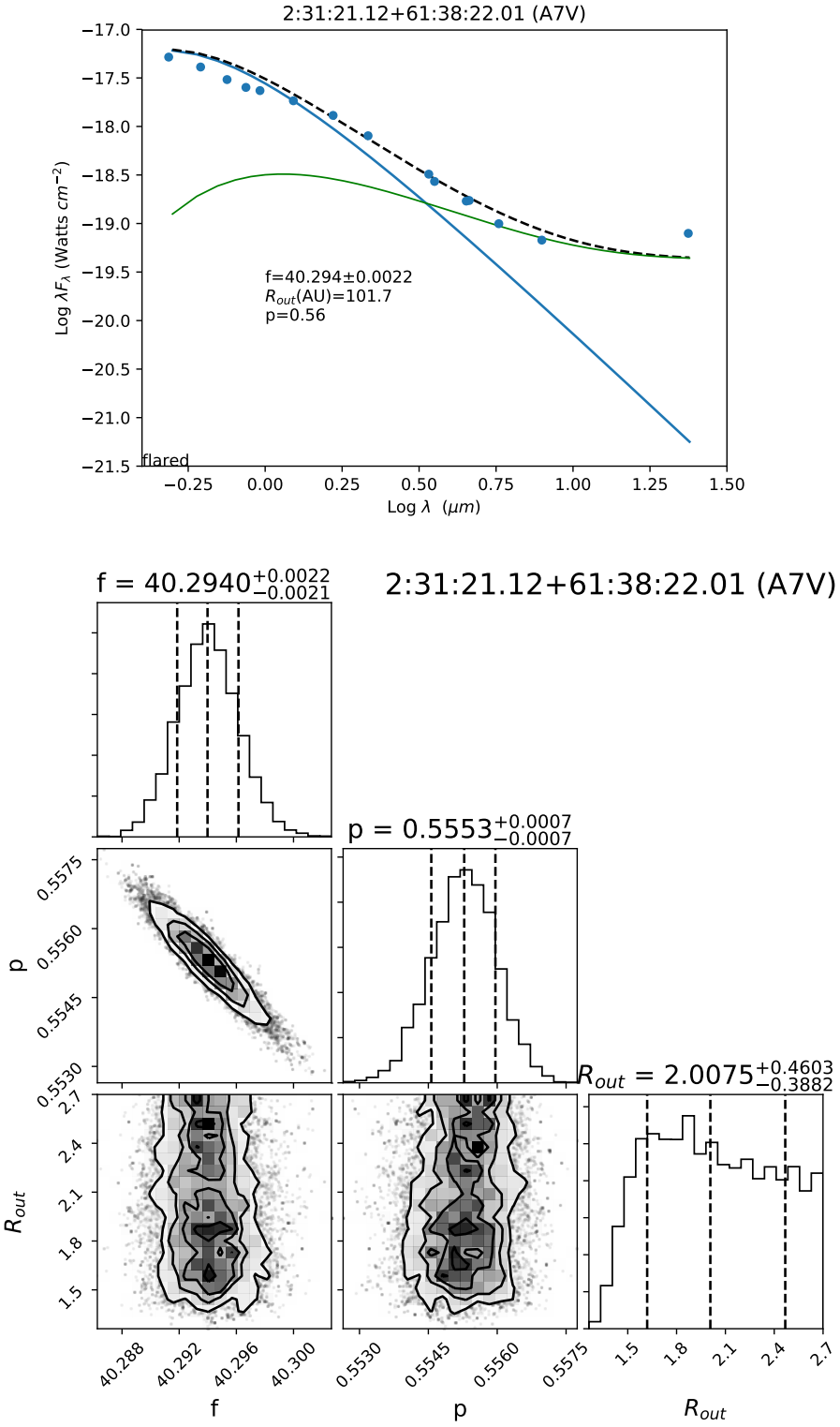

Figure 25. SED and corner plot of source 2:31:21.12+61:38:22.01 which is classified as a pt disk.

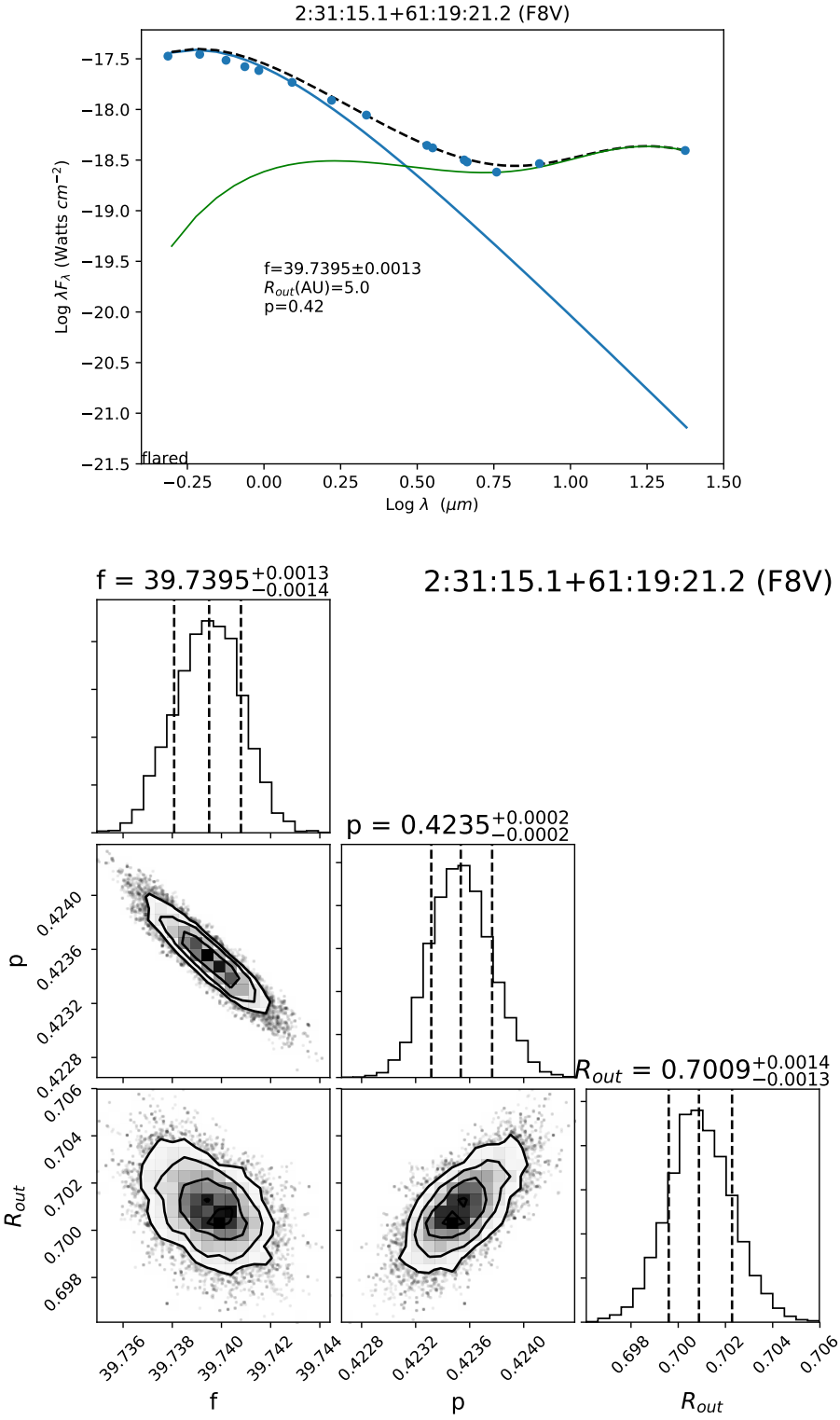

Figure 26. SED and corner plot of source 2:31:15.1+61:19:21.2 which is classified as a pt disk.

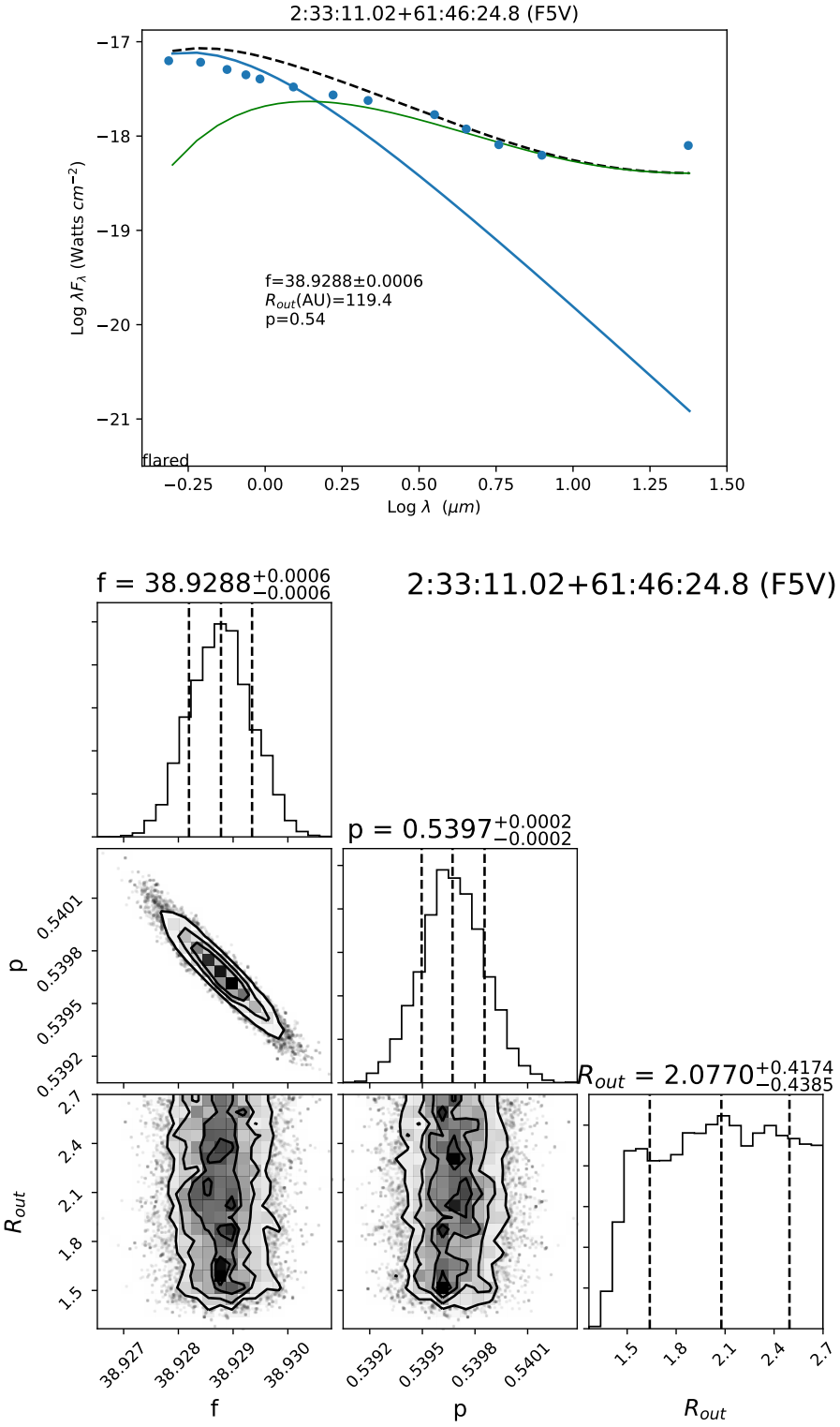

Figure 27. SED and corner plot of source 2:33:11.02+61:46:24.8 which is classified as a thick-pt disk.

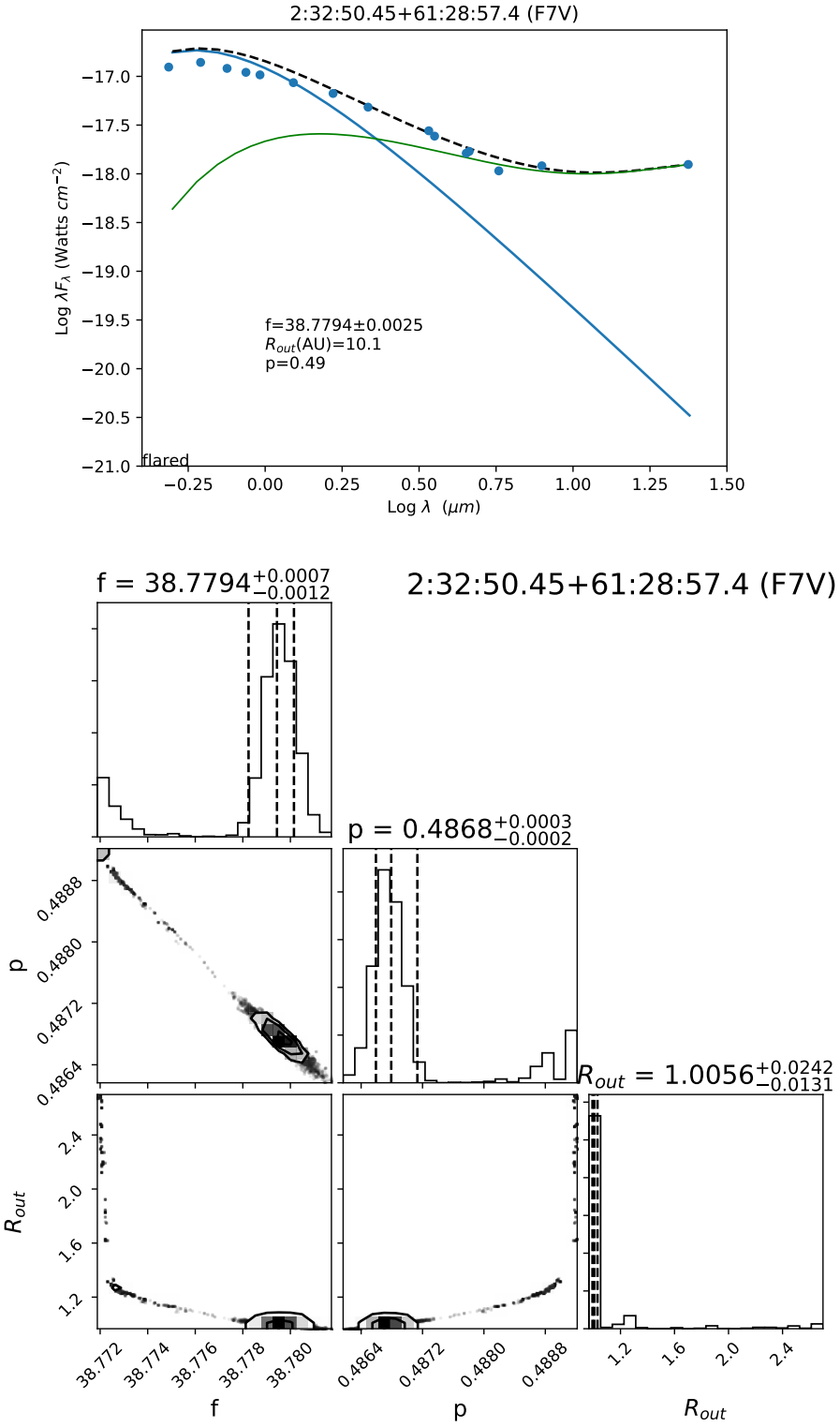

Figure 28. SED and corner plot of source 2:32:50.45+61:28:57.4 which is classified as a pt disk.

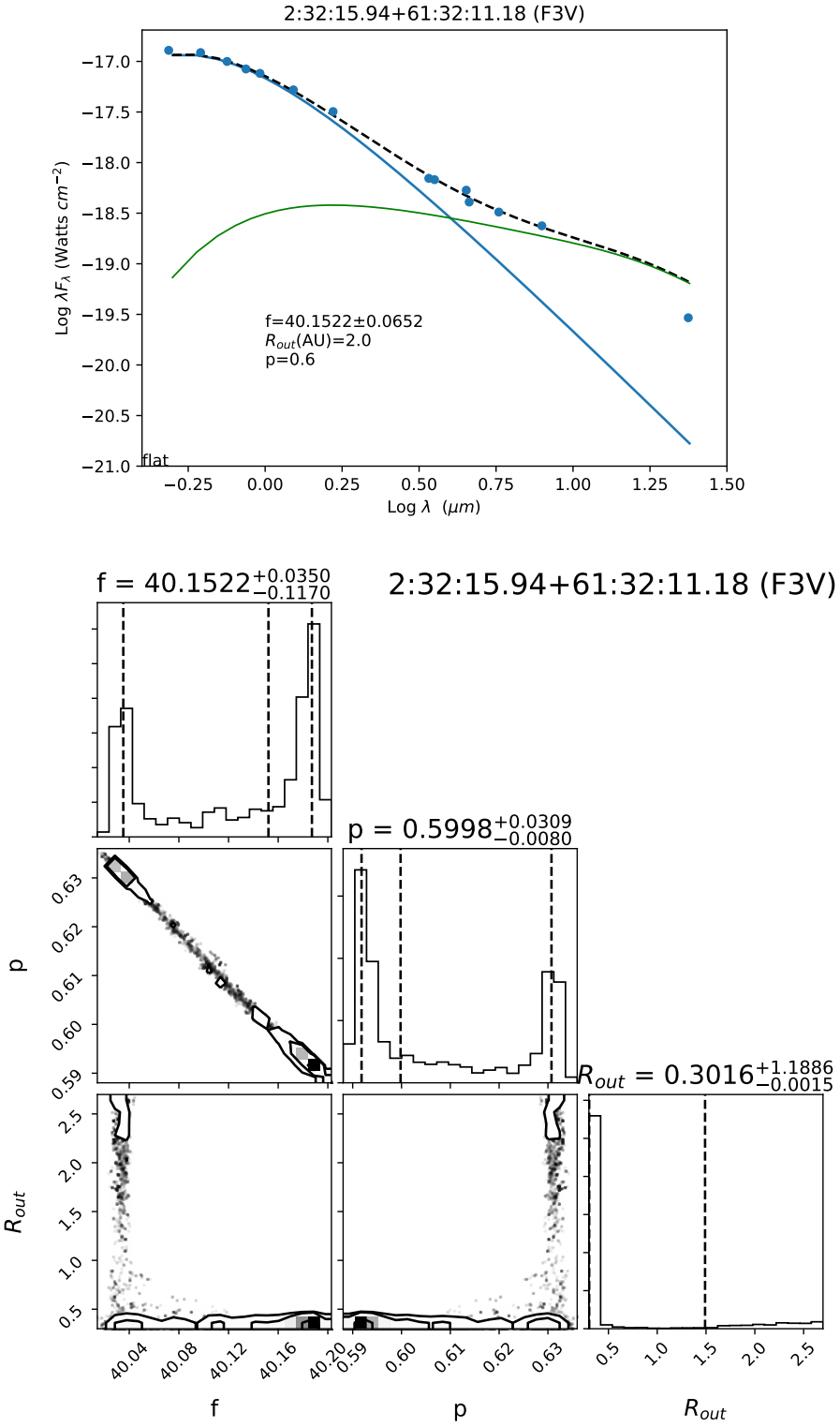

Figure 29. SED and corner plot of source 2:32:15.94+61:32:11.18 which is classified as a thin/trunc disk.

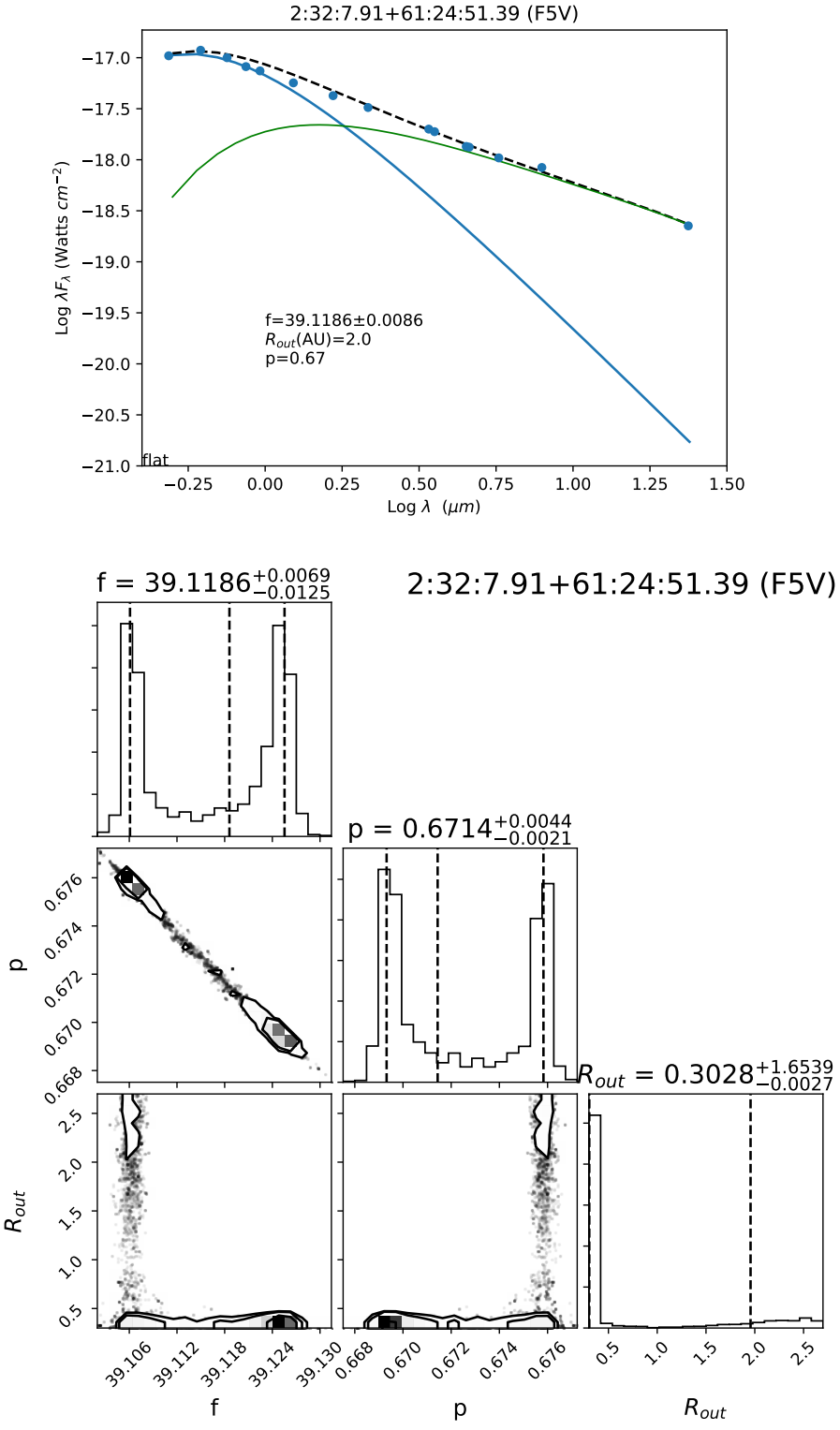

Figure 30. SED and corner plot of source 2:32:7.91+61:24:51.39 which is classified as a thin disk.

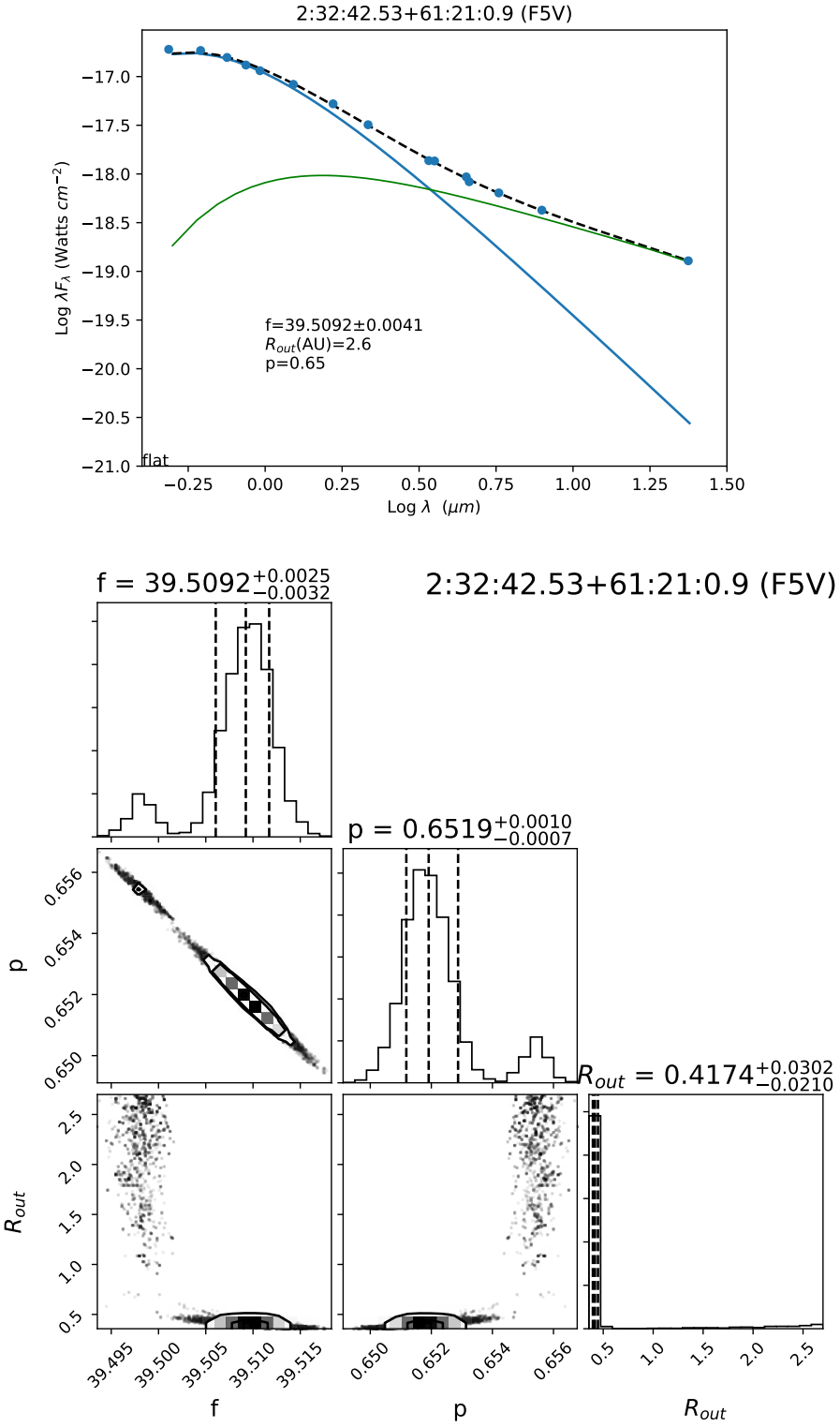

Figure 31. SED and corner plot of source 2:32:42.53+61:21:0.9 which is classified as a thin disk.

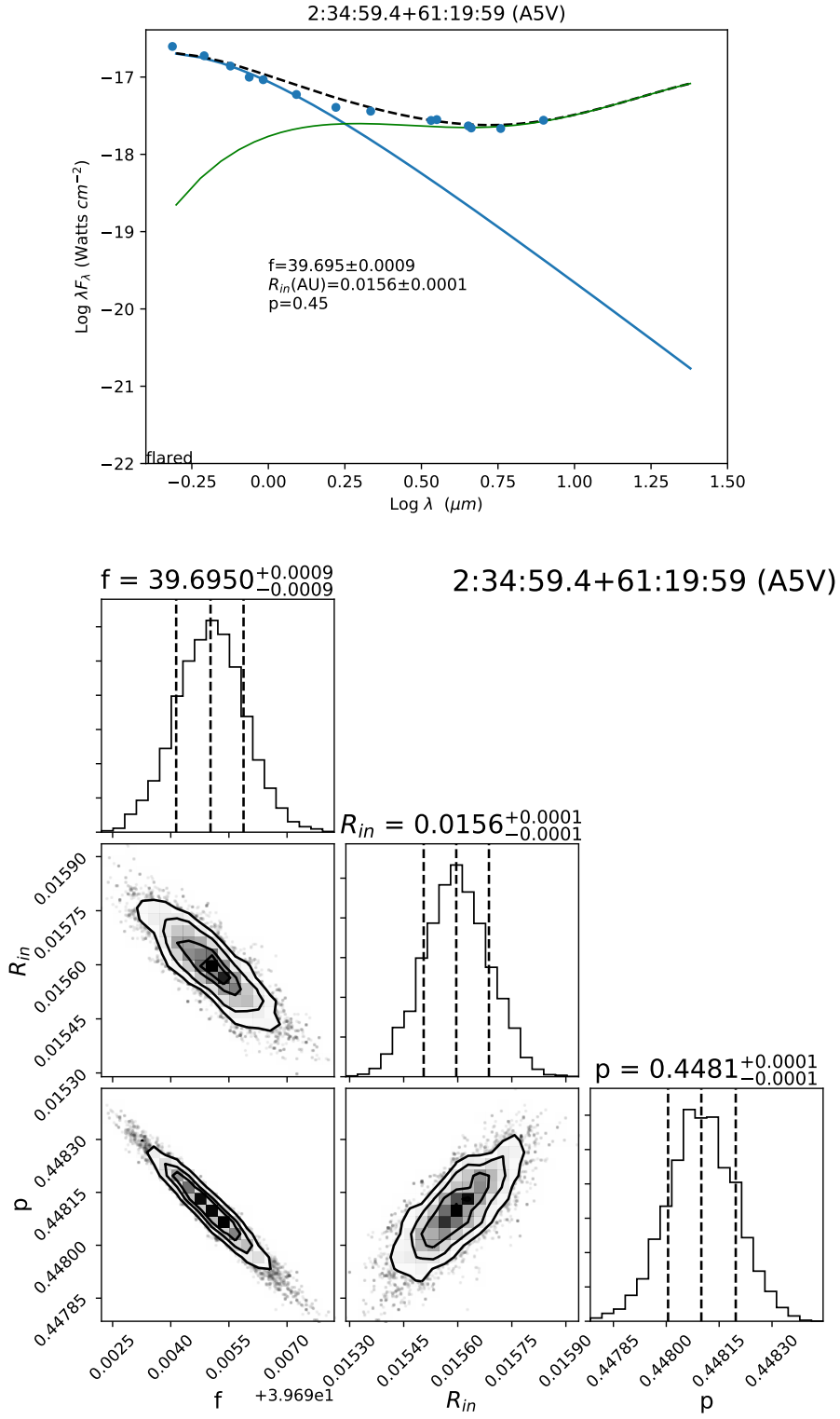

Figure 32. SED and corner plot of source 2:34:59.4+61:19:59 which is classified as a thick disk.

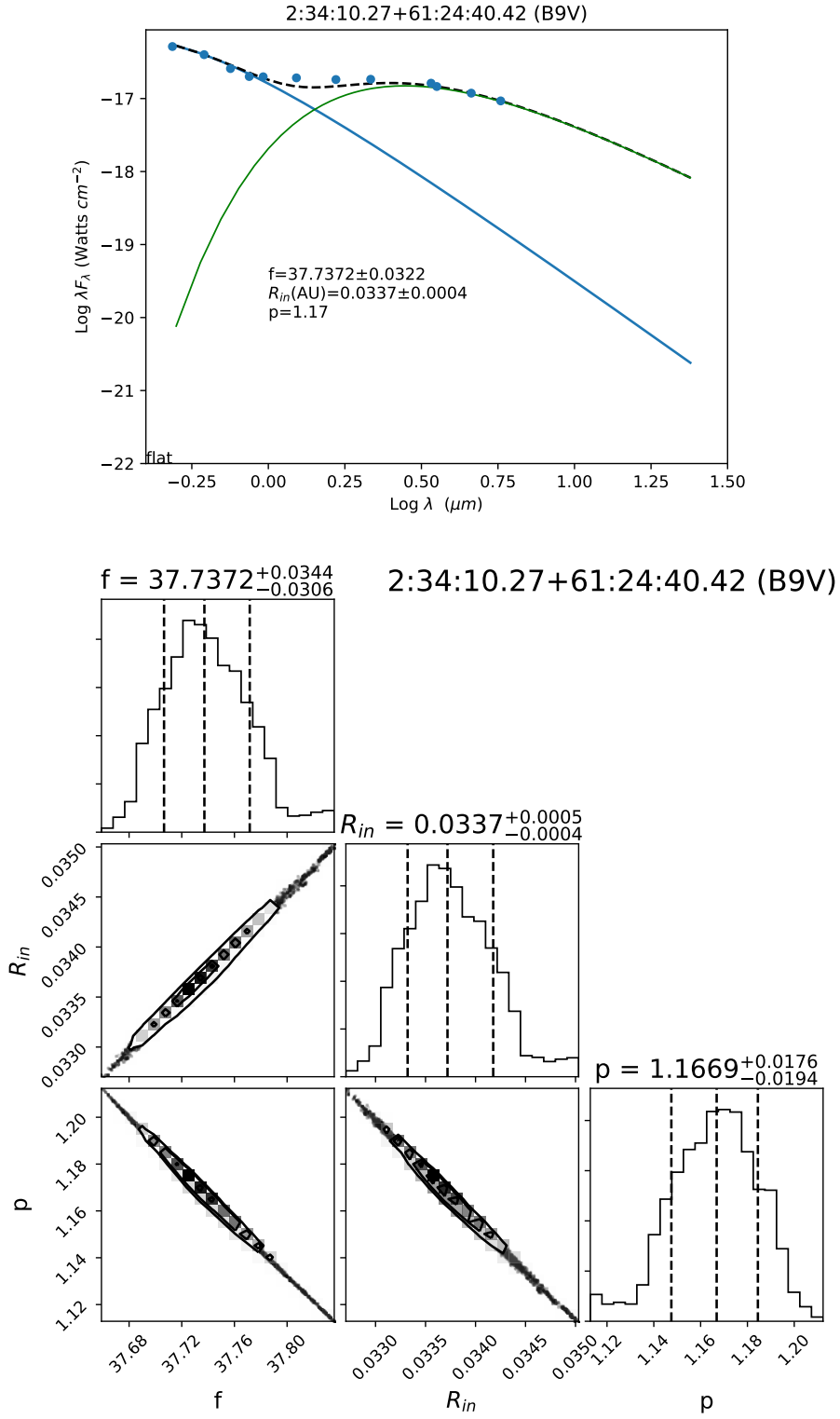

Figure 33. SED and corner plot of source 2:34:10.27+61:24:40.42 which is classified as a thick-pt disk.

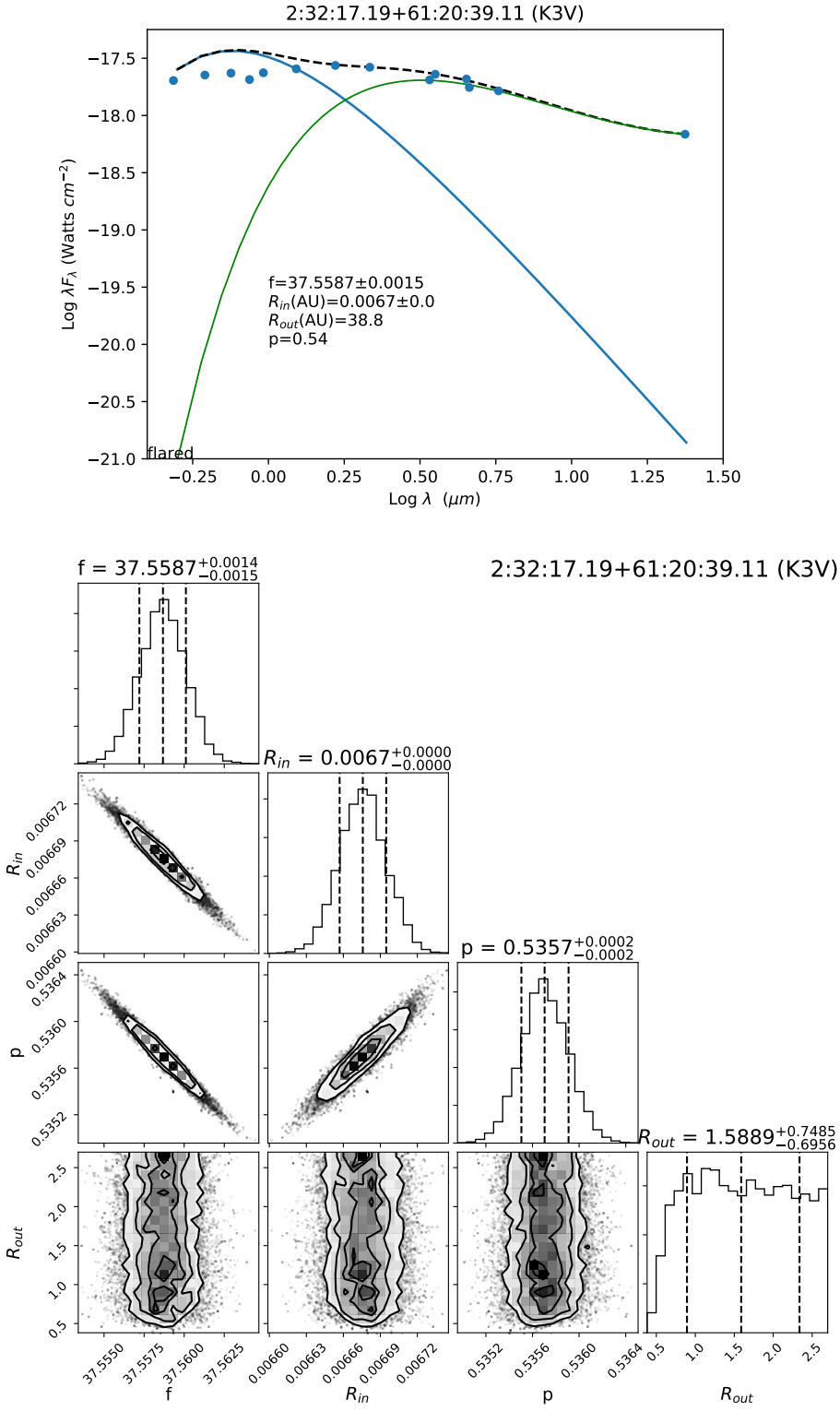

Figure 34. SED and corner plot of source 2:32:17.19+61:20:39.11 which is classified as a thick disk.

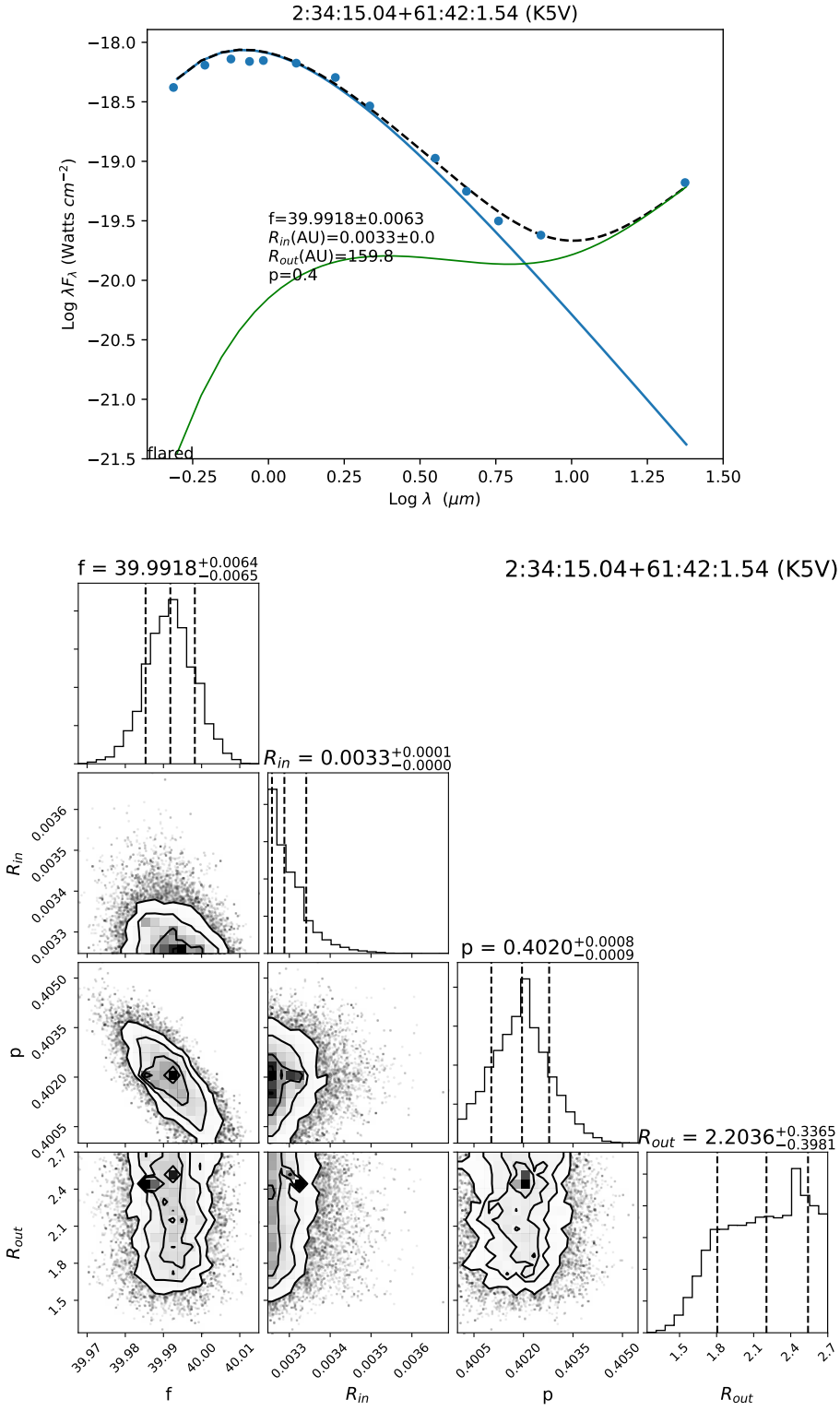

Figure 35. SED and corner plot of source 2:34:15.04+61:42:1.54 which is classified as a pt disk.

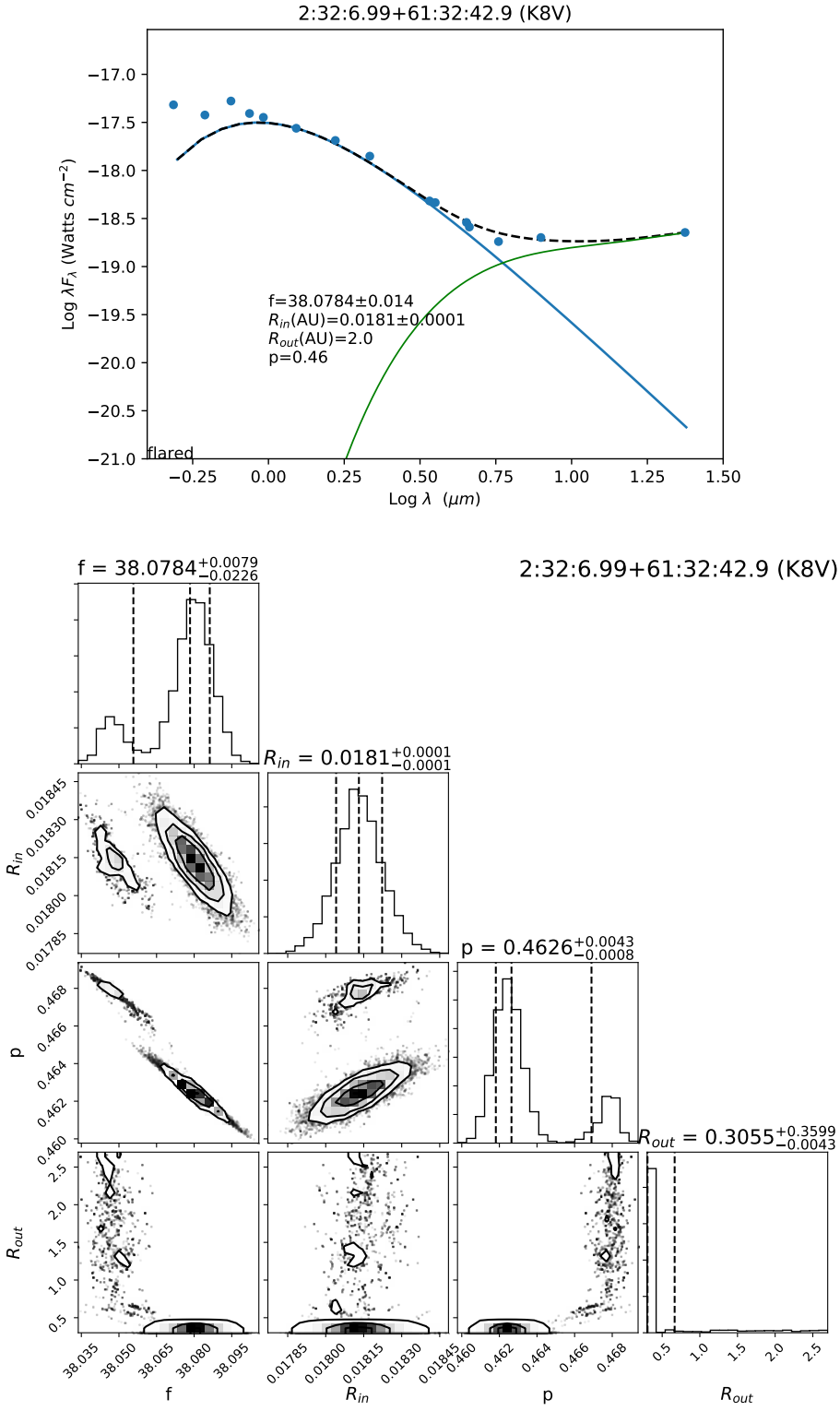

Figure 36. SED and corner plot of source 2:32:6.99+61:32:42.9 which is classified as a pt-t/enh disk.

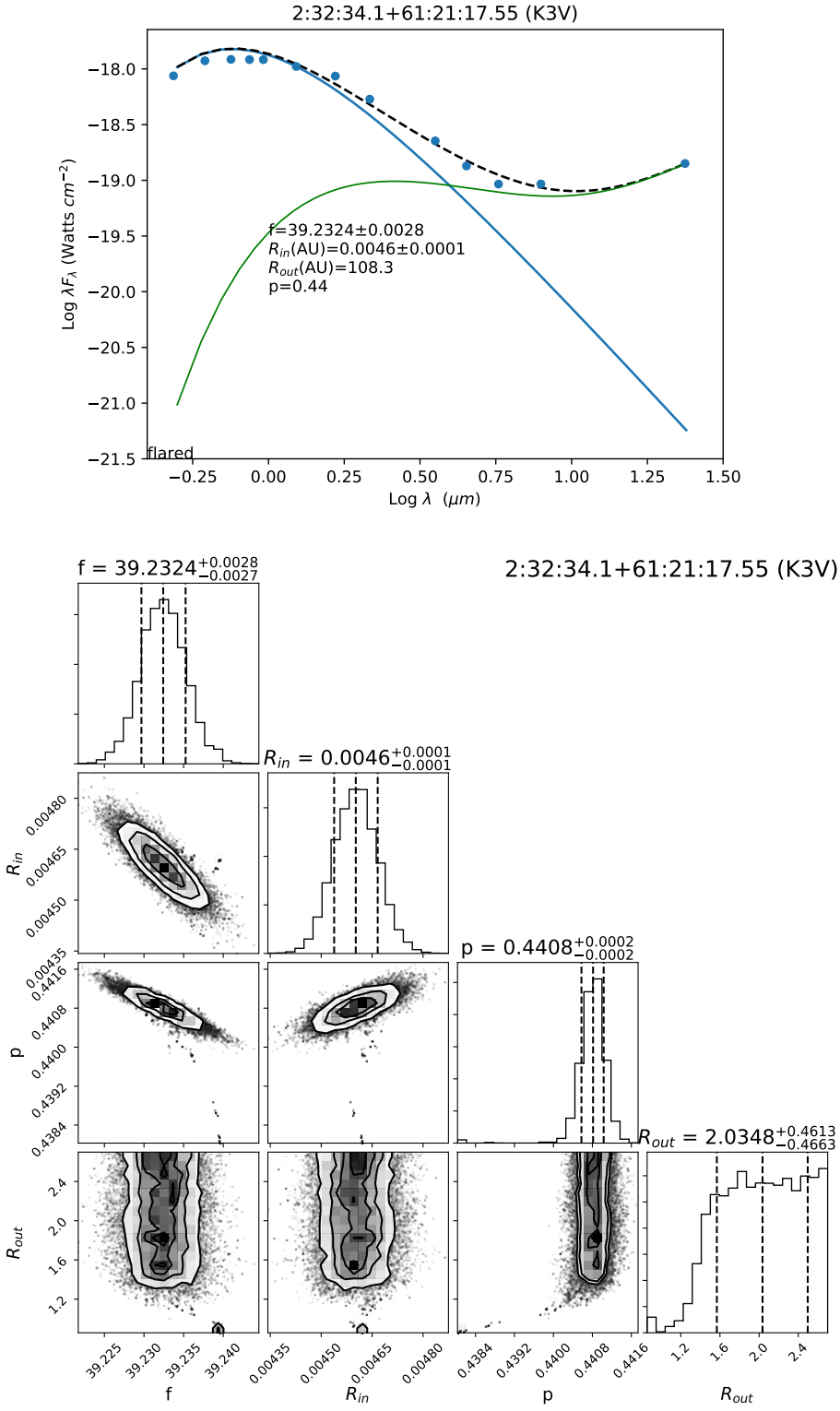

Figure 37. SED and corner plot of source 2:32:34.1+61:21:17.55 which is classified as a pt disk.

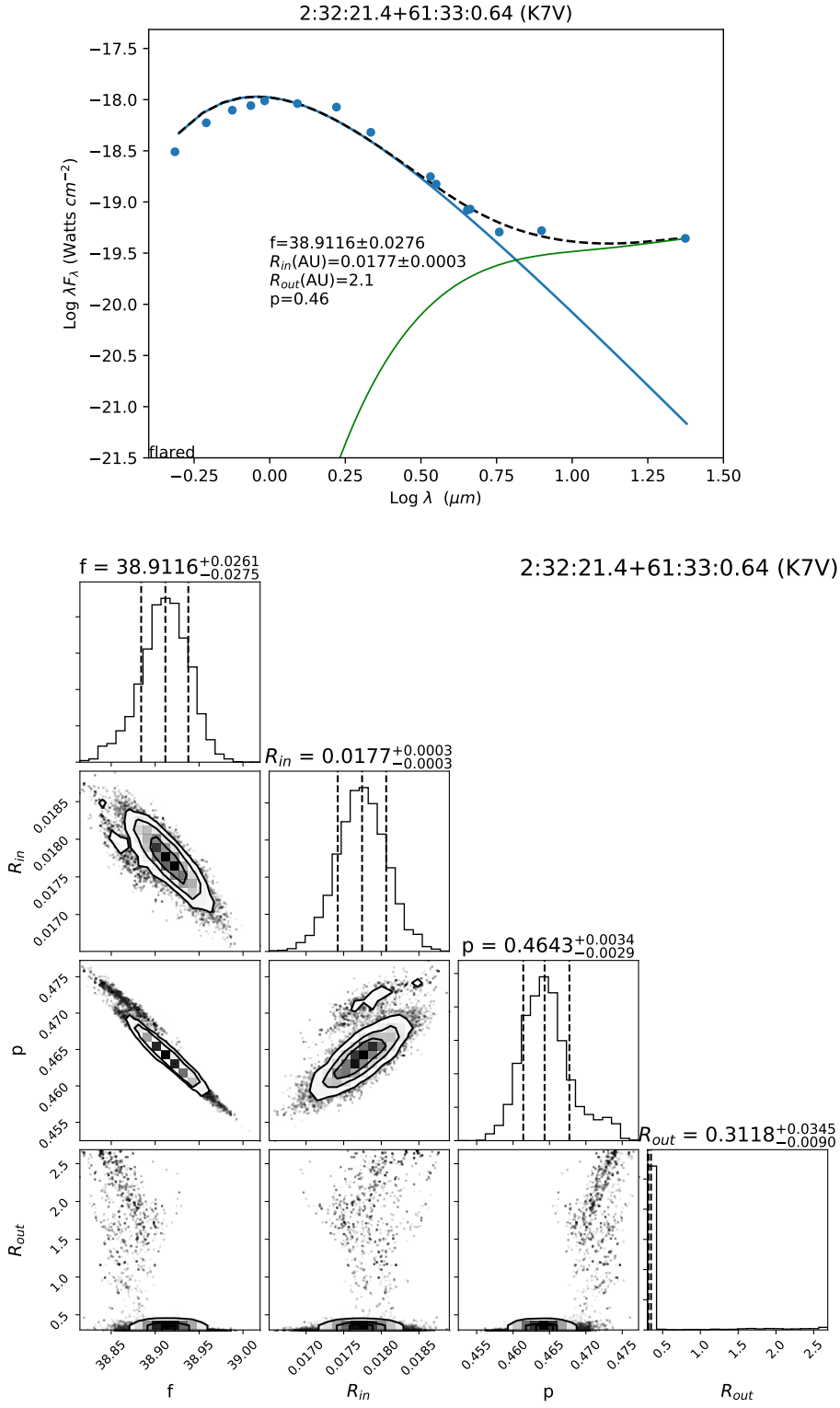

Figure 38. SED and corner plot of source 2:32:21.4+61:33:0.64 which is classified as a pt/enh disk.

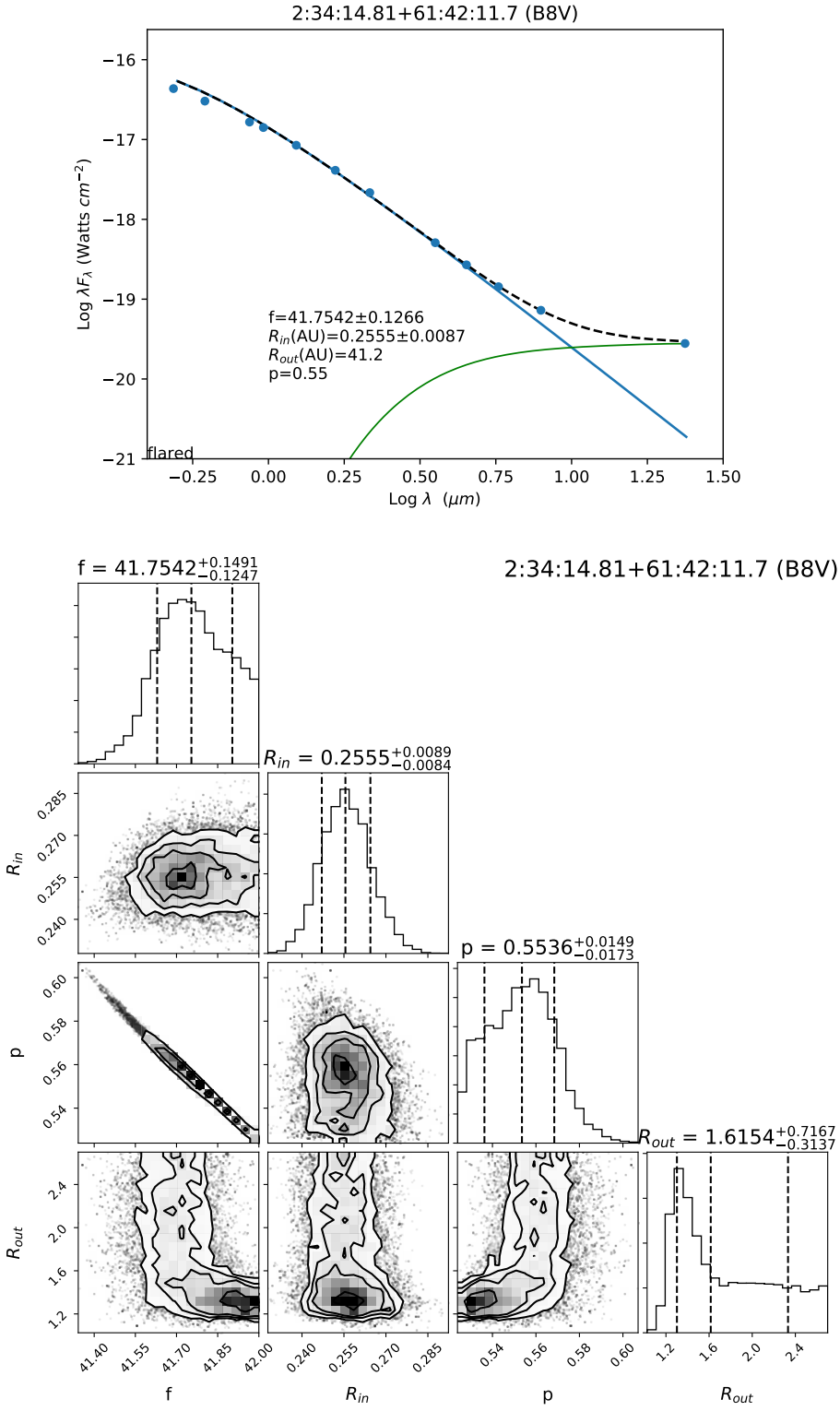

Figure 39. SED and corner plot of source 2:34:14.81+61:42:11.7 which is classified as a t disk.

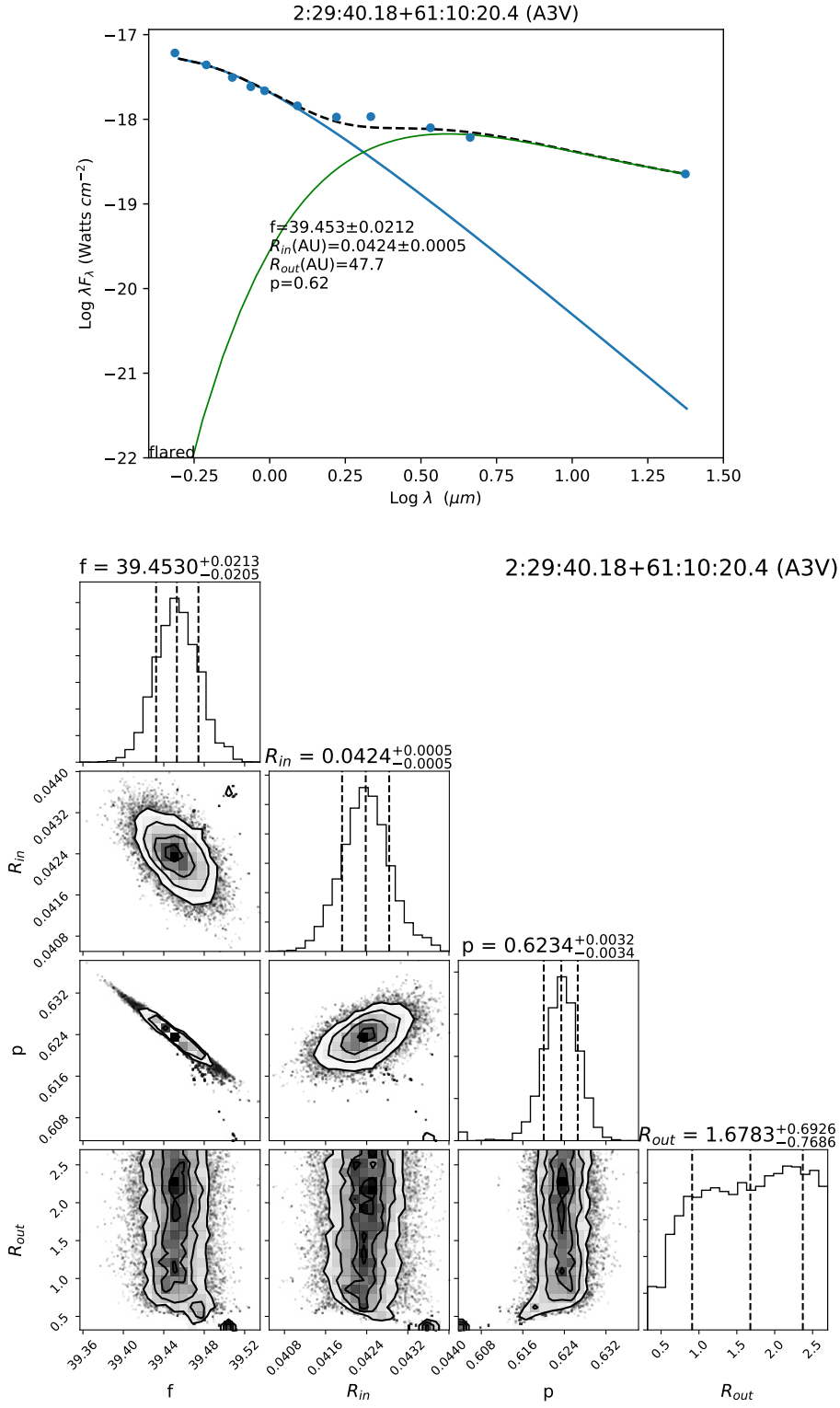

Figure 40. SED and corner plot of source 2:29:40.18+61:10:20.4 which is classified as a thick disk.

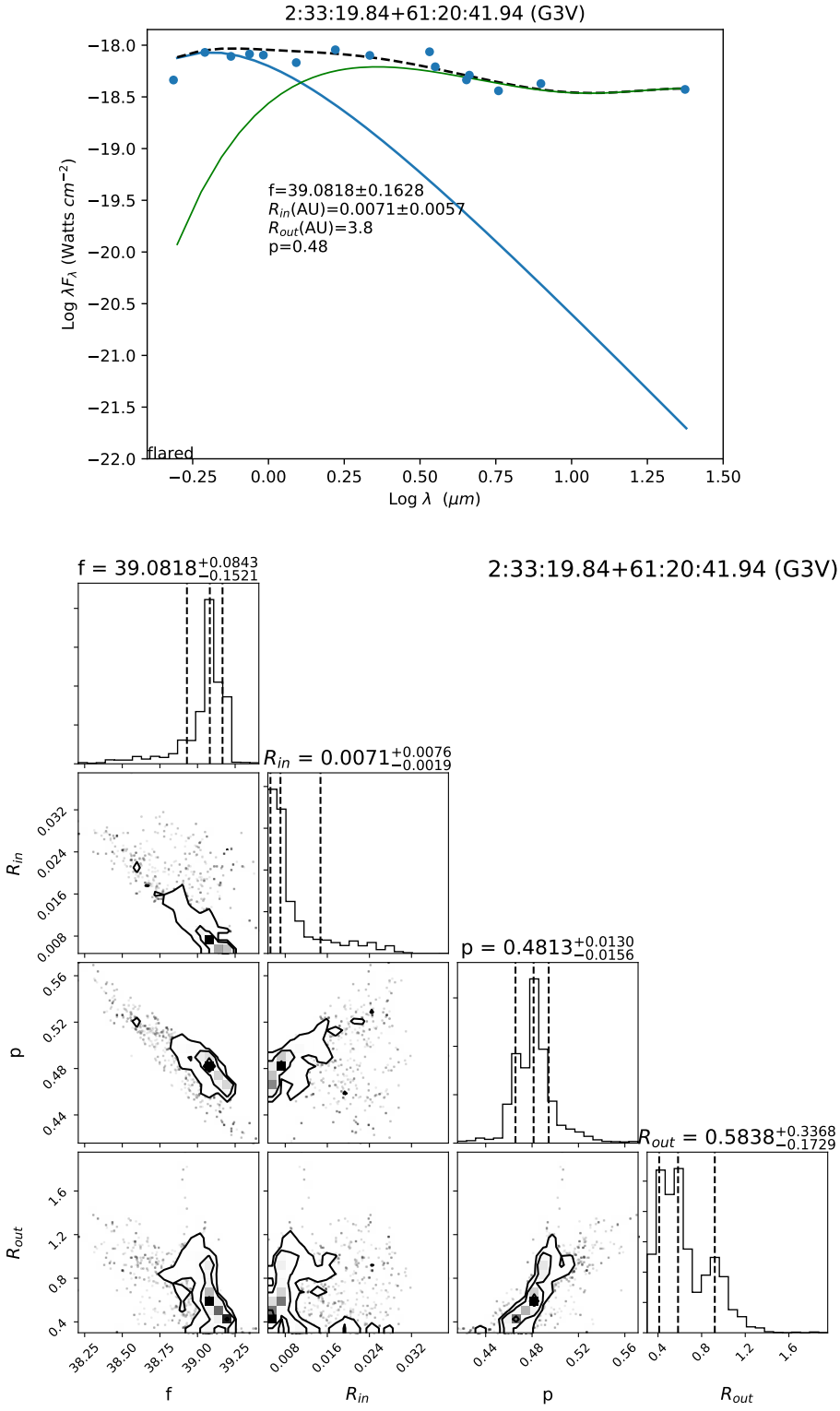

Figure 41. SED and corner plot of source 2:33:19.84+61:20:41.94 which is classified as a thick disk.

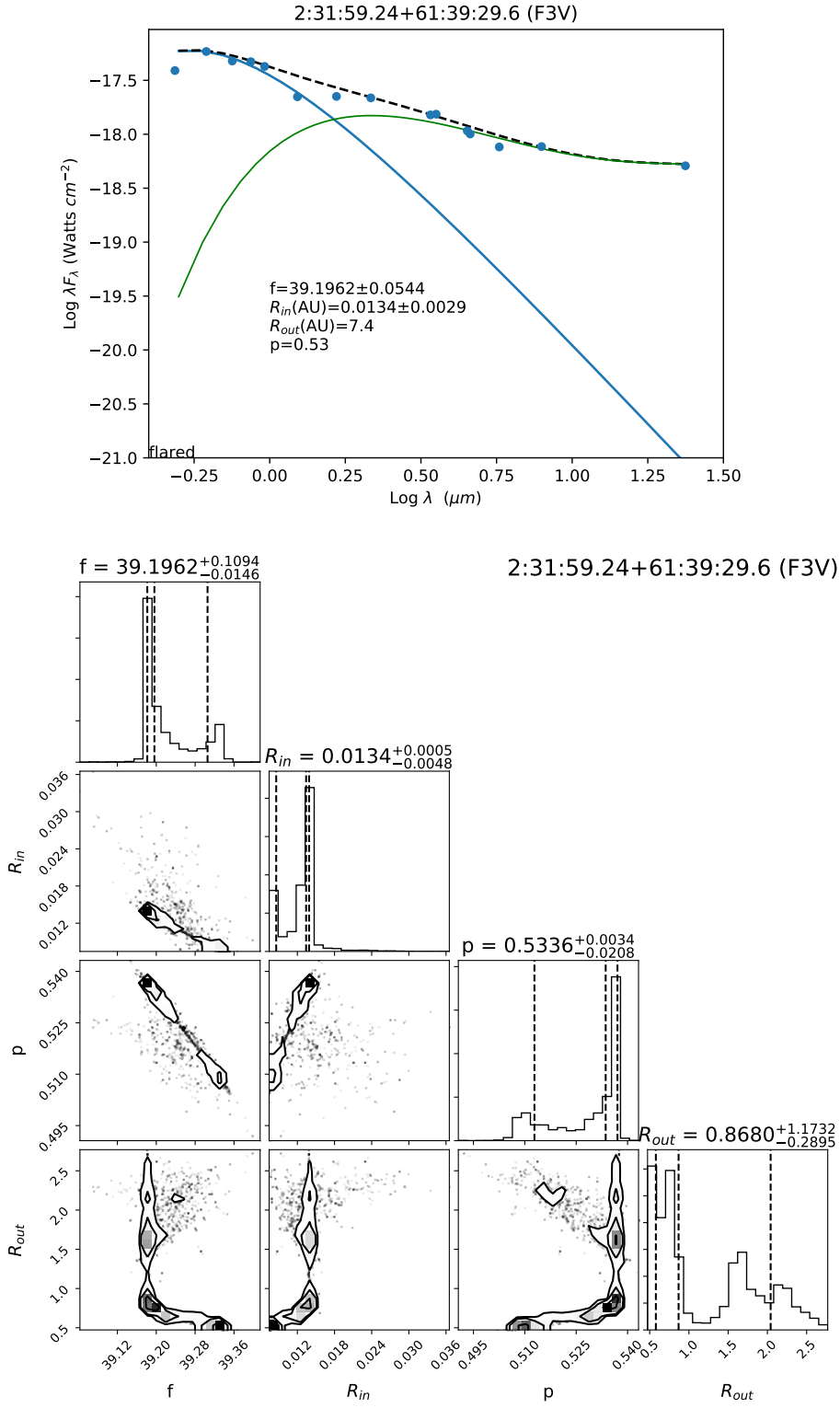

Figure 42. SED and corner plot of source 2:31:59.24+61:39:29.6 which is classified as a thick disk.

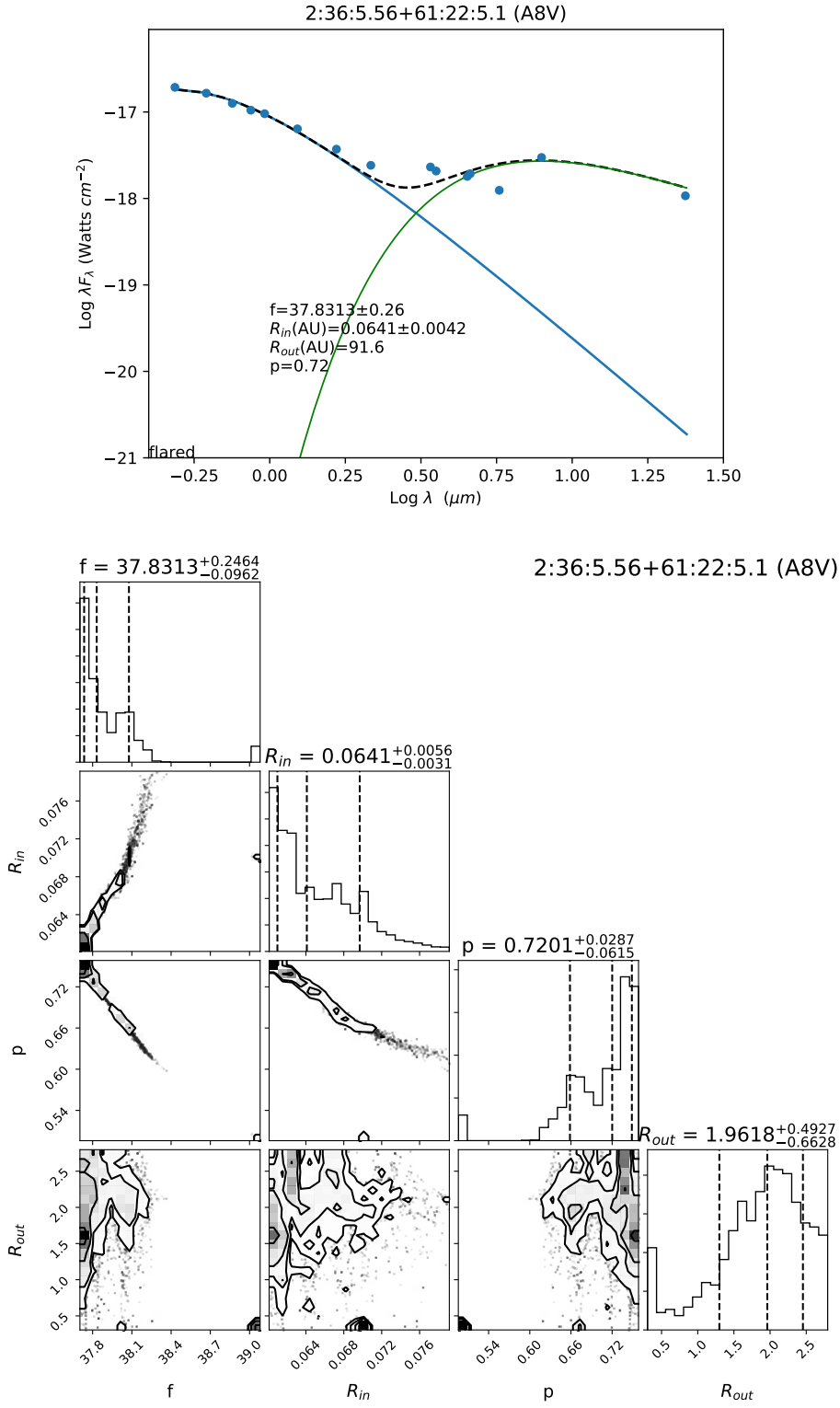

Figure 43. SED and corner plot of source 2:36:5.56+61:22:5.1 which is classified as a thick/trunc? disk.

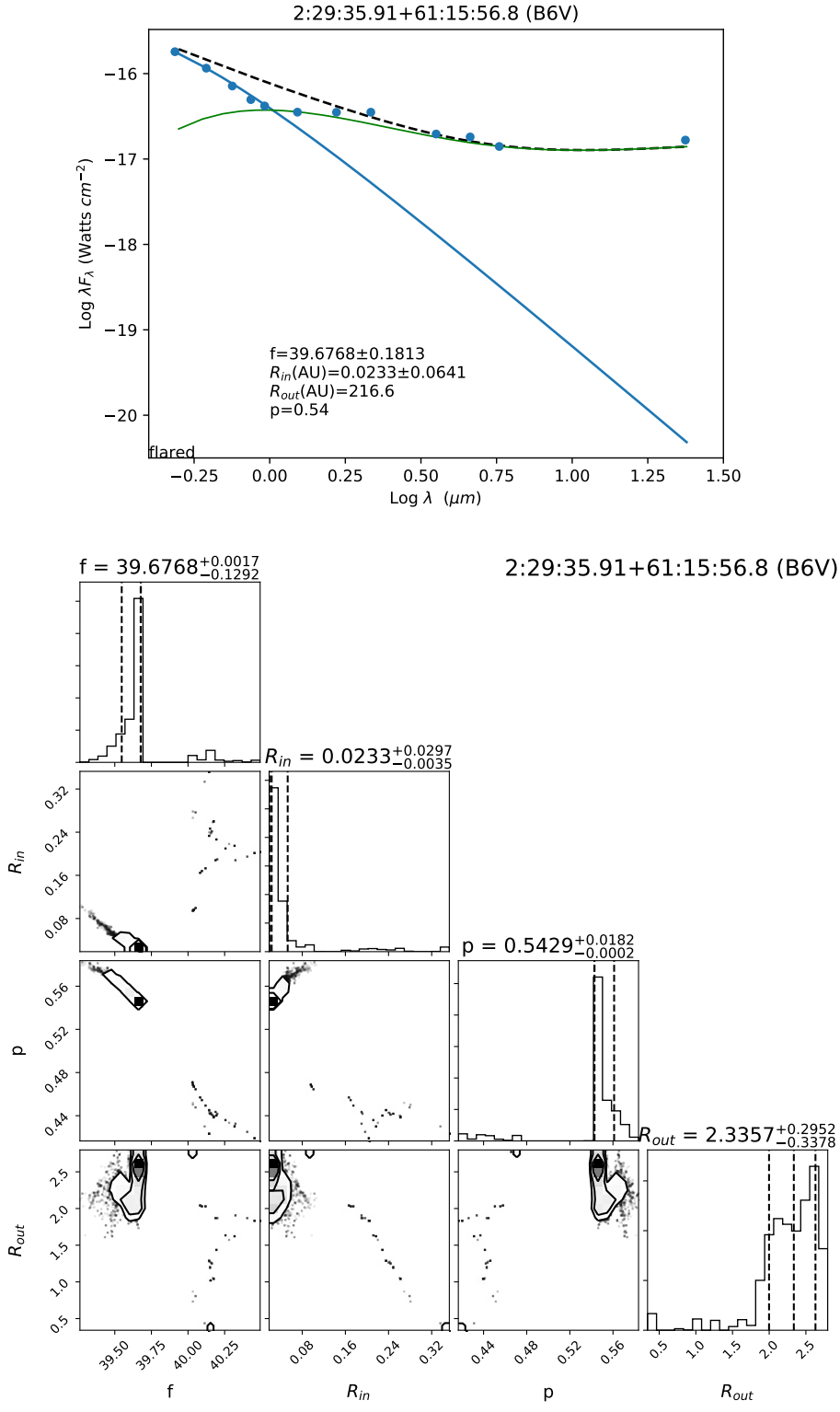

Figure 44. SED and corner plot of source 2:29:35.91+61:15:56.8 which is classified as a thick disk.

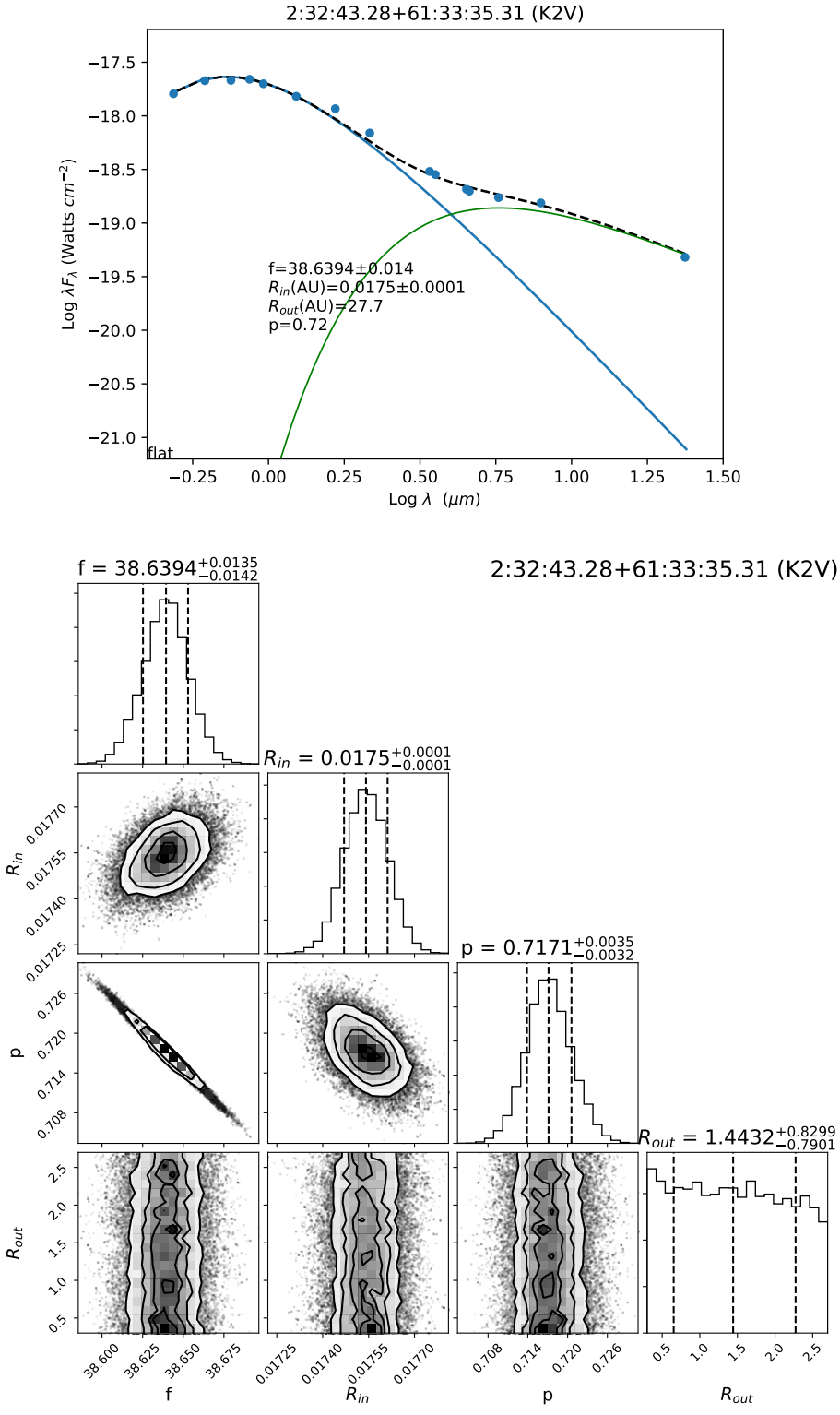

Figure 45. SED and corner plot of source 2:32:43.28+61:33:35.31 which is classified as a thick/trunc? disk.

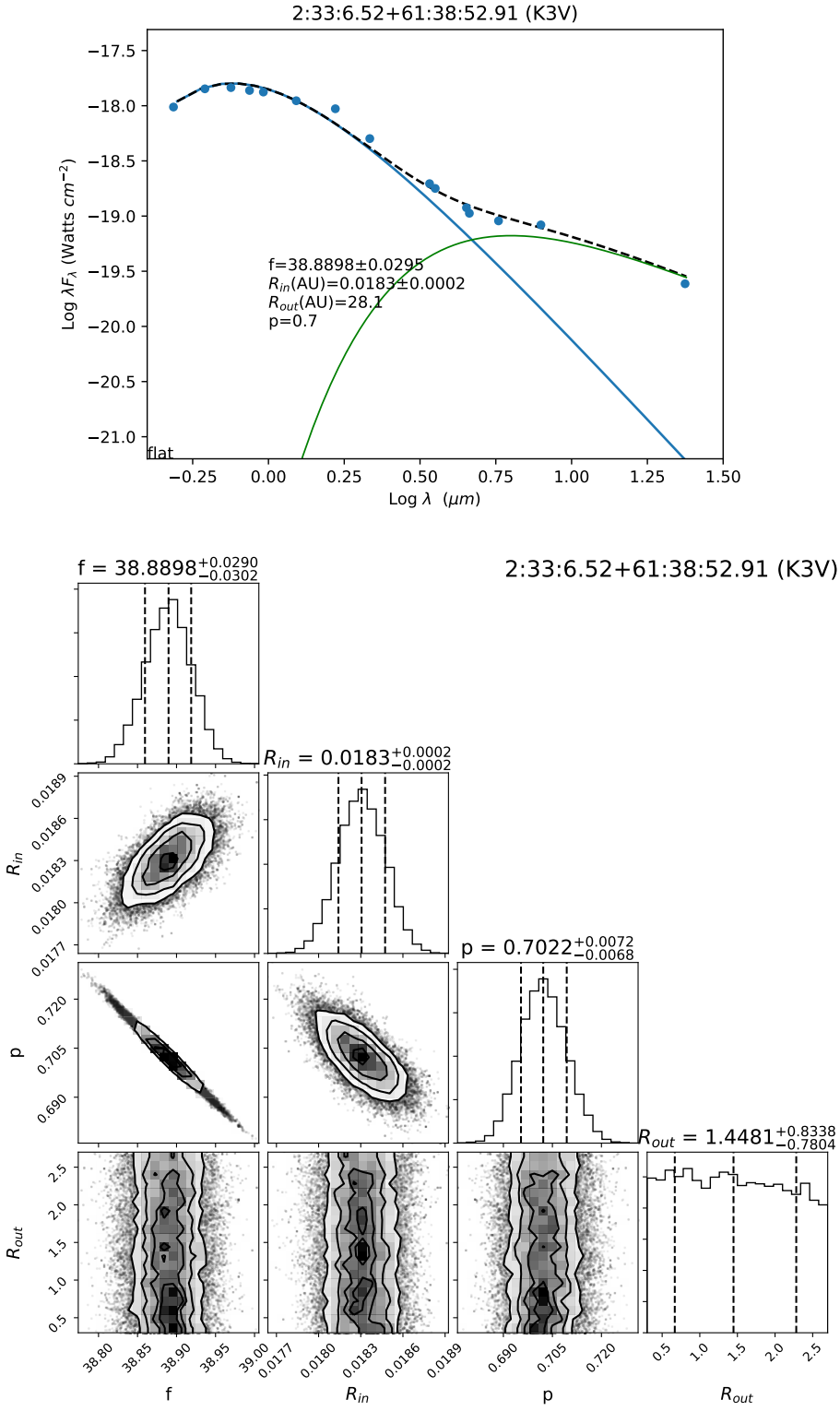

Figure 46. SED and corner plot of source 2:33:6.52+61:38:52.91 which is classified as a thin disk.

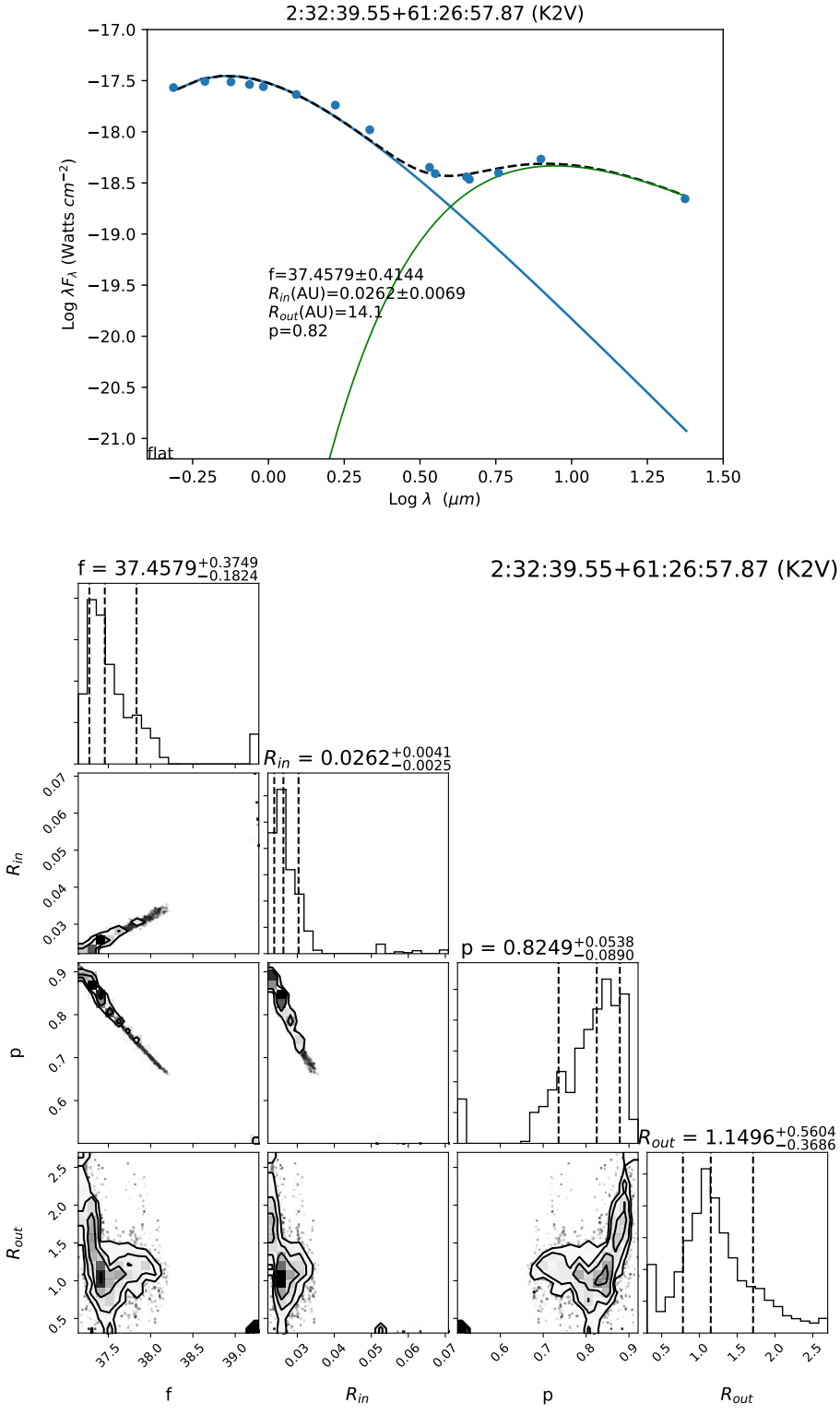

Figure 47. SED and corner plot of source 2:32:39.55+61:26:57.87 which is classified as a pt?-t?/trunc disk.

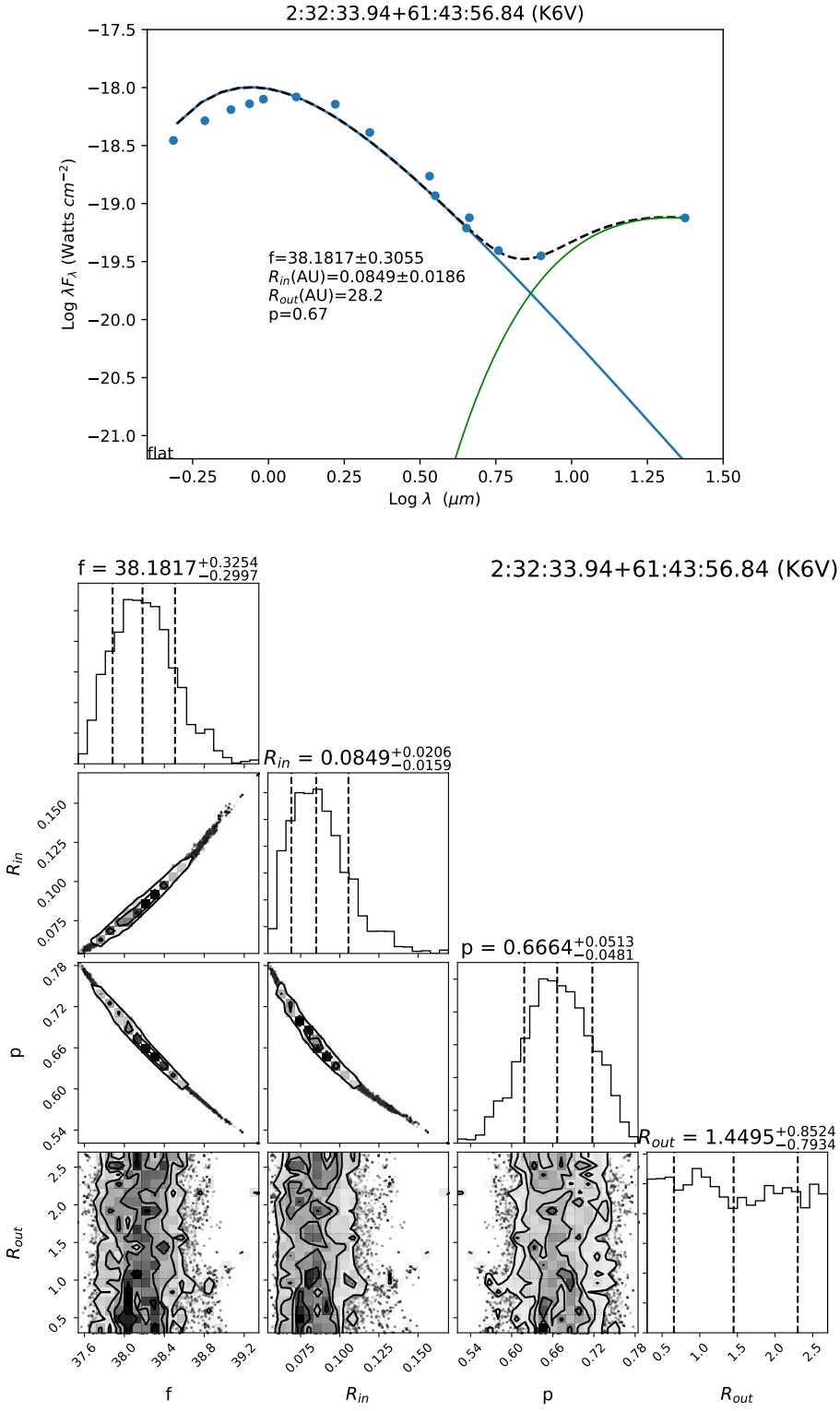

Figure 48. SED and corner plot of source 2:32:33.94+61:43:56.84 which is classified as a t disk.

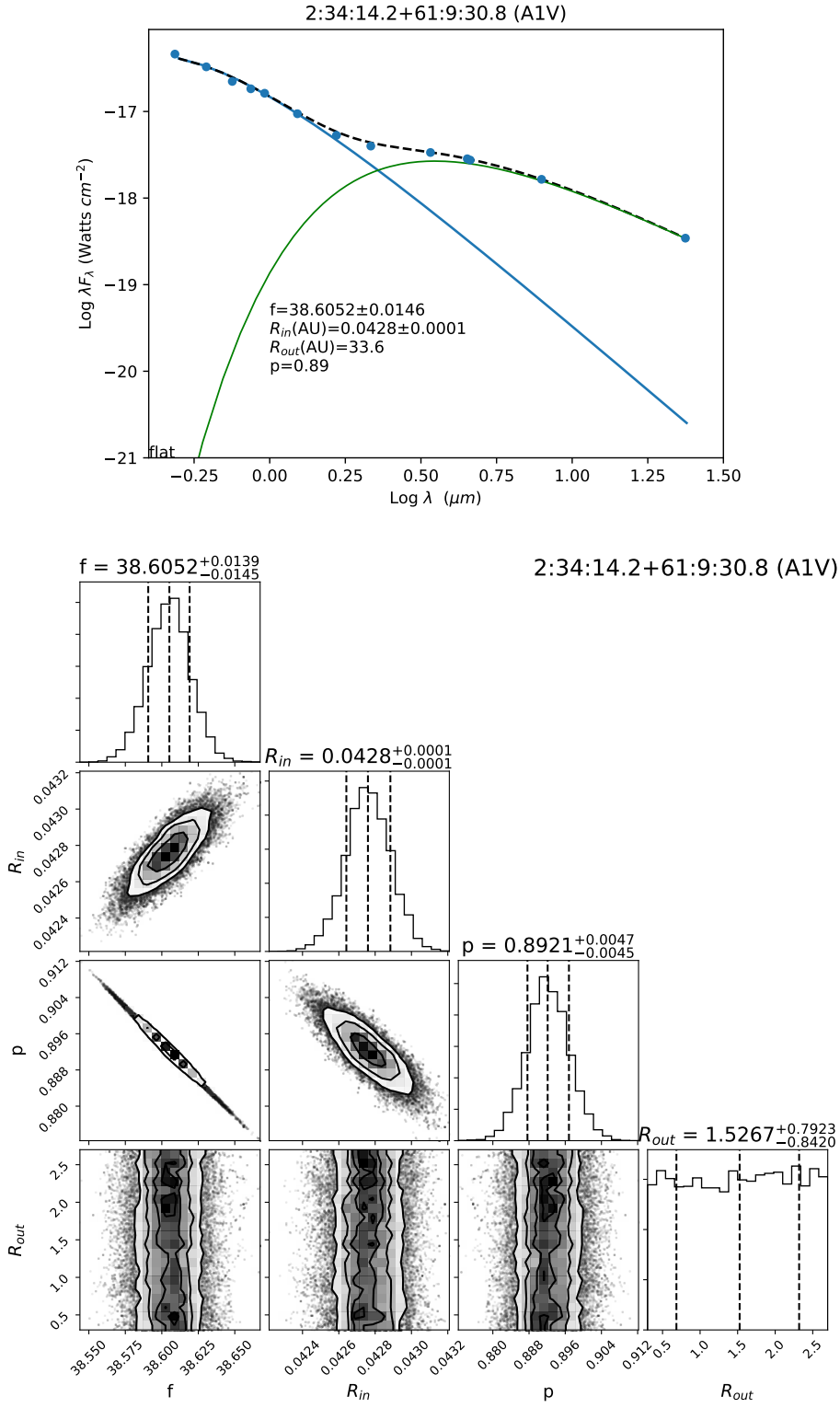

Figure 49. SED and corner plot of source 2:34:14.2+61:9:30.8 which is classified as a thick disk.

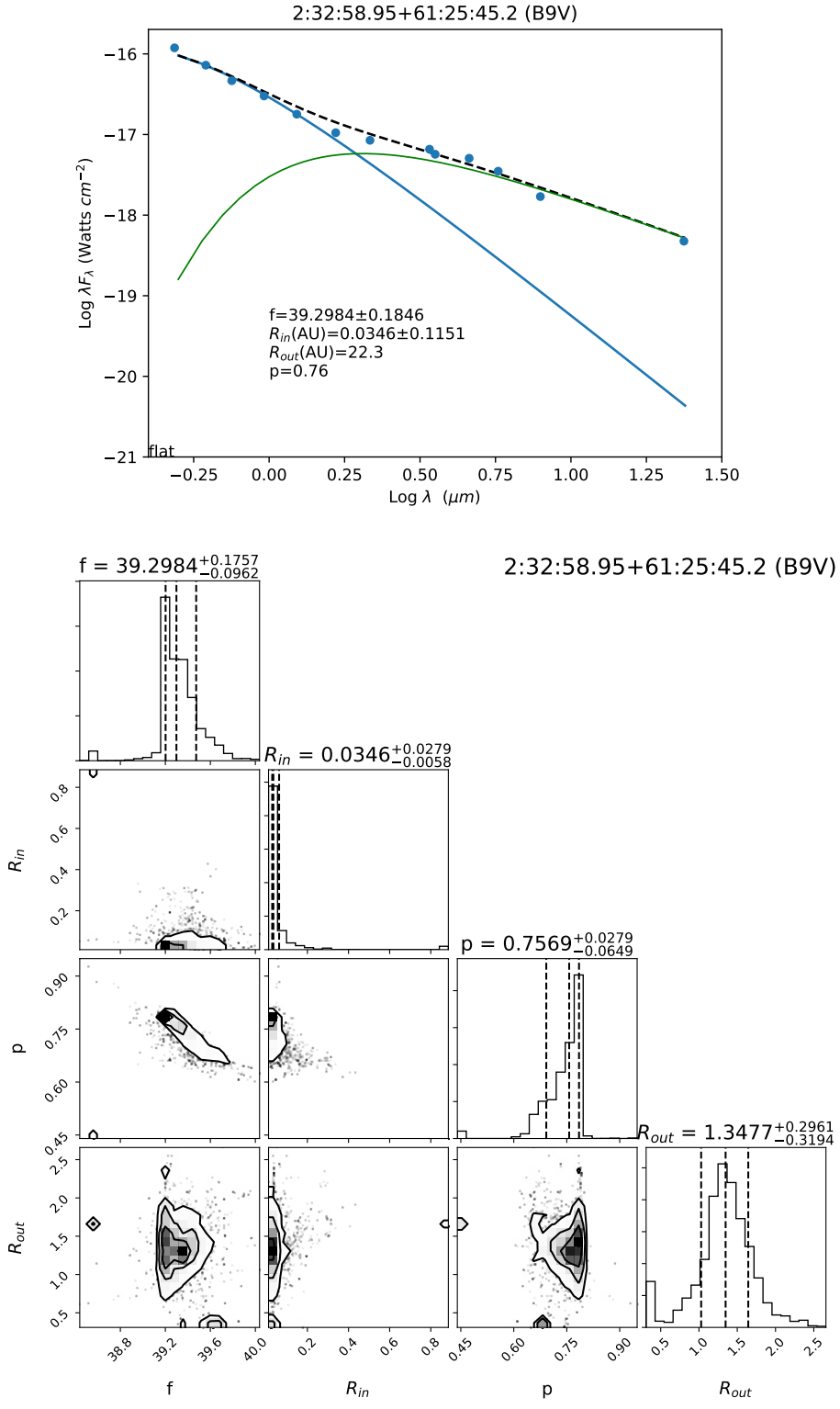

Figure 50. SED and corner plot of source 2:32:58.95+61:25:45.2 which is classified as a thin disk.

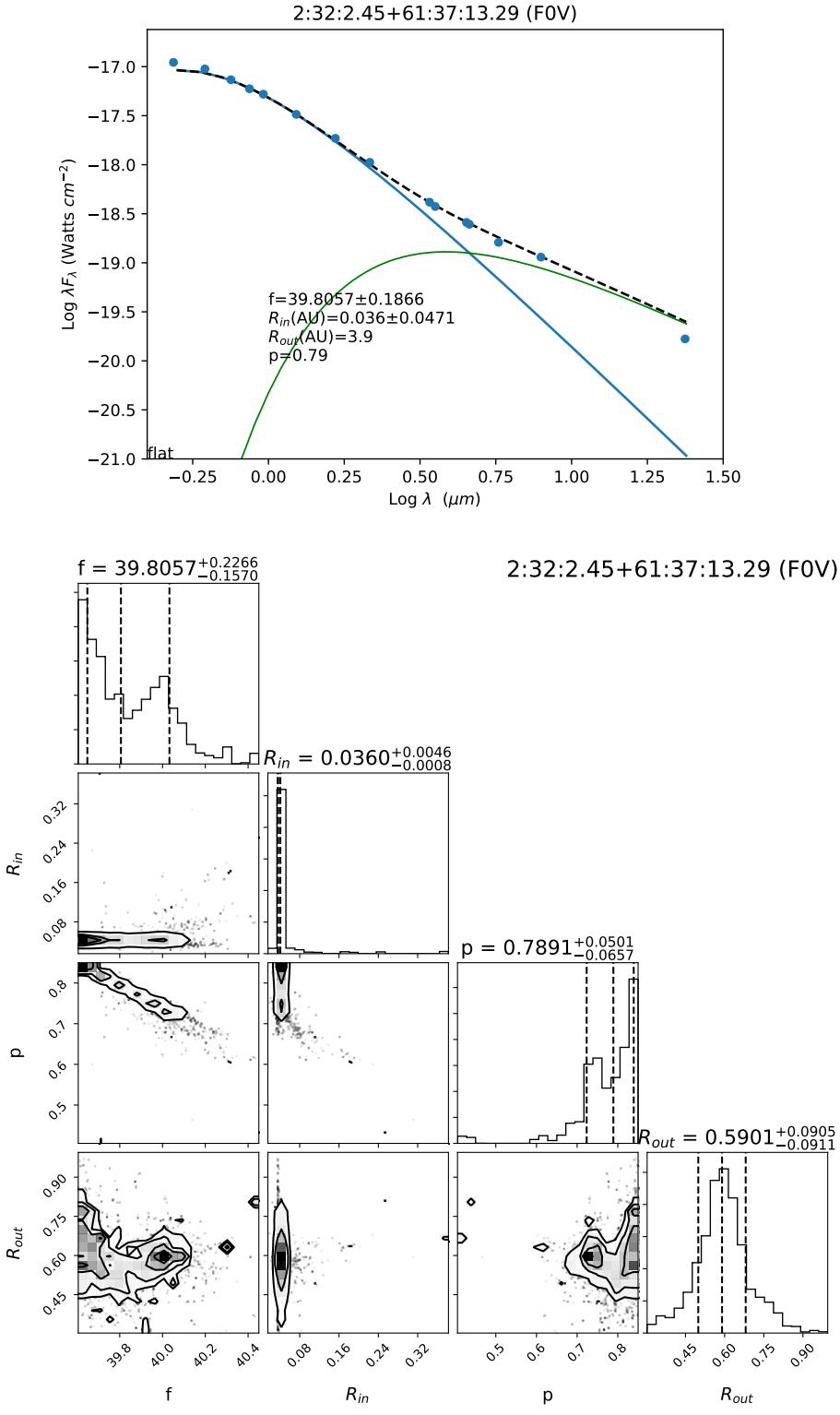

Figure 51. SED and corner plot of source 2:32:2.45+61:37:13.29 which is classified as a thin/trunc disk.

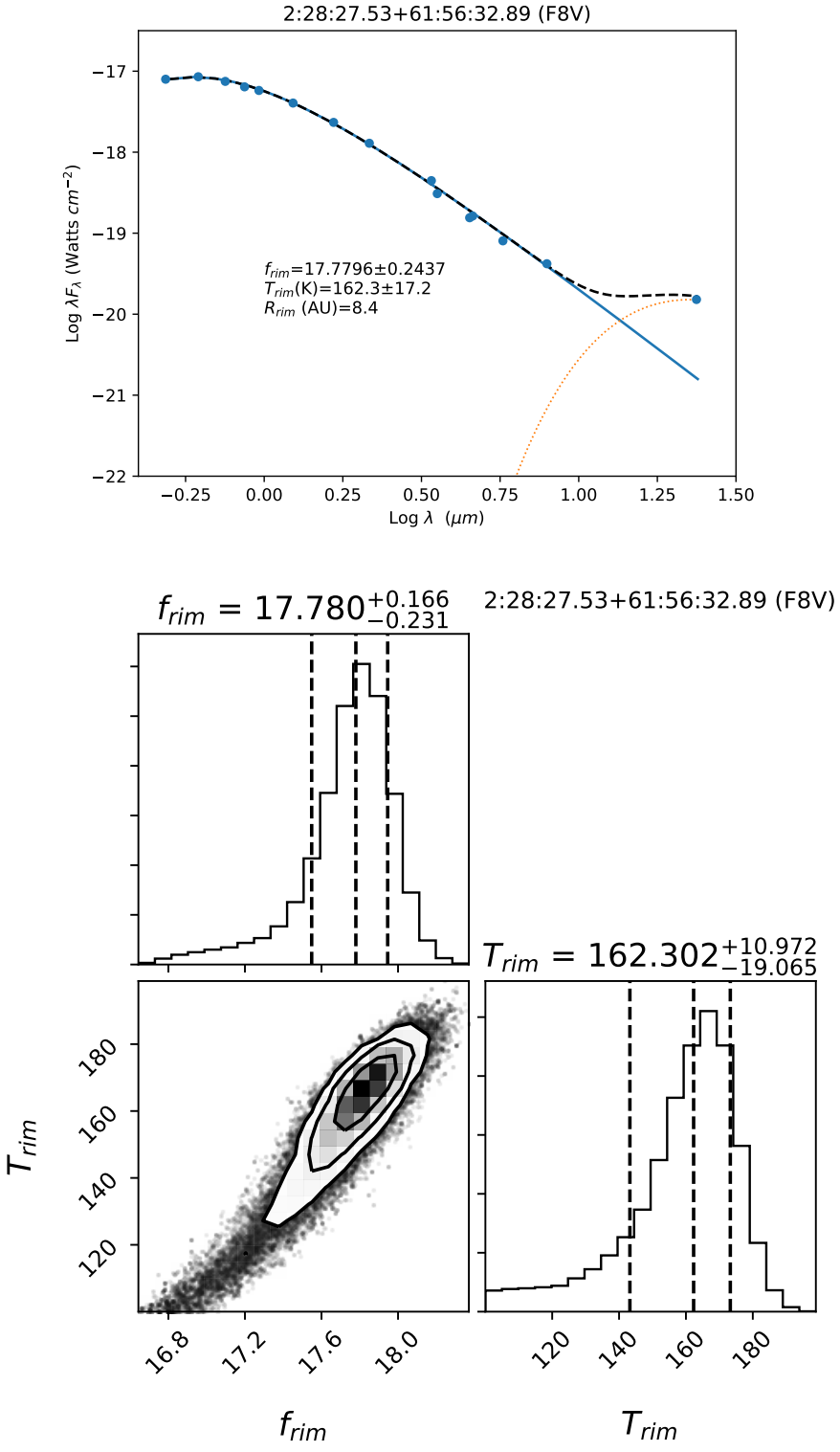

Figure 52. SED and corner plot of source 2:28:27.53+61:56:32.89 which is classified as a t disk.

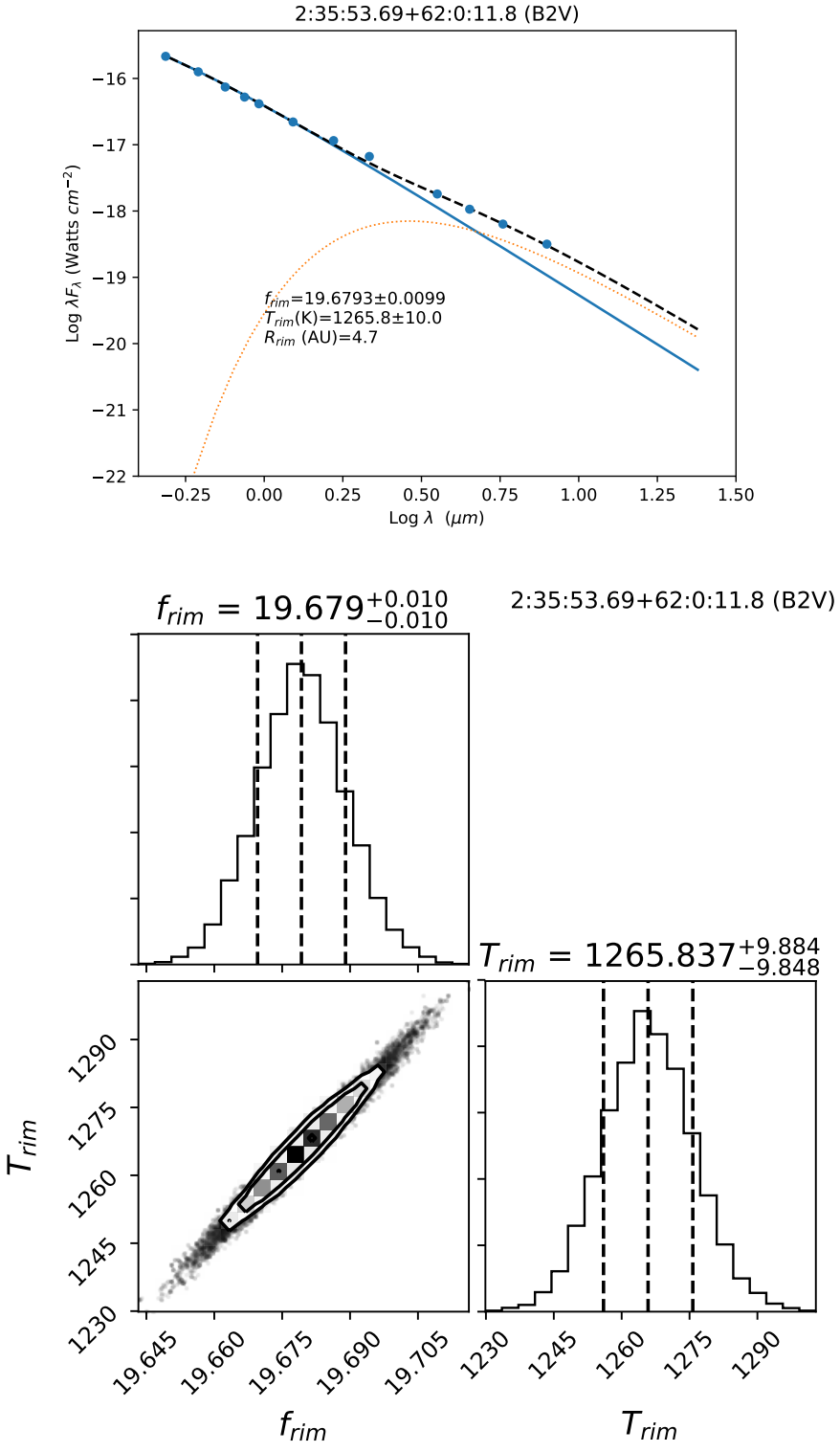

Figure 53. SED and corner plot of source 2:35:53.69+62:0:11.8 which is classified as a thin-t disk.

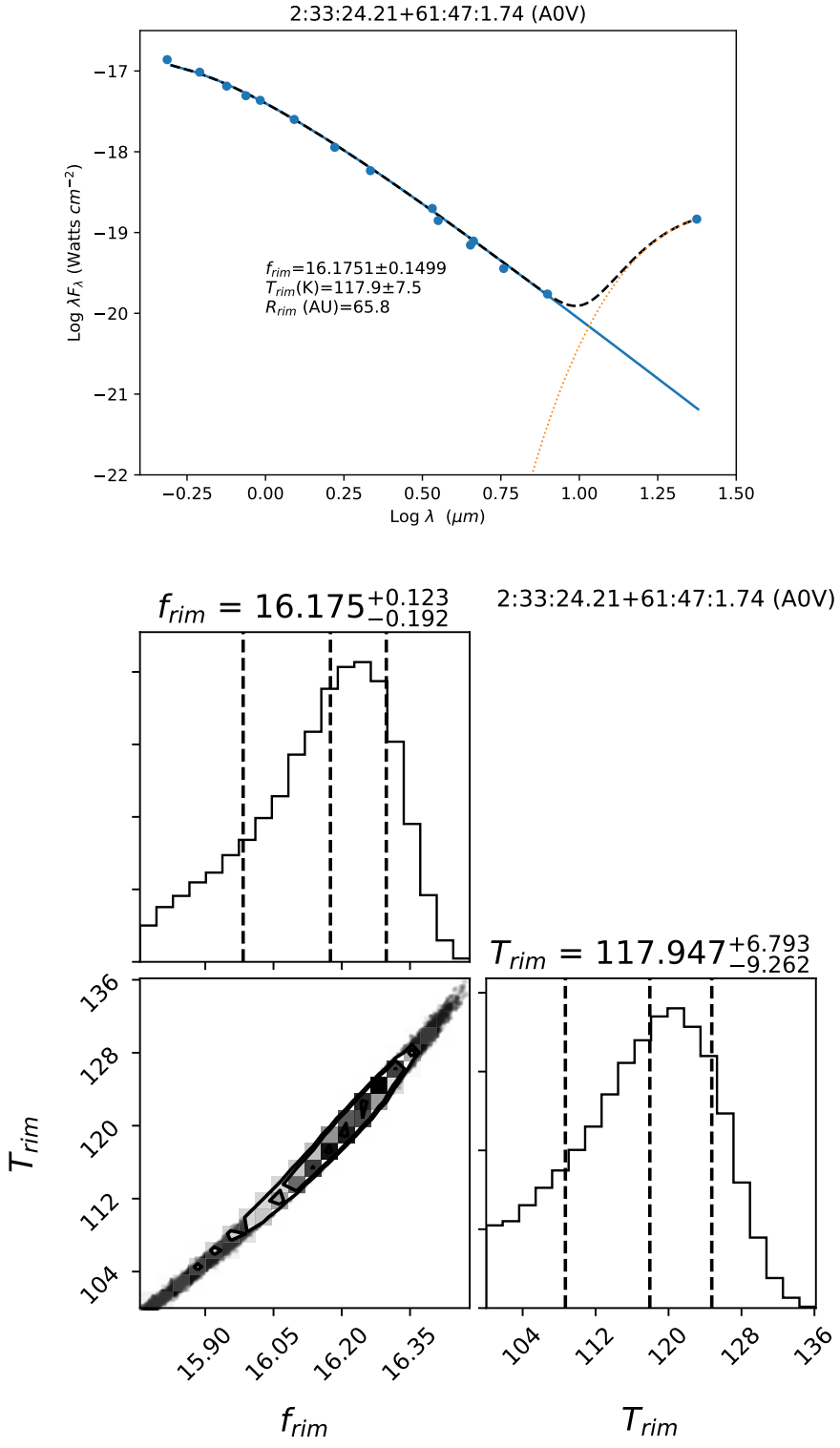

Figure 54. SED and corner plot of source 2:33:24.21+61:47:1.74 which is classified as a t disk.

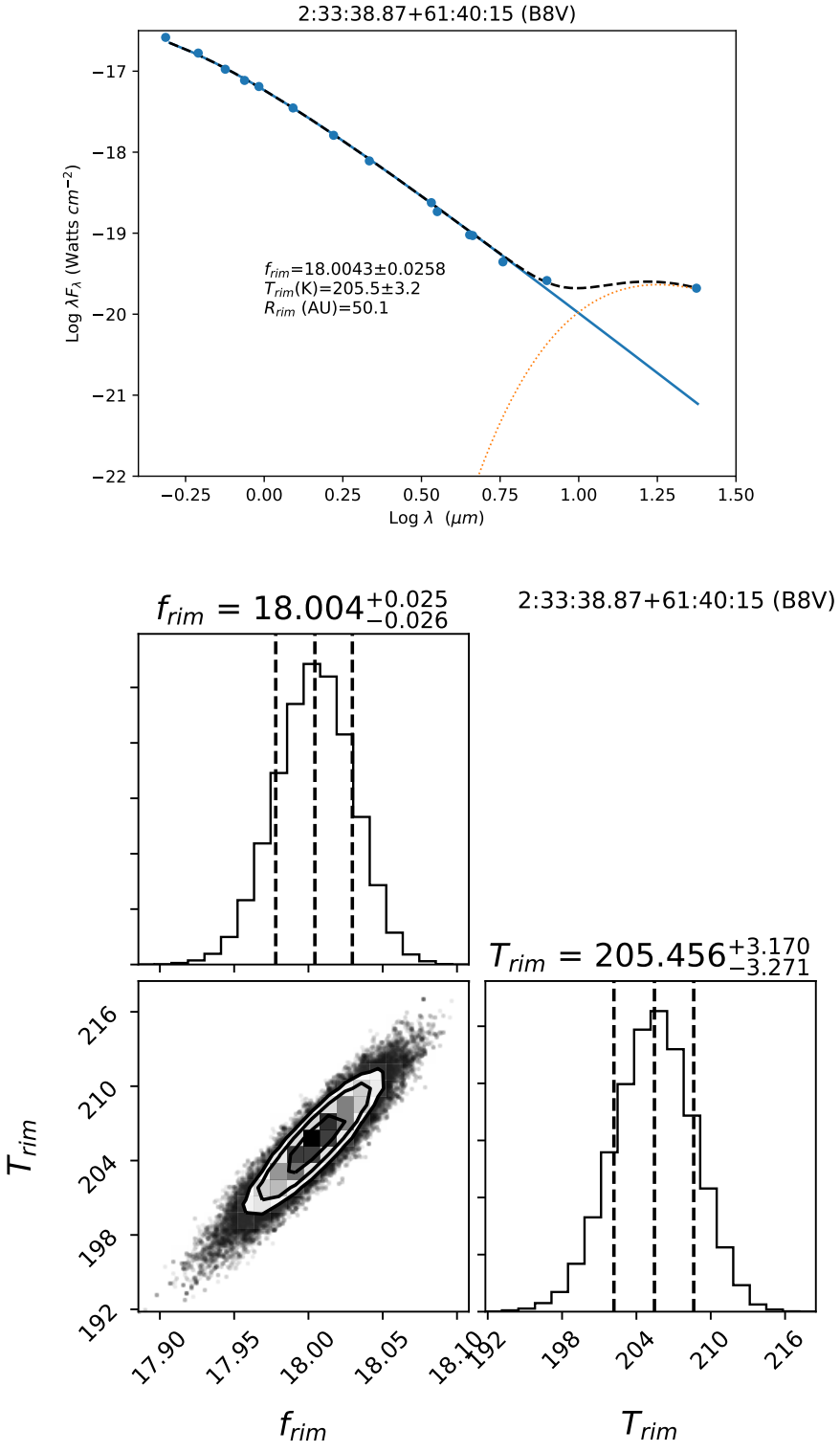

Figure 55. SED and corner plot of source 2:33:38.87+61:40:15 which is classified as a t disk.

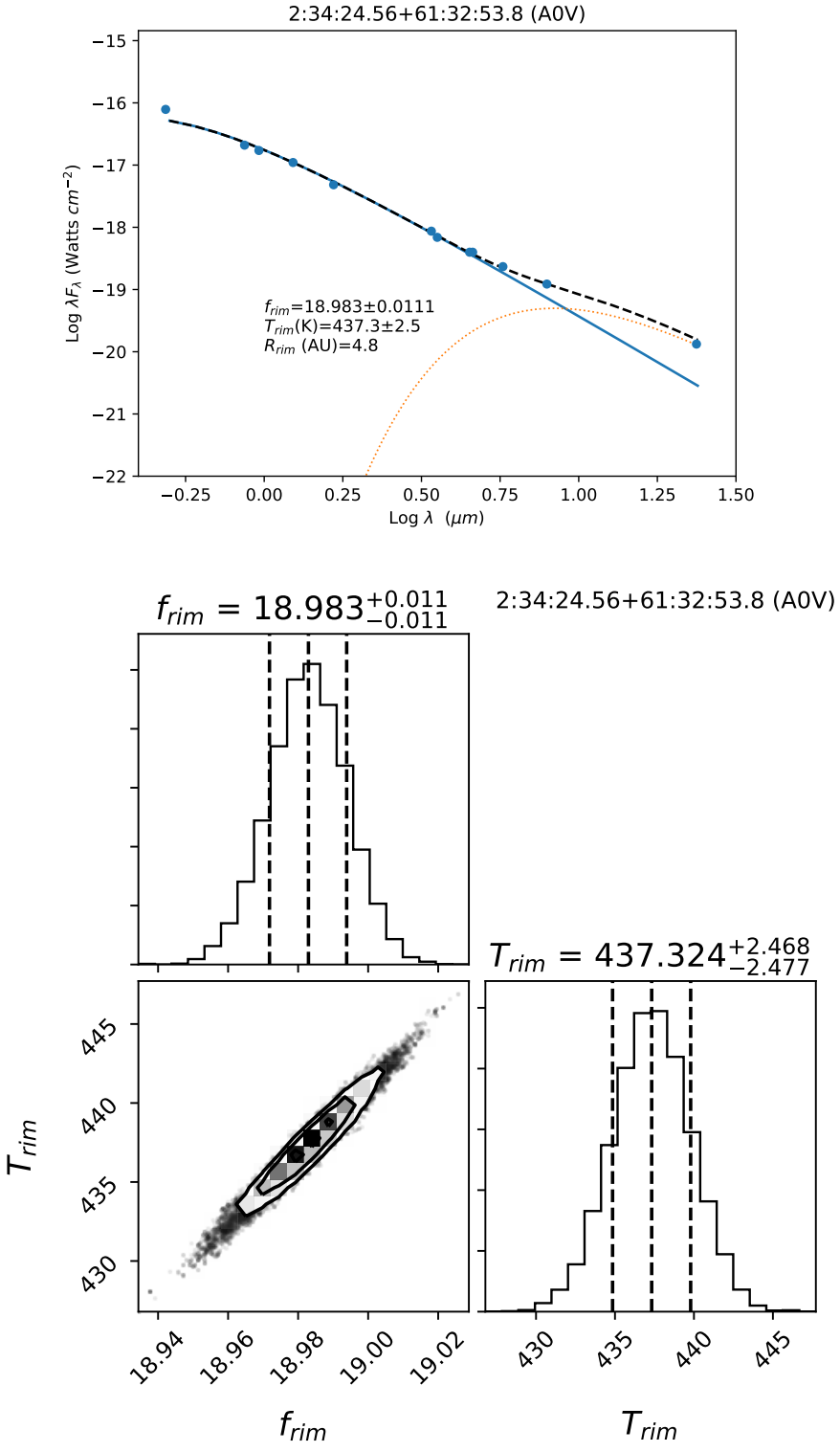

Figure 56. SED and corner plot of source 2:34:24.56+61:32:53.8 which is classified as a t disk.

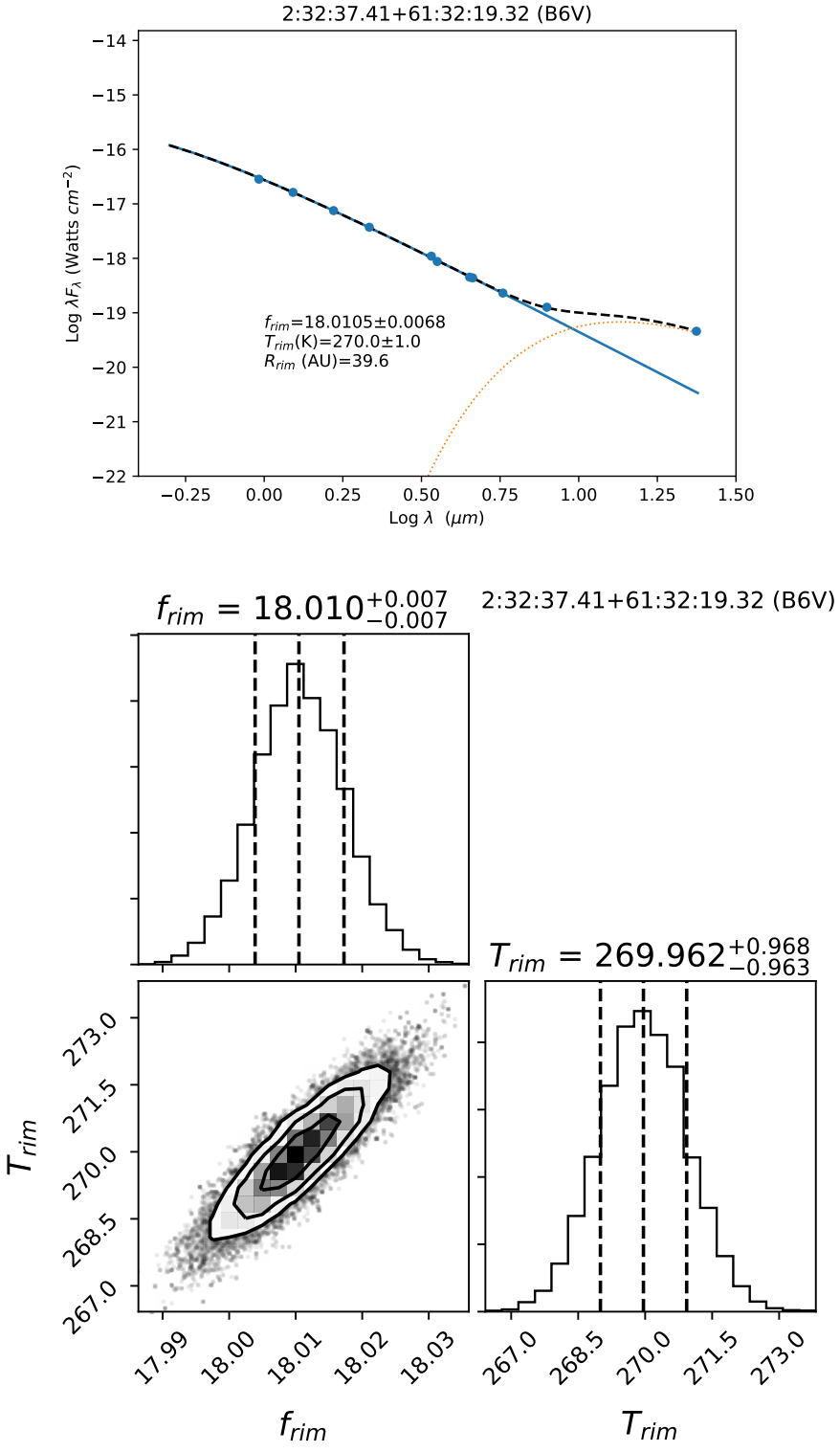

Figure 57. SED and corner plot of source 2:32:37.41+61:32:19.32 which is classified as a t disk.

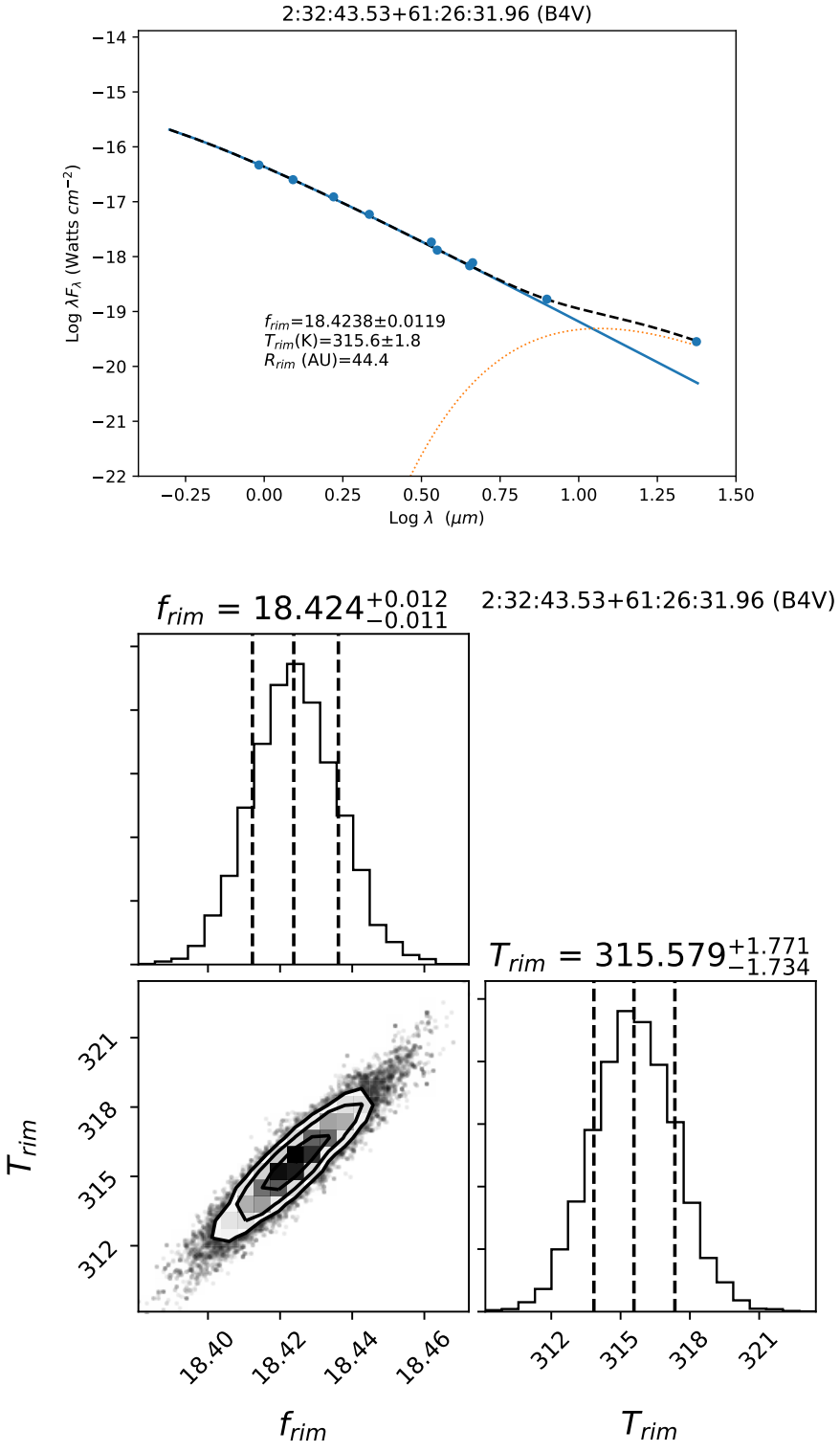

Figure 58. SED and corner plot of source 2:32:43.53+61:26:31.96 which is classified as a t disk.

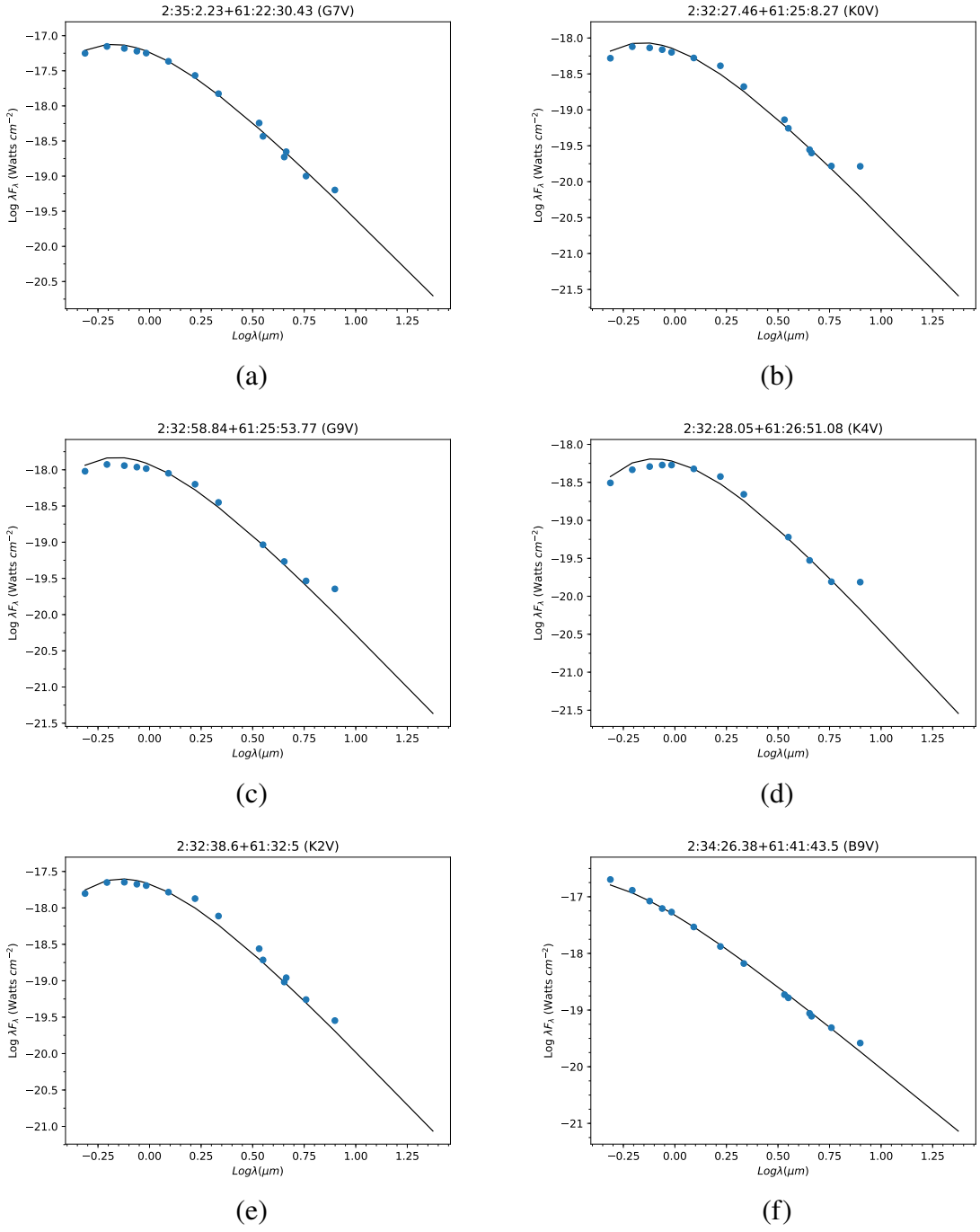

Figure 59. SEDs of sources not fit with a model. Source (a) 2:35:2.23+61:22:30.43, (b) 2:32:27.46+61:25:8.27, (c) 2:32:58.84+61:25:53.77, (d) 2:32:28.05+61:26:51.08, (e) 2:32:38.6+61:32:5, and (f) 2:34:26.38+61:41:43.5 are all classified as 8 μm infrared excesses.

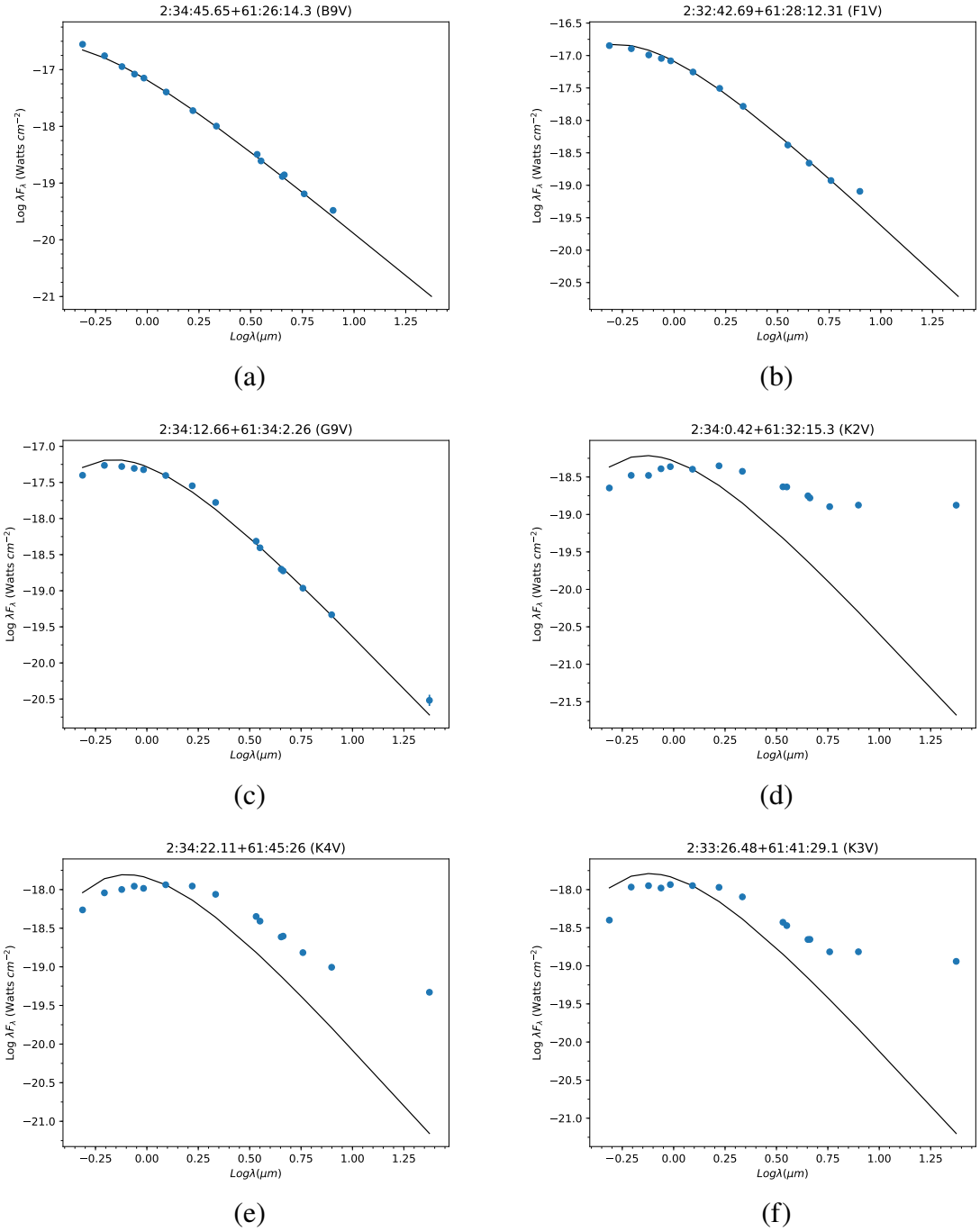

Figure 60. SEDs of sources not fit with a model. Source (a) 2:34:45.65+61:26:14.3 and (b) 2:32:42.69+61:28:12.31 are classified as 8 μm infrared excesses. Other sources are classified as (c) 2:34:12.66+61:34:2.26 a t disk, (d) 2:34:0.42+61:32:15.3 a pt-t disk, (e) 2:34:22.11+61:45:26 a t disk, and (f) 2:33:26.48+61:41:29.1 a t disk.

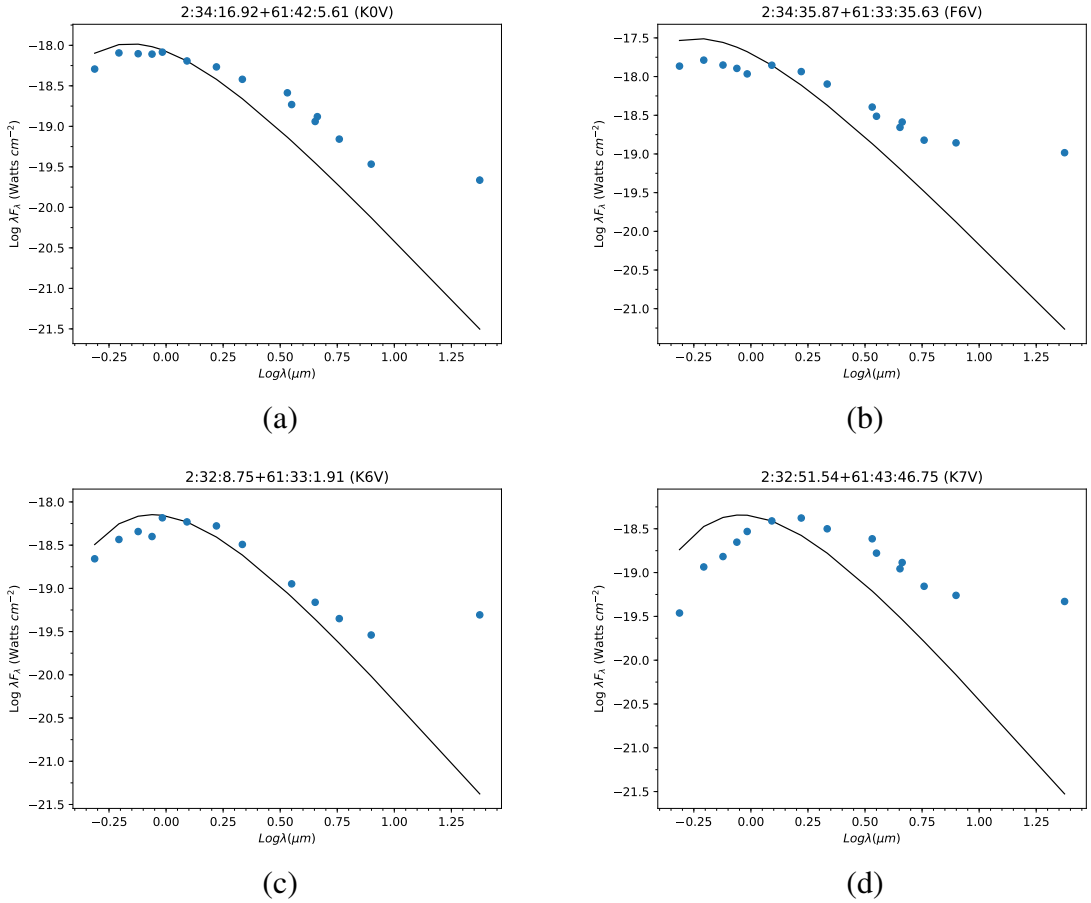

Figure 61. SEDs of sources not fit with a model. These are classified as (a) 2:34:16.92+61:42:5.61 a pt-t disk, (b) 2:34:35.87+61:33:35.63 a pt-t disk, (c) 2:32:8.75+61:33:1.91 a t/enh disk, and (d) 2:32:51.54+61:43:46.75 a pt-t disk.

REFERENCES

Adams, F. C., Lada, C. J., and Shu, F. H., 'Spectral Evolution of Young Stellar Objects,' Astrophysical Journal, 1987, **312**, p. 788.

Adams, F. C. and Shu, F. H., 'Infrared Spectra of Rotating Protostars,' Astrophysical Journal, 1986, **308**, p. 836.

Alexander, R. D., Clarke, C. J., and Pringle, J. E., 'Photoevaporation of protoplanetary discs - II. Evolutionary models and observable properties,' Monthly Notices of the Royal Astronomical Society, 2006, **369**(1), pp. 229–239.

Allen, L. E. and Strom, K. M., 'Moderate-Resolution Spectral Standards From λ5600 to λ9000 Angstrom,' Astronomical Journal, 1995, **109**, p. 1379.

Alonso-Albi, T., Fuente, A., Bachiller, R., Neri, R., Planesas, P., Testi, L., Berné, O., and Joblin, C., 'Circumstellar disks around Herbig Be stars,' Astronomy & Astrophysics, 2009, **497**(1), pp. 117–136.

Anderson, K. R., Adams, F. C., and Calvet, N., 'Viscous Evolution and Photoevaporation of Circumstellar Disks Due to External Far Ultraviolet Radiation Fields,' Astrophysical Journal, 2013, **774**(1), 9.

Andrews, S. M., 'Observations of Protoplanetary Disk Structures,' arXiv e-prints, 2020, arXiv:2001.05007.

Aragona, C., McSwain, M. V., Grundstrom, E. D., Marsh, A. N., Roettenbacher, R. M., Hessler, K. M., Boyajian, T. S., and Ray, P. S., 'The Orbits of the γ-Ray Binaries LS I +61 303 and LS 5039,' Astrophysical Journal, 2009, **698**(1), pp. 514–518.

Bailer-Jones, C. A. L., Rybizki, J., Fouesneau, M., Mantelet, G., and Andrae, R., 'Estimating Distance from Parallaxes. IV. Distances to 1.33 Billion Stars in Gaia Data Release 2,' Astronomical Journal, 2018, **156**(2), 58.

Bally, J., O'Dell, C. R., and McCaughrean, M. J., 'Disks, Microjets, Windblown Bubbles, and Outflows in the Orion Nebula,' Astronomical Journal, 2000, **119**(6), pp. 2919–2959.

Bans, A. and Königl, A., 'A Disk-wind Model for the Near-infrared Excess Emission in Protostars,' Astrophysical Journal, 2012, **758**(2), 100.

Baraffe, I., Chabrier, G., Allard, F., and Hauschildt, P. H., 'Evolutionary models for low-mass stars and brown dwarfs: Uncertainties and limits at very young ages,' Astronomy & Astrophysics, 2002, **382**, pp. 563–572.

Baraffe, I., Homeier, D., Allard, F., and Chabrier, G., 'New evolutionary models for pre-main sequence and main sequence low-mass stars down to the hydrogen-burning limit,' Astronomy & Astrophysics, 2015, **577**, A42.

Barentsen, G., Farnhill, H. J., Drew, J. E., and et al., 'VizieR Online Data Catalog: IPHAS DR2 Source Catalogue (Barentsen+, 2014),' VizieR Online Data Catalog, 2014, II/321.

Basu, S., Johnstone, D., and Martin, P. G., 'Dynamical Evolution and Ionization Structure of an Expanding Superbubble: Application to W4,' Astrophysical Journal, 1999, **516**(2), pp. 843–862.

Bonnarel, F., Fernique, P., Bienaymé, O., Egret, D., Genova, F., Louys, M., Ochsenbein, F., Wenger, M., and Bartlett, J. G., 'The ALADIN interactive sky atlas. A reference tool for identification of astronomical sources,' Astronomy & Astrophysics Supplement, 2000, **143**, pp. 33–40.

Boss, A. P., 'The Effect of the Approach to Gas Disk Gravitational Instability on the Rapid Formation of Gas Giant Planets,' Astrophysical Journal, 2019, **884**(1), 56.

Broos, P. S., Getman, K. V., Povich, M. S., Feigelson, E. D., Townsley, L. K., Naylor, T., Kuhn, M. A., King, R. R., and Busk, H. A., 'Identifying Young Stars in Massive Star-forming Regions for the MYStIX Project,' Astrophysical Journals, 2013, **209**(2), 32.

Carpenter, J. M., Heyer, M. H., and Snell, R. L., 'Embedded Stellar Clusters in the W3/W4/W5 Molecular Cloud Complex,' Astrophysical Journal Supplement Series, 2000, **130**(2), pp. 381–402.

Carroll, B. W. and Ostlie, D. A., *An introduction to modern astrophysics and cosmology*, Pearson, 2006.

Chiang, E. I. and Goldreich, P., 'Spectral Energy Distributions of T Tauri Stars with Passive Circumstellar Disks,' Astrophysical Journal, 1997, **490**(1), pp. 368–376.

Chiang, E. I. and Goldreich, P., 'Spectral Energy Distributions of Passive T Tauri Disks: Inclination,' Astrophysical Journal, 1999, **519**(1), pp. 279–284.

Choi, J., Dotter, A., Conroy, C., Cantiello, M., Paxton, B., and Johnson, B. D., 'Mesa Isochrones and Stellar Tracks (MIST). I. Solar-scaled Models,' Astrophysical Journal, 2016, **823**(2), 102.

Clarke, C. J., Gendrin, A., and Sotomayor, M., 'The dispersal of circumstellar discs: the role of the ultraviolet switch,' Monthly Notices of the Royal Astronomical Society, 2001, **328**(2), pp. 485–491.

Currie, T. and Kenyon, S. J., 'Deep MIPS Observations of the IC 348 Nebula: Constraints on the Evolutionary State of Anemic Circumstellar Disks and the Primordial-to-Debris Disk Transition,' Astronomical Journal, 2009, **138**(3), pp. 703–726.

Currie, T., Lada, C. J., Plavchan, P., Robitaille, T. P., Irwin, J., and Kenyon, S. J., 'The Last Gasp of Gas Giant Planet Formation: A Spitzer Study of the 5 Myr Old Cluster NGC 2362,' Astrophysical Journal, 2009, **698**(1), pp. 1–27.

Cutri, R. M. and et al., 'VizieR Online Data Catalog: AllWISE Data Release (Cutri+ 2013),' VizieR Online Data Catalog, 2013, II/328.

Cutri, R. M., Skrutskie, M. F., van Dyk, S., and et al., 'VizieR Online Data Catalog: 2MASS All-Sky Catalog of Point Sources (Cutri+ 2003),' VizieR Online Data Catalog, 2003, II/246.

D'Alessio, P., Calvet, N., and Hartmann, L., 'Accretion Disks around Young Objects. III. Grain Growth,' Astrophysical Journal, 2001, **553**(1), pp. 321–334.

Danks, A. C. and Dennefeld, M., 'An Atlas of Southern MK Standards from 5800 to 10,200A,' Publications of the Astronomical Society of the Pacific, 1994, **106**, p. 382.

Dennihy, E., Farihi, J., Fusillo, N. P. G., and Debes, J. H., 'A Word to the WISE: Confusion is Unavoidable for WISE-selected Infrared Excesses,' Astrophysical Journal, 2020, **891**(1), 97.

Dennison, B., Topasna, G. A., and Simonetti, J. H., 'Detection in Hα of a Supershell Associated with W4,' Astrophysical Journall, 1997, **474**(1), pp. L31–L34.

Dotter, A., 'MESA Isochrones and Stellar Tracks (MIST) 0: Methods for the Construction of Stellar Isochrones,' Astrophysical Journal Supplement Series, 2016, **222**(1), 8.

Dreyer, J. L. E., 'Index Catalogue of Nebulæ found in the years 1888 to 1894, with Notes and Corrections to the New General Catalogue,' Memoirs of the Royal Astronomical Society, 1895, **51**, p. 185.

Dullemond, C. P. and Dominik, C., 'Dust coagulation in protoplanetary disks: A rapid depletion of small grains,' Astronomy & Astrophysics, 2005, **434**(3), pp. 971–986.

Dullemond, C. P., Dominik, C., and Natta, A., 'Passive Irradiated Circumstellar Disks with an Inner Hole,' Astrophysical Journal, 2001, **560**(2), pp. 957–969.

Dullemond, C. P. and Monnier, J. D., 'The Inner Regions of Protoplanetary Disks,' Annual Review of Astronomy and Astrophysics, 2010, **48**, pp. 205–239.

Ekström, S., Georgy, C., Eggenberger, P., Meynet, G., Mowlavi, N., Wyttenbach, A., Granada, A., Decressin, T., Hirschi, R., Frischknecht, U., Charbonnel, C., and Maeder, A., 'Grids of stellar models with rotation. I. Models from 0.8 to 120 $M_\odot$ at solar metallicity (Z = 0.014),' Astronomy & Astrophysics, 2012, **537**, A146.

Elmegreen, B. G., 'Observations and Theory of Dynamical Triggers for Star Formation,' in C. E. Woodward, J. M. Shull, and J. Thronson, Harley A., editors, 'Origins,' volume 148 of *Astronomical Society of the Pacific Conference Series*, 1998 p. 150.

Espaillat, C., Ingleby, L., Hernández, J., Furlan, E., D'Alessio, P., Calvet, N., Andrews, S., Muzerolle, J., Qi, C., and Wilner, D., 'On the Transitional Disk Class: Linking Observations of T Tauri Stars and Physical Disk Models,' Astrophysical Journal, 2012, **747**(2), 103.

Espaillat, C., Muzerolle, J., Najita, J., Andrews, S., Zhu, Z., Calvet, N., Kraus, S., Hashimoto, J., Kraus, A., and D'Alessio, P., 'An Observational Perspective of Transitional Disks,' in H. Beuther, R. S. Klessen, C. P. Dullemond, and T. Henning, editors, 'Protostars and Planets VI,' 2014 p. 497.

Fabricant, D., Fata, R., Roll, J., and et al., 'Hectospec, the MMT's 300 Optical Fiber-Fed Spectrograph,' Publications of the Astronomical Society of the Pacific, 2005, **117**(838), pp. 1411–1434.

Federrath, C., 'Inefficient star formation through turbulence, magnetic fields and feedback,' Monthly Notices of the Royal Astronomical Society, 2015, **450**(4), pp. 4035–4042.

Feiden, G. A., 'Magnetic inhibition of convection and the fundamental properties of low-mass stars. III. A consistent 10 Myr age for the Upper Scorpius OB association,' Astronomy & Astrophysics, 2016, **593**, A99.

Ferriere, K. M., Mac Low, M.-M., and Zweibel, E. G., 'Expansion of a Superbubble in a Uniform Magnetic Field,' Astrophysical Journal, 1991, **375**, p. 239.

Flewelling, H. A., Magnier, E. A., Chambers, K. C., and et al., 'The Pan-STARRS1 Database and Data Products,' arXiv e-prints, 2016, arXiv:1612.05243.

Foreman-Mackey, D., Hogg, D. W., Lang, D., and Goodman, J., 'emcee: The MCMC Hammer,' Publications of the Astronomical Society of the Pacific, 2013, **125**(925), p. 306.

Friedjung, M., 'Accretion disks heated by luminous central stars.' Astronomy & Astrophysics, 1985, **146**, pp. 366–368.

Fukuda, N., Miao, J., Sugitani, K., Kawahara, K., Watanabe, M., Nakano, M., and Pickles, A. J., 'Triggered Star Formation in a Bright-rimmed Cloud (BRC 5) of IC 1805,' Astrophysical Journal, 2013, **773**(2), 132.

Gaia Collaboration, Brown, A. G. A., Vallenari, A., Prusti, T., and et al., 'Gaia Data Release 2. Summary of the contents and survey properties,' Astronomy & Astrophysics, 2018, **616**, A1.

Gaia Collaboration, Prusti, T., de Bruijne, J. H. J., Brown, A. G. A., and et al., 'The Gaia mission,' Astronomy & Astrophysics, 2016, **595**, A1.

Goodman, J. and Weare, J., 'Ensemble samplers with affine invariance,' Communications in Applied Mathematics and Computational Science, 2010, **5**(1), pp. 65–80.

Gras-Velázquez, À. and Ray, T., 'Weak-line T Tauri stars: circumstellar disks and companions. I. Spectral energy distributions and infrared excesses,' Astronomy & Astrophysics, 2005, **443**(2), pp. 541–556.

Gray, R. O. and Corbally, J., Christopher, *Stellar Spectral Classification*, Princeton University Press, 2009.

Green, G. M., Schlafly, E., Zucker, C., Speagle, J. S., and Finkbeiner, D., 'A 3D Dust Map Based on Gaia, Pan-STARRS 1, and 2MASS,' Astrophysical Journal, 2019, **887**(1), 93.

Guetter, H. H. and Vrba, F. J., 'Reddening and Polarimetric Studies toward IC 1805,' Astronomical Journal, 1989, **98**, p. 611.

Hachisuka, K., Brunthaler, A., Menten, K. M., Reid, M. J., Imai, H., Hagiwara, Y., Miyoshi, M., Horiuchi, S., and Sasao, T., 'Water Maser Motions in W3(OH) and a Determination of Its Distance,' Astrophysical Journal, 2006, **645**(1), pp. 337–344.

Haisch, J., Karl E., Lada, E. A., and Lada, C. J., 'Disk Frequencies and Lifetimes in Young Clusters,' Astrophysical Journal, 2001, **553**(2), pp. L153–L156.

Hartmann, L., Calvet, N., Gullbring, E., and D'Alessio, P., 'Accretion and the Evolution of T Tauri Disks,' Astrophysical Journal, 1998, **495**(1), pp. 385–400.

Hernández, J., Calvet, N., Briceño, C., Hartmann, L., and Berlind, P., 'Spectral Analysis and Classification of Herbig Ae/Be Stars,' Astronomical Journal, 2004, **127**(3), pp. 1682–1701.

Hernández, J., Morales-Calderon, M., Calvet, N., Hartmann, L., Muzerolle, J., Gutermuth, R., Luhman, K. L., and Stauffer, J., 'Spitzer Observations of the λ Orionis Cluster. II. Disks Around Solar-type and Low-mass Stars,' Astrophysical Journal, 2010, **722**(2), pp. 1226–1239.

Hillwig, T. C., Gies, D. R., Bagnuolo, J., William G., Huang, W., McSwain, M. V., and Wingert, D. W., 'Binary and Multiple O-Type Stars in the Cassiopeia OB6 Association,' Astrophysical Journal, 2006, **639**(2), pp. 1069–1080.

Hodapp, K.-W., 'A K Imaging Survey of Molecular Outflow Sources,' Astrophysical Journal Supplement Series, 1994, **94**, p. 615.

Hosokawa, T., Offner, S. S. R., and Krumholz, M. R., 'On the Reliability of Stellar Ages and Age Spreads Inferred from Pre-main-sequence Evolutionary Models,' Astrophysical Journal, 2011, **738**(2), 140.

Hueso, R. and Guillot, T., 'Evolution of protoplanetary disks: constraints from DM Tauri and GM Aurigae,' Astronomy & Astrophysics, 2005, **442**(2), pp. 703–725.

Hughes, A. M., Duchêne, G., and Matthews, B. C., 'Debris Disks: Structure, Composition, and Variability,' Annual Reviews of Astronomy and Astrophysics, 2018, **56**, pp. 541–591.

Hunter, J. D., 'Matplotlib: A 2d graphics environment,' Computing in Science & Engineering, 2007, **9**(3), pp. 90–95.

Ishida, K., 'U, B, V observations of IC 1805,' Monthly Notices of the Royal Astronomical Society, 1969, **144**, p. 55.

Jacoby, G. H., Hunter, D. A., and Christian, C. A., 'A library of stellar spectra.' Astrophysical Journal Supplement Series, 1984, **56**, pp. 257–281.

Jordi, K., Grebel, E. K., and Ammon, K., 'Empirical color transformations between SDSS photometry and other photometric systems,' Astronomy & Astrophysics, 2006, **460**(1), pp. 339–347.

Jose, J., Kim, J. S., Herczeg, G. J., Samal, M. R., Bieging, J. H., Meyer, M. R., and Sherry, W. H., 'Star Formation in W3—AFGL 333: Young Stellar Content, Properties, and Roles of External Feedback,' Astrophysical Journal, 2016, **822**(1), 49.

Kenyon, S. J. and Bromley, B. C., 'Variations on Debris Disks: Icy Planet Formation at 30-150 AU for 1-3 $M_{\odot}$ Main-Sequence Stars,' Astrophysical Journal Supplement Series, 2008, **179**(2), pp. 451–483.

Kenyon, S. J. and Hartmann, L., 'Spectral Energy Distributions of T Tauri Stars: Disk Flaring and Limits on Accretion,' Astrophysical Journal, 1987, **323**, p. 714.

Keppler, M., Benisty, M., Müller, A., and et al., 'Discovery of a planetary-mass companion within the gap of the transition disk around PDS 70,' Astronomy & Astrophysics, 2018, **617**, A44.

Kiminki, M. M., Kim, J. S., Bagley, M. B., Sherry, W. H., and Rieke, G. H., 'The O- and B-Type Stellar Population in W3: Beyond the High-Density Layer,' Astrophysical Journal, 2015, **813**(1), 42.

Kwon, S. M. and Lee, S.-W., 'Photoelectric Observations of Extremely Young Open Clusters,' Journal of Korean Astronomical Society, 1983, **16**(1), pp. 7–17.

Lada, C. J., 'Star formation: from OB associations to protostars.' in M. Peimbert and J. Jugaku, editors, 'Star Forming Regions,' volume 115 of *IAU Symposium*, 1987 p. 1.

Lada, C. J., Muench, A. A., Luhman, K. L., Allen, L., Hartmann, L., Megeath, T., Myers, P., Fazio, G., Wood, K., Muzerolle, J., Rieke, G., Siegler, N., and Young, E., 'Spitzer Observations of IC 348: The Disk Population at 2-3 Million Years,' Astronomical Journal, 2006, **131**(3), pp. 1574–1607.

Lada, C. J. and Wilking, B. A., 'The nature of the embedded population in the rho Ophiuchi dark cloud : mid-infrared observations.' Astrophysical Journal, 1984, **287**, pp. 610–621.

Le Borgne, J. F., Bruzual, G., Pelló, R., Lançon, A., Rocca-Volmerange, B., Sanahuja, B., Schaerer, D., Soubiran, C., and Vílchez-Gómez, R., 'STELIB: A library of stellar spectra at R ∼2000,' Astronomy & Astrophysics, 2003, **402**, pp. 433–442.

Lefloch, B. and Lazareff, B., 'Cometary globules. II. Observational tests of radiation-driven implosion: the case of CG7S.' Astronomy & Astrophysics, 1995, **301**, p. 522.

Lim, B., Hong, J., Yun, H.-S., Hwang, N., Kim, J. S., Lee, J.-E., Park, B.-G., and Park, S., 'The Origin of a Distributed Stellar Population in the Star-forming Region W4,' Astrophysical Journal, 2020, **899**(2), 121.

Lissauer, J. J., 'Planet formation.' Annual Review of Astronomy and Astrophysics, 1993, **31**, pp. 129–174.

Lynden-Bell, D. and Pringle, J. E., 'The evolution of viscous discs and the origin of the nebular variables.' Monthly Notices of the Royal Astronomical Society, 1974, **168**, pp. 603–637.

Mac Low, M.-M. and McCray, R., 'Superbubbles in Disk Galaxies,' Astrophysical Journal, 1988, **324**, p. 776.

Mamajek, E. E., 'Initial Conditions of Planet Formation: Lifetimes of Primordial Disks,' in T. Usuda, M. Tamura, and M. Ishii, editors, 'Exoplanets and Disks: Their Formation and Diversity,' volume 1158 of *American Institute of Physics Conference Series*, 2009 pp. 3–10.

Massey, P., Johnson, K. E., and Degioia-Eastwood, K., 'The Initial Mass Function and Massive Star Evolution in the OB Associations of the Northern Milky Way,' Astrophysical Journal, 1995, **454**, p. 151.

McKee, C. F. and Ostriker, E. C., 'Theory of Star Formation,' Annual Reviews of Astronomy and Astrophysics, 2007, **45**(1), pp. 565–687.

McKinney, W., 'Data structures for statistical computing in python,' in S. van der Walt and J. Millman, editors, 'Proceedings of the 9th Python in Science Conference,' 2010 pp. 56 – 61.

Mesa, D., Keppler, M., Cantalloube, F., and et al., 'VLT/SPHERE exploration of the young multiplanetary system PDS70,' Astronomy & Astrophysics, 2019, **632**, A25.

Millan-Gabet, R., Malbet, F., Akeson, R., Leinert, C., Monnier, J., and Waters, R., 'The Circumstellar Environments of Young Stars at AU Scales,' in B. Reipurth, D. Jewitt, and K. Keil, editors, 'Protostars and Planets V,' 2007 p. 539.

Mirabel, I. F., Rodrigues, I., and Liu, Q. Z., 'A microquasar shot out from its birth place,' Astronomy & Astrophysics, 2004, **422**, pp. L29–L32.

Morgan, L. K., Urquhart, J. S., and Thompson, M. A., 'CO observations towards bright-rimmed clouds,' Monthly Notices of the Royal Astronomical Society, 2009, **400**(4), pp. 1726–1733.

Ninkov, Z., Bretz, D. R., Easton, J., Roger L., and Shure, M. A., 'Imaging of the Central Region of IC 1805,' Astronomical Journal, 1995, **110**, p. 2242.

Normandeau, M., Taylor, A. R., and Dewdney, P. E., 'A galactic chimney in the Perseus arm of the Milky Way,' Nature, 1996, **380**(6576), pp. 687–689.

Ochsenbein, F., Bauer, P., and Marcout, J., 'The VizieR database of astronomical catalogues,' Astronomy & Astrophysics Supplement, 2000, **143**, pp. 23–32.

Oey, M. S., Watson, A. M., Kern, K., and Walth, G. L., 'Hierarchical Triggering of Star Formation by Superbubbles in W3/W4,' Astronomical Journal, 2005, **129**(1), pp. 393–401.

Osterbrock, D. E., *Astrophysics of gaseous nebulae and active galactic nuclei*, University Science Books, 1989.

Pandey, A. K., Upadhyay, K., Nakada, Y., and Ogura, K., 'Interstellar extinction in the open clusters towards galactic longitude around 130^{deg},' Astronomy & Astrophysics, 2003, **397**, pp. 191–200.

Panwar, N., Chen, W. P., Pandey, A. K., Samal, M. R., Ogura, K., Ojha, D. K., Jose, J., and Bhatt, B. C., 'Young stellar population of bright-rimmed clouds BRC 5, BRC 7 and BRC 39,' Monthly Notices of the Royal Astronomical Society, 2014, **443**(2), pp. 1614–1628.

Panwar, N., Samal, M. R., Pandey, A. K., Jose, J., Chen, W. P., Ojha, D. K., Ogura, K., Singh, H. P., and Yadav, R. K., 'Low-mass young stellar population and star formation history of the cluster IC 1805 in the W4 H II region,' Monthly Notices of the Royal Astronomical Society, 2017, **468**(3), pp. 2684–2698.

Panwar, N., Samal, M. R., Pandey, A. K., Singh, H. P., and Sharma, S., 'Understanding Formation of Young, Distributed Low-mass Stars and Clusters in the W4 Cloud Complex,' Astronomical Journal, 2019, **157**(3), 112.

Paxton, B., Schwab, J., Bauer, E. B., Bildsten, L., Blinnikov, S., Duffell, P., Farmer, R., Goldberg, J. A., Marchant, P., Sorokina, E., Thoul, A., Townsend, R. H. D., and Timmes, F. X., 'Modules for Experiments in Stellar Astrophysics (MESA): Convective Boundaries, Element Diffusion, and Massive Star Explosions,' Astrophysical Journal Supplement Series, 2018, **234**(2), 34.

Pecaut, M. J. and Mamajek, E. E., 'Intrinsic Colors, Temperatures, and Bolometric Corrections of Pre-main-sequence Stars,' Astrophysical Journal Supplement Series, 2013, **208**(1), 9.

Pecaut, M. J., Mamajek, E. E., and Bubar, E. J., 'A Revised Age for Upper Scorpius and the Star Formation History among the F-type Members of the Scorpius-Centaurus OB Association,' Astrophysical Journal, 2012, **746**(2), 154.

Peters, T., Banerjee, R., Klessen, R. S., Mac Low, M.-M., Galván-Madrid, R., and Keto, E. R., 'H II Regions: Witnesses to Massive Star Formation,' Astrophysical Journal, 2010, **711**(2), pp. 1017–1028.

Pinte, C., Price, D. J., Ménard, F., Duchêne, G., Dent, W. R. F., Hill, T., de Gregorio-Monsalvo, I., Hales, A., and Mentiplay, D., 'Kinematic Evidence for an Embedded Protoplanet in a Circumstellar Disk,' Astrophysical Journall, 2018, **860**(1), L13.

Pinte, C., van der Plas, G., Ménard, F., Price, D. J., Christiaens, V., Hill, T., Mentiplay, D., Ginski, C., Choquet, E., Boehler, Y., Duchêne, G., Perez, S., and Casassus, S., 'Kinematic detection of a planet carving a gap in a protoplanetary disk,' Nature Astronomy, 2019, **3**, pp. 1109–1114.

Pollack, J. B., Hubickyj, O., Bodenheimer, P., Lissauer, J. J., Podolak, M., and Greenzweig, Y., 'Formation of the Giant Planets by Concurrent Accretion of Solids and Gas,' Icarus, 1996, **124**(1), pp. 62–85.

Povich, M. S., Kuhn, M. A., Getman, K. V., Busk, H. A., Feigelson, E. D., Broos, P. S., Townsley, L. K., King, R. R., and Naylor, T., 'The MYStIX Infrared-Excess Source Catalog,' Astrophysical Journals, 2013, **209**(2), 31.

Rauw, G. and Nazé, Y., 'X-ray and optical spectroscopy of the massive young open cluster IC 1805,' Astronomy & Astrophysics, 2016, **594**, A82.

Reynolds, R. J., Sterling, N. C., and Haffner, L. M., 'Detection of a Large Arc of Ionized Hydrogen Far above the Cassiopeia OB6 Association: A Superbubble Blowout into the Galactic Halo?' Astrophysical Journall, 2001, **558**(2), pp. L101–L104.

Richert, A. J. W., Feigelson, E. D., Getman, K. V., and Kuhn, M. A., 'No Evidence for Protoplanetary Disk Destruction By OB Stars in the MYStIX Sample,' Astrophysical Journal, 2015, **811**(1), 10.

Richert, A. J. W., Getman, K. V., Feigelson, E. D., Kuhn, M. A., Broos, P. S., Povich, M. S., Bate, M. R., and Garmire, G. P., 'Circumstellar disc lifetimes in numerous galactic young stellar clusters,' Monthly Notices of the Royal Astronomical Society, 2018, **477**(4), pp. 5191–5206.

Rieke, G. and Lebofsky, M., 'The interstellar extinction law from 1 to 13 microns.' Astrophysical Journal, 1985, **288**, pp. 618–621.

Rivera-Ingraham, A., Martin, P. G., Polychroni, D., and Moore, T. J. T., 'Star Formation and Young Stellar Content in the W3 Giant Molecular Cloud,' Astrophysical Journal, 2011, **743**(1), 39.

Robin, A. C., Reylé, C., Derrière, S., and Picaud, S., 'A synthetic view on structure and evolution of the Milky Way,' Astronomy & Astrophysics, 2003, **409**, pp. 523–540.

Roccatagliata, V., Bouwman, J., Henning, T., Gennaro, M., Feigelson, E., Kim, J. S., Sicilia-Aguilar, A., and Lawson, W. A., 'Disk Evolution in OB Associations: Deep Spitzer/IRAC Observations of IC 1795,' Astrophysical Journal, 2011, **733**(2), 113.

Roman-Lopes, A., Román-Zúñiga, C. G., Tapia, M., Hernández, J., Ramírez-Preciado, V., Stringfellow, G. S., Ybarra, J. E., Kim, J. S., Minniti, D., Covey, K. R., Kounkel, M., Suárez, G., Borissova, J., García-Hernández, D. A., Zamora, O., and Trujillo, J. D., 'Massive Stars in the SDSS-IV/APOGEE-2 Survey. II. OB-stars in the W345 Complexes,' Astrophysical Journal, 2019, **873**(1), 66.

Ruden, S. P. and Pollack, J. B., 'The Dynamical Evolution of the Protosolar Nebula,' Astrophysical Journal, 1991, **375**, p. 740.

Salpeter, E. E., 'The Luminosity Function and Stellar Evolution.' Astrophysical Journal, 1955, **121**, p. 161.

Schaller, G., Schaerer, D., Meynet, G., and Maeder, A., 'New grids of stellar models from 0.8 to 120 Msolar at Z=0.020 and Z=0.001,' Astronomy & Astrophysics Supplement Series, 1992, **96**, p. 269.

Sharma, S., 'Markov Chain Monte Carlo Methods for Bayesian Data Analysis in Astronomy,' Annual Reviews of Astronomy and Astrophysics, 2017, **55**(1), pp. 213–259.

Shi, H. M. and Hu, J. Y., 'Spectroscopic observations of young open clusters: IC 1805, NGC 654 and NGC 6823,' Astronomy & Astrophysicss, 1999, **136**, pp. 313–331.

Sicilia-Aguilar, A., Henning, T., Dullemond, C. P., Patel, N., Juhász, A., Bouwman, J., and Sturm, B., 'Dust Properties and Disk Structure of Evolved Protoplanetary Disks in Cep OB2: Grain Growth, Settling, Gas and Dust Mass, and Inside-out Evolution,' Astrophysical Journal, 2011, **742**(1), 39.

Siess, L., Dufour, E., and Forestini, M., 'An internet server for pre-main sequence tracks of low- and intermediate-mass stars,' Astronomy & Astrophysics, 2000, **358**, pp. 593–599.

Silverberg, S. M., Kuchner, M. J., Wisniewski, J. P., and et al., 'Follow-up Imaging of Disk Candidates from the Disk Detective Citizen Science Project: New Discoveries and False Positives in WISE Circumstellar Disk Surveys,' Astrophysical Journal, 2018, **868**(1), 43.

Straižys, V., Boyle, R. P., Janusz, R., Laugalys, V., and Kazlauskas, A., 'The open cluster IC 1805 and its vicinity: investigation of stars in the Vilnius, IPHAS, 2MASS, and WISE systems,' Astronomy & Astrophysics, 2013, **554**, A3.

Sugitani, K., Fukui, Y., and Ogura, K., 'A Catalog of Bright-rimmed Clouds with IRAS Point Sources: Candidates for Star Formation by Radiation-driven Implosion. I. The Northern Hemisphere,' Astrophysical Journal Supplement Series, 1991, **77**, p. 59.

Sung, H., Bessell, M. S., Chun, M.-Y., Yi, J., Nazé, Y., Lim, B., Karimov, R., Rauw, G., Park, B.-G., and Hur, H., 'An Optical and Infrared Photometric Study of the Young Open Cluster IC 1805 in the Giant H II Region W4 ,' Astrophysical Journals, 2017, **230**(1), 3.

Sung, H. and Lee, S.-W., 'UBV(Ikc) CCD Photometry of Young Open Clusters. I. IC 1805,' Journal of Korean Astronomical Society, 1995, **28**(2), pp. 119–137.

Testa, P., Huenemoerder, D. P., Schulz, N. S., and Ishibashi, K., 'X-Ray Emission from Young Stellar Objects in the epsilon Chamaeleontis Group: The Herbig Ae Star HD 104237 and Associated Low-Mass Stars,' Astrophysical Journal, 2008, **687**(1), pp. 579–597.

Thompson, M. A., White, G. J., Morgan, L. K., Miao, J., Fridlund, C. V. M., and Huldtgren-White, M., 'Searching for signs of triggered star formation toward IC 1848,' Astronomy & Astrophysics, 2004, **414**, pp. 1017–1041.

Tielens, A. G. G. M., 'Interstellar polycyclic aromatic hydrocarbon molecules.' Annual Review of Astronomy and Astrophysics, 2008, **46**, pp. 289–337.

Torres-Dodgen, A. V. and Weaver, W. B., 'An Atlas of Low-Resolution Near-Infrared Spectra of Normal Stars,' Publications of the Astronomical Society of the Pacific, 1993, **105**, p. 693.

Townsley, L. K., Broos, P. S., Garmire, G. P., Bouwman, J., Povich, M. S., Feigelson, E. D., Getman, K. V., and Kuhn, M. A., 'The Massive Star-Forming Regions Omnibus X-Ray Catalog,' Astrophysical Journal Supplement Series, 2014, **213**(1), 1.

van der Walt, S., Colbert, S. C., and Varoquaux, G., 'The numpy array: A structure for efficient numerical computation,' Computing in Science & Engineering, 2011, **13**(2), pp. 22–30.

Vasilevskis, S., Sanders, W. L., and van Altena, W. F., 'Membership of the open cluster IC 1805.' Astronomical Journal, 1965, **70**, p. 806.

Vázquez-Semadeni, E., *Interstellar MHD Turbulence and Star Formation*, volume 407 of *Astrophysics and Space Science Library*, p. 401, Springer, 2015.

Virtanen, P., Gommers, R., Oliphant, T. E., and et al., S. . ., 'Scipy 1.0: Fundamental algorithms for scientific computing in python,' Nature Methods, 2020.

Wang, S. and Chen, X., 'The Optical to Mid-infrared Extinction Law Based on the APOGEE, Gaia DR2, Pan-STARRS1, SDSS, APASS, 2MASS, and WISE Surveys,' Astrophysical Journal, 2019, **877**(2), 116.

West, J. L., English, J., Normandeau, M., and Landecker, T. L., 'The Fragmenting Superbubble Associated with the H II Region W4,' Astrophysical Journal, 2007, **656**(2), pp. 914–927.

Westerhout, G., 'A survey of the continuous radiation from the Galactic System at a frequency of 1390 Mc/s,' Bulletin of the Astronomical Institutes of the Netherlands, 1958, **14**, p. 215.

Williams, G. G., Olszewski, E., Lesser, M. P., and Burge, J. H., '90prime: a prime focus imager for the steward observatory 90-in. telescope,' in A. F. M. Moorwood and M. Iye, editors, '90prime: a prime focus imager for the Steward Observatory 90-in. telescope,' volume 5492 of *Society of Photo-Optical Instrumentation Engineers (SPIE) Conference Series*, 2004 pp. 787–798.

Williams, J. P. and Cieza, L. A., 'Protoplanetary Disks and Their Evolution,' Annual Review of Astronomy and Astrophysics, 2011, **49**(1), pp. 67–117.

Wolff, S. C., Strom, S. E., and Rebull, L. M., 'The Evolution of Circumstellar Disks Surrounding Intermediate-mass Stars: IC 1805,' Astrophysical Journal, 2011, **726**(1), 19.

Xiao, L. and Chang, Q., 'Evolution and Photoevaporation of Protoplanetary Disks in Clusters: The Role of Pre-stellar Core Properties,' Astrophysical Journal, 2018, **853**(1), 22.

Xu, Y., Reid, M. J., Zheng, X. W., and Menten, K. M., 'The Distance to the Perseus Spiral Arm in the Milky Way,' Science, 2006, **311**(5757), pp. 54–57.

VITA

Matt Wentzel-Long was born in St. Charles, Missouri in 1990. In 2011, he finished his Associate of Arts degree from St. Charles Community, and in 2014 he finished his Bachelor of Science in Physics and Mathematics from Westminster College in Salt Lake City, Utah. He began his studies in the fall of 2014 at the University of Missouri - St. Louis where he then earned a Master of Science in Physics in 2016. He received his PhD from the University of Missouri – St. Louis and Missouri University of Science and Technology in December 2020.